

Synthesis and Photochemistry of Phenyl Substituted-1,2,4-Thiadiazoles; ¹⁵N-labeling Studies

by

Chuchawin Changtong

A Dissertation

Submitted to the Faculty of the

Worcester Polytechnic Institute

in partial fulfillment of the requirements for the

Degree of Doctor of Philosophy

in

Chemistry

by

Approved:

Dr. James W. Pavlik

Examining Committees:

Dr. Robert E. Connors

Dr. John C. MacDonald

Dr. Gary Weisman

University of New Hampshire

ABSTRACT

Photochemistry studies of phenyl substituted-1,2,4-thiadiazoles have revealed that 5-phenyl-1,2,4-thiadiazoles **31**, **90**, **98**, **54** and **47** undergo a variety of photochemical reactions including photofragmentation, phototransposition, and photo-ring expansion while irradiation of 3-phenyl-1,2,4-thiadiazoles **46**, **105** and **106** leads mainly to the formation of photofragmentation products. The formation of the phototransposition products has been suggested to arise from a mechanism involving electrocyclic ring closure and sigmatropic sulfur migration via a bicyclic intermediate: phenyl-1,3-diaza-5-thiabicyclo[2.1.0]pentene (**BC**). ^{15}N -Labeling experiments confirm that sulfur undergoes sigmatropic shifts around all four sides of the diazetine ring. Thus, irradiation of **31-4- ^{15}N** or **54-4- ^{15}N** leads to the formation of **31-2- ^{15}N** or **54-2- ^{15}N** and to an equimolar mixture of **46-2- ^{15}N** and **46-4- ^{15}N** or **57-2- ^{15}N** and **57-4- ^{15}N** . Work in this laboratory on ^{15}N -labeling of **46-2- ^{15}N** also shows that **46** does not undergo electrocyclic ring closure but reacts exclusively by photofragmentation of the thiadiazole ring. ^{15}N -Scrambling in the photofragmentation products observed after irradiation of **31-4- ^{15}N** or **54-4- ^{15}N** is greater than ^{15}N -scrambling in the starting thiadiazoles suggesting that these products cannot arise only from direct fragmentation of the thiadiazole rings. An additional pathway for the formation of these products is required.

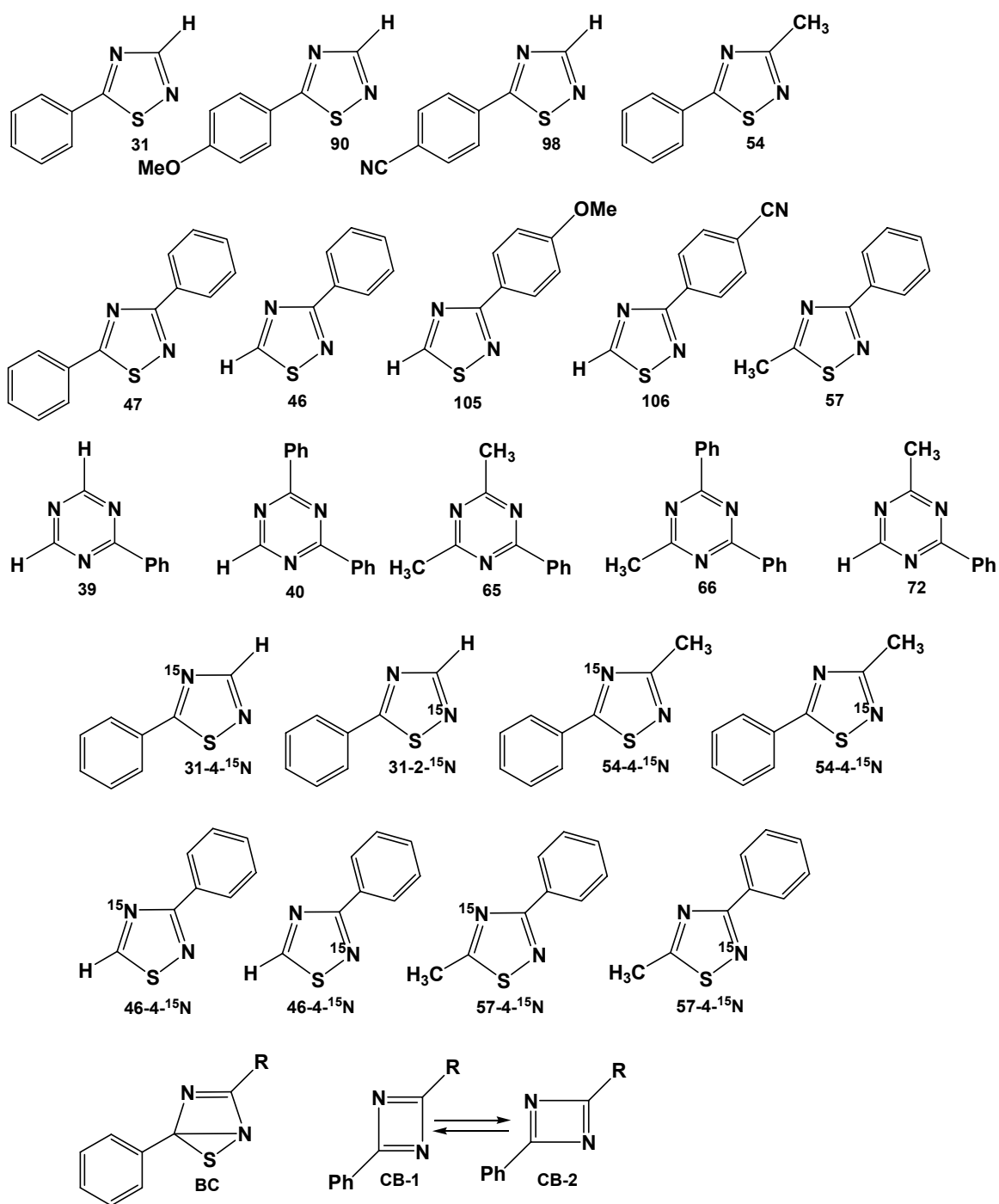
The formation of phenyltriazines, the photo-ring expansion products **39** and **40** or **65** and **66** from photolysis of **31** or **54** is proposed to arise via phenyldiazacyclobutadienes (**CB**), generated from elimination of atomic sulfur from the bicyclic intermediates. It is suggested that phenyldiazacyclobutadienes then undergo [4+2] cycloaddition self-coupling resulting in the formation of unstable tricyclic intermediates which finally cleave to give phenyltriazines

and nitriles. The observed ^{15}N distribution in the phenyltriazine photoproducts formed after photolysis of **31-4- ^{15}N** or **54-4- ^{15}N** and the formation triazine **72** after irradiation of a mixture of **31+54** are consistent with this mechanism. The formation of nitriles by this pathway would account for the additional ^{15}N -scrambling in the photofragmentation products.

The photochemically generated phenyl-1,3-diaza-5-thiabicyclo[2.1.0]pentenes are the key intermediates in this suggested mechanism. In the presence of furan, these intermediates are expected to be trapped as Diels-Alder adducts. Irradiation of phenylthiadiazoles **31**, **54** and **47** in furan solvent lead to increased consumption of these thiadiazoles, to quenching of the known photoproducts, and to the formation of new products suggested to result from furan trapping of the thiadiazoles followed by elimination of sulfur. Irradiation of **46** in furan solvent leads only to the formation of the photofragmentation product; no furan trapping adduct is observed. This result is consistent with the ^{15}N -labeling experiment indicating that **46** does not undergo electrocyclic ring closure after irradiation.

The photoreactivity of these phenylthiadiazoles in acetonitrile is substantially decreased when the phenyl ring at position 4 is substituted with an electron donating or withdrawing group. However, they are more photoreactive in cyclohexane solvent than in acetonitrile. The fluorescence emission spectra of these (4'-substituted)phenyl-1,2,4-thiadiazoles exhibit moderate - large Stokes' shifts in acetonitrile. The magnitudes of these Stokes' shifts decrease in cyclohexane. This suggests a charge transfer character associated with the excited states of these thiadiazoles. In acetonitrile, these charge transfer excited states would be stabilized and become the lowest energy excited state. These charge transfer excited states would not be photoreactive and, thus, fluorescence emission becomes an effective deactivation process. In cyclohexane solvent, the charge transfer excited states

would be less stabilized and, thus, the relaxed $S_{1(v0)}(\pi,\pi^*)$ would, then, become the lowest excited state. The relaxed $S_{1(v0)}(\pi,\pi^*)$ would be the state from which the observed photoproducts originate and the observed fluorescence with the smaller Stokes' shifts compared with the Stokes' shifts observed in acetonitrile.



ACKNOWLEDGEMENT

I would like to express my sincere gratitude to my advisor Prof. James W. Pavlik for his patient guidance, encouragement, assistance, suggestion and support through out the research project and in the preparation of this thesis. I am indebted to Prof. Alfred A. Scala for his many useful and friendly discussions in mass spectrometric analysis.

Financial support from the Department of Chemistry & Biochemistry, WPI is gratefully acknowledged. I also thank Dr. Jose Cruz and Dr. Yi Lui for their many useful discussions in NMR analysis and synthetic methodologies. Ernesto R. Soto is also acknowledged for his help on cyclic voltammetry measurements.

Finally, I would like to express my appreciation to my parents, brother, and friends for their support, devotion, and encouragement during this study.

CONTENTS

	Pages
ABSTRACT	i
ACKNOWLEDGEMENT.....	iv
CONTENTS.....	v
LIST OF FIGURES.....	xiv
LIST OF SCHEMES.....	xxxiii
LIST OF TABLES.....	xxxviii
CHAPTER 1 INTRODUCTION	
1.1 Photochemistry of isothiazoles and thiazoles.....	1
1.2 Photochemistry of 1,2,4-thiadiazoles.....	7
CHAPTER 2 RESULTS AND DISCUSSION	
2.1 Photochemistry of 5-phenyl-1,2,4-thiadiazole.....	8
2.1.1 Synthesis of 5-phenyl-1,2,4-thiadiazole.....	8
2.1.1.1 Synthesis of N-[(dimethylamino)methylene]thiobenzamide.....	9
2.1.1.2 Synthesis of 5-phenyl-1,2,4-thiadiazole.....	15
2.1.2 Synthesis of 2-phenyl- and 2,4-diphenyl-1,3,5-triazine.....	21
2.1.3 Photochemistry of 5-phenyl-1,2,4-thiadiazole.....	27
2.2 Photochemistry of 3-phenyl-1,2,4-thiadiazole.....	47
2.2.1 Synthesis of 3-phenyl-1,2,4-thiadiazole.....	47
2.2.1.1 Synthesis of 5-phenyl-1,3,4-oxathiazole-2-one.....	47
2.2.1.2 Synthesis of ethyl 3-phenyl-1,2,4-thiadiazole-5-carboxylate	51

2.2.1.3 Synthesis of 3-phenyl-1,2,4-thiadiazole.....	55
2.2.2 Photochemistry of 3-phenyl-1,2,4-thiadiazole.....	59
2.3 Photochemistry of 3-methyl-5phenyl-1,2,4-thiadiazole.....	67
2.3.1 Synthesis of 3-methyl-5-phenyl-1,2,4-thiadiazole.....	67
2.3.1.1 Synthesis of N-[(dimethylamino)ethylidene]thiobenzamide..	68
2.3.1.2 Synthesis of 3-methyl-5-phenyl-1,2,4-thiadiazole.....	74
2.3.2 Synthesis of 5-methyl-3-phenyl-1,2,4-thiadiazole.....	78
2.3.2.1 Synthesis of 5-chloro-3-phenyl-1,2,4- thiadiazole.....	79
2.3.2.2 Synthesis of diethyl 3-phenyl-1,2,4-thiadiazole-5-malonate..	84
2.3.2.3 Synthesis of 5-methyl-3-phenyl-1,2,4-thiadiazole.....	92
2.3.3 Synthesis of 2,4-dimethyl-6-phenyl-1,3,5-triazine and 2-methyl-4,6-diphenyl-1,3,5-triazine.....	97
2.3.3.1 Synthesis of N-[(dimethylamino)ethylidene]benzamide.....	98
2.3.3.2 Synthesis of 2,4-dimethyl-6-phenyl-1,3,5-triazine.....	104
2.3.3.3 Synthesis of 2-methyl-4,6-diphenyl-1,3,5-triazine.....	109
2.3.4 Photochemistry of 3-methyl-5-phenyl-1,2,4-thiadiazole.....	113
2.4 Photochemistry of 5-phenyl-1,2,4-thiadiazole- 4^{15}N	123
2.4.1 Synthesis of 5-phenyl-1,2,4-thiadiazole- 4^{15}N	123
2.4.1.1 Synthesis of thiobenzamide- ^{15}N	123
2.4.1.2 Synthesis of N-[(dimethylamino)methylene] thiobenzamide- ^{15}N	129
2.4.1.3 Synthesis of 5-phenyl-1,2,4-thiadiazole – 4^{15}N	134

2.4.2 Photochemistry of 5-phenyl-1,2,4-thiadiazole-4 ¹⁵ N.....	146
2.4.3 Preparative scale photolysis.....	165
2.4.3.1 Preparative gas chromatography.....	165
2.4.3.2 Preparative layer chromatography.....	171
2.5 Photochemistry of 3-methyl-5-phenyl-1,2,4-thiadiazole – 4 ¹⁵ N.....	174
2.5.1 Synthesis of 3-methyl-5-phenyl-1,2,4-thiadiazole – 4 ¹⁵ N.....	174
2.5.2 Photochemistry of 3-methyl-5-phenyl-1,2,4- thiadiazole – 4 ¹⁵ N.....	190
2.5.3 Preparative scale photolysis.....	207
2.6 Photolysis of 5-phenyl-1,2,4-thiadiazole in the presence of ethyl cyanoformate.....	213
2.7 Photolysis of 3-phenyl-1,2,4-thiadiazole in the presence of ethyl cyanoformate.....	220
2.8 Photolysis 3-methyl-5-phenyl-1,2,4-thiadiazole and 5-phenyl-1,2,4-thiadiazole mixture in acetonitrile.....	220
2.8.1 Synthesis of 2-methyl-4-phenyl-1,3,5-triazine.....	228
2.8.1.1 Synthesis of N-[(dimethylamino)methylene]benzamide.....	229
2.8.1.2 Synthesis of 2-methyl-4-phenyl-1,3,5-triazine.....	233
2.8.2 Irradiation of 5-phenyl- and 3-methyl-5-phenyl-1,2,4-thiadiazole mixture in acetonitrile.....	238

2.9 Photochemistry of phenyl substituted-1,2,4-thiadiazoles in furan solvent	251
2.9.1 Photochemistry of 5-phenyl-1,2,4-thiadiazoles in furan solvent....	254
2.9.1.1 Irradiation of 5-phenyl-1,2,4-thiadiazole in furan solvent...	254
2.9.1.2 Irradiation of 3-methyl-5-phenyl- and diphenyl-1,2,4- thiadiazole in furan solvent.....	260
2.9.1.3 Preparative scale photolysis of diphenyl-1,2,4-thiadiazole in Furan.....	269
2.9.2 Irradiation of 3-phenyl-1,2,4-thiadiazole in furan solvent.....	278
2.9.3 Irradiation of 3-phenyl-1,2,4-thiadiazole in tetrahydrofuran solvent	283
 2.10 Photochemistry of 5-(4'-substituted)phenyl- and 3-(4'-substituted)phenyl - 1,2,4-thiadiazoles.....	 290
2.10.1 Photochemistry of 5-(4'-substituted)phenyl-1,2,4-thiadiazole.....	290
2.10.1.1 Synthesis of 5-(4'-methoxy)phenyl-1,2,4-thiadiazole.....	290
2.10.1.1.1 Synthesis of 4-methoxythiobenzamide.....	291
2.10.1.1.2 Synthesis of N-[(dimethylamino)methylene] 4-methoxythiobenzamide.....	296
2.10.1.1.3 Synthesis of 5-(4'-methoxy)phenyl-1,2,4-thiadiazole...	300
2.10.1.2 Synthesis of 2-(4'-methoxy)phenyl-1,3,5-triazine.....	305
2.10.1.2.1 Synthesis of N-[(dimethylamino)methylene] 4-methoxybenzamide.....	305
2.10.1.2.2 Synthesis of 2-(4'-methoxy)phenyl-1,3,5-triazine.....	310

2.10.1.3 Synthesis of 5-(4'-cyano)phenyl-1,2,4-thiadiazole.....	315
2.10.1.3.1 Synthesis of 4-cyanobenzamide.....	316
2.10.1.3.2 Synthesis of 4-cyanothiobenzamide.....	320
2.10.1.3.3 Synthesis of N-[(dimethylamino)methylene] 4-cyanothiobenzamide.....	324
2.10.1.3.4 Synthesis of 5-(4'-cyano)phenyl-1,2,4-thiadiazole.....	329
2.10.1.4 Photochemistry of 5-(4'-substituted)phenyl- 1,2,4-thiadiazoles.....	336
2.10.2 Photochemistry of 3-(4'-substituted)phenyl-1,2,4-thiadiazoles...	358
2.10.2.1 Synthesis of 3-(4'-methoxy)phenyl-1,2,4-thiadiazole.....	358
2.10.2.1.1 Synthesis of 5-(4'-methoxy)phenyl-1,3,4- oxathiazole-2-one.....	359
2.10.2.1.2 Synthesis of ethyl 3-(4-methoxy)phenyl-1,2,4- thiadiazole-5-carboxylate.....	363
2.10.2.1.3 Synthesis of 3-(4'-methoxy)phenyl-1,2,4-thiadiazole.	367
2.10.2.2 Synthesis of 3-(4'-cyano)phenyl-1,2,4-thiadiazole.....	371
2.10.2.2.1 Synthesis of 5-(4'-cyano)phenyl-1,3,4- oxathiazole-2-one.....	372
2.10.2.2.2 Synthesis of ethyl 3-(4'-cyano)phenyl-1,2,4- thiadiazole-5-carboxylate.....	376
2.10.2.2.3 Synthesis of 3-(4'-cyano)phenyl-1,2,4-thiadiazole....	380

2.10.2.3 Photochemistry of 3-(4'-substituted)phenyl-1,2,4-thiadiazoles.....	385
2.11 Spectroscopic data of phenyl substituted-1,2,4-thiadiazoles.....	398
2.11.1 5-Phenyl-1,2,4-thiadiazole.....	398
2.11.2 5-(4'-Methoxy)phenyl-1,2,4-thiadiazole.....	407
2.11.3 5-(4'-Cyano)phenyl-1,2,4-thiadiazole.....	415
2.11.4 3-Methyl-5-phenyl-1,2,4-thiadiazole.....	423
2.11.5 3-Cyano-5-phenyl-1,2,4-thiadiazole.....	427
2.11.6 3-Amino-5-phenyl-1,2,4-thiadaizole.....	431
2.11.7 Diphenyl-1,2,4-thiadiazole.....	435
2.11.8 3-Phenyl-1,2,4-thiadiazole.....	440
2.11.9 3-(4'-Methoxy)phenyl-1,2,4-thiadiazole.....	449
2.11.10 3-(4'-Cyano)phenyl-1,2,4-thiadiazole.....	456
2.10.11 5-Cyano-3-phenyl-1,2,4-thiadiazole.....	461
2.10.12 5-Amino-3-phenyl-1,2,4-thiadiazole.....	465
2.10.13 Summary on spectroscopic properties of phenyl substituted-1,2,4-thiadiazoles.....	469
2.12 Triplet sensitizations.....	489
2.12.1 Triplet sensitization of 5-phenyl-1,2,4-thiadiazole.....	489
2.12.2 Triplet sensitization of 5-phenyl-1,2,4-thiadiazole.....	497

2.13 Photochemistry of phenyl substituted-1,2,4-thiadiazoles in the presence of tri-n-butylphosphine.....	504
2.13.1 Synthesis of tri-n-butylphosphine sulfide.....	506
2.13.2 Photochemistry of 5-phenyl-1,2,4-thiadiazole in the presence of tri-n-butylphosphine.....	512
2.13.3 Photochemistry of 5-(4'-methoxy)phenyl-1,2,4-thiadiazole in the presence of tri-n-butylphosphine.....	520
2.13.4 Photochemistry of 5-phenyl-1,2,4-thiadiazole in the presence of tri-n-butylphosphine.....	524
2.14 Photochemistry of phenyl substituted-1,2,4-thiadiazoles in the presence of triethylamine or propylamine.....	528
2.14.1 Irradiation of 5-phenyl-1,2,4-thiadiazole in the presence of triethylamine or propylamine.....	535
2.14.2 Irradiation of 3-phenyl-1,2,4-thiadiazole in the presence of triethylamine or propylamine.....	542

CHAPTER 3 EXPERIMENTAL

3.1 Synthesis of the phenyl-1,2,4-thiadiazoles and some expected photoproducts.....	549
3.1.1 General procedure.....	549
3.1.2 Synthesis of 5-phenyl-1,2,4-thiadiazole.....	550
3.1.3 Synthesis of 3-phenyl-1,2,4-thiadiazole.....	554
3.1.4 Synthesis of 3-methyl-5-phenyl-1,2,4-thiadiazole.....	556

3.1.5	Synthesis of diphenyl-1,2,4-thiadiazole.....	558
3.1.6	Synthesis of 5-phenyl-1,2,4-thiadiazole-4- ¹⁵ N.....	559
3.1.7	Synthesis of 3-methyl-5-phenyl-1,2,4-thiadiazole-4- ¹⁵ N.....	562
3.1.8	Synthesis of 5-(4'-methoxy)phenyl-1,2,4-thiadiazole.....	564
3.1.9	Synthesis of 5-(4'-cyano)phenyl-1,2,4-thiadiazole.....	566
3.1.10	Synthesis of 3-(4'-methoxy)phenyl-1,2,4-thiadiazole.....	569
3.1.11	Synthesis of 3-(4'-cyano)phenyl-1,2,4-thiadiazole.....	571
3.1.12	Synthesis of 5-methyl-3-phenyl-1,2,4-thiadiazole.....	574
3.1.13	Synthesis of 2-phenyl-1,3,5-triazine and 2,4-diphenyl-1,3,5-triazine.....	576
3.1.14	Synthesis of 2,4-dimethyl-6-phenyl-1,3,5-triazine and 2-methyl-4,6-diphenyl-1,3,5-triazine.....	578
3.1.15	Synthesis of 2-(4'-methoxy)phenyl-1,3,5-triazine.....	581
3.2	Photochemistry.....	583
3.2.1	Photolysis of 5-phenyl-1,2,4-thiadiazole.....	583
3.2.2	Photolysis of 5-phenyl-1,2,4-thiadiazole.....	585
3.2.3	Photolysis of 3-methyl-5-phenyl-1,2,4-thiadiazole.....	587
3.2.4	Photolysis of 5-phenyl-1,2,4-thiadiazole-4- ¹⁵ N.....	589
3.2.5	Photolysis of 3-methyl-5-phenyl-1,2,4-thiadiazole-4- ¹⁵ N.....	594
3.2.6	Photolysis of 5-phenyl-1,2,4-thiadiazole in the presence of ethyl cyanoformate.....	598
3.2.7	Photolysis of 3-phenyl-1,2,4-thiadiazole in the presence of	

ethyl cyanofornate.....	599
3.2.8 Photolysis of a mixture of 3-methyl-5-phenyl-1,2,4-thiadiazole and 5-phenyl-1,2,4-thiadiazole.....	600
3.2.9 Photochemistry of phenyl substituted-1,2,4-thiadiazoles in furan solvent	601
3.2.10 Photochemistry of 5-(4'-substituted)phenyl- and 3-(4'-substituted)phenyl-1,2,4-thiadiazoles	605
3.2.11 Spectroscopic data of phenyl-1,2,4-thiadiazoles.....	606
3.2.12 Triplet sensitization of phenyl-1,2,4-thiadiazole.....	607
3.2.13 Photochemistry of phenyl substituted-1,2,4-thiaidazoles in the presence of triethylamine or propylamine.....	608
3.2.14 Photochemistry of phenyl substituted-1,2,4-thiadiazoles in the presence of tri-n-butylphosphine.....	609
CHAPTER 4 CONCLUSION	612
REFERENCES.....	622
APPENDIX A – Calibration Curves.....	624
APPENDIX B – Ground States Geometry Optimization by AM1.....	627
APPENDIX C – List of Structures.....	630

LIST OF FIGURES

Figures	Pages
1a. GC-trace of the synthesized 32	10
1b. Mass spectrum of the compound eluted at a retention time of 33.9 min from the synthesis of 32	10
2. ¹ H-NMR spectrum of the synthesized 32	11
3. ¹³ C-NMR spectrum of the synthesized 32	12
4. ¹ H- ¹³ C-NMR correlation spectrum of the synthesized 32	14
5a. GC-trace of the synthesized 31	16
5b. Mass spectrum of the compound eluted at a retention time of 6.6 min from the synthesis of 31	17
5c. Mass spectrum of the compound eluted at a retention time of 10.9 min from the synthesis of 31	17
6. ¹ H-NMR spectrum of the synthesized 31	20
7a. GC-trace of the white solid A from the synthesis of 39 and 40	22
7b. Mass spectrum of the white solid A	23
8a. GC-trace of the white solid B from the synthesis of 39 and 40	23
8b. Mass spectrum of the white solid B	24
9. ¹ H-NMR spectrum of the white solid A.....	25
10. ¹ H-NMR spectrum of the white solid B.....	25
11a. UV-absorption spectrum of 31 in acetonitrile.....	27
11b. UV-overlay spectrum of the photolysis of 31 in acetonitrile.....	28
12a. UV-absorption spectrum of 31 in cyclohexane.....	27
12b. UV-overlay spectrum of the photolysis of 31 in cyclohexane.....	28
13a. GC-trace of solution of 31 before irradiation	31
13b. GC-trace of solution of 31 after irradiation	31
14a. GC-trace of the concentrated photolysate of 31 after 210 min of irradiation	32
14b. Mass spectrum of the photoproduct eluted at retention time 4 min.....	32

Figures	Pages
14c. Mass spectrum of the photoproduct eluted at retention time 10 min.....	35
14d. Mass spectrum of the photoproduct eluted at retention time 10.6 min...	36
14e. Mass spectrum of the photoproduct eluted at retention time 12.1 min....	37
14f. Mass spectrum of the photoproduct eluted at retention time 23.3 min....	39
14g. Mass spectrum of the photoproduct eluted at retention time 40 min....	40
14h. Mass spectrum of the photoproduct eluted at retention time 40.6 min....	42
14i. Mass spectrum of the photoproduct eluted at retention time 42.7 min....	42
14j. Mass spectrum of the photoproduct eluted at retention time 48.9 min....	43
15a. GC-trace of an authentic sample of 43	33
15b. Mass spectrum of an authentic sample of 43	34
16a. GC-trace of an authentic sample of 39	35
16b. Mass spectrum of an authentic sample of 39	36
17. Mass spectrum of the synthesized 46	38
18a. GC-trace of an authentic sample of 40	40
18b. Mass spectrum of an authentic sample of 40	41
19a. GC-trace of an authentic sample of 47	44
19b. Mass spectrum of an authentic sample of 47	44
20a. GC-trace of the white crystals from synthesis of 51	48
20b. Mass spectrum of the white crystals.....	48
21. ¹ H-NMR spectrum of the white crystals.....	50
22a. ¹³ C-NMR spectrum of the white crystals.....	50
22b. ¹³ C-DEPT 135 spectrum of the white crystals.....	50
23a. GC-trace of the synthesized 50	51
23b. Mass spectrum of the synthesized 50	52
24. ¹ H-NMR spectrum of the synthesized 50	53
25a. ¹³ C-NMR spectrum of the synthesized 50	54
25b. ¹³ C-DEPT 135 spectrum of the synthesized 50	54
26a. GC-trace of the synthesized 46	55
26b. Mass spectrum of the peak at RT 13.2 min	56

Figures	Pages
27. ¹ H-NMR spectrum of the synthesized 46	57
28a. ¹³ C-NMR spectrum of the synthesized 46	58
28b. ¹³ C-DEPT 135 spectrum of the synthesized 46	58
29a. UV-absorption spectrum of 46 in cyclohexane.....	60
29b. UV overlay spectrum of the photolysis of 46	60
30a. GLC analysis of 46 in acetonitrile before irradiation.....	62
30b. GLC analysis of 46 in acetonitrile after 120 min of irradiation.....	62
31a. GC-trace of the concentrated photolysate of 46 after 120 min of irradiation.....	63
31b. Mass spectrum of the peak at a retention time of 17.7 min.....	63
31c. Mass spectrum of the peak at a retention time of 7.5 min.....	64
31d. Mass spectrum of the peak at a retention time of 34.5 min.....	65
32a. GC-trace of 55	69
32b. Mass spectrum of the peak eluted at a retention time of 23.9 min; 55	69
33. ¹ H-NMR spectrum of 55	70
34a. ¹³ C-NMR spectrum of 55	71
34b. ¹³ C- Scale expansion exhibits the two singlets at δ 39.5 and 39.7.....	71
35. ¹ H- ¹³ C correlation spectrum of 55	73
36a. GC-trace of 54	75
36b. Mass spectrum of 54	75
37. ¹ H-NMR spectrum of 54	76
38a. ¹³ C-NMR spectrum of 54	77
38b. ¹³ C-DEPT 135 spectrum of 54	78
39a. GC analysis of 58	81
39b. Mass spectrum of 58	81
40. ¹ H-NMR spectrum of 58	82
41a. ¹³ C-NMR spectrum of 58	83
41b. ¹³ C-DEPT 135 spectrum of 58	83
42a. GC analysis of the yellow solid obtained in the synthesis of 59	85

Figures	Pages
42b. Mass spectrum of the component eluted at 18.5 min.....	85
43. ¹ H-NMR spectrum of 59	87
44. ¹ H- ¹ H coupling (COSY) spectrum of 59	88
45a. ¹³ C-NMR spectrum of 59	89
45b. ¹³ C-DEPT 135 spectrum of 59	90
46. ¹³ C- ¹ H correlation spectrum of 59	91
47a. GC-trace of the white solid from the synthesis of 57	92
47b. Mass spectrum of the component at RT of 9.5 min.....	93
48. ¹ H-NMR spectrum of 57	95
49. ¹³ C-NMR spectrum of 57	96
50a. GC-trace of the dark viscous liquid expected to be 67	99
50b. Mass spectrum of the peak eluted at a retention time of 17.4 min.....	99
51. ¹ H-NMR spectrum of the dark liquid from the synthesis of 67	100
52a. ¹³ C-NMR spectrum of the dark liquid from the synthesis of 67	101
52b. ¹³ C-scale expansion spectrum of the dark liquid.....	102
53. ¹ H- ¹³ C correlation spectrum of the dark liquid.....	103
54a. GC-trace of the crude product from the synthesis of 65	106
54b. Mass spectrum of the peak eluted with a retention time of 16.3 min.....	106
55. ¹ H-NMR spectrum of the yellow liquid expected to be 65	107
56a. ¹³ C – NMR spectrum of the yellow liquid expected to be 65	108
56b. ¹³ C-DEPT 135 spectrum of the yellow liquid expected to be 65	109
57a. GC-trace of the white solid expected to be 66	110
57b. Mass spectrum of the peak eluted at a retention time of 32.4 min.....	110
58. ¹ H-NMR spectrum of the white solid from the synthesis of 66	111
59a. ¹³ C-NMR spectrum of the white solid from the synthesis of 66	112
59b. ¹³ C-DEPT 135 spectrum of the white solid from the synthesis of 66	112
60a. UV-absorption spectrum of 54 in acetonitrile before irradiation.....	114
60b. UV-overlay spectrum of the photolysis of 54 in acetonitrile.....	114

Figures	Pages
61a. GLC analysis of 54 in acetonitrile before irradiation.....	115
61b. GLC analysis of the reaction mixture after 150 min of irradiation.....	116
62a. GC-analysis of the concentrated reaction mixture.....	117
62b. Mass spectrum of the peak eluted at a retention time of 4.1 min.....	117
62c. Mass spectrum of the peak eluted at a retention time of 29.2 min.....	118
62d. Mass spectrum of the peak eluted at a retention time of 13.0 min.....	119
62e. Mass spectrum of the peak eluted at a retention time of 14.0 min.....	122
63. Mass spectrum of an authentic sample of 65	120
64a. GC-trace (HP588) of 54 before irradiation.....	121
64b. Mass spectrum of 54 after irradiation.....	121
63a. Mass spectrum of 34-¹⁵N	125
63b. Mass spectrum of 34-¹⁴N	125
64a. ¹ H-NMR spectrum of the synthesized 34-¹⁵N	126
64b. ¹ H-scale expansion spectrum of the synthesized 34-¹⁵N	127
65. ¹³ C-NMR spectrum of the synthesized 34-¹⁵N	128
66. ¹⁵ N-NMR spectrum of the synthesized 34-¹⁵N	128
67. ¹ H-NMR spectrum of 32¹⁵N	130
68. ¹³ C-NMR spectrum of 32¹⁵N	130
69. Two-dimensional ¹ H- ¹³ C correlation spectrum of 32-¹⁵N	132
70. ¹⁵ N-NMR spectrum of 32-¹⁵N	133
71a. GC-trace of the synthesized 31-4¹⁵N	135
71b. Mass spectrum of the peak eluted at a retention time of 11.1 min.....	136
71c. Mass spectrum of the peak eluted at a retention time of 6.6 min.....	136
72. Mass spectrum of the synthetic 37	137
73a. GC-trace of the purified 31-4¹⁵N	138
73b. Mass spectrum of the peak eluted at a retention time of 11.1 min.....	139
74a. ¹ H-NMR spectrum of the purified 31-4¹⁵N	140
74b. ¹ H-scale expansion spectrum of the purified 31-4¹⁵N	140
75a. ¹³ C-NMR spectrum of the purified 31-4¹⁵N	141

Figures	Pages
75b. ¹³ C–scale expansion spectrum of purified 31-4¹⁵N showing the signal at δ 188.8 as singlet.....	142
75c. ¹³ C–scale expansion spectrum of purified 31-4¹⁵N showing the signal at δ 164.7 as doublet.....	142
76. Two-dimensional ¹ H– ¹³ C correlation spectrum of purified 31-4¹⁵N	144
77. ¹⁵ N–NMR spectrum of the purified 31-4¹⁵N	145
78a. GC-trace of solution of 31-4¹⁵N before irradiation	148
78b. Mass spectrum of 31-4¹⁵N before irradiation.....	148
79. GC-trace of the un-consumed reactant after 180 min of irradiation.....	150
80. GLC trace (PE9000) of 31-4¹⁵N solution after 16 min of irradiation.....	151
81a. GC trace (HP588) of 31-4¹⁵N solution after 16 min of irradiation.....	151
81b. Mass spectrum of the un-consumed reactant.....	152
81c. Mass spectrum of benzonitrile-photoproduct.....	154
81d. Mass spectrum of 3-phenyl-1,2,4-thiadiazole – photoproduct.....	157
81e. Mass spectrum of 2-phenyl-1,3,5-triazine photoproduct.....	158
81f. Mass spectrum of 2,4-diphenyl-1,3,5-triazine photoproduct.....	162
82. Plot of the ratio of the intensities of the 135/136 peaks.....	153
83. Plot of the ratio of the intensities of the 103/104 peaks.....	154
84. Mass spectrum of un-labeled 3-phenyl-1,2,4-thiadiazole.....	156
85. Plot of the ratio of the intensities of 135/136 peaks of 3-phenyl-1,2,4-thiadiazole- ¹⁵ N.....	156
86. Plot of the ratio of the intensities of the 158/159 peaks-phenyltriazine- ¹⁵ N.....	158
87. Mass spectrum of un-labeled 2-phenyl-1,3,5-triazine.....	159
88. Mass spectrum of regular 2,4-diphenyl-1,3,5-triazine.....	163
89. ¹ H-NMR spectrum of the isolated un-consumed 5-phenyl-1,2,4-thiadiazole- ¹⁵ N.....	166
90a. ¹⁵ N-NMR spectrum of 31-4¹⁵N before irradiation.....	167
90b. ¹⁵ N-NMR spectrum of the isolated un-consumed reactant after irradiation.....	167
91. ¹ H-NMR spectrum of the isolated 3-phenyl-1,2,4-thiadiazole- ¹⁵ N.....	169

Figures	Pages
92. ^{15}N -NMR spectrum of the isolated 3-phenyl-1,2,4-thiadiazole- ^{15}N	170
93. ^1H -NMR spectrum of the isolated un-consumed reactant after irradiation..	172
94. ^1H -NMR spectrum of a mixture of $46\text{-}4^{15}\text{N}$ and $46\text{-}2^{15}\text{N}$	173
95a. ^1H – NMR spectrum of $34\text{-}^{15}\text{N}$	175
95b. ^1H -NMR spectrum of $34\text{-}^{15}\text{N}$; scale expansion at δ 7.12-7.92.....	176
96. ^{13}C – NMR spectrum of $34\text{-}^{15}\text{N}$	176
97. ^1H – NMR spectrum of $55\text{-}^{15}\text{N}$	177
98a. ^{13}C – NMR spectrum of $55\text{-}^{15}\text{N}$	179
98b. ^{13}C -scale expansion spectrum of $55\text{-}^{15}\text{N}$	179
99. ^1H - ^{13}C correlation spectrum of $55\text{-}^{15}\text{N}$	180
100. ^{15}N -NMR spectrum of $55\text{-}^{15}\text{N}$	181
101a. GC-trace of orange crystals from synthesis of $55\text{-}^{15}\text{N}$	182
101b. Mass spectrum of the peak eluted at a retention time of 39.5 min.....	182
102a. GC-trace of $54\text{-}4^{15}\text{N}$	183
102b. Mass spectrum of $54\text{-}4^{15}\text{N}$	184
103. ^1H – NMR spectrum of $54\text{-}^{15}\text{N}$	185
104a. ^{13}C – NMR spectrum of $54\text{-}^{15}\text{N}$	187
104b. ^{13}C – DEPT 135 spectrum of $54\text{-}^{15}\text{N}$	188
105. ^{15}N -NMR spectrum of $54\text{-}4^{15}\text{N}$ and the scale expansion showing an un-resolved quartet.....	189
106a. GC-trace of $54\text{-}4^{15}\text{N}$ before irradiation.....	191
106b. Mass spectrum of $54\text{-}4^{15}\text{N}$ before irradiation.....	191
107. GLC analysis (PE9000) of the solution of $54\text{-}4^{15}\text{N}$ after 18 min of irradiation.....	194
108a. GC-trace (HP588) of the reaction solution at 18 min of irradiation.....	194
108b. Mass spectrum of the peak eluted at a retention time of 5 min.....	195
108c. Mass spectrum of the un-consumed reactant	197
108d. Mass spectrum of the peak eluted at a retention time of 40.5 min.....	198
108e. Mass spectrum of the peak eluted at a retention time of 42.7 min.....	201

Figures	Pages
108f. Mass spectrum of the peak eluted at a retention time of 57.7 min.....	204
109. Plot of 103/104 ratio as a function of irradiation.....	195
110. Plot of ratio of the 186/187 peaks as a function of irradiation.....	198
111. Mass spectrum of regular 2,4-dimethyl-6-phenyl-1,3,5-triazine.....	199
112. Mass spectrum of an authentic sample of 57	202
113. Formation of 66 contains 1 and 2 ¹⁵ N atoms.....	203
114. Mass spectrum of 2-methyl-4,6-diphenyl-1,3,5-triazine.....	204
117. ¹ H-spectrum of fractions 16-18.....	208
118a. ¹³ C-spectrum of fractions 16-18.....	208
118b. ¹³ C-scale expansion of a doublet at δ 18.0.....	209
118c. ¹³ C-scale expansion of a doublet at δ 129.4 and 129.5.....	210
119. Mass spectrum of the un-consumed reactant at 640 min of irradiation...	210
120. ¹⁵ N-NMR spectrum of fractions 16-18.....	212
121a. GLC analysis of solution of 31 containing 49 before irradiation.....	216
121b. GLC analysis of solution of 31 containing 49 after irradiation.....	216
121c. GLC analysis of the reaction solution spiked with an authentic 50	217
122a. GC-trace of the concentrated solution after 210 min of irradiation.....	218
122b. Mass spectrum of a suspected peak to be 50	218
123. Mass spectrum of an authentic sample of 50	219
124a. GLC analysis of the solution of 31+49 before irradiation.....	221
124b. GLC analysis of the solution of 31+49 after irradiation.....	222
124c. GLC analysis of the solution of 31+49 after irradiation spiked with an authentic 50	222
125a. GC-trace (HP588) of the un-concentrated reaction solution after irradiation.....	223
125b. Mass spectrum of the suspected product at RT 17 min.....	224
126. Mass spectrum of an authentic sample of 50	224
127a. GC (HP588) analysis of 31	229
127b. Mass spectrum of 31	230

Figures	Pages
128. ¹ H-spectrum of 31	231
129a. ¹³ C-spectrum of 31	232
129b. ¹³ C-DEPT 135 of 31	233
130a. GC analysis of the 72	234
130b. Mass spectrum of the 72	235
131. ¹ H-spectrum of 72	236
132a. ¹³ C-spectrum of 72	237
132b. ¹³ C-DEPT 135 of 72	237
133a. GLC analysis of 31 in acetonitrile before irradiation.....	239
133b. GLC analysis of 31 in acetonitrile after 650 min of irradiation.....	239
134a. GLC analysis of 54 in acetonitrile before irradiation.....	240
134b. GLC analysis of 54 in acetonitrile after 650 min of irradiation.....	240
135. GLC analysis of the mixture solution after 650 min of irradiation.....	241
136. GLC analysis of an authentic sample of 72	241
137. GLC analysis of the irradiated mixture solution spiked with an authentic sample 72	243
138a. GC-trace (HP588) of the mixture solution after 650 min of irradiation..	244
138b. Mass spectrum of the component eluted with a retention of 19.2 min...	244
139. GC-trace (HP588) of the irradiated mixture spiked with an authentic sample of 72	245
140a. GC analysis of the concentrated 1 photolysate after irradiation.....	246
140b. Mass spectrum of the Unk2 eluted with a retention time of 35 min.....	247
140c. Mass spectrum of the Unk1 eluted with a retention time of 18 min.....	248
141. GC (HP588) and mass spectrum of an authentic sample of 34	249
142a. GC-trace of 31+Furan before irradiation.....	255
142b. GC-trace of 31+Furan after 120 min of irradiation.....	255
143a. GC-trace of 31 in AcCN before irradiation.....	256
143b. GC-trace of 31 in AcCN after 120 min of irradiation.....	256
144a. GC-trace (HP588) of 31+Furan solution after 120 min of irradiation	257

Figures	Pages
144b. Mass spectrum of Unk1 (24.7 min).....	258
144c. Mass spectrum of Unk2 (26.2 min).....	258
145a. GC trace of photoreaction of 54 in furan after 210 min of irradiation....	260
145b. Mass spectrum of Unk3 ; 54+Furan reaction.....	261
145c. Mass spectrum of Unk4 ; 54+Furan reaction.....	261
146a. GC-trace of photoreaction of 47 in furan after 210 min of irradiation...	262
146b. Mass spectrum of Unk5 ; 47+Furan reaction.....	263
146c. Mass spectrum of Unk6 ; 47+Furan reaction.....	263
146d. Mass spectrum of Unk7 ; 47+Furan reaction.....	264
147a. Furan quenching of the formation of 43 in the photoreaction of 31	267
147b. Furan quenching of the formation of 46 in the photoreaction of 39	267
147c. Furan quenching of the formation of 39 in the photoreaction of 31	267
147d. Furan quenching of the formation of 40 in the photoreaction of 31	268
148a. GC-trace of the concentrated fraction 54	269
148b. Mass spectrum of the concentrated fraction 54	270
149a. ¹ H-NMR spectrum of the unknown sample F7 ; the expected adduct....	272
149b. ¹ H-NMR scale expansion of spectrum of the unknown sample F7	272
150a. ¹³ C-NMR spectrum of the unknown sample F7 ; the expected adduct...	277
150b. ¹³ C-DEPT 135 spectrum of the unknown sample F7 ; the expected adduct.....	277
151. GLC analysis of 46+Furan solution before irradiation.....	279
152. GC-trace of 46+Furan solution after 120 min of irradiation.....	280
153. Furan quenching of the formation of 43 in the photoreaction of 46	281
154. Plot between irradiation time <i>Vs</i> consumption of 46 in acetonitrile solvent	282
155. Plot between irradiation time <i>Vs</i> consumption 46 in furan solvent.....	282
156a. GC-trace of 46+THF solution before irradiation.....	283
156b. GC-trace of 46+THF solution after 90 min of irradiation.....	284
157a. GC trace of the concentrated 46+THF photolysate.....	285
157b. Mass spectrum of the component at retention time of 7 min.....	285

Figures	Pages
157c. Mass spectrum of the component at retention time of 17 min.....	286
157d. Mass spectrum of the component at retention time of 34.5 min.....	286
158. THF quenching of the formation of 43 in the photoreaction of 46	288
159. THF quenching of the consumption of 46	289
160a. GC analysis of the synthesized 91	292
160b. Mass spectrum of 91	292
161. ¹ H-NMR spectrum of 91	293
162a. ¹³ C-NMR spectrum of 91	295
162b. ¹³ C-DEPT 135 spectrum of 91	295
163. ¹ H-NMR spectrum of 93	297
164a. ¹³ C-NMR spectrum of 93	299
164b. ¹³ C-DEPT 135 spectrum of 93	299
165a. GC analysis of the synthesized 90	301
165b. Mass spectrum of the synthesized 90	301
166. ¹ H-NMR spectrum of 90	302
167a. ¹³ C-NMR spectrum of 90	304
167b. ¹³ C-DEPT 135 spectrum of 90	304
168a. GC analysis of the colorless crystals from synthesis of 96	306
168b. Mass spectrum of the synthesized 96	307
169. ¹ H-NMR spectrum of 96	308
170a. ¹³ C-NMR spectrum of 96	309
170b. ¹³ C-DEPT 135 spectrum of 96	309
171a. GC analysis of the colorless crystals B1 from synthesis of 94	311
171b. Mass spectrum of the colorless crystals B1	311
171c. ¹ H-NMR spectrum of the colorless crystals B1	312
172a. GC analysis of the colorless crystals B2 from synthesis of 94	313
172b. Mass spectrum of the colorless crystals B2 ; 94	313
173. ¹ H-NMR spectrum of the colorless crystals B2 ; 94	314
174a. GC analysis of 100	316

Figures	Pages
174b. Mass spectrum of 100	317
175. ¹ H-NMR spectrum of 100	318
176a. ¹³ C-NMR spectrum of 100	319
176b. ¹³ C-DEPT 135 spectrum of 100	319
177a. GC analysis of 99	320
177b. Mass spectrum of 99	321
178. ¹ H-NMR spectrum of 99	322
179a. ¹³ C-NMR spectrum of 99	323
179b. ¹³ C-DEPT 135 spectrum of 99	323
180a. GC analysis of 102	325
180b. Mass spectrum of 102	325
181. ¹ H-NMR spectrum of 102	326
182a. ¹³ C-NMR spectrum of 102	328
182b. ¹³ C-DEPT 135 spectrum of 102	328
183a. GC analysis of the light yellow solid from the synthesis of 98	330
183b. Mass spectrum of the major component at 13.1 min.....	330
183c. Mass spectrum of the minor component at 25.2 min.....	331
184a. GC analysis of the synthesized 98	331
184b. Mass spectrum of 98	332
185. Infrared absorption spectrum of 98	333
186. ¹ H-NMR spectrum of 98	334
187a. ¹³ C-NMR spectrum of 98	335
187b. ¹³ C-DEPT 135 spectrum of 98	335
188a. UV-absorption spectrum of 90 in acetonitrile.....	337
188b. UV-absorption overlay spectra of photolysis of 90 in acetonitrile.....	337
189a. UV-absorption spectrum of 90 in cyclohexane.....	338
189b. UV-absorption overlay spectra of photolysis of 90 in cyclohexane....	338
190a. UV-absorption spectrum of 98 in acetonitrile.....	339
190b. UV-absorption overlay spectra of photolysis of 98 in acetonitrile.....	339

Figures	Pages
191. UV-absorption spectrum of an authentic sample of 103 in acetonitrile..	340
192a. GLC analysis of 90 in acetonitrile before irradiation.....	342
192b. GLC analysis of 90 in acetonitrile after 120 min of irradiation.....	342
193a. GLC analysis of 98 in acetonitrile before irradiation.....	343
193b. GLC analysis of 98 in acetonitrile after 120 min of irradiation.....	343
194a. GC trace (HP588) of concentrated photolysate of 90	344
194b. Mass spectrum of the component at RT of 13.9 min.....	345
194c. Mass spectrum of the component at RT of 23.2 min.....	346
194d. Mass spectrum of the component at RT of 24.5 min.....	347
194e. Mass spectrum of the component at RT of 26.7 min.....	348
194f. Mass spectrum of the component at RT of 55.2 min.....	350
195. Mass spectrum of an authentic sample of 104	345
196. Mass spectrum of an authentic 94	346
197. Mass spectrum of an authentic 105	347
198a. GC trace (HP588) of concentrated photolysate of 98	350
198b. Mass spectrum of the component at RT of 12.5 min.....	351
198c. Mass spectrum of the component at RT of 17.3 min.....	354
198d. Mass spectrum of the component at RT of 18.1 min.....	353
198e. Mass spectrum of the component at RT of 19.3 min.....	354
199. Mass spectrum of an authentic 103	352
200. Mass spectrum of an authentic 106	355
201a. GC analysis of 109	360
201b. Mass spectrum of the component at RT of 4.4 min.....	360
202. ¹ H-NMR spectrum of 109	361
203a. ¹³ C-NMR spectrum of 109	362
203b. ¹³ C-DEPT 135 spectrum of 109	362
204a. GC analysis of 111	363
204b. Mass spectrum of 111	364
205. ¹ H-NMR spectrum of 111	365

Figures	Pages
206a. ¹³ C-NMR spectrum of 111	366
206b. ¹³ C-DEPT 135 spectrum of 111	366
207a. GC analysis of 105	367
207b. Mass spectrum of 105	368
208. ¹ H-NMR spectrum of 105	369
209a. ¹³ C-NMR spectrum of 105	370
209b. ¹³ C-DEPT 135 spectrum of 105	370
210a. GC analysis of 114	372
210b. Mass spectrum of the component at RT of 8 min.....	373
211. ¹ H-NMR spectrum of 114	374
212a. ¹³ C-NMR spectrum of 114	375
212b. ¹³ C-DEPT 135 spectrum of 114	375
213a. GC analysis of 115	376
213b. Mass spectrum of 115	377
214. ¹ H-NMR spectrum of 115	378
215a. ¹³ C-NMR spectrum of 115	379
215b. ¹³ C-DEPT 135 spectrum of 115	379
216. Infrared spectrum of 116	381
217a. GC analysis of 106	382
217b. Mass spectrum of 106	382
218. ¹ H-NMR spectrum of 106	383
219a. ¹³ C-NMR spectrum of 106	384
219b. ¹³ C-DEPT 135 spectrum of 106	384
220a. UV-absorption spectrum of 105 in acetonitrile before irradiation.....	385
220b. UV-absorption overlay spectra of photolysis of 105 in acetonitrile.....	386
221. UV-absorption of an authentic sample of 104 in acetonitrile.....	387
222. The overlay spectra between authentic 104 on the photolysis of 105 in acetonitrile.....	387
223a. UV-absorption spectrum of 106 in acetonitrile before irradiation.....	388

Figures	Pages
223b. UV-absorption overlay spectra of photolysis of 106 in acetonitrile.....	388
224. UV-absorption of an authentic sample of 103 in acetonitrile.....	389
225. GC-trace of the solution of 105 in acetonitrile before of irradiation.....	390
226. GC-trace of the solution of 106 in acetonitrile before irradiation.....	390
227a. GC-trace of concentrated photolysate of 105	391
227b. Mass spectrum of the component at RT 7.5 min.....	392
227c. Mass spectrum of the component at RT 15.5 min.....	391
228a. GC-trace of concentrated photolysate of 106	393
228b. Mass spectrum of the component at RT 8 min.....	394
228c. Mass spectrum of the component at RT 15.8 min.....	395
228d. Mass spectrum of the component at RT 16.2 min.....	393
229. UV-absorption spectrum of 31 in acetonitrile.....	399
230. UV-absorption overlay spectra of 31 in acetonitrile at various concentrations.....	399
231. Fluorescence spectrum of 31 in acetonitrile.....	400
232. UV-absorption spectrum of 31 in acetonitrile.....	402
233. Fluorescence spectrum of 37 in acetonitrile.....	402
234a. Phosphorescence emission spectrum of 31 in methanol/ethanol.....	404
234b. Phosphorescence excitation overlay spectra of 31 in methanol/ethanol.	405
235. Infrared spectrum of 31 (neat liquid).....	405
236. State diagram of 31	406
237. UV-absorption spectrum of 90 in acetonitrile.....	408
238. UV-absorption overlay spectra of 90 in acetonitrile at various concentrations.....	408
239. Fluorescence spectrum of 90 in acetonitrile.....	410
240. UV-absorption spectra of 90 in acetonitrile and cyclohexane.....	410
241. Fluorescence spectrum of 90 in cyclohexane.....	411
242a. Phosphorescence emission spectrum of 90 in methanol/ethanol.....	412
242b. Phosphorescence excitation overlay spectra of 90	414

Figures	Pages
243. Infrared spectrum of 90 (neat solid).....	413
244. State diagram of 90	414
245. UV-absorption spectrum of 98 in acetonitrile.....	416
246. UV-absorption overlay spectra of 98 in acetonitrile at various concentrations.....	416
247a. Fluorescence spectrum of 98 in acetonitrile.....	417
247b. Fluorescence emission overlay spectra of 98 at various excitation wavelengths.....	419
248a. Phosphorescence emission spectrum of 98 in methanol/ethanol.....	420
248b. Phosphorescence excitation overlay spectra of 98	420
249. Infrared spectrum of 98 (neat solid).....	421
250. State diagram of 98	422
251. UV-absorption spectrum of 54 in acetonitrile.....	424
252. UV-absorption overlay spectra of 54 in acetonitrile at various concentrations.....	424
253a. Fluorescence spectrum of 54 in acetonitrile.....	425
253b. Fluorescence emission overlay spectra of 54 at various excitation wavelengths.....	425
254. UV-absorption spectrum of 117 in acetonitrile.....	428
255. UV-absorption overlay spectra of 117 in acetonitrile at various concentrations.....	428
256. Fluorescence spectrum of 117 in acetonitrile.....	430
257. UV-absorption spectrum of 118 in acetonitrile.....	432
258. UV-absorption overlay spectra of 118 in acetonitrile at various concentrations.....	432
259. Fluorescence spectrum of 118 in acetonitrile.....	434
260. UV-absorption spectrum of 47 in acetonitrile.....	436
261. UV-absorption overlay spectra of 47 in acetonitrile at various concentrations.....	436

Figures	Pages
262. UV-absorption spectra of 47 in acetonitrile and cyclohexane.....	437
263. Fluorescence spectrum of 47 in acetonitrile.....	438
264. 259. Fluorescence spectrum of 47 in cyclohexane.....	439
265. UV-absorption spectrum of 46 in acetonitrile.....	440
266. UV-absorption spectra of 46 at various concentrations.....	441
267. UV-absorption spectra of 46 after re-purification in various solvents.....	442
268a. Fluorescence spectrum of 46 in acetonitrile.....	444
268b. Fluorescence emission overlay spectra of 46 in acetonitrile.....	444
268c. Fluorescence spectrum of 46 in methanol at various excitation wavelengths.....	445
269a. Phosphorescence emission spectrum of 46 in methanol/ethanol.....	447
269b. Phosphorescence excitation spectra of 46 at various emission wavelengths.....	447
269c. Phosphorescence emission spectra of 46 at various excitation wavelengths.....	448
270. State diagram of 46	448
271. UV-absorption spectrum of 105 in acetonitrile.....	450
272. UV-absorption overlay spectra of 105 at various concentrations.....	450
273. Fluorescence spectrum of 105 in acetonitrile.....	451
274. UV-absorption overlay spectra of 105 in acetonitrile and cyclohexane...	452
275. Fluorescence spectrum of 105 in cyclohexane.....	452
276a. Phosphorescence emission spectrum of 5 in methanol/ethanol.....	454
276b. Phosphorescence excitation spectra of 105 in methanol/ethanol.....	454
277. State diagram of 105	455
281. UV-absorption overlay spectra of 106 before and after purification in acetonitrile.....	457
282. UV-absorption overlay spectra of 106 after purification at various concentrations.....	457
283. Fluorescence spectrum of 106 in acetonitrile after purification.....	458

284a. Phosphorescence emission spectrum of 106 in methanol/ethanol.....	459
284b. Phosphorescence emission overlay spectra of 106 in methanol/ethanol.	460
285. State diagram of 106	460
286. UV-absorption spectrum of 119 in acetonitrile.....	462
287. UV-absorption spectra of 119 in acetonitrile at various concentrations..	462
288. Fluorescence spectrum of 119 in acetonitrile.....	463
289. UV-absorption spectrum of 120 in acetonitrile.....	466
290. UV-absorption spectrum of 120 in acetonitrile at various concentrations	466
291a. Fluorescence spectrum of 120 in acetonitrile.....	467
291b. Scale expansion of fluorescence spectrum of 120 in acetonitrile.....	467
292. UV-absorption overlay spectra of 5-phenyl-1,2,4-thiadiazoles in acetonitrile.....	471
293. UV-absorption overlay spectra of 3-phenyl-1,2,4-thiadiazoles in acetonitrile.....	475
294. UV-absorption spectra of butyrophenone in acetonitrile at various concentrations.....	491
295. UV-absorption spectrum of 31 in acetonitrile.....	491
296a. GLC analysis of butyrophenone solution before irradiation.....	493
296b. GLC analysis of butyrophenone solution after 90 min of irradiation....	493
297a. GLC analysis of solution of 31 before irradiation.....	494
297b. GLC analysis of solution of 31 after 90 min of irradiation.....	494
298a. GLC analysis of solution of 31 +Butyrophenone before irradiation.....	495
298b. GLC analysis of solution of 31 +Butyrophenone after irradiation.....	495
299. UV-absorption spectrum of 46 in acetonitrile.....	498
300a. GLC analysis of solution of 46 before irradiation.....	499
300b. GLC analysis of solution of 46 after 120 min of irradiation.....	499
301a. GLC analysis of butyrophenone solution before irradiation.....	500
301b. GLC analysis of butyrophenone solution after irradiation.....	500
302a. GLC analysis of solution of 46 +Butyrophenone before irradiation.....	501
302b. GLC analysis of solution of 46 +Butyrophenone after irradiation.....	501
303a. GC-trace of the viscous liquid product from synthesis of 128	507

Figures	Pages
303b. Mass spectrum of the viscous liquid product.....	507
304. ¹ H-NMR spectrum of the viscous colorless liquid.....	509
305a. ¹³ C-NMR spectrum of the viscous colorless liquid.....	510
305b. ¹³ C-NMR spectrum of the viscous colorless liquid; scale expansion.....	511
305c. ¹³ C-DEPT 135 spectrum of the viscous colorless liquid.....	512
306. GC-trace of 31+127 mixture in acetonitrile before irradiation.....	513
307. UV-absorption spectrum of 31 in acetonitrile.....	515
308. UV-absorption spectrum of 127 in acetonitrile.....	516
309. UV-absorption spectrum of a mixture of 31+127 in acetonitrile.....	516
310a. GC-trace of 31+127 mixture after 180 min of irradiation.....	517
310b. Mass spectrum of the component at RT 26.7 min.....	518
311. GC-trace of 90+127 mixture before irradiation.....	520
312. GC-trace of 90+127 mixture after 180 min of irradiation.....	521
313. Fluorescence quenching of the excited state of 90 by 127	522
314. GC-trace of a mixture of 46+127 before irradiation.....	525
315a. GC-trace of a mixture of 46+127 after 120 min of irradiation.....	526
315b. Mass spectrum of the component at RT of 26.7 min.....	526
316. Cyclic voltametry of 31 in acetonitrile.....	529
317. Cyclic voltametry of 46 in acetonitrile.....	529
318. Cyclic voltametry of 90 in acetonitrile.....	530
319. Cyclic voltametry of 47 in acetonitrile.....	530
320. GC-trace of the Solution 31+TEA after 30 min of irradiation.....	536
321. GC-trace of Solution 31+PA after 30 min of irradiation.....	536
322. GC-trace of the 31+TEA mixture after 30 min of irradiation.....	539
323. GC-trace of 31+PA mixture after 30 min of irradiation.....	539
324. GLC analysis of the 46+TEA mixture after 120 min of irradiation.....	543
325. GLC analysis of the 46+PA mixture after 120 min of irradiation.....	543
326. GC-trace of the 46+TEA mixture after 120 min of irradiation.....	545
327. GLC analysis of the 4+PA mixture after 120 min of irradiation.....	54

LIST OF SCHEMES

Schemes	Pages
1. Phototransposition of isothiazoles <i>via</i> tricyclic zwitterionic intermediates..	2
2. Phototransposition of phenylisothiazoles and phenylthiazoles <i>via</i> tricycliczwitterionic intermediates.....	2
3. Electrocyclic ring closure heteroatom migration mechanism of thiazoles and isothiazoles	4
4. Photocleavage of the S–N bond in isothiazoles.....	6
5. Particular pathway for the synthesis of 1,2,4-thiadiazole ring system.....	8
6. Synthesis of N-[(dimethylamino)methylene]thiobenzamide.....	9
7. Mechanism for the formation 5-phenyl-1,2,4-thiadiazole.....	15
8. Major fragmentation pathways of 1,2,4-thiadiazoles.....	18
9. Possible fragmentation pathway of 3-amino-5-phenyl-1,2,4-thiadiazole and 5-phenyl-1,2,4-thiadiazole.....	19
10. Synthesis of 2-phenyl- and 2,4-diphenyl-1,3,5-triazine.....	21
11. Photochemistry of 5-phenylthiazole and 5-phenylisothiazole.....	26
12. The photoreaction of 5-phenyl-1,2,4-thiadiazole.....	45
14. Synthesis of 5-phenyl-1,3,4-oxathiazole-2-one	47
15. Synthesis of ethyl 3-phenyl-1,2,4-thiadiazole-5-carboxylate.....	51
16. Synthesis of 3-phenyl-1,2,4-thiadiazole.....	55
17. Synthesis of 3-methyl-5-phenyl-1,2,4-thiadiazole.....	67
18. Synthesis of N-[(dimethylamino)ethylidene]thiobenzamide.....	68
19. Synthesis of 3-methyl-5-phenyl-1,2,4-thiadiazole.....	74
20. Synthesis of 5-methyl-3-phenyl-1,2,4-thiadiazole.....	79
21. Synthesis of 5-chloro-3-phenyl-1,2,4-thiadiazole.....	80
22. Synthesis of diethyl 3-phenyl-1,2,4-thiadiazole-5-malonate.....	84
23. Synthesis of 5-methyl-3-phenyl-1,2,4-thiadiazole	92
24. Fragmentation pathways of 7 and 53	94

Schemes	Pages
25. The recent synthetic method of un-symmetrically substituted-s-triazines..	97
26. Synthesis of N-[(dimethylamino)ethylidene]benzamide.....	98
27. Synthesis of 2,4-dimethyl-6-phenyl-1,3,5-triazine.....	105
28. Possible synthetic method of 2-methyl-4,6-diphenyl-1,3,5-triazine.....	109
29. Synthesis of thiobenzamide- ¹⁵ N.....	124
30. Synthesis of N-[(dimethylamino)methylene]thiobenzamide- ¹⁵ N.....	129
31. Synthesis of 5-phenyl-1,2,4-thiadiazole – 4 ¹⁵ N.....	135
32. The plausible pathway for the formation of 5-phenyl-1,2,4-oxadiazole – 4 ¹⁵ N.....	146
33. The proposed mechanism for the formation of the phototransposition product.....	146
34. Possible fragmentation pathways of 5-phenyl-1,2,4-thiadiazole-4- ¹⁵ N....	149
35. Major possible fragmentation pathways of regular 2-phenyl-1,3,5-triazine	160
36. Possible structures and fragmentation patterns of 2-phenyl-1,3,5-triazine containing one ¹⁵ N and two ¹⁵ N atoms.....	161
37. Possible fragmentation pathways of 2,4-diphenyl-s-triazine- ¹⁵ N.....	164
38. Synthesis of 3-methyl-5-phenyl-1,2,4-thiadiazole.....	174
39. Synthetic pathway of 3-methyl-5-phenyl-1,2,4-thiadiazole-4 ¹⁵ N.....	175
40. The N-scrambling mechanism.....	190
41. Two major fragmentation pathways of 7-4 ¹⁵ N.....	192
42. Possible fragmentation pathways for the triazine containing one and two ¹⁵ N atoms.....	200
45. Possible fragmentation pathways of 2-methyl-4,6-diphenyl-1,3,5-triazine- ¹⁵ N.....	206
46. N-2 and C-3 interchange photochemical pathway of isothiazoles.....	213
47. N-2 and C-3 interchange photochemical pathway of 5-phenyl-1,2,4-thiadiazole.....	213

Schemes	Pages
48. Possible mechanism for the formation of benzonitrile sulfide.....	214
49. Trapping of thermally generated 13 by 1,3-dipolar cycloaddition reaction	215
50. The predicted mechanism for the formation of isothiocyanic acid.....	220
51. The proposed mechanism for the formation of 13 upon irradiation of 4 ...	225
52. The proposed mechanism for phenyl-s-triazines formation.....	226
53. The proposed formation of unsymmetrical phenyltriazine via [4+2] cycloaddition cross-coupling of phenyldiazacyclobutadiene intermediates	227
54. The possible photoproducts predicted to observe upon irradiation of a mixture of 5-phenyl-1,2,4-thiadiazole and 3-methyl-5-phenyl-1,2,4- thiadiazole.....	228
55. Total synthesis of 2-methyl-4-phenyl-1,3,5-triazine.....	228
56. Synthesis of N-[(dimethylamino)methylene]benzamide.....	229
57. Synthesis of 2-methyl-4-phenyl-1,3,5-triazine.....	233
58. The proposed formation of benzamide upon irradiation of 1	250
59. 1,3-Diaza-5-thiabicyclo[2.1.0]pentene; Key intermediate upon irradiation of 5-phenyl-1,2,4-thiadiazole.....	251
60. Photochemistry of 3-cyanothiophene in furan solvent.....	252
61. Photochemistry of 1-methyl-5-phenylpyrazole in methanol.....	252
62. Irradiation of 1-methyl-5-phenylpyrazole in furan solvent.....	253
63. Formation of furan-phenyldiazacyclobutadiene adduct upon irradiation of 10+Furan	259
64. Formation of furan-phenyldiazacyclobutadiene adduct upon irradiation of 7+Furan	262
65. Formation of furan-phenyldiazacyclobutadiene adduct upon irradiation of 12+Furan	264
66. Possible formation of the observed adducts.....	265
67. The expected ¹⁵ N-scrambling in 3-phenyl-1,2,4-thiadiazole-2- ¹⁵ N.....	278
68. Possible formation of banzamide upon irradiation of 4	287

Schemes	Pages
69. Total synthesis of 5-(4'-methoxy)phenyl-1,2,4-thiadiazole.....	291
70. Synthesis of 4-methoxythiobenzamide.....	291
71. Synthesis of N-[(dimethylamino)methylene]4-methoxythiobenzamide....	296
72. Synthesis of 5-(4-methoxy)phenyl-1,2,4-thiadiazole.....	300
73. Total synthetic scheme of 2-(4'-methoxy)phenyl-1,3,5-triazine.....	305
74. Synthesis of N-[(dimethylamino)methylene]4-methoxybenzamide.....	305
75. Synthesis of 2-(4'-methoxy)phenyl-1,3,5-triazine.....	310
76. Total synthesis of 5-(4'-cyano)phenyl-1,2,4-thiadiazole.....	315
77. Synthesis of 4-cyanobenzamide.....	316
78. Synthesis of 4-cyanothiobenzamide	320
79. Synthesis of N-[(dimethylamino)methylene]4-cyanothiobenzamide.....	324
80. Synthesis of 5-(4'-cyano)phenyl-1,2,4-thiadiazole.....	329
81. Photoreaction of 5(4'-methoxy)- and 5(4'-cyano)-phenyl-1,2,4- thiadiazole.....	357
82. Total synthesis of 3-(4-methoxy)phenyl-1,2,4-thiadiazole.....	358
83. Synthesis of 5-(4'-methoxy)phenyl-1,3,4-oxathiazole-2-one.....	359
84. Synthesis of ethyl 3-(4'-methoxy)phenyl-1,2,4-thiadiazole- 5-carboxylate.....	363
85. Synthesis of 3-(4'-methoxy)phenyl-1,2,4-thiadiazole.....	367
86. Total synthesis of 3-(4'-cyano)phenyl-1,2,4-thiadiazole.....	371
87. Synthesis of 5-(4'-cyano)phenyl-1,3,4-oxathiazole-2-one.....	372
88. Synthesis of ethyl 3-(4'-cyano)phenyl-1,2,4-thiadiazole-5-carboxylate....	376
89. Synthesis of 3-(4'-cyano)phenyl-1,2,4-thiadiazole.....	380
90. Photoreaction of 3(4'-methoxy)- and 3(4'-cyano)-phenyl-1,2,4-thiadiazole	396
91. Solvent reorganization resulting in lowering of the excited state energy level.....	479
92. Energy difference between absorbing and emitting states due to geometry change upon excitation.....	480

Schemes	Pages
93. Photostability of Tinuvin P (reprinted from ref. 32).....	481
94. A large Stokes' shift due to emission from a TICT excited state.....	482
95. Photoinduced intramolecular charge transfer in biaryl systems.....	485
96. Possible energy diagram of phenylthiadiazoles in acetonitrile or cyclohexane solvent.....	486
97. Major photochemical reaction of butyrophenone.....	492
98. Triplet sensitization of 1 by butyrophenone photosensitizer.....	497
99. Triplet sensitization of 4 by butyrophenone photosensitizer.....	503
100. Possible pathway for the formation of irradiation of 92 in the presence of 90	504
101. BC-1 intermediate – the key intermediate in the photoreaction of 1	505
102. Synthesis of tri-n-butylphosphine sulfide.....	506
103. Possible fragmentation pathway of tri-n-butylphosphine sulfide.....	508
104. A possible ground state interaction between 1 and 90	514
105. Thermodynamic feasibilities of electron transfer between TEA and some thiadiazoles.....	533
106. Thermodynamic feasibilities of electron transfer between PA and some thiadiazoles.....	534
107. Possible mechanism for the formation of the phototransposition product	614
108. Possible formation of the observed adducts.....	615
109. Phenyl diazacyclobutadiene formation.....	616
110. Possible orientations for this cycloaddition-cleavage pathway.....	617
111. [4+2] cycloaddition cross-coupling of phenyl diazacyclobutadiene intermediates.....	618
112a. Possible photofragmentation pathways of 3-phenyl-1,2,4-thiadiazole...	619
112b. Possible photofragmentation pathways of 3-phenyl-1,2,4- thiadiazole-2- ¹⁵ N.....	619
113. Evidences for the intermediacy of benzonitrile sulfide upon irradiation of 4	620

LIST OF TABLES

Tables	Pages
1. ^{13}C -chemical shifts of 7-oxabicyclo[2.2.1]hept-2-ene and some derivatives.....	273
2. UV-absorption properties of 5-phenyl-1,2,4-thiadiazoles in acetonitrile....	470
3. Fluorescence properties of 5-phenyl-1,2,4-thiadiazoles in acetonitrile.....	472
4. Phosphorescence properties of 5-phenyl-1,2,4-thiadiazoles in ethanol/methanol (4:1) at 77 K.....	473
5. UV-absorption properties of 3-phenyl-1,2,4-thiadiazoles in acetonitrile....	475
6. Fluorescence properties of 3-phenyl-1,2,4-thiadiazoles in acetonitrile.....	477
7. Phosphorescence properties of 3-phenyl-1,2,4-thiadiazoles in ethanol/methanol (4:1) at 77 K.....	478
8. Quantitative analysis of triplet sensitization reaction of 31	496
9. Quantitative analysis of triplet sensitization reaction of 46	502
10. Reduction potentials and E_{00} (eV) of some phenyl-1,2,4-thiadiazoles in acetonitrile.....	531
11. Quantitative analysis of the photoreaction of 1 in AcCN with the presence of TEA or PA	538
12. Quantitative analysis of the photoreaction of 31 in acetonitrile and methanol with the presence of TEA or PA	541
13. Quantitative analysis of irradiation of 46 in the presence of TEA or PA in acetonitrile or methanol solvent.....	546
14. Photolysis of 5-phenyl-1,2,4-thiadiazole in acetonitrile.....	584
15. Photolysis of 5-phenyl-1,2,4-thiadiazole in cyclohexane.....	585
16. Photolysis of 3-phenyl-1,2,4-thiadiazole in acetonitrile.....	586
17. Photolysis of 3-methyl-5-phenyl-1,2,4-thiadiazole in acetonitrile.....	588
18. Photolysis of 3-methyl-5-phenyl-1,2,4-thiadiazole in methanol.....	588

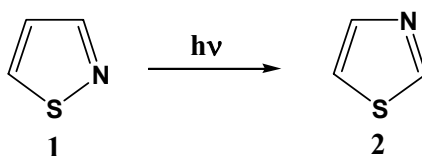
Tables	Pages
19. Time (min) <i>V</i> s ratio of 103/104 peaks of benzonitrile-photoproduct.....	589
20. Time (min) <i>V</i> s ratio of 158/159 peaks of 2-phenyl-1,3,5-triazine-photoproduct.....	590
21. Time (min) <i>V</i> s ratio of 135/136 peaks of un-consumed 5-phenyl-1,2,4-thiadiazole-4 ¹⁵ N.....	590
22. Time (min) <i>V</i> s ratio of 135/136 peaks of 3-phenyl-1,2,4-thiadiazole-photoproduct.....	591
23. Time (min) <i>V</i> s ratio of 234/235 peaks of 2,4-diphenyl-1,3,5-triazine-photoproduct	591
24. Time (min) <i>V</i> s ratio of 103/104 peaks of benzonitrile-photoproduct.....	595
25. Time (min) <i>V</i> s of 186/187 ratio of 2,4-dimethyl-6- phenyl-1,3,5-triazine-photoproduct	595
26. Time (min) <i>V</i> s of 135/136 ratio of un-consumed 3-methyl-5-phenyl-1,2,4-thiadiazole-4 ¹⁵ N	596
27. Time (min) <i>V</i> s of 135/136 ratio of 5-methyl-3-phenyl- 1,2,4-thiadiazole-photoproduct.....	596
28. Time (min) <i>V</i> s of 248/249 ratio of 2-methyl-4,6-diphenyl-1,3,5- triazine-photoproduct.....	597

CHAPTER 1

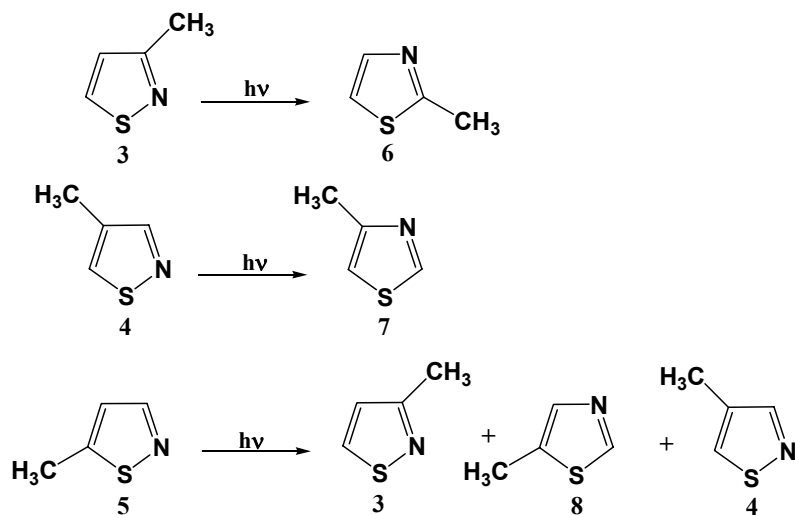
INTRODUCTION

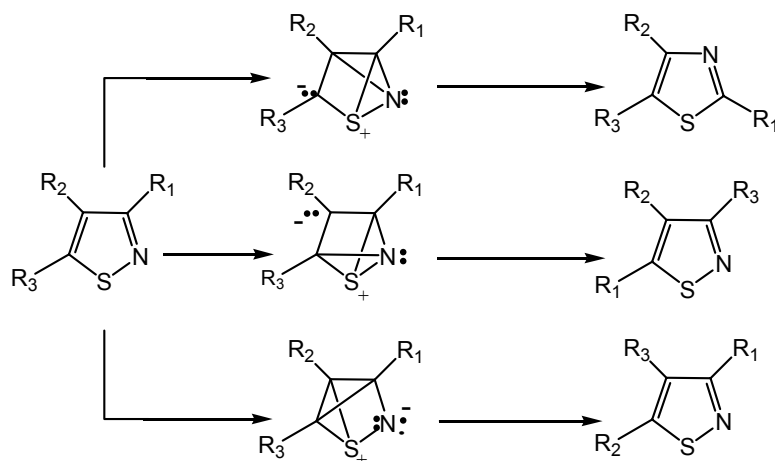
1.1 Photochemistry of isothiazoles and thiazoles

The photoreaction of isothiazole (**1**) was first reported to undergo phototransposition to yield thiazole (**2**).¹ The reverse transposition of isothiazole (**2**) was, however, reported not to take place.



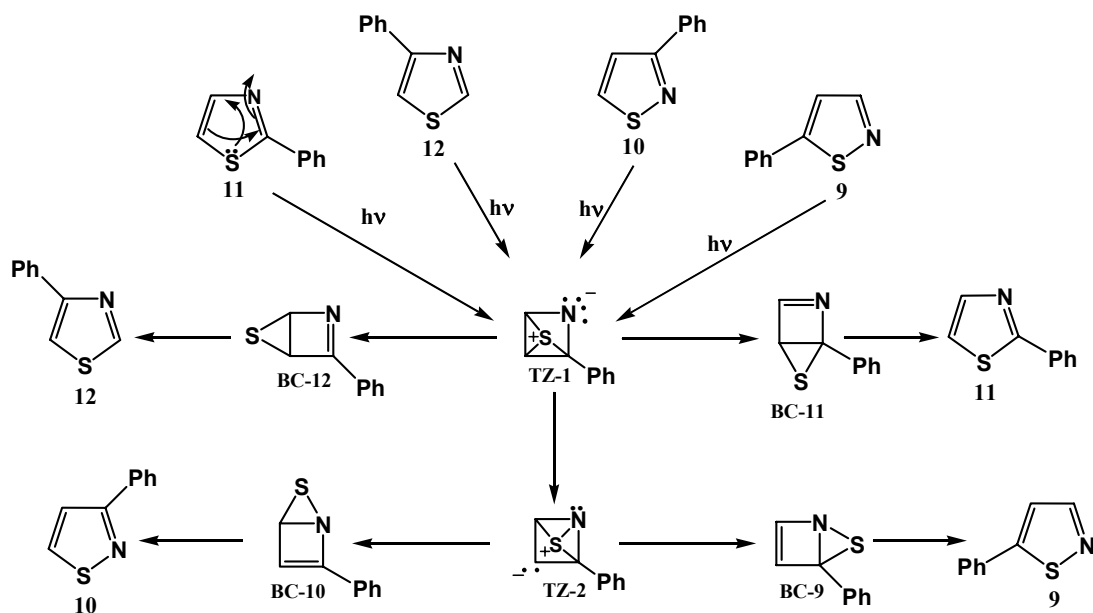
Lablache-Combiere and co-workers² reported that 3- and 4-methylisothiazole (**3**) and (**4**) each transposes to a single N2-C3 interchanged thiazole product (**6**) and (**7**). But 5-methylthiazole (**5**) transposes to the thiazole (**8**), and isomeric isothiazoles (**3**) and (**4**). These methylisothiazoles were suggested to result from a mechanism involving tricyclic zwitterionic intermediates, as shown in Scheme 1, based on the known phototransposition reaction of 2-phenylthiophene.³





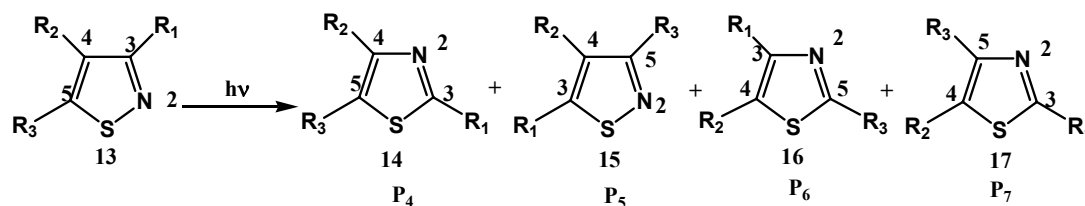
Scheme 1: Phototransposition of isothiazoles *via* tricyclic zwitterionic intermediates

Research groups in France⁴ and Japan⁵ further extended the study to phenylisothiazoles and phenylthiazoles and proposed that the phototransposition of phenylisothiazoles and phenylthiazoles takes place by a mechanism, which involves tricyclic zwitterionic intermediates as shown in Scheme 2.

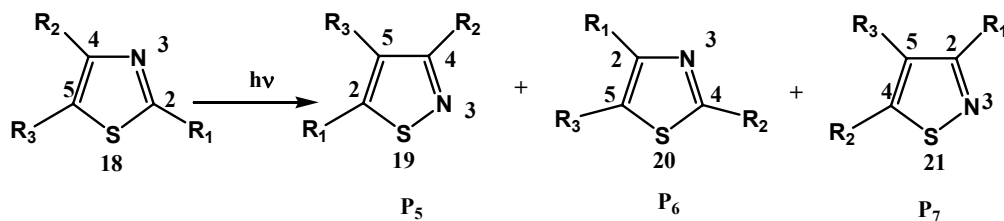


Scheme 2: Phototransposition of phenylisothiazoles and phenylthiazoles *via* tricyclic zwitterionic intermediates

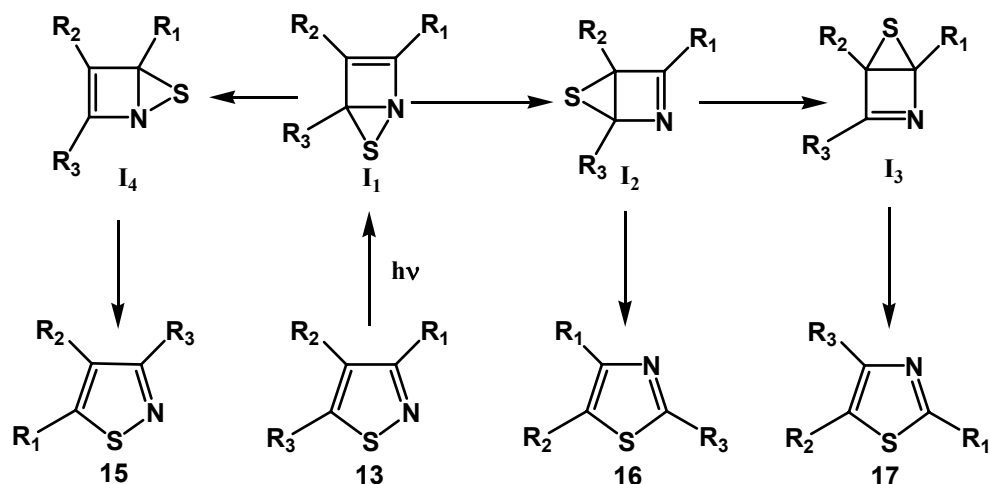
Pavlik and colleagues later found several ambiguities in those previous reports. Thus, a reinvestigation of the photochemistry of phenylisothiazoles and phenylthiazoles was carried out.⁶ Their studies revealed that the mechanism involving tricyclic zwitterionic intermediates did not correspond to some of their results. They reported that isothiazoles transposed by four different transposition patterns, which can be labeled as P₄, P₅, P₆ and P₇, respectively leading to the isomeric thiazoles and isothiazoles.⁶



Similarly, thiazoles were observed to transpose to isomeric isothiazoles and thiazoles by the P₅, P₆ and P₇ transposition patterns.⁶



Although the P₅, P₆ and P₇ pathways involve the largest number of atom interchanges, the formation of all of these products were explained by the electrocyclic ring closure–heteroatom migration mechanism,⁶ as shown in Scheme 3.



Scheme 3: Electrocyclic ring closure heteroatom migration mechanism of thiazoles and isothiazoles

Pavlik and colleagues suggested that sulfur migration in the initially formed 1-aza-5-thiabicyclopentane intermediate, **I**₁, occurred by successive 1,3-sigmatropic shifts of sulfur in both directions allowing sulfur to migrate around all four sides of the azetine ring. Thus, sulfur migration followed by rearomatization allows sulfur insertion into all four different sites in the carbon–nitrogen sequence resulting in the formation of the P₅, P₆ and P₇ phototransposition products.

Although the P₄ phototransposition involves the interchange of fewer ring atoms (i.e. N₂ and C₃) than the P₅, P₆ and P₇ pathways, it is mechanistically more complicated, involving both photocleavage and photo-ring contraction pathways.⁷ 4-Substituted-isothiazoles react exclusively via these pathways while the photochemistry of 3- and 5-substituted-isothiazoles involve a competition between this pathway and the electrocyclic ring closure heteroatom migration mechanism.⁸

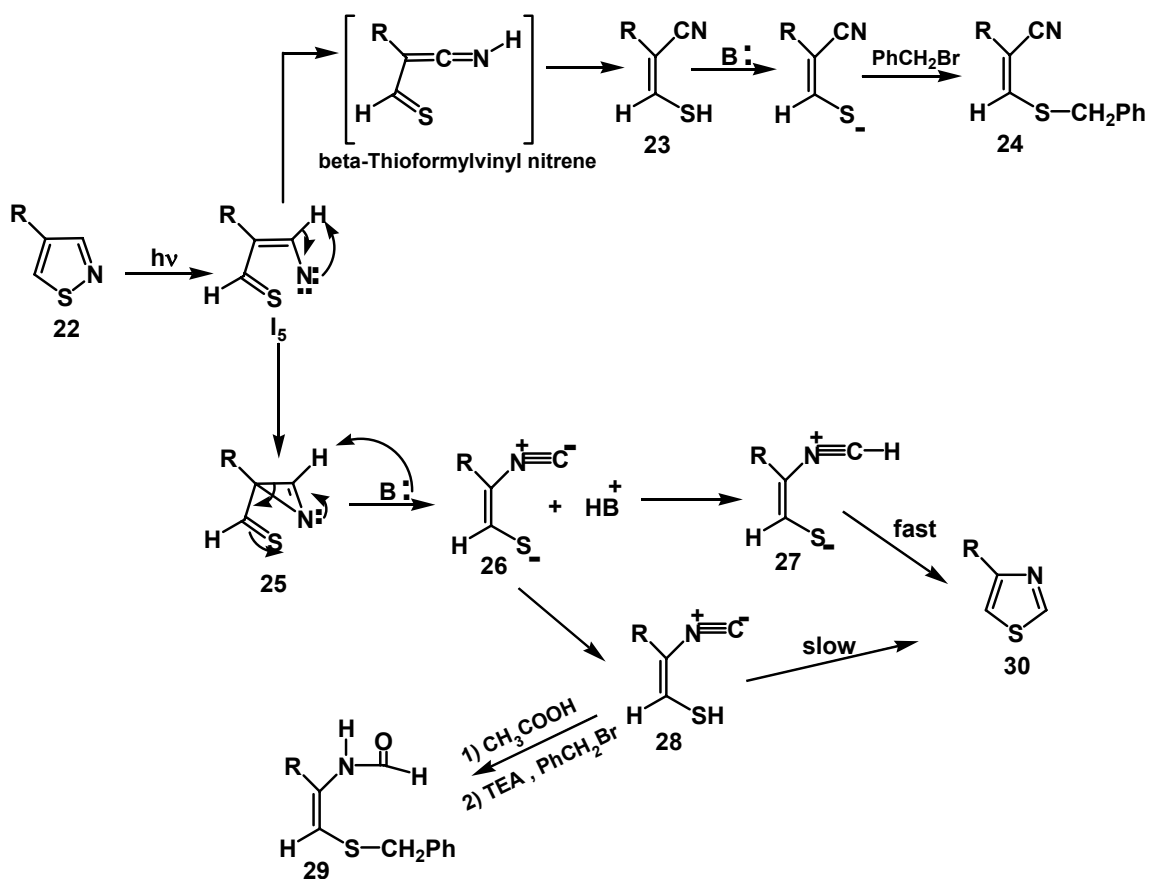
According to Pavlik and Tongcharoensirikul,⁶⁻⁸ electrocyclic ring closure (the first step of the electrocyclic ring closure heteroatom migration pathway) is in competition with cleavage of the S–N bond in the isothiazole reactant. This cleavage results in the formation of a species **I**₅ (Scheme 4). It can be viewed as a β-thioformylvinyl nitrene.

Vinyl nitrenes are known to rearrange to nitriles. Therefore, as expected, upon irradiation 4-substituted-isothiazoles undergo this photocleavage reaction to yield a substituted cyanothiol (**23**), which can be detected spectroscopically, trapped and characterized as their benzyl thioether derivatives (**24**).

Vinyl nitrenes are also known to be in equilibrium with their isomeric azirines. The β -thioformylvinyl nitrene, **I₅**, formed from 4-substituted-isothiazoles (**22**), would be in equilibrium with the substituted thioformylazirines (**25**). In the presence of an external base such as triethylamine, ammonia or aqueous bicarbonate, Pavlik and Tongcharoensirikul suggested that the azirine (**25**) undergoes deprotonation by the added base resulting in the formation of an isocyanosulfide, **26**.

The fate of isocyanide **26** depends on the natures of the substituent originally at C-4 of the isothiazole ring. If the substituent is aromatic (**26**; R = Ph), the extended conjugation of the sulfide and aryl group lowers the basicity of the sulfide, leaving the isocyanide carbon as the more basic site. The effect of protonation at this position to form **27** and to render the carbon more susceptible to nucleophilic attack by the negative sulfur. As the result, these substituted isocyanides cyclize spontaneously to 4-arylthiazoles (**30**; R = Ph) and cannot be detected or chemically trapped.

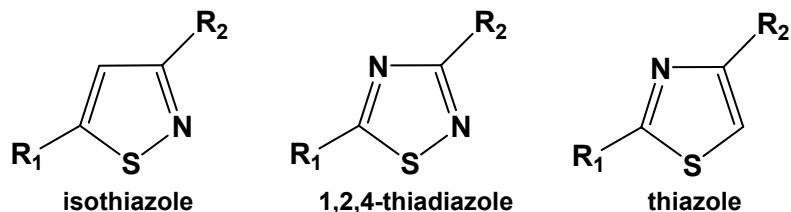
If the C-4 substituent is allyl or substituted allyl (**26**, R = PhCH₂ or CH₃), the reduced conjugation raises the energy of the sulfide so that sulfide is more basic. Thus, protonation at this position leads to **28**, which reduces the nucleophilic character of the sulfur and leaves the negative charged isocyanide carbon less susceptible to nucleophilic attack. As a result, cyclization requires a higher energy of activation, and hence, the allyl-substituted isocyanothiols can be detected spectroscopically, trapped and characterized as their N-formylaminobenzyl thioether derivatives (**29**).



Scheme 4: Photocleavage of the S-N bond in 4-substituted isothiazoles

1.2 Photochemistry of 1,2,4-thiadiazoles

Although the photochemistry of thiazoles and isothiazoles has been extensively studied in this and other laboratories, no reports concerning the photochemistry of 1,2,4-thiadiazoles were available in the literature at the beginning of this research project. The photochemistry of 1,2,4-thiadiazoles is of interest because the ring system can be viewed



as a combination of a thiazole and an isothiazole. Therefore, 1,2,4-thiadiazoles would be expected to undergo phototransposition reaction, via sulfur migration around four sides of the photochemically generated bicyclic intermediates, and photocleavage of the S-N bond similar to those of thiazoles and isothiazoles.

In order to extend the knowledge on photochemistry of five-membered ring heterocycles containing sulfur and nitrogen atoms, the goal of this research is to investigate the primary photochemical reaction of phenyl substituted-1,2,4-thiadiazoles.

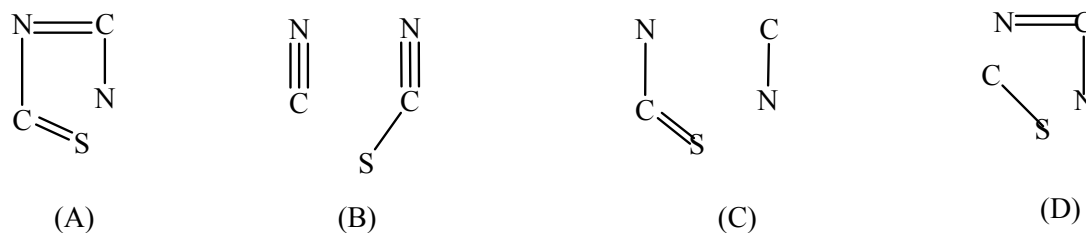
CHAPTER 2

Results and Discussion

2.1 Photochemistry of 5-phenyl-1,2,4-thiadiazole

2.1.1 Synthesis of 5-phenyl-1,2,4-thiadiazole

The 1,2,4-thiadiazole ring can be synthesized by the four following methods; (1) oxidative cyclization of an N-thioacyl amidine⁹ (method A), (2) cycloaddition of nitrile sulfides with a nitrile⁹ (method B), (3) oxidation of thioamides or thioureas⁹ (method C), (4) condensation of amidines with halogenated methylmercaptans⁹ (method D).



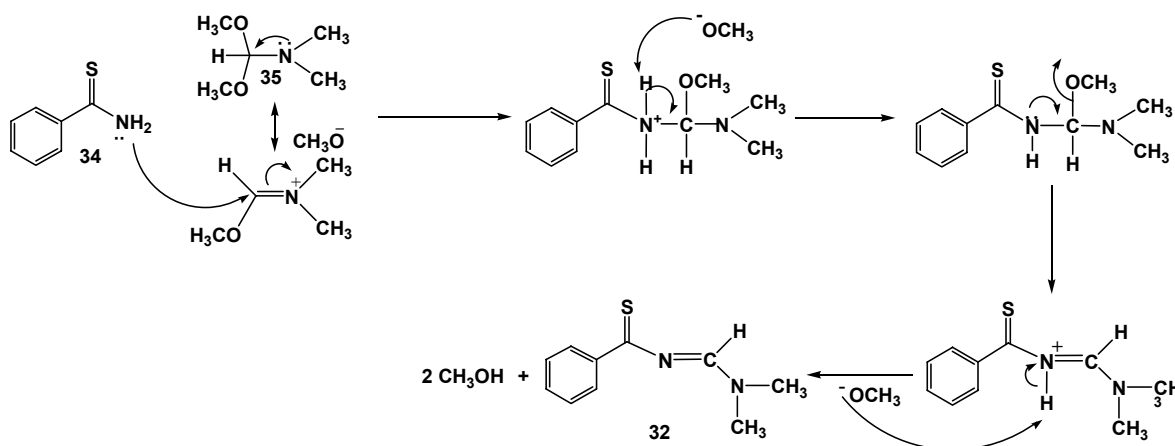
Scheme 5: Particular pathway for the synthesis of 1,2,4-thiadiazole ring system

These methods, however, do not allow the preparation of 5-monosubstituted-1,2,4-thiadiazoles. Therefore, 5-phenyl-1,2,4-thiadiazole (**31**) was synthesized by the method described by Yang-i Lin and colleagues.⁹ According to this approach, the amination cyclization of N-[(dimethylamino)methylene]thiobenzamide (**32**) with the aminating agent,

hydroxylamine-O-sulfonic acid (**33**), resulted in the formation of **31** as a colorless viscous liquid in 70% yield.

2.1.1.1 Synthesis of N-[(dimethylamino)methylene]thiobenzamide

According to the synthetic method for **1** described by Yang-i Lin and colleagues,⁹ N-[(dimethylamino)methylene]thiobenzamide (**32**) was required as the starting material. Therefore, **32** was synthesized in 87.5% by the condensation between thiobenzamide (**34**) and N,N-dimethylformamide dimethylacetal (**35**) as shown in Scheme 6.



Scheme 6: Synthesis of N-[(dimethylamino)methylene]thiobenzamide

The orange crystalline product was identified by GC-MS, ¹H- and ¹³C-NMR spectroscopy. The GC-trace of the sample, shown in Figure 1a, [140°C (5 min), 10°C/min to 240°C (50 min)] indicated the presence of some impurities. The mass spectrum of the major peak, which eluted with a retention time of 33.9 min (Figure 1b), exhibits the molecular ion at m/z 192 corresponding to the molecular weight of **32** (MW 192). It also

shows a base peak at m/z 44 due to the $[\text{CH}_3]_2\text{N}^+$ fragment, which is consistent with the structure of this compound, **32**.

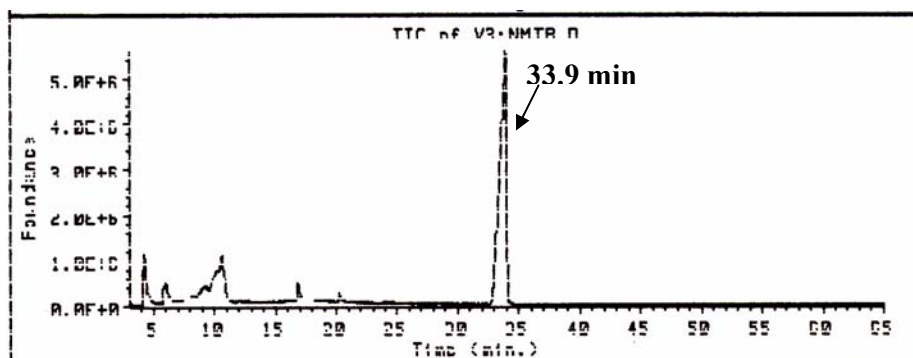


Figure 1a: GC-trace of the synthesized N-[(dimethylamino)methylene]thiobenzamide

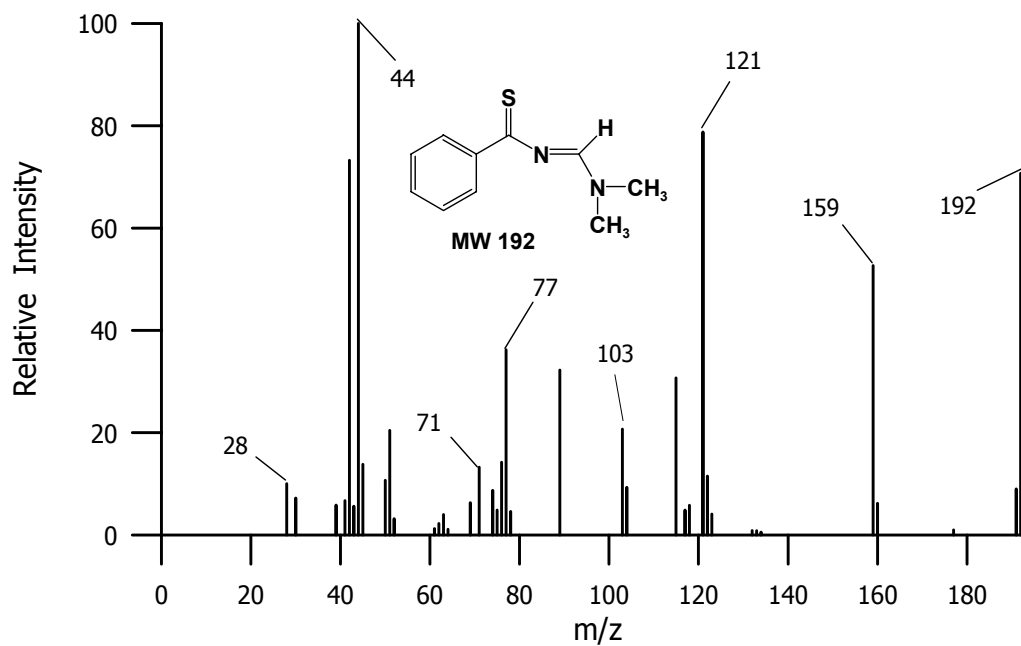


Figure 1b: Mass spectrum of the peak at retention time 33.9 min

The $^1\text{H-NMR}$ spectrum of this amidine **32**, as shown in Figure 2, exhibits a singlet (1H) at δ 8.73 due to the imine proton. The two non-equivalent methyl groups are shown as two singlets (3H) at δ 3.24 and 3.25. The phenyl ring protons appear as two multiplets at δ 7.32-7.36 (3H) and 8.39-8.41 (2H) due to the meta-, para- and ortho-ring protons, respectively.

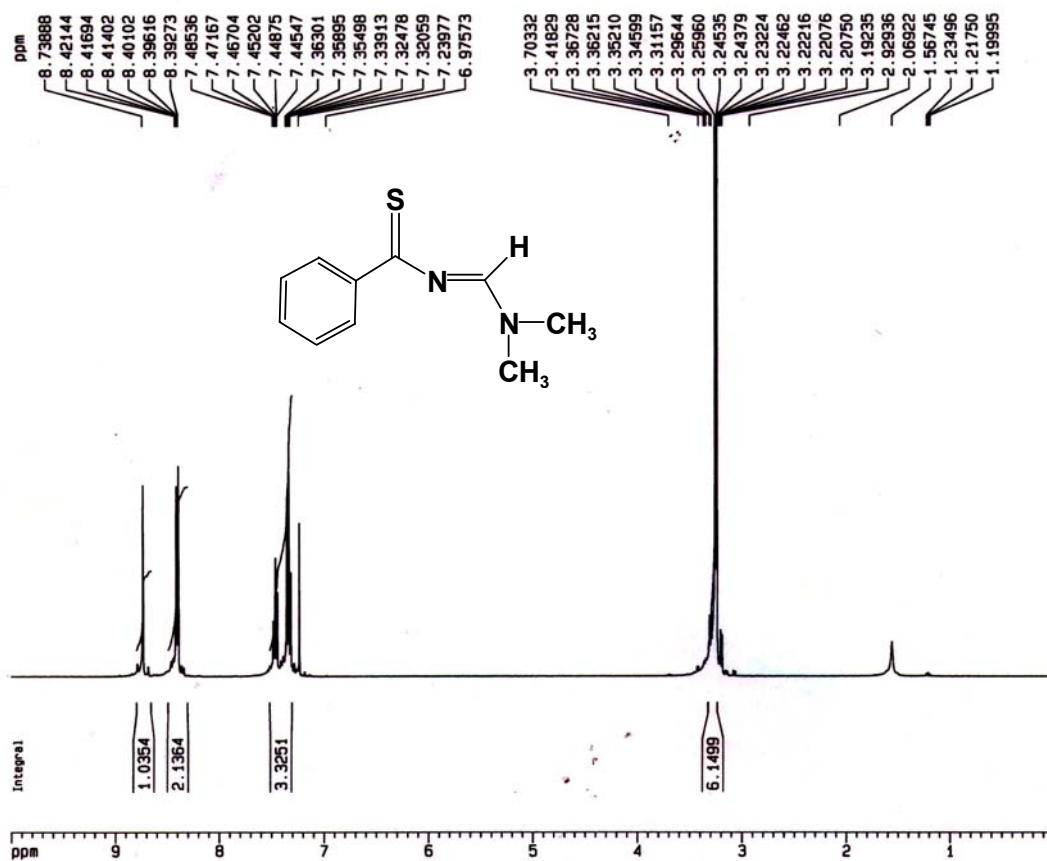


Figure 2: $^1\text{H-NMR}$ spectrum of the synthesized N-[(dimethylamino)methylene]thiobenzamide

The ^{13}C -NMR spectrum, shown in Figure 3, exhibits signals due to the two non-equivalent methyl carbons at δ 36.81 and 42.37. The four singlets at δ 128.12, 129.27, 132.33 and 143.47 were assigned to phenyl ring carbons. The imine carbon absorbs at δ 159.49. The thiocarbonyl carbon appears downfield at δ 216.66.

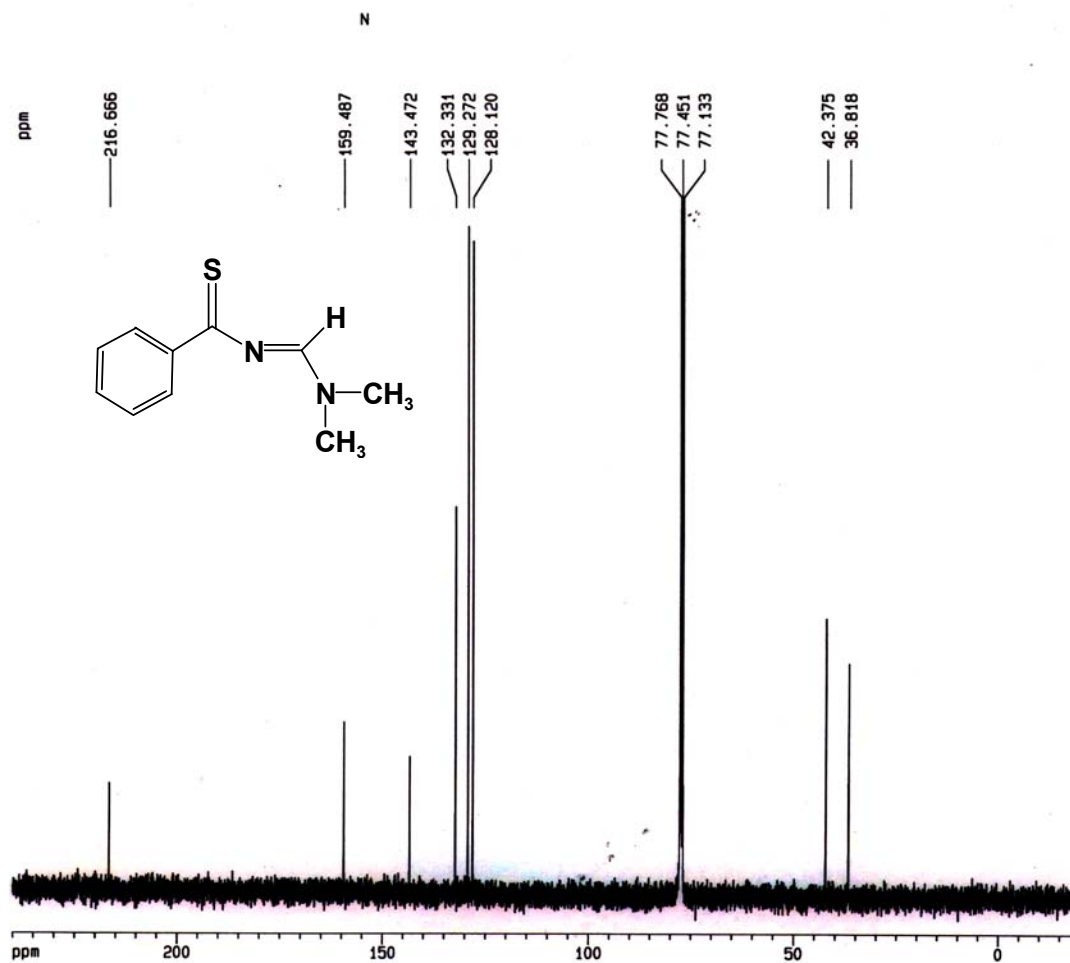


Figure 3: ^{13}C -NMR spectrum of the synthesized N-[(dimethylamino)methylene]thiobenzamide

In order to confirm the ^1H - and ^{13}C -NMR spectral assignments, the two dimensional ^1H - ^{13}C correlation spectrum was recorded. The spectrum, shown in Figure 4, reveals that the two carbon signals at δ 36.8 and 42.4, that were assigned to the non-equivalent methyl carbons, correlate with the two singlets at δ 3.24 and 3.25 in the ^1H -spectrum, that were assigned to the protons of the two non-equivalent methyl groups. In addition, the signal in the ^{13}C -spectrum at δ 159.5, assigned to the imine carbon, correlates with the downfield singlet in the ^1H -spectrum at δ 8.74, assigned to the imine proton. The signal at δ 143.47 in the ^{13}C -spectrum, which was assigned to one of the phenyl ring carbons, is not present in the two dimensional spectrum. This shows that this signal is due to the quaternary carbon of the phenyl ring at position 1. As expected, the three additional signals in the ^{13}C -spectrum due to the phenyl ring carbons still appear in the two dimensional spectrum. The signals in the ^{13}C -spectrum at δ 128.1 and 132.3 can be assigned to the meta- and para-carbons of the phenyl ring, respectively, since they correlate with the multiplet (3H) at δ 7.32-7.36 in the ^1H -spectrum assigned to the meta- and para-protons. Finally, the last signal at δ 129.3 in the ^{13}C -spectrum can be assigned to the ortho carbons of the phenyl ring since this signal correlates with the multiplet (2H) at δ 8.39-8.41 in the ^1H -spectrum assigned to the ortho protons.

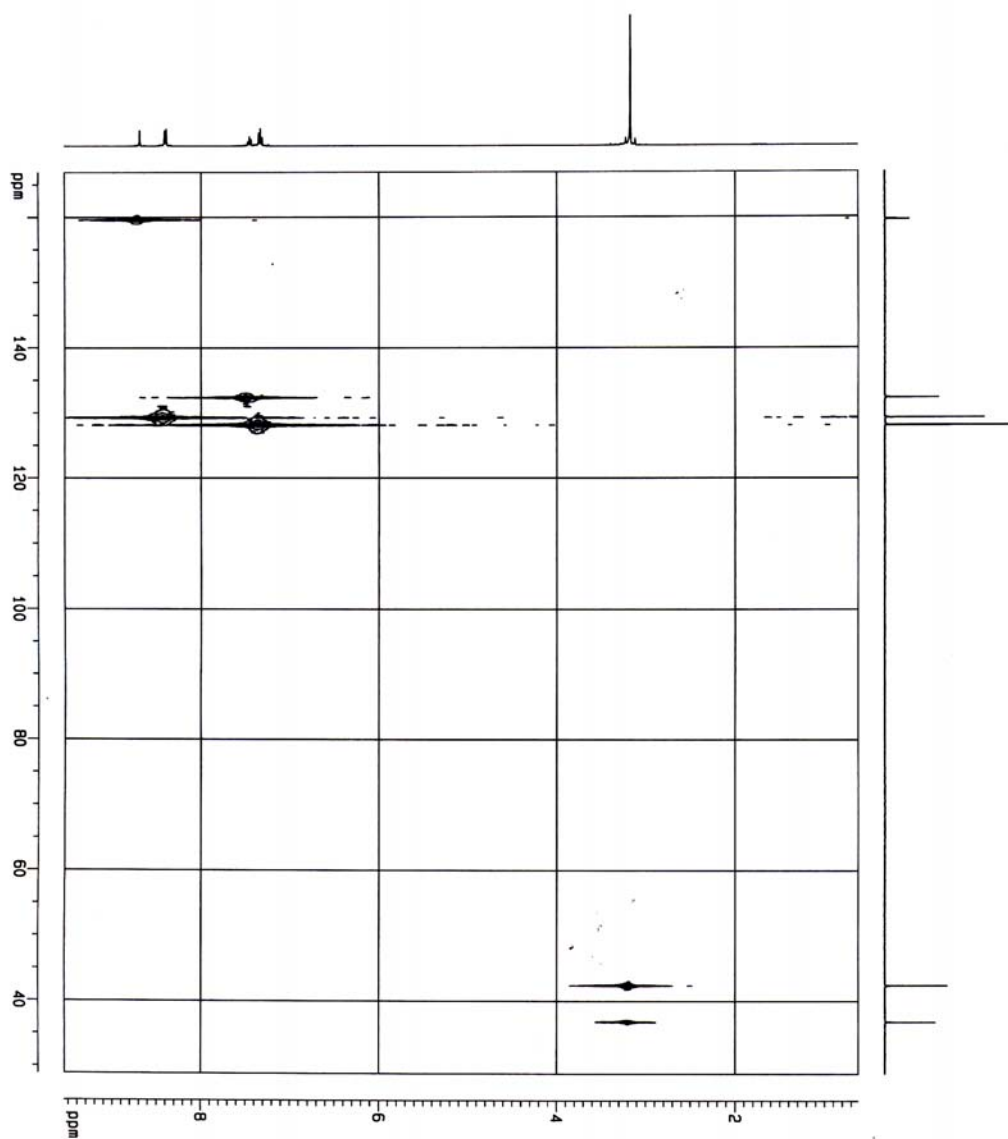
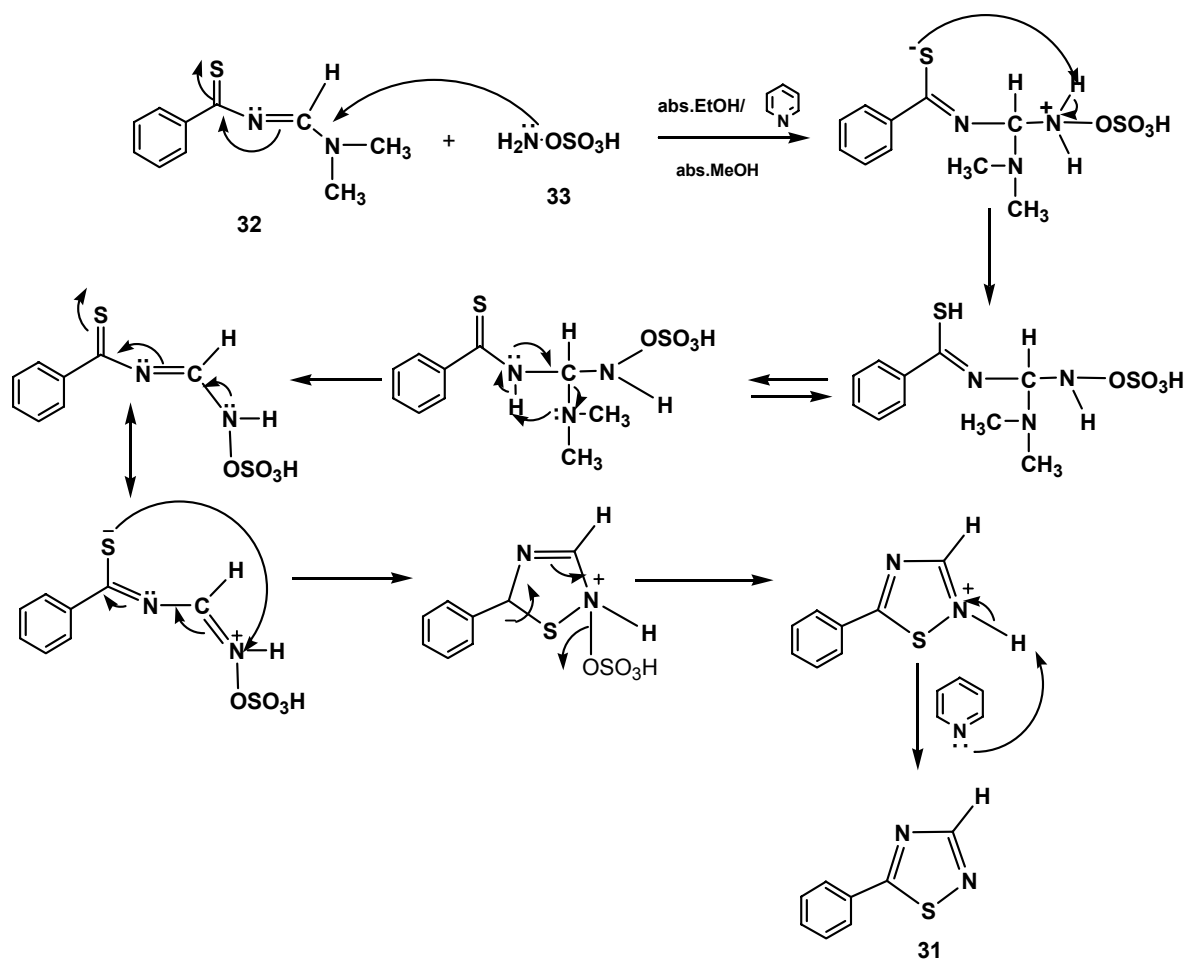


Figure 4: Two dimensional ^1H - ^{13}C correlation spectrum of the N-[(dimethylamino)methylene]thiobenzamide

2.1.1.2 Synthesis of 5-phenyl-1,2,4-thiadiazole

The amination cyclization of N-[(dimethylamino)methylene]thiobenzamide (**32**) using hydroxylamine-O-sulfonic acid (**33**) and pyridine as basic catalyst led to the formation of 5-phenyl-1,2,4-thiadiazole (**31**) as shown in Scheme 7.



Scheme 7: Mechanism for the formation 5-phenyl-1,2,4-thiadiazole

5-Phenyl-1,2,4-thiadiazole (**31**) was obtained as a light yellow viscous liquid and characterized by GC-MS, ^1H - and ^{13}C -NMR spectroscopy.

According to the synthetic method described by Yang-i Lin,⁹ **31** was reported as a colorless liquid. But in this synthesis, **31** was obtained as a light yellow viscous liquid. Therefore, there might be an impurity in this product.

The GC-trace (Figure 5a) indicates the presence of an impurity which eluted at a retention time of 6.6 min. Its mass spectrum (Figure 5b) exhibits a molecular ion at m/z 146 and a base peak at m/z 103. The major gc-volatile component eluted with a retention time of 10.9 min. The mass spectrum (Figure 5c) of this compound exhibits a molecular ion at m/z 162, corresponding to the molecular weight of **31** (MW 162). Moreover, the spectrum exhibits a base peak at m/z 135 and an intense peak at m/z 104 which indicates that **31** undergoes fragmentation in the mass spectrometer to yield $[\text{C}_6\text{H}_7\text{CNS}]^{*\dagger}$ and $[\text{C}_6\text{H}_7\text{CNH}]^+$ fragments, respectively.

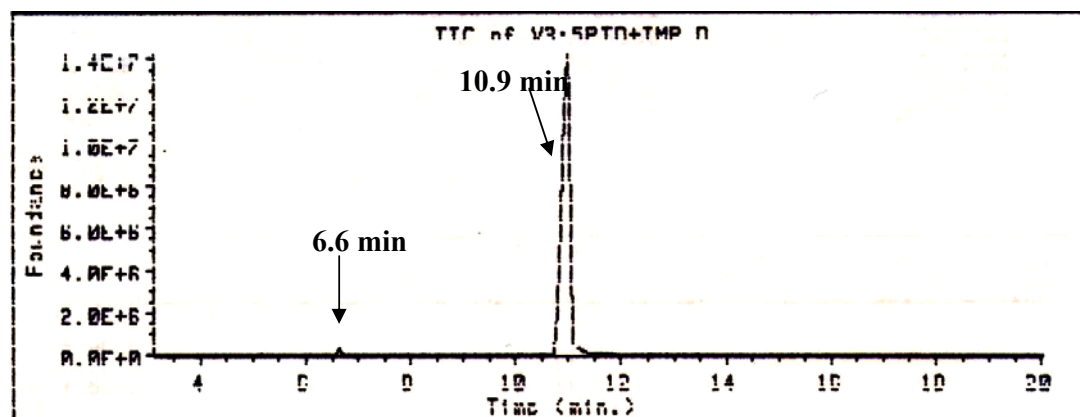


Figure 5a: GC-trace of the synthesized 5-phenyl-1,2,4-thiadiazole

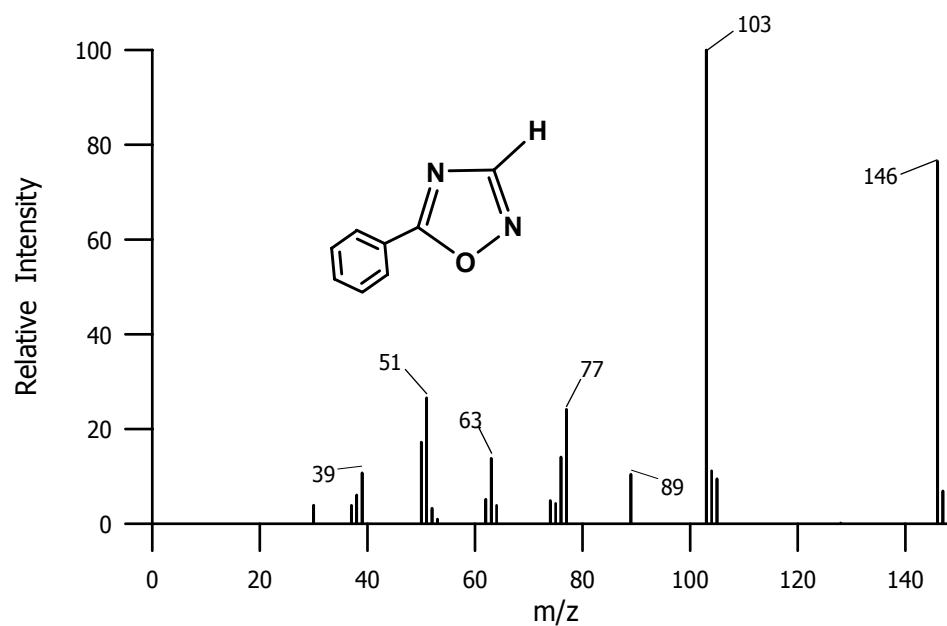


Figure 5b: Mass spectrum of the peak at retention time 6.6 min

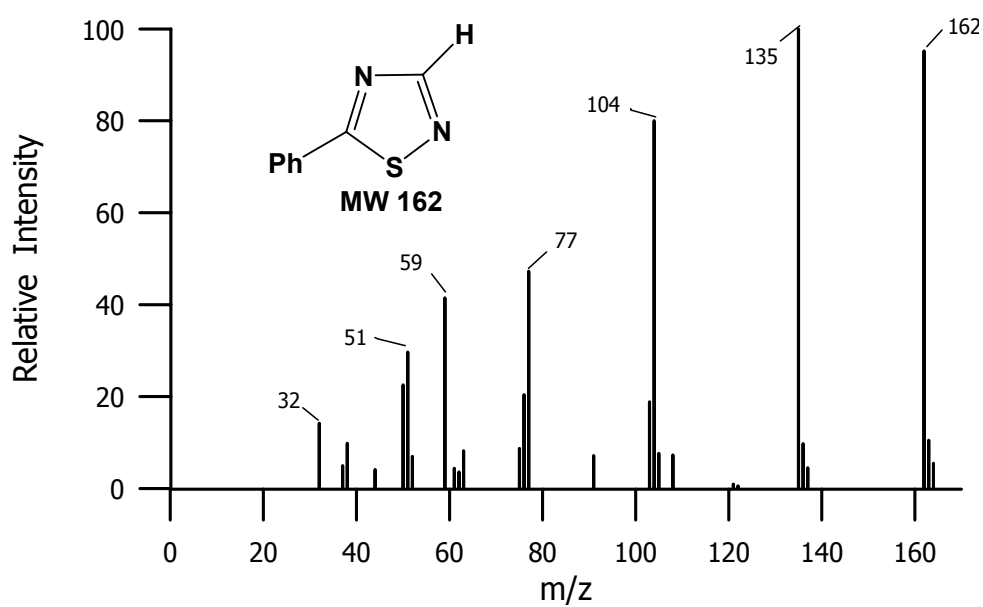
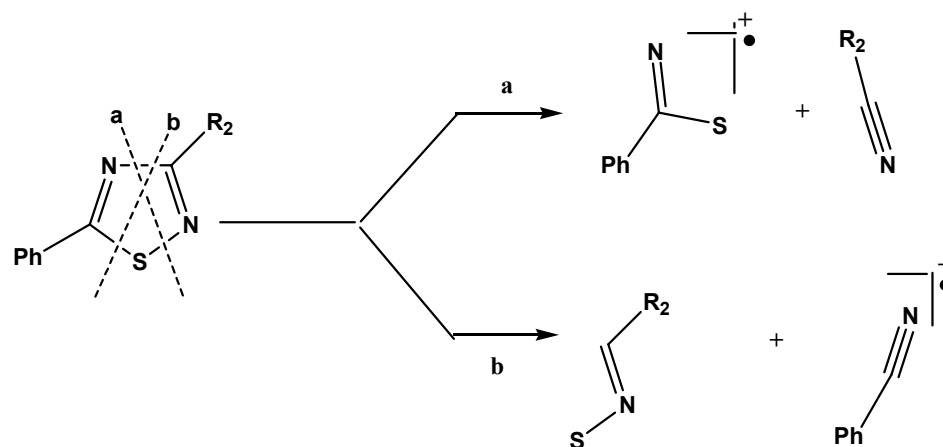


Figure 5c: Mass spectrum of the peak at retention time 10.9 min

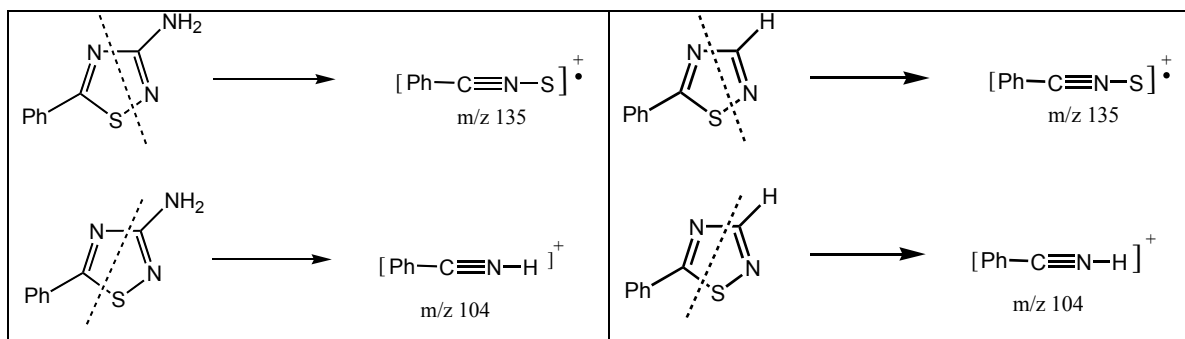
Interestingly, based on the reported fragmentation pathways of phenyl-1,2,4-thiadiazoles¹⁰ (shown in Scheme 8), the cleavage of $[\text{C}_6\text{H}_5\text{CN}]^{\bullet+}$ was expected to be one of the major fragments. But according to the mass spectrum, shown in Figure 5c, the peak at m/z 104 is much more intense than the peak at m/z 103.



Scheme 8: Major fragmentation pathways of 1,2,4-thiadiazoles

However, the mass spectrum of 3-amino-5-phenyl-1,2,4-thiadiazole was also reported to reveal a peak at m/z 104 as one of intense peaks.¹⁰ This was suggested to be due to the cleavage of $[\text{C}_6\text{H}_5\text{CNH}]^+$ fragment with a proton from the amino group at position 3 on the thiadiazole ring, as shown in Scheme 9.

Consequently, based on these suggestions, the intense peak at m/z 104 is due to the $[\text{C}_6\text{H}_5\text{CNH}]^+$ fragment and the base peak at m/z 135 is due to the $[\text{C}_6\text{H}_5\text{CNS}]^{\bullet+}$ fragment which can also be expected as a major fragmentation pathway for 5-phenyl-1,2,4-thiadiazole (**31**) ($\text{R}_1 = \text{Ph}$, $\text{R}_2 = \text{H}$), as shown in Scheme 9,



Scheme 9: Possible fragmentation pathway of 3-amino-5-phenyl-1,2,4-thiadiazole and 5-phenyl-1,2,4-thiadiazole

The $^1\text{H-NMR}$ spectrum (Figure 6) also shows the presence of an impurity that was also observed by GC-MS. The spectrum shows a singlet at δ 8.53 due to the proton at position 3 of the thiadiazole ring and 3H and 2H multiplets at δ 7.32-7.38 and δ 7.80-7.82 due to the meta-, para-protons and the ortho-protons of the phenyl ring, respectively. In addition, the spectrum also exhibits a singlet of low intensity at δ 8.31 and a multiplet of low intensity in the phenyl region, which must be due to the observed impurity in the sample.

Based on the observed molecular ion at m/z 146 and the $^1\text{H-NMR}$ spectrum, this impurity was suspected to be 5-phenyl-1,2,4-oxadiazole (**37**). In order to investigate this possibility, **37** was synthesized by the same procedure that was used to synthesized **1** except that benzamide (**38**) was used as the starting material instead of thiobenzamide (**34**).

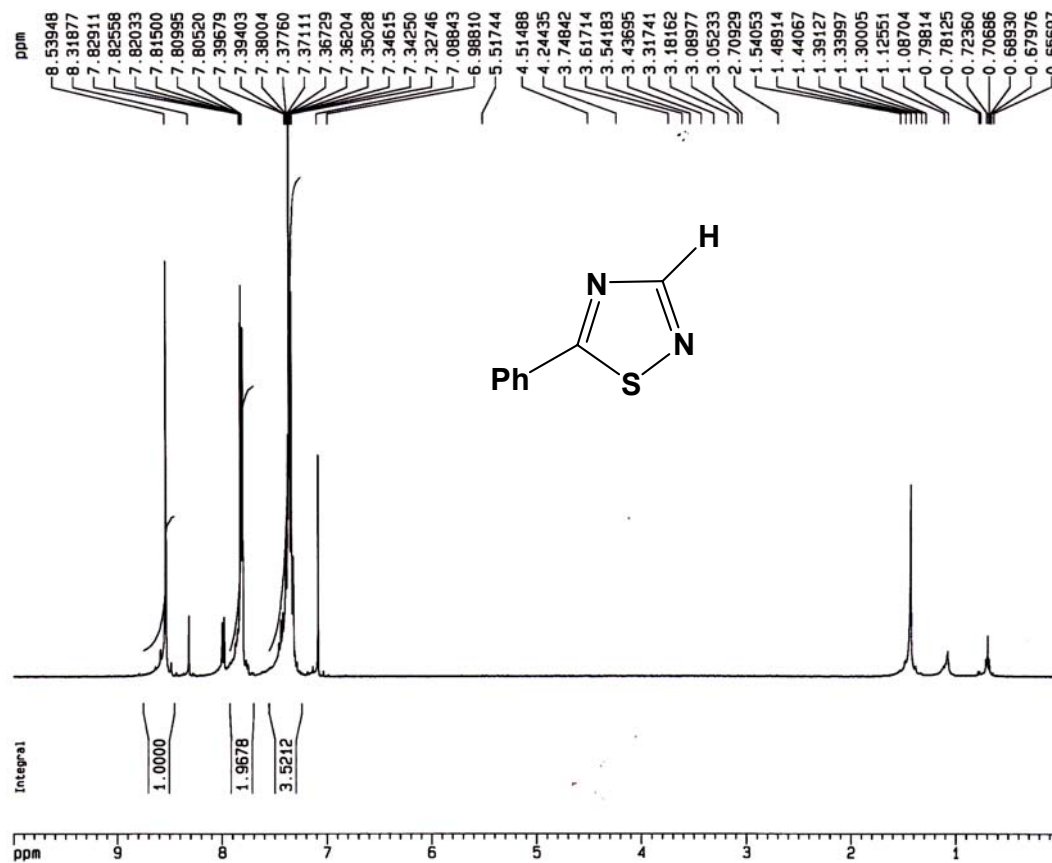
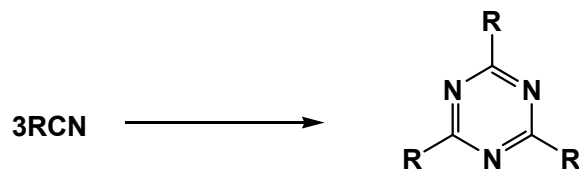


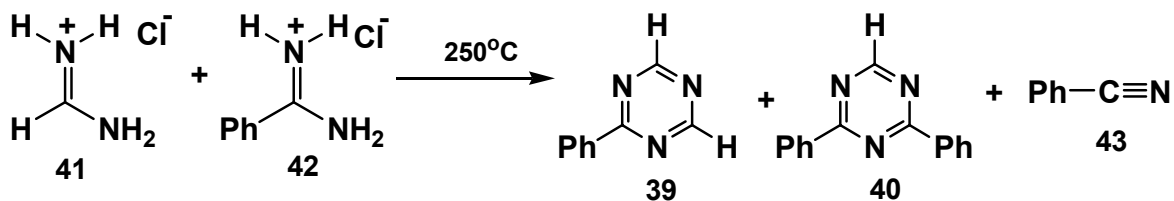
Figure 6: $^1\text{H-NMR}$ spectrum of the synthesized 5-phenyl-1,2,4-thiadiazole

2.1.2 Synthesis of the photoproducts: 2-phenyl-1,3,5-triazine and 2,4-diphenyl-1,3,5-triazine

It has been reported that 1,3,5-triazines can be prepared via cyclotrimerization of nitriles¹¹ where the R group can be hydrogen, alkyl, aryl, halogen or other substituent groups. This method is not effective, however, when the substituents are different.



F.C Schaefer and I. Hechenbleiner reported¹¹ the synthesis of sym-triazines with different substituent groups by trimerization and co-trimerization of amidines. According to their report, 2-phenyl- and 2,4-diphenyl-1,3,5-triazine (**39**) and (**40**) can be prepared in 20% and 50 %, respectively, by the co-trimerization of formamidine hydrochloride (**41**) and benzamidine hydrochloride (**42**), shown in Scheme 10.



Scheme 10: Synthesis of 2-phenyl- and 2,4-diphenyl-1,3,5-triazine

By employing their procedure, both triazines **39** and **40** were obtained as a mixture and separated by steam distillation. Both isolated triazines (**39**) and (**40**) were obtained as white solids which were different in their melting points (white solid A; mp 62-64 °C and white solid B; mp 80-82°C).

The GC-analysis of the white solid A [isothermal 170 °C (30 min)] (Figure 7a) shows only one component, which eluted with a retention time of 8.5 min. The mass spectrum of this peak (Figure 7b) exhibits a molecular ion at m/z 157 corresponding to the molecular weight of 2-phenyl-1,3,5-triazine (**39**; MW 157) which was additionally supported by a base peak at m/z 104 due to the $[C_6H_5CNH]^+$ fragment, which could be expected as the major fragmentation pathway of **39** rather than the cleavage of benzonitrile fragment (m/z 103).

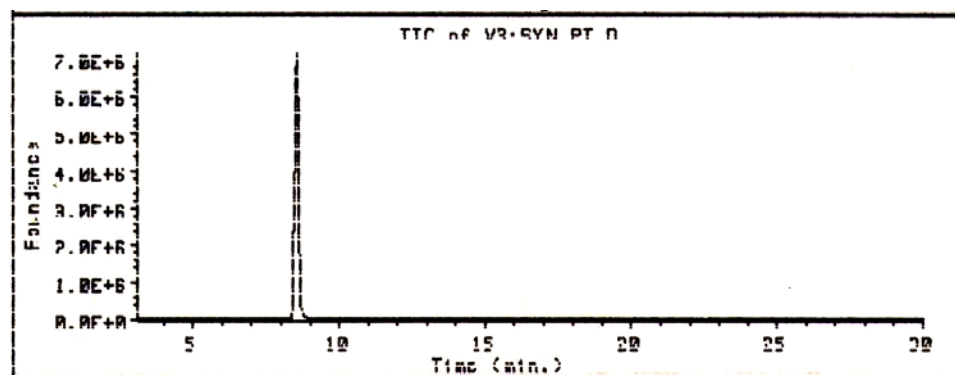


Figure 7a: GC-trace of the white solid A

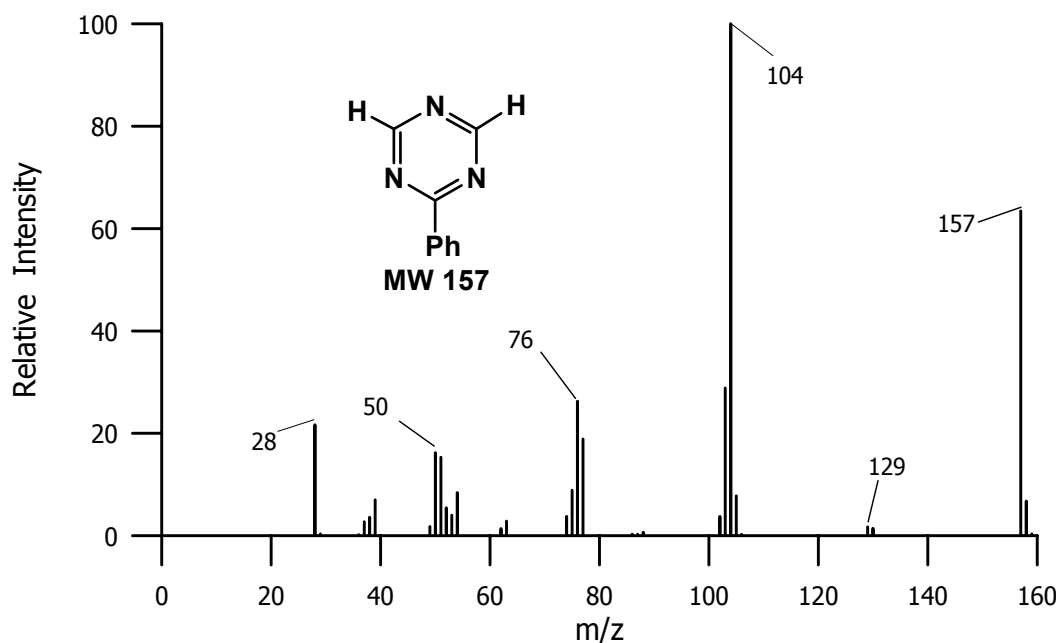


Figure 7b: Mass spectrum of the white solid A

The GC-trace of the white solid B [isothermal 240°C (30 min)] (Figure 8a) also shows only one gc-volatile component which eluted with a retention time of 16.2 min. As expected, the mass spectrum of this peak exhibits (Figure 8b) a molecular ion at m/z 233, which is consistent with the molecular weight of 2,4-diphenyl-1,3,5-triazine (**40**; MW 233). In this case the base peak that is observed at m/z 103 instead of m/z 104, which was observed in the mass spectrum of 2-phenyl-1,3,5-triazine (**39**). This base peak at m/z 103 is probably due to the cleavage of $[\text{C}_6\text{H}_5\text{CN}]^{*+}$ fragment.

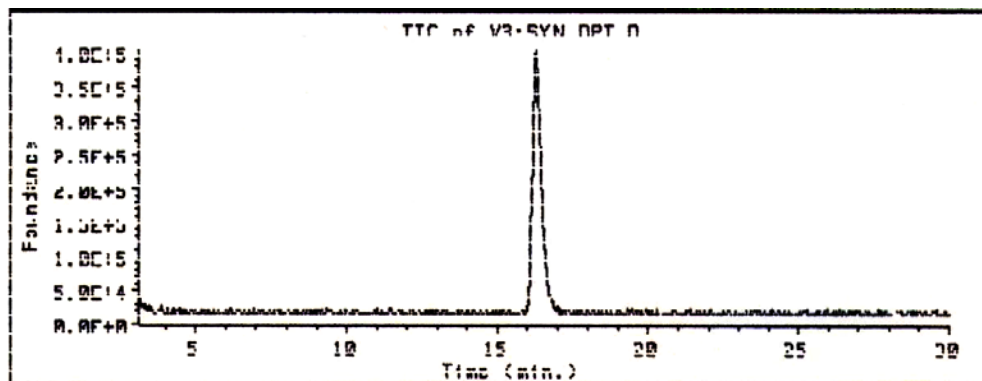


Figure 8a: GC-trace of the white solid B

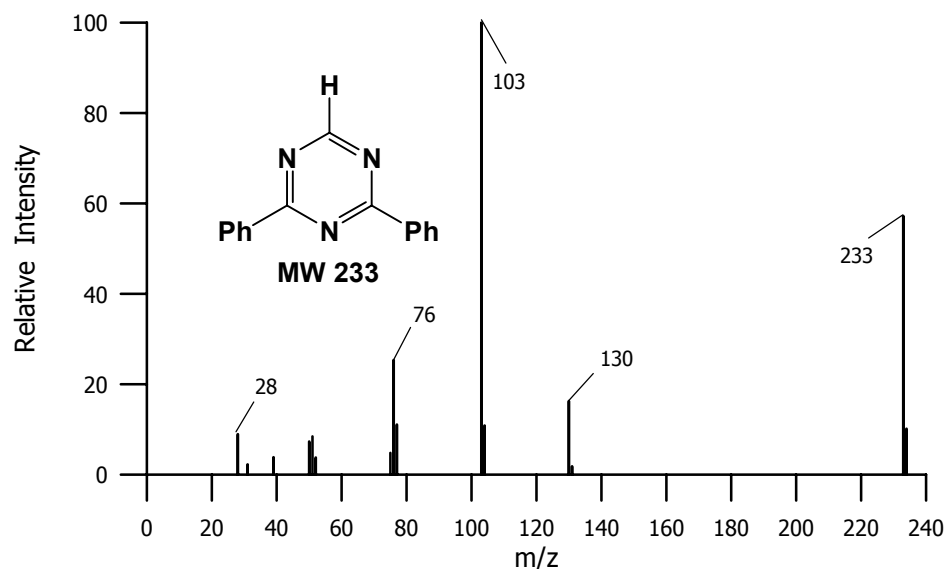


Figure 8b: Mass spectrum of the white solid B

The $^1\text{H-NMR}$ spectrum of the white solid A, shown in Figure 9, exhibits a downfield singlet (2H) at δ 9.14 and two multiplets at δ 7.43-7.54 (3H) and δ 8.43-8.45 (2H). In the case of the white solid B, the $^1\text{H-NMR}$ spectrum exhibits a singlet (1H) at δ 9.28 and two multiplets at δ 7.56-7.63 (6H) and δ 8.66-8.68 (4H). The $^1\text{H-NMR}$ spectrum of white solid A is consistent with the assignment as 2-phenyl-1,3,5-triazine (**39**), in which, the two equivalent triazine ring protons appear downfield as a singlet (2H) and the phenyl ring protons appear as two multiplet (2H due to meta protons and 3H due to ortho-para protons). Also the $^1\text{H-NMR}$ spectrum of the white solid B, shown in Figure 10, is consistent with the assignment as 2,4-diphenyl-1,3,5-triazine (**40**), in which the triazine ring proton absorbs at δ 9.28 as a singlet (1H) and the two multiplet at δ 7.56-7.63 (6H) and δ 8.66-8.68 (4H) were assigned to the two sets of equivalent phenyl ring protons of 2,4-diphenyl-1,3,5-triazine (**40**).

Consequently, according to the above mass spectra and $^1\text{H-NMR}$ spectra, the white solid A can be identified as 2-phenyl-1,3,5-triazine (**39**) and the white solid B can be identified as 2,4-diphenyl-1,3,5-triazine (**40**).

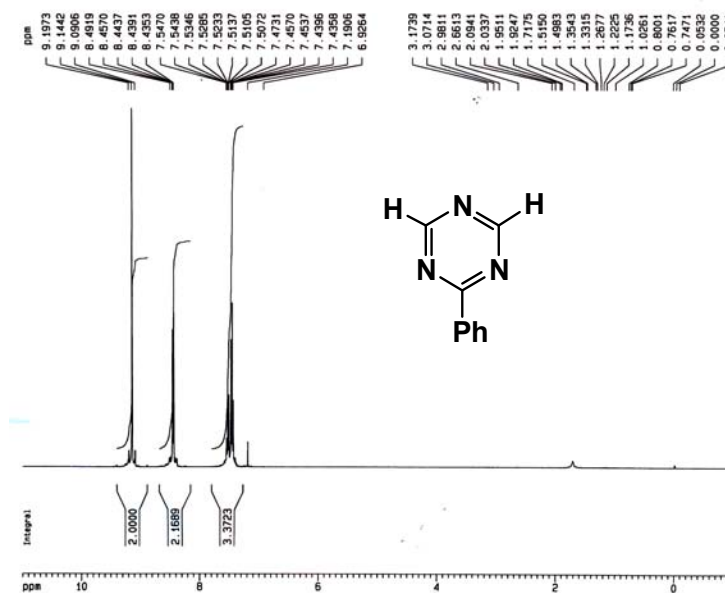


Figure 9: $^1\text{H-NMR}$ spectrum of the white solid A

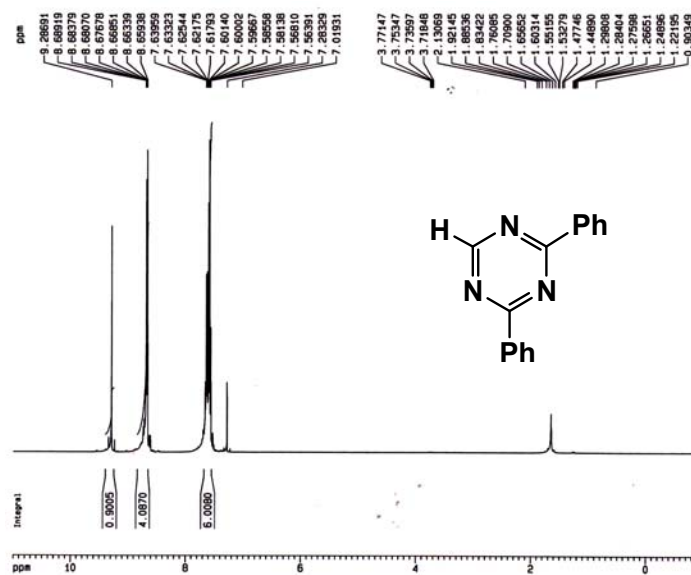
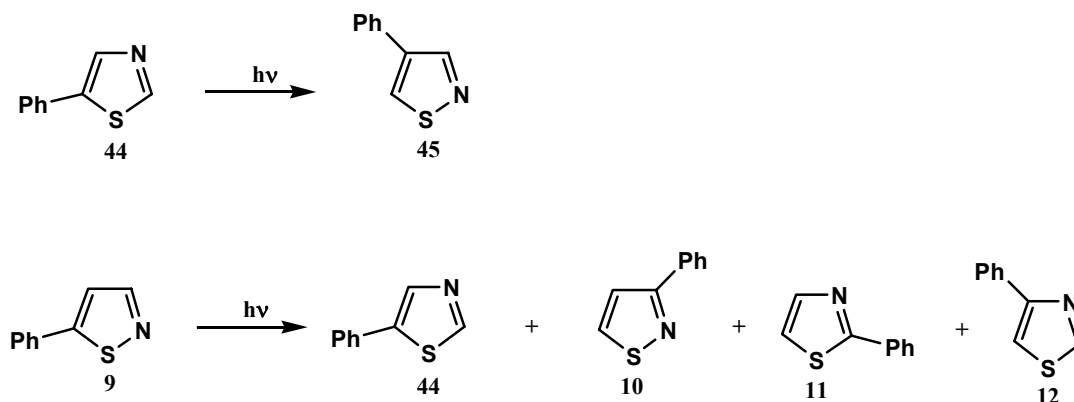


Figure 10: $^1\text{H-NMR}$ spectrum of the white solid B

2.1.3 Photochemistry of 5-phenyl-1,2,4-thiadiazole

5-Phenyl-1,2,4-thiadiazole (**31**) can be viewed as a combination between 5-phenylthiazole (**44**) and 5-phenylisothiazole (**9**). 5-Phenylthiazole (**44**) and 5-phenylisothiazole (**9**) have been reported to undergo the phototransposition reactions,⁶ shown in Scheme 11. Therefore, the photochemistry of **31** might be expected to exhibit the same type of photochemistry.



Scheme 11: Photochemistry of 5-phenylthiazole and 5-phenylisothiazole

The photolysis of **31** was first monitored by ultraviolet absorption spectroscopy. Solutions of **31** (5×10^{-5} M) in acetonitrile and cyclohexane were prepared. The solutions were irradiated with three > 290 nm lamps and monitored by ultraviolet absorption spectroscopy at 60 seconds intervals. Figure 11a and 12a show the UV-absorption spectra of **31** in acetonitrile and cyclohexane, respectively. The λ_{\max} is shown at the same wavelength of 273.2 nm in both solvents with an extinction coefficient of $13,880 \text{ L mol}^{-1} \text{ cm}^{-1}$ in cyclohexane and $13,873 \text{ L mol}^{-1} \text{ cm}^{-1}$ in acetonitrile.

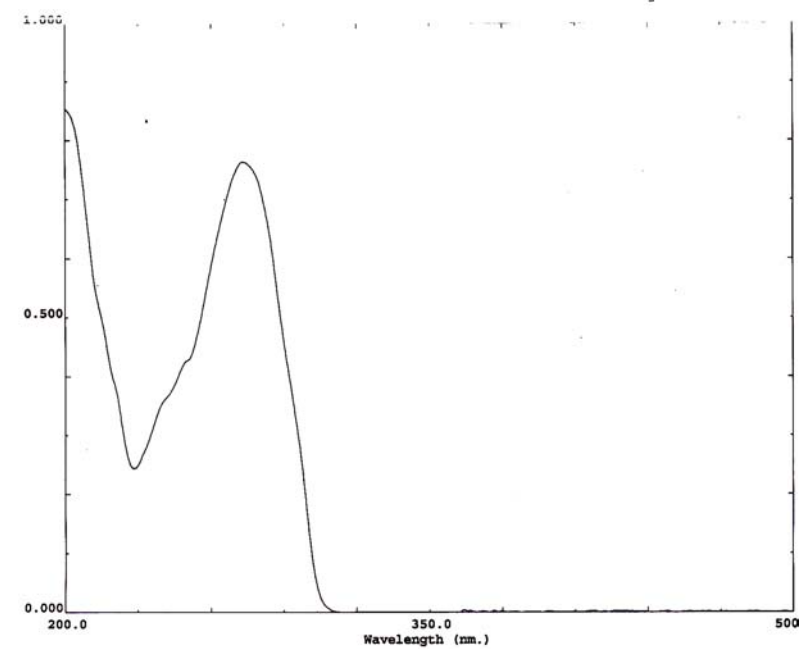


Figure 11a: UV-absorption spectrum of **31** in acetonitrile

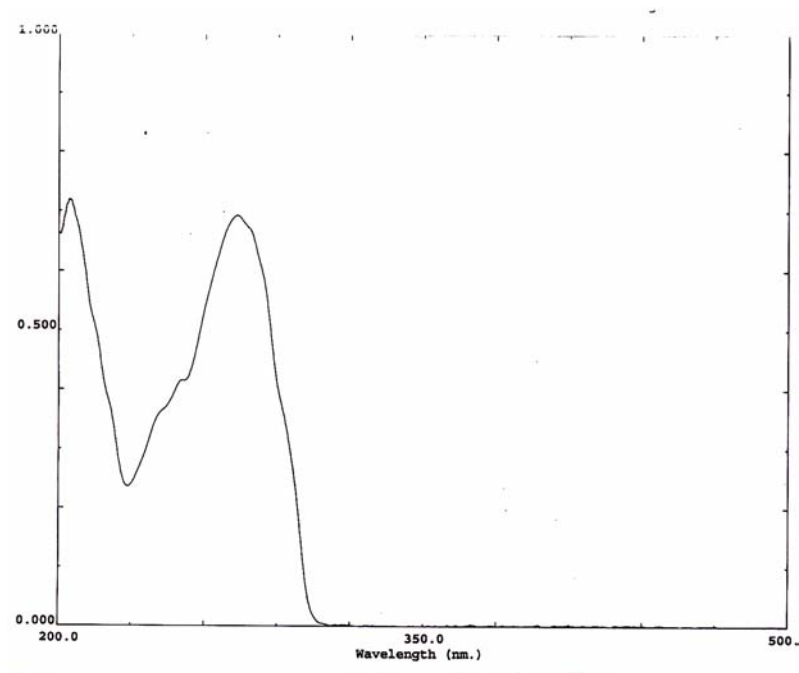


Figure 12a: UV-absorption spectrum of **31** in cyclohexane

The UV overlay spectrum of the photolysis in acetonitrile (Figure 11b) exhibits the decreasing in the absorption band at the λ_{max} 273.2 nm from 0.76 to 0.68 after 240 sec. After 1,560 sec of irradiation, the UV-absorption overlay spectrum (Figure 11b) reveals the absorption band at the λ_{max} 273.2 nm shifted to λ_{max} 260.2 nm. The spectrum also reveals the increasing in the absorption band at λ 230 nm.

The UV overlay spectrum of the photolysis in cyclohexane exhibits (Figure 12b) the same spectral pattern. But the absorption band at λ_{max} 264.4 nm was being formed slower than the absorption band observed from the photolysis in acetonitrile. Also the absorption band at λ 230 nm is increasing more slowly than during the photolysis in acetonitrile.

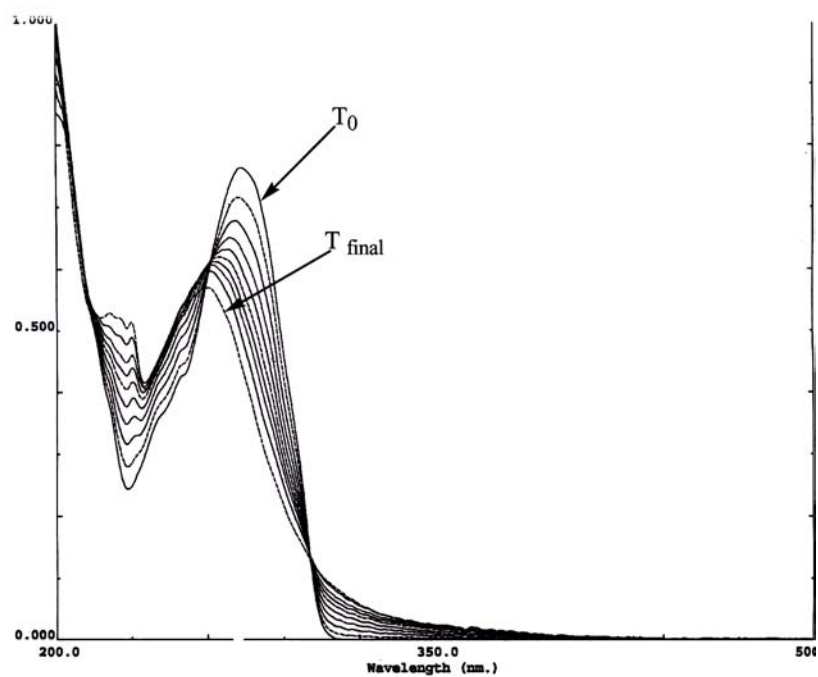


Figure 11b: UV-overlay spectrum of the photolysis of **31** in acetonitrile

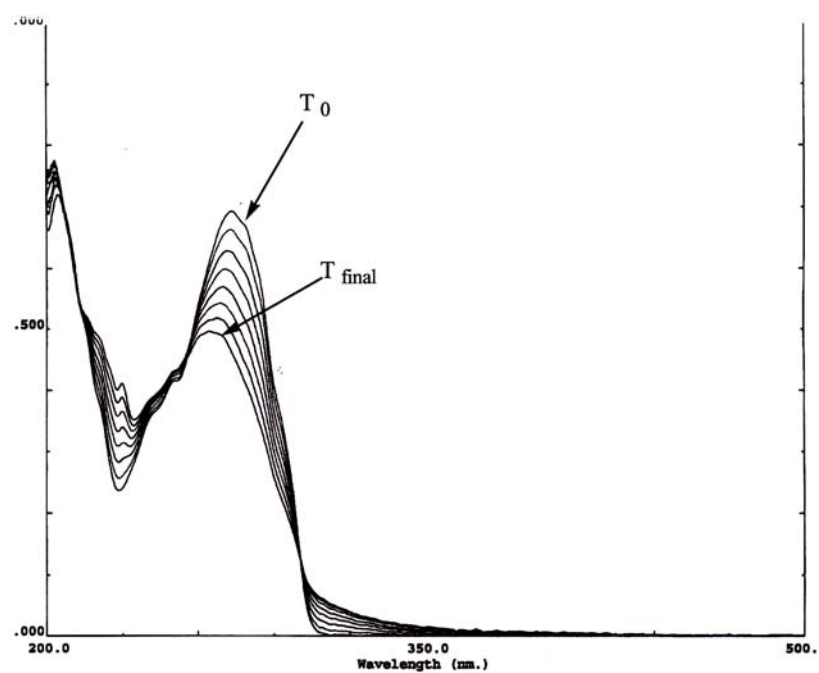


Figure 12b: UV-overlay spectrum of the photolysis in cyclohexane

The photochemical reaction of **31** was also monitored by gas chromatography. A solution of **31** in acetonitrile (2.0×10^{-2} M; 17 mL) was placed in a Pyrex tube (20 cm \times 0.7 cm). The GLC analysis of this solution [140 (4 min), 20°C/min to 180°C (14 min), 20°C/min to 240 (30 min)] shows (Figure 13a) one major peak with a retention time of 12 min and a small peak with a retention time of 8 min due to the presence of an impurity. The tube was sealed with a rubber septum, purged with argon for 15 min, and irradiated with sixteen > 290 nm lamps for 210 min. The GLC analysis of the resulting solution (Figure 13b) shows the consumption of 33.4% of the reactant and the appearance of six new peaks with retention times of 4, 11, 18, 39 and 40 min.

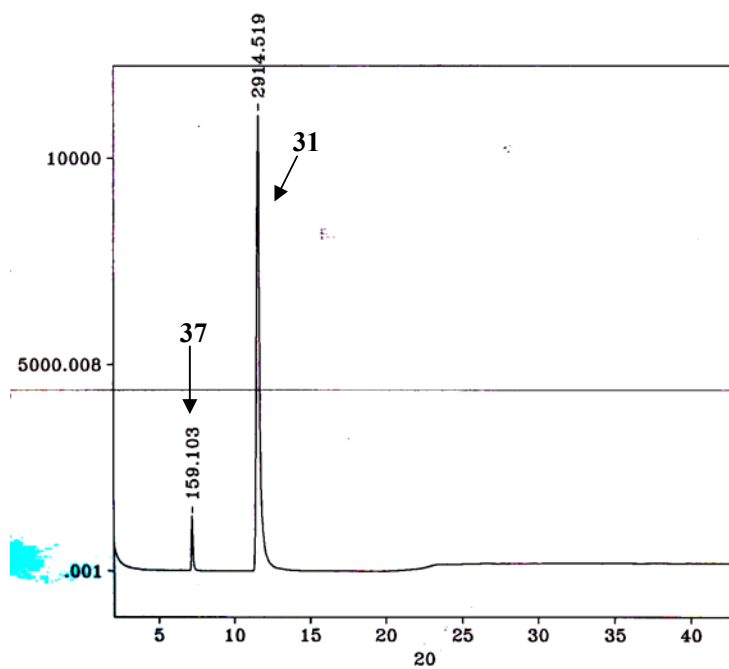


Figure 13a: GC-trace of solution of **31** before irradiation

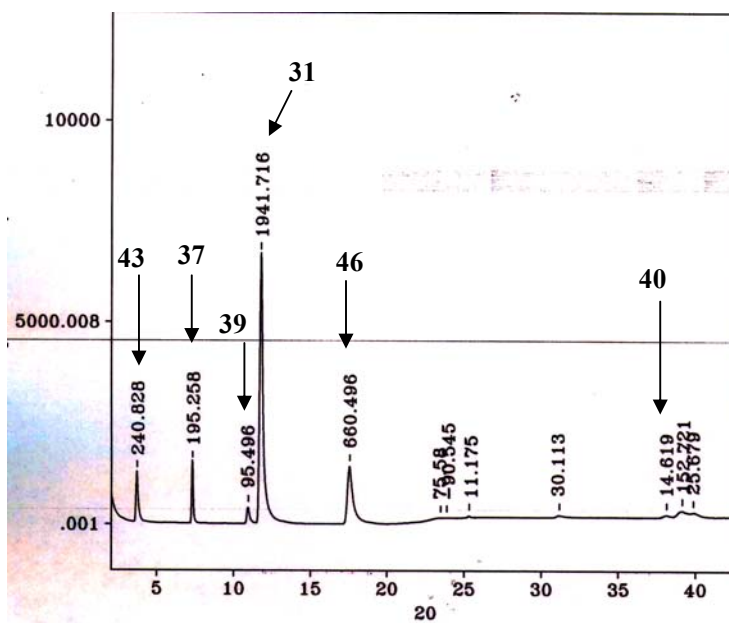


Figure 13b: GC-trace of the solution of **31** after 210 min of irradiation

The reaction solution was concentrated by rotary evaporation at room temperature and analyzed by the GC interfaced with a mass spectrometer.

The GC-trace, shown in Figure 14a, [140 (5 min), 20°C/min to 200°C (20 min), 10°C/min to 240 (20 min)] exhibits seven gc-volatile components with retention times of 4, 7.5, 10, 10.6, 12.1, 23.3 and 40 min.

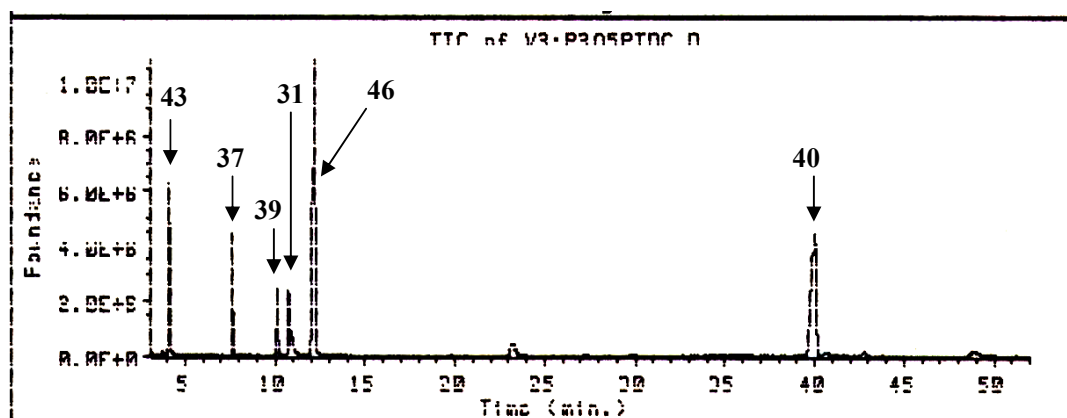


Figure 14a: GC-trace of the concentrated photolysate of **31** after 210 min of irradiation time

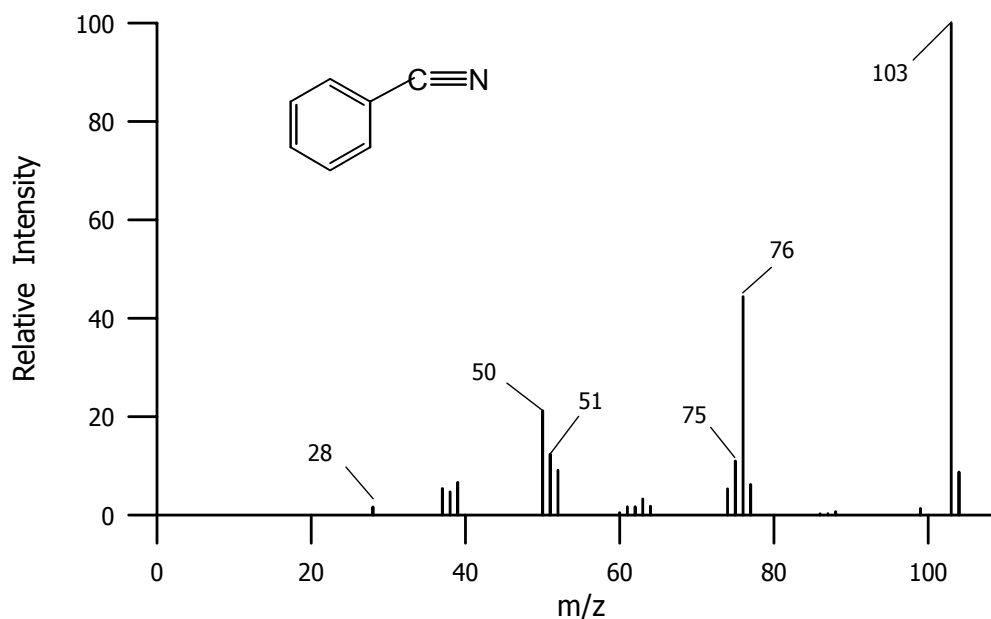


Figure 14b: Mass spectrum of the photoproduct eluted at retention time 4 min

The mass spectrum of the first peak with a retention time of 4 min (Figure 14b) shows a base molecular ion peak at m/z 103. This product was assumed to be benzonitrile (**43**).

In order to prove this assumption, an authentic sample of **43** was analyzed by the GC interfaced with a mass spectrometer under the same temperature program (Figure 15a-b). Figure 15a shows that **43** was eluted with the same retention time as the first eluted photoproduct. Furthermore, Figure 15b shows that the fragmentation pattern and molecular ion from both the photoproduct and authentic benzonitrile (**43**) are also identical. Therefore, based on these chromatographic and mass spectroscopic results, the first eluted photoproduct was identified as benzonitrile (**43**), a photofragmentation product.

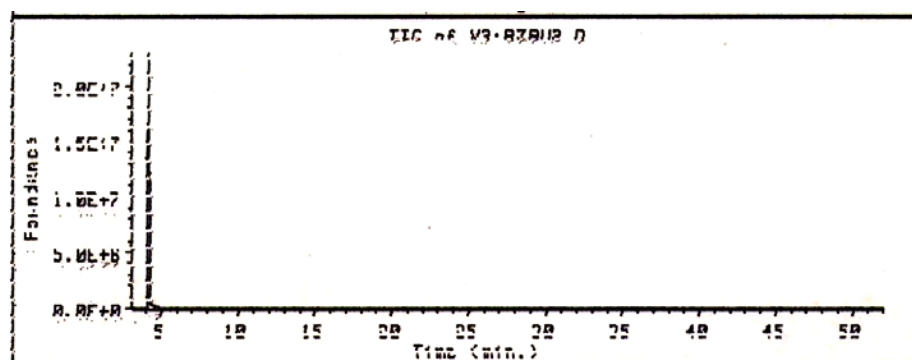


Figure 15a: GC-trace of an authentic sample of **50**

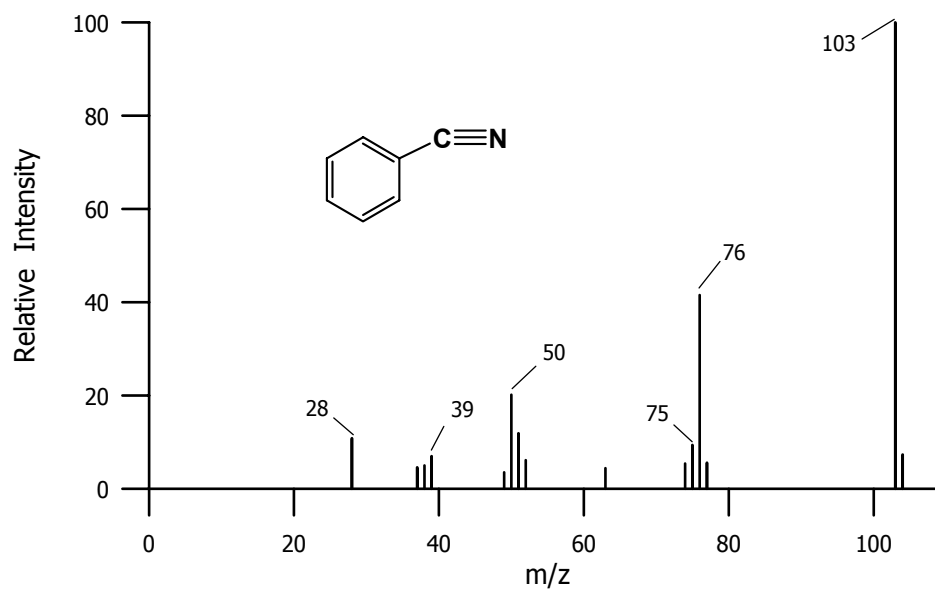


Figure 15b: Mass spectrum of an authentic sample of **43**

The peak at retention time of 7.5 min was identified as 5-phenyl-1,2,4-oxadiazole (**37**) which was formed as a minor product during the synthesis of **31** (as discussed in the synthesis of section). The GLC analysis showed no significant decrease in the peak area of this compound after irradiation. Therefore, none of the observed photoproducts could result from a reaction of this compound.

The mass spectrum of the product that eluted with a retention time of 10.0 min (Figure 14c) exhibits a molecular ion at m/z 157, consistent with the molecular formula of $C_9H_7N_3$, and a base peak at m/z 104, consistent with the elimination of $[C_6H_5CNH]^+$ as the major fragment. This photoproduct was suggested to be 2-phenyl-1,3,5-triazine (**39**), a unique ring expansion product. This was confirmed by a direct comparison with the retention time and mass spectrum of an authentic sample of **39**, shown in Figure 16a-b.

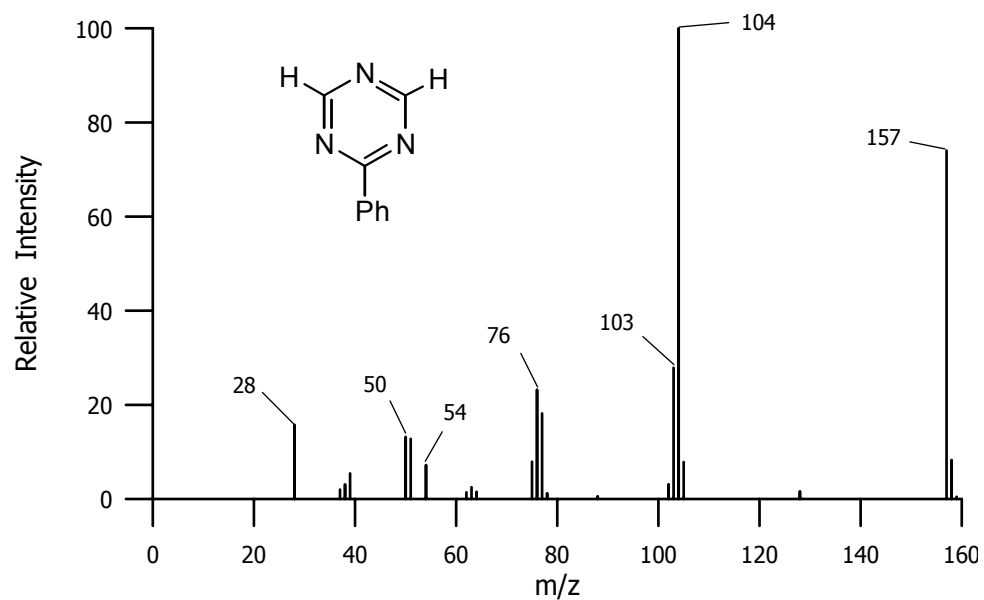


Figure 14c: Mass spectrum of the product eluted at a retention time of 10.0 min; expected to be **39**

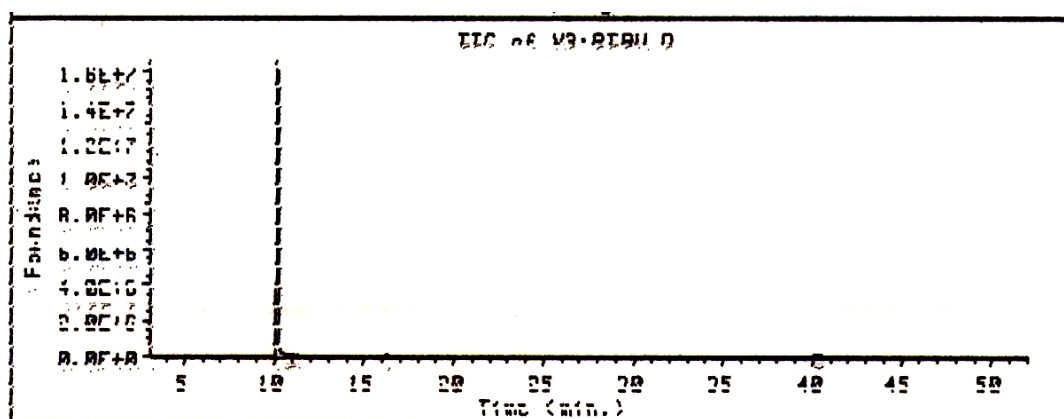


Figure 16a: GC-trace of an authentic sample of **39**

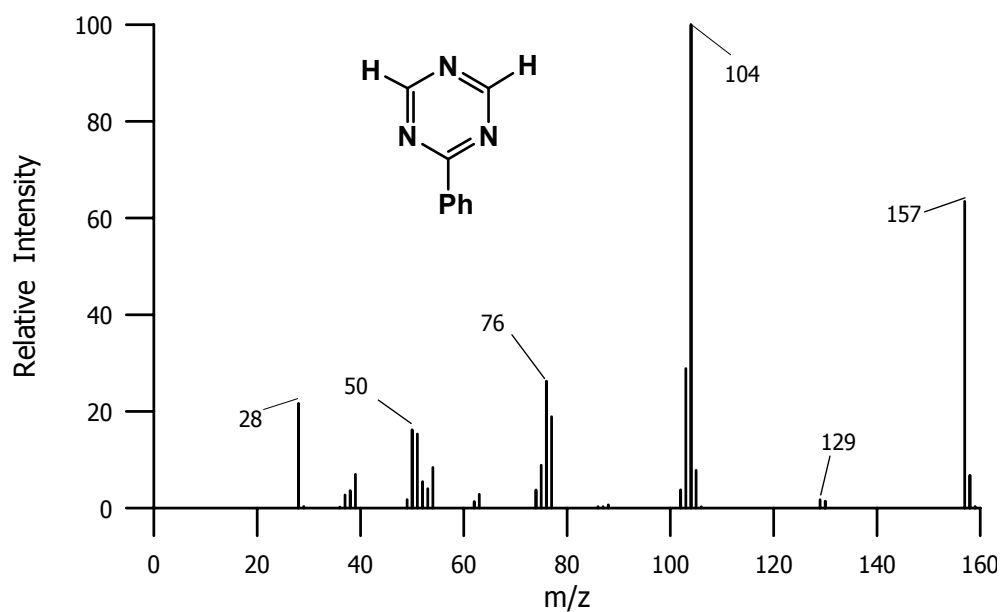


Figure 16b: Mass spectrum of an authentic sample of **39**

The peak with a retention time of 10.6 min is the starting material since it has a retention time and a mass spectrum (Figure 4d) identical to the reactant, **31**.

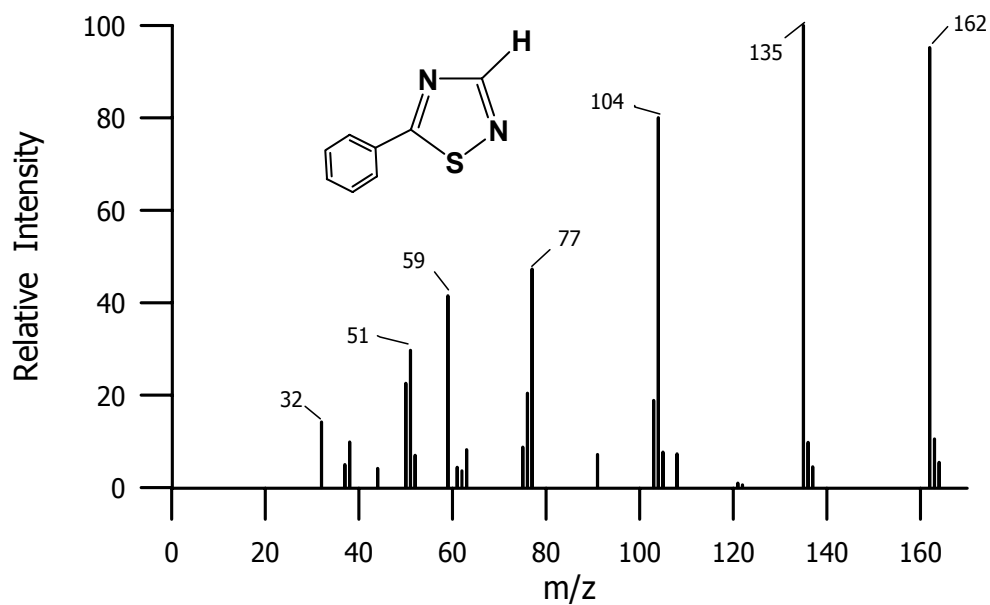


Figure 14d: Mass spectrum of the component at a retention time of 10.6 min; the reactant

The mass spectrum of the next photoproduct, which eluted with a retention time of 12.1 min, also exhibits a molecular ion at m/z 162 (Figure 14e) which is also consistent with the molecular formula of $C_8H_6N_2S$, identical to the formula of the reactant, **31**. Comparison of these mass spectra clearly shows, however, that although the mass spectrum of the photoproduct is different than the mass spectrum of **31**, Figure 14d, it is identical to the mass spectrum of 3-phenyl-1,2,4-thiadiazole (**46**), shown in Figure 17. This photoproduct is thus the phototransposition product, 3-phenyl-1,2,4-thiadiazole (**46**).

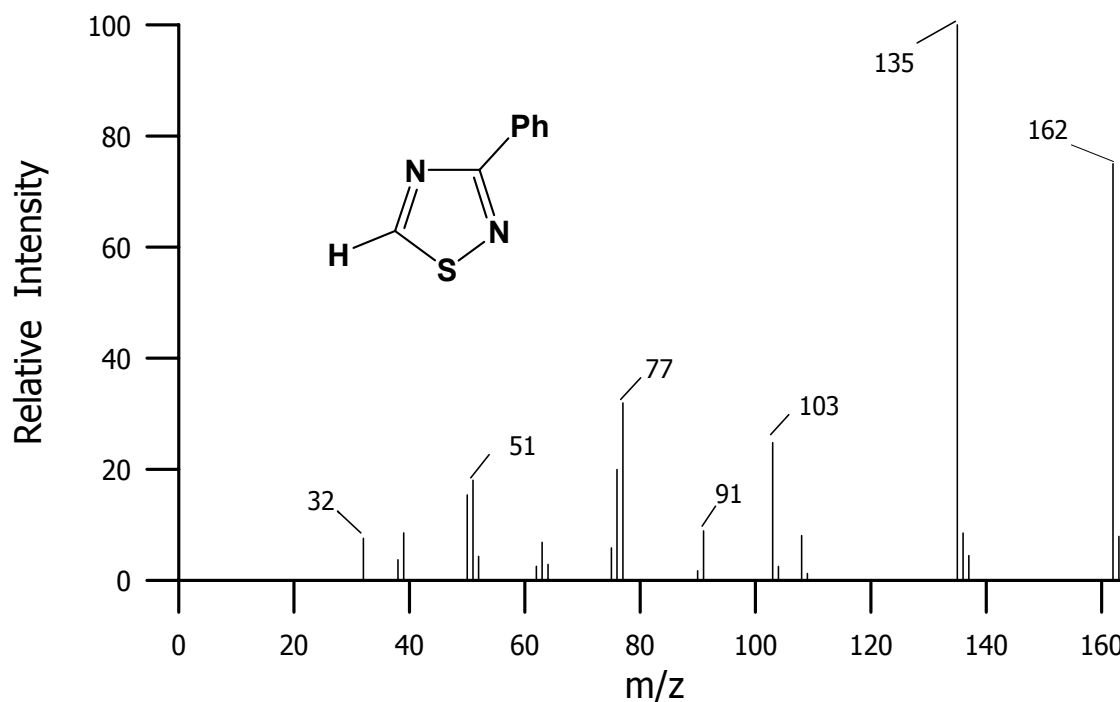


Figure 14e: Mass spectrum of the peak eluted with a retention time of 12.1 min; expected to be **46**

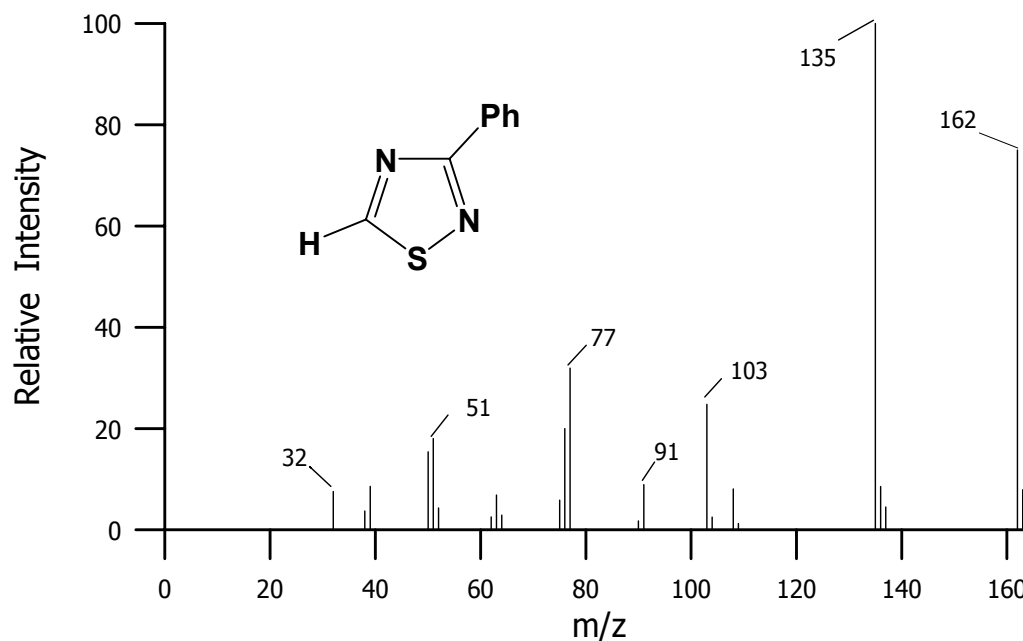


Figure 17: Mass spectrum of the synthesized **46**

The mass spectrum of the peak that eluted with a retention time of 23.3 min (Figure 14f) exhibits a base molecular ion at m/z 172 and two medium intensity peaks at m/z 103 and 104. Due to the presence of these two peaks, the structure of this product is suggested to contain a system similar to 5-phenyl-1,2,4-thiadiazole (**31**) which can cleave to give two fragments; $[C_6H_5CN]^+\bullet$ and $[C_6H_5CNH]^+$, as discussed previously. However, the absolute structure of this product has not been identified.

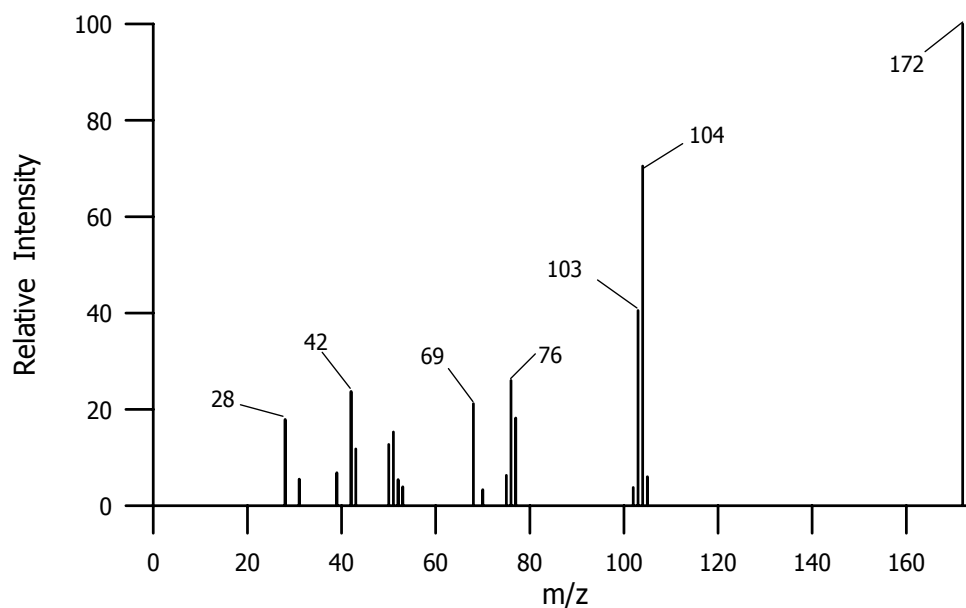


Figure 14f: Mass spectrum of the peak eluted with a retention time of 23.3min

The mass spectrum of the photoproduct that eluted with a retention time of 40 min (Figure 14g) exhibits a molecular ion at m/z 233, which is consistent with a molecular formula of $C_{15}H_{11}N_3$, and a base molecular peak at m/z 103, consistent with the formation of $[C_6H_5CN]^{\bullet+}$ as the major fragment. Based on this information the photoproduct was suggested to be 2,4-diphenyl-1,3,5-triazine (**40**), a ring expansion product. This was confirmed by direct comparison of the retention time and the mass spectrum of an authentic sample of **40**, shown in Figure 18a-b.

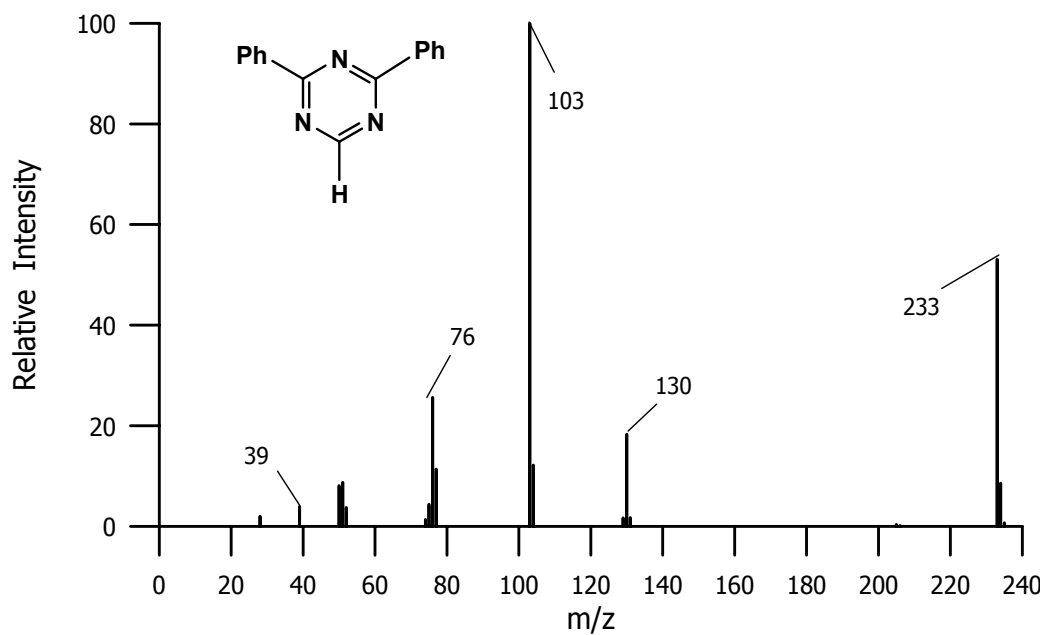


Figure 14g: Mass spectrum of the peak eluted with a retention time 40 min; expected to be 40

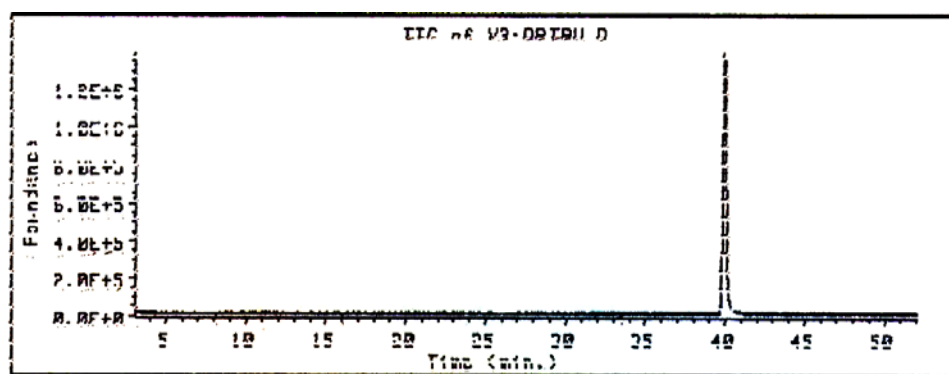


Figure 18a: GC-trace of an authentic sample of 40

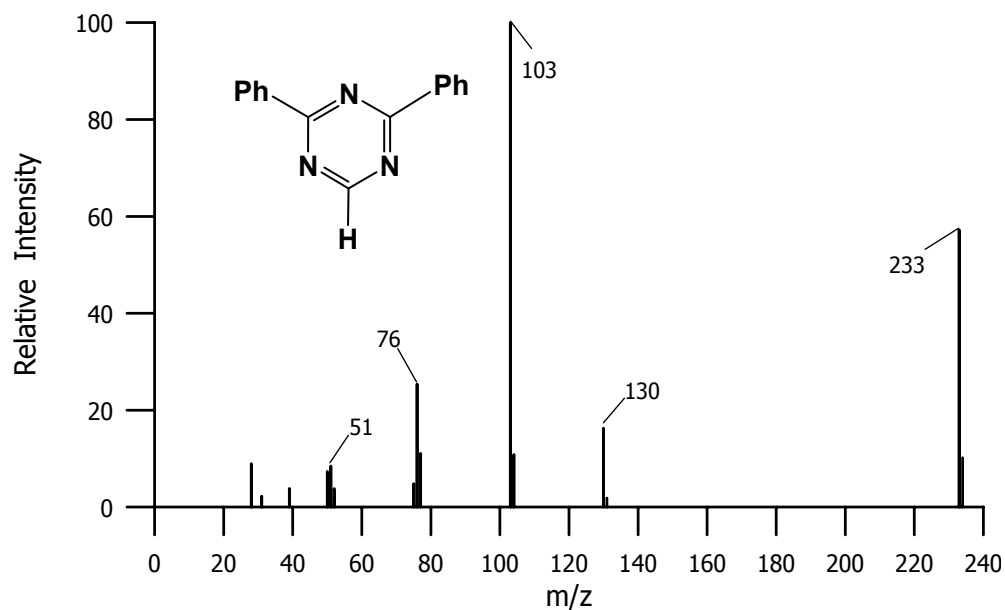


Figure 18b: Mass spectrum of an authentic sample of **40**

Beside the four major photoproducts shown in Figure 14a, the trace also shows three minor peaks which eluted with retention times of 40.6, 42.7 and 48.9 min. Their mass spectra, shown in Figure 14h, i, j, exhibit molecular ions at m/z 187, 238, 205, respectively. These peaks could be due to some impurities in the solvent. However, their mass spectra exhibit peaks at m/z 77, 103 and 104 which could be due to the cleavage of $[C_6H_5]^+$, $[C_6H_5CN]^{\bullet+}$ and $[C_6H_5CNH]^+$ fragments as previously discussed. Especially, the mass spectra of the peaks that eluted with retention times of 42.7 and 48.9 min also exhibit a peak at m/z 135 as a base peak. This peak has been previously assigned due to $[C_6H_5CNS]^{\bullet+}$ fragment. Therefore, these three minor peaks can also be expected as photoproducts formed upon irradiation of 5-phenyl-1,2,4-thiadiazole (**31**) (in acetonitrile).

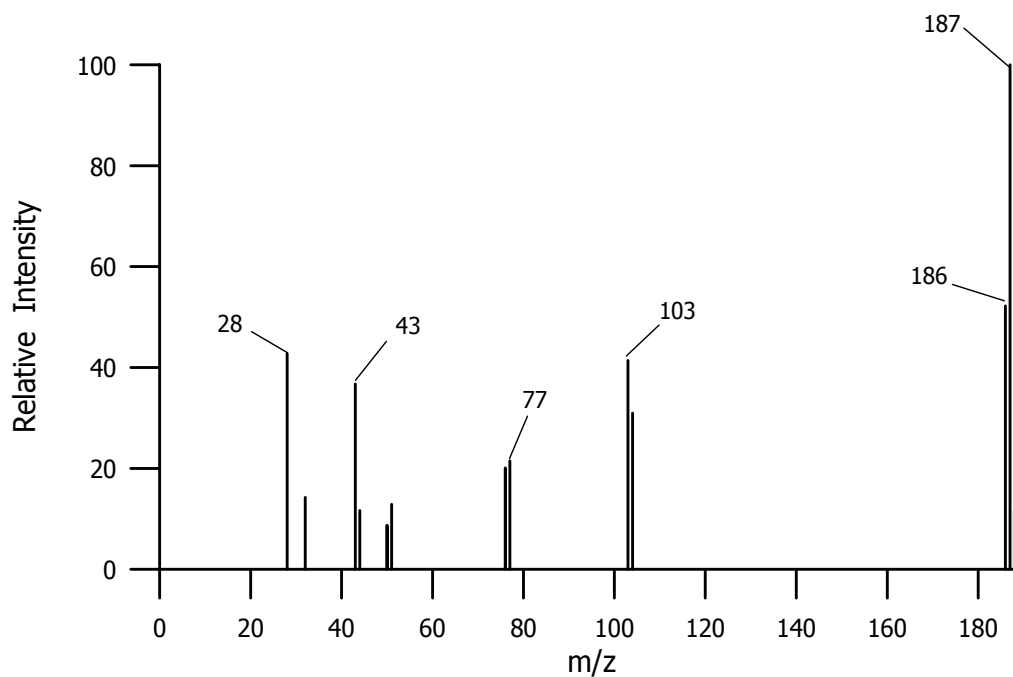


Figure 14h: Mass spectrum of the peak eluted with a retention time of 40.6 min

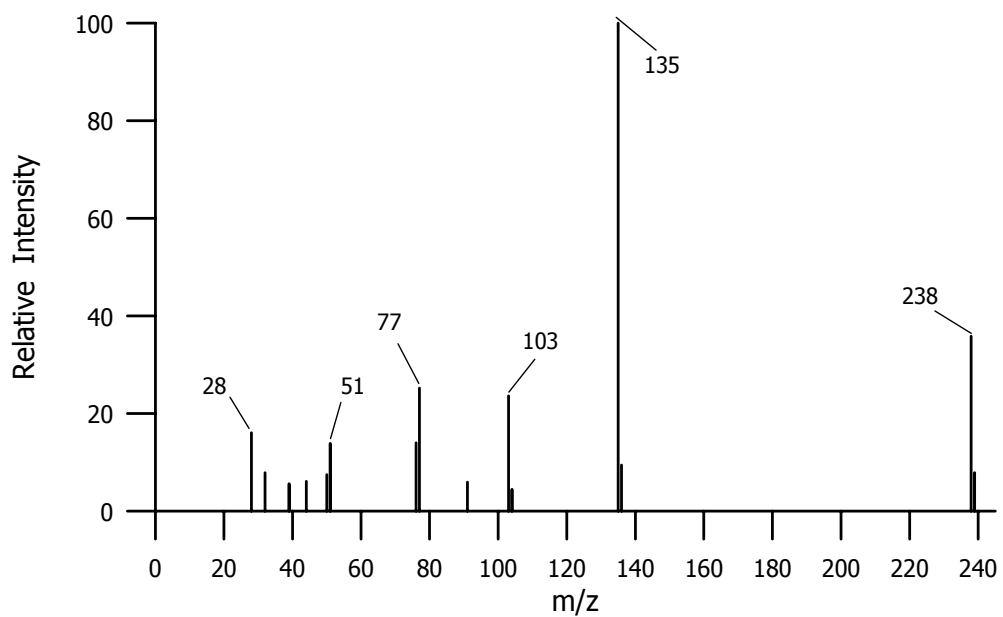


Figure 14i: Mass spectrum of the peak at a retention time of 42.7 min

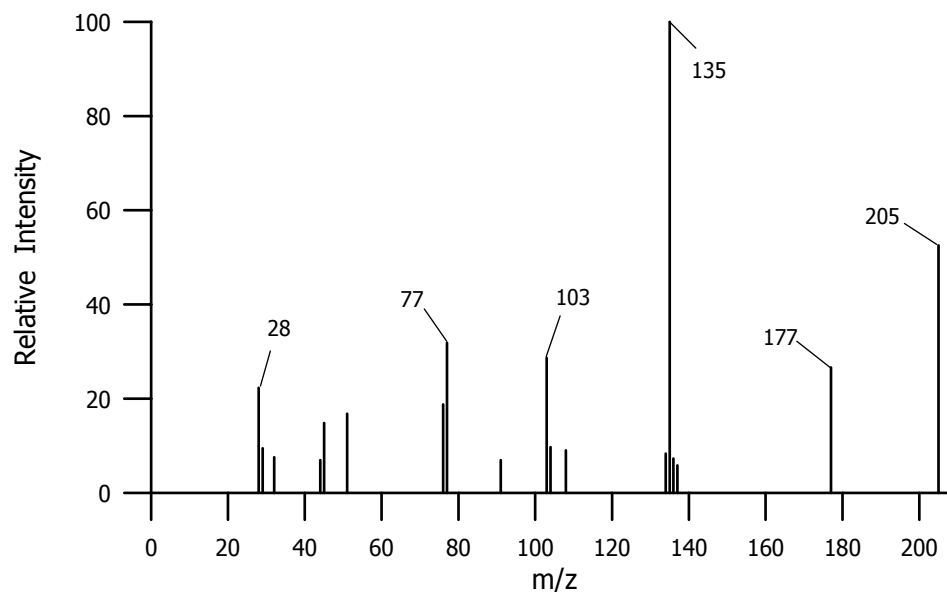


Figure 14j: Mass spectrum of the peak eluted with a retention time of 48.9 min

The mass spectrum of the peak eluted with a retention time of 42.7 min (Figure 4i) exhibits a molecular ion at m/z 238 which corresponds to the molecular weight of diphenyl-1,2,4-thiadiazole (**47**; MW 238). By direct comparison between the GC-retention time and fragmentation pattern of this product and the GC-retention time and fragmentation pattern of an authentic sample of **47** (shown in Figure 19a-b), this photoproduct was identified as diphenyl-1,2,4-thiadiazole (**47**).

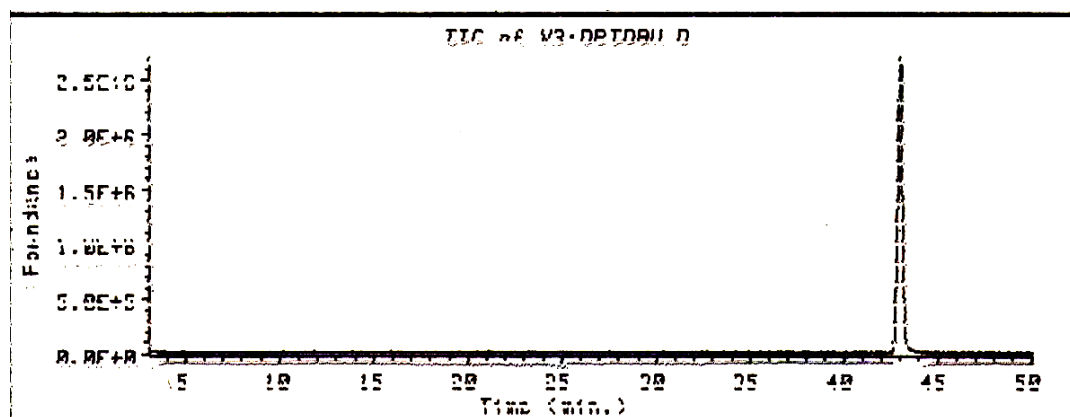


Figure 19a: GC-trace of an authentic sample of 47

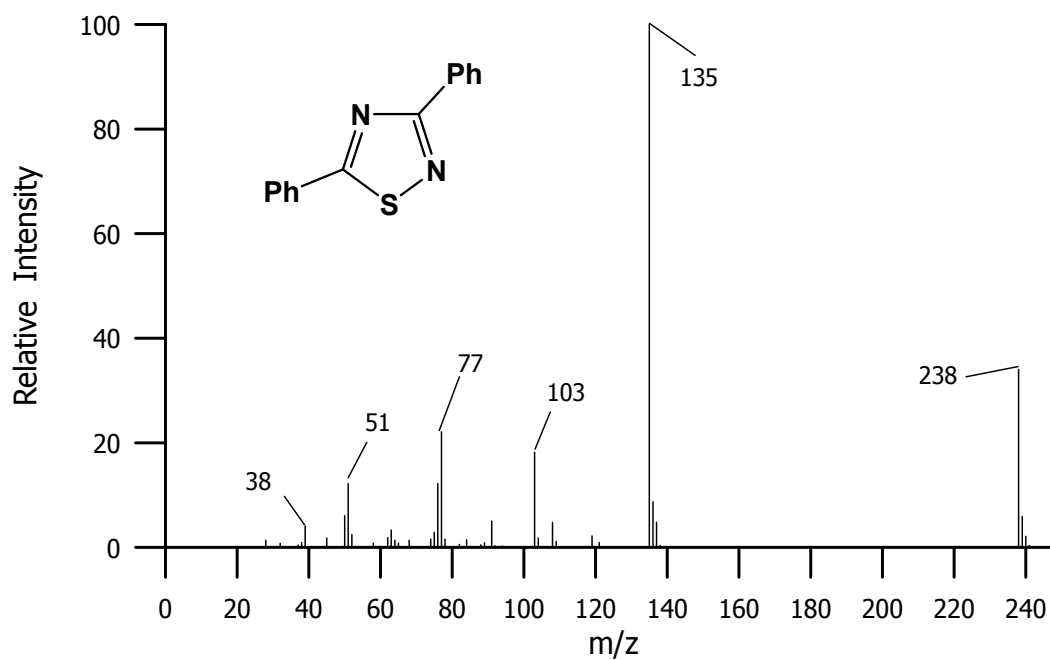
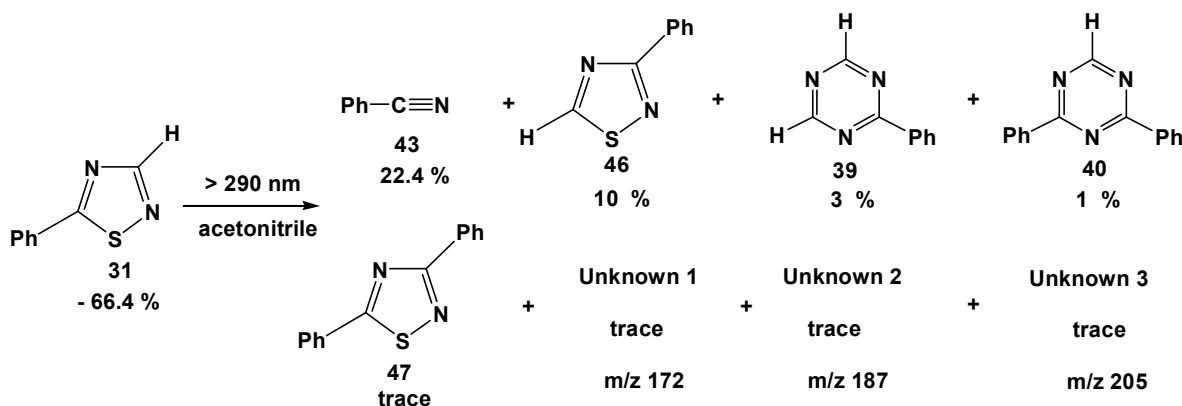


Figure 19b: Mass spectrum of an authentic sample of 47

These results conclusively show that irradiation of 5-phenyl-1,2,4-thiadiazole (**31**) in acetonitrile solvent at > 290 nm leads to the formation of eight gc-volatile products. Five of these products have been identified as benzonitrile (**43**; photofragmentation product), 2-phenyl- and 2,4-diphenyl-1,3,5-triazine [(**39**) and (**40**); photo ring expansion products], 3-phenyl-1,2,4-thiadiazole (**46**; phototransposition product) and diphenyl-1,2,4-thiadiazole (**47**). The three minor photoproducts have not been identified.

In order to determine the chemical yield of these photoproducts, a solution (4 mL, 2×10^{-2} M) of **31** in acetonitrile was irradiated with sixteen > 290 nm lamps and monitored by gas-liquid chromatography every 30 min for a total of 150 min. The GC- calibration curves for the four identified photoproducts were constructed by plotting concentration V_s peak area. Scheme 12 shows the photoreaction of 5-phenyl-1,2,4-thiadiazole (**31**).



Scheme 12: Photoreaction of 5-phenyl-1,2,4-thiadiazole

3-Phenyl-1,2,4-thiadiazole (**46**), the phototransposition product was found to be formed in 10% yield. Benzonitrile (**43**), the photofragmentation product, was formed in 22.4% yield. The two unique ring expansion photoproducts, 2-phenyl- and 2,4-diphenyl-1,3,5-triazine (**39**) and (**40**), were formed in 3% and 1% yield, respectively. The GC-trace obtained from the GC-HP588 interfaced with a mass spectrometer of the concentrated reaction solution revealed the presence of trace amount of three unidentified photoproducts which were not observed in the GC-analysis on GC-PE9000 of the reaction mixture before concentration.

2.2 Photochemistry of 3-phenyl-1,2,4-thiadiazole

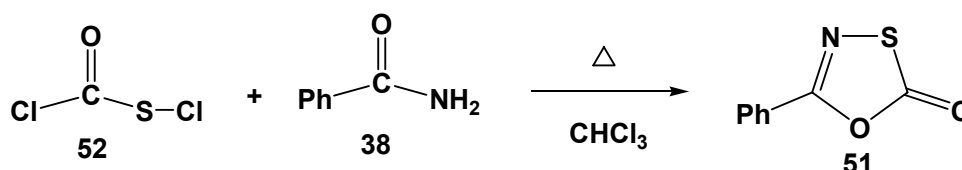
2.2.1 Synthesis of 3-phenyl-1,2,4-thiadiazole

The 1,2,4-thiadiazoles can be prepared from a 1,3-dipolar cycloaddition reaction of a nitrile sulfide with a nitrile as described by Howe and Franz.¹²

In the case of 3-phenyl-1,2,4-thiadiazole (**46**), a cycloaddition of benzonitrile sulfide (**48**) with ethyl cyanofornate (**49**) led to the formation of ethyl 3-phenyl-1,2,4-thiadiazole-5-carboxylate (**50**). Base catalyzed ester hydrolysis of **50** followed by decarboxylation of the resulting carboxylic acid produced **46** in 72% as a white solid.

2.2.1.1 Synthesis of 5-phenyl-1,3,4-oxathiazole-2-one

According to the method described by Howe and Franz¹², **46** could be synthesized by cycloaddition of benzonitrile sulfide (**48**), which can be in situ generated by decarboxylation of 5-phenyl-1,3,4-oxathiazole-2-one (**51**). 5-Phenyl-1,3,4-oxathiazole-2-one (**51**) was prepared by a coupling between chlorocarbonyl chloride (**52**) and benzamide (**38**) in refluxing chloroform under anhydrous condition, described by Howe and Franz,¹² to yield the desired oxathiazole in 95.5% yield as white crystals. Scheme 14 shows the synthesis of **51**.



Scheme 14: Synthesis of 5-phenyl-1,3,4-oxathiazole-2-one

The GC analysis of the white crystals (Figure 20) exhibited two components eluted with a retention time of 4.1 min and 17.2 min. The mass spectrum of the major peak at retention time 17.2 min (Figure 20b) exhibits a molecular ion at m/z 179 which is consistent with the molecular formula of $C_8H_5NO_2S$ and a base peak at m/z 105 which is also consistent with $[C_6H_5CNS]^+$ fragment which is due to the loss of CO_2 .

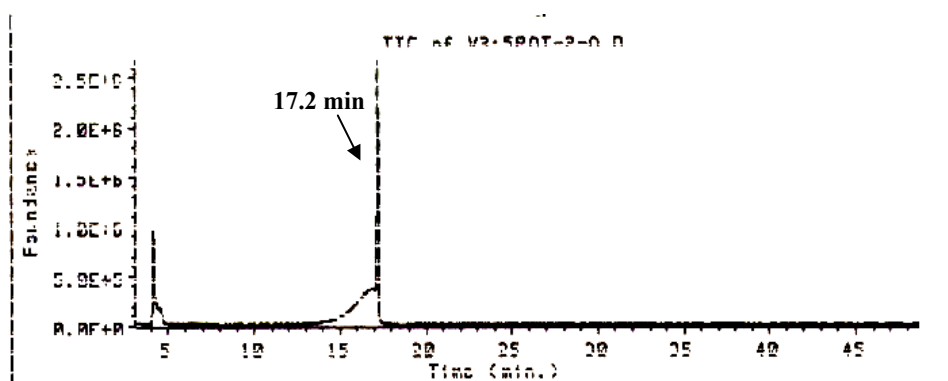


Figure 20a: GC-trace of the white crystals

The $^1\text{H-NMR}$ spectrum of this compound (Figure 21) exhibits two multiplets: δ 7.45-7.54 (2H), which is assigned to the ortho phenyl-ring protons, and δ 7.93-7.95 (3H), which is assigned to the meta-para phenyl-ring protons.

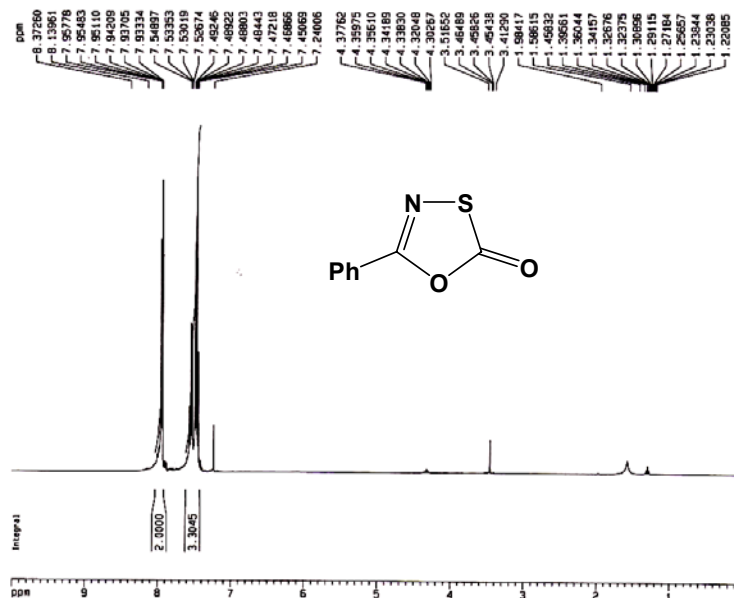


Figure 21: $^1\text{H-NMR}$ spectrum of the white crystals

The $^{13}\text{C-NMR}$ spectrum (Figure 22a) exhibits the carbon signals corresponding to the structure of 5-phenyl-1,3,4-oxathiazole-2-one (**51**). The carbonyl carbon on the oxathiazole ring absorbs downfield at δ 174.3. The carbon at position 5 of the oxathiazole ring appears at δ 157.8. The phenyl ring carbons appear as four singlets at δ 126.2, 127.8, 129.4 and 133.1. These assignments are consistent with the $^{13}\text{C-DEPT}$ 135 spectrum (Figure 22b). The two signals at δ 157.8 and 174.3 disappeared in the $^{13}\text{C-DEPT}$ 135 spectrum, which were consistent with the assignment of the two signals to the two quaternary carbons on the oxathiazole ring.

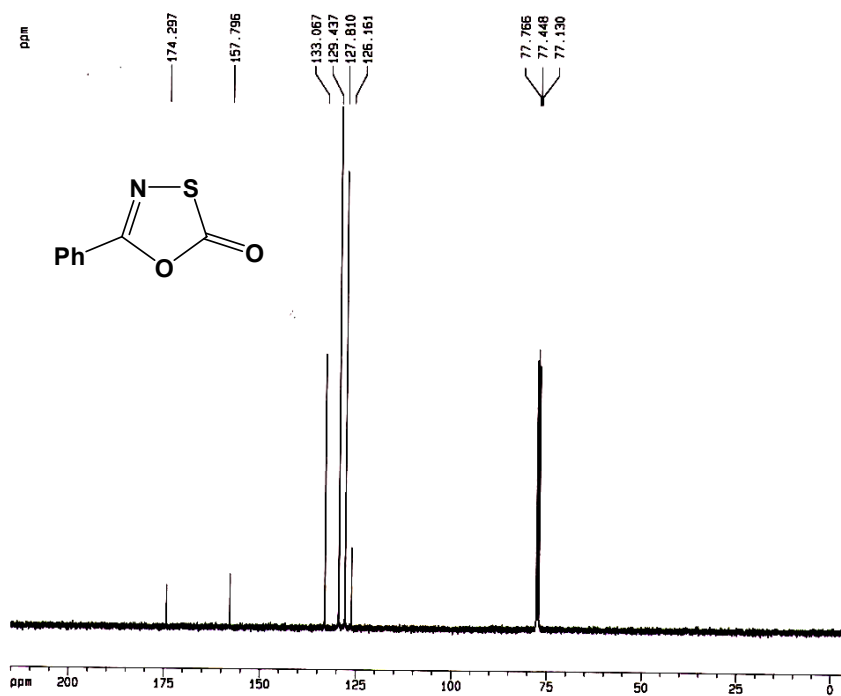


Figure 22a: ^{13}C -NMR spectrum of the white crystals

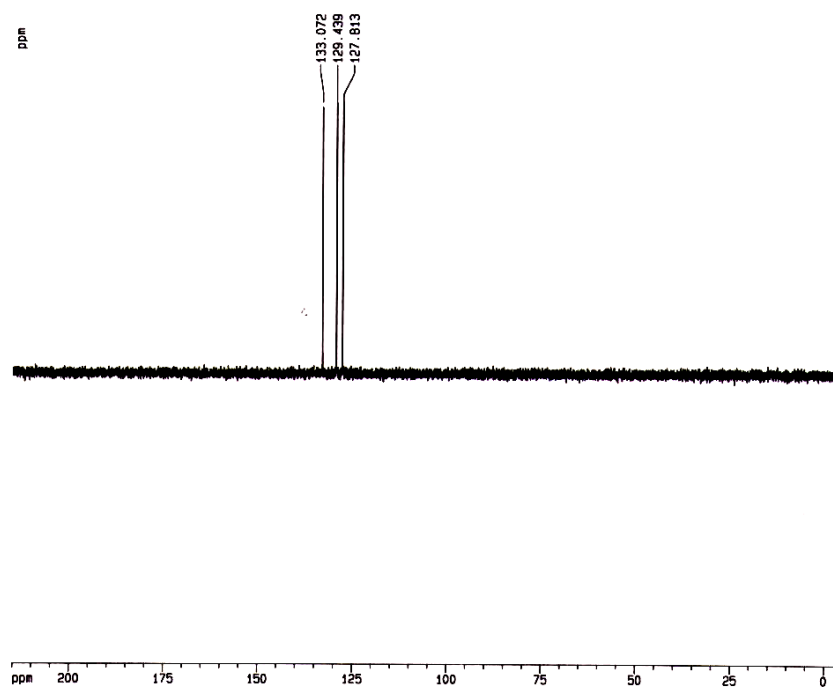
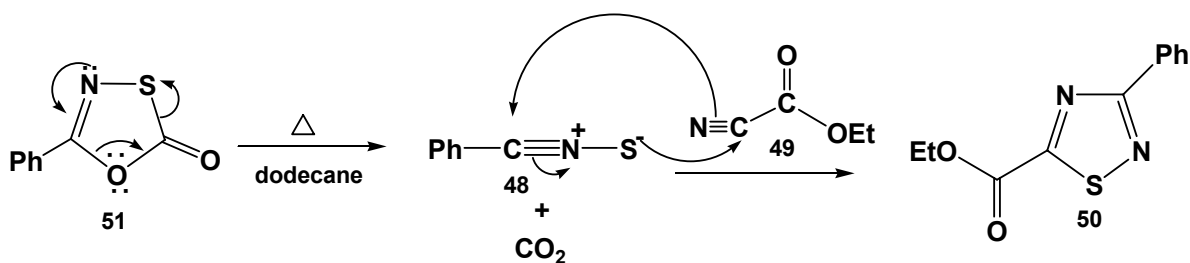


Figure 22b: ^{13}C -DEPT 135 spectrum of the white crystals

2.2.1.2 Synthesis of ethyl 3-phenyl-1,2,4-thiadiazole-5-carboxylate

Decarboxylation of **51** has been reported to result in in situ generation of benzonitrile sulfide (**48**). Thus, ethyl 3-phenyl-1,2,4-thiadiazole-5-carboxylate (**50**) was prepared in 80% as light brown crystals by trapping of **48**, formed upon decarboxylation of **51**, with ethyl cyanoformate (**49**) as shown in Scheme 15.



Scheme 15: Synthesis of ethyl 3-phenyl-1,2,4-thiadiazole-5-carboxylate

The GC-trace [isothermal 220°C (30 min)] of the cycloaddition product shows only one gc-volatile component, which eluted with a retention time of 12.4 min (shown in Figure 23a). The mass spectrum (Figure 23b) of this compound exhibits a molecular ion at m/z 234 which corresponds to the molecular weight of ethyl 3-phenyl-1,2,4-thiadiazole-5-carboxylate (**50**) (MW 234). The spectrum also shows a base peak at m/z 135 due to the $[\text{C}_6\text{H}_5\text{CNS}]^{*+}$ fragment.

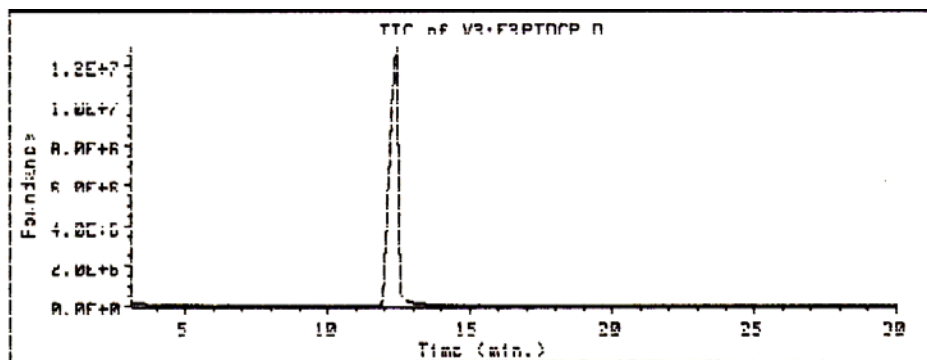


Figure 23a: GC-trace of the synthesized **15**

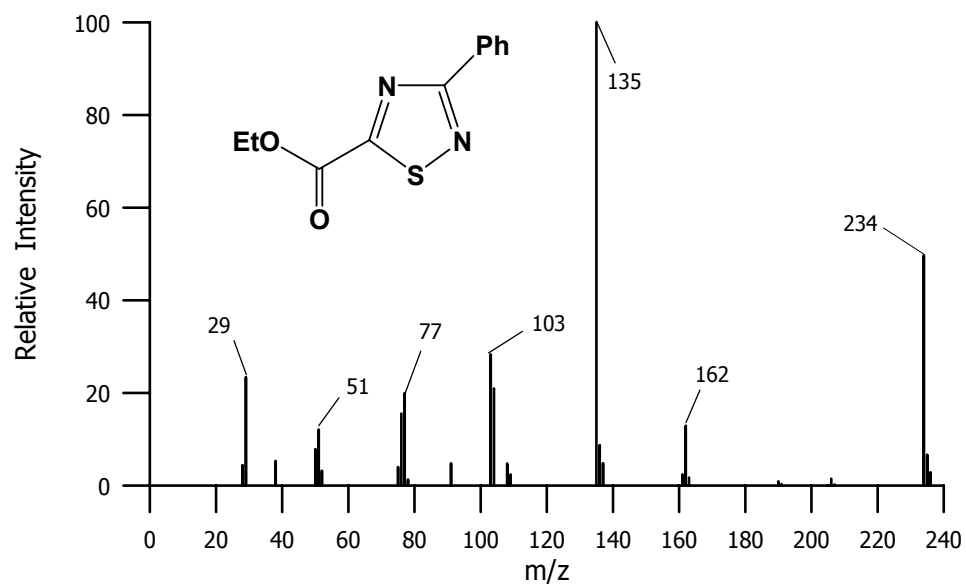


Figure 23b: Mass spectrum of the peak at retention time 12.4 min

The $^1\text{H-NMR}$ spectrum of this synthesized **15** (Figure 24) exhibits the phenyl ring protons as two multiplets at δ 7.43-7.44 (3H) and δ 8.28-8.29 (2H) due to the meta-para and ortho ring protons, respectively. The ethyl ester protons are shown at δ 4.51 as a quartet (2H; $J = 7.07$ Hz) and at δ 1.41 as a triplet (3H; $J = 7.07$ Hz).

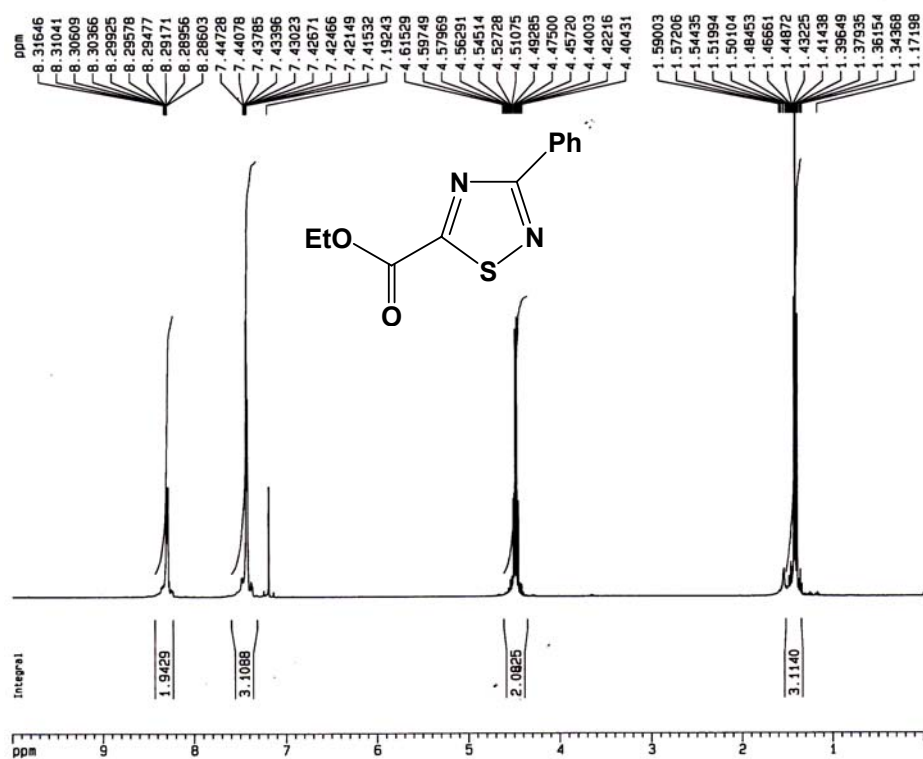


Figure 24: ^1H -NMR spectrum of the synthesized **15**

The ^{13}C -NMR spectrum (shown in Figure 25a) exhibits the two carbons of the ethyl ester group at δ 14.6 (CH_3 -) and 63.8 ($-\text{CH}_2$ -). The ring phenyl carbons appear as four singlets at δ 128.9, 129.2, 131.3 and 132.4. The signal at δ 179.4 is assigned to the ester carbonyl carbon. The two carbons of the thiadiazole ring appear at δ 158.9 for the carbon at position 3 and at δ 175.1 for the carbon at ring position 5. These assignments can be supported by the ^{13}C -DEPT 135 spectrum, shown in Figure 25b. The signals at δ 14.6 and 63.8 absorb in positive and negative directions in the ^{13}C -DEPT 135 spectrum, respectively, which is consistent with their assignments as methyl and methylene carbons, respectively. Three signals at δ 158.9, 175.1 and 179.4 disappeared in the ^{13}C -DEPT 135 spectrum confirming that they are all quaternary carbons.

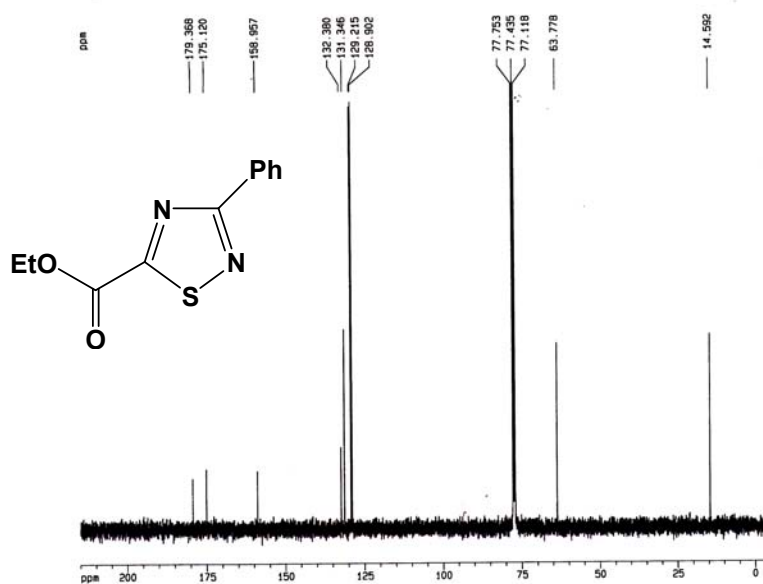


Figure 25a: ^{13}C – NMR spectrum of the synthesized **50**

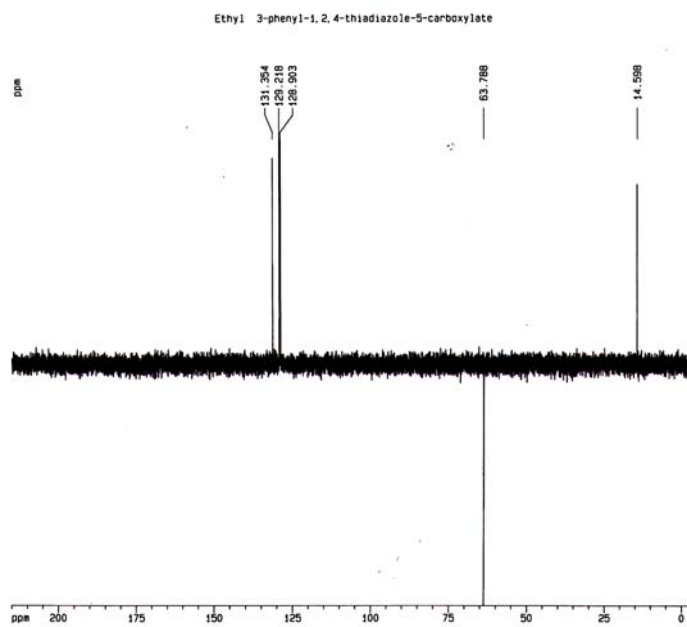
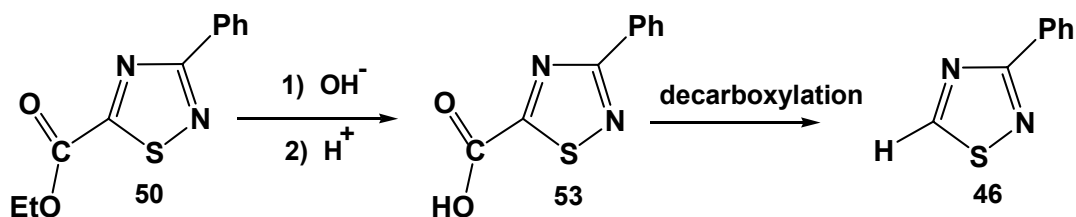


Figure 25b: ^{13}C – DEPT 135 spectrum of the synthesized **50**

2.2.1.3 Synthesis of 3-phenyl-1,2,4-thiadiazole

Base catalyzed ester hydrolysis of **50** led to the formation of 3-phenyl-1,2,4-thiadiazole-5-carboxylic acid (**53**). Decarboxylation of **53** produced 3-phenyl-1,2,4-thiadiazole (**46**) as a white solid in 72% yield as shown in Scheme 16.



Scheme 16: Synthesis of 3-phenyl-1,2,4-thiadiazole

The GC-trace [150°C (5 min), 30°C/min to 180°C (17 min)], as shown in Figure 26a, shows that only one component eluted with a retention time of 13.2 min. The mass spectrum (Figure 26b) of this product exhibits a molecular ion at m/z 162 and the base peak at m/z 135, which corresponds to both its molecular weight (MW 162) and to the possible fragment $[\text{C}_6\text{H}_5\text{CNS}]^{*+}$ as the base peak. The mass spectrum also corresponds with the reported molecular ion of this compound.¹²

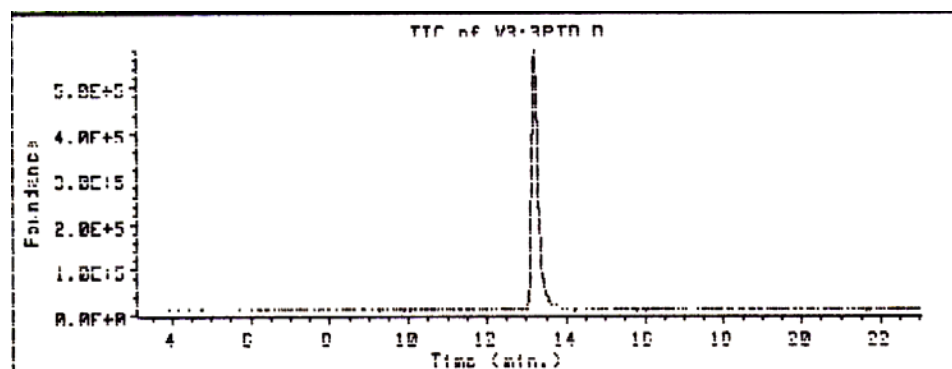


Figure 26a: GC-trace of the synthesized **46**

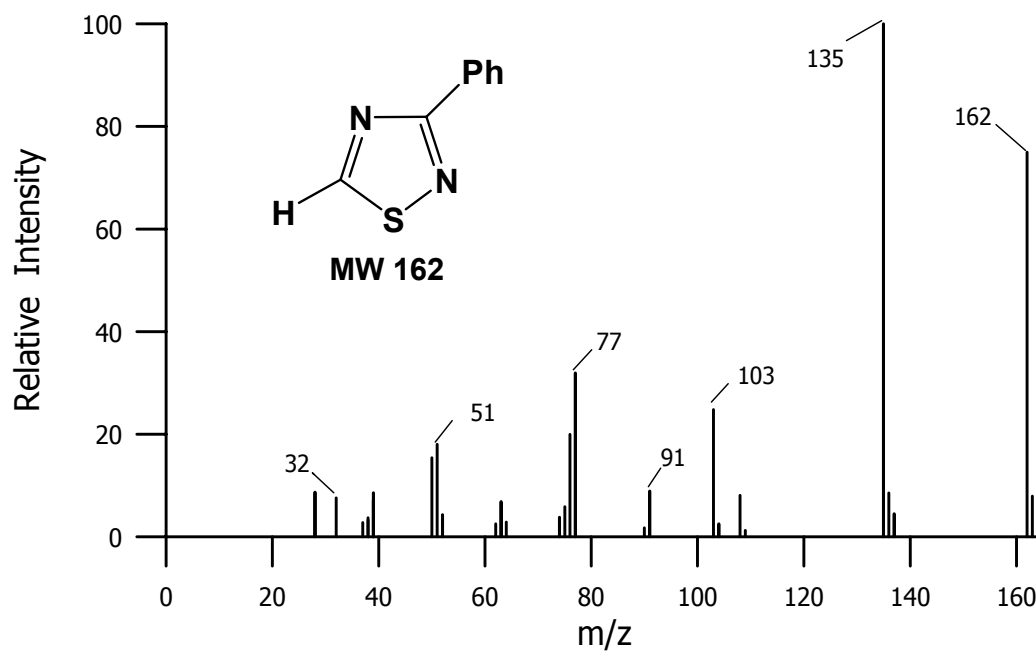


Figure 26b: Mass spectrum of the peak at retention time of 13.2 min

The ^1H -NMR spectrum, as shown in Figure 27, exhibits a very clear spectrum. The proton of the thiazole ring at position 5 absorbs downfield at δ 10.27 as a singlet (1H). The phenyl ring protons appear as two multiplets at δ 7.49-7.55 (3H) assigned to the meta- and para-ring protons and δ 8.33-8.36 (2H) assigned to the ortho-ring protons.

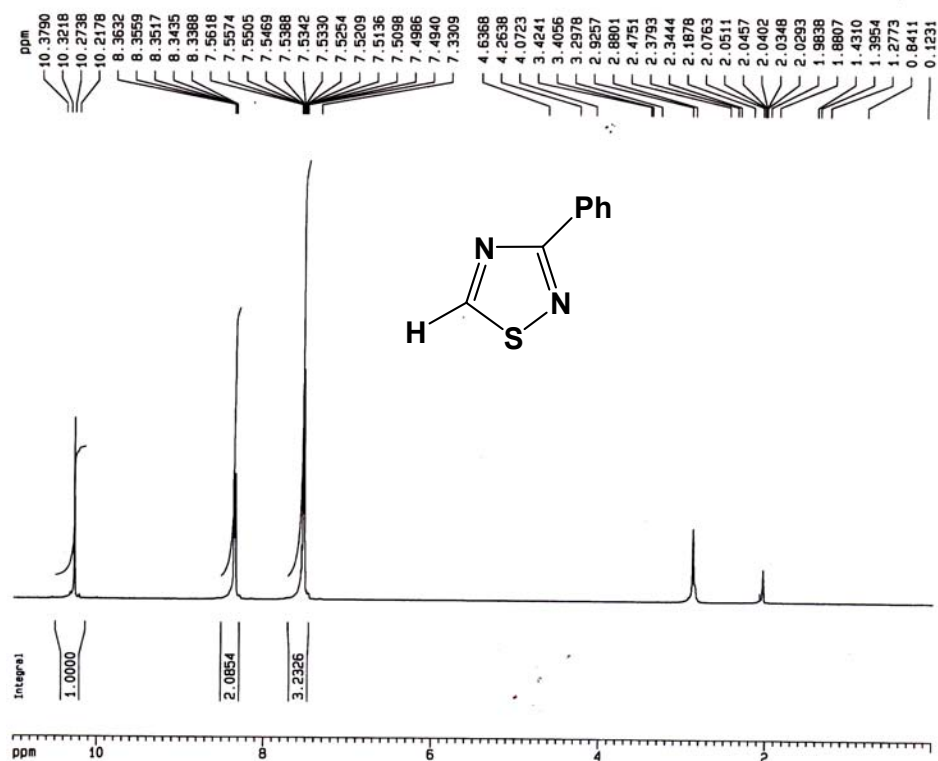


Figure 27: $^1\text{H-NMR}$ spectrum of the synthesized **46**

The $^{13}\text{C-NMR}$ spectrum, as shown in Figure 28a, shows that the two carbons of the thiadiazole ring absorb at δ 174.9 and 175.0. The former signal was assigned to the carbon at ring position 3, while the latter signal was assigned to the carbon at ring position 5. These assignments are consistent with the $^{13}\text{C-DEPT}$ 135 spectrum (Figure 28b), which confirms that the signal at δ 174.9 is due to a quaternary carbon. The signal at δ 175.0 still appears in the $^{13}\text{C-DEPT}$ 135 spectrum and that must be due to the carbon at ring position 5 of the thiadiazole ring.

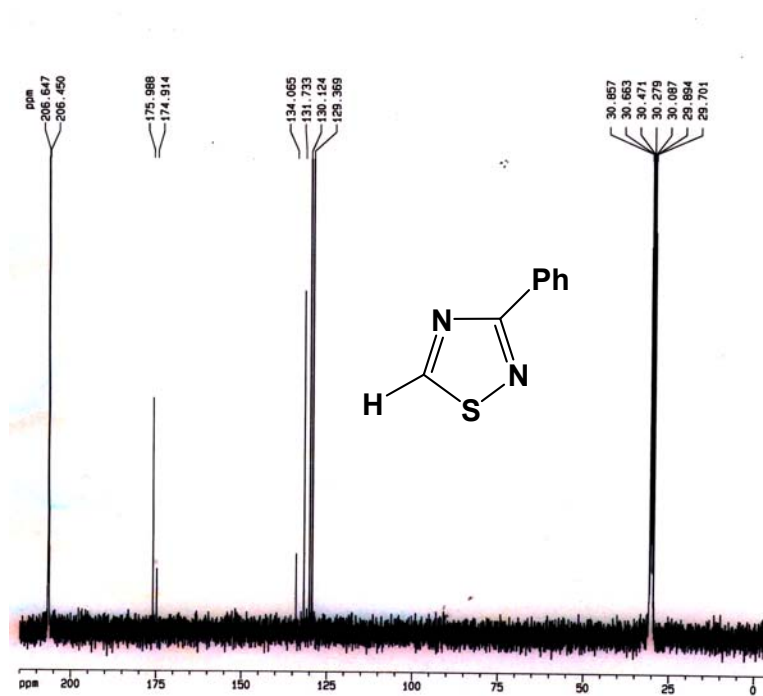


Figure 28a: ^{13}C -NMR spectrum of the synthesized 46

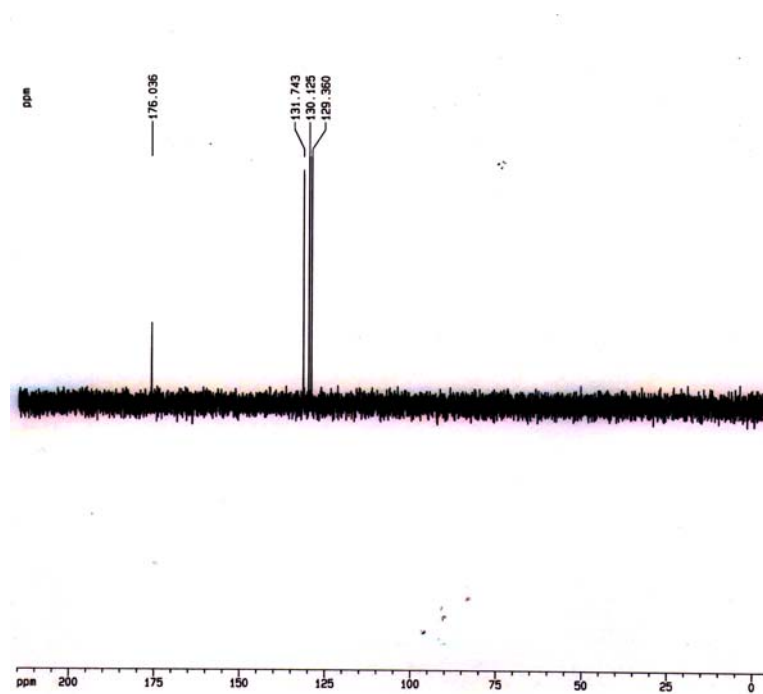
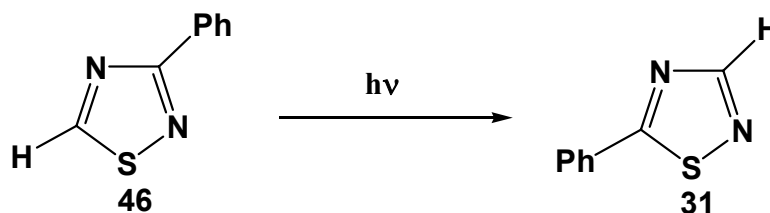


Figure 28b: ^{13}C -DEPT 135 spectrum of the synthesized 46

2.2.2 Photochemistry of 3-phenyl-1,2,4-thiadiazole

This study has shown that 5-phenyl-1,2,4-thiadiazole (**31**) undergoes phototransposition to 3-phenyl-1,2,4-thiadiazole (**46**) in 10 % yield and to the formation of other photofragmentation and photo ring-expansion products. In order to determine the effect of changing the position of the phenyl substituent from position 5 to 3, the photochemistry of **46** has also been studied.



The photolysis of **46** was first monitored by ultraviolet-absorption spectroscopy. A solution of **46** (5.0×10^{-5} M) in cyclohexane was placed in a quartz cell and irradiated with three > 290 nm lamps through a Pyrex filter. The solution was monitored by ultraviolet absorption spectroscopy at 40 sec intervals.

Figure 29a shows the UV-absorption spectrum of **46** in cyclohexane before irradiation. The UV overlay spectrum (Figure 29b) shows the continuous consumption of the reactant, as indicated by the decrease in the optical density of the absorption band at λ 263.60 nm from 0.51 to 0.34 after 280 sec of irradiation and also shows an increase in the optical density at λ_{\max} 229.8 nm. This new absorption maximum suggests the formation of benzonitrile (**43**) in this reaction since **43** is known to absorb at λ_{\max} 224 nm in acetonitrile.

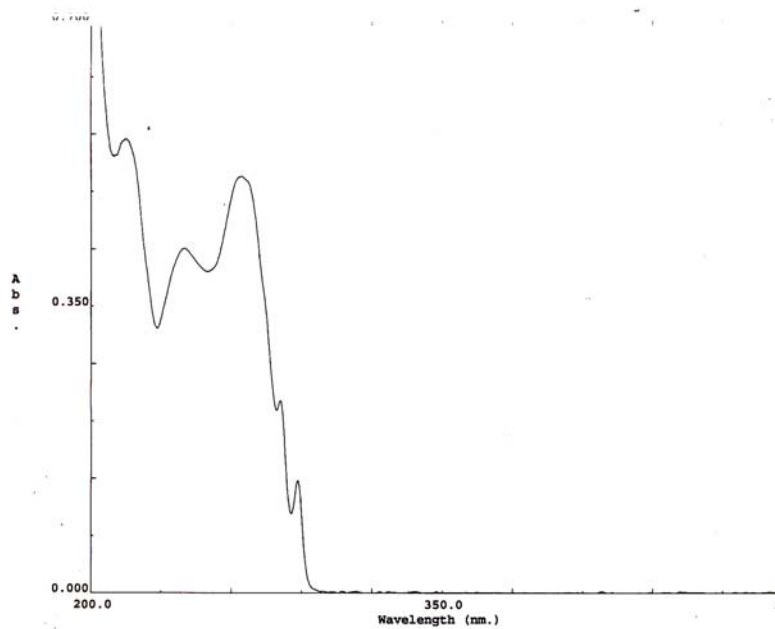


Figure 29a: UV-absorption spectrum of **46** in cyclohexane

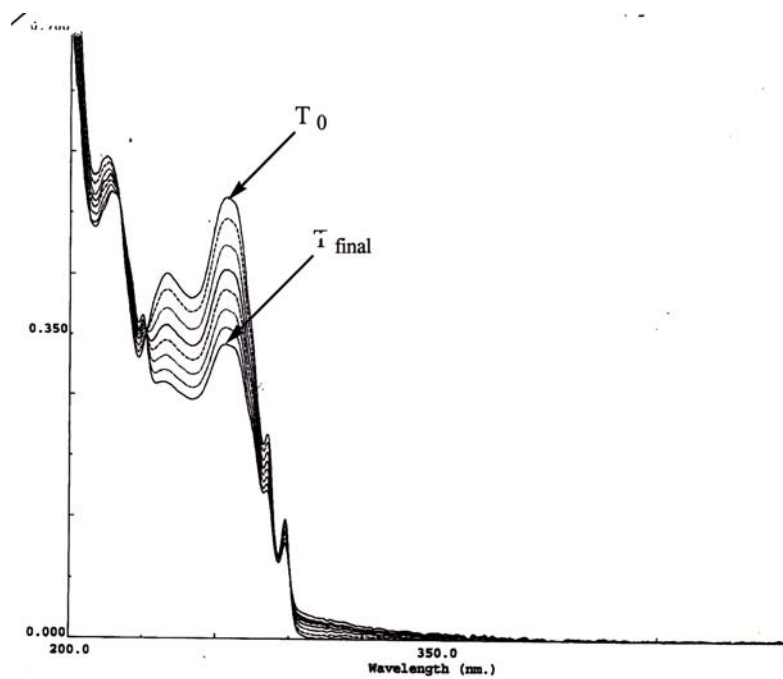


Figure 29b: UV overlay spectrum of the photolysis of **46**

The photoreaction of **46** was also monitored by gas-liquid chromatography. A solution of **46** (2.0×10^{-2} M) in acetonitrile was placed in a Pyrex tube, sealed with a rubber septum and purged with argon gas for 15 min. GLC analysis [140°C (4 min), 15 min/°C to 180°C (14 min)] of this solution (Figure 30a) indicated the presence of only one component in the sample, which eluted with a retention time of 18 min. The solution was irradiated with sixteen > 290 nm lamps and monitored by gas-liquid chromatography every 15 min. Figure 30b shows the GC-chromatogram of the reaction after 120 min of irradiation. The chromatogram exhibits two volatile components in this sample. One component which eluted with a retention time of 18 min, is the reactant **46**. The second component, which eluted with a retention time of 4 min is the only photoproduct observed upon irradiation of **46**. The GLC analysis was carried out at a higher oven temperature but no sign of any other photoproduct was observed.

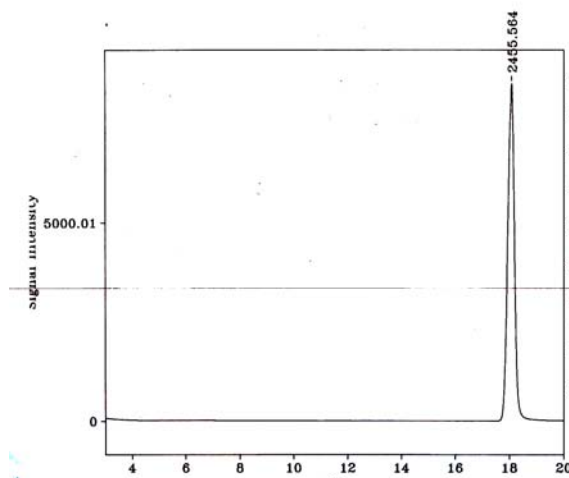


Figure 30a: GLC analysis of **46** in acetonitrile before irradiation

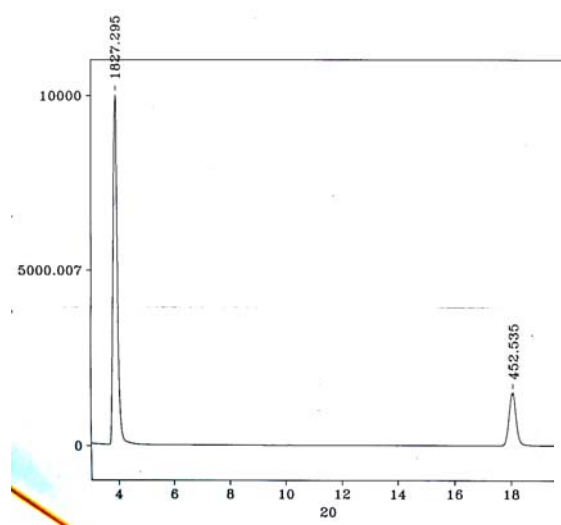


Figure 30b: GLC analysis of **46** in acetonitrile after 120 min of irradiation

The reaction solution after 120 min of irradiation was concentrated by rotary evaporation at room temperature and analyzed by the GC interfaced with a mass spectrometer. The GC trace (Figure 31a) again exhibits two components in the sample. The mass spectrum of the compound, which eluted with a retention time of 17.7 min (Figure 31b), reveals a molecular ion at m/z 162 and a fragmentation pattern identical to the mass spectrum of the reactant, **46**. Therefore, this peak is due to the reactant **46**. The mass

spectrum of the peak, which eluted with a retention time of 7.5 min (Figure 31c), reveals a molecular ion at m/z 103.

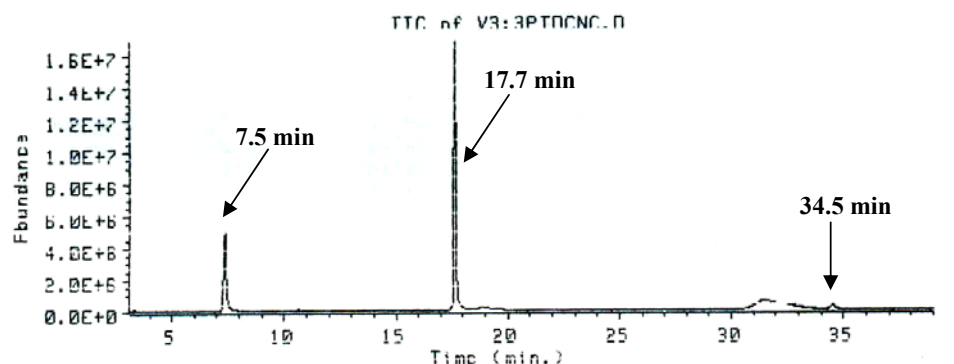


Figure 31a: GC-trace of the concentrated photolysate of **46** after 120 min of irradiation

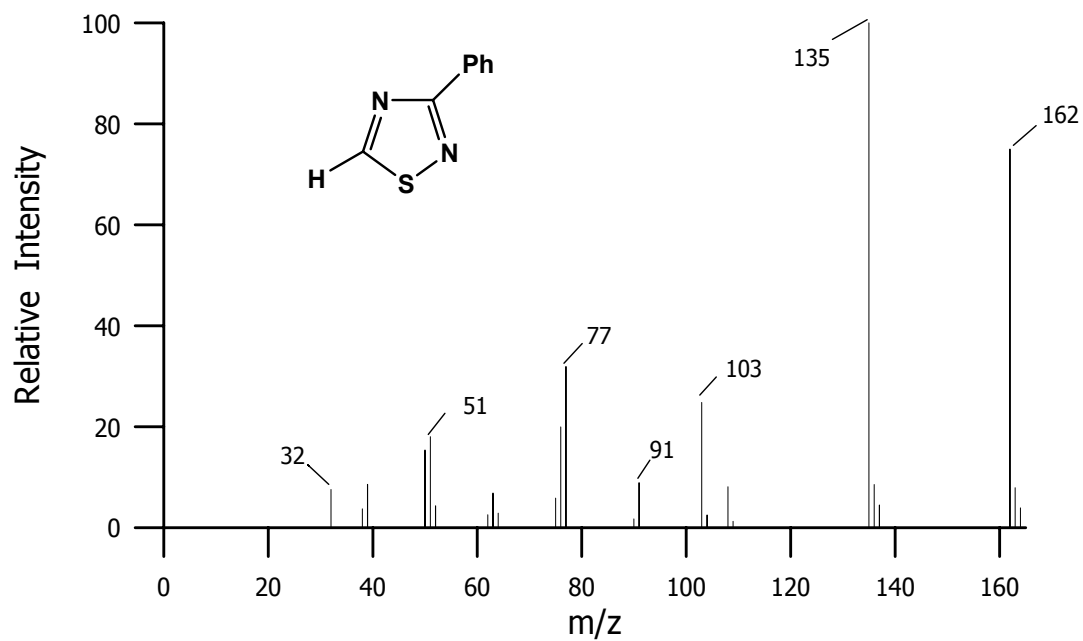


Figure 31b: Mass spectrum of the peak at a retention time of 14.3 min, the reactant **46**

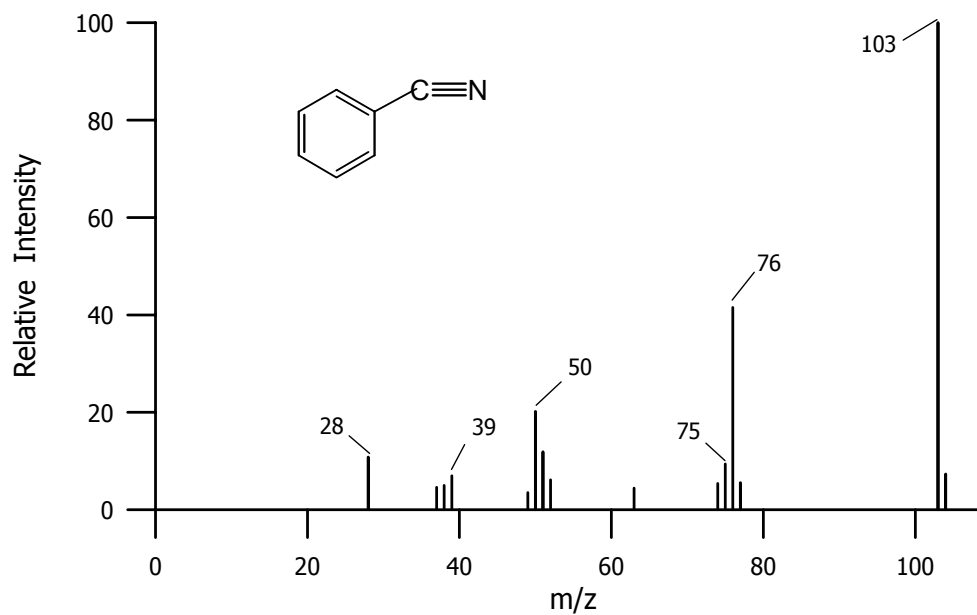


Figure 31c: Mass spectrum of the peak at a retention time of 4.1 min

By direct comparison of the mass spectrum and GC-trace of this peak with the mass spectrum and GC-trace of an authentic sample of benzonitrile (**43**), it was determined that both fragmentation patterns and retention times are identical. This shows that the only photoproduct observed upon irradiation of 3-phenyl-1,2,4-thiadiazole (**46**) is benzonitrile (**43**). This result also indicates that 5-phenyl-1,2,4-thiadiazole (**31**) is not formed as a phototransposition product as expected.

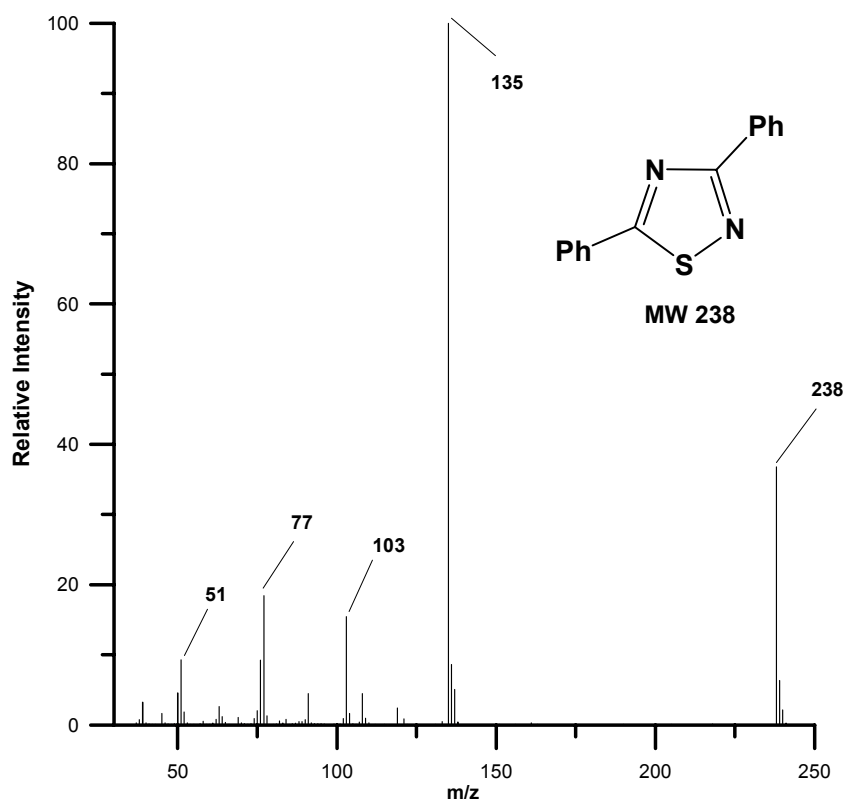
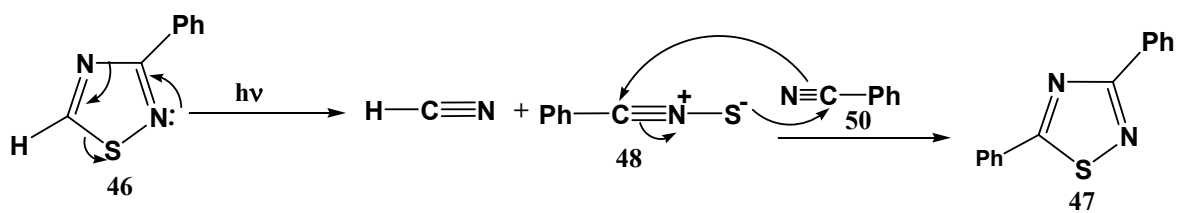


Figure 31d: Mass spectrum of the component at retention time of 34.5 min

Unlike the GLC analysis of the solution before concentration, Figure 31 also reveals trace quantity of a gc-volatile material which eluted at high oven temperature with a retention time of 34.5 min. The mass spectrum of this component (Figure 31d) exhibits a molecular ion at m/z 238 and a base peak at m/z 135. Comparison of its mass spectrometric and chromatographic properties with those of the available authentic samples of phenyl-1,2,4-thiadiazoles indicates that this trace quantity product is diphenyl-1,2,4-thiadiazole (**47**). The observed formation of **47** upon irradiation of **46** in acetonitrile was proposed to arise from a 1,3-dipolar cycloaddition of benzonitrile sulfide (**48**) with benzonitrile (**43**), the observed major product in this photoreaction.



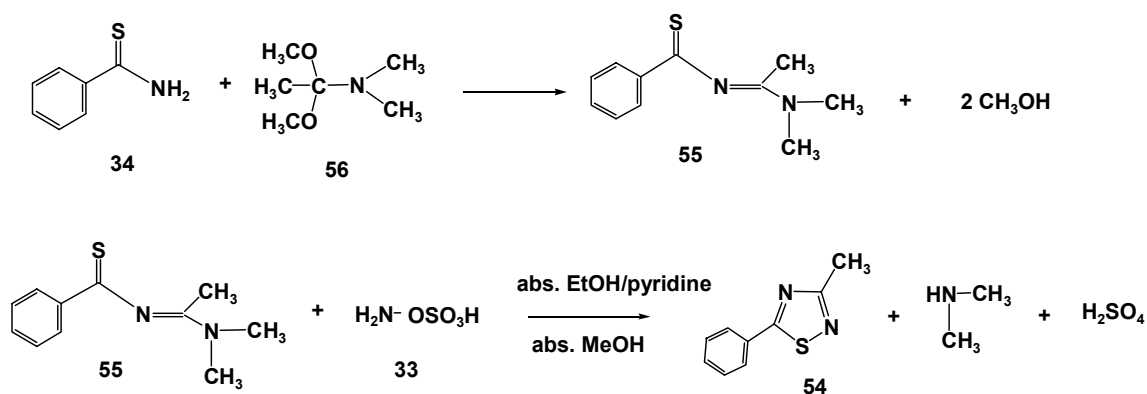
The percent yield of **43** was determined by using the same benzonitrile calibration curve previously constructed. After 120 min of irradiation, the trace showed 81.6% consumption of the reactant **46** and the formation of benzonitrile (**43**) in 74.1% yield.

2.3 Photochemistry of 3-methyl-5-phenyl-1,2,4-thiadiazole

2.3.1 Synthesis of 3-methyl-5-phenyl-1,2,4-thiadiazole

5-Phenyl-1,2,4-thiadiazole (**31**) can be synthesized by the amination cyclization of N-[(dimethylamino)methylene]thiobenzamide (**32**) with hydroxylamine-O-sulfonic acid (**33**). This synthesis not only allows the synthesis of 5-monosubstituted-1,2,4-thiadiazole but it also allows the synthesis of 3,5-disubstituted-1,2,4-thiadiazoles.

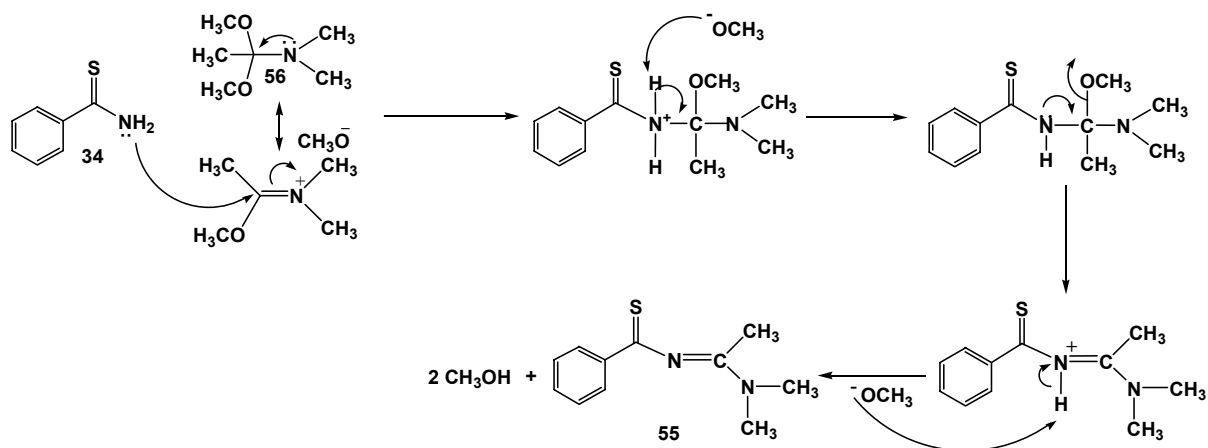
Therefore, 3-methyl-5-phenyl-1,2,4-thiadiazole (**54**) was synthesized the amination cyclization of the corresponding amidine, N-[(dimethylamino)ethylidene]thiobenzamide (**55**). Scheme 17 shows the total synthesis of 3-methyl-5-phenyl-1,2,4-thiadiazole (**54**).



Scheme 17: Synthesis of 3-methyl-5-phenyl-1,2,4-thiadiazole

2.3.1.1 Synthesis of N-[(dimethylamino)ethylidene]thiobenzamide

N-[(dimethylamino)ethylidene]thiobenzamide (**24**) was prepared in 89.8 % as an orange crystalline solid by the condensation between thiobenzamide (**22**) and N,N-dimethylacetamide dimethylacetal (**27**), as shown in Scheme 18.



Scheme 18: Synthesis of N-[(dimethylamino)ethylidene]thiobenzamide

The obtained orange crystals were characterized by ^1H -, ^{13}C -NMR and mass spectrometry.

The product from this reaction was analyzed by GC-MS [140°C (5 min), 20°C/min to 180°C (10 min), 20°C/min to 240°C (30 min)] (Figure 32a). The mass spectrum of the peak that eluted with a retention time of 23.9 minutes (Figure 32b) exhibited a molecular ion at m/z 206, which corresponds to the molecular weight of the desired product, **55**. The trace also exhibits the presence of some impurities.

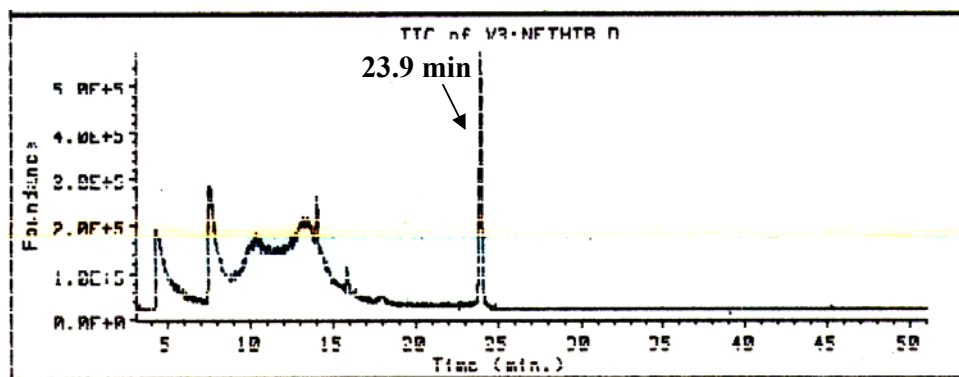


Figure 32a: GC-trace of N-[(dimethylamino)ethylidene]thiobenzamide

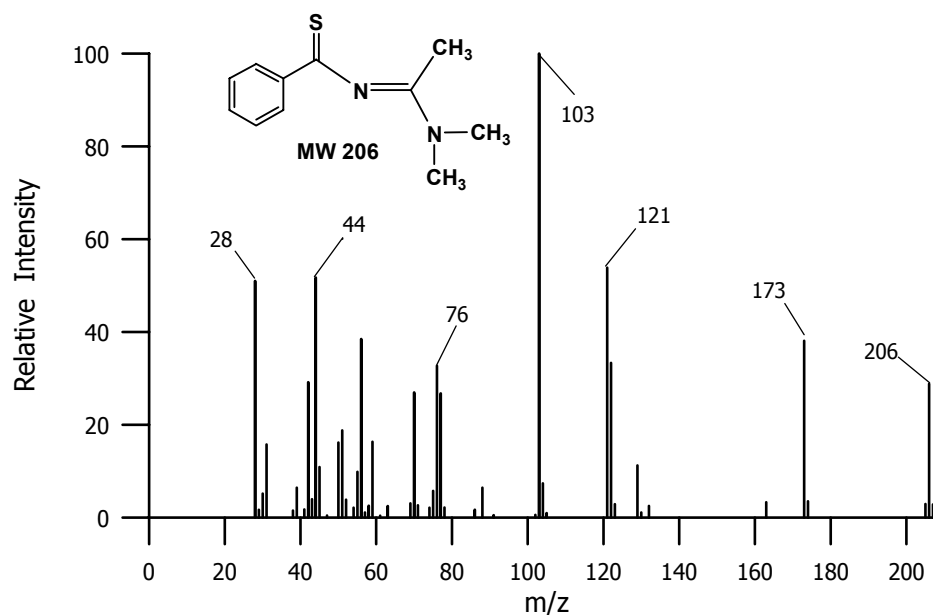


Figure 32b: Mass spectrum of the peak eluted at a retention time of 23.9 min

This orange crystalline solid, expected to be **55**, is different from N-[(dimethylamino)methylene]thiobenzamide (**32**) since the substituent at the imine carbon in this case is methyl group instead of hydrogen. Therefore, as expected, the $^1\text{H-NMR}$ spectrum of this orange solid (Figure 33) exhibits a 3H singlet at δ 2.45, which can be assigned to the methyl protons of the methyl group attached to the imine carbon. The two singlets (3H) at δ 3.20 and 3.22 are the absorptions due to the two non-equivalent methyls

bonded to the amino group. The two multiplets at δ 7.31-7.41 (3H) and δ 8.22-8.28 (2H) were assigned to para-meta and ortho- phenyl ring protons, respectively.

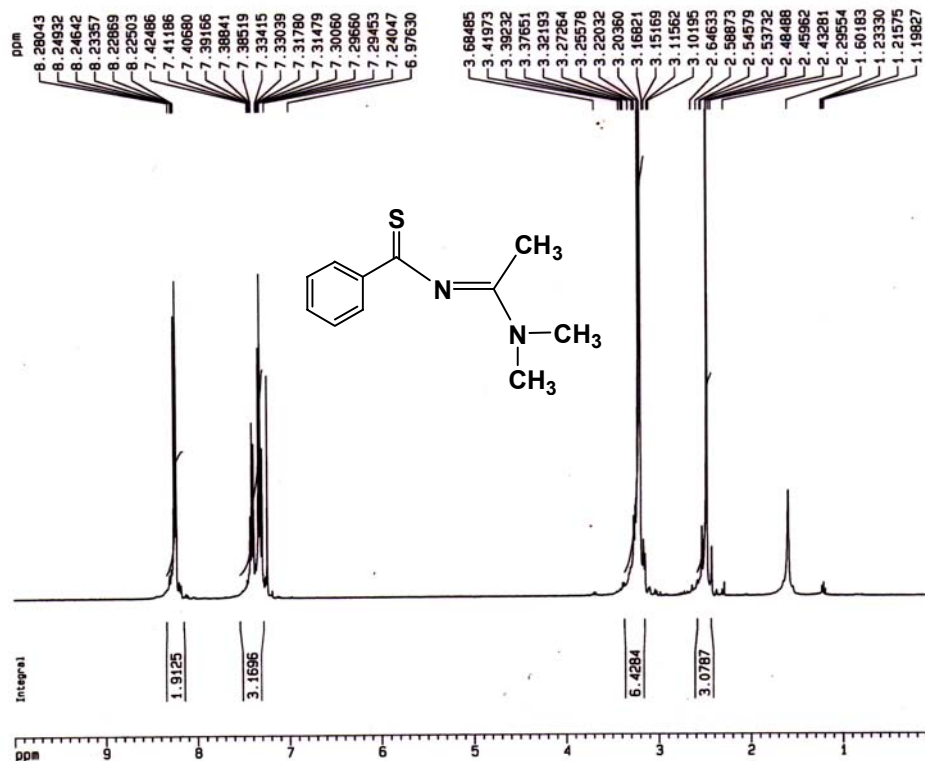


Figure 33: $^1\text{H-NMR}$ spectrum of N-[(dimethylamino)ethylidene]thiobenzamide

In the $^{13}\text{C-NMR}$ spectrum (Figure 34a), the most down field signal at δ 202.8 is assigned to the thiocarbonyl carbon. The imine carbon absorbs at δ 168.3. The four signals at δ 128.0, 128.9, 131.3 and 142.7 were assigned to the phenyl ring carbons. The spectrum reveals the two non-equivalent methyl carbons of the amino group as two singlets at δ 39.5 and 39.7. Figure 34b shows the scale expansion revealing the two singlet signals. The methyl carbon attached to the imine carbon appears at δ 18.4.

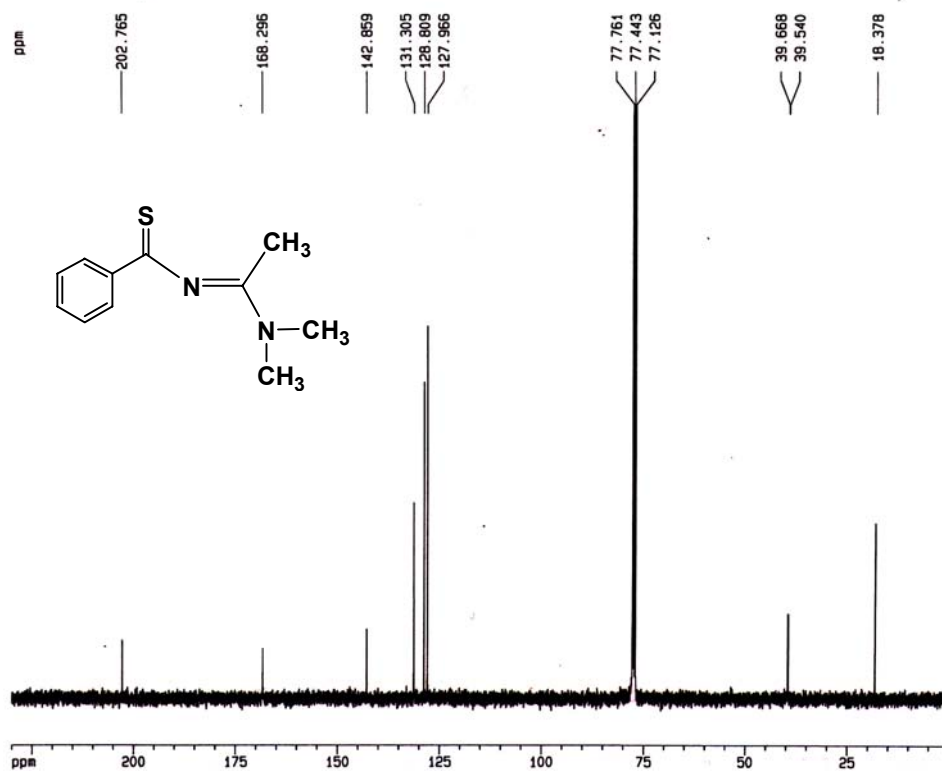


Figure 34a: ^{13}C -NMR spectrum of N-[(dimethylamino)ethylidene]thiobenzamide

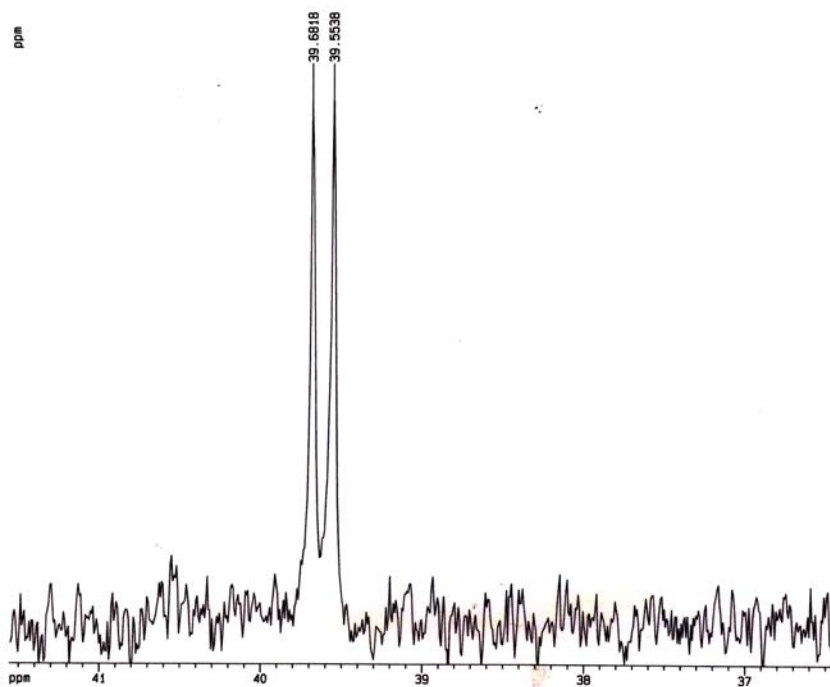


Figure 34b: Scale expansion exhibits the two singlets at δ 39.5 and 39.7

The above ^{13}C -spectral assignments are consistent with the ^1H - ^{13}C correlation spectrum (Figure 35). The carbon signal at δ 18.4, which was assigned to the methyl carbon attached to the imine carbon, correlates with the 3H singlet proton signal at δ 2.48, which was assigned to the protons of the methyl group attached to the imine carbon. The two singlet at δ 39.5 and 39.7, which were assigned to the two non-equivalent methyl carbons of the amino group, correlate with the two 3H singlet protons assigned to the two non-equivalent methyl protons of the amino group. Although, the GC-analysis of this sample exhibited the presence of some impurities, all NMR results are consistent with the structure of the desired product, N-[(dimethylamino)ethylidene]thiobenzamide (**55**).

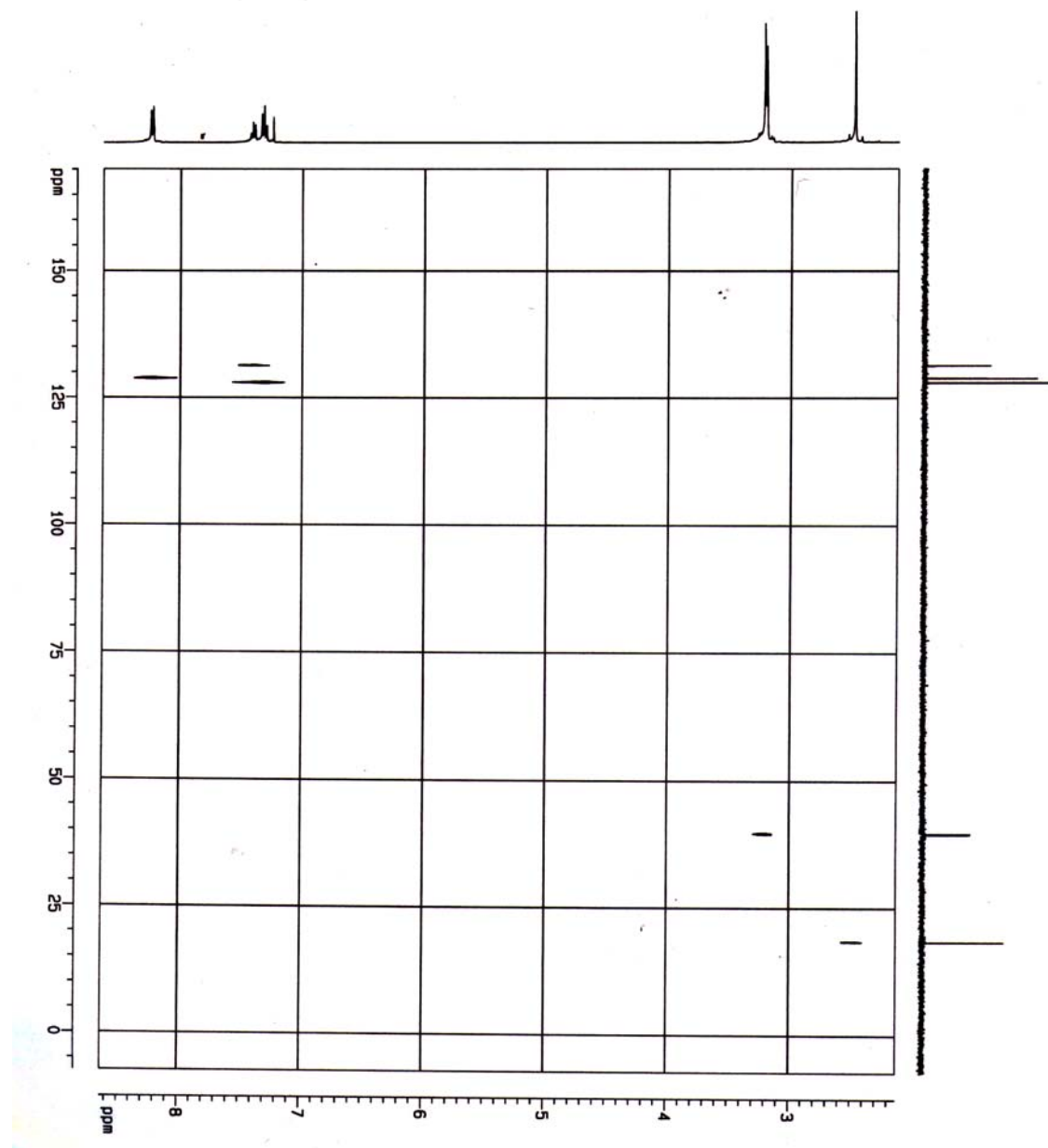
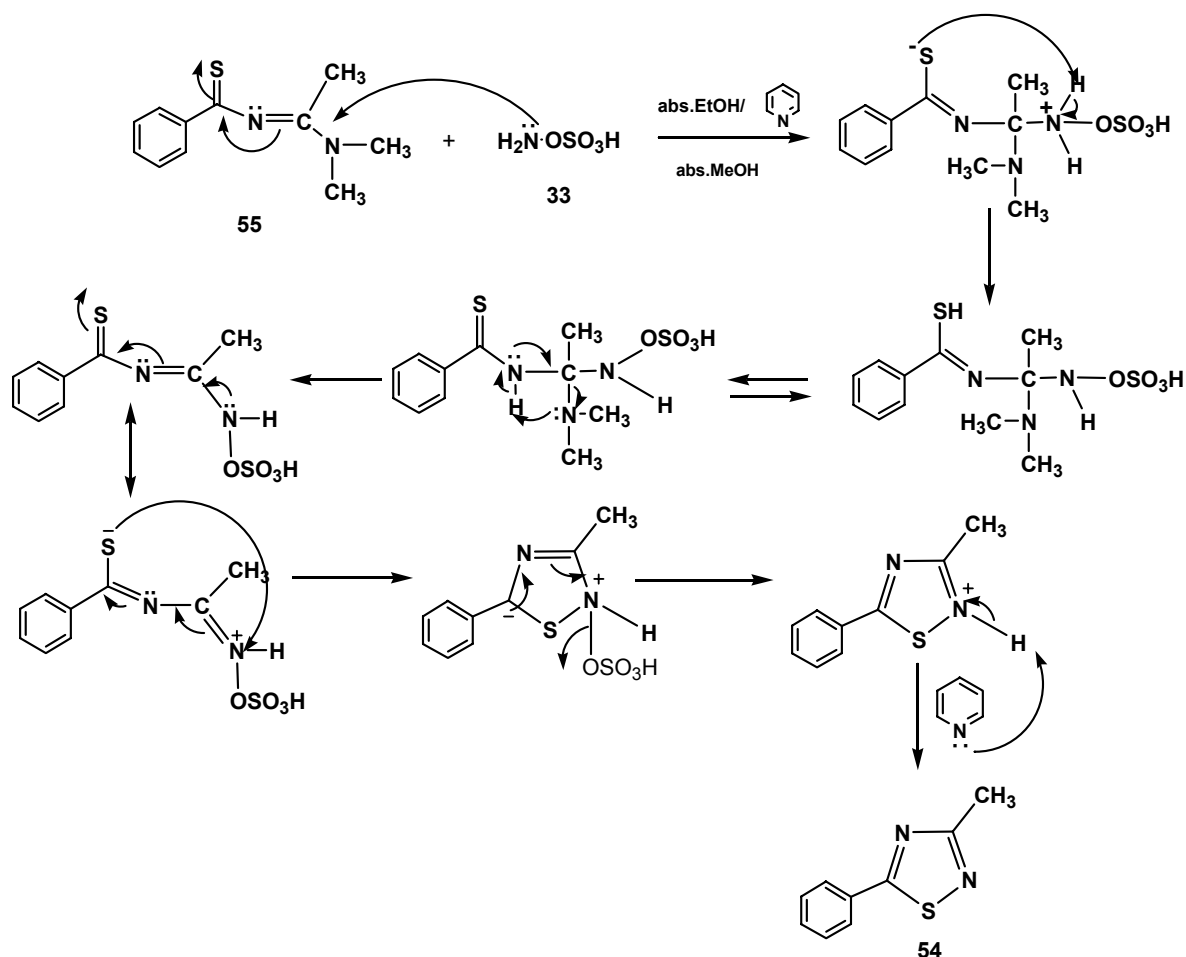


Figure 35: ^1H - ^{13}C correlation spectrum of N-[(dimethylamino)ethylidene]thiobenzamide

2.3.1.2 Synthesis of 3-methyl-5-phenyl-1,2,4-thiadiazole

3-Methyl-5-phenyl-1,2,4-thiadiazole (**54**) can be synthesized by the same method as described by Yang-i Lin and colleagues⁹ for the synthesis of 5-phenyl-1,2,4-thiadiazoles. But in the case of **54**, the amination cyclization will employ **55** as the starting material instead of **32**, as shown in Scheme 19.



Scheme 19: Synthesis of 3-methyl-5-phenyl-1,2,4-thiadiazole

3-Methyl-5-phenyl-1,2,4-thiadiazole (**54**) was obtained in 75 % as white colorless crystals. This crystalline solid was characterized by ¹H-, ¹³C-NMR and mass spectroscopy.

The GC-trace (isothermal 170°C) of these colorless crystals (Figure 36a) exhibits a major peak with a retention time of 15.6 min. The mass spectrum of this peak (Figure 36b) exhibits a molecular ion at m/z 176, which is consistent with the molecular weight of **54** (MW 176). The spectrum also exhibits a base peak at m/z 135 and a peak at m/z 73, which are consistent with the cleavage of $[\text{C}_6\text{H}_5\text{CNS}]^{*+}$ and $[\text{CH}_3\text{CNS}]^{*+}$, respectively.

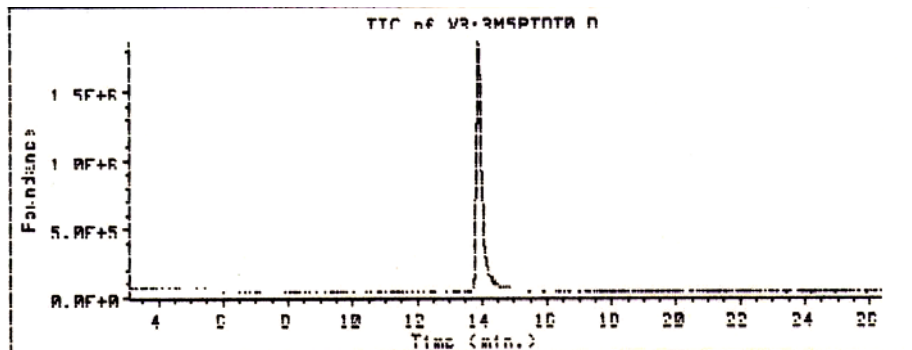


Figure 36a: GC-trace of 3-methyl-5-phenyl-1,2,4-thiadiazole

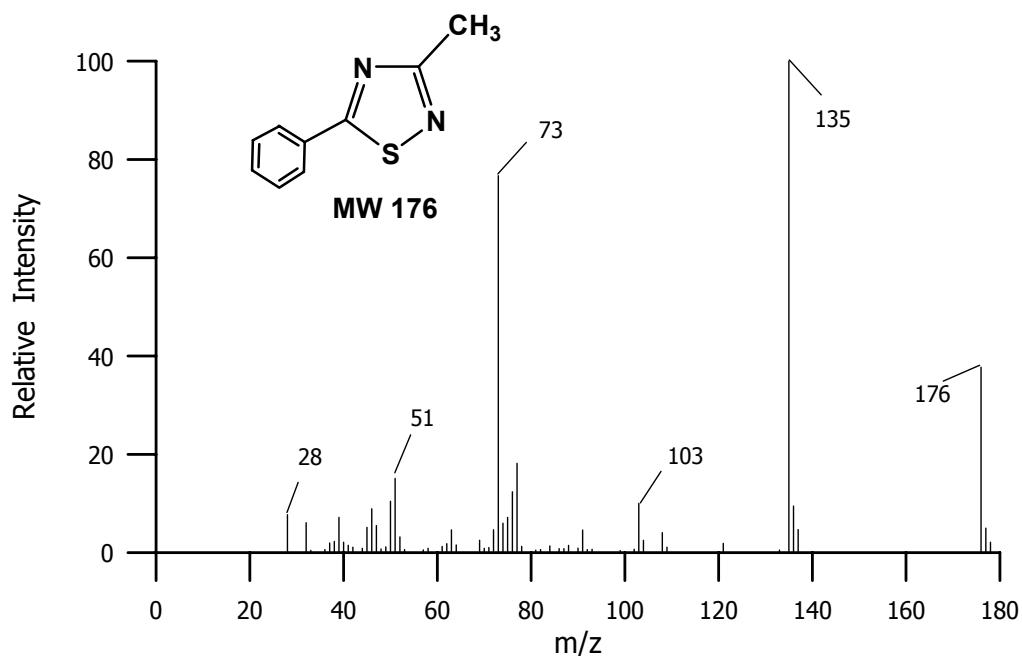


Figure 36b: Mass spectrum of the peak eluted at a retention time of 15.6 min

The $^1\text{H-NMR}$ spectrum (Figure 37) shows the methyl group as a 3H singlet at δ 2.70. The phenyl ring protons appear as two multiplets at δ 7.46-7.51 (3H) assigned to para-meta phenyl ring protons and δ 7.90-7.93 (2H) assigned to ortho phenyl ring protons.

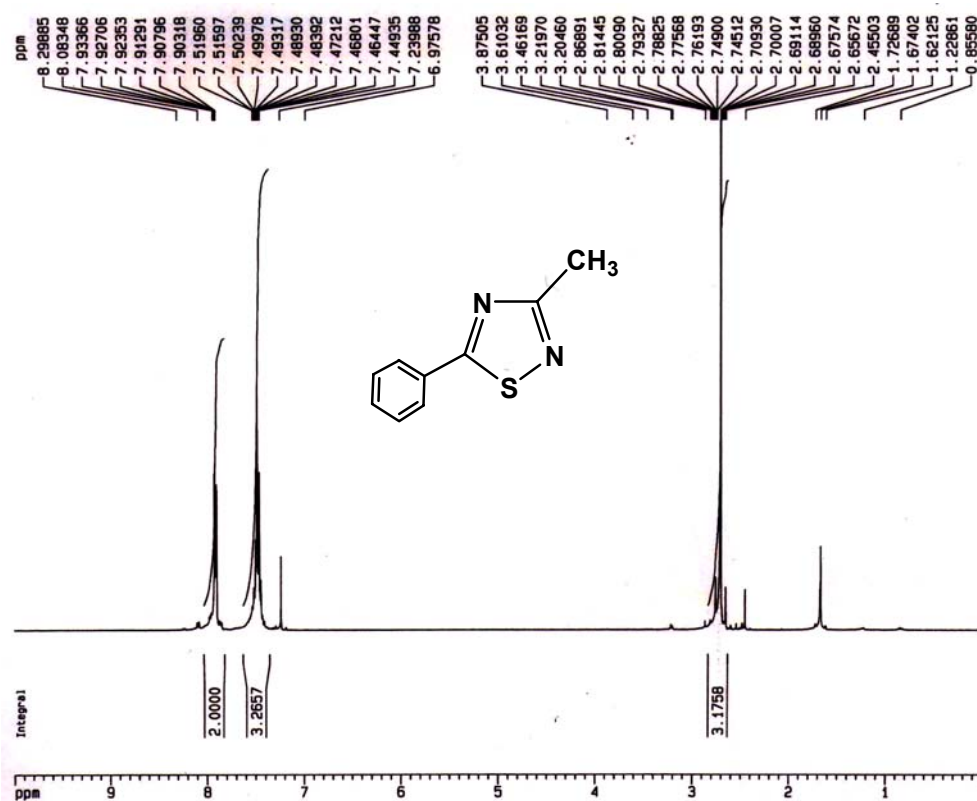


Figure 37: $^1\text{H-NMR}$ spectrum of 3-methyl-5-phenyl-1,2,4-thiadiazole

The $^{13}\text{C-NMR}$ spectrum (Figure 38a) reveals the methyl carbon at δ 19.5. The two thiadiazole ring carbons at positions 3 and 5 absorb at δ 174.6 and 188.5, respectively. The four signals at δ 127.8, 129.7, 130.9 and 132.3 are assigned to the phenyl ring carbons. These spectral assignments were confirmed by the $^{13}\text{C-DEPT}$ 135 spectrum, shown in Figure 38b. The signal at δ 19.5 still appears in the $^{13}\text{C-DEPT}$ 135 spectrum, which is consistent with the assignment to the methyl carbon. The two signals at δ 174.6 and 188.5, which were assigned to the two carbons at positions 3 and 5 of the thiadiazole ring, are not

observed in the ^{13}C -DEPT 135 spectrum since these signals are due to quaternary carbons. Three of the four singlets, which absorb in the phenyl region, still appear in the ^{13}C -DEPT 135 spectrum. Thus, these signals can be assigned to the ortho-, meta- and para-phenyl ring carbons. The signal at δ 130.9 was however not observed in the ^{13}C -DEPT 135 spectrum and, therefore, can be assigned to the phenyl carbon at the ring position 1.

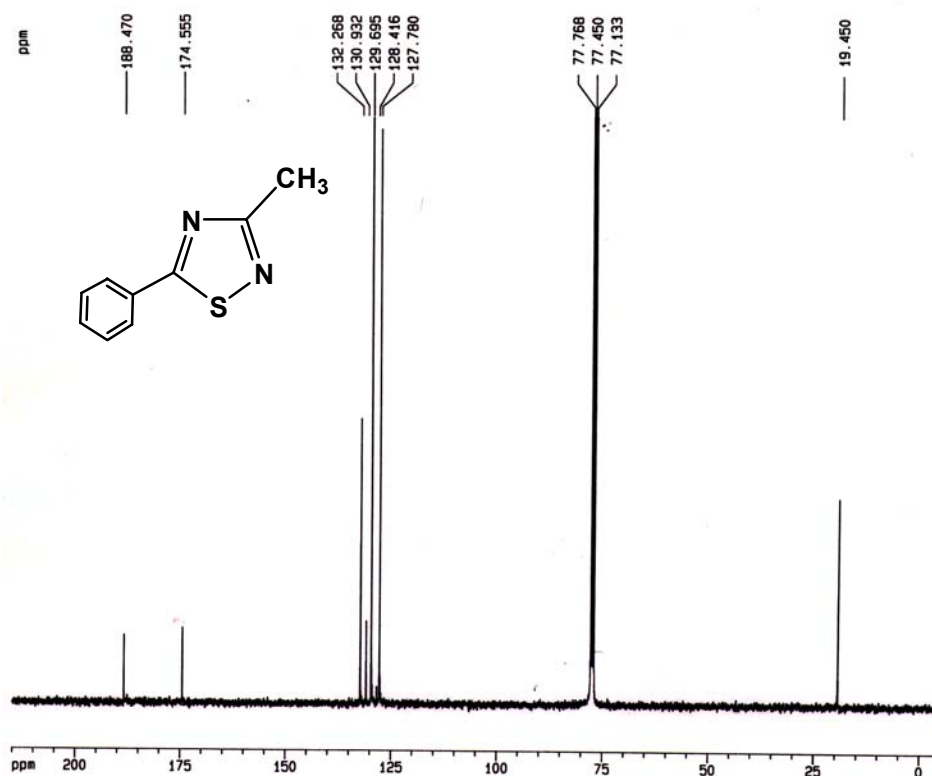


Figure 38a: ^{13}C -NMR spectrum of 3-methyl-5-phenyl-1,2,4-thiadiazole

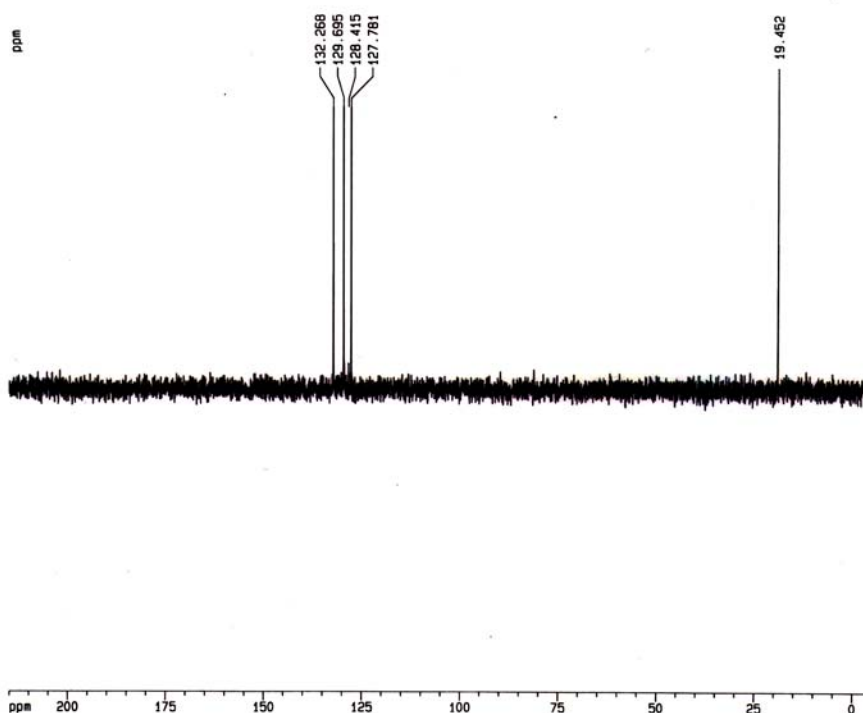
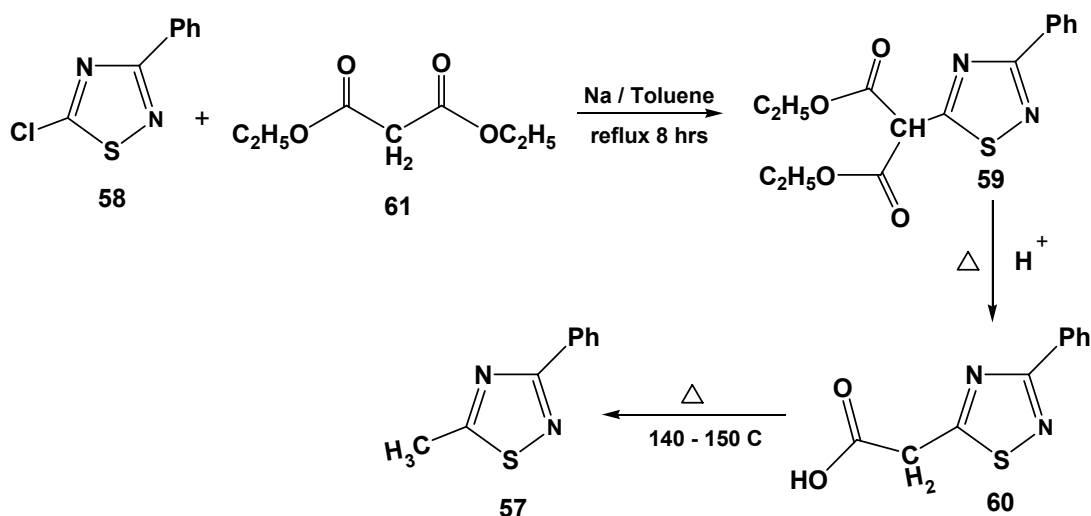


Figure 38b: ^{13}C -DEPT 135 spectrum of 3-methyl-5-phenyl-1,2,4-thiadiazole

2.3.2 Synthesis of 5-methyl-3-phenyl-1,2,4-thiadiazole

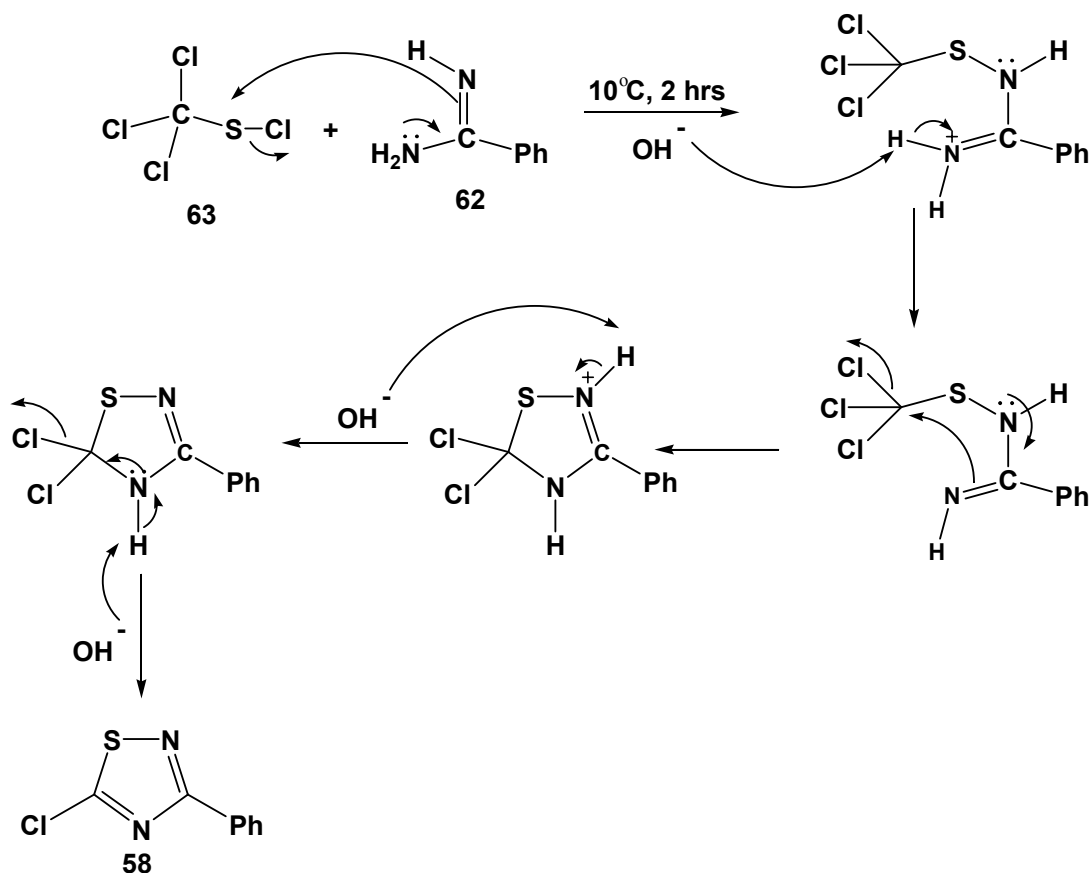
The synthesis of 5-methyl-3-phenyl-1,2,4-thiadiazole (**57**) has been reported by Goerdeler and Hammen¹⁶ involving a nucleophilic substitution of a malonate ester group at the ring position 5 of 5-chloro-3-phenyl-1,2,4-thiadiazole (**58**) followed by acid catalyzed hydrolysis of **59** and decarboxylation of **60** to give **57** in high yield. Scheme 20 shows the total synthetic route of **57**. Thus, **57** was prepared by this method to give the desired thiadiazole as a white solid, however, in very low yield.



Scheme 20: Synthesis of 5-methyl-3-phenyl-1,2,4-thiadiazole

2.3.2.1 Synthesis of 5-chloro-3-phenyl-1,2,4-thiadiazole

According to the synthetic route shown in Scheme 20, **58** is required as a starting material. 5-Chloro-3-phenyl-1,2,4-thiadiazole (**58**) could be synthesized by a procedure described by Goerdeler and co-workers¹⁶ via a coupling between benzamidine (**62**) with perchloromethyl mercaptan (**63**) in the presence of a base leading to the formation of **58** as a white solid in 41 % yield. The white solid was characterized by ¹H-, ¹³C-NMR and mass spectroscopy. Scheme 21 shows the synthesis of **58**.



Scheme 21: Synthesis of 5-chloro-3-phenyl-1,2,4-thiadiazole

GC analysis of this white solid (Figure 39a) shows a single gc-volatile component that eluted with a retention time of 10.3 min. The mass spectrum (Figure 39b) of this compound exhibits a molecular ion at m/z 196 which is consistent with the molecular weight of **58** (MW 196.5). A base peak at m/z 135 corresponds to the cleavage of [ClCN] from the molecular ion. The cleavage that results in the formation of $[C_6H_5CNS]^{\bullet+}$ is a characteristic fragmentation pathways of 5- and 3-phenyl-1,2,4-thiadiazoles as presented in other synthesis sections of this thesis. Furthermore, the presence of a chlorine atom in a molecule can be characterized by the presence of a P+2 peak, which is due to a fragment containing natural abundance of isotopic $^{37.5}\text{Cl}$ atom. The intensity of the P+2 peak will appear as 1/3 less intense than of the molecular ion for the existence of one chlorine atom in the molecule.

The mass spectrum in Figure 39b reveals a P+2 peak at m/z 198 with an intensity approximately 1/3 less intense than of the peak at m/z 196. Thus, this confirms that this compound contains one chlorine atom in the molecule.

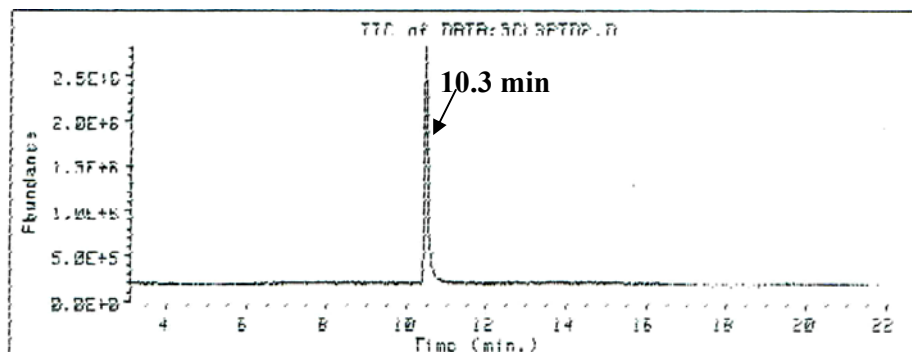


Figure 39a: GC analysis of 5-chloro-3-phenyl-1,2,4-thiadiazole

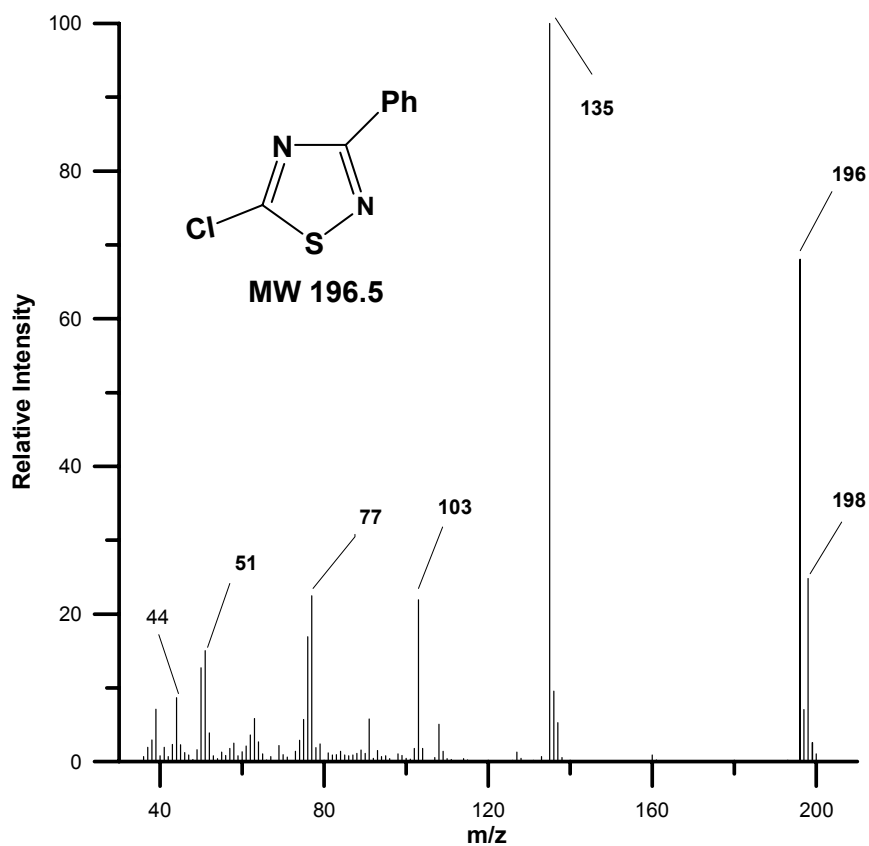


Figure 39b: Mass spectrum of 5-chloro-3-phenyl-1,2,4-thiadiazole

The ^1H -NMR spectrum, as shown in Figure 40, exhibits a clear spectrum. The phenyl ring protons appear as two multiplets at δ 7.36-7.43 (3H) assigned to the meta and para ring protons and δ 8.15-8.22 (2H) assigned to the ortho ring protons.

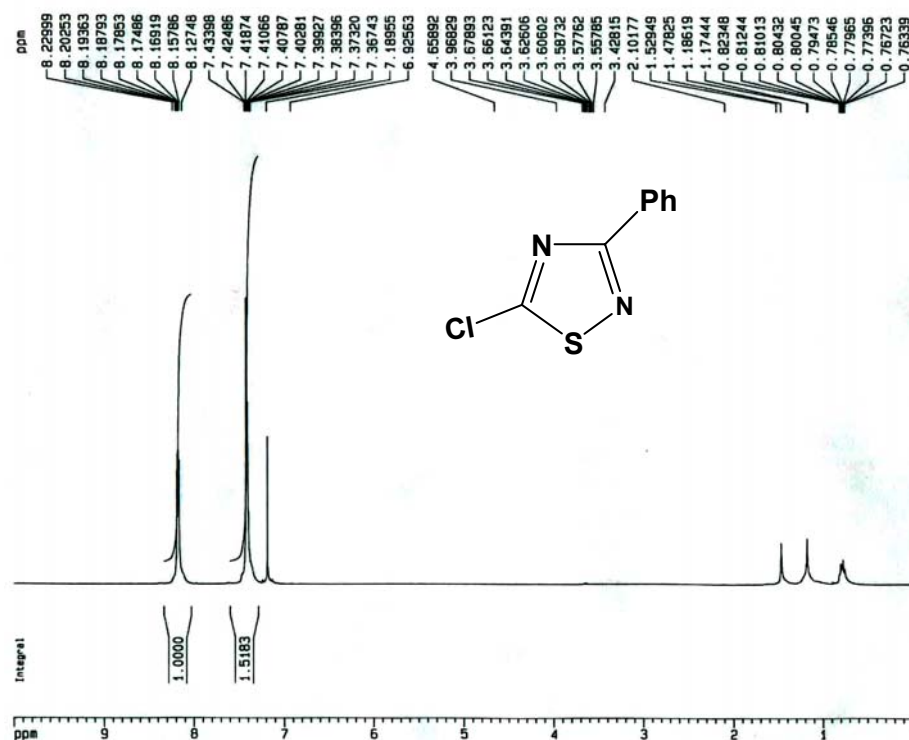


Figure 40: ^1H -NMR spectrum of 5-chloro-3-phenyl-1,2,4-thiadiazole

The ^{13}C -NMR spectrum, as shown in Figure 41a, shows that the two carbon atoms of the thiadiazole ring absorb at δ 172.5 and 173.4. The former signal was assigned to the carbon at ring position 3, while the latter signal was assigned to the carbon at ring position 5. These assignments were based on the previous spectral assignments of 3-phenyl-1,2,4-thiadiazole (**46**). The signals at δ 128.4, 129.2, 131.3 and 132.2 were assigned to the phenyl ring carbons. The signal at δ 132.2 disappears in the ^{13}C -DEPT 135 spectrum and that must be due to the carbon on phenyl ring at position 1. The signals at δ 128.4, 129.2 and 131.3 still remain in the ^{13}C -DEPT 135 spectrum. Thus, this confirms

that these signals are due to absorption of phenyl ring carbons at position 2 and 6, 3 and 5, and 4, respectively.

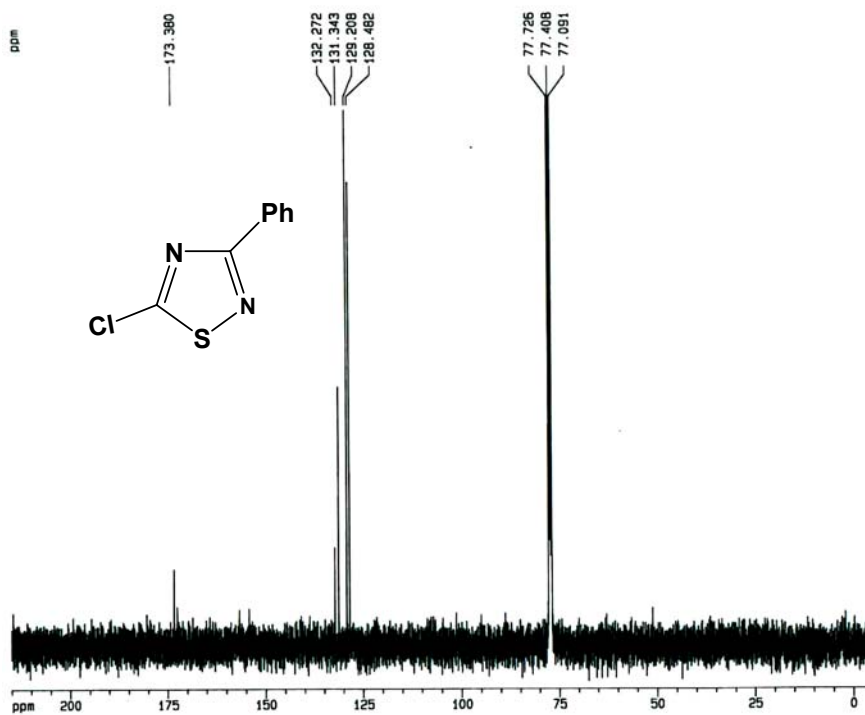


Figure 41a: ^{13}C -NMR spectrum of 5-chloro-3-phenyl-1,2,4-thiadiazole

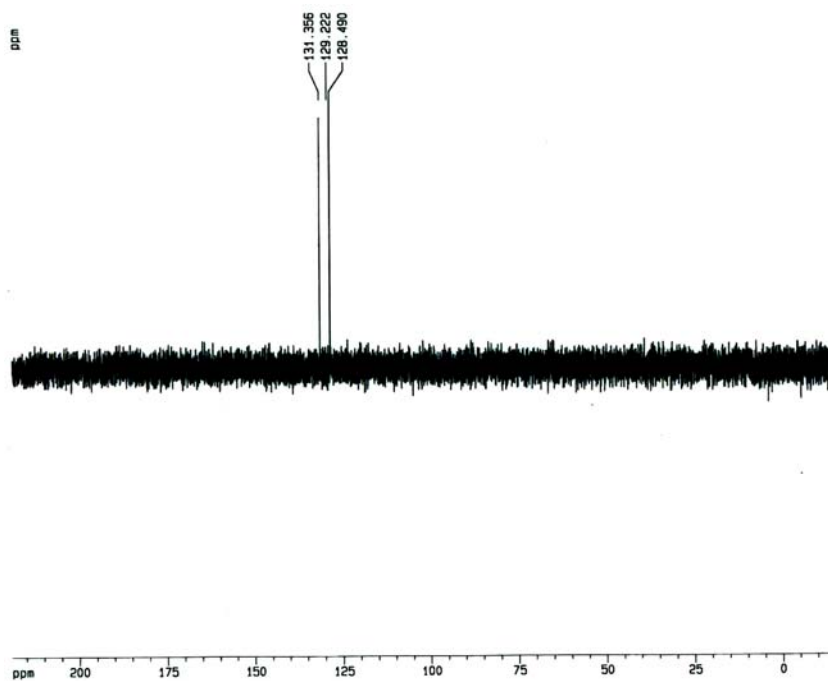
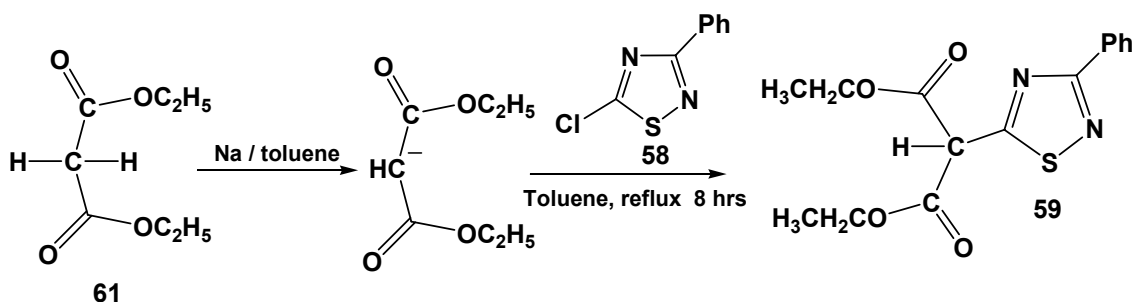


Figure 41b: ^{13}C -DEPT 135 spectrum of 5-chloro-3-phenyl-1,2,4-thiadiazole

2.3.2.2. Synthesis of diethyl 3-phenyl-1,2,4-thiadiazole-5-malonate

In this synthesis, a malonate ester anion was generated in situ by a reaction of sodium metal with the malonate ester (**61**) in toluene at room temperature. Addition of **58** to the solution of the malonate ester anion and subsequent refluxing in toluene for 8 hours gave the thiadiazole malonate ester (**59**) as light yellow crystals in 20% yield.



Scheme 22: Synthesis of diethyl 3-phenyl-1,2,4-thiadiazole-5-malonate

GC analysis of the yellow crystals (Figure 42a) shows a major component eluted at a retention time of 18.5 min. The mass spectrum of this component (Figure 42b) exhibits a molecular ion at m/z 240 which is not consistent with a molecular weight of the desired thiadiazole malonate ester **59** (MW 320). The spectrum, however, reveals a base peak at m/z 135 which is a characteristic fragmentation of 3-phenyl-1,2,4-thiadiazoles. Thus, this may indicate that **59** would undergo a reaction under the GC-MS analytical condition to give a product with a structure corresponding to the ester **64** (MW 248; Figure 42b). This GC-MS analysis result, however, is still unclear and, thus, structural determination of **59** cannot be confirmed by this GC-MS analysis.

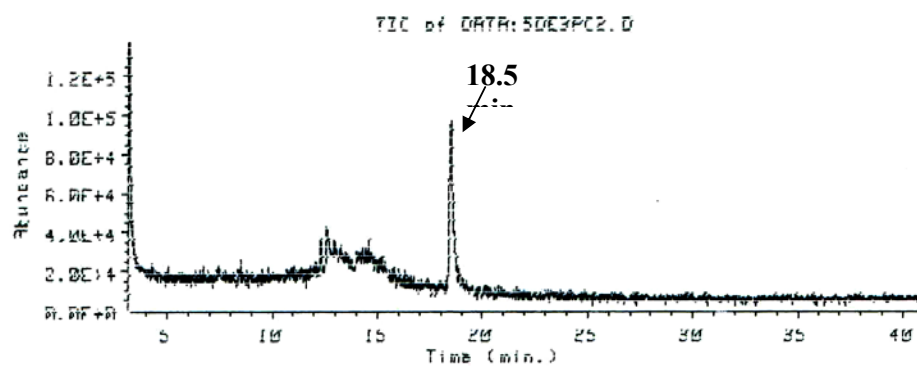


Figure 42a: GC analysis of the yellow solid obtained in the synthesis of **59**

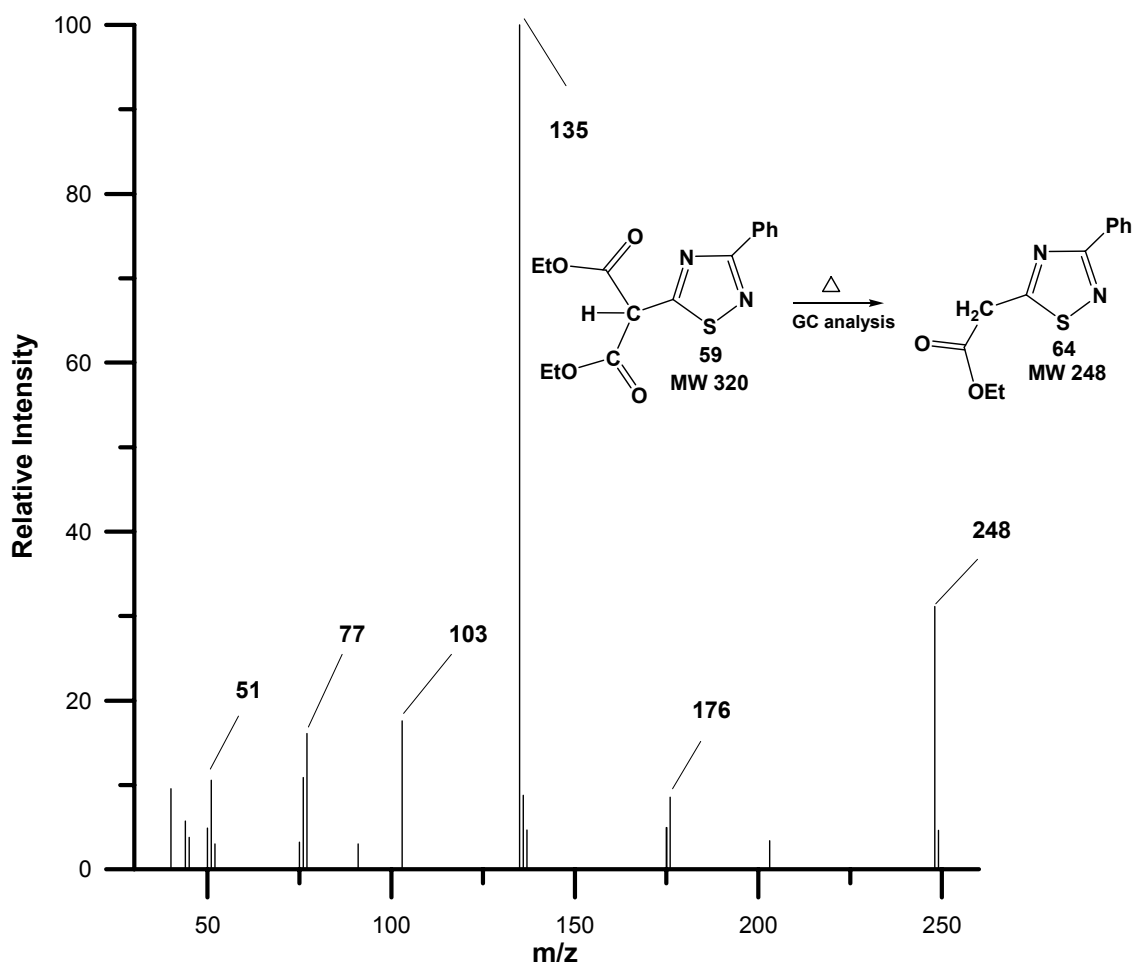


Figure 42b: Mass spectrum of the component eluted at 18.5 min

Although, mass spectral analysis of the yellow crystals did not provide fragmentation information corresponding to the structure of **59**, the $^1\text{H-NMR}$ analysis shown in Figure 43 exhibits a clear spectrum consistent with the structure of **59**. The spectrum reveals a broad singlet (1H) very downfield at δ 13.78. This broad downfield signal is a characteristic signal for a proton of a hydroxyl group. Thus, it indicates that the structure of this compound contains a hydroxyl group which corresponds to the structure of **59** in an enol form in CDCl_3 solution. A typical keto-enol equilibrium is fast and would not be observed on NMR time scale at room temperature. The $^1\text{H-NMR}$ of this product clearly shows that the structure of this product in CDCl_3 would be dominated at only one form. If **59** is in an enol form in chloroform-d solution associated with a hydrogen bonding with a nitrogen on thiadiazole ring as shown, the protons on ethyl ester groups will become non-equivalent. The absorption in the region of δ 1.33-.140 were assigned to absorptions of two overlapping triplets at δ 1.355 ($J = 7.07$ Hz) and 1.375 ($J = 7.07$ Hz) due to the two non-equivalent methyl protons of the ethyl ester groups. This assignment corresponds to the signal integration of six protons. The absorption in the region of δ 4.25-4.35 were assigned to absorptions of two overlapping quartets at δ 4.30 ($J = 7.07$ Hz) and 4.315 ($J = 7.07$ Hz) due to the two non-equivalent methylene protons of the ethyl ester groups. This assignment corresponds to the signal integration of four protons. The two multiplets at δ 7.46-7.52 (3H) and δ 7.89-7.92 (2H) are due to absorptions of the phenyl ring protons. Figure 44 shows a two-dimensional $^1\text{H-}^1\text{H}$ coupling (COSY) spectrum. This spectrum confirms that the protons which absorb in the region of δ 1.33-.140 (6H) coupled only with the protons that absorb in the region of δ 4.25-4.35 (4H) and *vice versa* without any additional coupling from the other protons.

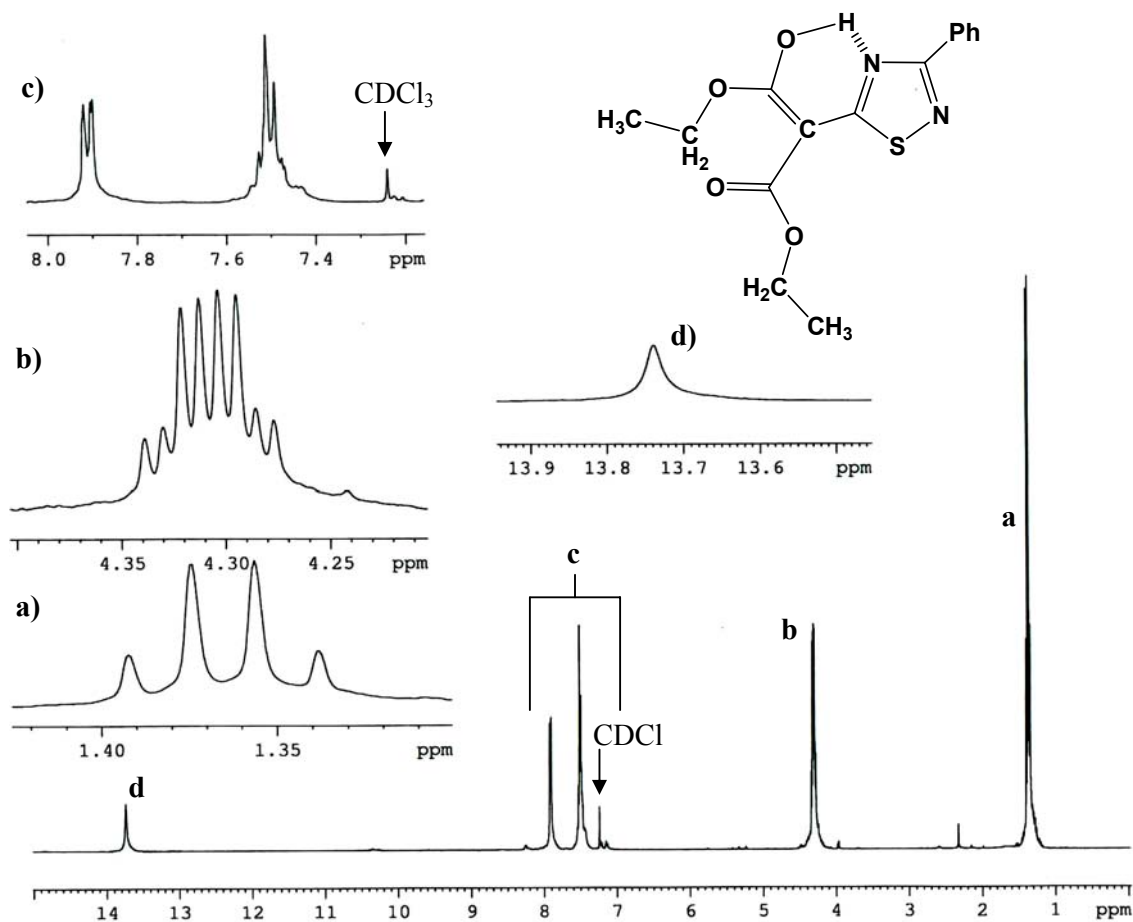


Figure 43: $^1\text{H-NMR}$ spectrum of diethyl 3-phenyl-1,2,4-thiadiazole-5-malonate

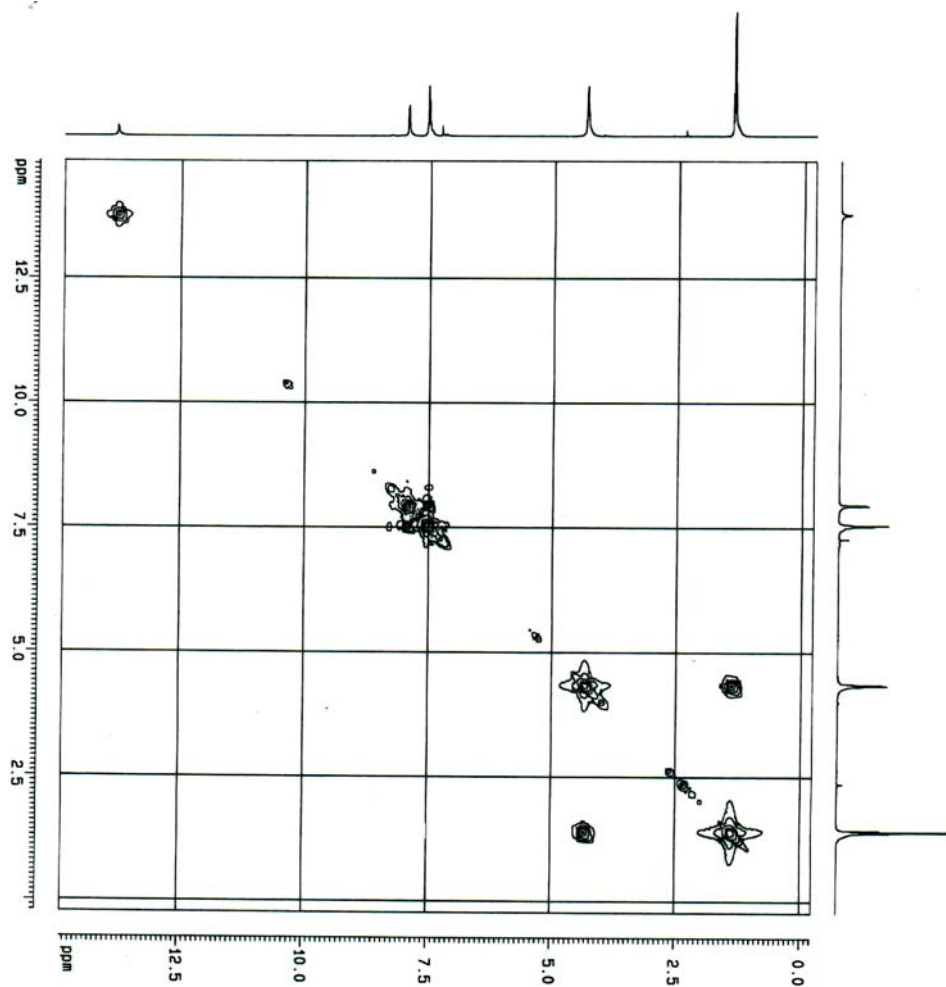


Figure 44: ^1H - ^1H coupling (COSY) spectrum of **59**

The ^{13}C -NMR spectrum, shown in Figure 45a, exhibits signals due to the two non-equivalent methyl carbons at δ 14.3 and 14.4 and the two non-equivalent methylene carbons at δ 60.7 and 61.0. The α -carbon of the malonate ester group absorbs at δ 85.7. The singlets at δ 126.8, 127.5, 129.2 and 131.7 were assigned to phenyl ring carbons. The carbons on thiadiazole ring at position 3 and 5 appear at δ 155.2 and 167.9, respectively. Since the enol equilibrium is fast, thus, the carbonyl carbon and enol carbon will become equivalent on the NMR time scale and appears as a singlet at δ 178.0. These assignments are consistent with the ^{13}C -DEPT 135 spectrum (Figure 45b). The four signals at δ 127.5, 155.2, 167.9 and 178.0 disappear in the ^{13}C -DEPT 135 spectrum which is consistent with

their assignment to the four quaternary carbons of phenyl ring carbon at position 1, the carbons on the thiadiazole ring at positions 3 and 5, and the equivalent carbonyl-enol carbon, respectively. The two singlets at δ 14.3 and 14.4 appear in the positive direction while the signals at δ 60.7 and 61.0 appear in negative direction in the ^{13}C -DEPT 135 spectrum. These are consistent to the assignments to the two non-equivalent methyl carbons and the two non-equivalent methylene carbons of the malonate ester group, respectively.

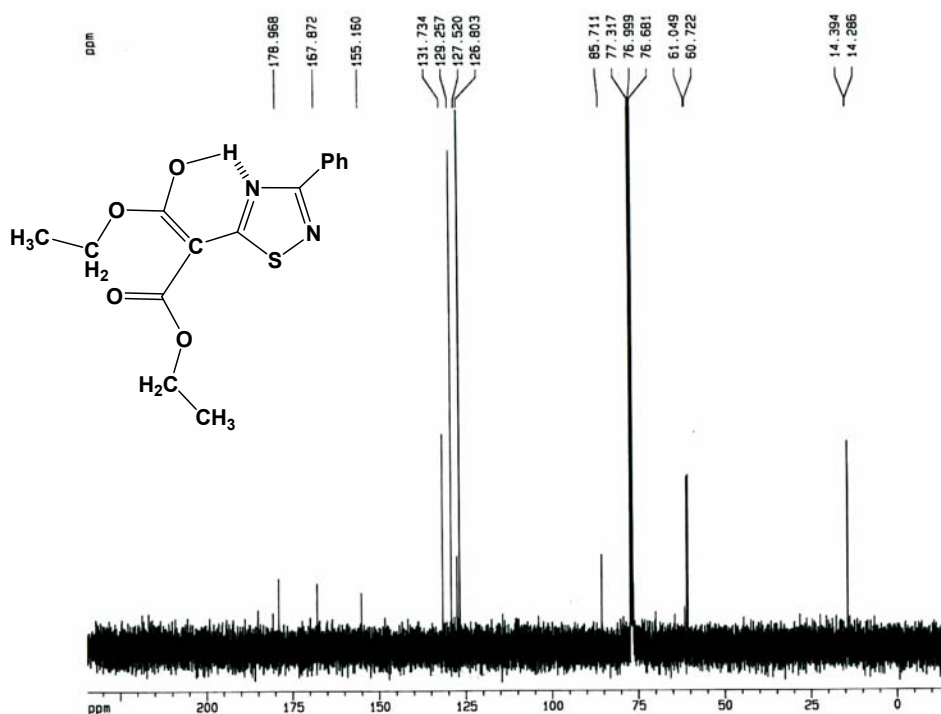


Figure 45a: ^{13}C -NMR spectrum of diethyl 3-phenyl-1,2,4-thiadiazole-5-malonate

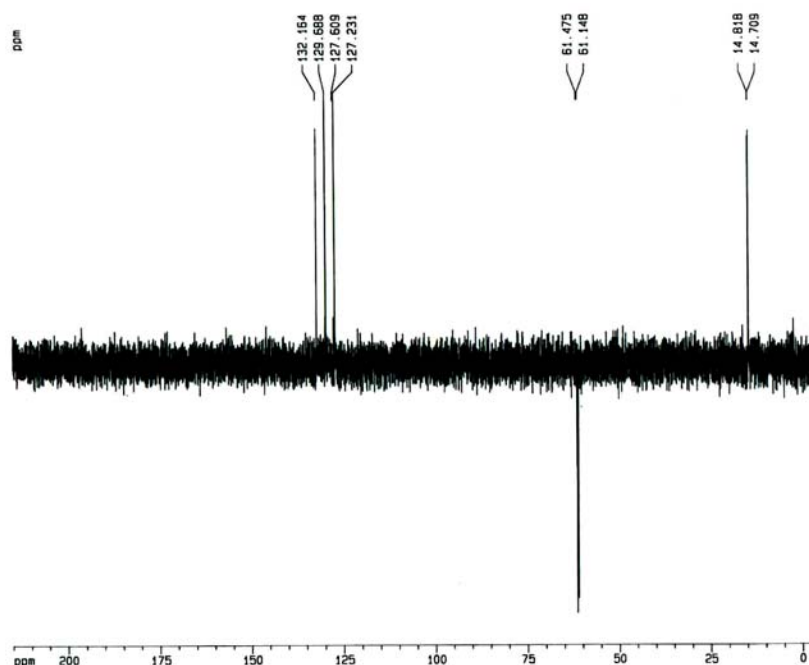


Figure 45b: ^{13}C -DEPT 135 spectrum of diethyl 3-phenyl-1,2,4-thiadiazole-5-malonate

Figure 46 shows the two dimensional ^1H - ^{13}C correlation spectrum of the yellow crystals. This spectrum exhibits correlation between ^1H and ^{13}C supporting the previous ^1H and ^{13}C -spectral assignments. The spectrum reveals that the two carbon signals at δ 14.3 and 14.4, which were assigned to the non-equivalent methyl carbons, correlate with the quartet (6H) at δ 1.36 in the ^1H -spectrum, which was assigned to the protons of the two non-equivalent methyl groups. In addition, the signals in the ^{13}C -spectrum at δ 60.7 and 61.0, assigned to the two non-equivalent methylene carbons, correlate with the multiplet (4H) in the ^1H -spectrum at δ 4.31, assigned to the protons of the two non-equivalent methylene groups. The spectrum also reveals no correlation of the broad down filed singlet in the ^1H -spectrum with any carbon signal confirming that this proton is not attaching to any carbon and corresponds to absorption of the hydroxyl proton in enol form of **59**.

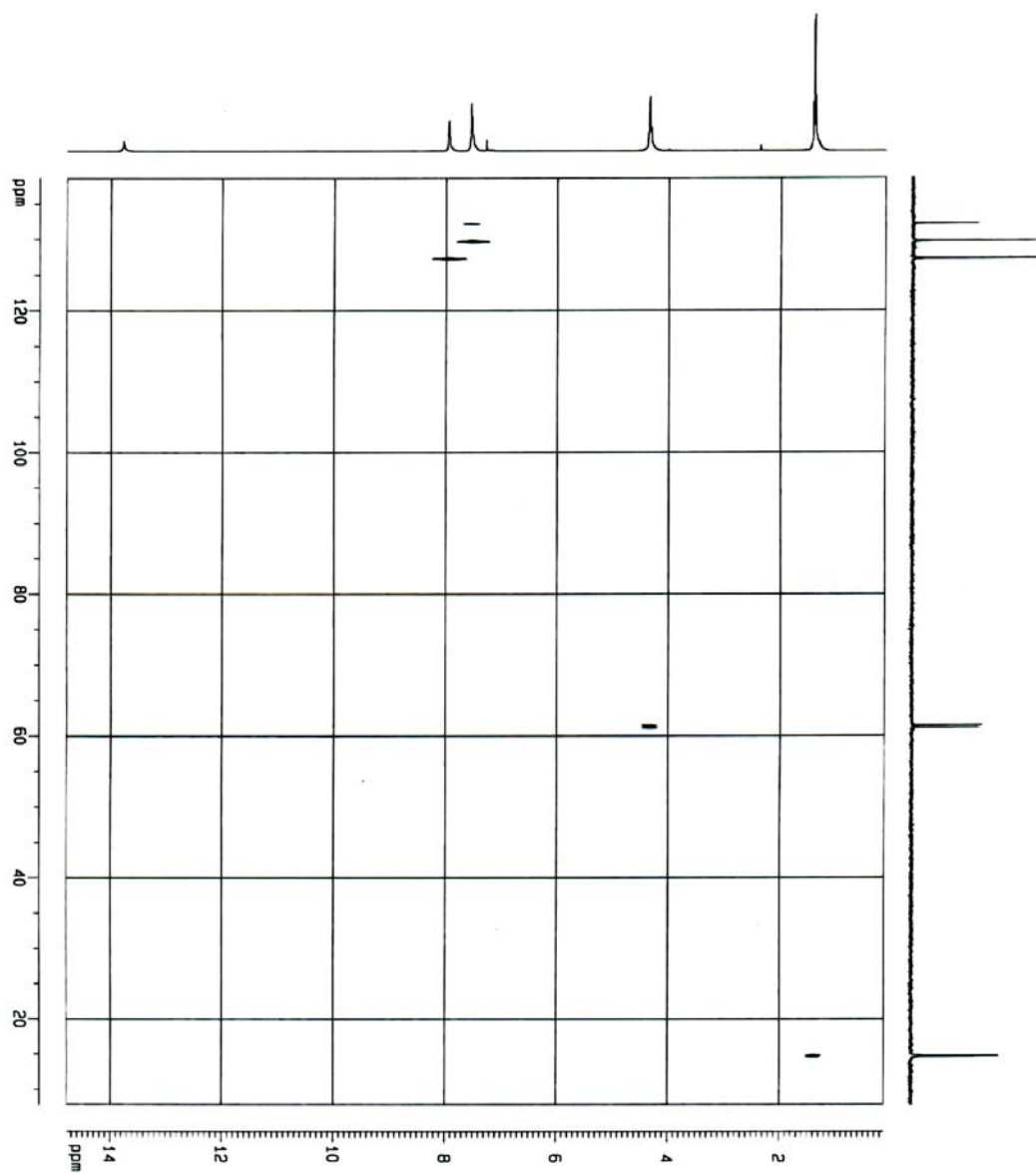
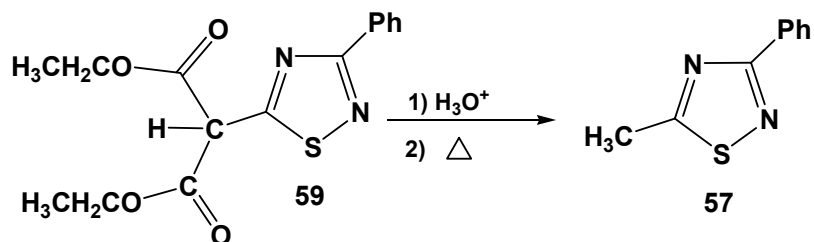


Figure 46: ^{13}C - ^1H correlation spectrum of diethyl 3-phenyl-1,2,4-thiadiazole-5-malonate

2.3.2.3 Synthesis of 5-methyl-3-phenyl-1,2,4-thiadiazole

Acid catalyzed hydrolysis of the ester **59** followed by decarboxylation led to the formation of 5-methyl-3-phenyl-1,2,4-thiadiazole (**57**) as a white solid, however, in a very low yield.



Scheme 23: Synthesis of 5-methyl-3-phenyl-1,2,4-thiadiazole

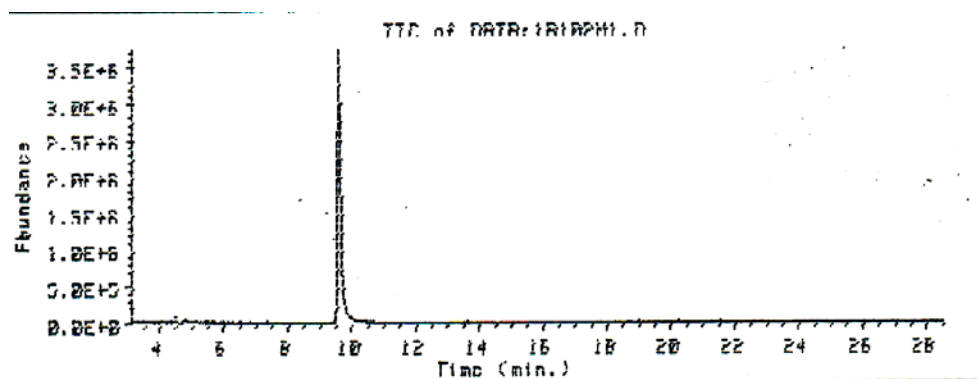


Figure 47a: GC-trace of the white solid

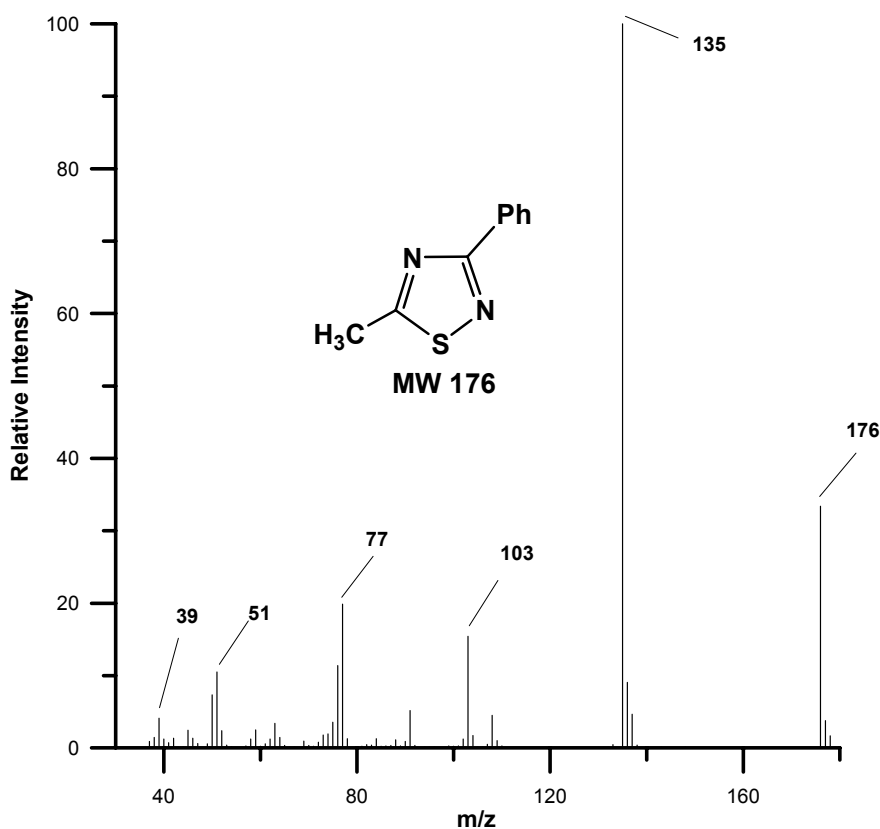
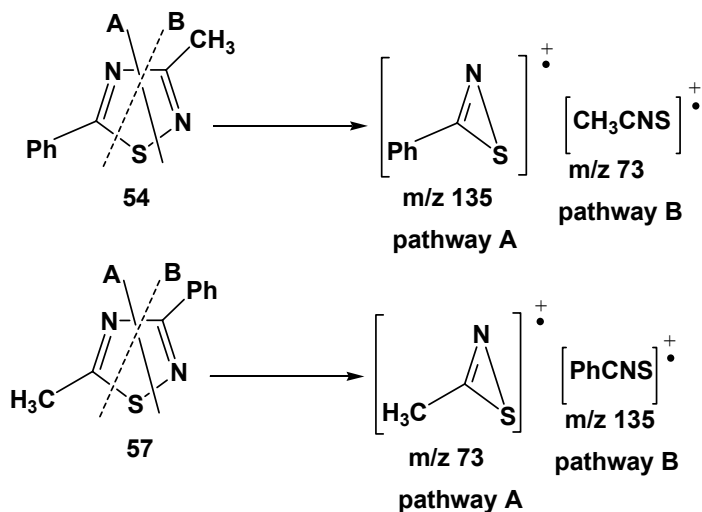


Figure 47b: Mass spectrum of the white solid

The white solid was characterized by ^1H -, ^{13}C -NMR and mass spectroscopy. The GC-trace (Figure 47a) of this white solid shows the presence of one gc-volatile component eluted with a retention time of 9.5 min. The mass spectrum (Figure 47b) of this component shows a molecular ion peak at m/z 176 which corresponds to a molecular weight of the desired thiadiazole **57** (MW 176). The spectrum also exhibits a base peak at m/z 135. Unlike, the mass spectrum of 3-methyl-5-phenyl-1,2,4-thiadiazole (**54**), no peak at m/z 73 was observed in Figure 47b. In the case of **54**, the peaks at m/z 73 and 135 were suggested to result from fragmentation pathways A and B, respectively, as shown in Scheme 24. Fragmentation pathway A in **54** would give a fragment with m/z 135 that could be stabilized by the phenyl group leading to a stable radical cation (m/z 135) which could be detected by the mass spectrometer. In contrast, under this similar fragmentation pathway for **57**, the

peak at m/z 73 could not be detected in the mass spectrometer which was possibly due to the lack of stabilization of the generated radical cation and, thus, it might undergo further fragmentation before detection by the mass spectrometer. Thus, the absence of the peak at m/z 73 is characteristic fragmentation pathway of **57**. Therefore, it can be concluded that this white solid is 5-methyl-3-phenyl-1,2,4-thiadiazole (**57**).



Scheme 24: Fragmentation pathways of **54** and **57**

The ^1H -NMR spectrum (Figure 48) shows the methyl group as a 3H singlet at δ 2.84. The phenyl ring protons appear as two multiplets at δ 7.34-7.48 (3H) assigned to para- and meta-phenyl ring protons and δ 8.17-8.27 (2H) assigned to ortho phenyl ring protons.

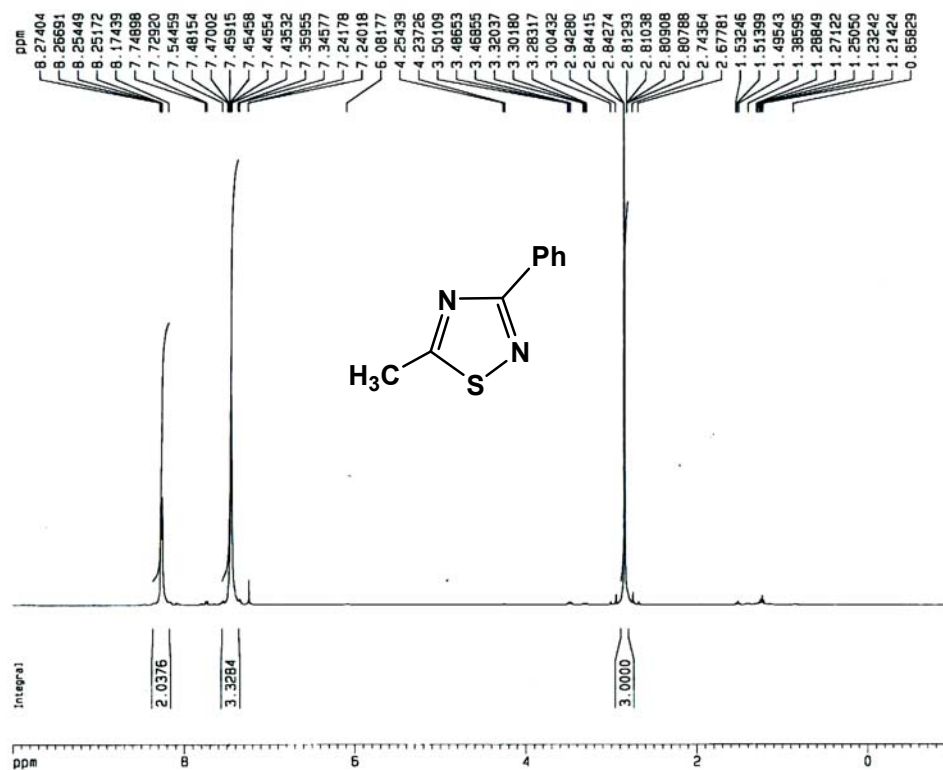


Figure 48: ¹H-NMR spectrum of 5-methyl-3-phenyl-1,2,4-thiadiazole

The ¹³C-NMR spectrum (Figure 49) reveals the methyl carbon of **57** at δ 16.9 which is slightly upfield compared with the methyl carbon that attaches to the thiadiazole ring carbon at position 3. The two thiadiazole ring carbons at positions 3 and 5 absorb at δ 186.4 and 173.1, respectively. The four signals at δ 128.1, 128.7, 130.2 and 132.7 are assigned to the phenyl ring carbons.

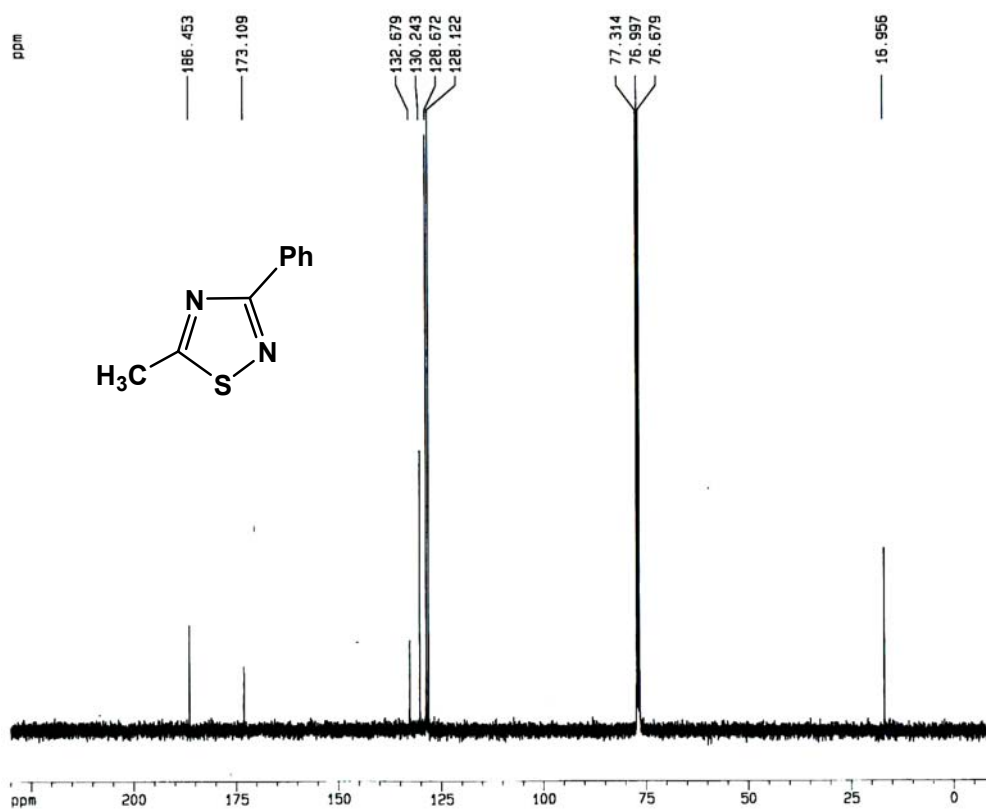
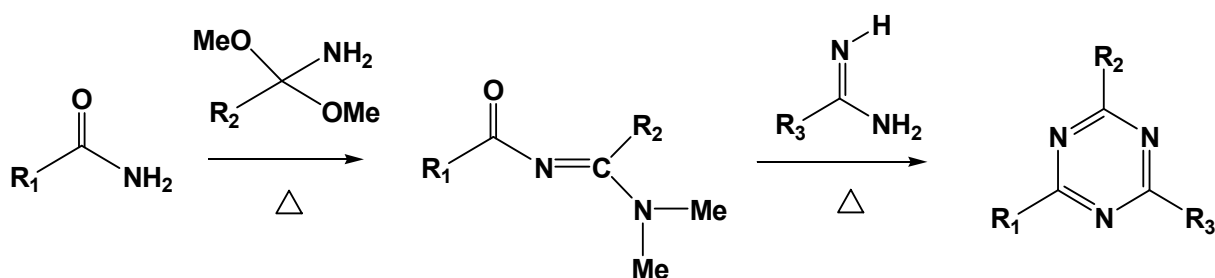


Figure 49: ^{13}C -NMR spectrum of 3-methyl-5-phenyl-1,2,4-thiadiazole

2.3.3 Synthesis of 2,4-dimethyl-6-phenyl-1,3,5-triazine and 2-methyl-4,6-diphenyl-1,3,5-triazine

The procedure for the synthesis of sym-triazines by the cotrimerization of amidines described by Schaefer and colleagues¹⁰ is suitable for the synthesis of mono substituted-sym-triazines. Additional studies by these same researchers also revealed that the cotrimerization of amidines and imidates also allows the synthesis of un-symmetrically substituted-s-triazines. Since the cotrimerization is a random process, this procedure leads to mixtures of sym-triazines products.

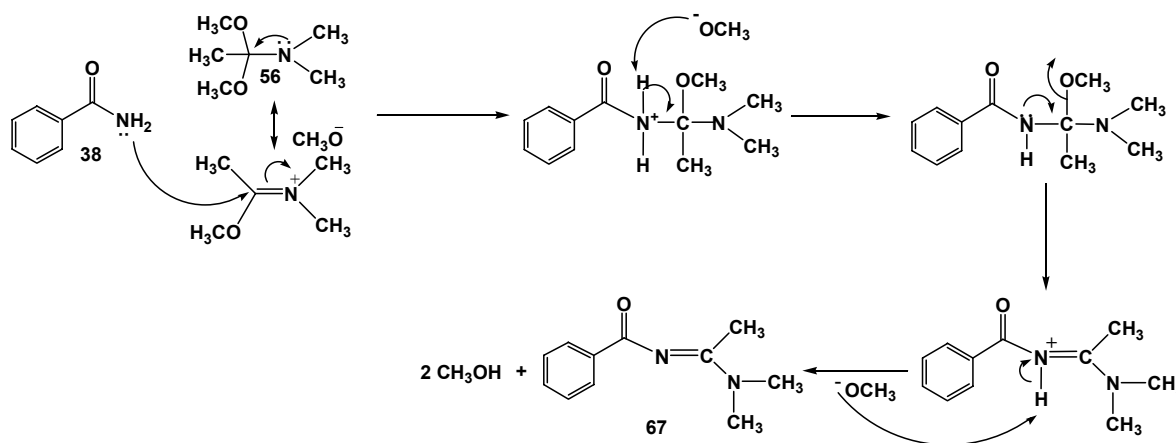
However, more recently, a new synthesis of unsymmetrically substituted-s-triazines was reported. This method involves the condensation of N-acylamidines and amidines or guanidines in aprotic solvent,¹³ as shown in Scheme 25. Therefore, both 2,4-methyl-6-phenyl-1,3,5-triazine (**65**) and 2-methyl-4,6-diphenyl-1,3,5-triazine (**66**) were synthesized by this more recent method.



Scheme 25: The recent synthetic method of un-symmetrically substituted-s-triazines

2.3.3.1 Synthesis of N-[(dimethylamino)ethylidene]benzamide

In order to synthesize 2,4-dimethyl-6-phenyl-1,3,5-triazine (**65**) and 2-methyl-4,6-dimethyl-1,3,5-triazine (**66**) by the method described by Raymond Dengino and colleagues, required the acylamidine, N-[(dimethylamino)ethylidene]benzamide (**67**). This amidine was prepared in 90% as a dark viscous liquid by the condensation of benzamide (**38**) and N,N-dimethylacetamide dimethylacetal (**56**), as shown in Scheme 26.



Scheme 26: Synthesis of N-[(dimethylamino)ethylidene]benzamide

The product was identified by ^1H -, ^{13}C -NMR and mass spectroscopy. The GC-chromatogram of this dark liquid [180°C (5min), 10°C/min to 240°C (30 min)] shows (Figure 50a) the presence of only one component with a retention time of 17.4 min. The mass spectrum (Figure 50b) of this material exhibits a molecular ion at m/z 190, a base peak at m/z 105, and two strong intensity peaks at m/z 44 and 77. The molecular ion at m/z 190 is consistent with the molecular weight of **67** (MW 190). Furthermore, the base peak at m/z 105 corresponds to the cleavage of $[\text{C}_6\text{H}_5\text{CO}]^+$ and the two strong intensity peaks at m/z 44 and 77 correspond to the cleavage of $[\text{C}_2\text{H}_6\text{N}]^+$ and $[\text{C}_6\text{H}_5]^+$, respectively.

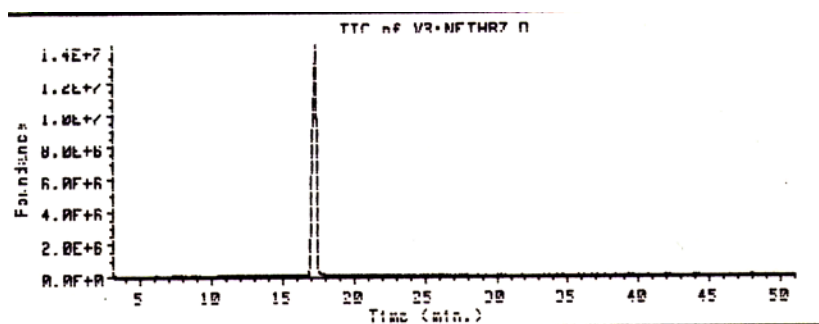


Figure 50a: GC-trace of the dark viscous liquid expected to be **67**

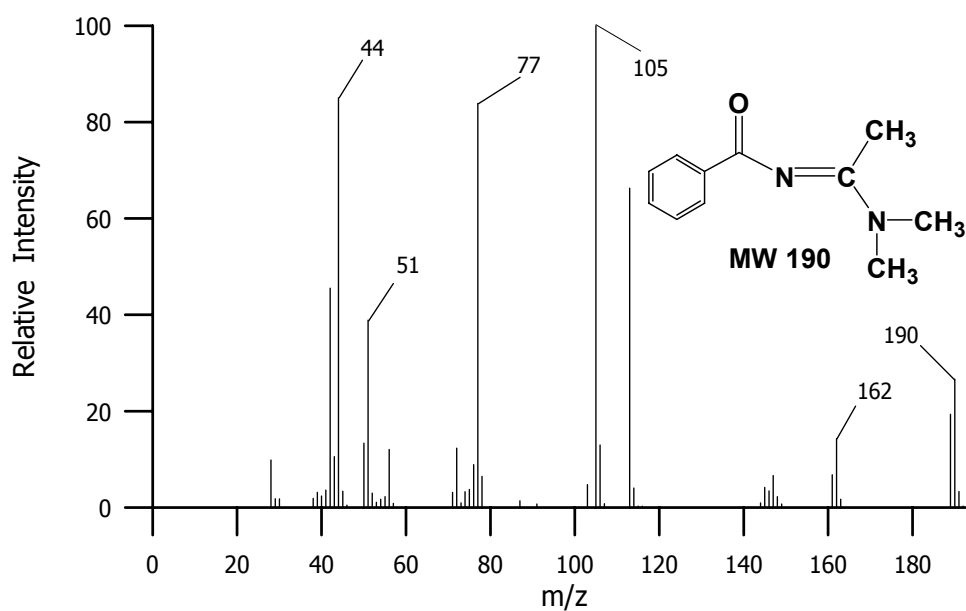


Figure 50b: Mass spectrum of the peak eluted at a retention time of 17.4 min

The $^1\text{H-NMR}$ spectrum of this liquid (Figure 51) exhibits two multiplets at δ 7.31-7.39 (3H) and δ 8.07-8.12 (2H) and three singlets at δ 2.23 (3H), 2.97 (3H) and 3.07 (3H). This spectrum is consistent with the structure of N-[(dimethylamino)ethylidene]benzamide (**67**). The two multiplets at δ 7.31-7.39 and δ 8.07-8.12 were assigned to the meta-para and ortho-phenyl ring protons, respectively. The 3H singlet at δ 2.23 can be assigned to the methyl protons bonded to the imine carbon. The additional two 3H singlets were assigned to the two non-equivalent methyl groups bonded to the amino group.

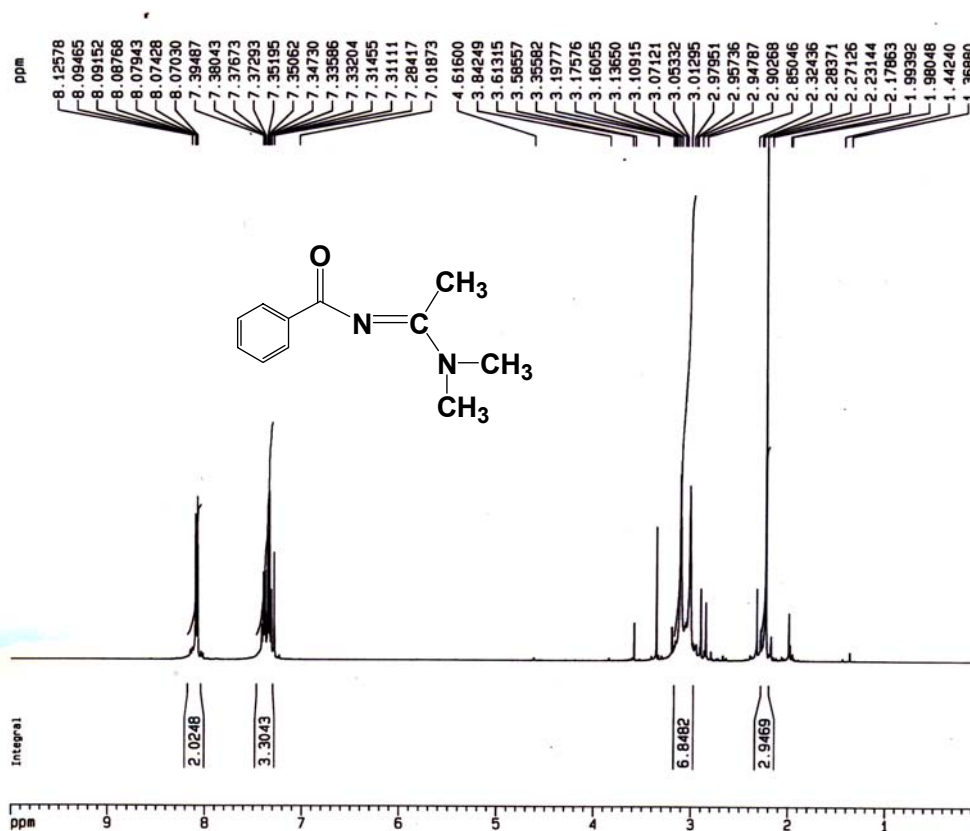


Figure 51: $^1\text{H-NMR}$ spectrum of the dark liquid

The ^{13}C -NMR spectrum of this liquid (Figure 52a) also reveals signals consistent with the structure of **67**. The methyl carbon bonded to the imine carbon appears at δ 18.7. The two non-equivalent N-methyl carbons were observed to absorb at δ 38.6 and 38.7. In the normal scale spectrum, these two absorptions appear as only one signal. But upon scale expansion (Figure 52b), this signal is resolved into two peaks. The signals at δ 128.2, 129.7, 131.7 and 137.9 were assigned to the phenyl ring carbons. Also the signals at δ 165.7 and 176.4 were assigned to the imine carbon and the carbonyl carbon, respectively.

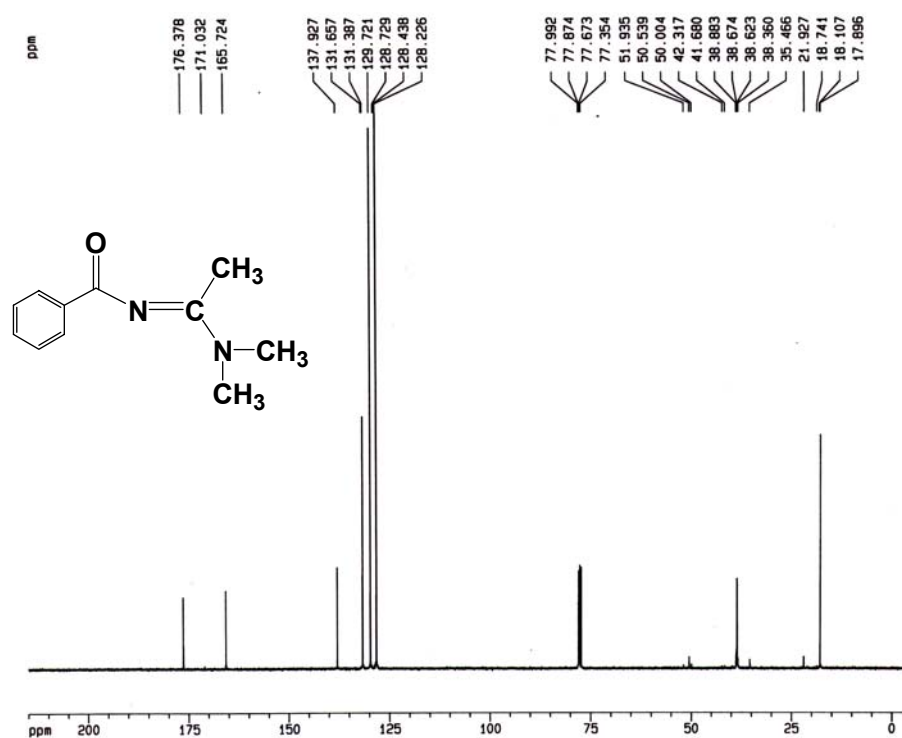


Figure 52a: ^{13}C -NMR spectrum of the dark liquid

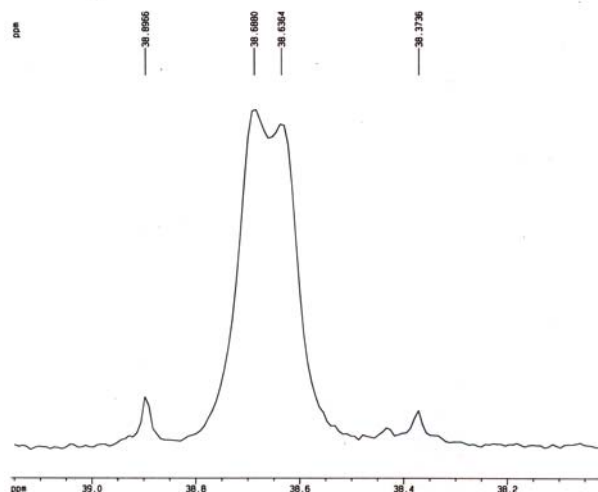


Figure 52b: ^{13}C -scale expansion spectrum of the dark liquid

In order to confirm the above spectral assignments, the ^1H - ^{13}C NMR correlation spectrum was recorded. This spectrum (Figure 53) reveals that the signal at δ 18.7 in the ^{13}C -spectrum, which was assigned to the methyl carbon bonded to the imine carbon, correlates with the singlet (3H) at δ 2.23 in the ^1H -spectrum, which was assigned to the protons of the methyl group bonded to the imine carbon. The signals at δ 38.63 and 38.68 in the ^{13}C -spectrum, which were assigned to the two non-equivalent methyl carbons of the amino group, correlate with the two singlets (3H) at δ 2.97 and 3.07 in the ^1H -spectrum, which were also assigned to the two non-equivalent methyl groups bonded to the amino group. The spectrum also reveals that the signals at δ 128.2, 129.7 and 131.7 in ^{13}C -spectrum correlate with the two multiplets at δ 7.31-7.39 and δ 8.07-8.12 in the ^1H -spectrum, which were assigned to the protons of the phenyl group. The spectrum also allows to assign the signals at δ 128.2 and 131.7 in the ^{13}C -spectrum to the para-meta phenyl ring carbons. Thus, the signal at δ 129.7 can be assigned to the ortho-phenyl ring carbons.

The signal at δ 137.9 in the ^{13}C -spectrum disappears in the ^1H - ^{13}C spectrum, this indicates that this signal is due to the phenyl ring carbon at position 1. The signals at δ 165.7 and 176.7 in the ^{13}C -spectrum also disappear in the ^1H - ^{13}C spectrum, this is consistent with the assignment of these two quaternary carbons to the imine carbon and the carbonyl carbon.

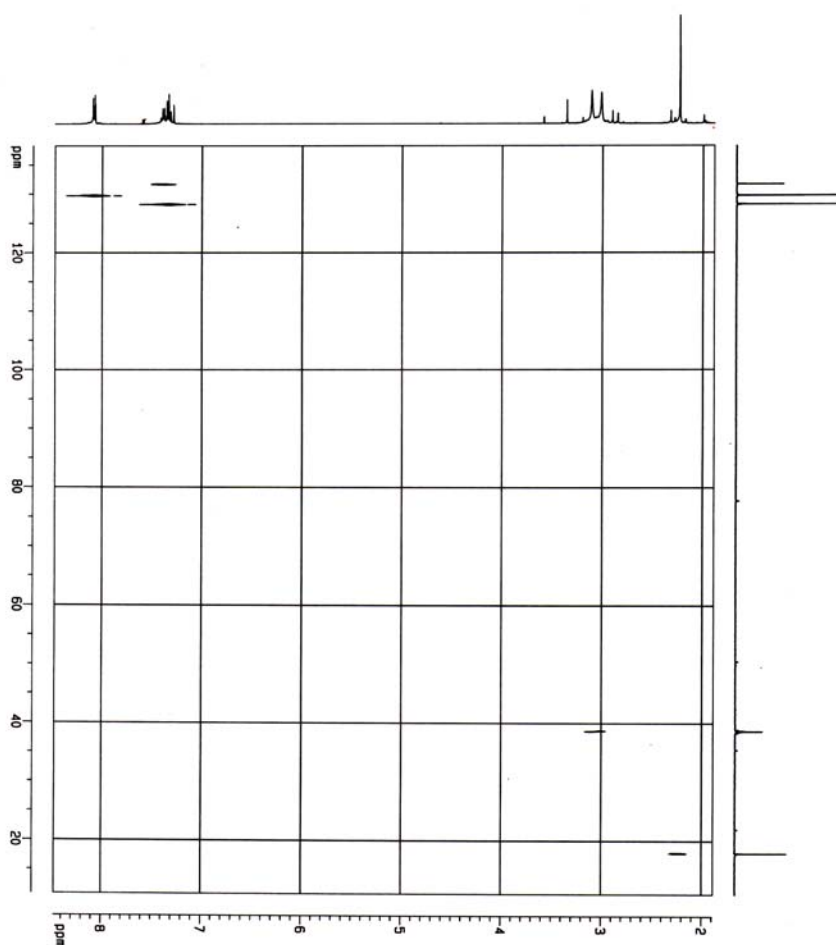
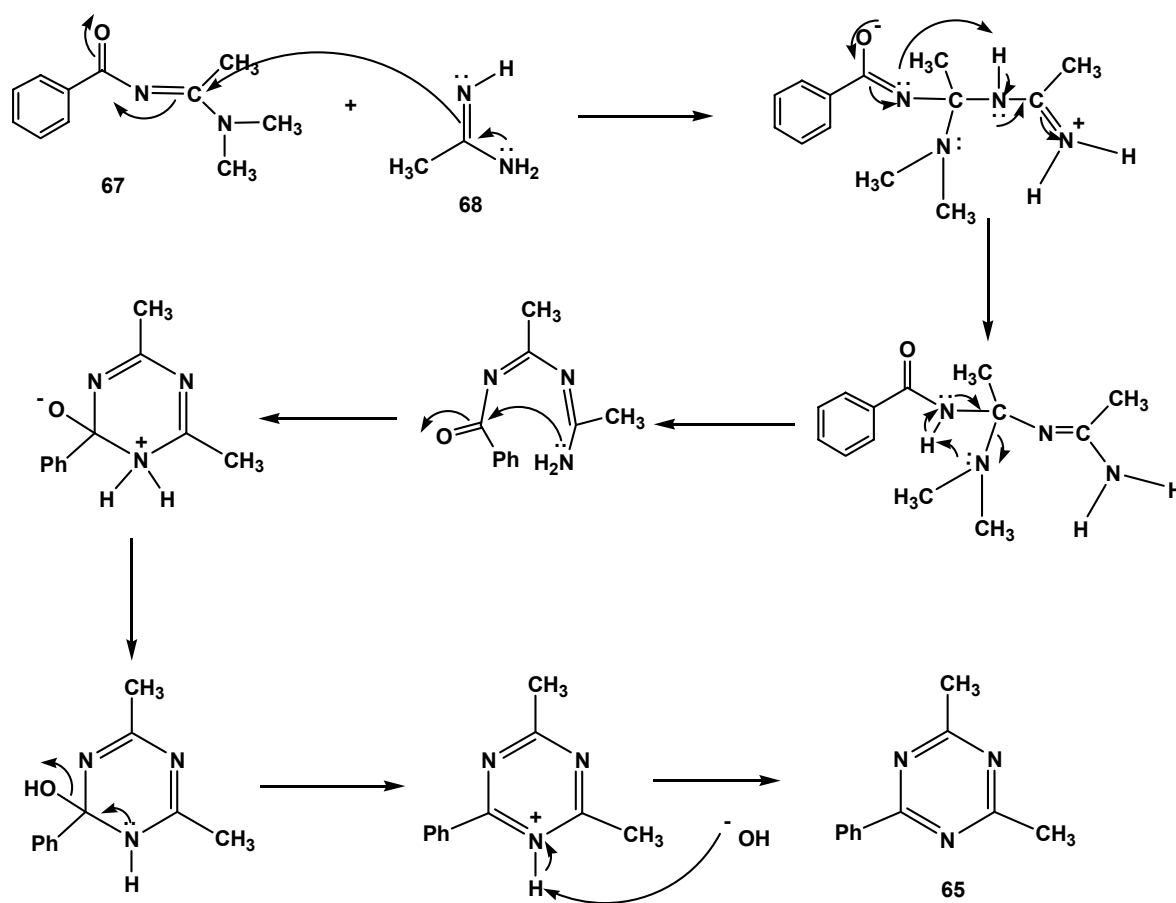


Figure 53: ^1H - ^{13}C correlation spectrum of the dark liquid

According to the literature,¹⁴ the melting point of this compound was reported at 47°C, thus, in this synthesis the amidine product was expected to obtain as a solid. But in this synthesis, even though the product was obtained as a dark viscous liquid, however, all the NMR and mass spectroscopic results are consistent with the assignment of this product to N-[(dimethylamino)ethylidene]benzamide (**67**).

2.3.3.2 Synthesis of 2,4-dimethyl-6-phenyl-1,3,5-triazine

The condensation between **67** and acetamidine (**68**) in refluxing anhydrous tetrahydrofuran led to the formation of 2,4-dimethyl-6-phenyl-1,3,5-triazine (**65**) in 14.6% as a light yellow liquid. Scheme 27 shows the proposed mechanism for the formation of 2,4-dimethyl-6-phenyl-1,3,5-triazine (**65**).



Scheme 27: Synthesis of 2,4-dimethyl-6-phenyl-1,3,5-triazine

The GC-trace [110°C (10 min), 10°C/min to 240°C (30 min)] of the crude product (Figure 54a) indicates the presence of more than one product. The mass spectrum of the peak that eluted with a retention time of 16.3 min (Figure 54b) exhibits a molecular ion at m/z 185, thus, this peak was expected to be the desired triazine **65** (MW 185).

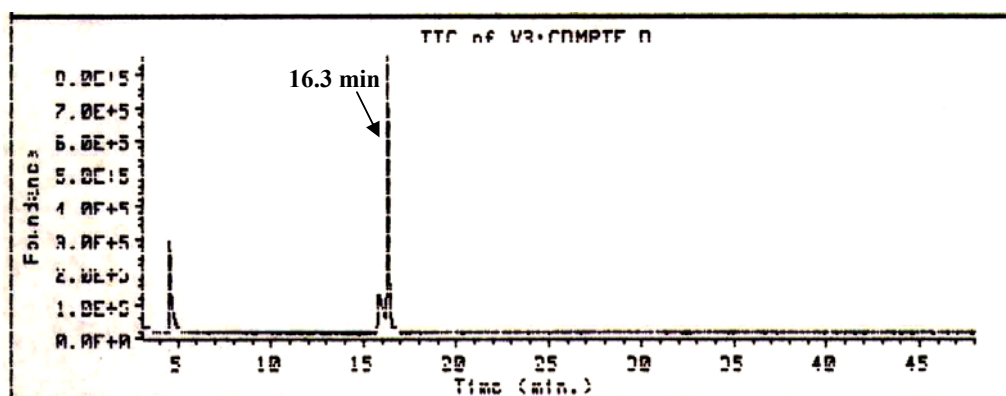


Figure 54a: GC-trace of the crude product from the synthesis of **65**

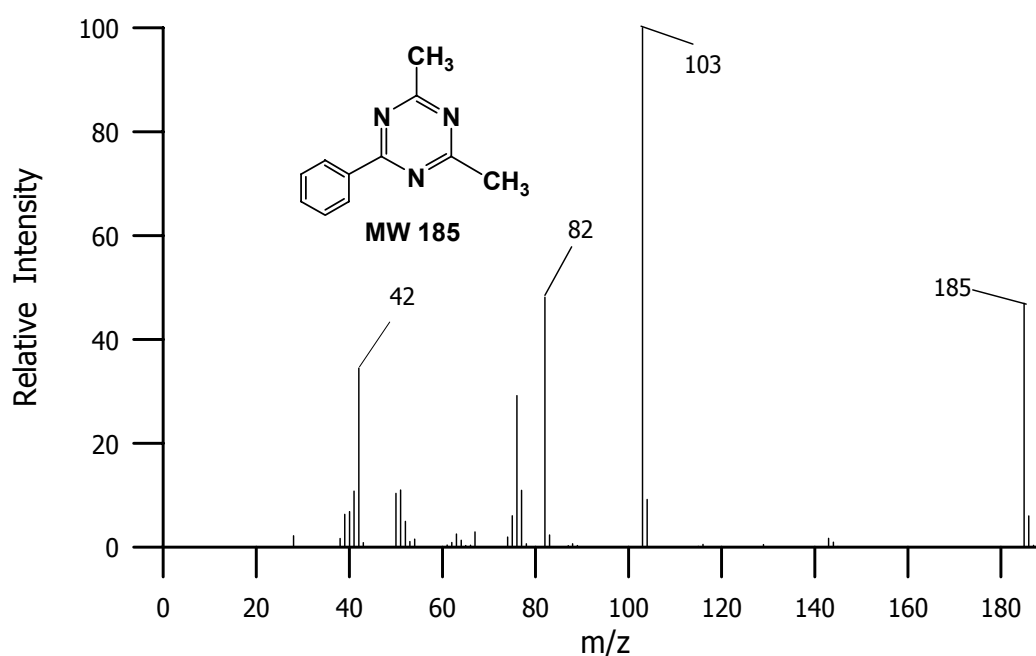


Figure 54b: Mass spectrum of the peak eluted with a retention time of 16.3 min

This crude product was purified by preparative thin-layer chromatography. The highest band with a R_f of 0.79 was removed and extracted with ethyl acetate. The solvent was removed to give a light yellow viscous liquid. This liquid was analyzed by the GC interfaced with a mass spectrometer. The GC-chromatogram exhibited a major component with a retention time of 16.3 min. The mass spectrum of this component was identical to the mass spectrum shown in Figure 54b, which showed a molecular ion at

m/z 185 which is consistent with the molecular weight of **65**. The spectrum also showed a base peak at m/z 103 and a peak at m/z 82, which corresponded to the cleavage of $[\text{C}_6\text{H}_5\text{CN}]^+$ and $[\text{C}_4\text{H}_6\text{N}_2]^+$, respectively, from **65**.

The $^1\text{H-NMR}$ spectrum of this yellow liquid (Figure 55) exhibits a singlet at δ 2.67, which is expected due to the absorption of the protons of the two equivalent methyl groups substituted on the triazine ring. The two multiplets at δ 7.44-7.55 (3 H) and δ 8.47-8.49 (2H) were assigned to para-meta and ortho-phenyl ring protons, respectively.

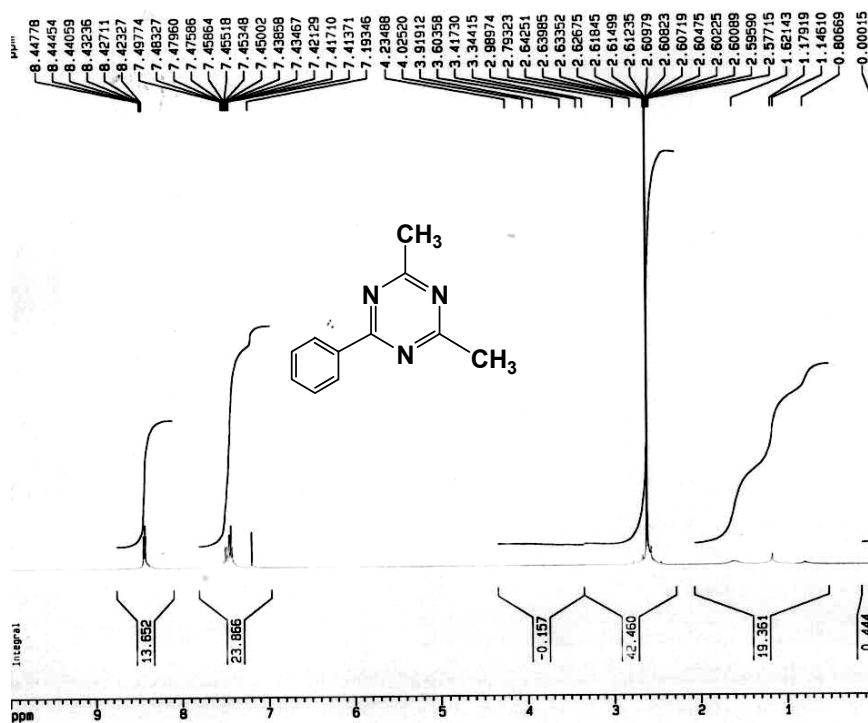


Figure 55: $^1\text{H-NMR}$ spectrum of the yellow liquid expected to be **65**

The ^{13}C - NMR spectrum of this yellow liquid (Figure 56a) also reveals the signals correspond to the structure of **65**. The signal at δ 25.7 was assigned to the two equivalent methyl carbons on the triazine ring. The signal at δ 171.2 was assigned to the triazine ring carbon at position 6. The two equivalent triazine ring carbons at positions 2 and 4 absorb at the same chemical shift of δ 176.3. The four signals at δ 128.6, 128.8, 132.5 and 135.5 were assigned to the phenyl ring carbons. This assignment also corresponds to the signals appear in the ^{13}C -DEPT 135 spectrum (Figure 56b). The signal at δ 25.7 still appears in the ^{13}C -DEPT 135 spectrum. This is consistent with the assignment to the two equivalent methyl carbons. The two signals at δ 171.2 and 176.4 disappear in the ^{13}C -DEPT 135 spectrum, which corresponds to the assignment of the three quaternary triazine ring carbons.

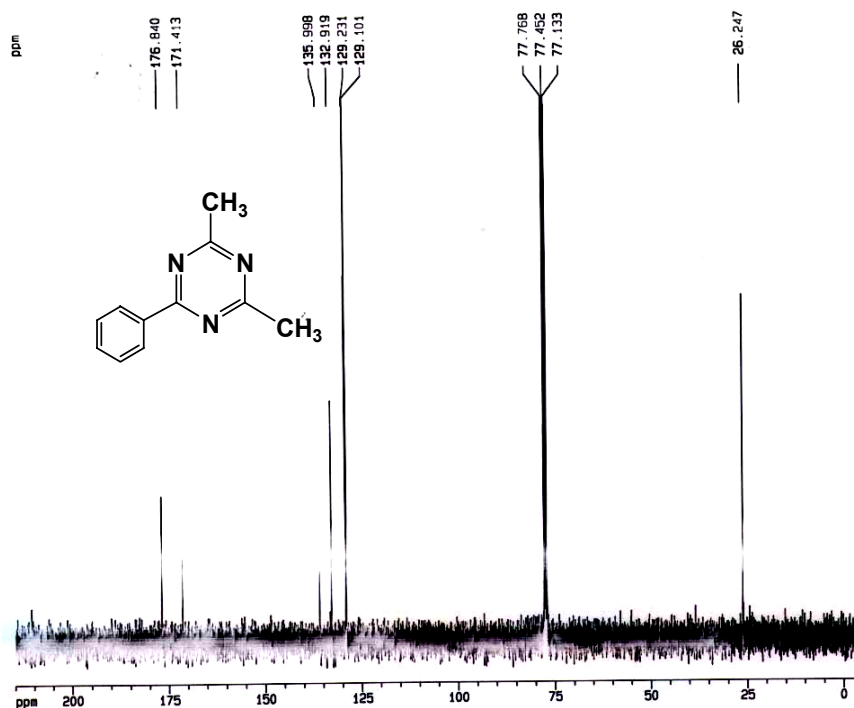


Figure 56a: ^{13}C - NMR spectrum of the yellow liquid expected to be **65**

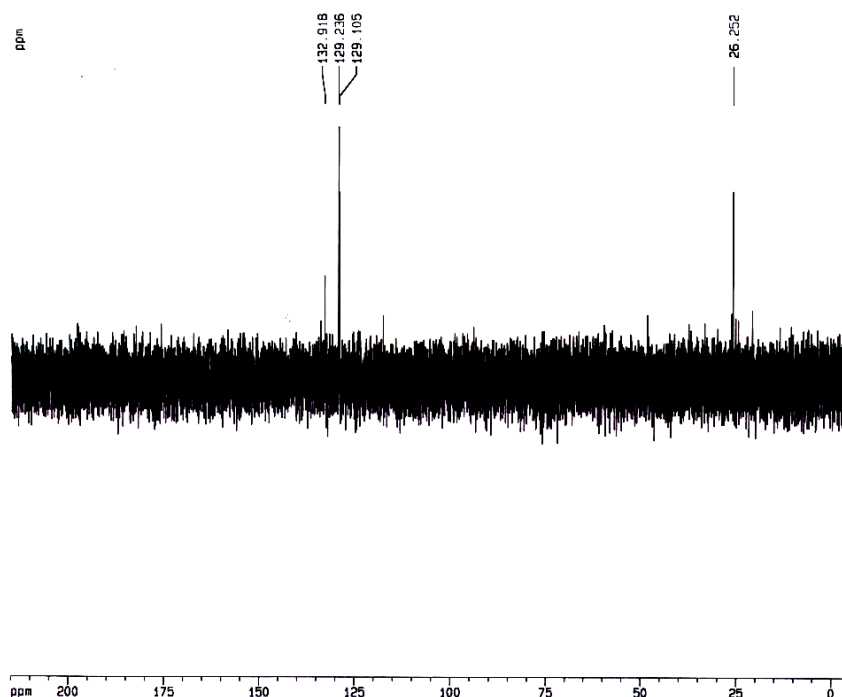
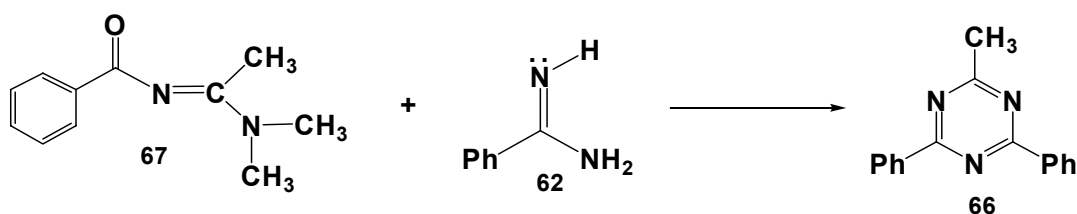


Figure 56b: ^{13}C -DEPT 135 spectrum of the yellow liquid expected to be **65**

2.3.3.3 Synthesis of 2-methyl-4,6-diphenyl-1,3,5-triazine

Raymond Dengino and colleagues did not report the synthesis of 2-methyl-4,6-diphenyl-1,3,5-triazine (**66**). However, by analogy with the synthesis of **65**, it should be possible to synthesize **66** by the reaction of N-[(dimethylamino)ethylidene]benzamide (**67**) with benzamidine (**62**) instead of acetamidine (**68**), as shown in Scheme 28.



Scheme 28: Possible synthetic method of 2-methyl-4,6-diphenyl-1,3,5-triazine

Thus, by using this procedure, 2-methyl-4,6-diphenyl-1,3,5-triazine (**66**) was synthesized from **67** and **62**. The product was obtained in 12.5 % as a white solid and was characterized by ^1H -, ^{13}C -NMR and mass spectrometry.

The GC-analysis [110°C (5 min), 10°C/min to 240°C (30 min)] of the white solid (Figure 57a) shows the presence of two components. The mass spectrum of the major peak (Figure 57b), which eluted with a retention time of 32.4 min, exhibits a molecular ion at m/z 247, which corresponds to the molecular weight of **66** (MW 247). The spectrum also exhibits a base peak at m/z 103, which is consistent with the cleavage of $[\text{C}_6\text{H}_5\text{CN}]^{\bullet+}$.

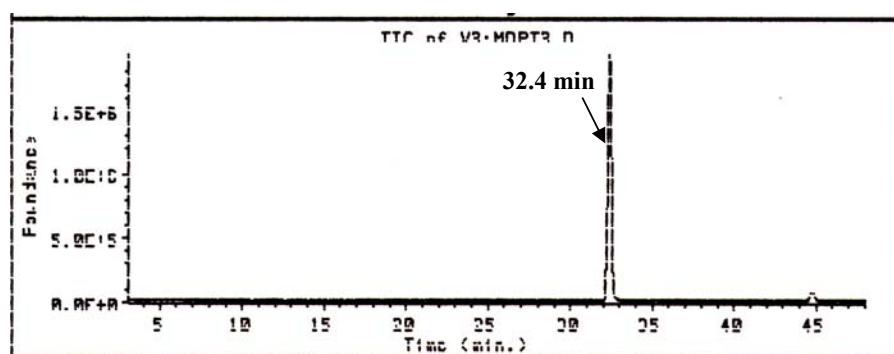


Figure 46a: GC-trace of the white solid expected to be **66**

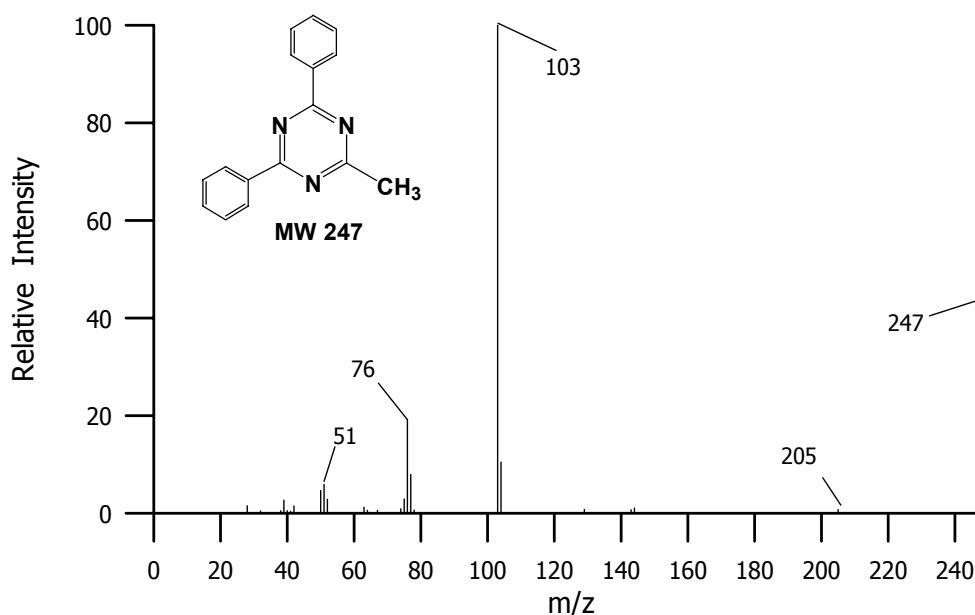


Figure 46b: Mass spectrum of the peak eluted at a retention time of 32.4 min

The ^1H -NMR spectrum of this white solid (Figure 58) exhibits a 3H singlet at δ 2.77, which was assigned to the proton of the methyl group substituted on the triazine ring. The two multiplets at δ 7.46-7.57 (6H) and δ 8.61-8.64 (4H) were assigned to the meta-para and ortho-phenyl ring protons, respectively.

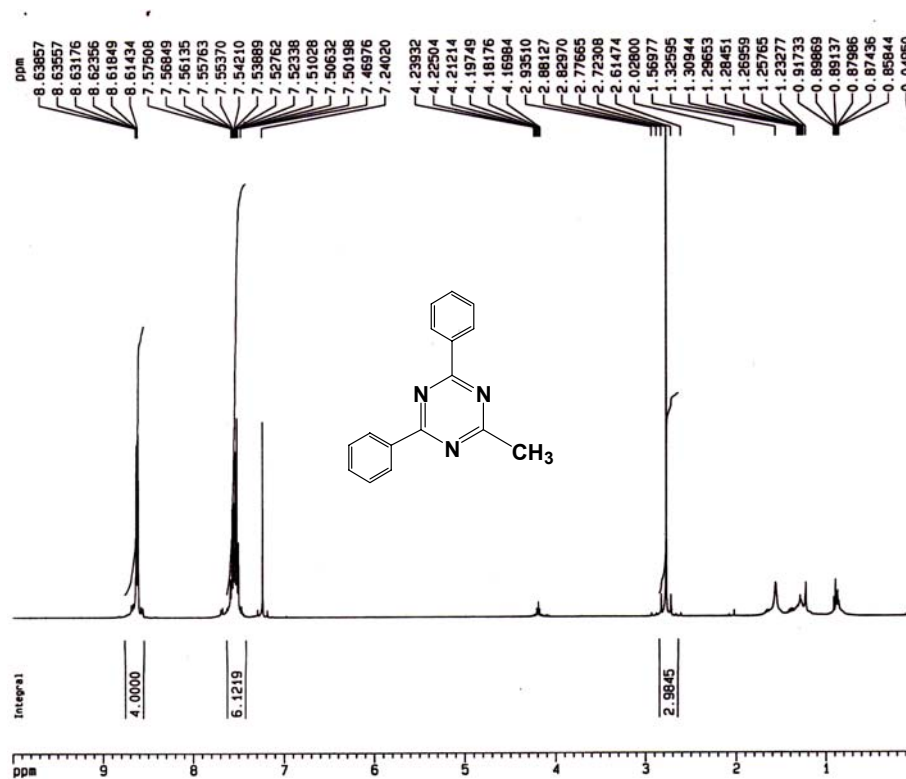


Figure 58: ^1H -NMR spectrum of the white solid

The ^{13}C -NMR spectrum (Figure 59a) reveals the methyl signal at δ 26.5. The two equivalent phenyl ring carbons absorb at δ 129.1, 129.3, 132.9 and 136.3. The triazine ring carbon at position 2 appears at δ 177.5 while the two equivalent triazine ring carbons at positions 4 and 6 absorb at δ 171.6. These ^{13}C -spectral assignments can be confirmed by the ^{13}C -DEPT 135 spectrum. The spectrum (Figure 59b) still reveals the signal at δ 26.5 as expected for a signal due to a methyl carbon. The two signals at δ 171.6 and 177.5, however, disappear in the ^{13}C -DEPT 135 spectrum. This is consistent with the assignment

of these signals to the three quaternary carbons of the triazine ring. In the phenyl region, the signal at δ 136.3 disappears in the ^{13}C -DEPT 135 spectrum and can, therefore, be assigned to the carbon at position 1 of the phenyl ring.

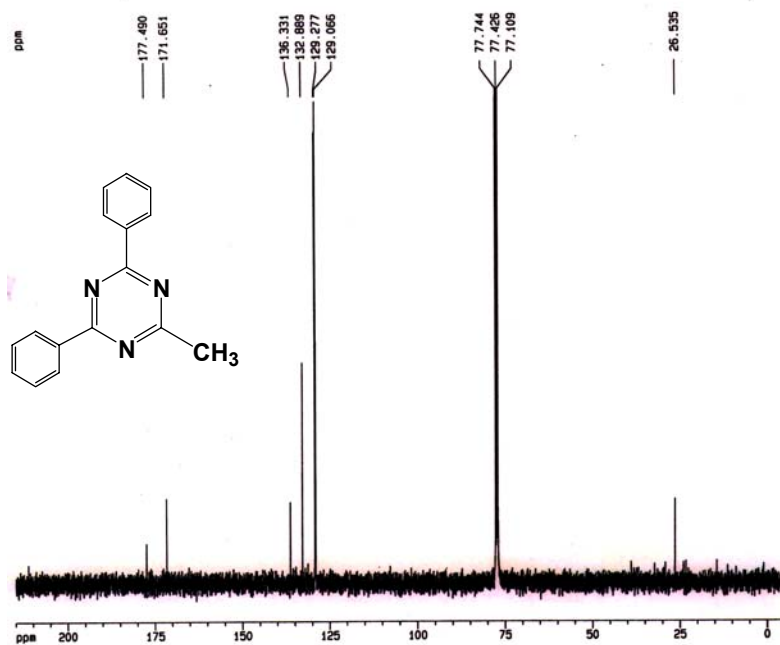


Figure 59a: ^{13}C -NMR spectrum of the white solid

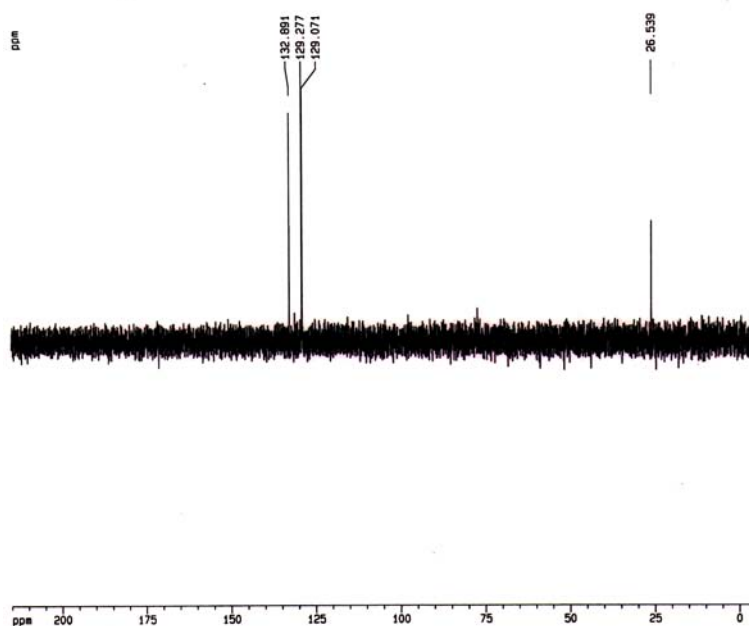


Figure 59b: ^{13}C -DEPT 135 spectrum of the white solid

2.3.4 Photochemistry of 3-methyl-5-phenyl-1,2,4-thiadiazole

The studies presented in this thesis have indicated that 5-phenyl-1,2,4-thiadiazole (**31**) undergoes phototransposition leading to the formation of 3-phenyl-1,2,4-thiadiazole (**46**). It also undergoes photofragmentation leading to the formation of benzonitrile (**43**) and photo ring-expansion leading to the formation of 2-phenyl- and 2,4-diphenyl-1,3,5-triazine (**39**) and (**40**). However, in the case of **46**, only **43** was observed in 75% upon irradiation of this compound. There is no evidence indicating the formation of **31**, the phototransposition product expected upon irradiation of **46**.

This work was also extended to study the photochemistry of disubstituted 3-methyl-5-phenyl-1,2,4-thiadiazole. Based on the observed photochemistry of **31**, the photoproducts expected upon irradiation of **54** would be benzonitrile (**43**), 5-methyl-3-phenyl-1,2,4-thiadiazole (**57**), 2,4-dimethyl-6-phenyl-1,3,5-triazine (**65**) and 2-methyl-4,6-diphenyl-1,3,5-triazine (**66**).

The photochemistry of **54** was first studied in acetonitrile solvent. A solution of **54** (6.0×10^{-5} M, 10 mL) was placed in a quartz cuvette. This solution was irradiated with three > 290 nm lamps through a Pyrex filter. The reaction was monitored by ultraviolet absorption spectroscopy at 40 sec intervals. Figure 60a shows the ultraviolet absorption spectrum of the solution before irradiation. The spectrum reveals the λ_{max} at 278 nm with an extinction coefficient of $14,100 \text{ L mol}^{-1} \text{ cm}^{-1}$. Figure 60b exhibits the UV-overlay spectrum of the photolysis of this compound. The spectrum reveals the decreasing of the absorption band at λ 278 nm from 0.85 to 0.7 which is due to the consumption of the reactant **54**. It also reveals the increasing of the absorption band at λ 261 nm from 0.56 to 0.65.

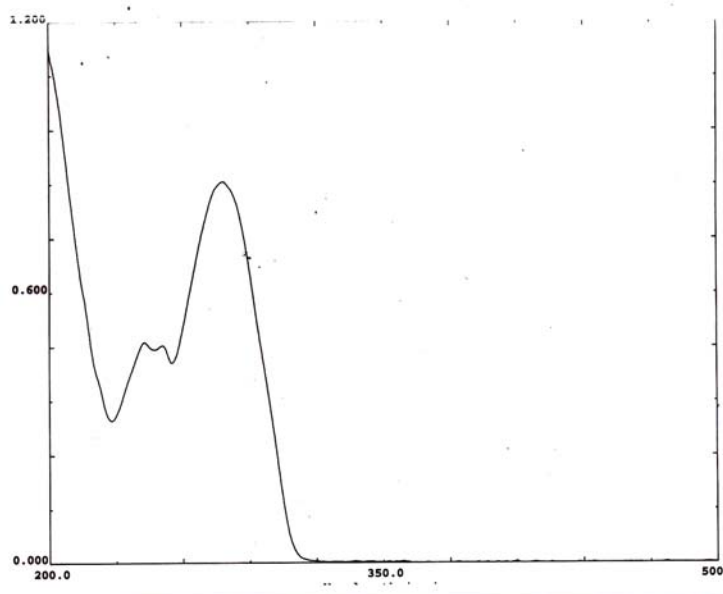


Figure 60a: UV-absorption spectrum of **54** in acetonitrile before irradiation

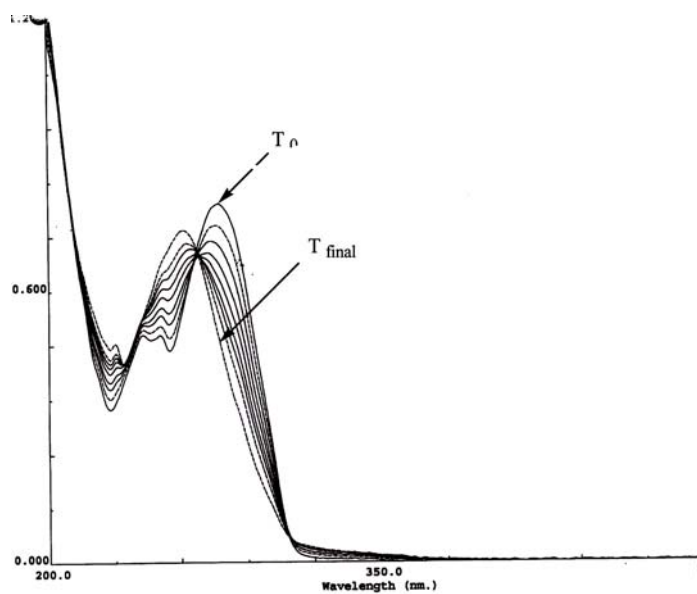


Figure 60b: UV-overlay spectrum of the photolysis of **54** in acetonitrile

The photolysis was also monitored by GLC. A solution of **54** (2.0×10^{-2} M, 4 mL) was placed into a Pyrex tube (0.7 cm \times 13.5 cm), sealed with a rubber septum and purged with argon for 30 min. The solution was irradiated with sixteen > 290 nm lamps and monitored by gas liquid chromatography [140°C (4 min), 10°C/min to 240°C (20 min)] at 40 min intervals. Figure 61a shows the GLC analysis of the solution before irradiation. The trace exhibits a major peak with a retention time of 12 min, which is due to the reactant **54**. Figure 61b shows the GC-trace of the reaction mixture after 150 min of irradiation time. The trace reveals the consumption of 76.4 % of the reactant and the formation of four new peaks with retention time of 5, 11.5, 13.5 and 28 min.

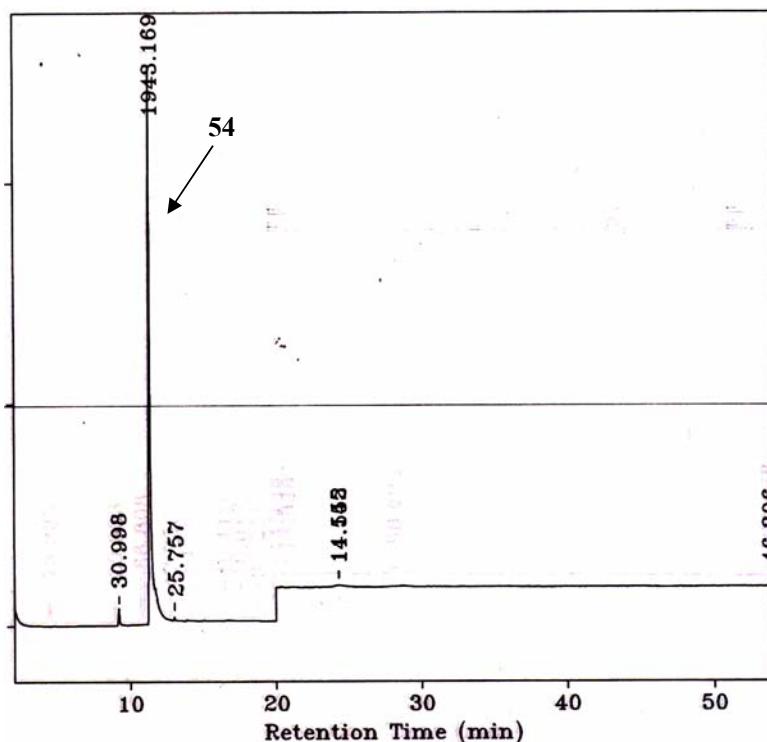


Figure 61a: GLC analysis of **54** in acetonitrile before irradiation

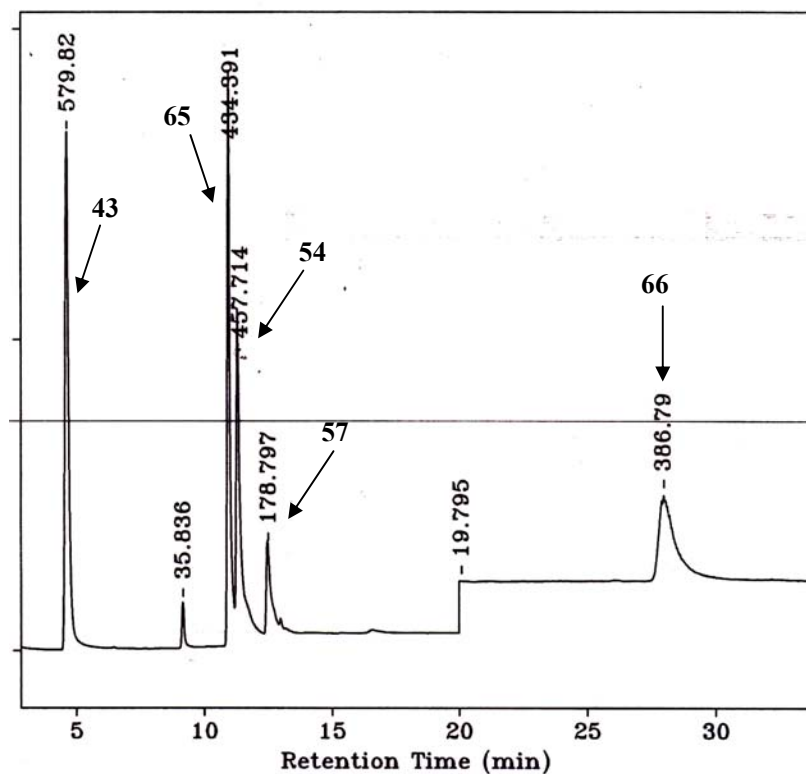


Figure 61b: GLC analysis of the reaction mixture after 150 min of irradiation

The reaction mixture was concentrated by rotary evaporation at room temperature and analyzed again by GC-MS [140°C (5 min), 10°C/min to 240°C (30 min)]. Figure 62a exhibits GC-trace of this concentrated reaction mixture. The trace shows four major gc-volatile components with retention times of 4.1, 13.0, 14 and 29.2 min. The mass spectrum of the first eluted component (Figure 62b) exhibits a base molecular ion peak at m/z 103, which could be due to **43**. This was confirmed by comparison of the chromatographic and mass spectrometric properties of this component with an authentic sample of **43**.

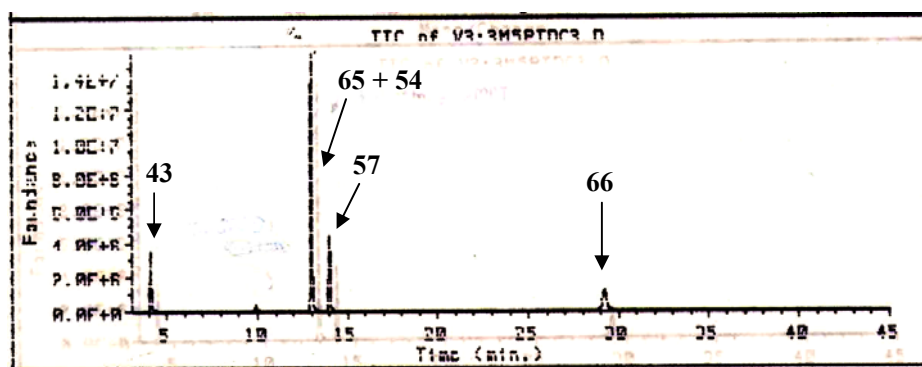


Figure 62a: GC-analysis of the concentrated reaction mixture

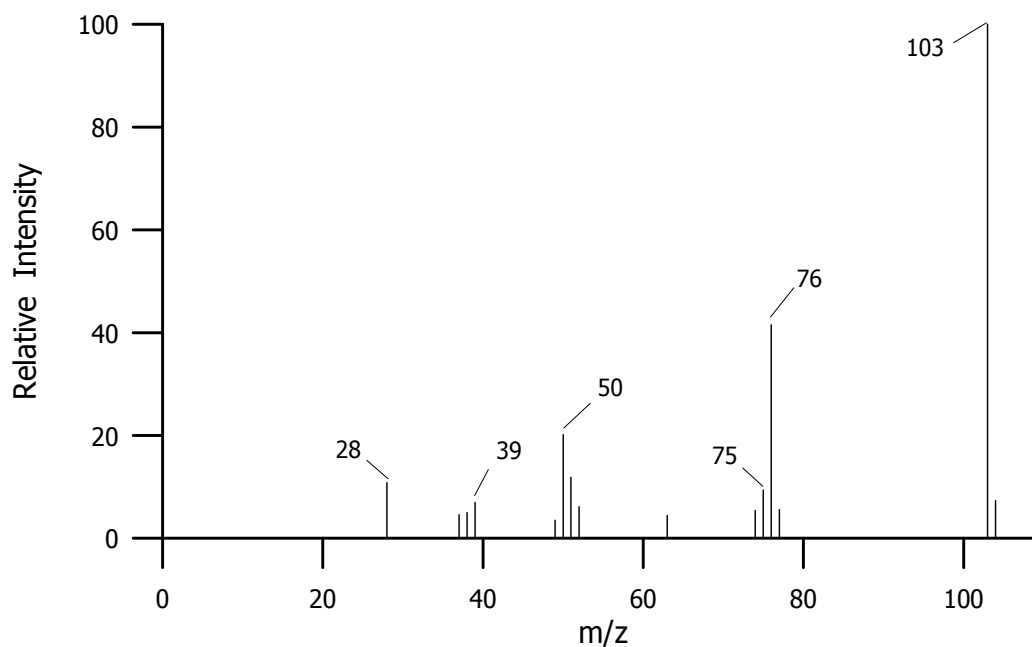


Figure 62b: Mass spectrum of the peak eluted at a retention time of 4.1 min

By direct comparison of the mass spectrum and GC-retention time of the first eluted photoproduct with these of an authentic sample of **43**, it confirms that the first eluted photoproduct is benzonitrile (**43**).

The mass spectrum of the peak that eluted with a retention time of 29.2 min (Figure 62c) exhibits a molecular ion at m/z 247. This photoproduct was expected, by analogy of the results from the photolysis of **31**, to be 2-methyl-4,6-diphenyl-1,3,5-triazine (**66**). The molecular ion at m/z 247 corresponds to the molecular weight of **66** (MW 247).

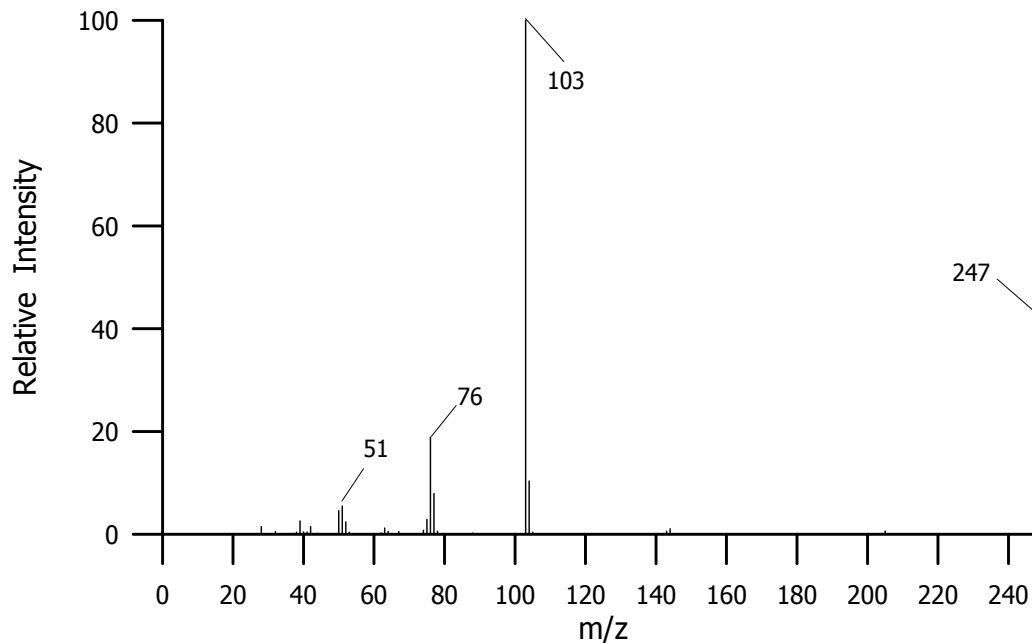


Figure 62c: Mass spectrum of the peak eluted at a retention time of 29.2 min

In order to confirm the formation of this photoproduct, an authentic sample of **66** was analyzed by GC-MS. This compound eluted with a retention time of 29.3 min, which is the same as the retention time of the product peak. The mass spectrum of this authentic sample also exhibited a molecular ion at m/z 247 and a base peak at m/z 103, which was due to $[C_6H_5CN]^+$. The fragmentation pattern of this authentic sample was identical to the fragmentation pattern of the photoproduct. According to this information, the peak that eluted with a retention time of 29.2 minutes can be identified as 2-methyl-4,6-diphenyl-1,3,5-triazine (**66**).

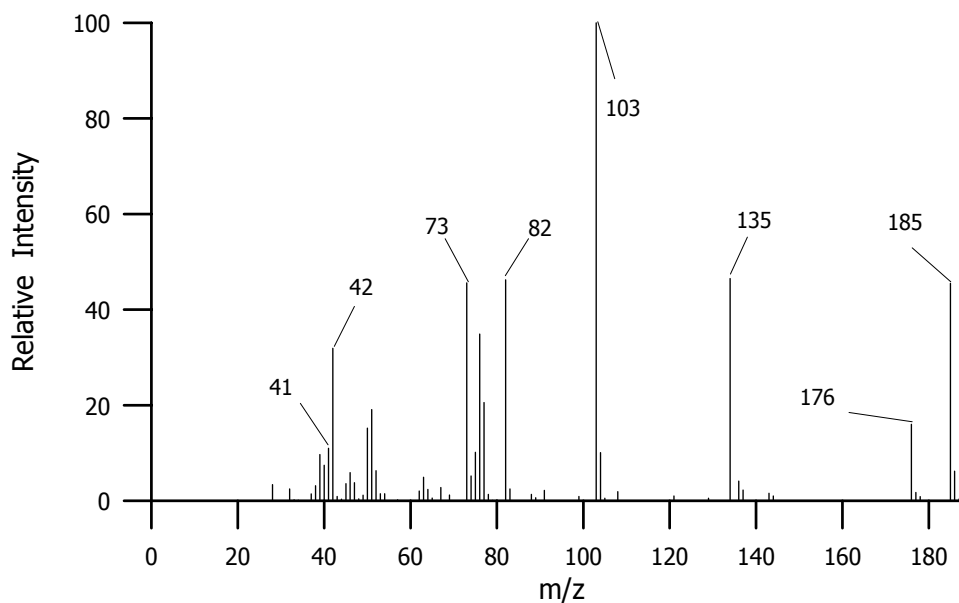


Figure 62d: Mass spectrum of the peak eluted at a retention time of 13 min

The mass spectrum of the peak, which eluted with a retention time of 13 min (Figure 62d) exhibits a molecular ion at m/z 185 and a base peak at m/z 103. Based on the molecular weight and the fragmentation pattern, this compound was suspected to be 2,4-dimethyl-6-phenyl-1,3,5-triazine (**65**), another possible photoproduct. Therefore, an authentic sample of **65** was analyzed by GC-MS in order to compare its chromatographic and mass spectral properties with those of the photoproducts. Authentic 2,4-dimethyl-6-phenyl-1,3,5-triazine also eluted with a retention time of 13 min.

The mass spectrum of an authentic sample of **65** (Figure 63) shows a molecular ion at m/z 185, a base peak at m/z 103 which is due to $[C_6H_5CN]^{*+}$ and a peak at m/z 82 with an intensity of 49.1% of the base peak which is due to $[C_4H_6N_2]^+$.

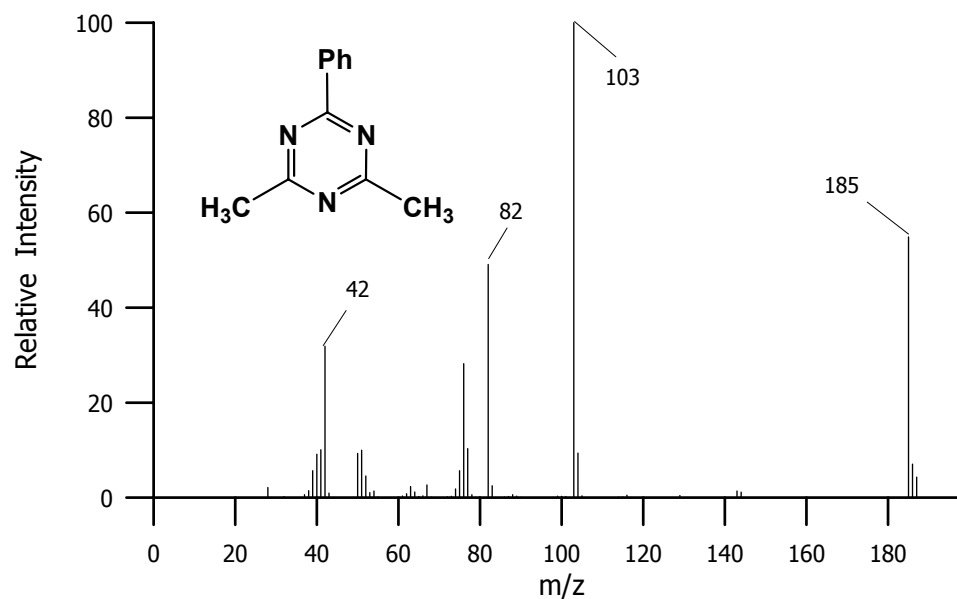


Figure 63: Mass spectrum of an authentic sample of **65**

Comparison between Figures 62d and 63, the mass spectrum of an authentic sample of **65** is not totally identical with the mass spectrum of the photoproduct. Although, the mass spectrum of the photoproduct (Figure 62d) exhibits a molecular ion at m/z 185, a base peak at m/z 103, a peak at m/z 82, the spectrum also reveals peaks at m/z 135 and m/z 73. These two peaks are certainly not due to **65**. However, it was suspected that this peak may be due to an overlap of the peaks due to **65** and the reactant **54**. Since the GC-analysis and the mass spectrum of **54** before irradiation (Figure 64a-b) show that **54** also has a retention time of 13 min. Furthermore, the mass spectrum (Figure 64b) exhibits a molecular ion at m/z 176, a base peak at m/z 135 which is due to $[\text{C}_6\text{H}_5\text{CNS}]^{+\bullet}$, a peak at m/z 73 which is due to $[\text{C}_2\text{H}_3\text{NS}]^{+\bullet}$. All of these major fragments are observed in the mass spectrum of the photoproduct peak.

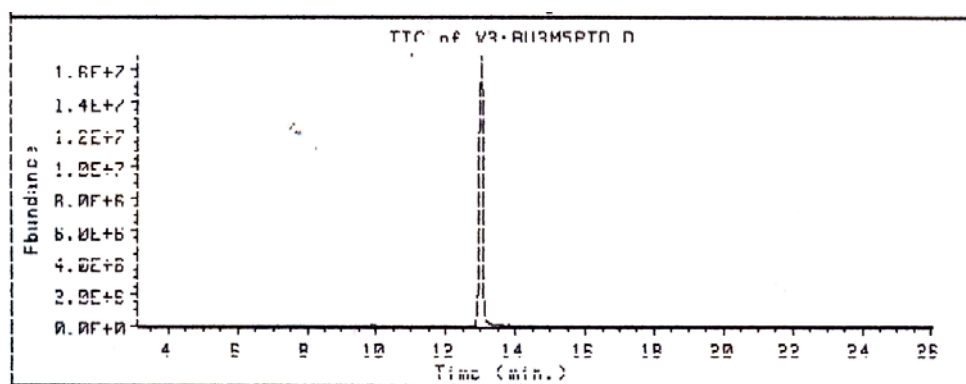


Figure 64a: GC-trace of 3-methyl-5-phenyl-1,2,4-thiadiazole before irradiation

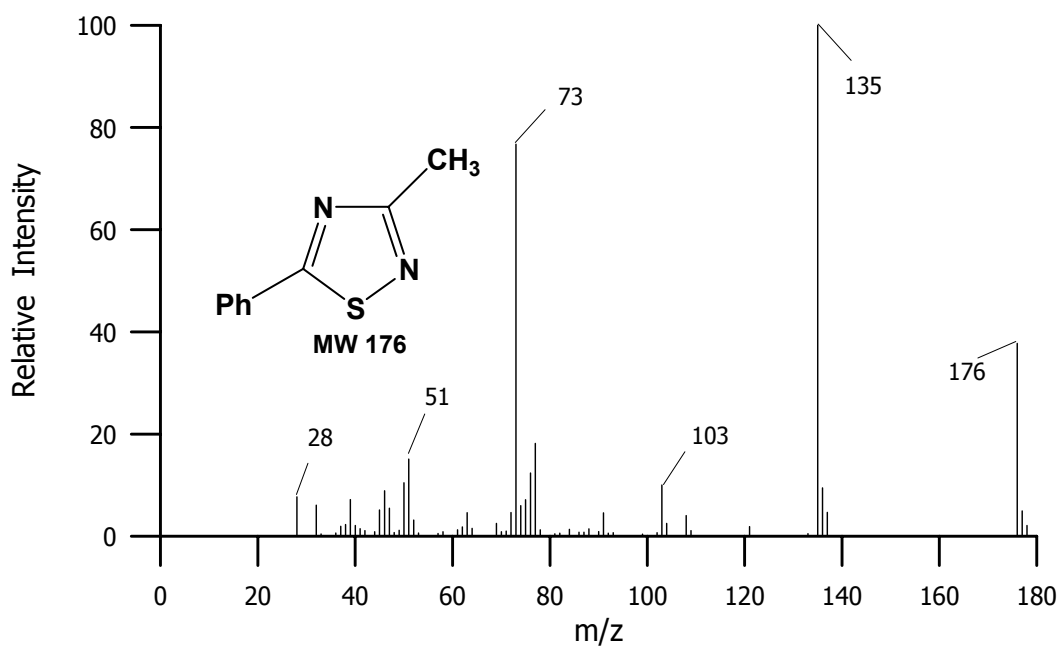


Figure 64b: Mass spectrum of 3-methyl-5-phenyl-1,2,4-thiadiazole

Moreover, according to the GC-trace (PE-9000) of the mixture after 150 min of irradiation, which is shown in Figure 61b, reveals two partially resolved peaks at retention time of approximately 13 min. One of these peaks is due to the reactant, **54**, and another one is due to a photoproduct. Although these two compounds are resolved in the GC PE-9000, they are not resolved on the gas chromatograph interfaced to the mass detector. Thus, the mass spectrum shown in Figure 62d is the mass spectrum of a mixture of 2,4-dimethyl-6-phenyl-1,3,5-triazine (**65**) and 3-methyl-5-phenyl-1,2,4-thiadiazole (**54**).

The mass spectrum of the peak which eluted with a retention time of 14 min (Figure 62e) exhibits a molecular ion at m/z 176, and is therefore isomeric with **54**. This product was expected to be 5-methyl-3-phenyl-1,2,4-thiadiazole (**57**), the expected transposition product. By comparison of GC-retention time and mass spectral pattern of this product with those of an authentic sample of **57**, this product could, therefore, be identified as the phototransposition product, 5-methyl-3-phenyl-1,2,4-thiadiazole (**57**).

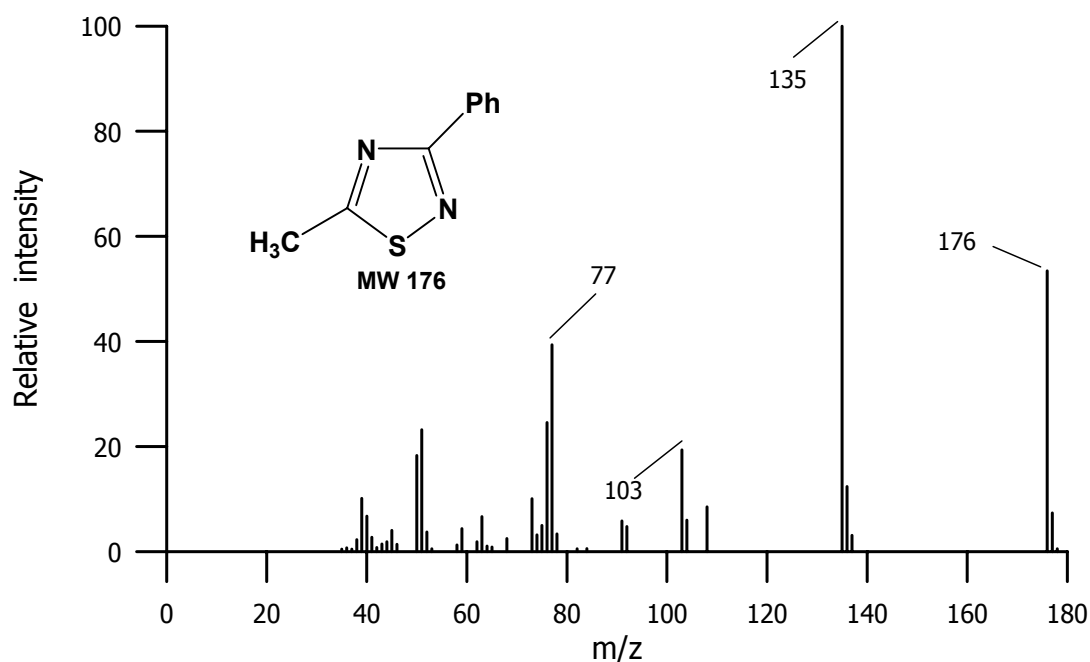


Figure 62e: Mass spectrum of the peak eluted with a retention time of 14 min

2.4 Photochemistry of 5-phenyl-1,2,4-thiadiazole-4¹⁵N

2.4.1 Synthesis of 5-phenyl-1,2,4-thiadiazole-4¹⁵N

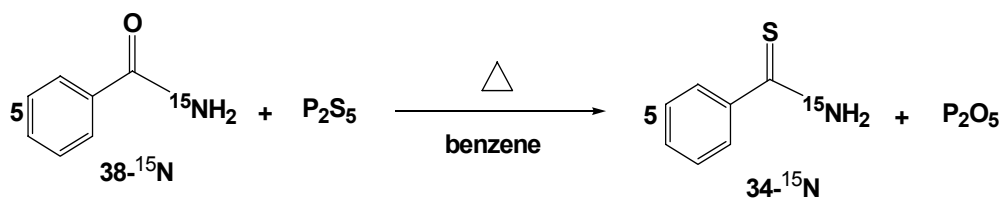
5-phenyl-1,2,4-thiadiazole (**31**) was synthesized in two steps according to the procedure described by Yang-I Lin and colleagues.⁹ The first step was to synthesize N-[(dimethylamino)methylene]thiobenzamide (**32**) by the reaction of thiobenzamide (**34**) with N,N-dimethylformamide dimethylacetal (**35**). Then, amination cyclization of **32** with hydroxylamine-O-sulfonic acid (**33**) gave **31** as a colorless viscous liquid.

Thus, in the synthesis of 5-phenyl-1,2,4-thiadiazole-4¹⁵N (**31-4¹⁵N**), thiobenzamide-¹⁵N (**34-¹⁵N**) was required. Since this compound was commercially not available, it was synthesized by thionation of benzamide-¹⁵N (**38-¹⁵N**) with phosphorus pentasulfide.

2.4.1.1 Synthesis of thiobenzamide-¹⁵N

There are several methods for the synthesis of thioamides. The classical method is a thionation of the corresponding carboamide compound by reaction with phosphorus pentasulfide. Up to now, although there are several other thionating agents available for the conversion of a carboamide to thioamide, phosphorus pentasulfide is still one of the most widely used thionating agent.

Thiobenzamide-¹⁵N (**34-¹⁵N**) was synthesized in 51.3% by the thionation of **38-¹⁵N** (Scheme 29) with phosphorus pentasulfide in refluxing benzene solvent. Thiobenzamide-¹⁵N (**34-¹⁵N**) was identified by ¹H-, ¹³C-, ¹⁵N-NMR and mass spectrometry.



Scheme 29: Synthesis of thiobenzamide-¹⁵N

The mass spectrum of the synthetic **34-¹⁵N** (Figure 63a) exhibits the base molecular ion peak at m/z 138, which corresponds to the molecular weight of **34-¹⁵N**. The spectrum also exhibits a peak at m/z 137 with an intensity of 17.8% of the peak at m/z 138. This peak at m/z 137 could be due to an M-1 peak resulting from loss of hydrogen from the molecular ion or from the presence of thiobenzamide-¹⁴N (**34-¹⁴N**) in the sample. Figure 63b, however, shows that the mass spectrum of **34-¹⁴N** also exhibits a molecular ion at m/z 137 and an M-1 peak at m/z 136 with an intensity of 18.1% of the molecular ion peak. This confirms that loss of hydrogen is a normal fragmentation pathway for **34-¹⁴N** and therefore will also be a normal fragmentation pathway for **34-¹⁵N**. The peak at m/z 137 in the mass spectrum of **34-¹⁵N** is therefore not due to the presence of **34-¹⁴N** in the sample.

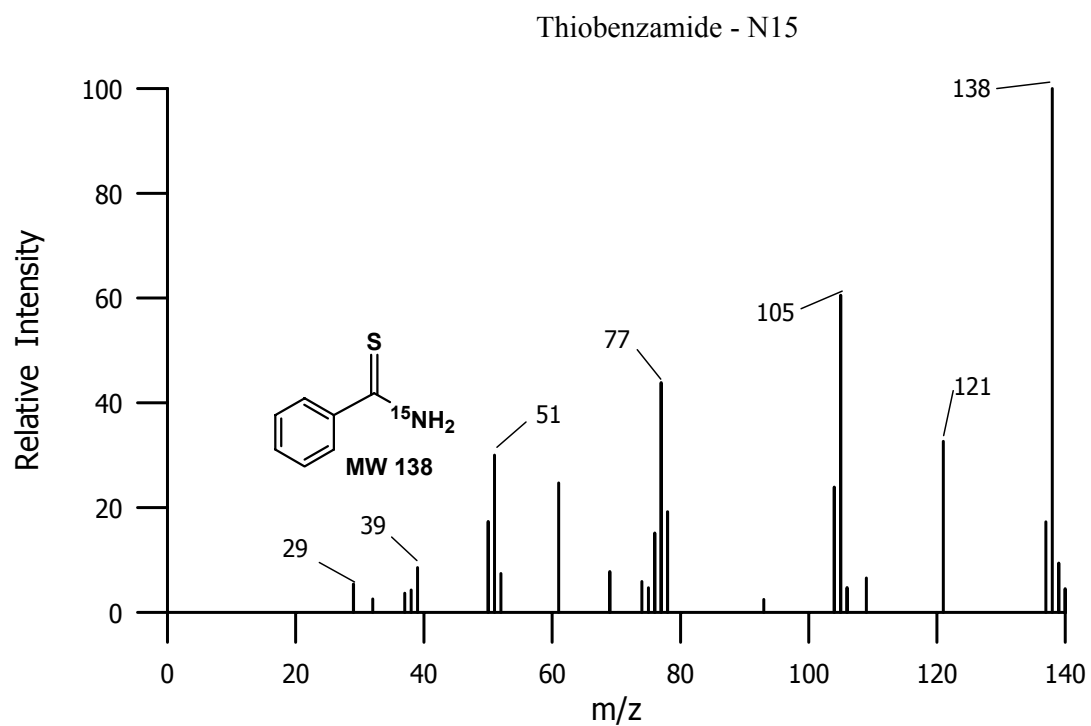


Figure 63a: Mass spectrum of thiobenzamide - ^{15}N

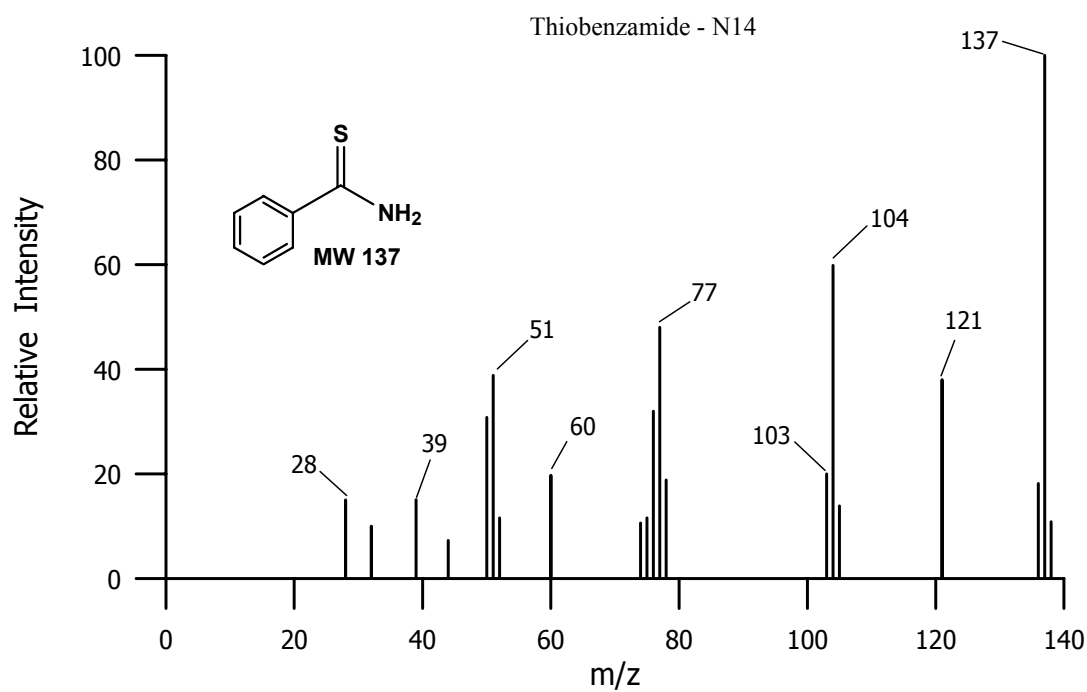


Figure 63b: Mass spectrum of thiobenzamide- ^{14}N

The ^1H -NMR spectrum (Figure 64a-b) of this synthesized thiobenzamide- ^{15}N ($34\text{-}^{15}\text{N}$) is more complicated than ^1H -NMR spectrum of $34\text{-}^{14}\text{N}$ due to the heteronuclear coupling between ^1H and ^{15}N . The two protons of the amino group are not equivalent due to the partial double bond character of the C-N bond. Therefore, these two protons will have different chemical shifts. These two signals appear (see Figure 64b) as double doublet at δ 7.06–7.30 and δ 7.70–7.94 due to ^1H - ^1H coupling ($J = 4.29$ Hz) and ^1H - ^{15}N coupling ($J = 89.2$ Hz) for the signal at δ 7.06–7.30 and $J = 92.7$ Hz for the signal at δ 7.70–7.94.

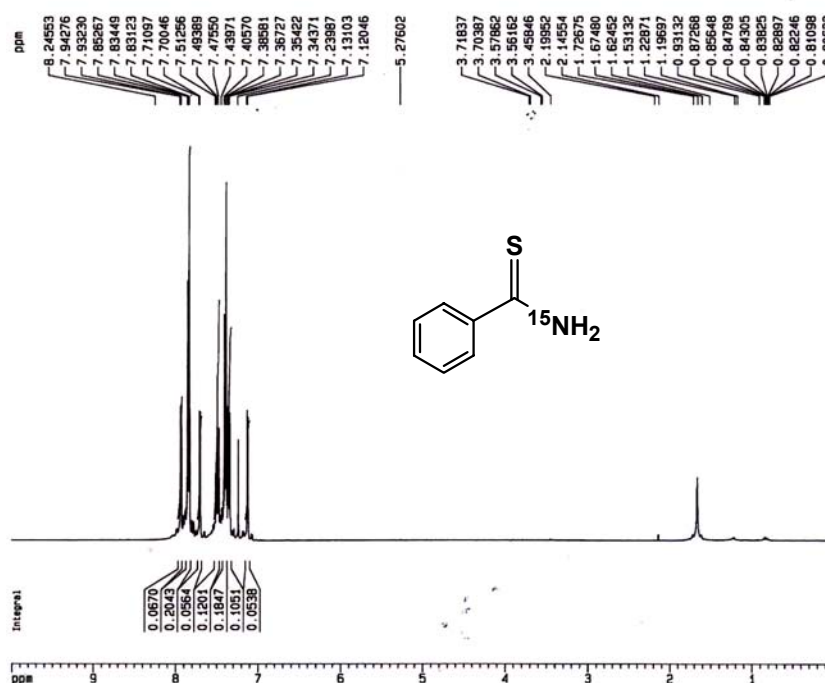


Figure 64a: ^1H -NMR spectrum of the synthesized thiobenzamide- ^{15}N

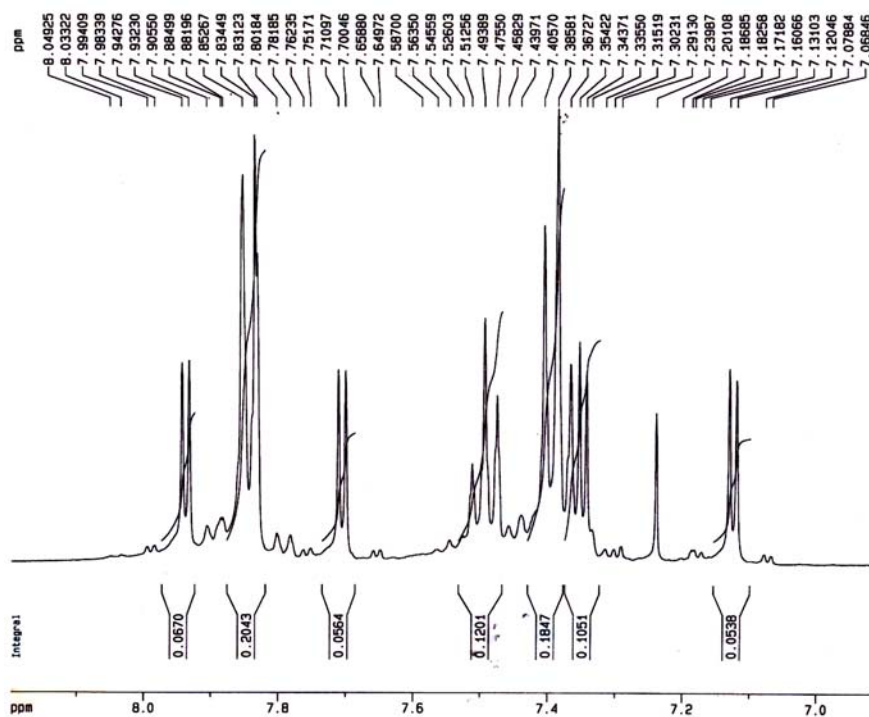


Figure 64b: ^1H -scale expansion spectrum of the synthesized thiobenzamide- ^{15}N

In addition to the signals expected for the ring carbon atoms, the ^{13}C -NMR spectrum of **34**- ^{15}N (Figure 65) exhibits a doublet for the thiocarbonyl carbon at δ 202.8 (d ; $J = 13.80$ Hz) due to ^{13}C - ^{15}N coupling.

The amide nitrogen of **34**- ^{15}N appears in the ^{15}N -NMR spectrum (Figure 66) as a triplet ($J = 91.20$ Hz) at δ 132.88 due to its one bond heteronuclear coupling with the two attached hydrogens. The nitrogen shielding referred to neat nitromethane is at + 279.8 ppm.

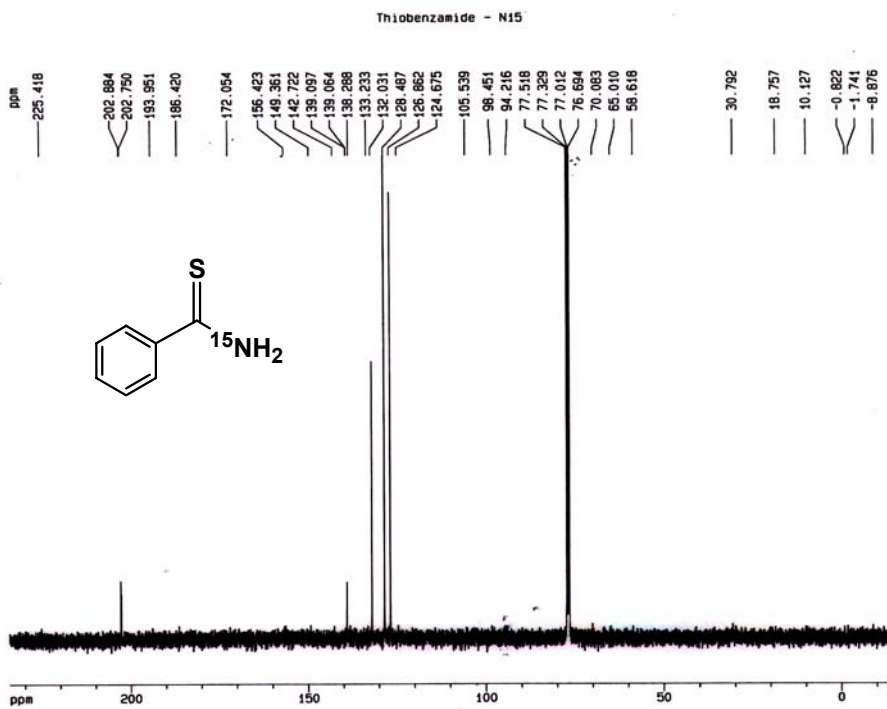


Figure 65: ¹³C-NMR spectrum of the synthesized thiobenzamide-¹⁵N

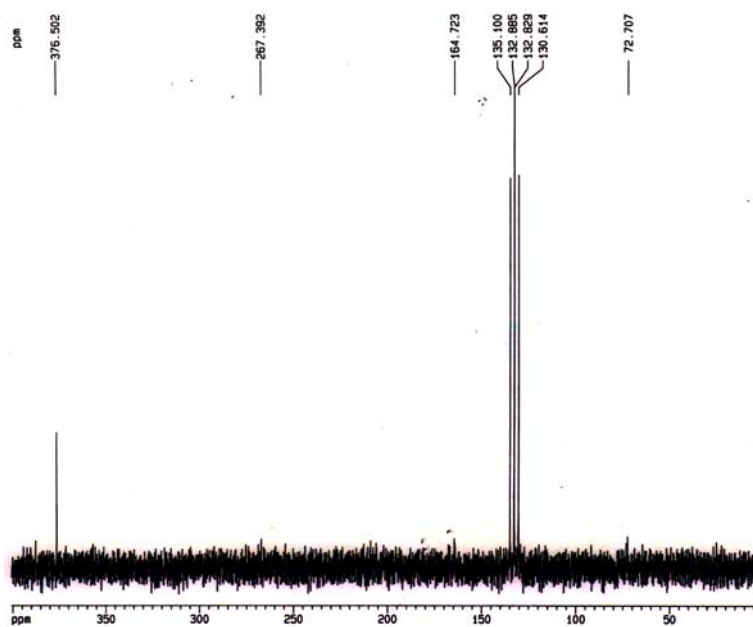
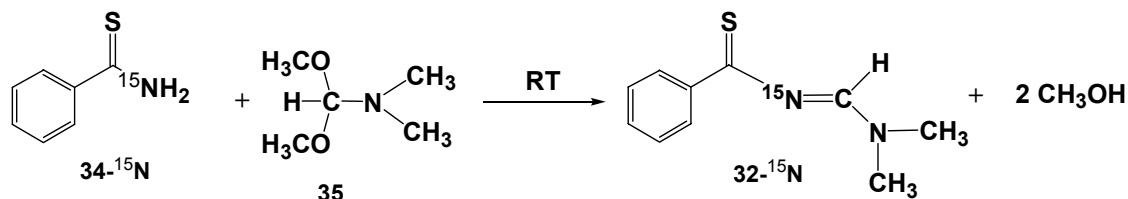


Figure 66: ¹⁵N-NMR spectrum of the synthesized thiobenzamide-¹⁵N

2.4.1.2 Synthesis of N-[(dimethylamino)methylene]thiobenzamide-¹⁵N

N-[(dimethylamino)methylene]thiobenzamide-¹⁵N (**32-¹⁵N**) was synthesized in 83% by the condensation of thiobenzamide-¹⁵N (**34-¹⁵N**) and N,N-dimethylformamide dimethylacetal (**35**) at room temperature as shown in Scheme 30.



Scheme 30: Synthesis of N-[(dimethylamino)methylene]thiobenzamide-¹⁵N

The ¹H-NMR spectrum (Figure 67) of N-[(dimethylamino)methylene]thiobenzamide-¹⁵N (**32-¹⁵N**) exhibits a singlet at δ 8.78. Although this proton would be expected to couple with the imine ¹⁵N nucleus, no sign of any coupling was observed upon scale expansion of this signal. The two non-equivalent methyl protons appear in the spectrum as two singlets at δ 3.24 and 3.25. The phenyl protons appear as a 3H multiplet from δ 7.29-7.52 assigned to the meta and para protons and 2H multiplet from δ 8.36 – 8.41 assigned to the ortho protons.

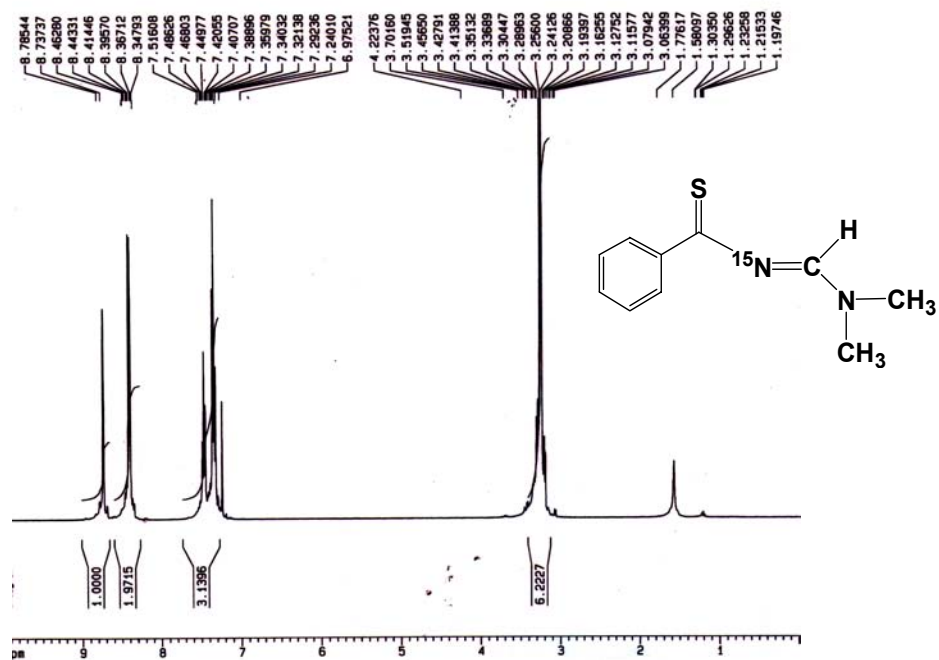


Figure 67: ^1H -NMR spectrum of N-[(dimethylamino)methylene]thiobenzamide- ^{15}N

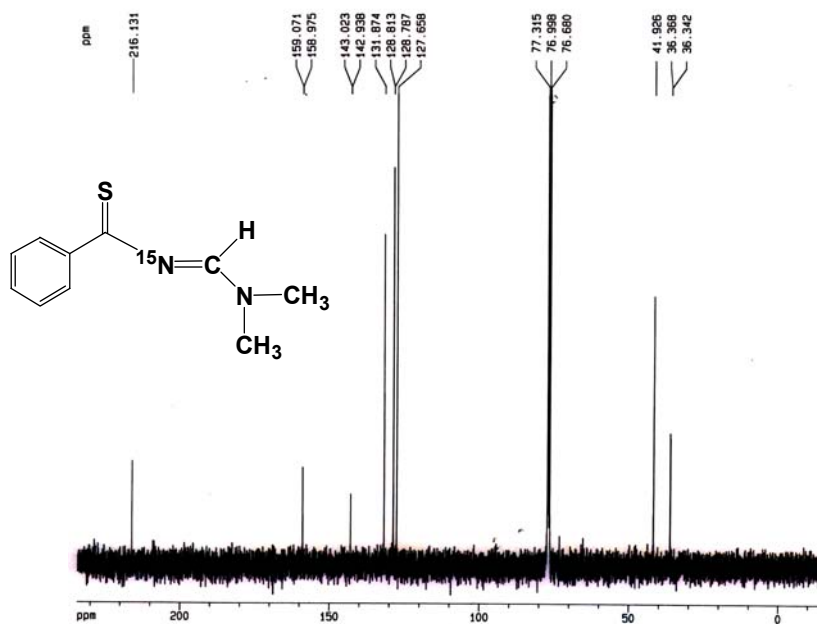


Figure 68: ^{13}C -NMR spectrum of N-[(dimethylamino)methylene]thiobenzamide- ^{15}N

The ^{13}C -NMR spectrum shown in Figure 68 exhibits a singlet at δ 216.1 for the thiocarbonyl carbon. It is surprising that this signal shows no sign of the coupling with the adjacent ^{15}N nucleus since in **32- ^{15}N** , the thiocarbonyl carbon appeared in the ^{13}C -spectrum at δ 202.8 as a doublet ($J = 13.8$ Hz) due to its coupling with the ^{15}N nucleus. The ^{13}C -NMR spectrum of **32- ^{15}N** does exhibit a doublet ($J = 10.0$ Hz) for the imine carbon at δ 159.0 indicating that this carbon is coupling with the adjacent ^{15}N nucleus. The two non-equivalent methyl carbons appear in the spectrum as sharp singlets. The former absorption appears as a doublet ($J = 2.3$ Hz), presumably due to a long range coupling with the ^{15}N . The spectrum also exhibits unusual long range couplings between the ^{15}N and C-1 of the phenyl ring, which appears as a doublet ($J = 8.40$ Hz) at δ 143.0 and between ^{15}N and the two equivalent ortho carbon of the phenyl ring, which appear as a doublet ($J = 3.10$ Hz) at δ 128.8.

The two-dimensional ^1H - ^{13}C correlation spectrum shown in Figure 69 is consistent with these spectral assignments. Thus, as shown in Figure 60, the doublet at δ 36.4 and the singlet at δ 41.9 in the ^{13}C -spectrum that were assigned to the two non-equivalent methyl groups correlate with the signals in the ^1H -spectrum at δ 3.24 and 3.25 assigned to the two sets of methyl hydrogens. Furthermore, the ^1H - ^{13}C correlation spectrum allows the assignments of the carbon absorptions of the phenyl ring to be confirmed. Thus, as can be seen in Figure 60, the doublet at δ 128.8 in the ^{13}C -spectrum assigned to the two equivalent ortho-ring carbon atoms correlate with 2H multiplet at δ 8.39-8.44 in the ^1H -spectrum assigned to the ortho-ring protons. In addition, the singlets in the ^{13}C - spectrum at δ 127.7 and 131.9 which were assigned to the meta- and para-ring carbons, respectively, correlate with the 3H multiplet at δ 7.29-7.46 in the ^1H -spectrum due to the

meta- and para- protons. As expected, the doublet in ^{13}C -spectrum at δ 130.0 assigned to the quaternary carbon of the phenyl ring is not observed in the ^1H - ^{13}C correlation spectrum.

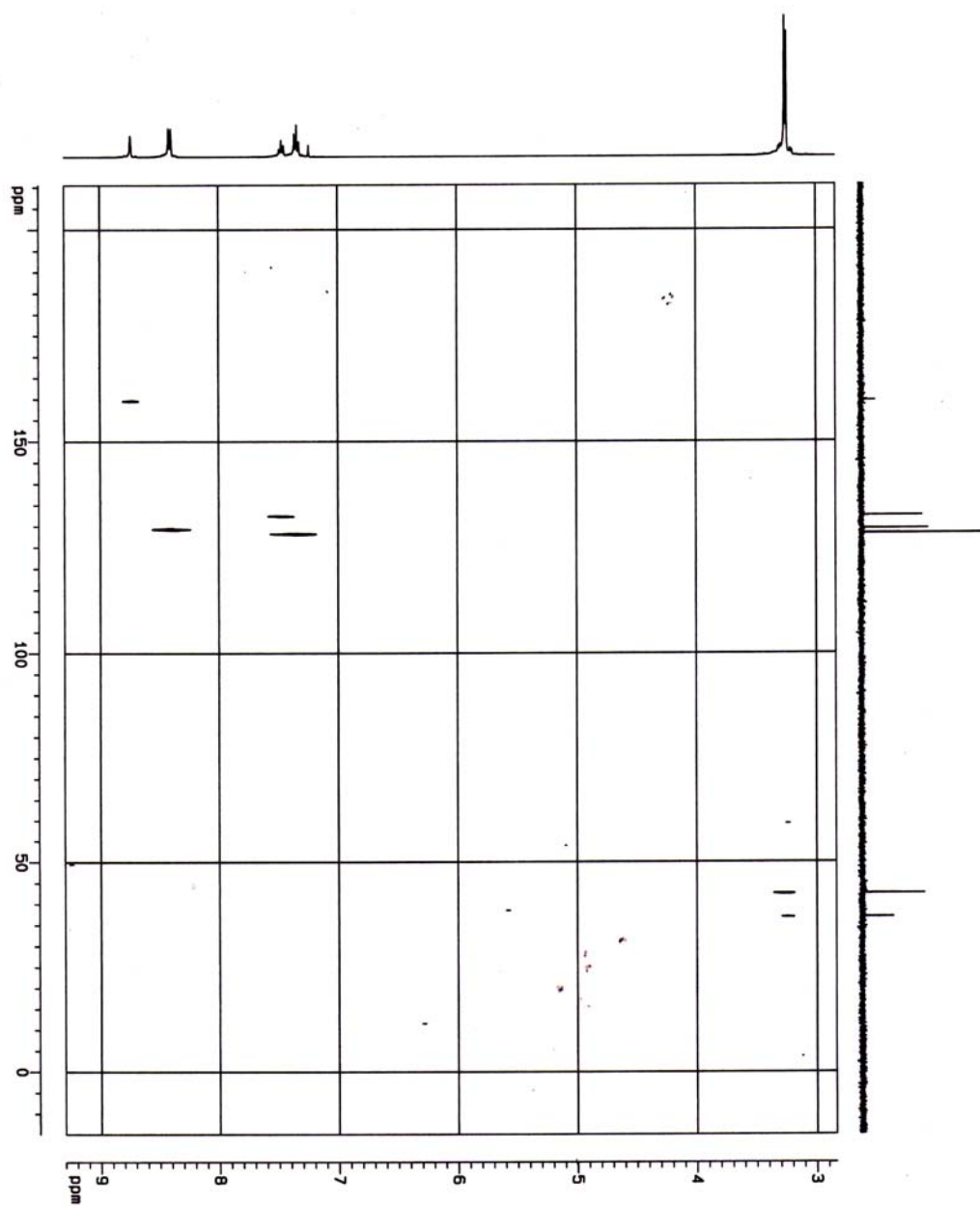


Figure 69: Two-dimensional ^1H - ^{13}C correlation spectrum of $32\text{-}^{15}\text{N}$

Finally, the ^{15}N -NMR spectrum, shown in Figure 70, exhibits a doublet ($J = 2\text{Hz}$) at δ 266.8 due to the coupling between ^{15}N and the imine proton. The nitrogen shielding is referred to neat nitromethane at δ 109.7. The geometry of this compound could be the trans-isomer since the calculated coupling constant for the trans-isomer has been reported at 2 Hz.¹⁵

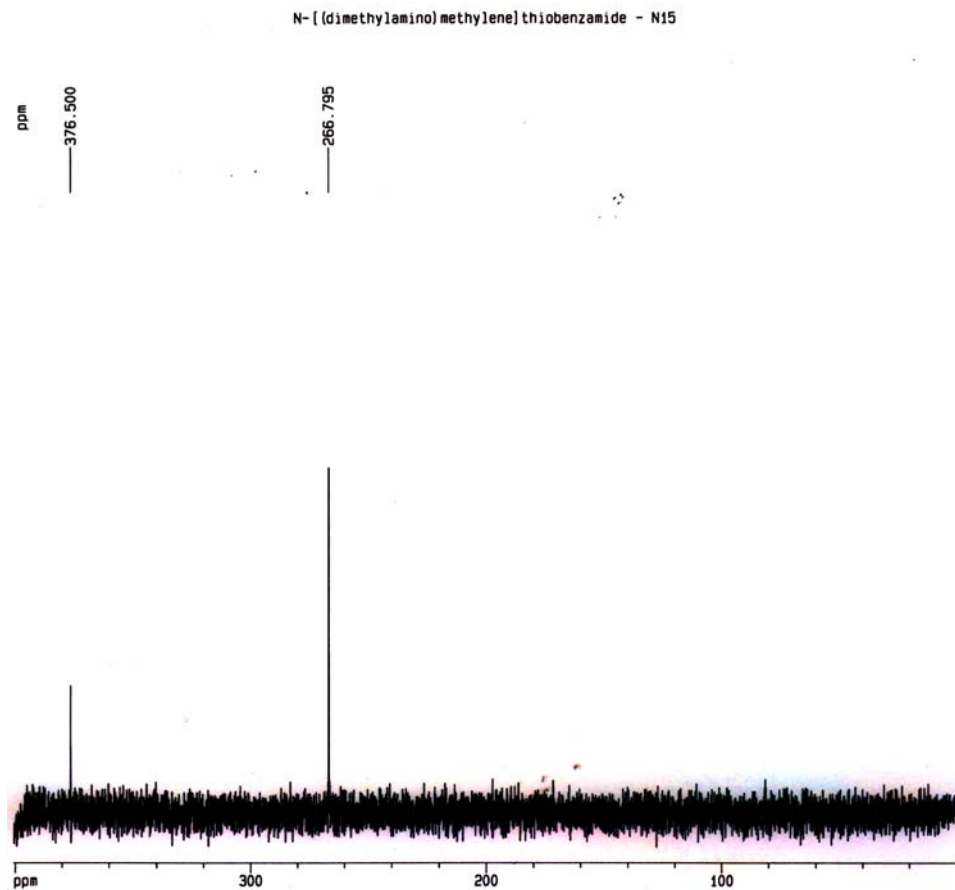
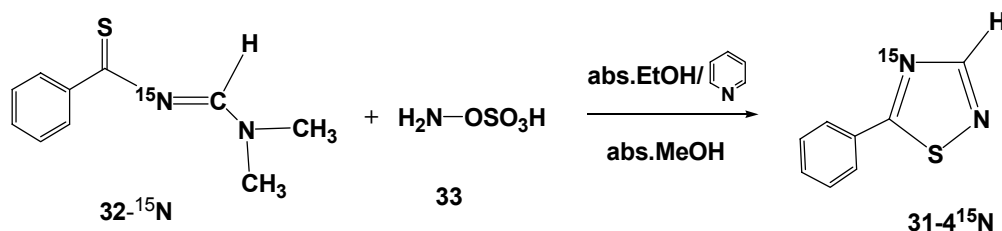


Figure 70: ^{15}N -NMR spectrum of N-[(dimethylamino)methylene]thiobenzamide- ^{15}N

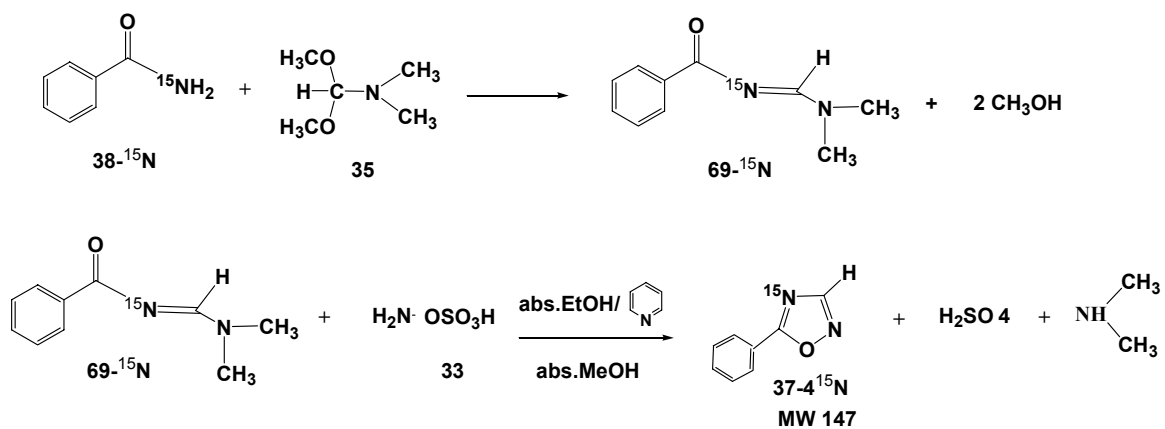
2.4.1.3 Synthesis of 5-phenyl-1,2,4-thiadiazole – 4^{15}N

5-phenyl-1,2,4-thiadiazole- 4^{15}N (**31- 4^{15}N**) was synthesized by the reaction of **32- ^{15}N** with **33** in absolute ethanol and methanol at room temperature using pyridine as basic catalyst (Scheme 31). Amination cyclization of **32- ^{15}N** resulted in the formation of **31- 4^{15}N** as colorless viscous liquid.



Scheme 31: Synthesis of 5-phenyl-1,2,4-thiadiazole – 4^{15}N

The GC-chromatogram [150°C (5 min), 30°C/min to 180°C (14 min)] of the synthetic **31- 4^{15}N** (Figure 71a) indicates the presence of two components. The major product eluted with a retention time of 11.1 min. The mass spectrum (Figure 71b) of this product exhibits a molecular ion at m/z 163 indicating that this component is the desired thiadiazole **31- 4^{15}N** . The minor component eluted with a retention time of 6.6 min and exhibits a molecular ion in the mass spectrum (Figure 71c) at m/z 147 and a base peak at m/z 104. This impurity was expected to be 5-phenyl-1,2,4-oxadiazole- 4^{15}N (**37- 4^{15}N**). It was presumed to be formed by the reaction of benzamide- ^{15}N (**38- ^{15}N**) present in the thiobenzamide- ^{15}N (**34- ^{15}N**) (Scheme 32).



Scheme 32: The plausible pathway for the formation of 5-phenyl-1,2,4-oxadiazole – 4¹⁵N

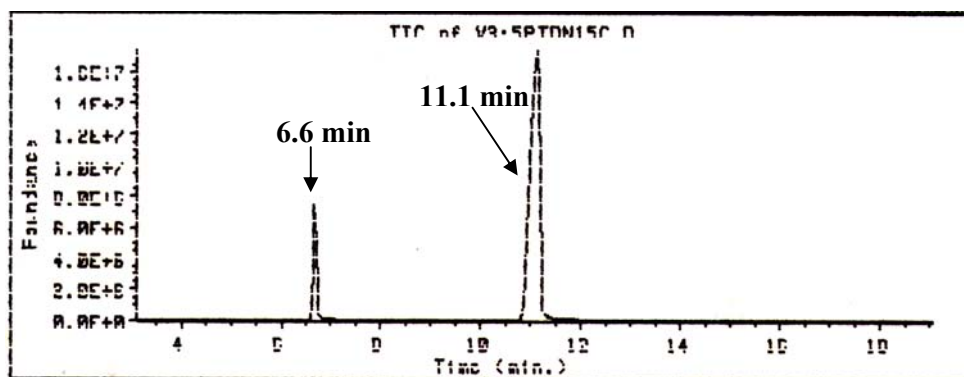


Figure 71a: GC-trace of the synthesized 5-phenyl-1,2,4-thiadiazole – 4¹⁵N

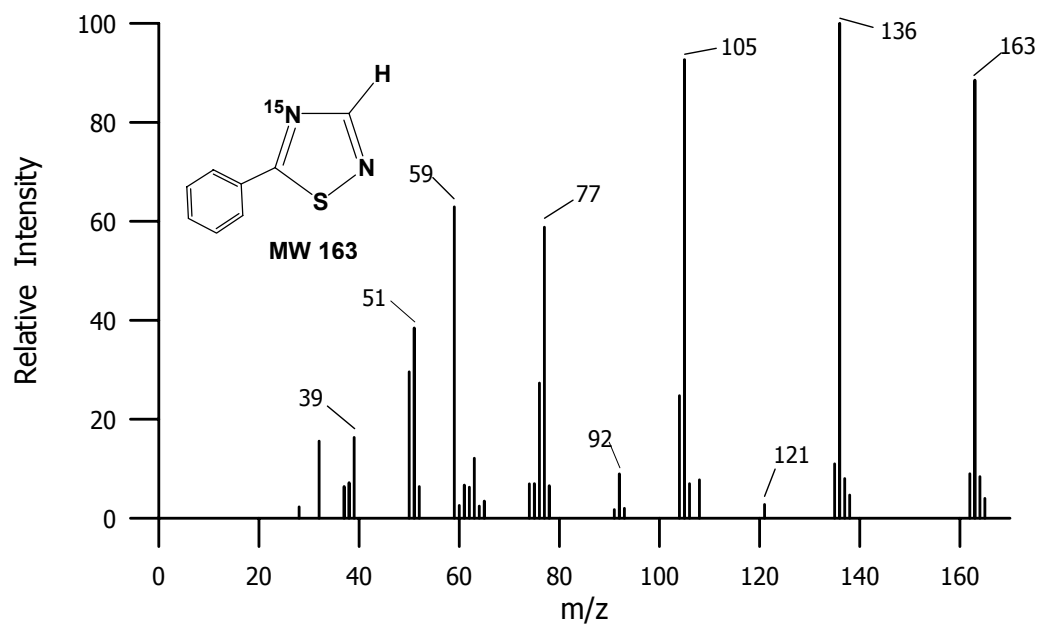


Figure 71b: Mass spectrum of the peak eluted at a retention time of 11.1 min

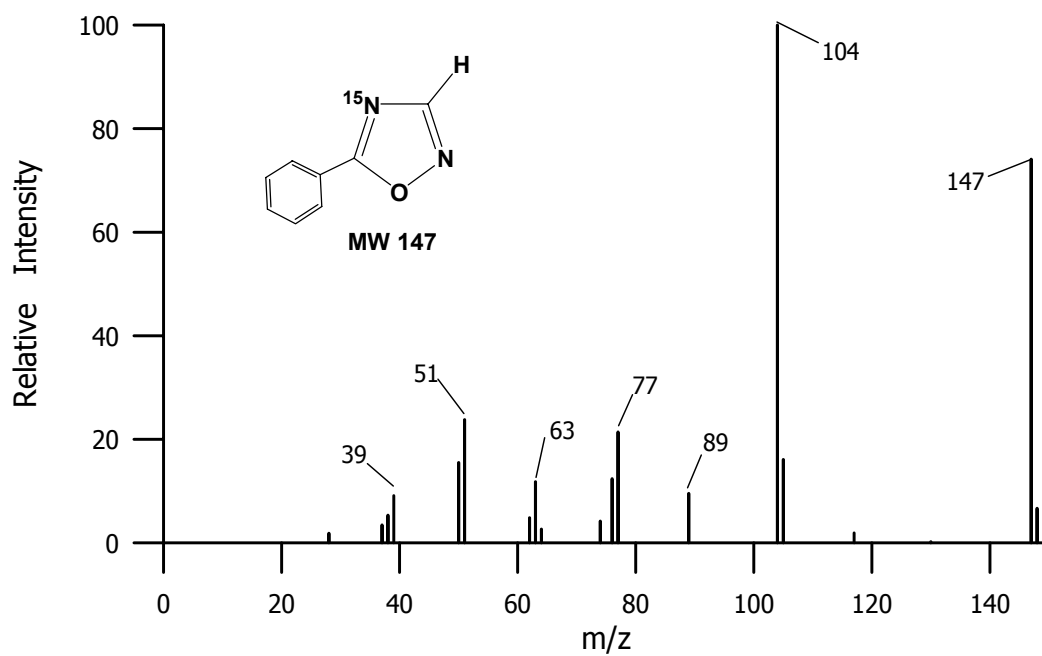


Figure 71c: Mass spectrum of the peak eluted at a retention time of 6.6 min

By direct comparison of the mass spectrum of this impurity with the mass spectrum of the previously synthesized 5-phenyl-1,2,4-oxadiazole (**37**), it revealed that the fragmentation of this impurity was identical to the fragmentation pattern of the synthetic 5-phenyl-1,2,4-oxadiazole. Some fragments of in the mass spectrum of this impurity were different due to the presence of ^{15}N -atom in those fragments. For example, the molecular ion was exhibited at m/z 147 and the base peak was exhibited at m/z 104. These results indicated that the impurity in the synthesized 5-phenyl-1,2,4-thiadiazole- 4^{15}N (**31- 4^{15}N**) was 5-phenyl-1,2,4-oxadiazole - 4^{15}N (**37- 4^{15}N**).

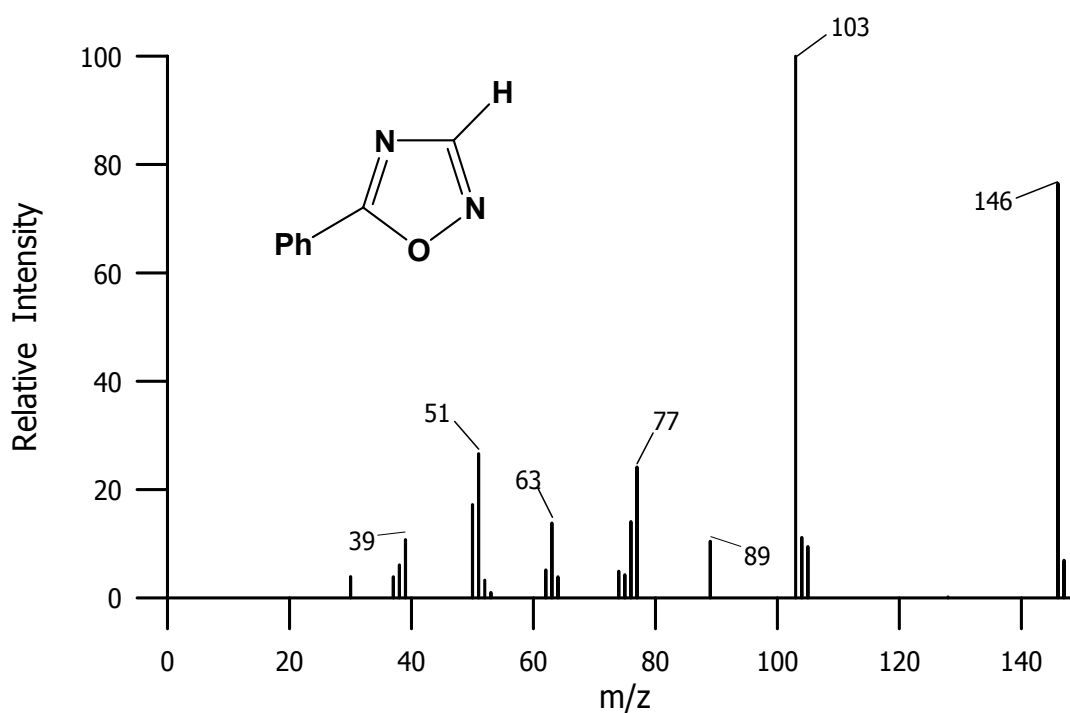


Figure 72: Mass spectrum of the synthetic 5-phenyl-1,2,4-oxadiazole

After the synthesized **31-4¹⁵N** was purified by preparative gas chromatography, the GC-analysis (Figure 73a) indicates the presence of only the desired product with a retention time of 11.1 min and no sign of any peak at retention time 6.6 min where the impurity was expected to be eluted. The mass spectrum (Figure 73b) exhibits a molecular ion at m/z 163 and two intense peaks at m/z 136 and 105 due to $[\text{C}_6\text{H}_5\text{C}^{15}\text{NS}]^+$ and $[\text{C}_6\text{H}_5\text{C}^{15}\text{NH}]^+$ fragments, respectively, which confirm the presence of only **31-4¹⁵N**. The mass spectrum also exhibits a peak at m/z 162 with relative intensity of 9 % and a peak at m/z 135 with relative intensity of 11%. This indicated the presence of 5-phenyl-1,2,4-thiadiazole-¹⁴N (**31**).

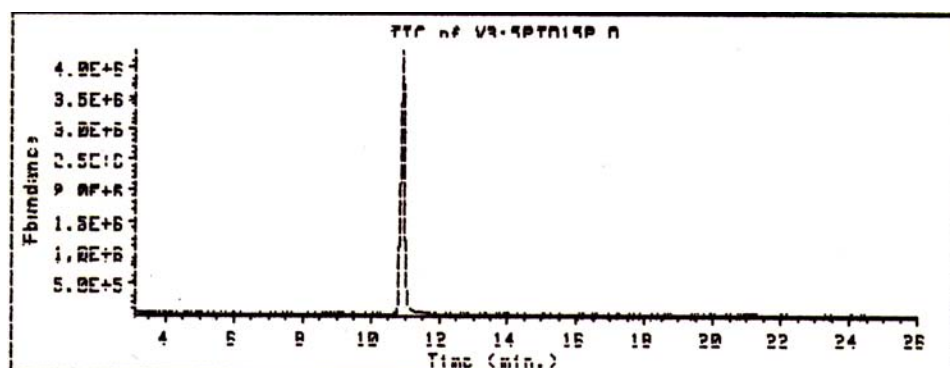


Figure 73a: GC-trace of the purified 5-phenyl-1,2,4-thiadiazole-⁴¹⁵N

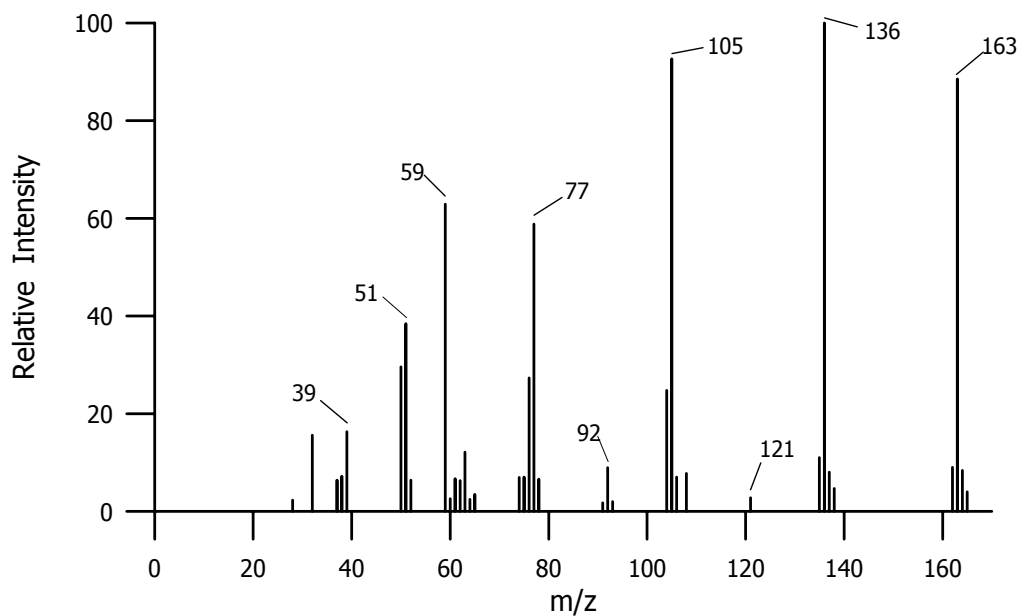


Figure 73b: Mass spectrum of the peak eluted at a retention time of 11.1 min

The ^1H -NMR spectrum of the synthetic **31**- 4^{15}N is shown in Figure 74a. In addition to 3H and 2H multiplets due to the phenyl protons at δ 7.58-7.61 and at δ 8.06-8.08, respectively, the spectrum exhibits a doublet ($J = 13.90$ Hz) at δ 8.84 due to the C-3 proton of the thiadiazole ring coupling with the ^{15}N at ring position 4. Interestingly, scale expansion of this signal shown in Figure 65b reveals the presence of a small amount of 5-phenyl-1,2,4-thiadiazole- 4^{14}N (**31**) in the sample as shown by mass spectrometry. Thus, in the absence of ^{15}N , the C-3 proton appears only as a singlet.

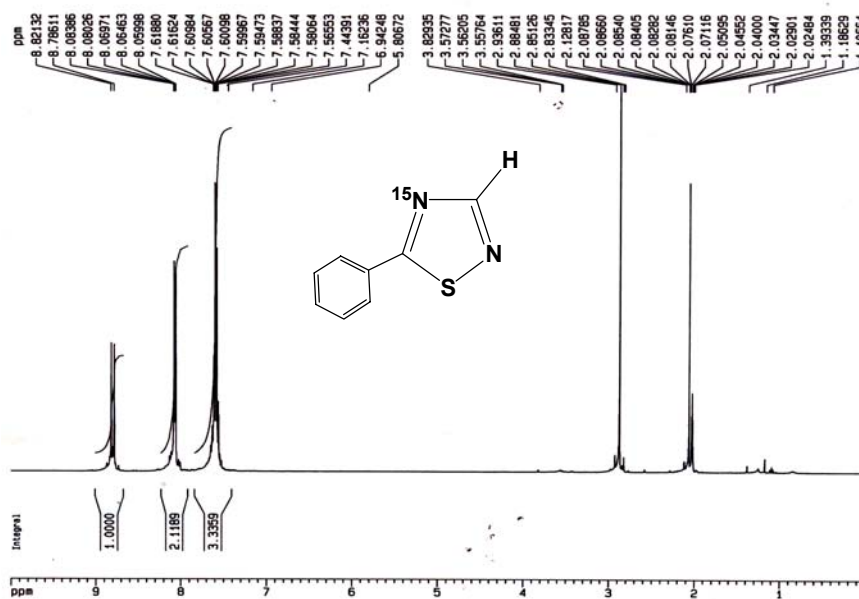


Figure 74a: ^1H -NMR spectrum of purified 5-phenyl-1,2,4-thiadiazole – 4^{15}N

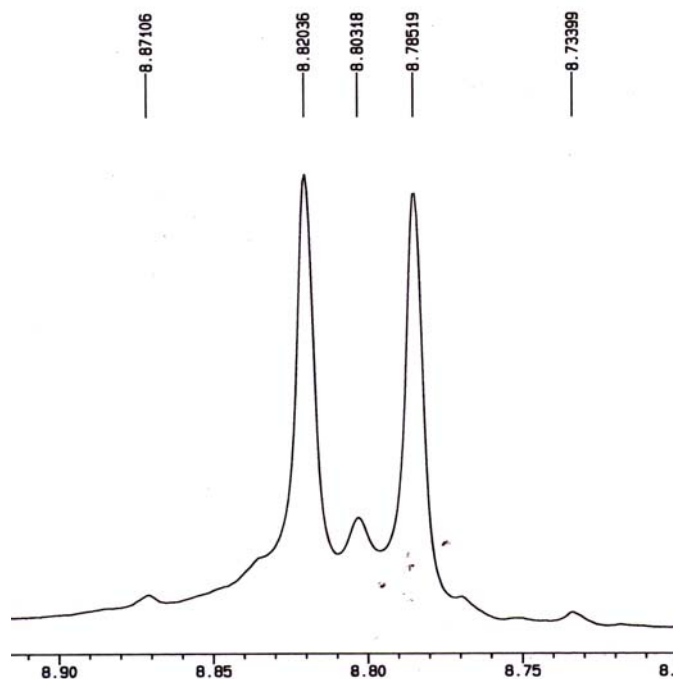


Figure 74b: ^1H -scale expansion spectrum of purified 5-phenyl-1,2,4-thiadiazole – 4^{15}N

The ^{13}C -NMR spectrum, shown in Figure 75a, exhibits a singlet at δ 188.8 assigned to the carbon at position 5 of the thiadiazole ring. The carbon at position 3 of the ring appears as a doublet at δ 164.7 ($J = 3.80$ Hz) due to the coupling with ^{15}N atom at the ring position 4 (Figure 75c). Surprisingly, the C-5 carbon signal does not appear as a doublet (Figure 75b), which was expected due to the coupling of this C-5 with ^{15}N .

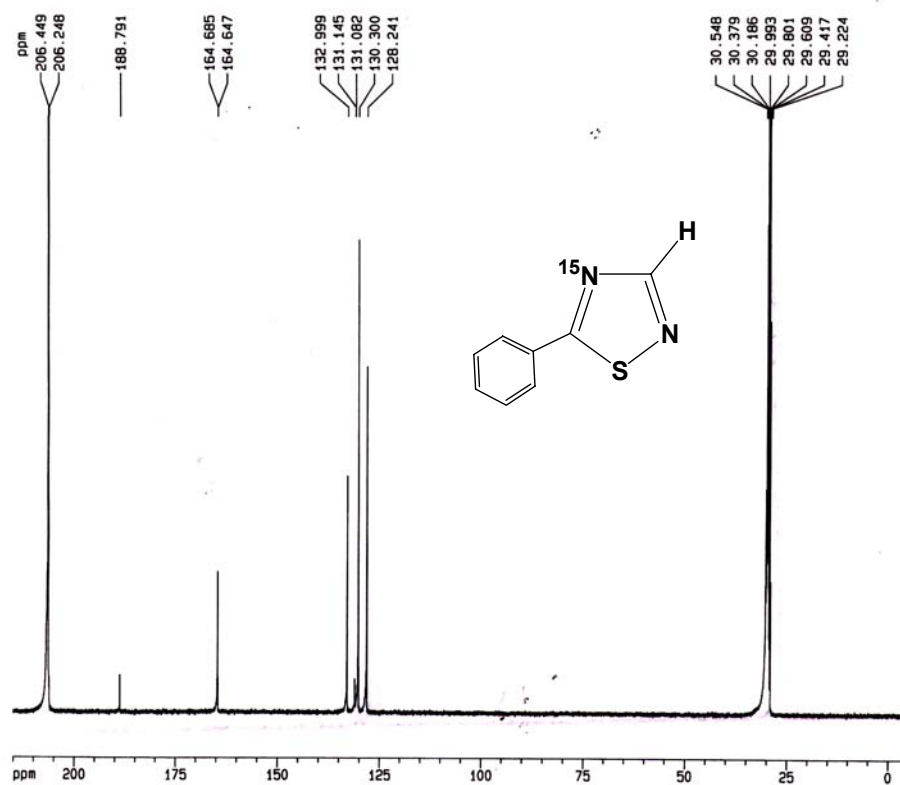


Figure 75a: ^{13}C -NMR spectrum of purified 5-phenyl-1,2,4-thiadiazole - 4^{15}N

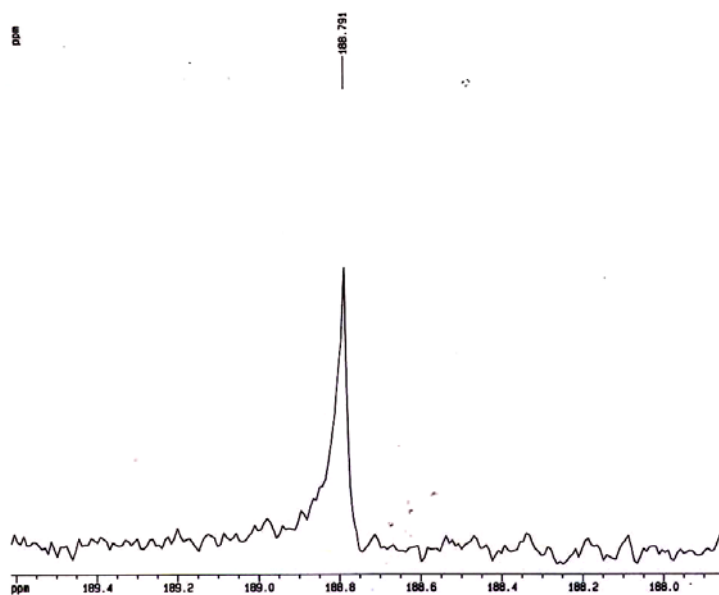


Figure 75b: ^{13}C -scale expansion spectrum of purified $31\text{-}4^{15}\text{N}$ showing the signal at δ 188.8 as singlet

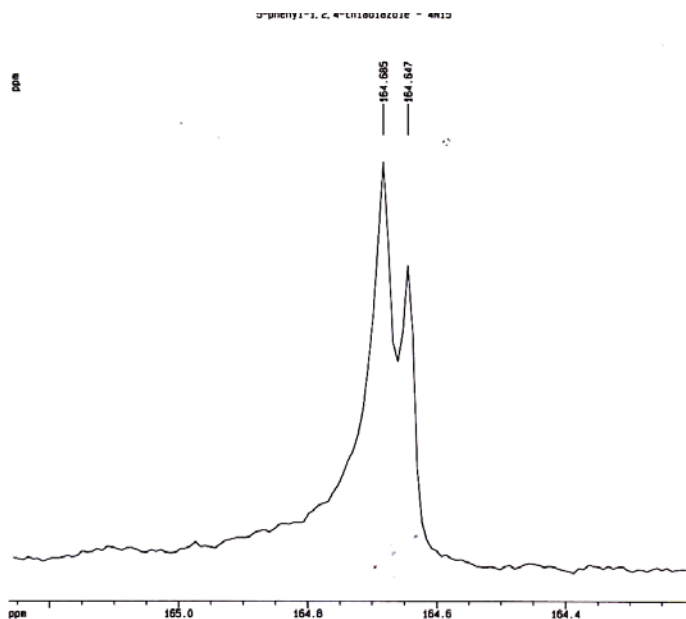


Figure 75c: ^{13}C -scale expansion spectrum of purified $31\text{-}4^{15}\text{N}$ showing the signal at δ 164.7 as doublet

As shown in Figure 75a, the doublet in the ^{13}C -spectrum at δ 164.6 ($J = 3.80$) that was assigned to the carbon in position 3 of the thiadiazole ring correlates with the doublet in the ^1H -spectrum at δ 8.80 ($J = 13.90$ Hz) that was assigned to the proton at position 3 of the thiadiazole ring. Furthermore, the ring phenyl carbon signals in the ^{13}C -spectrum can also be assigned from the correlation spectrum. Thus, the signal at δ 128.2 in the carbon spectrum can be assigned to the two equivalent ortho-ring carbons since this signal correlates with the 2H multiplet due to the ortho-protons at δ 8.05–8.08 in the ^1H -spectrum. In addition, the two signals in the ^{13}C -spectrum at δ 130.3 and 133.0 can be assigned to the meta- and para-carbons, respectively, since these signals correlate with the 3H multiplet in the ^1H -spectrum at δ 7.59–7.61 that is due to the meta- and para-protons. Furthermore, the doublet in the ^{13}C -spectrum at δ 131.05 ($J = 6.3$ Hz) can be assigned to the quaternary phenyl carbon since it is not observed in the ^1H - ^{13}C correlation spectrum (Figure 76).

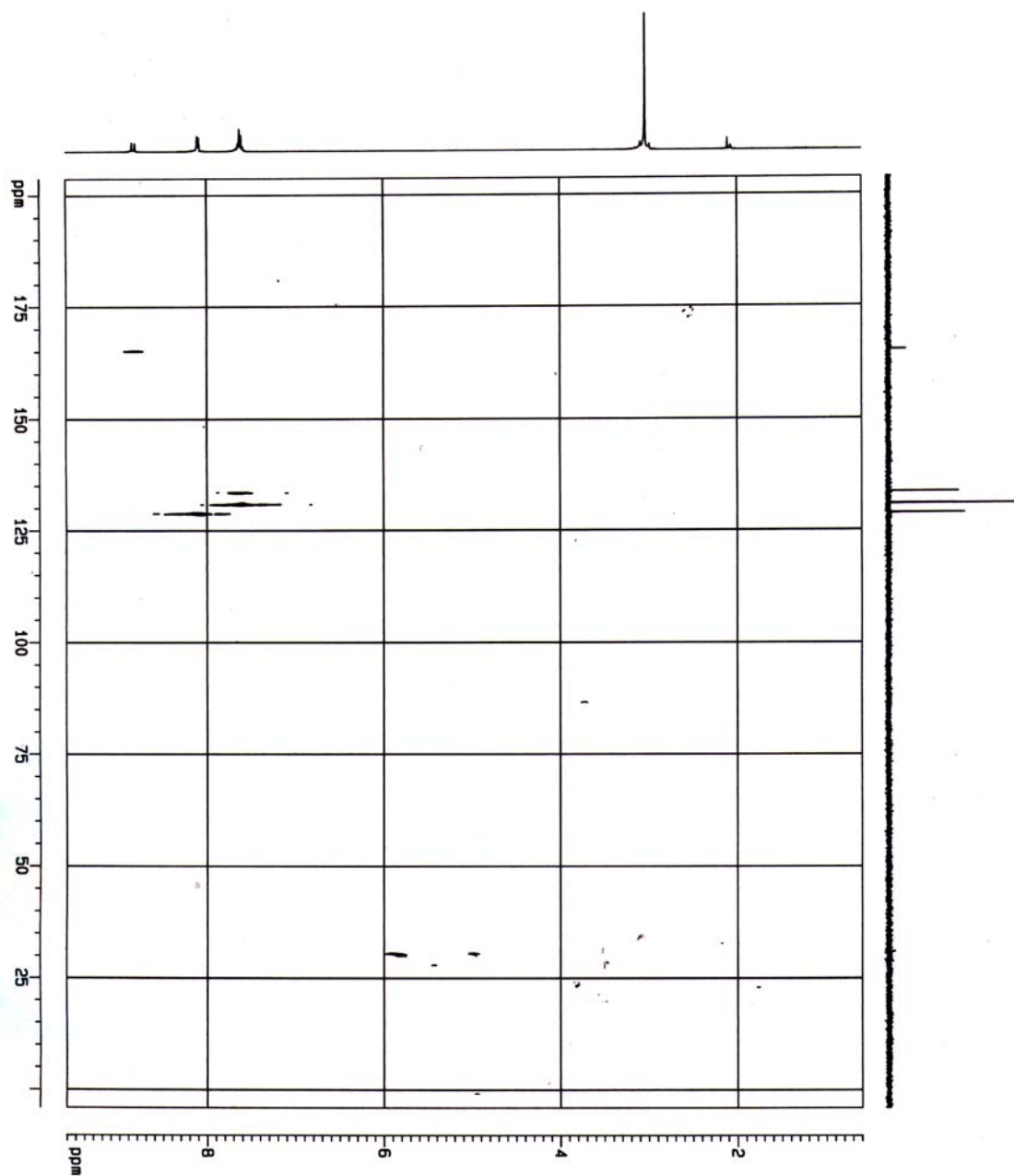


Figure 76: Two-dimensional ^1H - ^{13}C correlation spectrum of purified **31-4** ^{15}N

The ^{15}N -NMR spectrum (Figure 77) exhibits the signal of $^{15}\text{N-4}$ at δ 302.2 as doublet ($J = 13.90$ Hz) due to the coupling between $^{15}\text{N-4}$ and $^1\text{H-3}$. The signal of this $^{15}\text{N-4}$ in the term of nitrogen shielding is at + 74.2 ppm, which corresponds to the reported nitrogen shielding of $^{15}\text{N-4}$ on 1,2,4-thiadiazole at + 70 ppm (in dimethyl ether).¹⁵

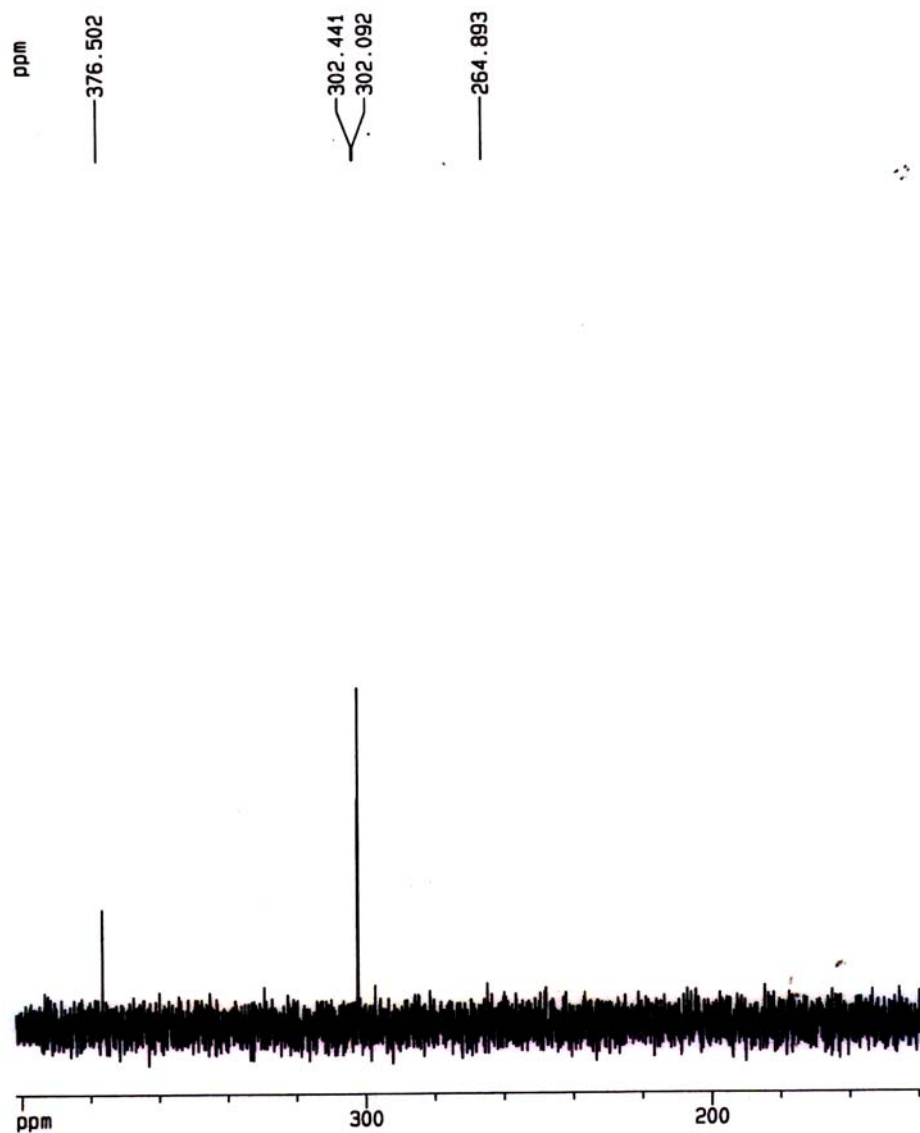
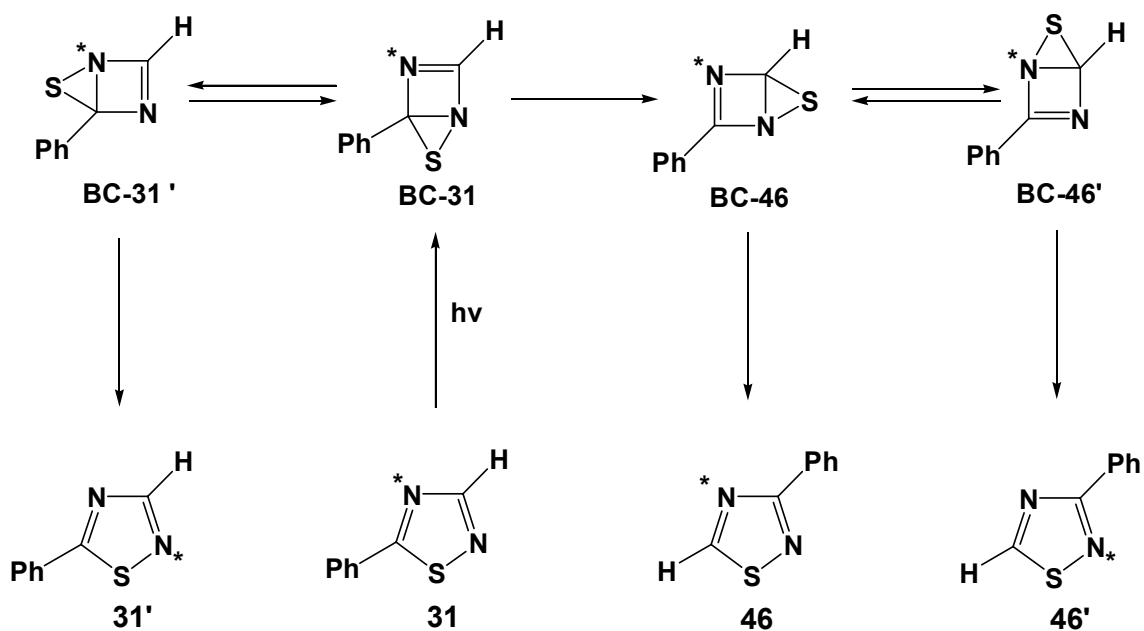


Figure 77: ^{15}N -NMR spectrum of the purified 5-phenyl-1,2,4-thiadiazole- ^{15}N

2.4.2 Photochemistry of 5-phenyl-1,2,4-thiadiazole-4-¹⁵N

In the previous photochemistry study of 5-phenyl-1,2,4-thiadiazole (**31**), the results indicated that five photoproducts were formed upon irradiation of this compound. They were identified as benzonitrile (**43**), 3-phenyl-1,2,4-thiadiazole (**46**), diphenyl-1,2,4-thiadiazole (**47**), 2-phenyl-1,3,5-triazine (**39**), and 2,4-diphenyl-1,3,5-triazine (**40**). Scheme 33 shows the proposed mechanism for the formation of **46** upon irradiation of **31**.



Scheme 33: The proposed mechanism for the formation of the phototransposition product

The phototransposition of **31** can be rationalized by the mechanism shown in Scheme 33. According to this mechanistic pathway, upon photochemical excitation, **31** is predicted to undergo electrocyclic ring closure leading to the formation of bicyclic intermediate, **BC-31**. One or two sigmatropic shifts of sulphur would lead to an equilibrium mixture of **BC-46** and **BC-46'**, which are identical except for the scrambling of the two nitrogens. Rearomatization of either **BC-46** or **BC-46'** would lead to the observed phototransposition product, **46**. In addition, **BC-31** would be expected to be in equilibrium with **BC-31'** via sulfur migration in the opposite direction. Again, **BC-31** and **BC-31'** are identical except for the scrambling of the two nitrogen atoms. Rearomatization of either of these two bicyclic species would lead back to the starting heterocycle, 5-phenyl-1,2,4-thiadiazole (**31**). Since, it is not possible to distinguish between the two nitrogen atoms in an unlabelled reactant **31**, it is not possible to distinguish between formation of **46** by the one or two sulfur migrations. Similarly, it is not possible to detect sulfur migration in the opposite direction leading back to **31**.

Scheme 33 shows, however, that nitrogen labelling can resolve these ambiguities. Thus, if the ^{14}N at ring position 4 is replaced with ^{15}N , then the one and two step sulfur migrations lead to the formation of 3-phenyl-1,2,4-thiadiazole-4- ^{15}N (**46-4 ^{15}N**) and 3-phenyl-1,2,4-thiadiazole-2- ^{15}N (**46-2 ^{15}N**), respectively. Furthermore, sulfur migration in the opposite direction will result in the formation of 5-phenyl-1,2,4-thiadiazole-2- ^{15}N (**31-2 ^{15}N**).

Figure 78a-b show GC trace and mass spectrum of the solution of **31-4 ^{15}N** before irradiation, respectively.

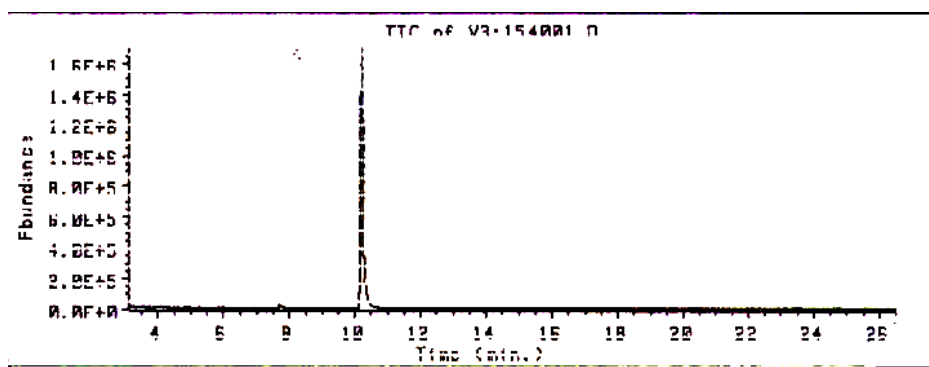


Figure 78a: GC-trace of 5-phenyl-1,2,4-thiadiazole-4-¹⁵N solution before irradiation

The mass spectrum of the starting material **31-4**¹⁵N before irradiation (Figure 78b) exhibits a molecular ion peak at m/z 163, which is consistent with the molecular weight of **31-4**¹⁵N (MW 163). The spectrum also exhibits an intense peak at m/z 136 due to the loss of HC^{14}N but no signal at m/z 135, which would result if HC^{15}N was lost from the molecule. The mass spectrum also exhibits peaks at m/z 105 and 104 due to the formation of $[\text{PhC}^{15}\text{N}]^{+\bullet}$ and $[\text{PhC}^{15}\text{NH}]^+$, respectively, but no significant signal at m/z 103, which would indicate the formation of $[\text{PhC}^{14}\text{N}]^{+\bullet}$. Scheme 34 shows the possible fragmentation pathways of **31-4**¹⁵N.

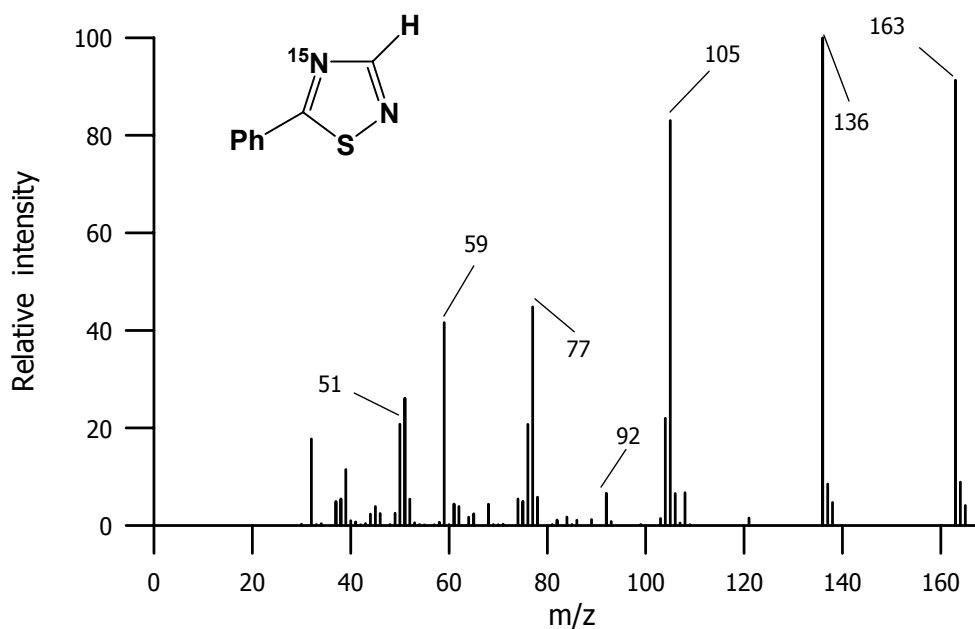
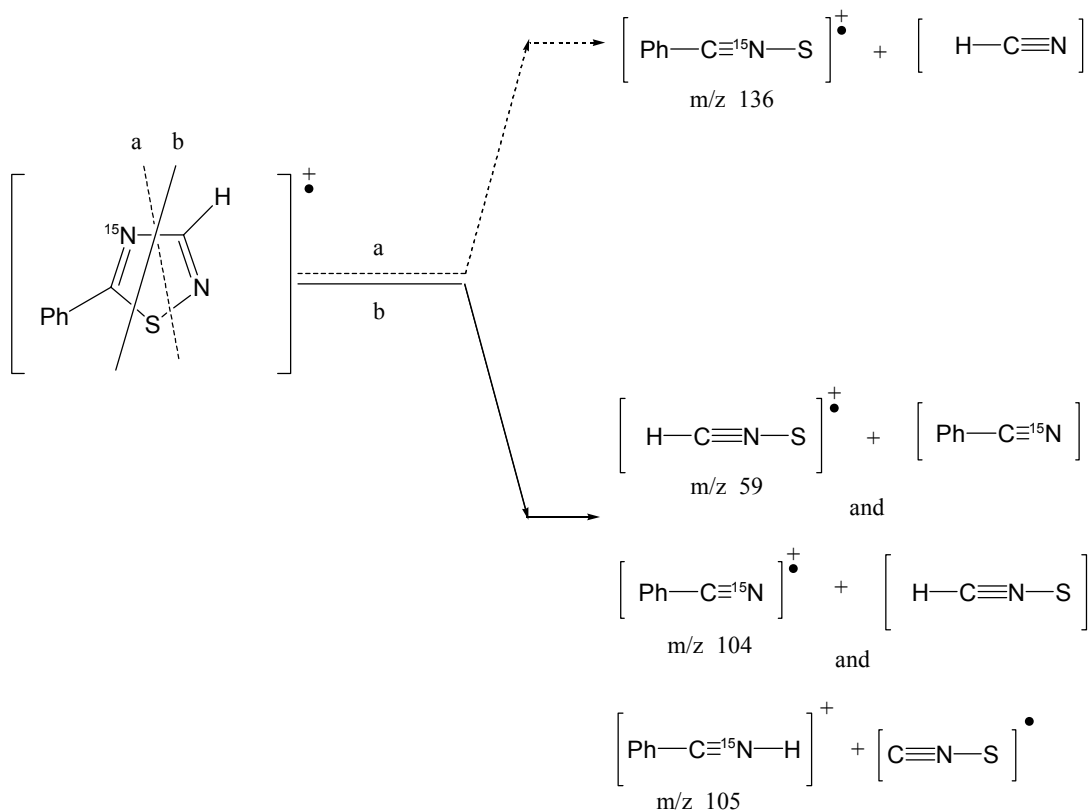


Figure 78b: Mass spectrum of 5-phenyl-1,2,4-thiadiazole-4-¹⁵N before irradiation



Scheme 34: Possible fragmentation pathways of 5-phenyl-1,2,4-thiadiazole-4-¹⁵N

In the initial photochemical experiment, a solution of **31-4**¹⁵N (4 mL, 3×10^{-2} M) was placed in a Pyrex tube (12 cm \times 0.7 cm). The tube was sealed with a rubber septum, purged with argon for 15 min, and irradiated with sixteen > 290 nm mercury lamps for a total of 180 min. The mass spectrum of the unconsumed reactant (Figure 79), which eluted with a retention time of 11.5 min, again shows a molecular ion at m/z 163 and an intense signal at m/z 136 due to the loss of HC^{14}N . In addition, however, the mass spectrum also shows a peak at m/z 135 due to the loss of HC^{15}N . This peak was not observed in the mass spectrum of **31-4**¹⁵N before irradiation. This reveals that **31-4**¹⁵N has been converted to **31-2**¹⁵N during the irradiation. The corrected ratio of the 135:136 signals is 1:2.47. This shows that after 180 min of irradiation the unconsumed reactant is a mixture of 29% of **31-2**¹⁵N and 71 % of **31-4**¹⁵N.

Mass spectrum analysis of the ^{15}N -labelled 3-phenyl-1,2,4-thiadiazole and 2-phenyl- and 2,4-diphenyl-1,3,5-triazine photoproducts obtained after this prolong irradiation also exhibited ^{15}N scrambling. The origin of this scrambling is unclear, however, due to the extensive scrambling in the reactant **31-4** ^{15}N .

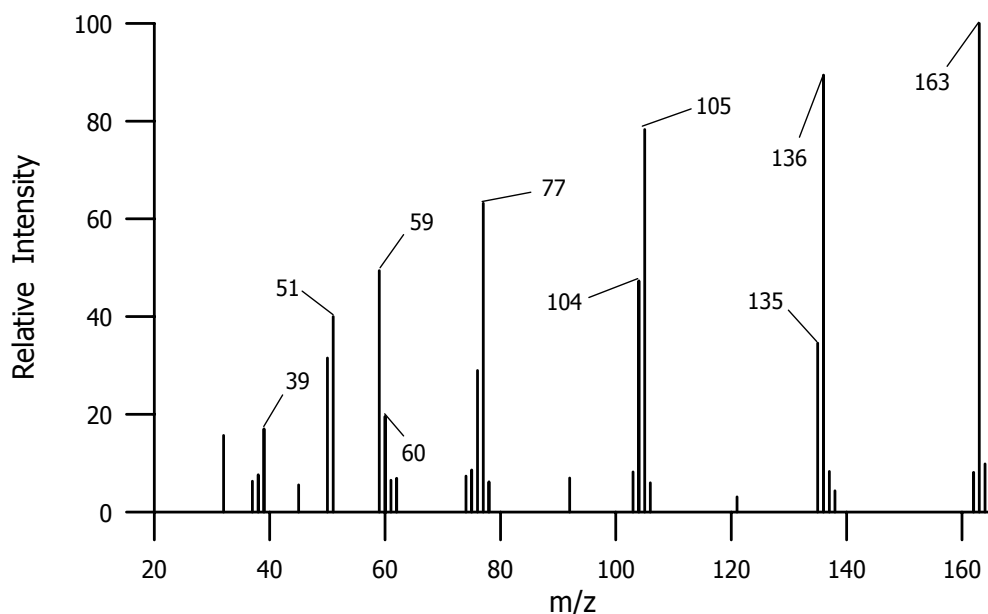


Figure 79: GC-trace of the un-consumed reactant after 180 min of irradiation

In order to minimize the extent of ^{15}N scrambling in the reactant, the irradiation was carried out for a shorter period of time. In this experiment the sample (4 mL, 3×10^{-2} M) was irradiated with sixteen > 290 nm lamps for a total of 16 min. Aliquots of the reaction solution were removed after every four min of irradiation, concentrated, and analyzed by the GC (HP588) interfaced with a mass spectrometer [140°C (5 min), 20°C/min to 240°C (20 min)].

GLC analysis on GC-PE9000 (Figure 80) shows that only a trace quantity of the reactant had been consumed after 16 min of irradiation and that only a trace amount of photoproducts had been formed. Although the consumption of the starting material and

the formation of the products are clearly observed by the GC-PE9000 analysis, the quantities consumed and formed are too small for accurate measurement. The GC-trace (HP588) of this irradiated solution (Figure 81a) shows five volatile components with retention times of 4.2, 10.7, 11.7, 14.0, and 33.5 min.

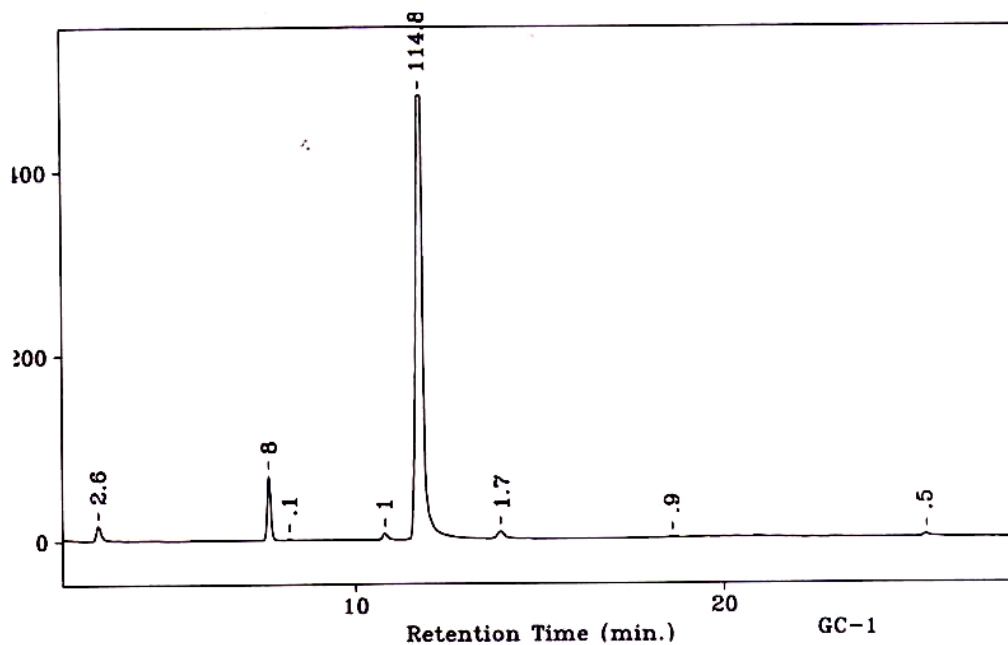


Figure 80: GLC trace (PE9000) of $31\text{-}4^{15}\text{N}$ solution after 16 min of irradiation

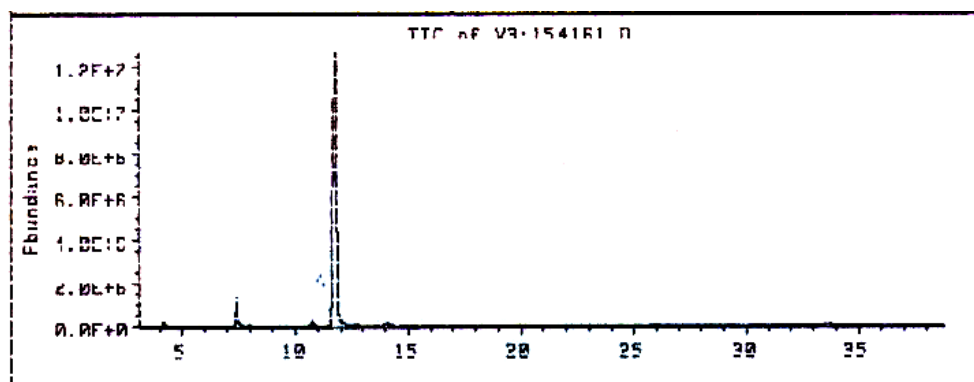


Figure 81a: GC-trace (HP588) of $31\text{-}4^{15}\text{N}$ solution after 16 min of irradiation

The un-consumed 5-phenyl-1,2,4-thiadiazole- ^{15}N eluted with a retention time of 11.7 min. The mass spectrum of this compound (Figure 81b) exhibits a molecular ion at m/z 163 and a base peak at m/z 136 due to the loss of HC^{14}N from the molecular ion. Moreover, the spectrum also reveals the presence of a peak at m/z 135 with an intensity of 7.8 % of the base peak, which is due to the loss of HC^{15}N from the molecular ion. This signal was not present in the mass spectrum of $31\text{-}4^{15}\text{N}$ before photolysis. The formation of this peak during irradiation indicates that some $31\text{-}4^{15}\text{N}$ has been photochemically converted to $31\text{-}2^{15}\text{N}$. Figure 82 is a plot of the ratio of the observed intensities of 135/136 peaks as a function of irradiation time, which shows that the ratio slowly increase from 0 before irradiation to 0.07 after 16 min of irradiation. This indicates that at this point the un-consumed reactant consists of 93.5% $31\text{-}4^{15}\text{N}$ and 6.5% $31\text{-}2^{15}\text{N}$.

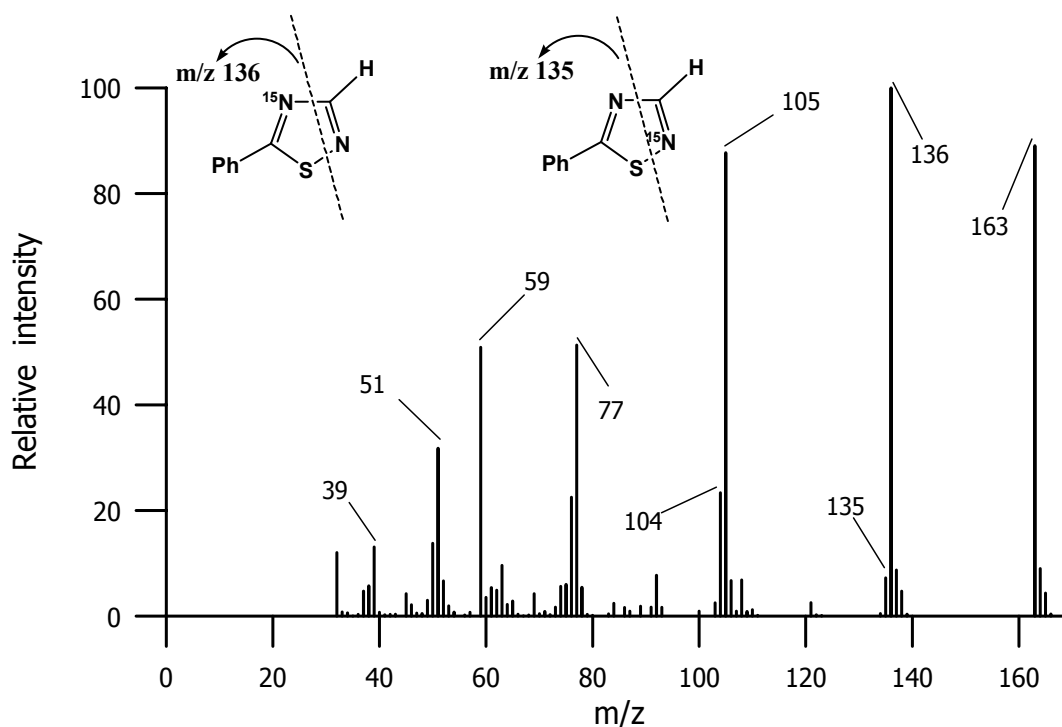


Figure 81b: Mass spectrum of the un-consumed reactant

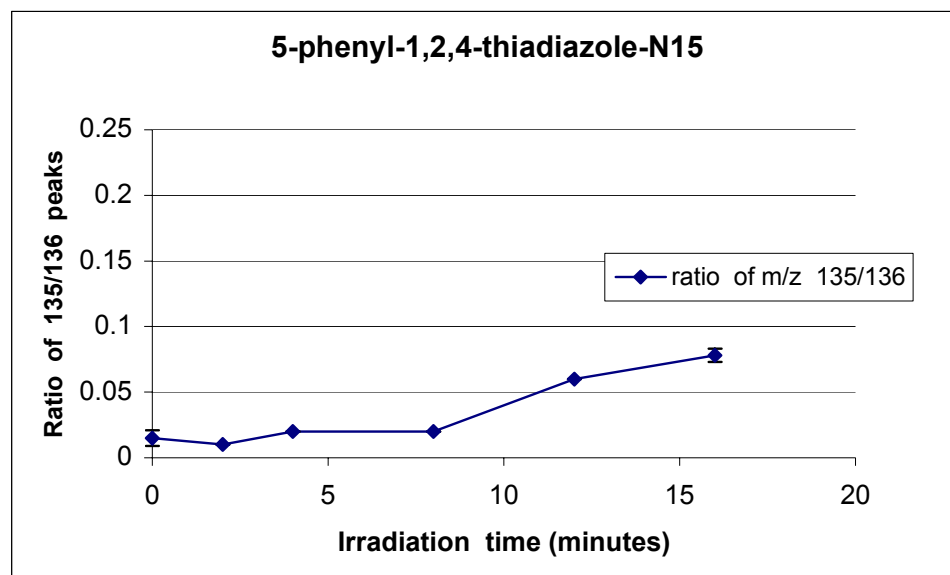


Figure 82: Plot of the ratio of the intensities of the 135/136 peaks

The mass spectrum of the compound that eluted with a retention time of 4.2 min (Figure 81c) exhibits peaks at m/z 103 and 104, which are consistent with the molecular ions of benzonitrile- ^{14}N ($43\text{-}^{14}\text{N}$) and benzonitrile- ^{15}N ($43\text{-}^{15}\text{N}$). Figure 83 is a plot of the ratio of the observed intensities of the 103/104 peaks as a function of irradiation time. It reveals that the ratio gradually increased from a value of 0.17 after two min of irradiation to a ratio of 0.31 after 16 min of irradiation. The corrected ratio at this time is 0.32.

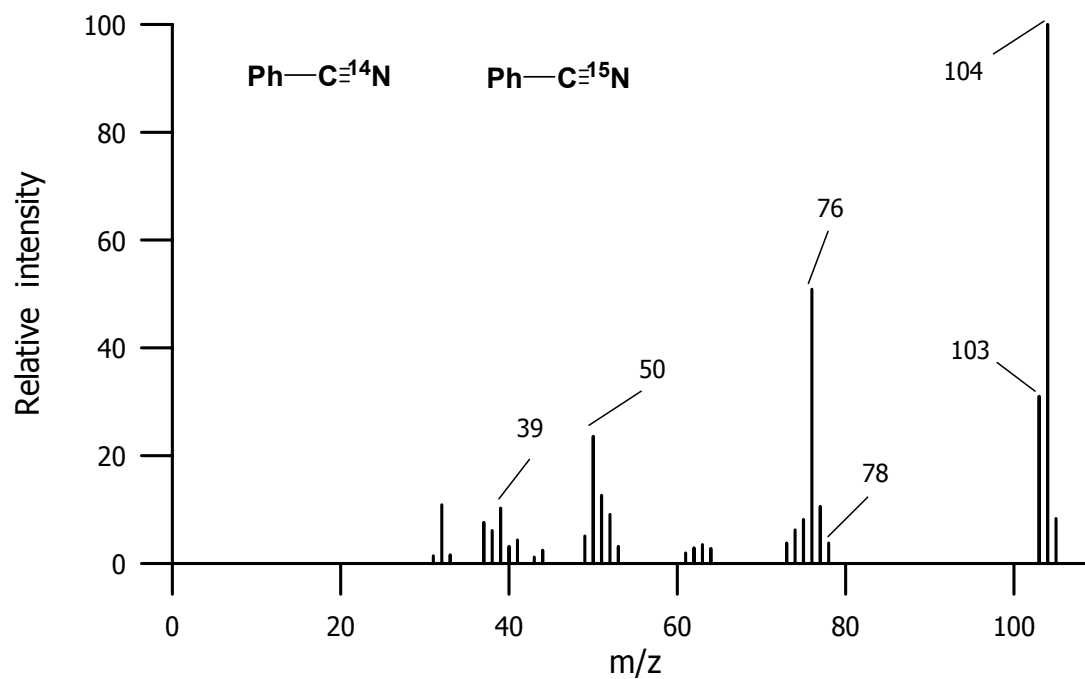


Figure 81c: Mass spectrum of benzonitrile-photoproduct at 16 min of irradiation

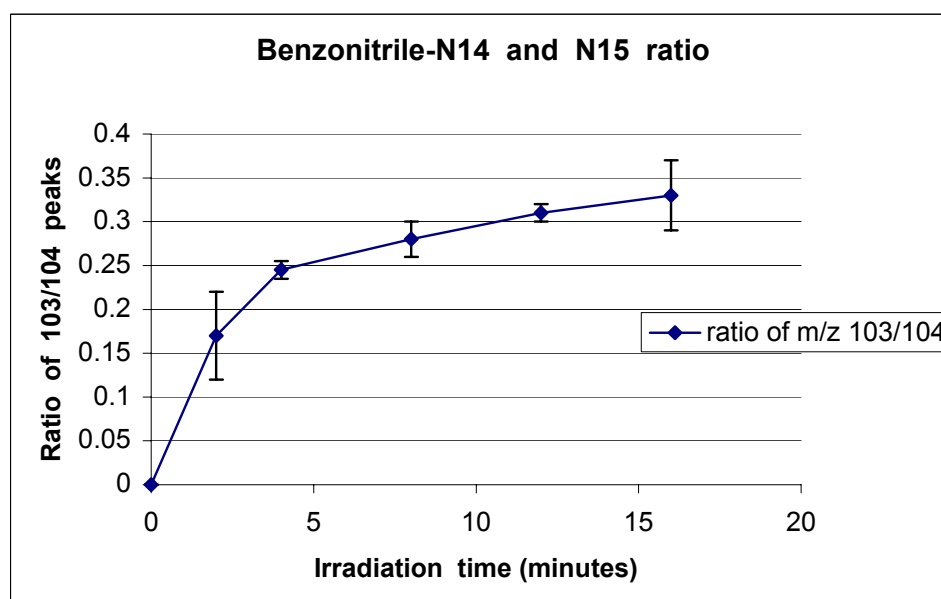


Figure 83: Plot of the ratio of the intensities of the 103/104 peaks

It should be pointed out that if the benzonitrile formed in this photoreaction came only directly from 5-phenyl-1,2,4-thiadiazole- ^{15}N , the benzonitrile- ^{14}N to benzonitrile- ^{15}N ratio should also be 0.07. As previously stated, however, the observed corrected ratio is 0.32. This indicates that the benzonitrile formed consists of 24 % $43\text{-}^{14}\text{N}$ and 76 % $43\text{-}^{15}\text{N}$.

The photoproduct which eluted with a retention time of 11.7 min was identified as 3-phenyl-1,2,4-thiadiazole- ^{15}N , the phototransposition product. As previously discussed (see synthetic section), the mass spectrum of 3-phenyl-1,2,4-thiadiazole **46** (Figure 84) exhibits major fragmentation pathways involving the loss of HCNS to form $[\text{PhCN}]^{*+}$ with an intense signal at m/z 103 and the loss of HCN to form $[\text{PhCNS}]^{*+}$ which has an intense signal at m/z 135.

The mass spectrum of the ^{15}N -labelled 3-phenyl-1,2,4-thiadiazole photoproduct, shown in Figure 81d, exhibits a molecular ion at m/z 163 and two intense peaks at m/z 135 and 136 with a corrected 135/136 ratio of 1.13. Whereas the peak at m/z 135 is consistent with the loss of HC^{15}N from the molecular ion, the signal at m/z 136 results from the loss of HC^{14}N . This mass spectral data indicates that the ^{15}N -labelled phototransposition product is a mixture of 53% $46\text{-}4^{15}\text{N}$ and 47% of $46\text{-}2^{15}\text{N}$.

Figure 85 is a plot of the ratio of the m/z 135 and 136 peak as a function of irradiation time. This plot shows that the ratio is constant over the entire time monitored. Thus, even very early in the photoreaction when the product can first be detected, it is formed with essentially complete scrambling of the ^{15}N between position 2 and 4.

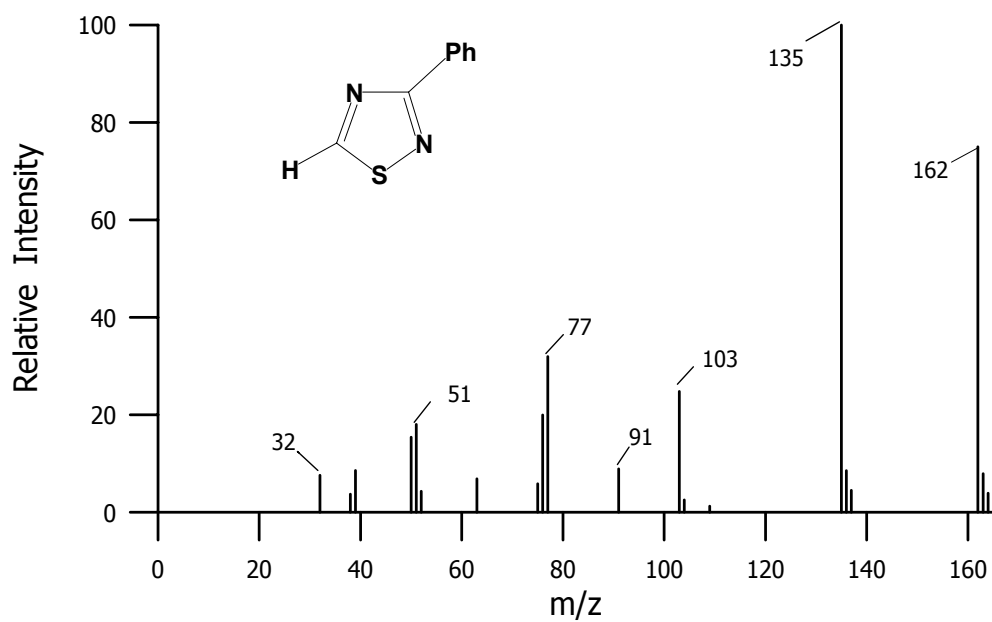


Figure 84: Mass spectrum of un-labelled 3-phenyl-1,2,4-thiadiazole

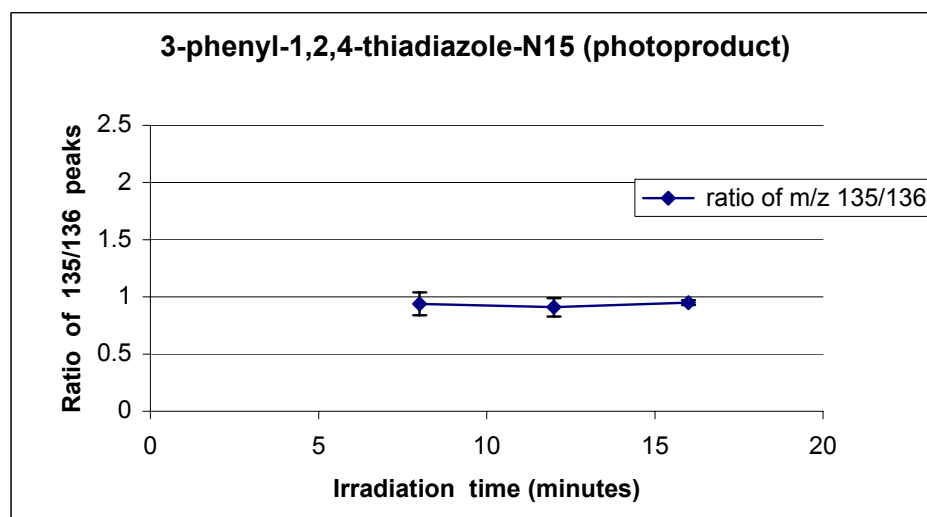


Figure 85: Plot of the ratio of the intensities of 135/136 peaks of 3-phenyl-1,2,4-thiadiazole-¹⁵N (photoproduct)

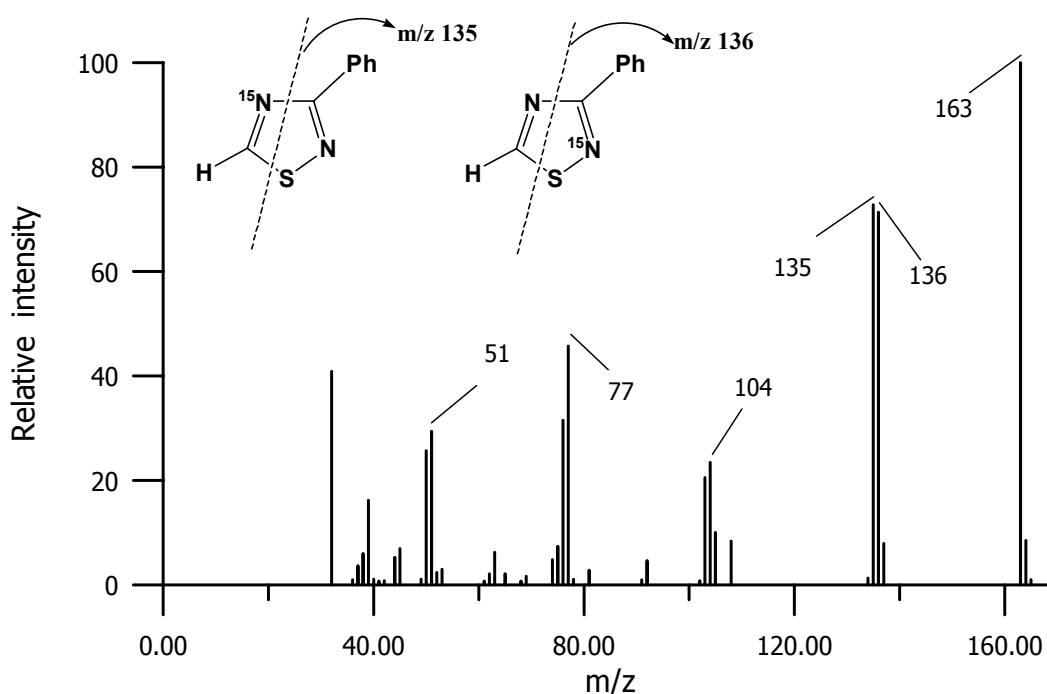


Figure 81d: Mass spectrum of 3-phenyl-1,2,4-thiadiazole - photoproduct upon irradiation of 5-phenyl-1,2,4-thiadiazole-4- ^{15}N

The photo ring-expansion products, 2-phenyl- and 2,4-diphenyl-1,3,5-triazine eluted with retention times of 10.7 and 35.5 min, respectively. The mass spectrum of the first eluted triazine, shown in Figure 81e, exhibits molecular ions at m/z 158 and 159 which indicate the formation of 2-phenyl-1,3,5-triazine molecules containing one ^{15}N and two ^{15}N atoms. Figure 86 shows a plot of the ratio of the intensities of the 158/159 peaks as a function of irradiation time. This plot reveals that the ratio of the 158:159 peaks is constant at a value of 0.8 from 8 min to 16 min of irradiation. The observed corrected ratio at 16 min is 0.84. This indicates that the photoproduct is a mixture with 46% of the 2-phenyl-1,3,5-triazine molecules containing one ^{15}N atom and 54% containing two ^{15}N atoms per molecule.

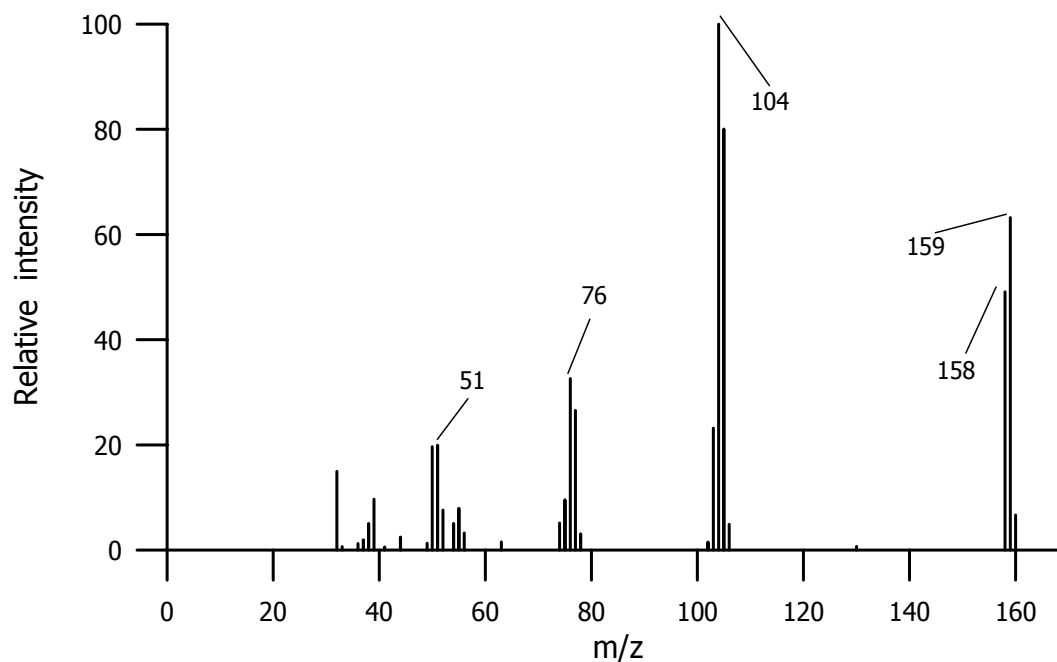


Figure 81e: Mass spectrum of 2-phenyl-1,3,5-triazine photoproduct containing one ^{15}N and two ^{15}N atoms

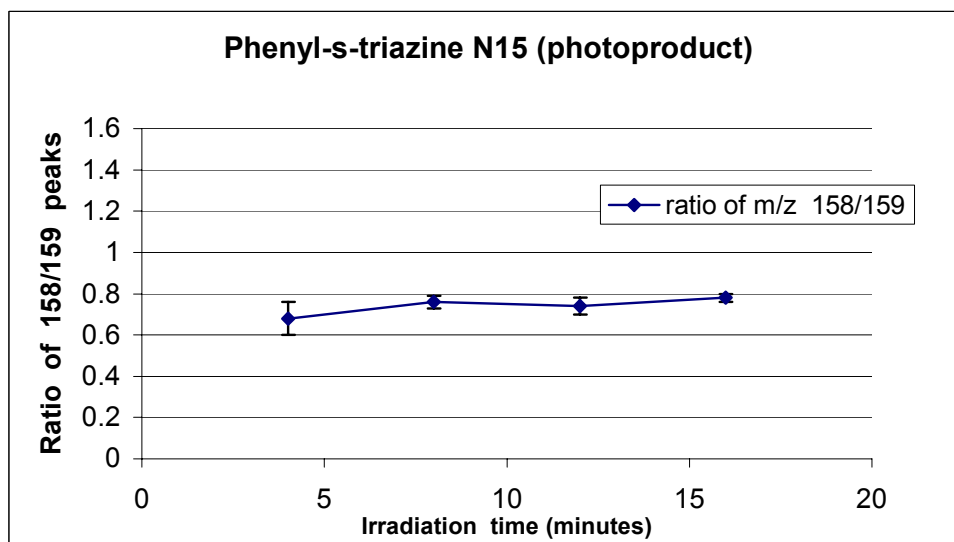


Figure 86: Plot of the ratio of the intensities of the 158/159 peaks

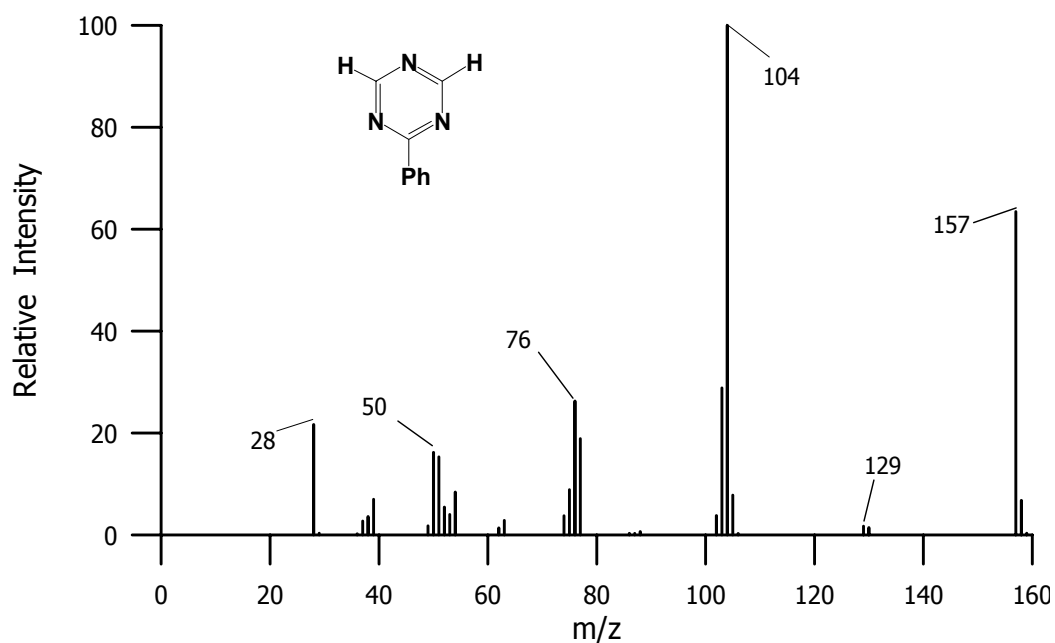
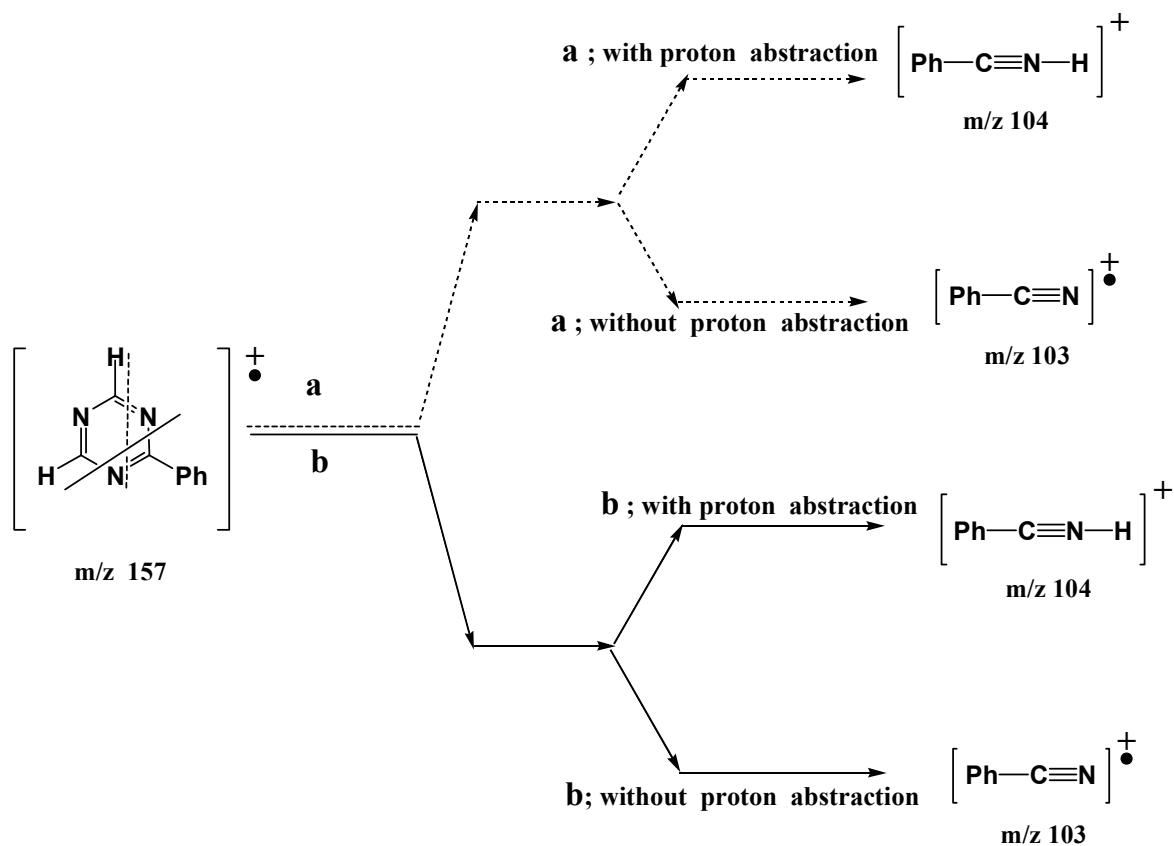


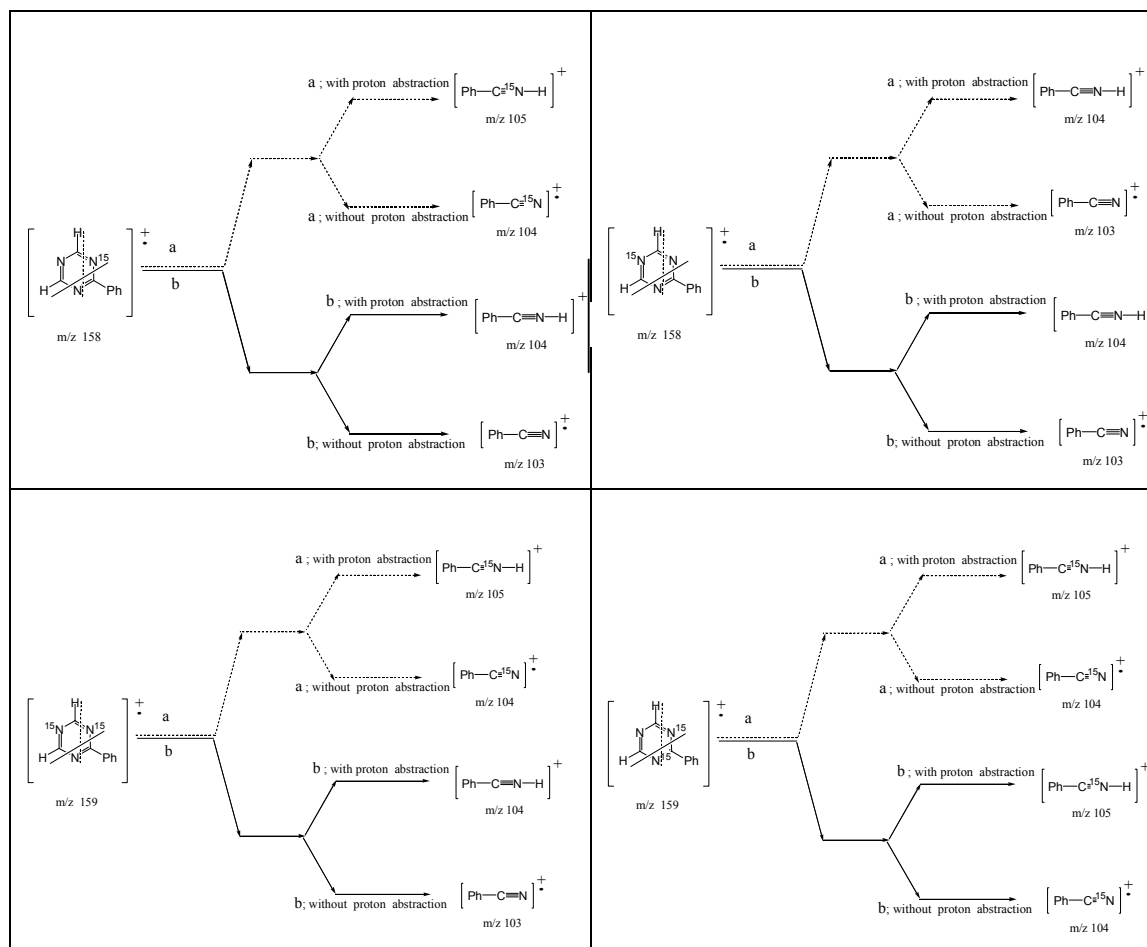
Figure 87: Mass spectrum of un-labeled 2-phenyl-1,3,5-triazine

The mass spectrum of the un-labelled triazine **52** (Figure 87) reveals a molecular ion at m/z 157 and a base peak at m/z 104. The major possible fragmentation pathways could be expected as shown in Scheme 35.



Scheme 35: Major possible fragmentation pathways of regular 2-phenyl-1,3,5-triazine

According to the fragmentation patterns of the un-labelled triazine **39** in Scheme 35, this could lead to the structures of 2-phenyl-1,3,5-triazine photoproduct containing one ^{15}N and two ^{15}N atoms, which are shown in Scheme 36.



Scheme 36: Possible structures and fragmentation patterns of 2-phenyl-1,3,5-triazine containing one ^{15}N and two ^{15}N atoms

The fragmentation patterns in Scheme 36 reveals the ratio of 103 : 104 : 105 peaks at 1 : 2 : 1. However, the formation of 2-phenyl-1,3,5-triazine containing one ^{15}N and two ^{15}N atoms was presented with the corrected ratio of 0.84, thus, the actual ratio of 103 : 104 : 105 peaks would be 1 : 2.1 : 1.1. However, the observed corrected ratio is observed at value of 1 : 4.4 : 3.2 .

The mass spectrum of the second eluted triazine **40**, which is shown in Figure 81f, exhibits molecular ions at m/z 234 and 235 which indicate the formation of 2,4-diphenyl-1,3,5-triazine molecules containing one ^{15}N and two ^{15}N atoms. This triazine was unable to be detected before 8 min of irradiation. However, at irradiation times from 8 to 16 min the corrected ratio of the 234/235 peaks is constant at a value of 1.2. This indicates that the photoproduct is a mixture with 54% of the 2,4-diphenyl-1,3,5-triazine molecules containing one ^{15}N atom and 46 % containing two ^{15}N atoms per molecule.

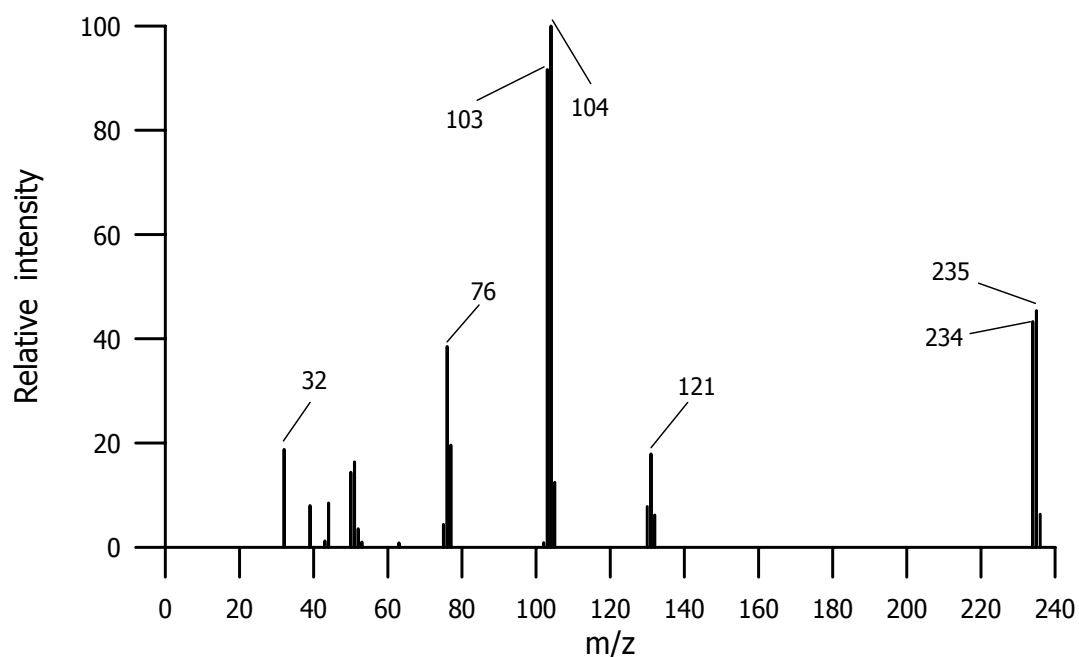


Figure 81f: Mass spectrum of 2,4-diphenyl-1,3,5-triazine photoproduct containing one ^{15}N and two ^{15}N atoms

The mass spectrum of the un-labelled triazine **40** (Figure 88) reveals a molecular ion at m/z 233 and a base peak at m/z 103. In the mass spectrum of triazine containing ^{15}N , it reveals a peak at m/z 104 as a base peak. The observed corrected ratio of 103/104 peaks is 1.03. Scheme 32 shows the possible fragmentation pathways of this triazine **40** containing one and two ^{15}N atoms. According to Scheme 32, the ratio of 103/104 fragments should be 1 : 1. Interestingly, the observed corrected ratio of 103/104 peaks is consistent with the ratio predicted in Scheme 37.

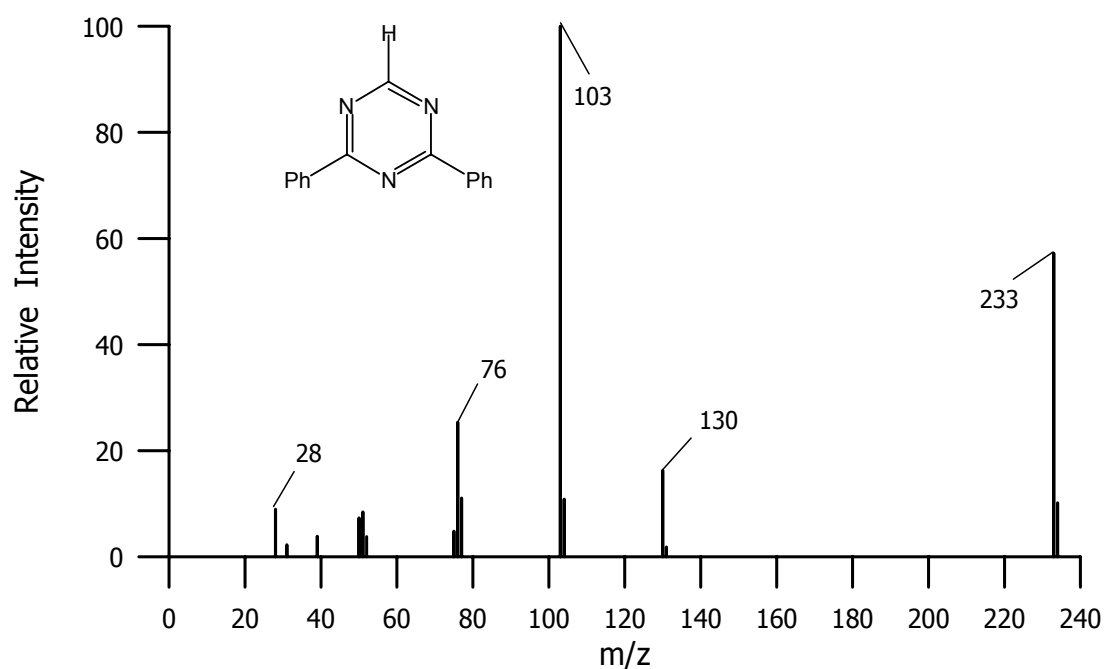


Figure 88: Mass spectrum of regular 2,4-diphenyl-1,3,5-triazine

2.4.3 Preparative scale photolysis

2.4.3.1 Preparative gas chromatography: isolation of the un-consumed reactant and the phototransposition product

A solution of 5-phenyl-1,2,4-thiadiazole-4-¹⁵N (**31-4¹⁵N**) in acetonitrile (1.8×10^{-2} M; 25 mL) was irradiated with sixteen > 290 nm lamps for 180 min while the solution was continuously purged with a fine stream of argon gas. The resulting reaction solution turned to a light brown clear solution with a fine solid precipitate. This preparative scale photolysis was focused on the isolation of the un-consumed reactant and the phototransposition product, 3-phenyl-1,2,4-thiadiazole-¹⁵N, by preparative gas chromatography and preparative thin layer chromatography.

The un-consumed reactant, 5-phenyl-1,2,4-thiadiazole-¹⁵N, eluted with a retention time of 9.5 min. TLC analysis indicated the presence of two components which expected to be the un-consumed reactant and 2-phenyl-1,3,5-triazine-¹⁵N. Thus, this mixture was subjected to preparative layer chromatography [hexane:chloroform (3:2)]. The un-consumed reactant, which had an R_f of 0.8 (10 runs), was removed from the plate. Figure 89 shows ¹H-NMR spectrum of the isolated un-consumed reactant. The spectrum indicates the presence of 5-phenyl-1,2,4-thiadiazole-¹⁵N with two multiplets at δ 7.58-7.62 (m, 3H), δ 8.06-8.09 (m, 3H) and a doublet at δ 8.803 (d, 1H, $J = 13.89$ Hz). The ¹⁵N-spectrum of the reactant, 5-phenyl-1,2,4-thiadiazole-4-¹⁵N (**31-4¹⁵N**), before irradiation (Figure 90a) exhibits a signal due to the ¹⁵N atom at position 4 as a doublet at δ 300.9 ($J = 13.9$ Hz) while the ¹⁵N-spectrum of the isolated un-consumed reactant (after 180 min of irradiation) (Figure 90b) reveals an additional signal at δ 254.7 as a singlet. Since mass spectral analysis indicated that **31-4¹⁵N** had undergone photo-¹⁵N-scrambling to **31-2¹⁵N**, the new signal at δ 254.7 is expected to be due to the ¹⁵N at position 2 in **31-2¹⁵N**.

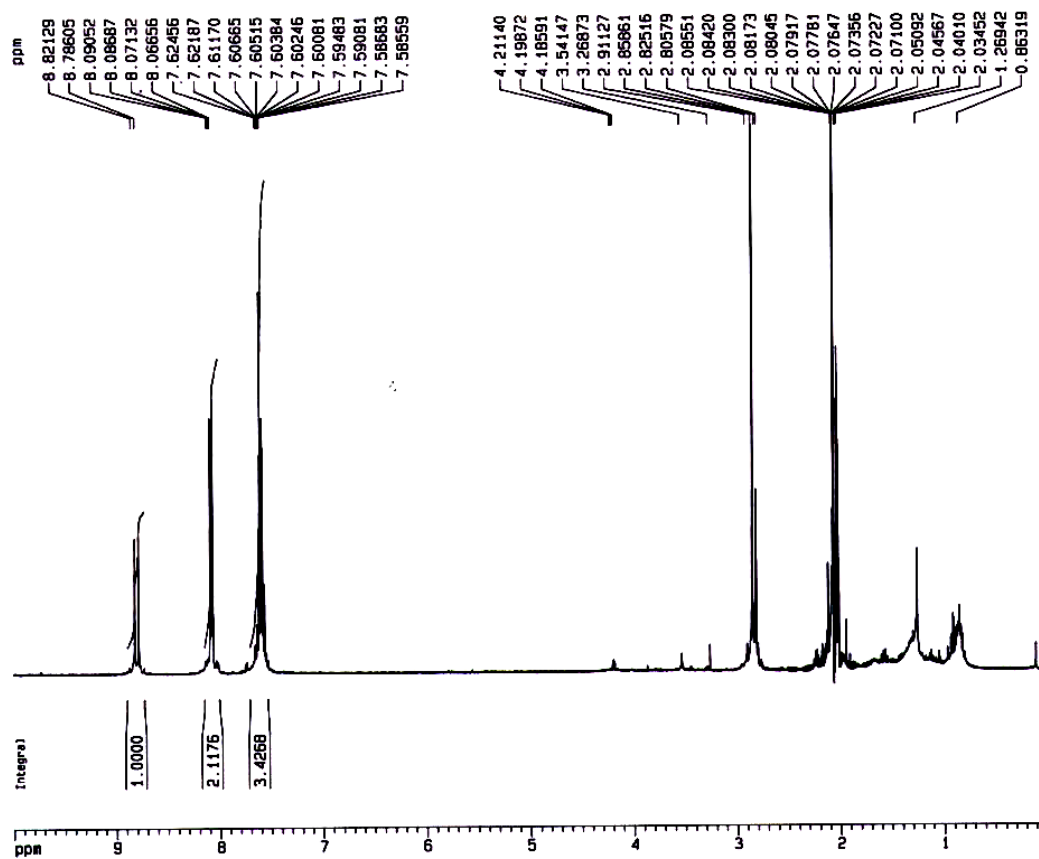


Figure 89: $^1\text{H-NMR}$ spectrum of the isolated un-consumed 5-phenyl-1,2,4-thiadiazole- ^{15}N

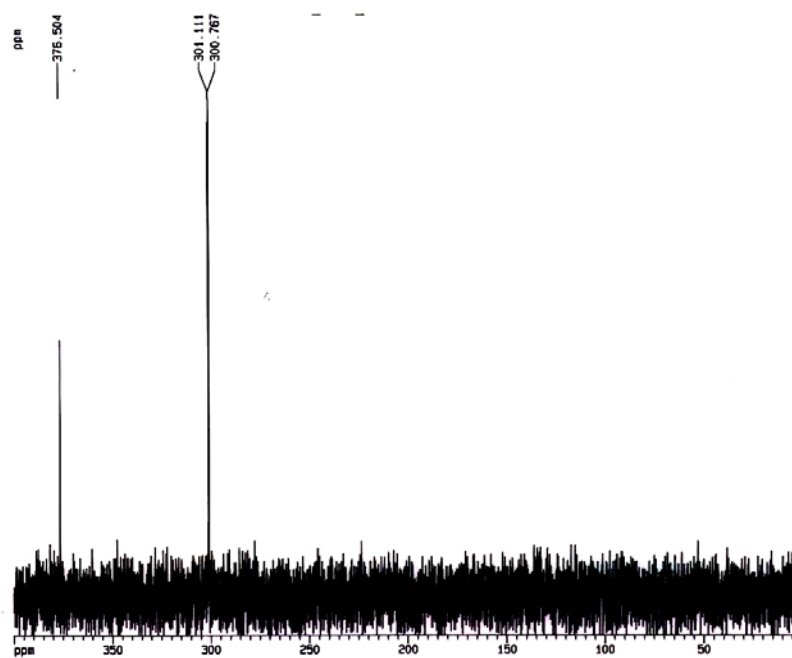


Figure 90a: ^{15}N -NMR spectrum of 5-phenyl-1,2,4-thiadiazole-4- ^{15}N before irradiation

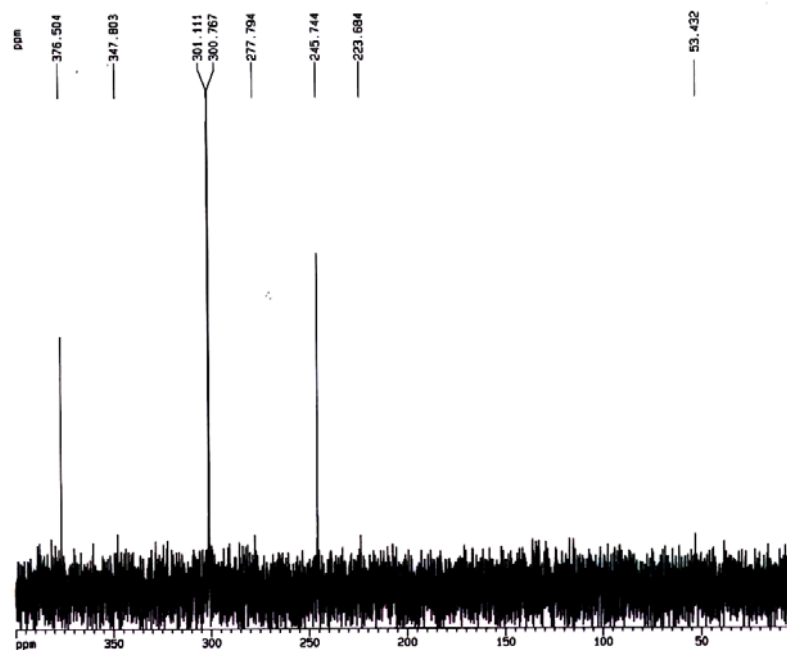


Figure 90b: ^{15}N -NMR spectrum of the isolated un-consumed reactant after irradiation

The phototransposition product was isolated from the reaction mixture by preparative gas chromatography with a retention time of 17 min. TLC analysis of this isolated product indicated the presence of at least two components in this sample. The $^1\text{H-NMR}$ spectrum of this isolated product (Figure 91) exhibits three multiplets at δ 7.52-7.62, 8.06-8.09, and 8.34-8.78 and three doublets at δ 8.80 ($J = 13.89$ Hz), δ 10.27 ($J = 11.62$), and δ 10.275 ($J = 1.52$ Hz). This $^1\text{H-NMR}$ spectrum reveals that this sample is a mixture between 5- and 3-phenyl-1,2,4-thiadiazole- ^{15}N , which indicates an unsuccessful isolation. The doublet at δ 8.80 ($J = 13.89$ Hz) is due to the presence of the unconsumed reactant. By comparison with the ^1H -spectrum of 3-phenyl-1,2,4-thiadiazole- ^{14}N , the ring proton at position 5 of thiadiazole ring is known to appear as a singlet at δ 10.3. Thus, the two overlapping doublets at δ 10.27 ($J = 11.62$), and δ 10.275 ($J = 1.52$ Hz) are due to the presence of 3-phenyl-1,2,4-thiadiazole-4- ^{15}N (**46-4 ^{15}N**) and 3-phenyl-1,2,4-thiadiazole-2- ^{15}N (**46-2 ^{15}N**), respectively, confirming ^{15}N -scrambling in 3-phenyl-1,2,4-thiadiazole- ^{15}N . The doublet at δ 10.27 with the larger coupling constant ($J = 11.62$ Hz) is expected due to the ring proton at position 5 of **46-4 ^{15}N** coupling with the ^{15}N nucleus at ring position 4 while the doublet at δ 10.275 with smaller coupling constant ($J = 1.52$ Hz) is expected due to the ring proton at position 5 of **46-2 ^{15}N** coupling with the ^{15}N nucleus at position 2. The ^{15}N -spectrum (Figure 92) also reveals a signal due to the presence of **31-4 ^{15}N** as a doublet at δ 302.3 ($J = 13.9$ Hz) and **31-2 ^{15}N** as a singlet at δ 261.4. The spectrum also reveals a doublet at δ 307.76 ($J = 11.9$ Hz), which is expected due to the presence of **46-4 ^{15}N** based on the corresponding coupling constant in the ^1H -spectrum, which was proposed due to this compound. However, according to the previous GC analysis results indicated the 50 % ^{15}N -scrambling in the phototransposition, therefore, this ^{15}N -spectrum should also present a doublet with a small coupling constant due to 3-phenyl-1,2,4-thiadiazole-2- ^{15}N . But there is no any signal indicates the presence of this product.

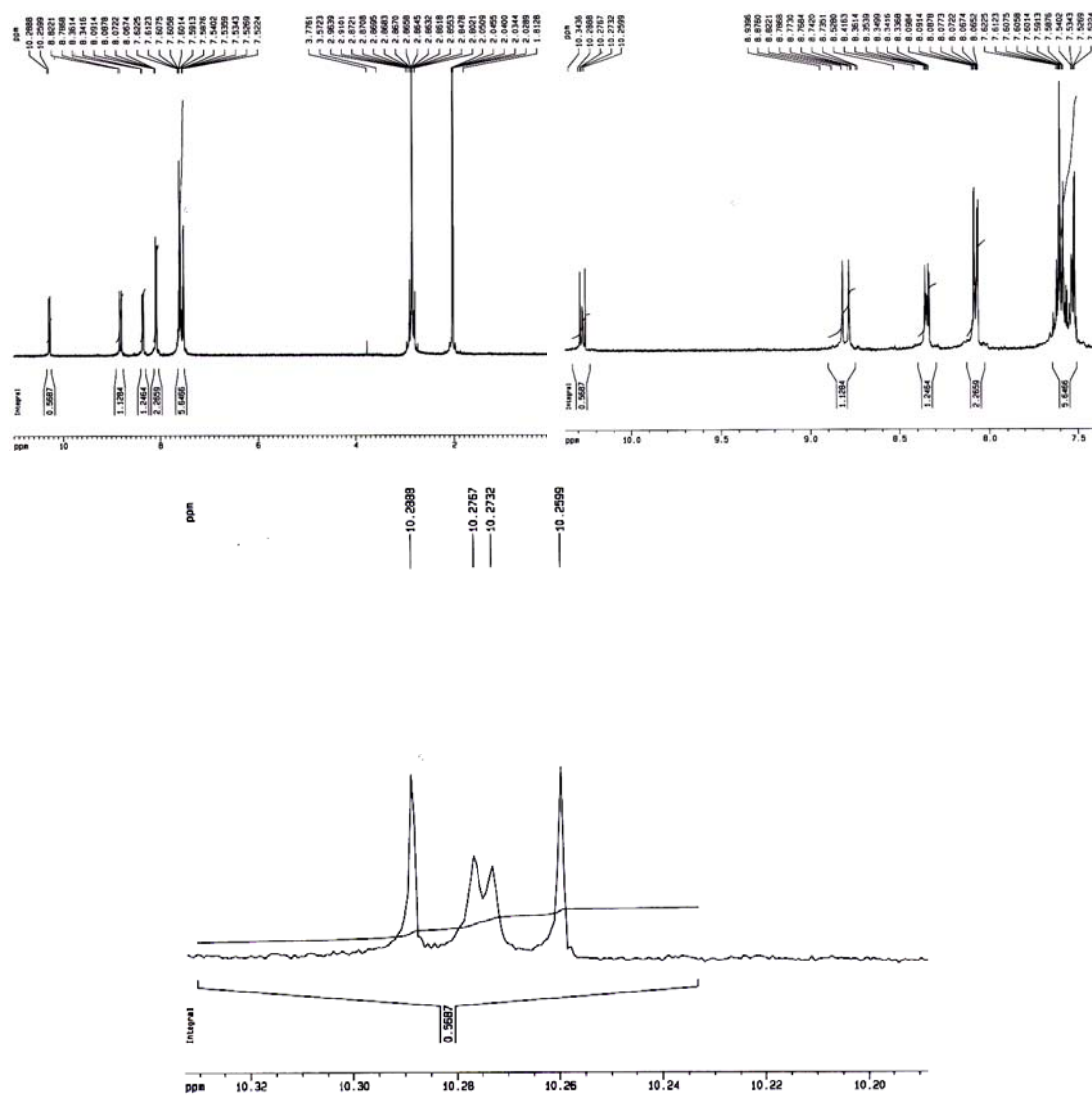


Figure 91: $^1\text{H-NMR}$ spectrum of the isolated 3-phenyl-1,2,4-thiadiazole- ^{15}N

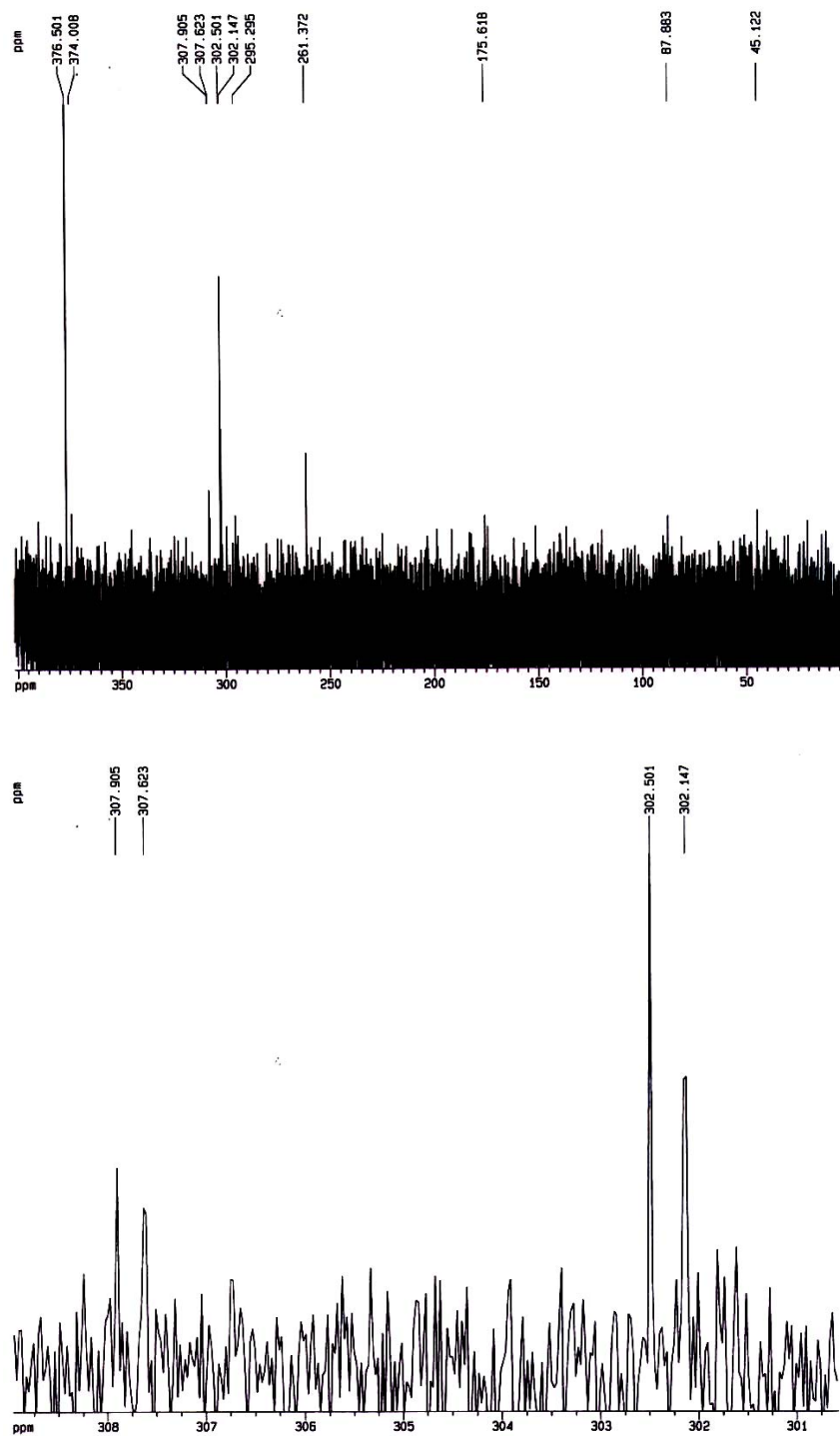


Figure 92: ^{15}N -NMR spectrum of the isolated 3-phenyl-1,2,4-thiadiazole- ^{15}N

2.3.4.2 Preparative layer chromatography: isolation of the unconsumed reactant and the phototransposition product.

A solution of purified 5-phenyl-1,2,4-thiadiazole-4-¹⁵N (**31-4¹⁵N**) (2×10^{-2} M, 8 mL) was photolysed to 40% consumption of the reactant. The reaction solution was concentrated to dryness (42 mg), re-dissolved in small amount of dichloromethane and subjected to preparative layer chromatography. Dichloromethane:hexane (4:1) was employed as a developing solvent. The un-consumed reactant was removed from the plate with a R_f of 0.39 (4 runs) and the phototransposition product was removed with a R_f of 0.69 (4 runs). The ¹H-NMR spectrum of the band with R_f of 0.69 (Figure 93) exhibits two multiplets at δ 7.28-7.53 (m, 3H), δ 7.95-7.98 (m, 2H) and a doublet at δ 8.69 (d, 1H, $J = 13.89$ Hz) which are indicating the presence of the un-consumed reactant, 5-phenyl-1,2,4-thiadiazole-¹⁵N. The ¹H-NMR spectrum of the band with R_f of 0.39 (Figure 94) exhibits two multiplets at δ 7.23-7.50 (m, 3H), δ 7.82-8.34 (m, 2H) and two overlapping doublets at δ 9.875 (d, $J = 11.12$ Hz) and δ 9.875 (d, $J = 1.52$ Hz). These signals indicate the presence of 3-phenyl-1,2,4-thiadiazole-¹⁵N with ¹⁵N atom in both position 2 ($J_{H15N} = 1.52$ Hz) and 4 ($J_{H15N} = 11.12$ Hz).

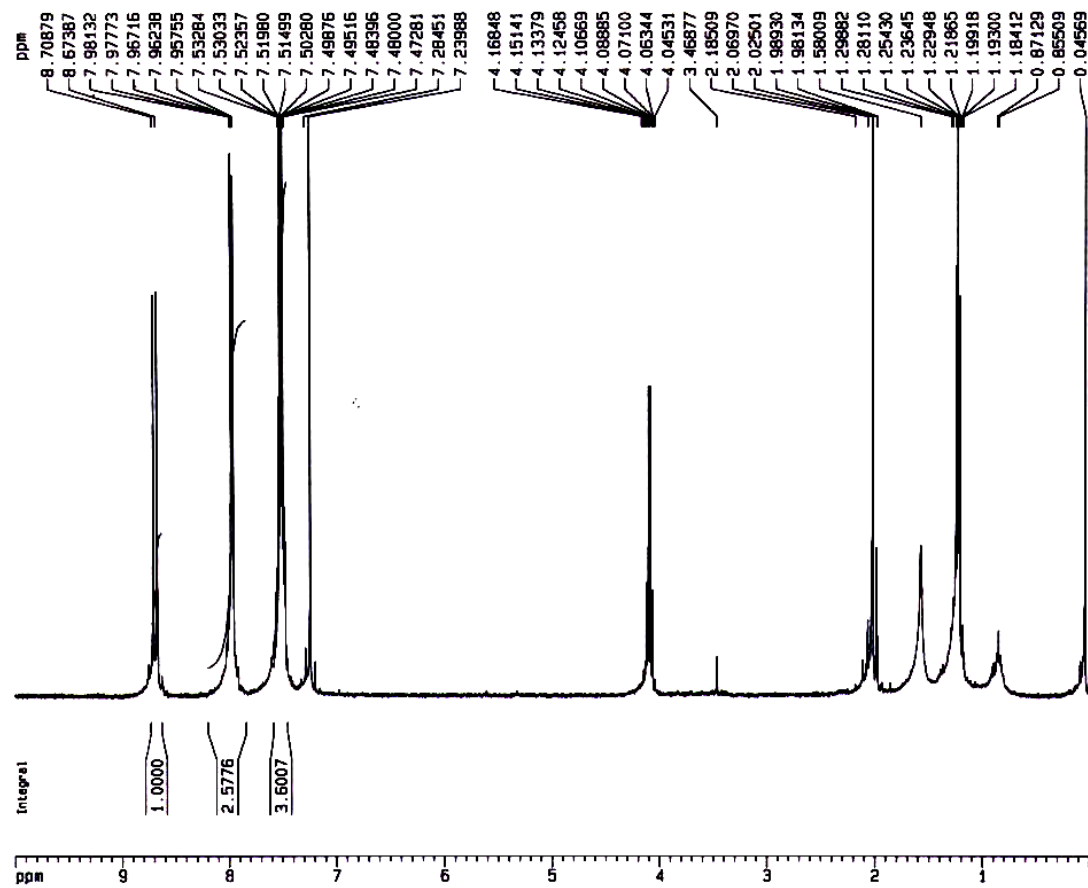


Figure 93: $^1\text{H-NMR}$ spectrum of the isolated unconsumed reactant after 180 min of irradiation

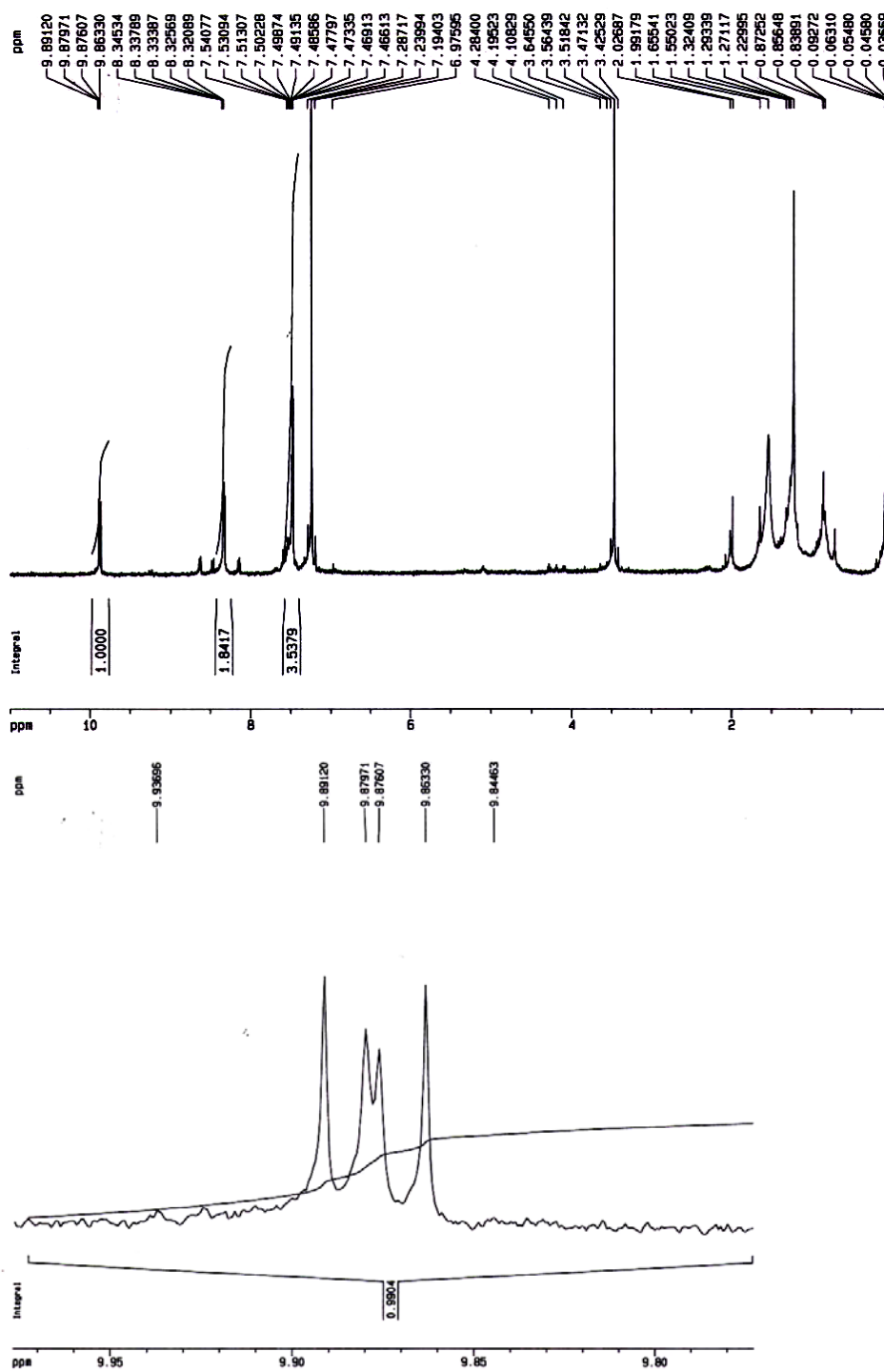
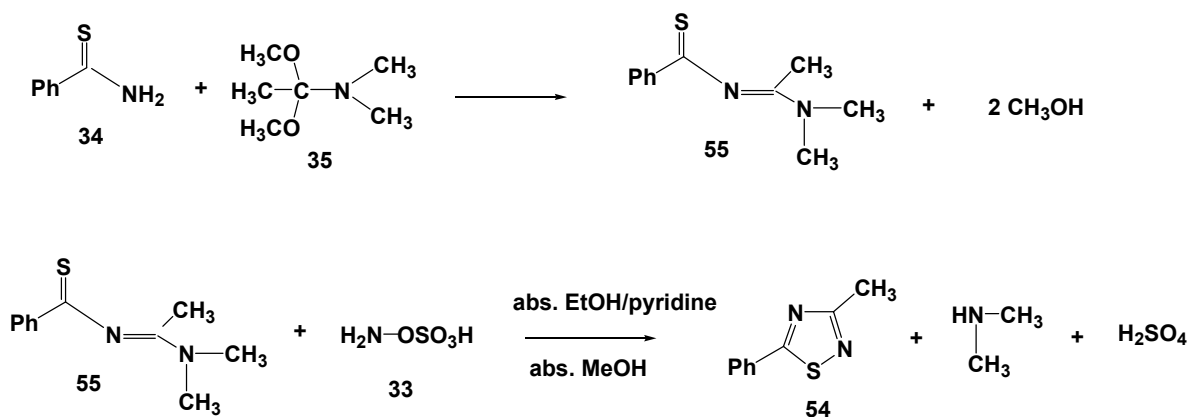


Figure 94: $^1\text{H-NMR}$ spectrum of a mixture of $46\text{-}4^{15}\text{N}$ and $46\text{-}2^{15}\text{N}$

2.5 Photochemistry of 3-methyl-5-phenyl-1,2,4-thiadiazole-4¹⁵N

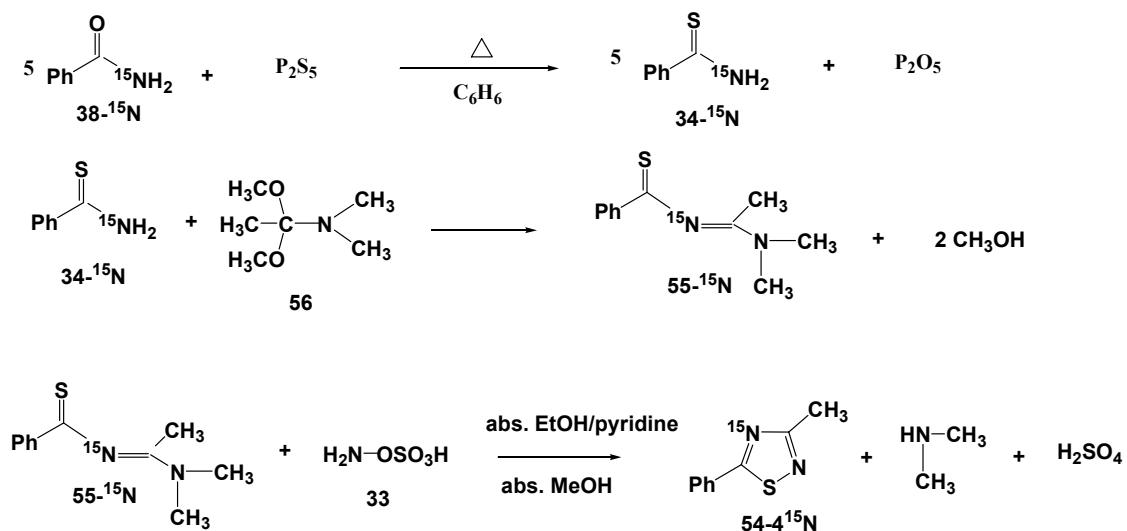
2.5.1 Synthesis of 3-methyl-5-phenyl-1,2,4-thiadiazole-4¹⁵N

3-Methyl-5-phenyl-1,2,4-thiadiazole (**54**) was previously synthesized by the cyclization of **55** with **33** as shown in Scheme 38.



Scheme 38: Synthesis of 3-methyl-5-phenyl-1,2,4-thiadiazole

3-methyl-5-phenyl-1,2,4-thiadiazole-4-¹⁵N (**54-4¹⁵N**) was synthesized from commercially available benzamide-¹⁵N (**38-¹⁵N**) by the procedure outlined in Scheme 39.



Scheme 39: Synthetic pathway of 3-methyl-5-phenyl-1,2,4-thiadiazole-4- ^{15}N

Figure 95a-b and 96 exhibit the ^1H -NMR and ^{13}C -NMR spectra of $34\text{-}^{15}\text{N}$, respectively. The spectra reveal the complicated couplings similar to the ^1H -NMR spectra of $34\text{-}^{15}\text{N}$ previously synthesized as the starting material for the synthesis of $31\text{-}4\text{-}^{15}\text{N}$.



Figure 95a: ^1H – NMR spectrum of thiobenzamide- ^{15}N

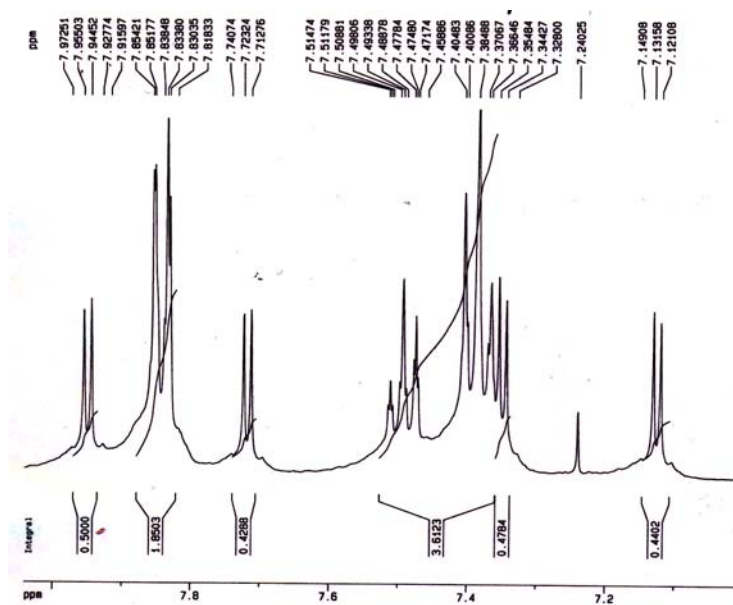


Figure 95b: ^1H -NMR spectrum of thiobenzamide- ^{15}N ; scale expansion at δ 7.12-7.92

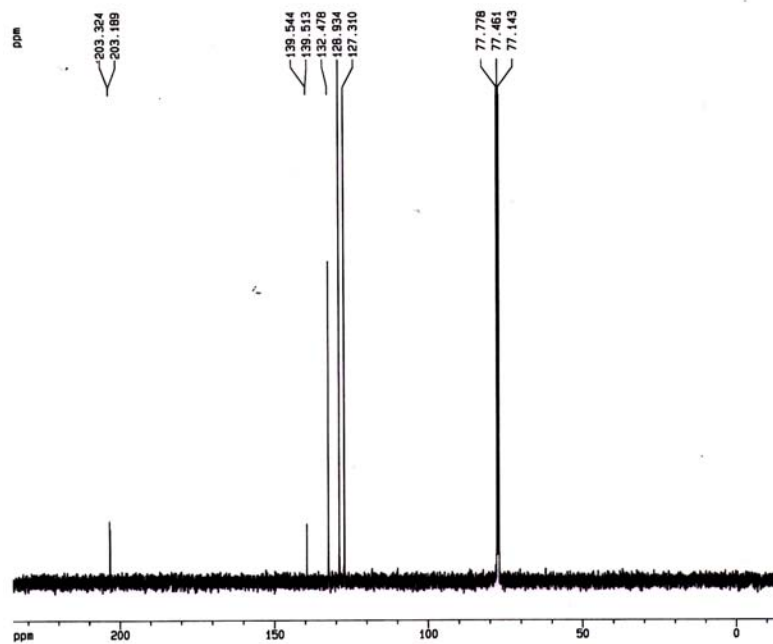


Figure 96: ^{13}C -NMR spectrum of thiobenzamide- ^{15}N

The second step in this synthetic pathway was the preparation of N-[(dimethylamino)ethylidene]thiobenzamide- ^{15}N (**55- ^{15}N**) by a condensation reaction of **34- ^{15}N** with **56**. The desired ^{15}N -labeled-amidine **55- ^{15}N** was obtained as orange crystals in 82.3% yield with the melting point of 110-113°C. The ^1H -NMR spectrum of these crystals (Figure 97) exhibits the two multiplets at δ 7.29-7.42 (3H) and δ 8.22-8.24 (2H), which were assigned to para-meta and ortho-phenyl protons, respectively. The two singlets (3H) at δ 3.19 and 3.21 are the absorptions due to the two sets of the non-equivalent methyl protons bonded to the amino group. The protons of the methyl group which is bonded to the imine carbon is revealed as a singlet (3H) at δ 2.47.

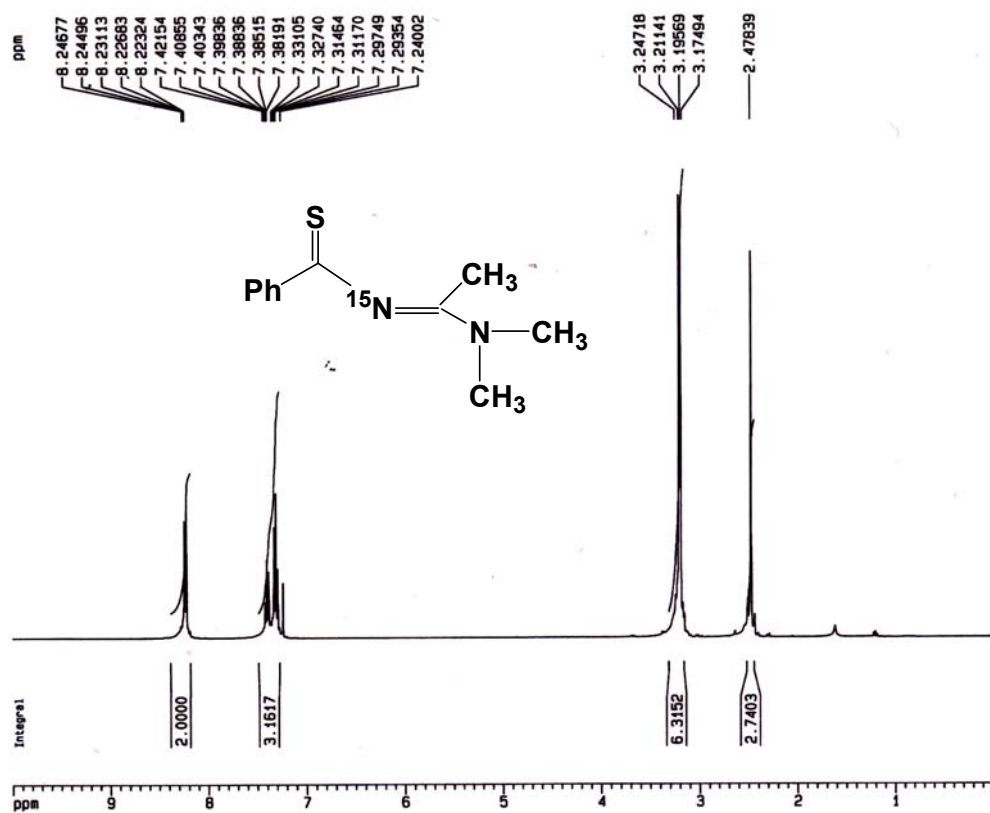


Figure 97: ^1H -NMR spectrum of N-[(dimethylamino)ethylidene]thiobenzamide- ^{15}N

In the ^{13}C -NMR spectrum (Figure 98a), the most down field doublet at δ 202.7 ($J = 6.90$ Hz) is assigned to the thiocarbonyl. It appears as a doublet due to the coupling of this carbon with ^{15}N atom. The imine carbon absorbs at δ 168.3. This signal also appears as a doublet ($J = 12.30$ Hz) due to the coupling of this carbon with ^{15}N atom. The four signals at δ 128.0, 128.8, 131.3 and 142.9 were assigned to the ring phenyl carbons. However, upon the scale expansion (Figure 98b) the spectrum also reveals a pair of doublets at δ 128.8 and 142.9 with coupling constants of 2.30 and 8.40 Hz, respectively. According to the ^1H - ^{13}C correlation spectrum (Figure 99), the signal at δ 128.8 ($J = 2.30$ Hz) is assigned as ortho-phenyl ring carbon since this signal correlates with the signal at δ 8.22-8.24 (multiplet, 2H) in the ^1H -spectrum which was assigned to ortho-phenyl ring protons. The signal at δ 142.9 ($J = 8.4$ Hz) can also be assigned to the meta-phenyl ring carbon since this signal correlates with the signal at δ 7.29-7.42 (3H) in the ^1H - spectrum which was assigned to the para- and meta- phenyl ring protons. The intensity of this signal is also consistent with the assignment to meta-phenyl ring carbons. These two phenyl-carbon signals appear as two doublets, presumably due to a long-range coupling of these carbons with ^{15}N atom. The spectrum reveals the two non-equivalent methyl carbons of the amino group as two singlets at δ 39.5 and 39.7. The methyl carbon attached to the imine carbon appears at δ 18.4.

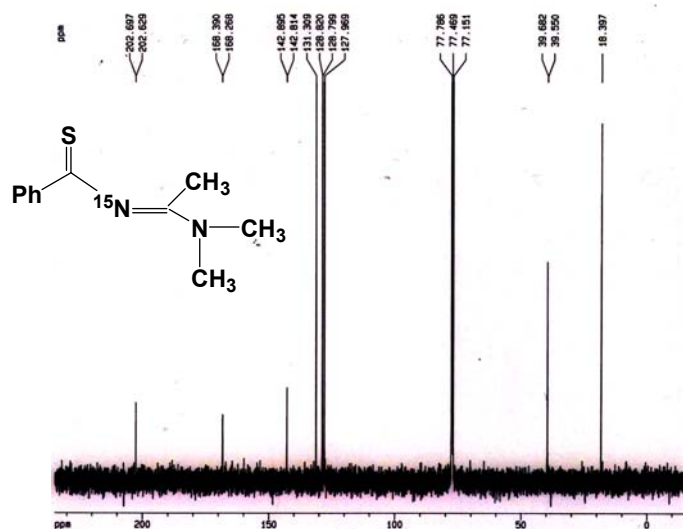


Figure 98a: ^{13}C -NMR spectrum of N-[(dimethylamino)ethylidene]thiobenzamide- ^{15}N

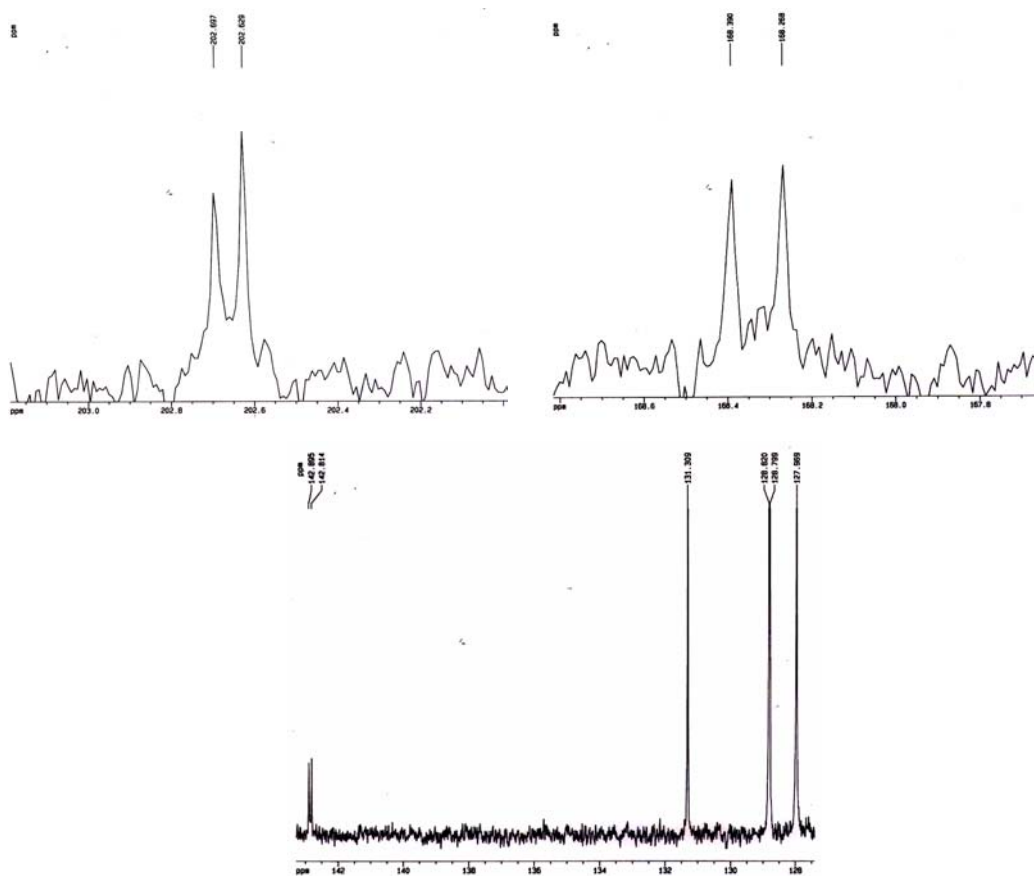


Figure 98b: ^{13}C -scale expansion spectrum of 55- ^{15}N

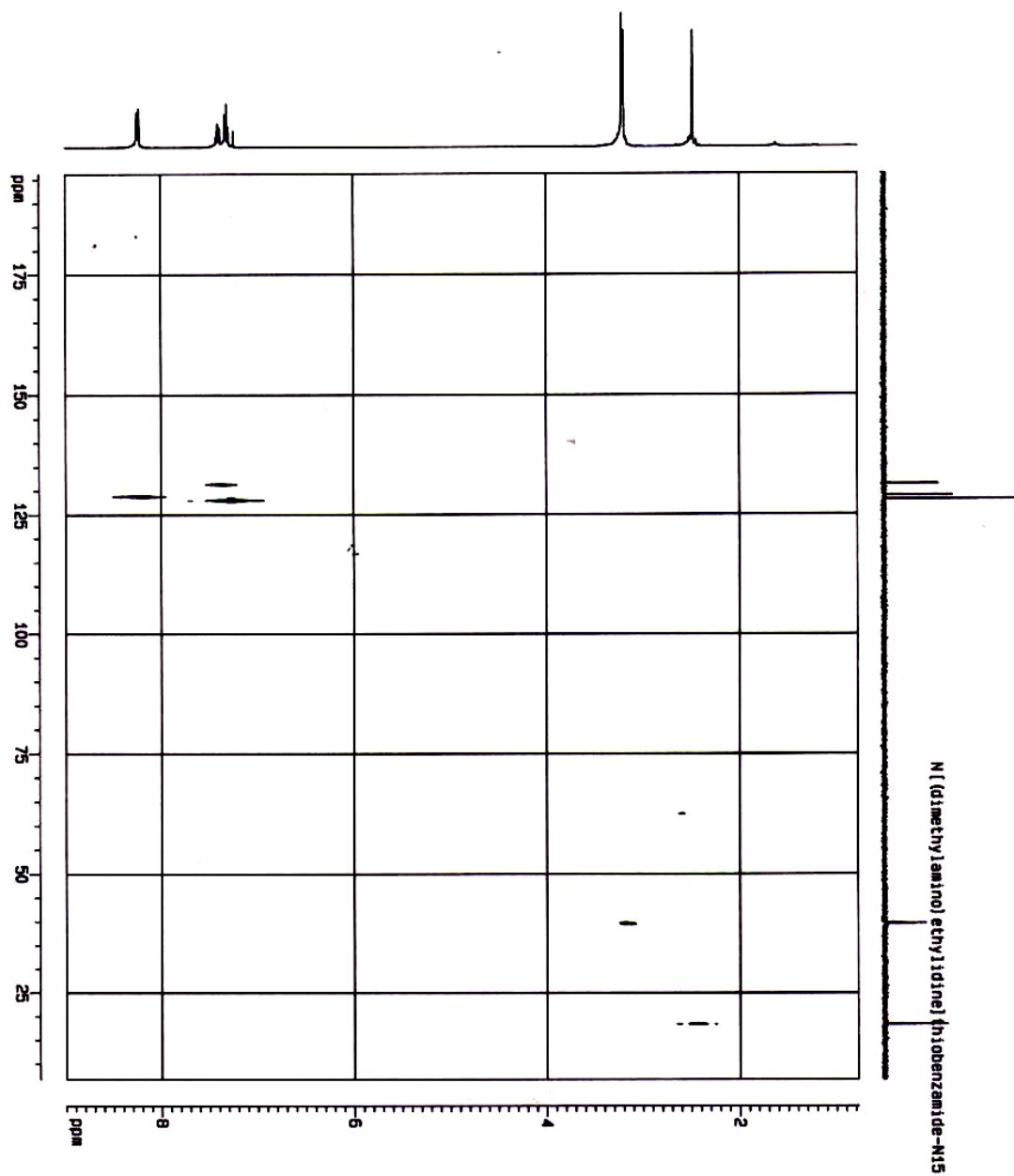


Figure 99: ^1H - ^{13}C correlation spectrum of $^{55}\text{-}^{15}\text{N}$

The ^{15}N -NMR spectrum (Figure 100) exhibits a singlet at δ 289.5 which is due to the single ^{15}N atom in the molecule. Surprisingly, the spectrum does not exhibit the splitting of this signal which could be expected due to the coupling of ^{15}N with ^{13}C as showing in ^{13}C -NMR spectrum. This is most likely due to the very low concentration of ^{13}C in the compound.

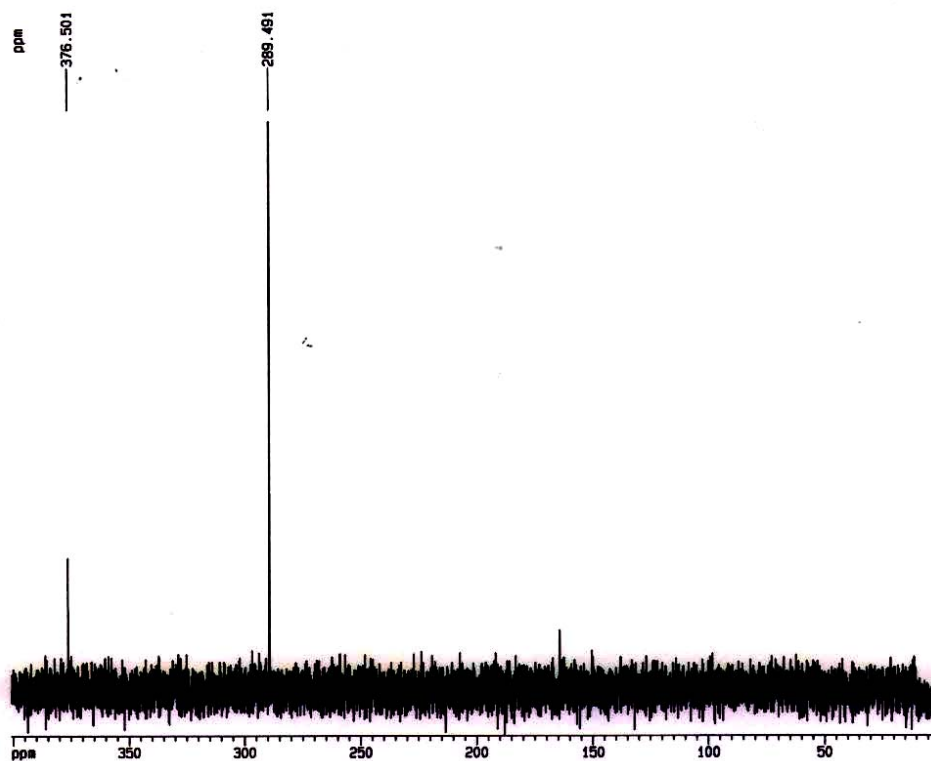


Figure 100: ^{15}N -NMR spectrum of N-[(dimethylamino)ethylidene]thiobenzamide- ^{15}N

The orange crystals were also analyzed by GC-MS [120°C (10 min), 20°C /min to 240°C (30 min)] (Figure 101a). The mass spectrum of the peak that eluted with a retention time of 39.5 min (Figure 101b) shows a molecular ion at m/z 207, which corresponds to the molecular weight of the desired product, N-[(dimethylamino)ethylidene]thiobenzamide- ^{15}N ($55\text{-}^{15}\text{N}$). The trace also exhibits the presence of some impurities.

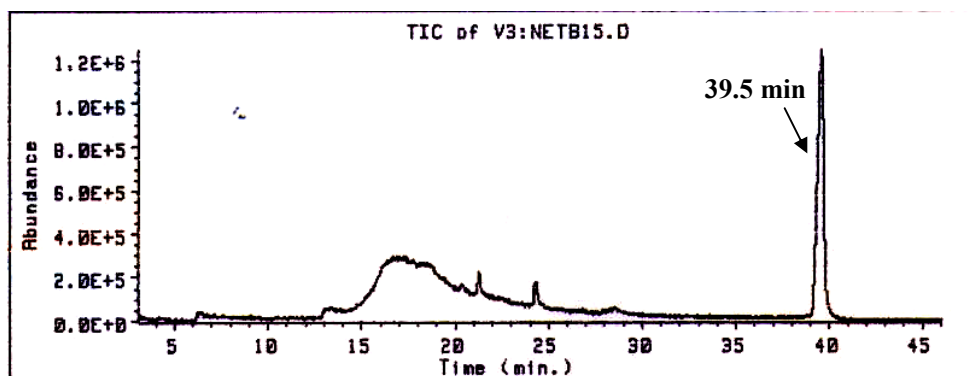


Figure 101a: GC-trace of N-[(dimethylamino)ethylidene]thiobenzamide- ^{15}N

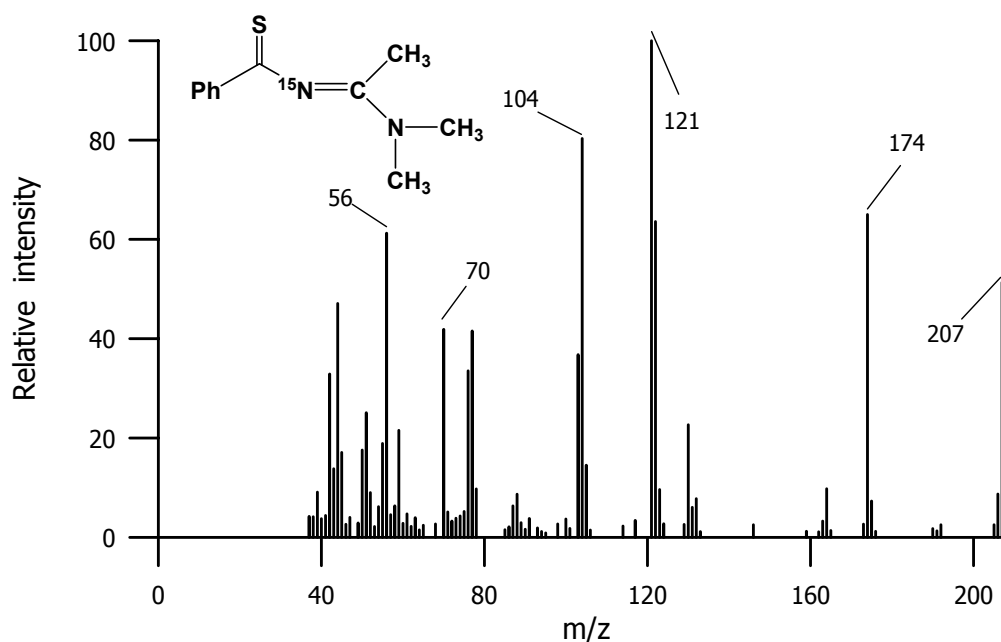


Figure 101b: Mass spectrum of the peak eluted at a retention time of 39.5 min

The third step of this pathway is the amination cyclization of $55\text{-}^{15}\text{N}$ with **33** using pyridine as a basic catalyst. 3-Methyl-5-phenyl-1,2,4-thiadiazole- 4^{15}N ($54\text{-}4^{15}\text{N}$) was obtained as a colorless crystals in 80% yield with the melting point of $50\text{-}52^\circ\text{C}$.

The GC-chromatogram [140°C (5 min), 20°C/min to 240°C (20 min)] of these colorless crystals (Figure 102a) exhibits a major peak with a retention time of 10.8 min. The mass spectrum of this peak (Figure 102b) exhibits a molecular ion at m/z 177, which is consistent with the molecular weight of $54\text{-}4^{15}\text{N}$ (MW 177). The spectrum also exhibits a base peak at m/z 136, which is consistent with the cleavage of $[\text{C}_6\text{H}_5\text{C}^{15}\text{NS}]^{*+}$ and a peak at m/z 73, which is consistent with the cleavage $[\text{CH}_3\text{CNS}]^{*+}$.

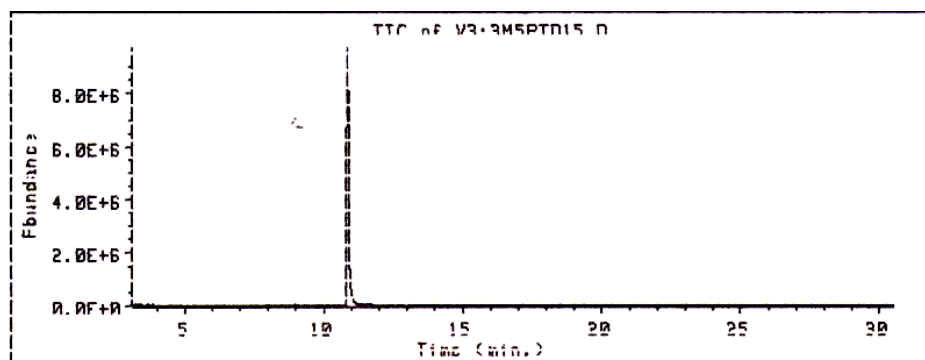


Figure 102a: GC-trace of 3-methyl-5-phenyl-1,2,4-thiadiazole- 4^{15}N

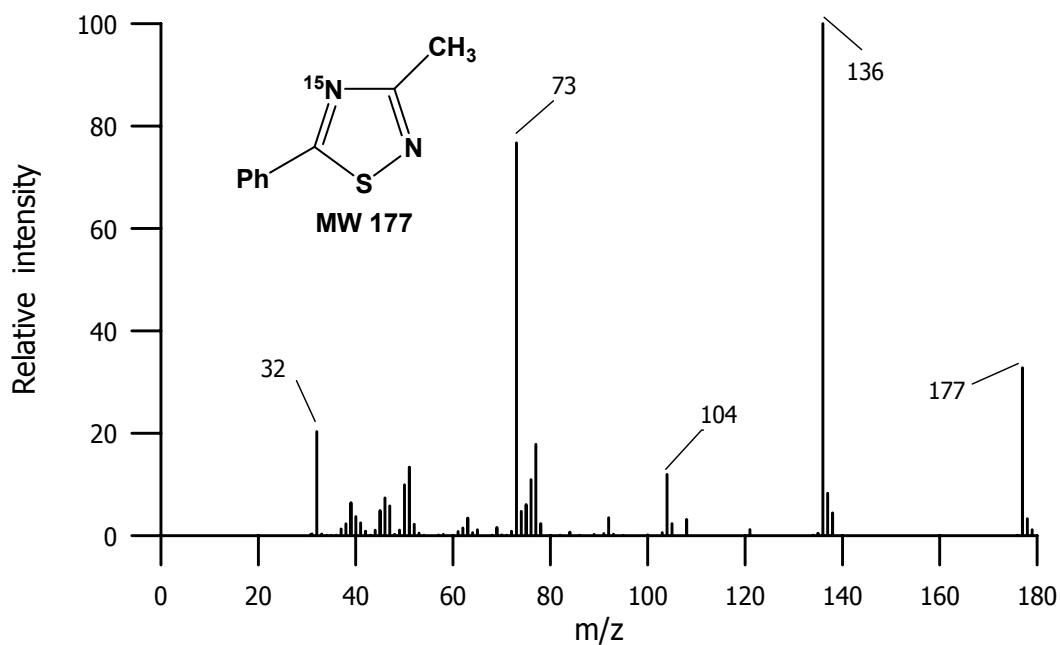


Figure 102b: Mass spectrum of the peak eluted at a retention time of 10.8 min

The ^1H -NMR of this solid (Figure 103) shows two multiplets at δ 7.46-7.50 (3H) and δ 7.90-7.92 (2H), which could be assigned to the para-meta and ortho-phenyl ring protons, respectively. The doublet at δ 2.71 ($J = 2.27$ Hz) is assigned to the protons of methyl group attached to C-3 of thiadiazole ring. This signal appears as a doublet due to a long-range coupling of these protons with ^{15}N atom at position 4.

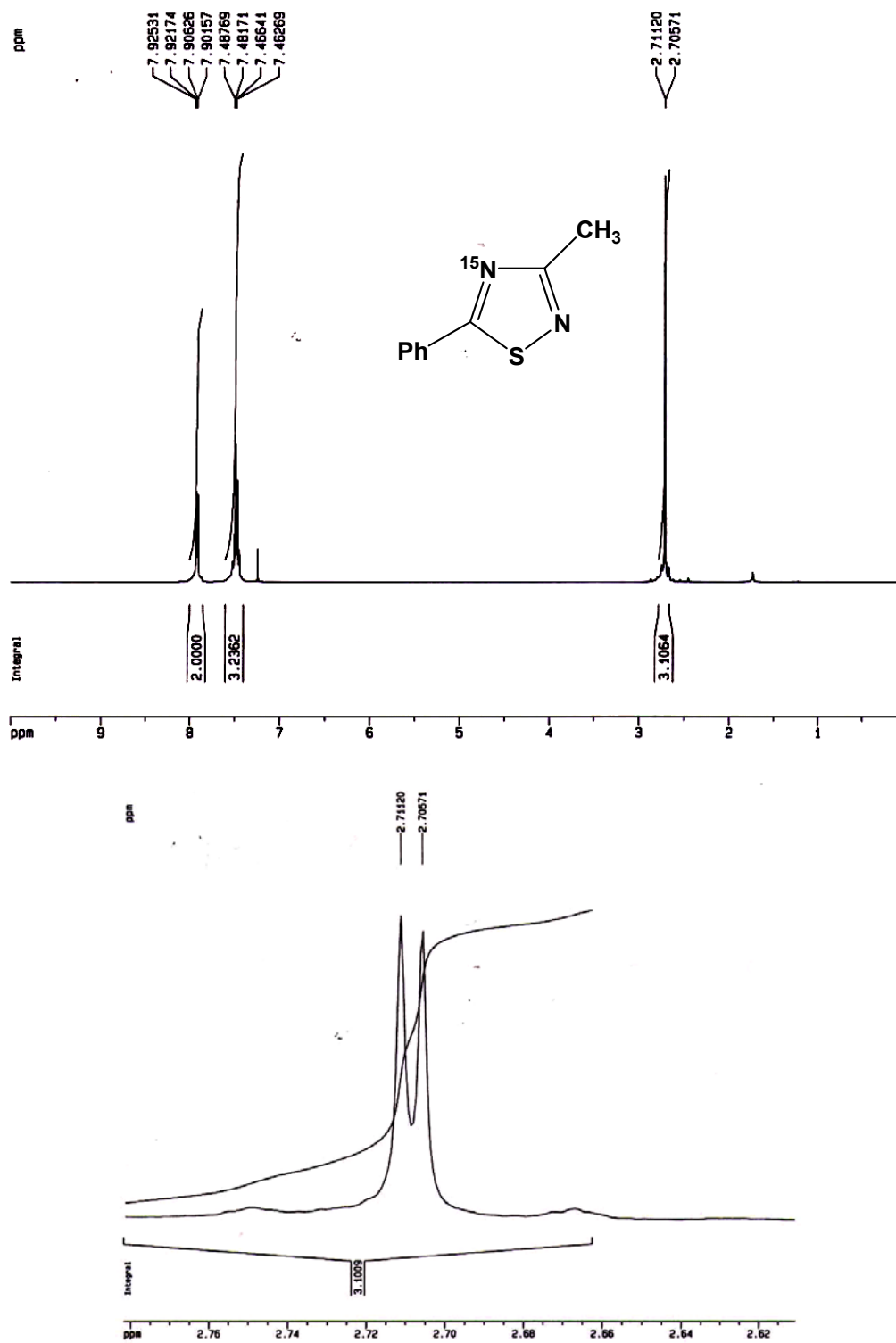


Figure 103: ^1H -NMR spectrum of 3-methyl-5-phenyl-1,2,4-thiadiazole-4- ^{15}N

The ^{13}C -NMR (Figure 104a) reveals the signal of carbon at position 5 on the thiadiazole at δ 188.5. The signal at δ 174.5, which appears as a doublet ($J = 2.30$ Hz), can be assigned to the carbon at position 3 of the thiadiazole ring. The assignment of these two carbons is based on the previous ^{13}C -NMR spectral assignment of 5-phenyl-1,2,4-thiadiazole-4 ^{15}N (**31-4 ^{15}N**). The doublet at δ 174.5 ($J = 2.30$ Hz) can be due to the coupling of this carbon with ^{15}N atom at position 4. Surprisingly, the carbon at position 5 is also bonded to ^{15}N atom at position 4 but the spectrum does not exhibit the coupling of this carbon with ^{15}N atom. The four signals at δ 127.8 (d; $J = 2.30$ Hz), 129.7, 130.9 (d; $J = 6.16$ Hz) and 132.3 were assigned to the phenyl ring carbons. The doublet at δ 19.5 (d; $J = 8.40$ Hz) was assigned to the methyl carbon bonded to the position 3 of the thiadiazole ring. These spectral assignments were confirmed by the ^{13}C -DEPT 135 spectrum, shown in Figure 104b. The doublet at δ 19.5 ($J = 8.40$ Hz) still appears in the ^{13}C -DEPT 135 spectrum, which is consistent with the assignment to the methyl carbon. The two signals at δ 174.5 and 188.6, which were assigned to the two carbons at positions 3 and 5 of the thiadiazole ring, are not observed in the ^{13}C -DEPT 135 spectrum since these signals are due to quaternary carbons. Three of the four signals, which absorb in the phenyl region, still appear in the ^{13}C -DEPT 135 spectrum. Thus, these signals can be assigned to the ortho-, meta- and para-phenyl ring carbons. The doublet at δ 130.9 (d; $J = 6.16$ Hz), which was, however, not observed in the ^{13}C -DEPT 135 spectrum, and therefore can be assigned to the phenyl carbon at ring position 1. The observed splitting in some phenyl carbon signals is presumably due to a long-range couplings with ^{15}N atom.

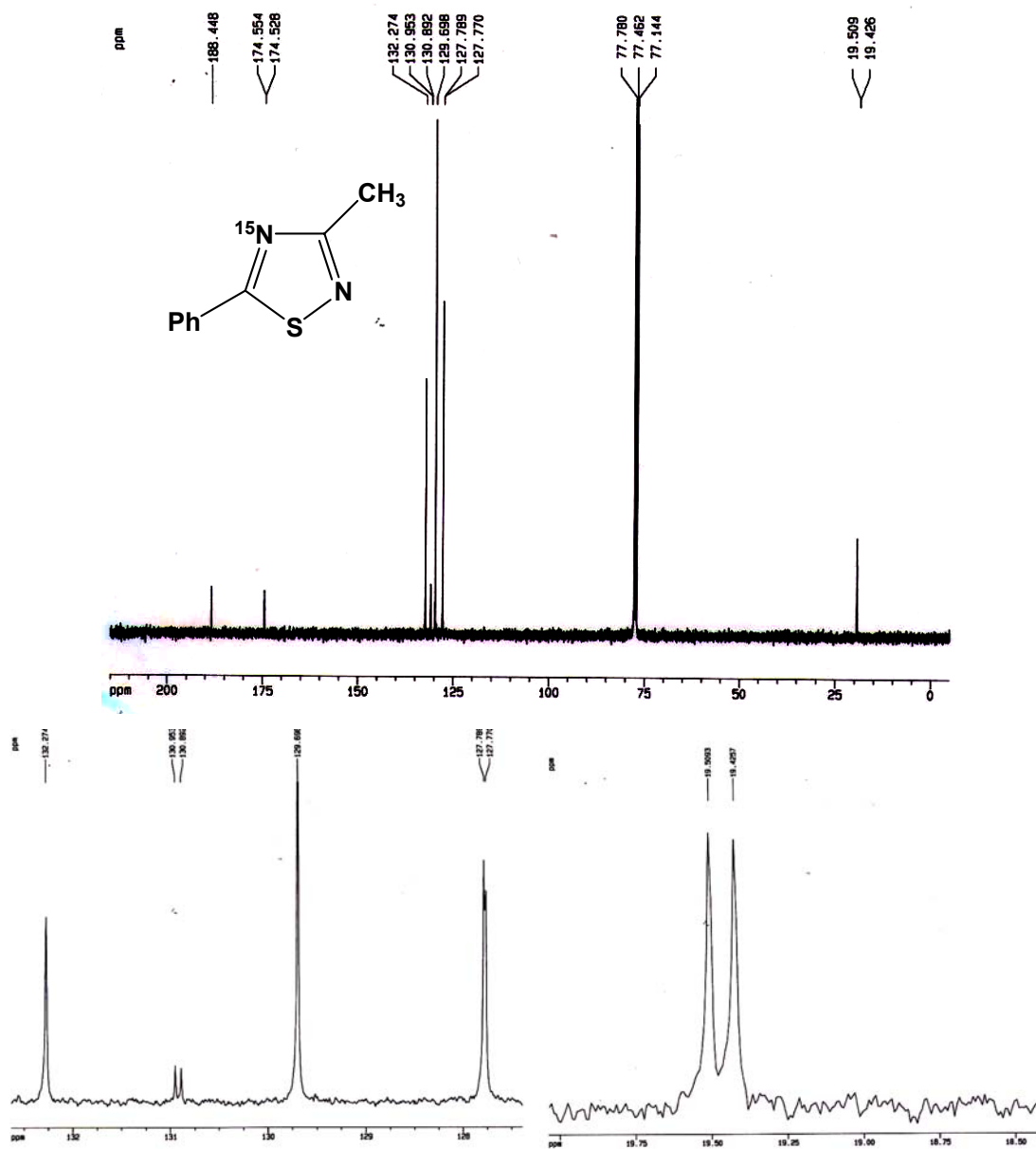


Figure 104a: ^{13}C -NMR spectrum of 3-methyl-5-phenyl-1,2,4-thiadiazole-4- ^{15}N

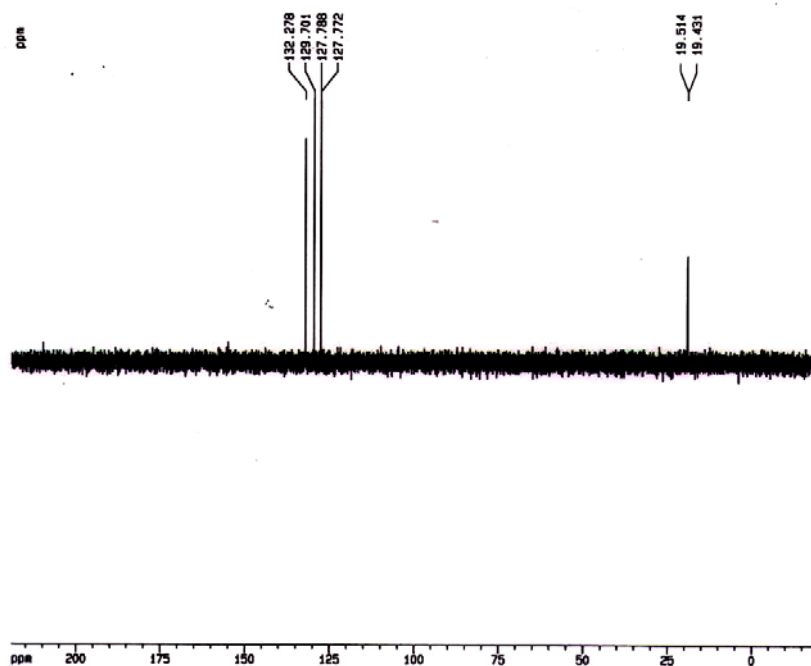


Figure 104b: ^{13}C -DEPT 135 spectrum of 3-methyl-5-phenyl-1,2,4-thiadiazole- 4^{15}N

The ^{15}N -NMR spectrum (Figure 105) reveals a doublet at δ 301.7 ($J = 2.00$ Hz), which can be assigned to the ^{15}N atom at position 4 on the thiadiazole ring. This doublet could be due to a long range coupling of this ^{15}N atom with the protons of the methyl group bonded to the carbon at position 3 of the thiadiazole ring. If this was true then the ^{15}N signal should appear as a quartet and, in fact, it does appear to be a quartet with very small coupling constant and unable to be resolved as a clear quartet. This assignment is consistent with the observed coupling constant of the methyl protons in the ^1H -spectrum ($J = 2.27$ Hz).

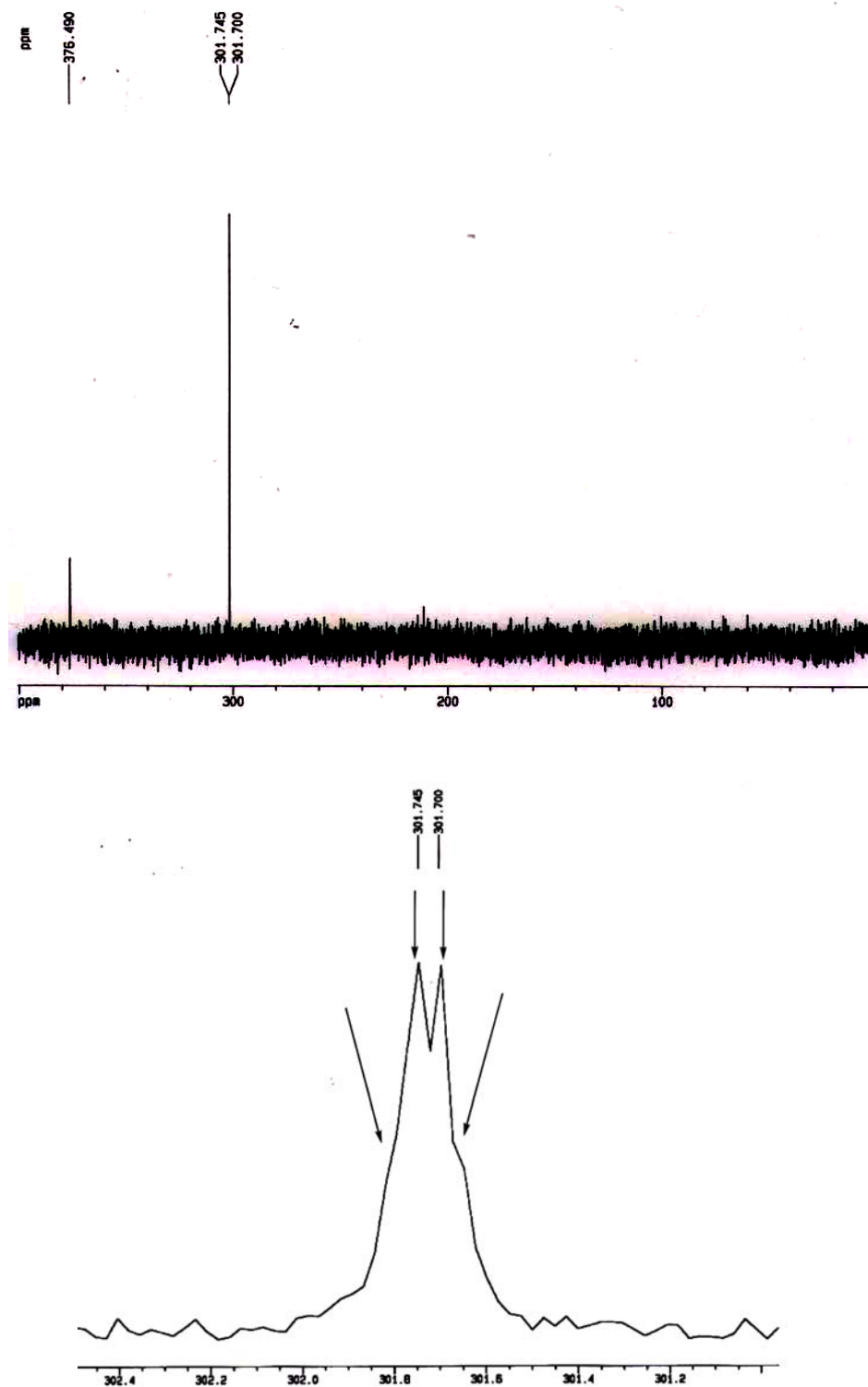
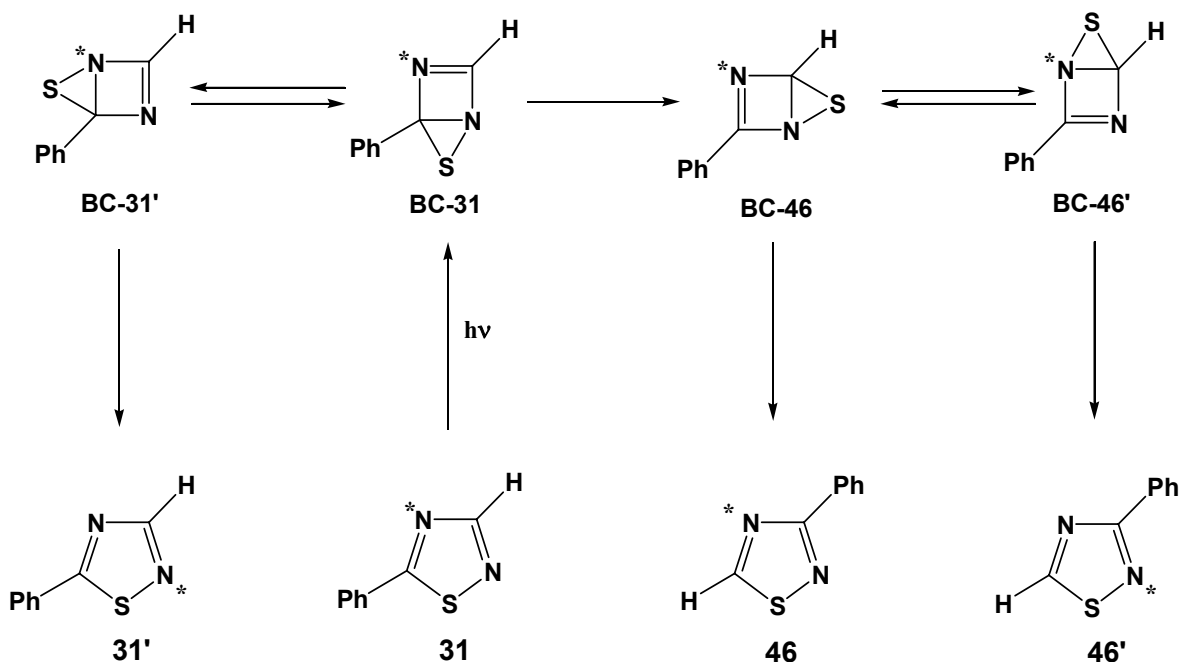


Figure 105: ^{15}N -NMR spectrum of $54\text{-}4^{15}\text{N}$ and the scale expansion showing an un-resolved quartet

2.5.2 Photochemistry of 3-methyl-5-phenyl-1,2,4-thiadiazole-4-¹⁵N

In an earlier part of this thesis it was shown that 5-phenyl-1,2,4-thiadiazole-4-¹⁵N (**31-4¹⁵N**) undergoes phototransposition to 3-phenyl-1,2,4-thiadiazole-¹⁵N with complete scrambling of ¹⁵N between position 2 and 4 of the thiadiazole ring. Upon more prolonged irradiation, ¹⁵N scrambling between rings position 2 and 4 in the un-consumed reactant was also observed. These observations are consistent with the mechanism shown in Scheme 40.

It has also been previously shown in this thesis that 3-methyl-5-phenyl-1,2,4-thiadiazole (**54**) undergoes photoreaction to yield benzonitrile (**43**) in 66%, 5-methyl-3-phenyl-1,2,4-thiadiazole (**57**) in 10%, 2,4-dimethyl-6-phenyl-1,3,5-triazine (**65**) in 33% and 2-methyl-4,6-diphenyl-1,3,5-triazine (**66**) in 6.6%. In this section the results of a study of the photochemistry of 3-methyl-5-phenyl-1,2,4-thiadiazole-4-¹⁵N (**54-4¹⁵N**) is presented.



Scheme 40: The N-scrambling mechanism

A solution of $54\text{-}4^{15}\text{N}$ (2.5×10^{-2} M) in acetonitrile was placed in a Pyrex tube (12 cm \times 0.7 cm). The tube was sealed with a rubber septum, purged with argon gas for 30 min, and irradiated with sixteen > 290 nm mercury lamps for a total of 18 min. Aliquots of the reaction solution were removed after every 4 min of irradiation, concentrated, and analysed by GC-MS [130°C (35 min), 10°C/min to 240°C (20 min)]. Figure 106a-b show GC analysis and mass spectrum of the solution of $54\text{-}4^{15}\text{N}$ before irradiation.

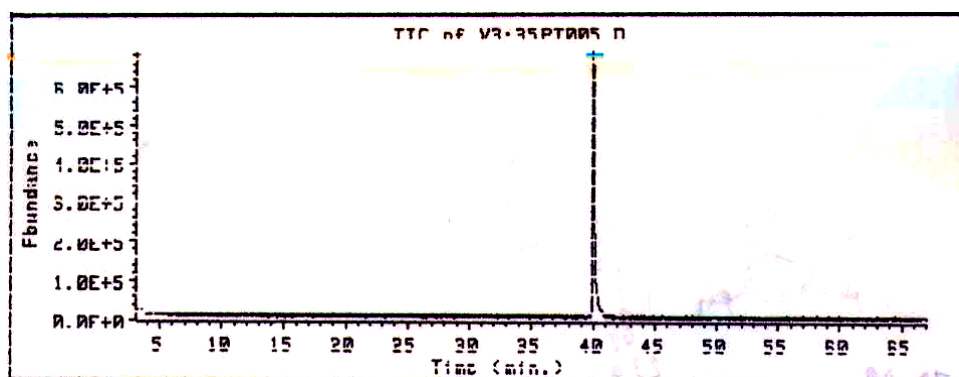


Figure 106a: GC-trace of 3-methyl-5-phenyl-1,2,4-thiadiazole-4 ^{15}N before irradiation

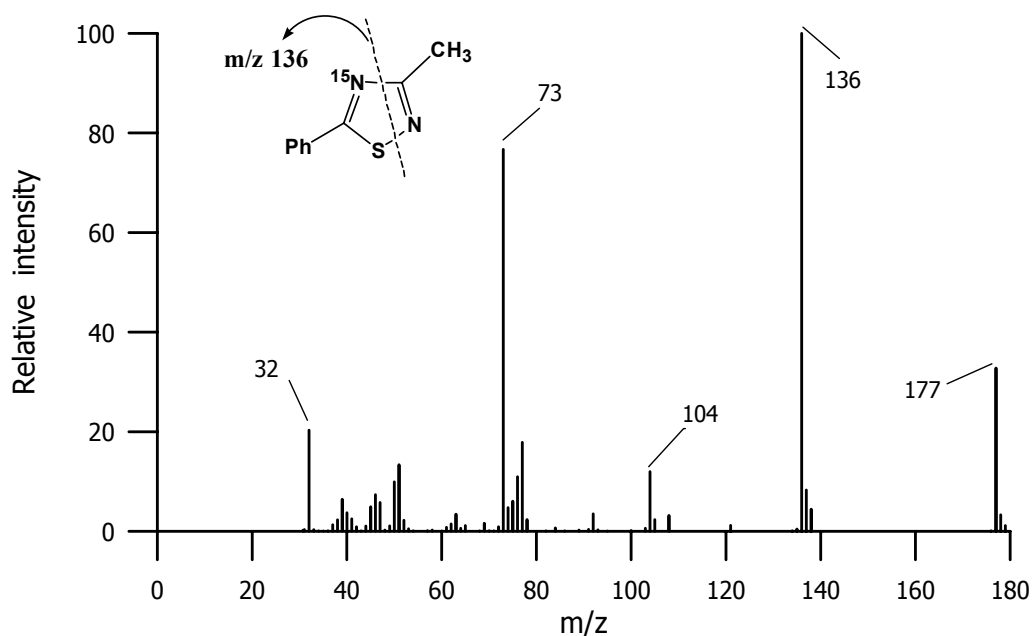
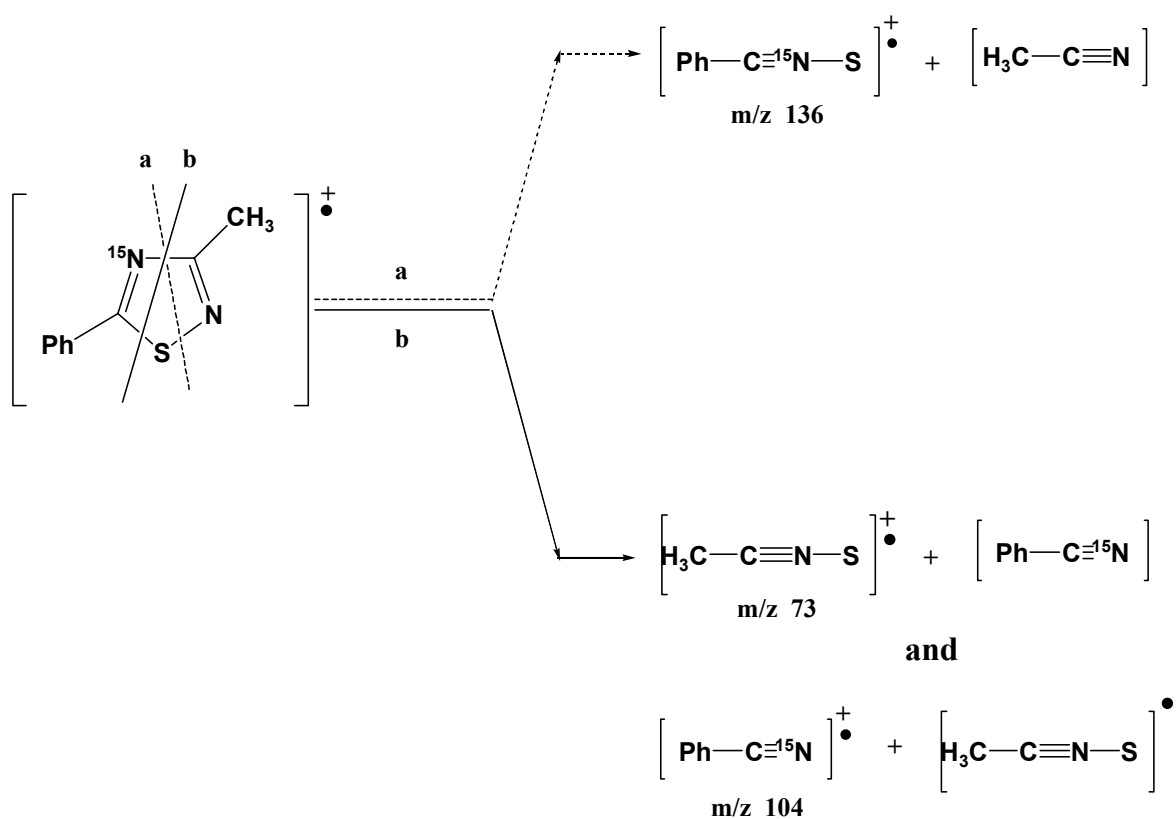


Figure 106b: Mass spectrum of 3-methyl-5-phenyl-1,2,4-thiadiazole-4 ^{15}N before irradiation

The mass spectrum of the starting material before irradiation (Figure 106b) exhibits a peak at m/z 177, which is consistent with the molecular weight of $54\text{-}4^{15}\text{N}$ (MW 177). The fragmentation pattern of this compound is analogous to the fragmentation of 5-phenyl-1,2,4-thiadiazole- 4^{15}N ($31\text{-}4^{15}\text{N}$) with two major pathways. As shown in Scheme 41, fragmentation pattern **a** leads to the base peak at m/z 136 due to the loss of $\text{CH}_3\text{C}^{14}\text{N}$. No signal, however, is observed at m/z 135, which would result from the loss of $\text{CH}_3\text{C}^{15}\text{N}$. Pathway **b** leads to an intense signal at m/z 73 due to the loss of PhC^{15}N .



Scheme 41: Two major fragmentation pathways of $54\text{-}4^{15}\text{N}$

GLC analysis (PE9000) (Figure 107) shows that only trace quantity of the reactant $54\text{-}4^{15}\text{N}$ had been consumed after 18 min of irradiation and that only trace amounts of the photoproducts had been formed. Although the consumption of the starting material and the formation of the products are clearly observed by the GLC analysis, the quantities consumed and formed are too small for accurate measurement. GC (HP588) analysis of the irradiated solution (Figure 108a) shows five volatile components with retention times of 5.0, 40.2, 40.5, 42.7, and 57.7 min.

The mass spectrum of the compound, which eluted with a retention time of 5.0 min (Figure 108b), exhibits signals at m/z 103 and 104 with an observed 103/104 ratio of 0.77 which are consistent with the molecular ions of benzonitrile- ^{14}N ($43\text{-}^{14}\text{N}$) and benzonitrile- ^{15}N ($43\text{-}^{15}\text{N}$). After the intensity of the 104 peak is corrected for $p+1$ contribution (8.03 % of the 103 peak), the ratio is 0.83. Figure 109 is a plot of the ratio of the intensities of the 103/104 peaks as a function of irradiation time. Although it was not possible to detect this photoproduct until after 5 min of irradiation, the plot shows that the 103:104 ratio is essentially constant at a value of 0.83 from 5 min to 18 min of irradiation.

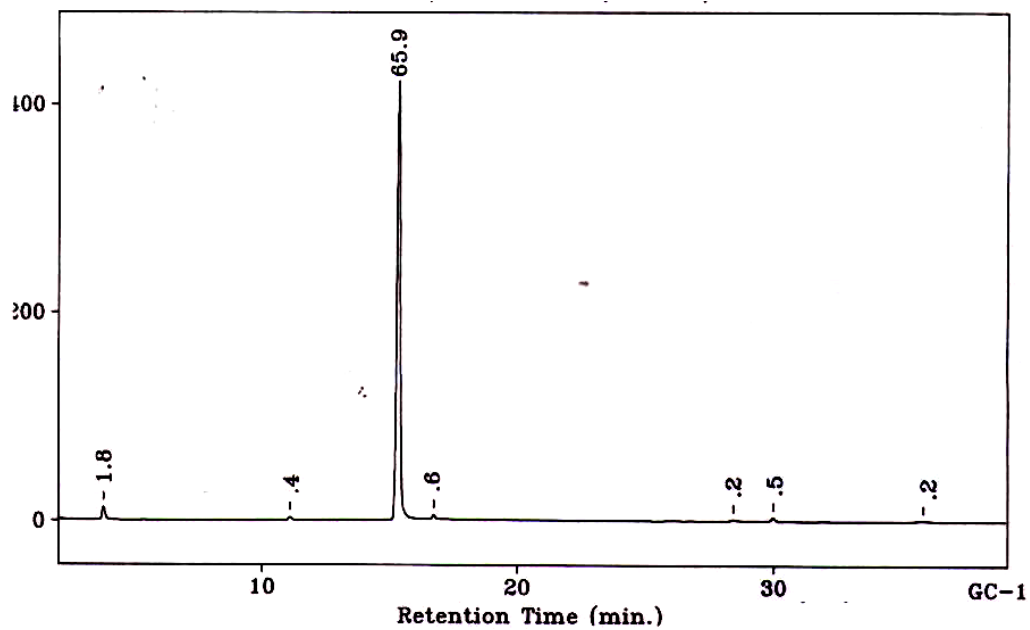


Figure 107: GLC analysis (PE9000) of the solution of $54\text{-}4^{15}\text{N}$ after 18 min of irradiation

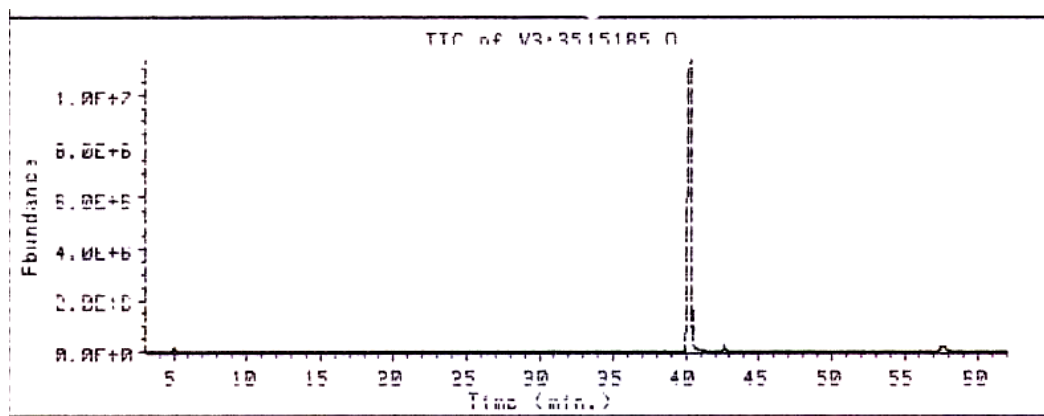


Figure 108a: GC-trace (HP588) of the reaction solution at 18 min of irradiation

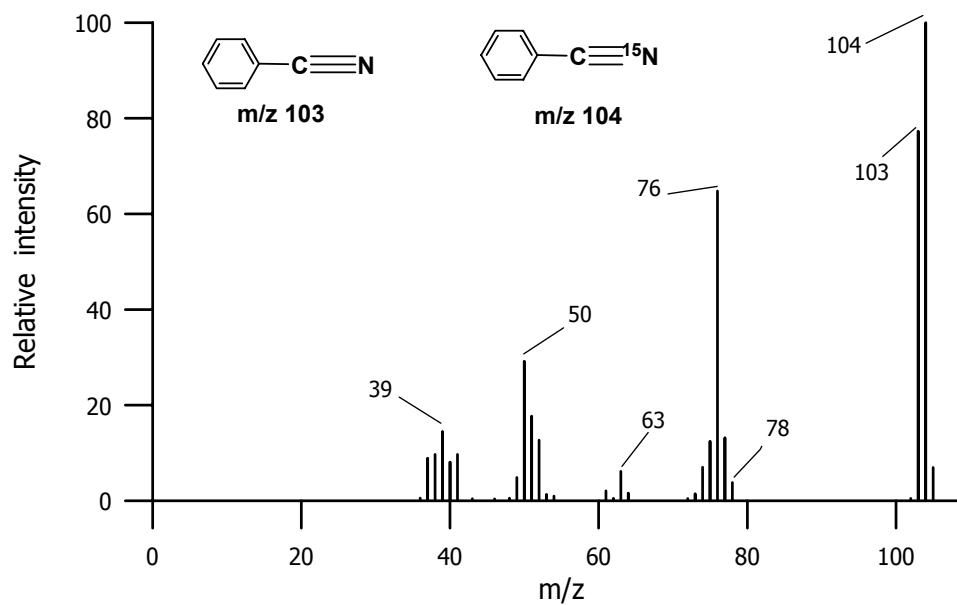


Figure 108b: Mass spectrum of the peak eluted at a retention time of 5 min; benzonitrile-¹⁴N and benzonitrile-¹⁵N

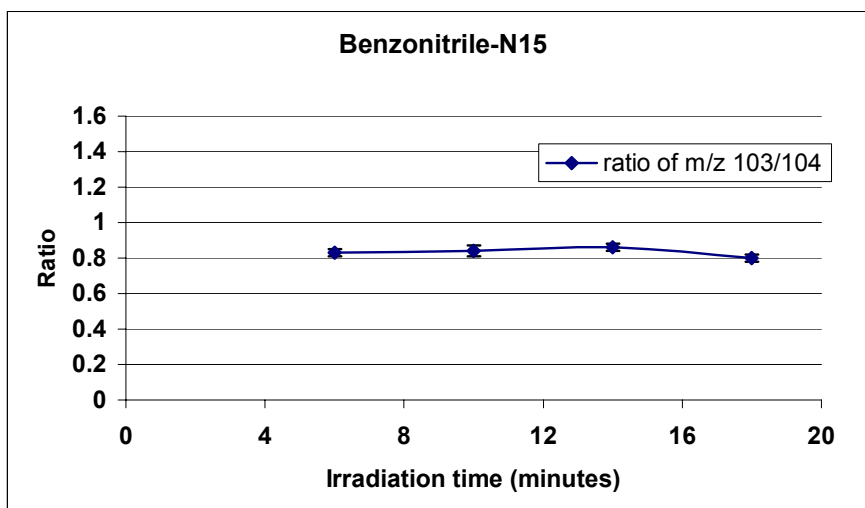


Figure 109: Plot of 103/104 ratio as a function of irradiation

Un-converted 3-methyl-5-phenyl-1,2,4-thiadiazole-¹⁵N eluted with a retention time of 40.2 min. The mass spectrum of this compound (Figure 108c) exhibits a molecular ion at m/z 177 and a base peak at m/z 136 due to the loss of [CH₃C¹⁴N]. Interestingly, the mass spectrum also exhibits a peak at m/z 135 due to the loss of [CH₃C¹⁵N], which was not present in the mass spectrum before irradiation. The corrected 135:136 ratio is 0.1 from 5 to 18 min. The formation of the signal at m/z 135 after irradiation indicates that some of **54-4**¹⁵N has been photochemically converted to **54-2**¹⁵N.

It is of interest to compare the extent of ¹⁵N scrambling in the reactant, **54-4**¹⁵N, with the degree of scrambling in benzonitrile photoproduct. Mass spectral analysis shows that after 18 min of irradiation the un-consumed reactant is 90% **54-4**¹⁵N and 10% of **54-2**¹⁵N. If the observed benzonitrile (**43**) is being formed only from 3-methyl-5-phenyl-1,2,4-thiadiazole-¹⁵N, the benzonitrile-¹⁴N : benzonitrile-¹⁵N ratio should be 0.1. As previously presented, the actual observed corrected ratio was 0.82 indicating that some or all of benzonitrile is formed from a different source by a pathway, which results in a much greater extent of ¹⁵N scrambling.

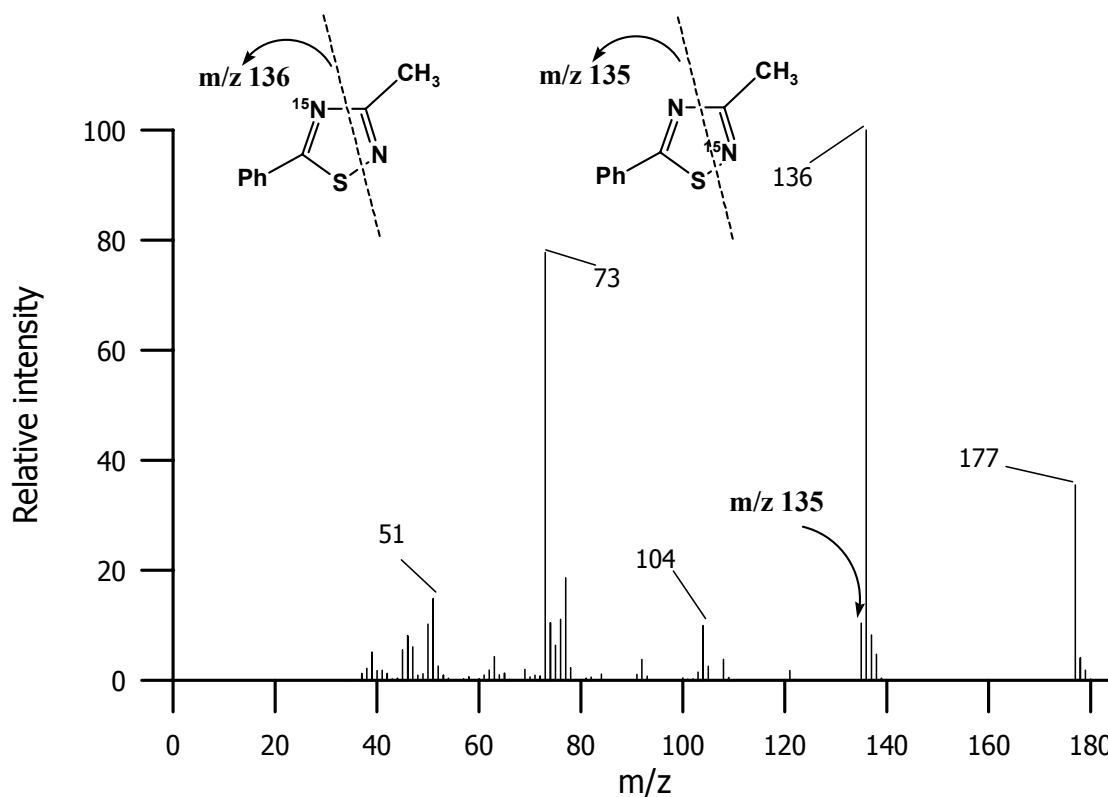


Figure 108c: Mass spectrum of the un-consumed reactant eluted at a retention time of 40.2 min

The compound which eluted with a retention time of 40.5 min has previously been identified as 2,4-dimethyl-6-phenyl-1,3,5-triazine (**65**), which has a molecular weight of 185. The mass spectrum of this photoproduct (Figure 108d) exhibits molecular ions at m/z 186 and 187 with an observed 186/187 ratio of 0.76 and a corrected ratio of 0.86. Figure 110 is a plot of the ratio of the intensities of the 186/187 peaks as a function of irradiation time. The plot shows that the ratio of the 186/187 peaks is constant at a value of 0.76 from 5 min to 18 min of irradiation. This reveals that 2,4-dimethyl-6-phenyl-1,3,5-triazine has been formed with both one ^{15}N and two ^{15}N atoms per molecule. Although it may be a coincidence, it is also interesting to note that the corrected observed one ^{15}N : two ^{15}N ratio of 0.86 is very similar to the benzonitrile- ^{14}N : benzonitrile- ^{15}N ratio which was observed to be 0.83.

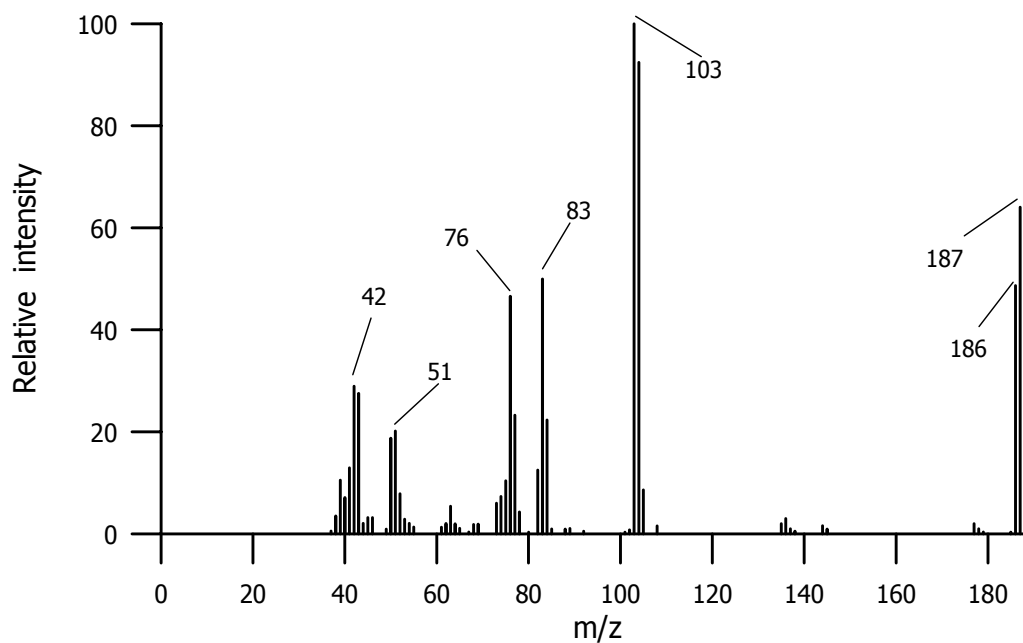


Figure 108d: Mass spectrum of the peak eluted at a retention time of 40.5 min

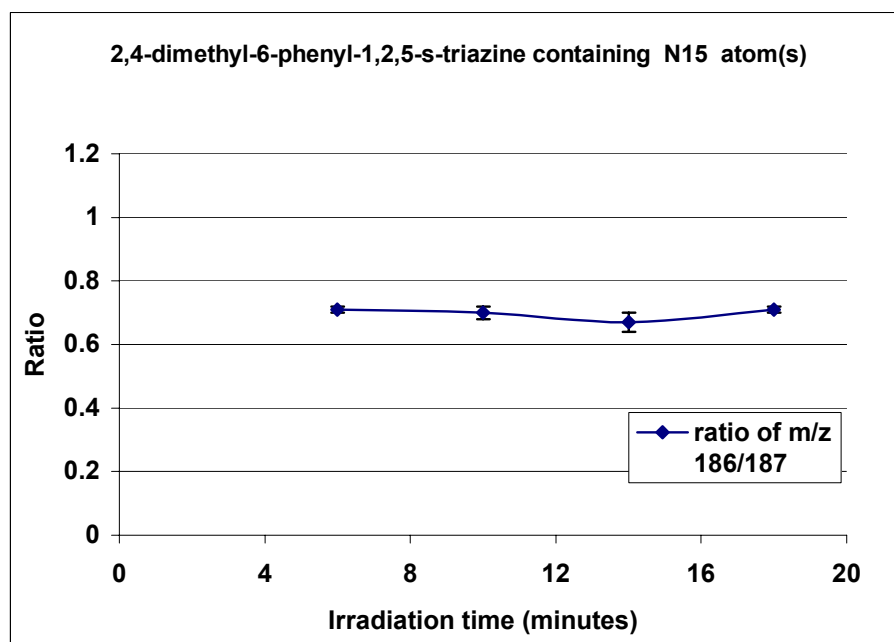


Figure 110: Plot of ratio of the 186/187 peaks as a function of irradiation

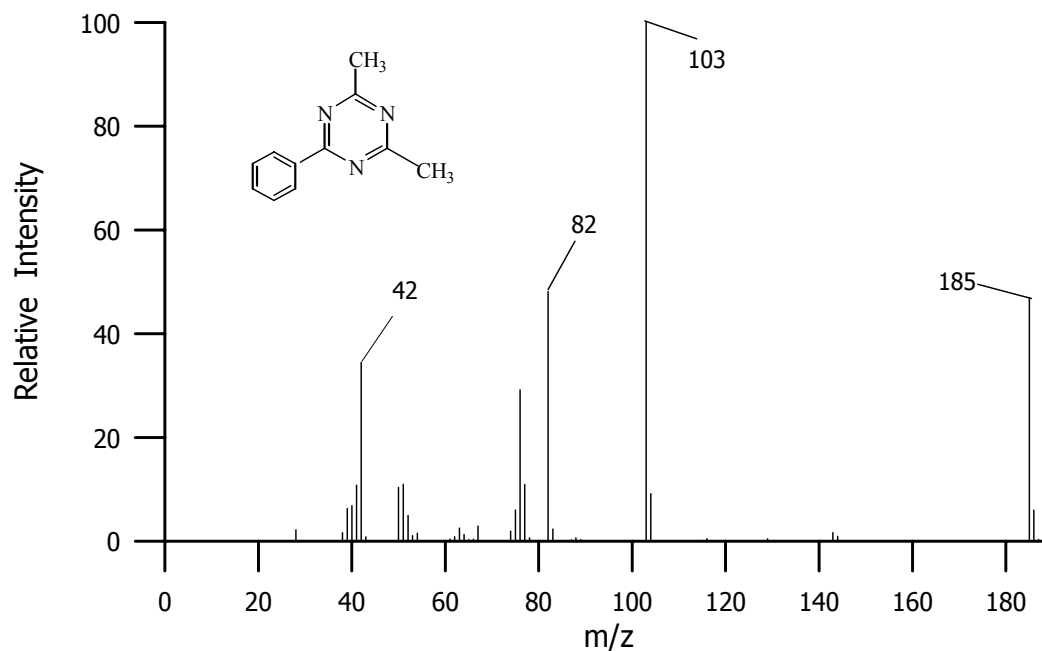
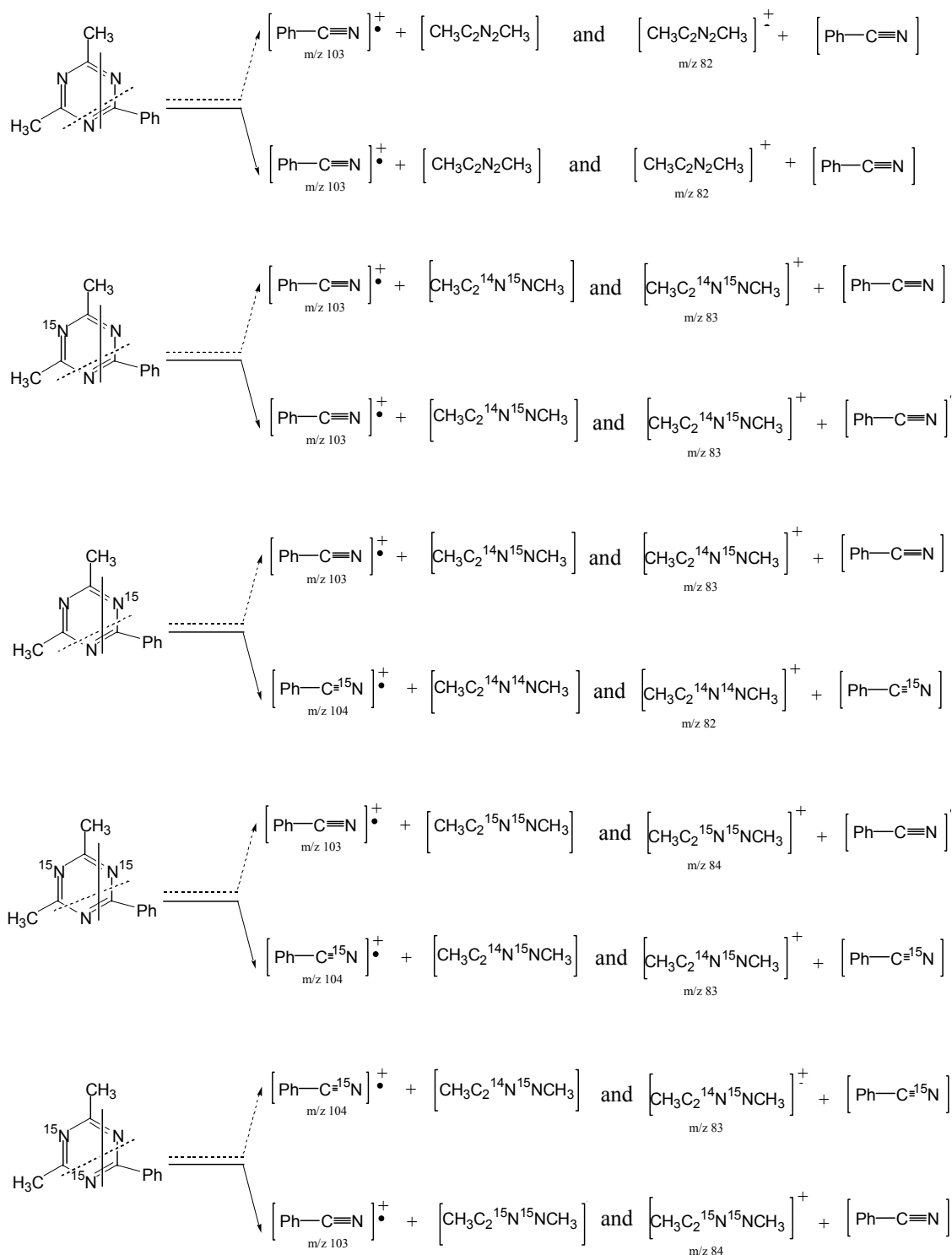


Figure 111: Mass spectrum of regular 2,4-dimethyl-6-phenyl-1,3,5-triazine

The mass spectrum of un-labelled 2,4-dimethyl-6-phenyl-1,3,5-triazine (**65**) is shown in Figure 111. This spectrum exhibits a molecular ion at m/z 185 and major fragments with m/z 103 (base peak) and 82 due to the formation of $[\text{PhCN}]^{\bullet+}$ and $[\text{C}_4\text{H}_6\text{N}_2]^+$ fragment, respectively. Scheme 42 shows the possible fragmentation pathways for the triazine containing one and two ^{15}N atoms per molecule. According to Scheme 42, it is expected that the ratio of the m/z 82 : 83 : 84 signals in the mass spectrum would be 1 : 5 : 2. Interestingly, the actual spectrum, shown in Figure 108d, shows that the corrected observed ratio is observed to be 1 : 5.4 : 2.4. Scheme 42 also reveals the expected ratio of 103/104 peaks at value of 1.7. The observed corrected ratio of 103/104 peaks is 1.6, which is consistent with this scheme.



Scheme 42: Possible fragmentation pathways for the triazine containing one and two ^{15}N atoms

The mass spectrum of the compound which eluted with a retention time of 42.7 min (Figure 108e) exhibits a molecular ion peak at m/z 177. This indicates that this compound is isomeric with the reactant, **54-4¹⁵N** which has a retention time of 40.2 min. This photoproduct was assigned to the structure of the phototransposition product, ¹⁵N-labelled 5-methyl-3-phenyl-1,2,4-thiadiazole (**57-¹⁵N**). The fragmentation pattern of this compound without ¹⁵N-labelling, shown in Figure 112, consists of the two major pathways as previously discussed for 3-methyl-5-phenyl-1,2,4-thiadiazole (**54**). The mass spectrum (Figure 112) of an authentic sample of **57** reveals a molecular ion peak at m/z 176. It also reveals two peaks at m/z 135 (base peak) due to the loss of CH₃CN and at 103 due to the formation of [PhCN]⁺• fragment corresponding to the two major fragmentation pathways.

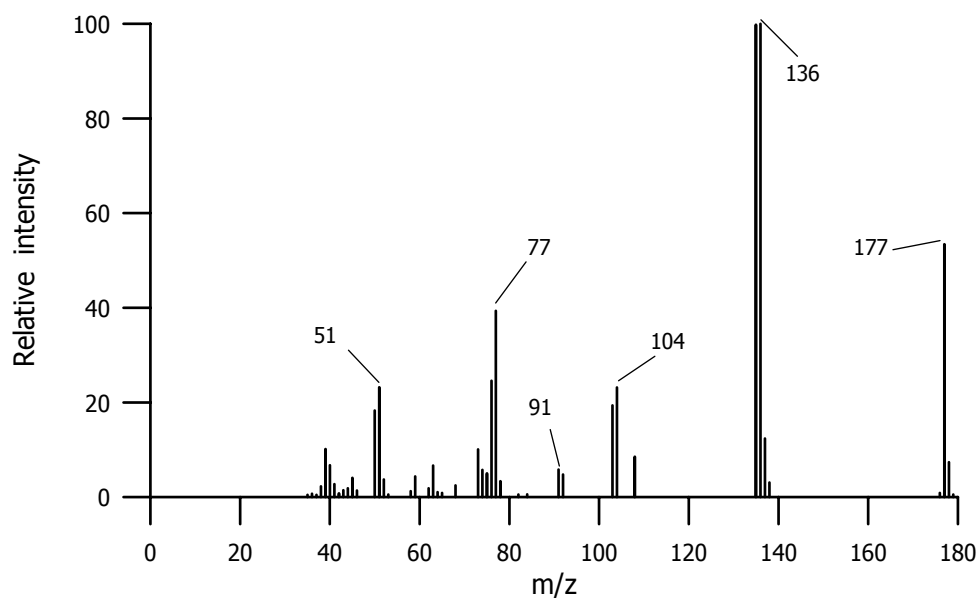


Figure 108e: Mass spectrum of the peak eluted at a retention time of 42.7 min; 5-methyl-3-phenyl-1,2,4-thiadiazole contains ¹⁵N atom

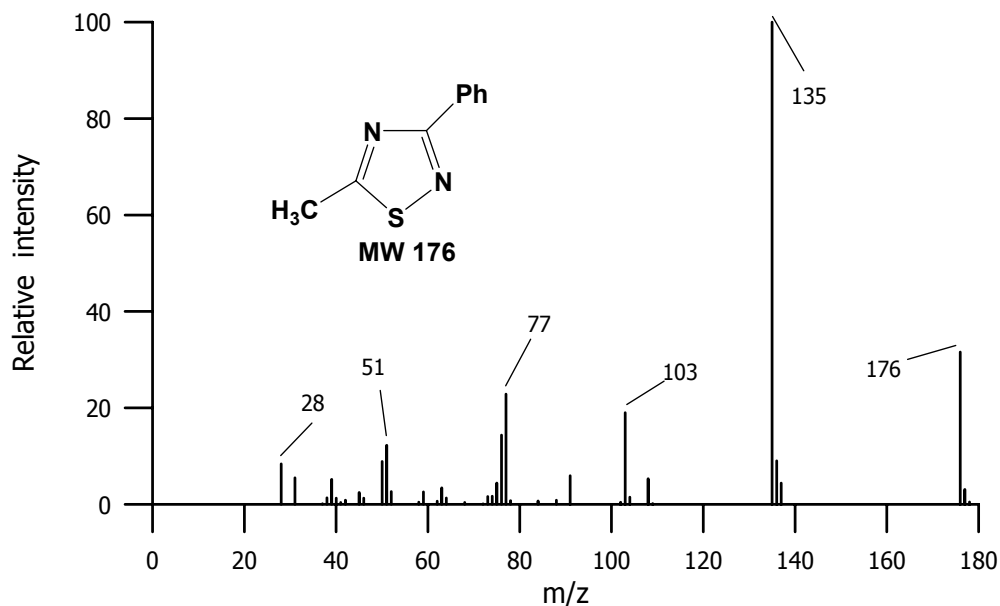


Figure 112: Mass spectrum of an authentic sample of 5-methyl-3-phenyl-1,2,4-thiadiazole

The mass spectrum of the 5-methyl-3-phenyl-1,2,4-thiadiazole-¹⁵N formed upon photolysis of **54-4¹⁵N**, shown in figure 108e, also exhibited an intense signal at m/z 135 due to the loss of CH₃C¹⁴N and also a signal of an equal intensity at m/z 136 due to the loss of CH₃C¹⁵N. The corrected ratio of these signals was 1.10. This ratio indicates that the phototransposition product consists of 52 % of **57-4¹⁵N**, which would split out CH₃C¹⁵N leaving a m/z 135 fragment, and 48 % of **57-2¹⁵N**, which would loose CH₃C¹⁴N leaving m/z 136 fragment. The mass spectrum also exhibits a signal at m/z 103 due to the formation of the [PhC¹⁴N]^{+•} fragment and a signal of almost equal intensity at m/z 104 due to the formation of [PhC¹⁵N]^{+•} fragment in a corrected ratio of 0.95 consistent with a mixture of 49% **57-4¹⁵N** and 51% **57-2¹⁵N**. These results show that the phototransposition product is very close to a mixture of equal amounts of **57-4¹⁵N** and **57-2¹⁵N**. The ¹⁵N scrambling in the phototransposition of **54-4¹⁵N** is identical to the ¹⁵N scrambling that was observed during the phototransposition of 5-phenyl-1,2,4-thiadiazole-4-¹⁵N (**31-4¹⁵N**).

By comparison with the photoproducts obtained from un-labelled 3-methyl-5-phenyl-1,2,4-thiadiazole (**54**), the product which eluted with a retention time of 57.7 min was identified as ^{15}N -labelled 2-methyl-4,6-diphenyl-1,3,5-triazine. The mass spectrum of this product, shown in Figure 108f, exhibits a molecular ion at m/z 248 and 249 indicating that the triazine has been formed with one or two ^{15}N atoms per molecule. The ratio of the 248/249 peaks observed in the spectrum is 1 : 1.2. When the intensity of the m/z 249 peak is corrected for $p+1$ contribution (18.64%), the corrected ratio is 1:1. This shows that 2-methyl-4,6-diphenyl-1,3,5-triazine- $^{15}\text{N}_1$, and - $^{15}\text{N}_2$ are being formed in equal amounts. Furthermore, Figure 113 shows that the ratio is consistent over the time monitored.

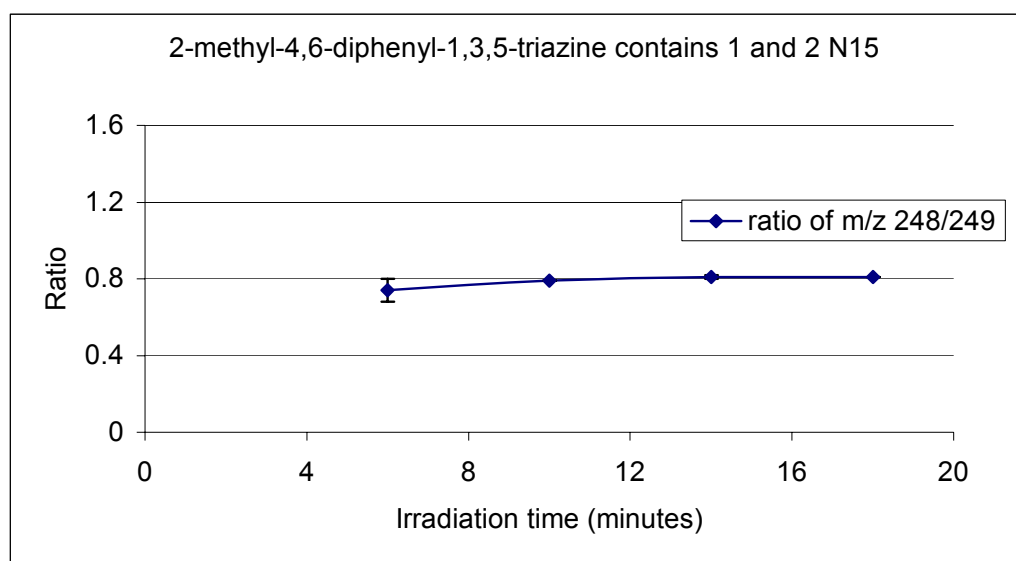


Figure 113: Formation of 2-methyl-4,6-diphenyl-1,3,5-triazine contains 1 and 2 ^{15}N atoms

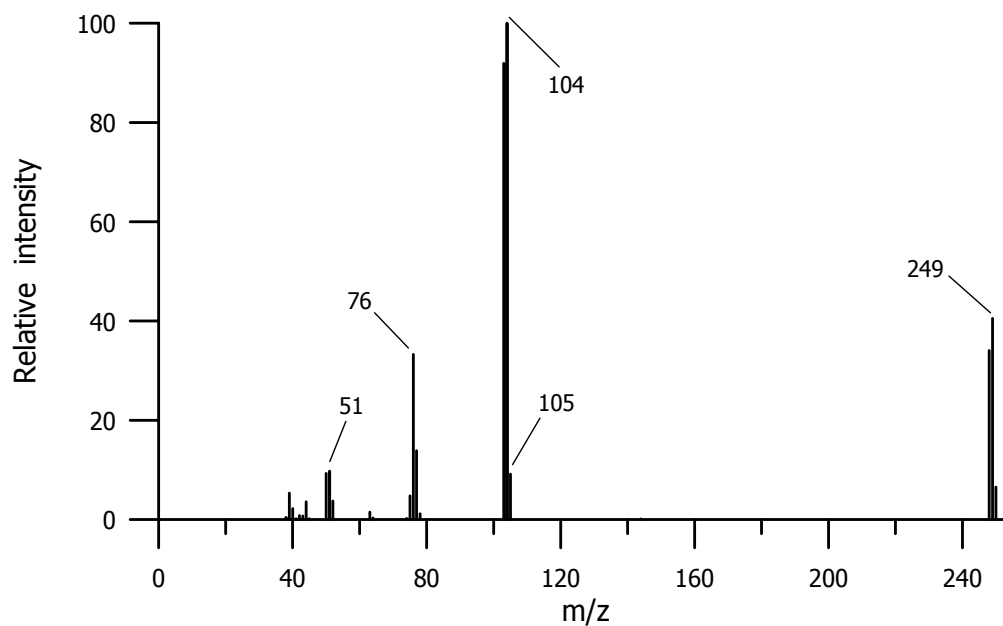


Figure 109f: Mass spectrum of the peak eluted at a retention time of 57.7 min; 2-methyl-4,6-diphenyl-1,3,5-triazine contains 1 and 2 ^{15}N atoms

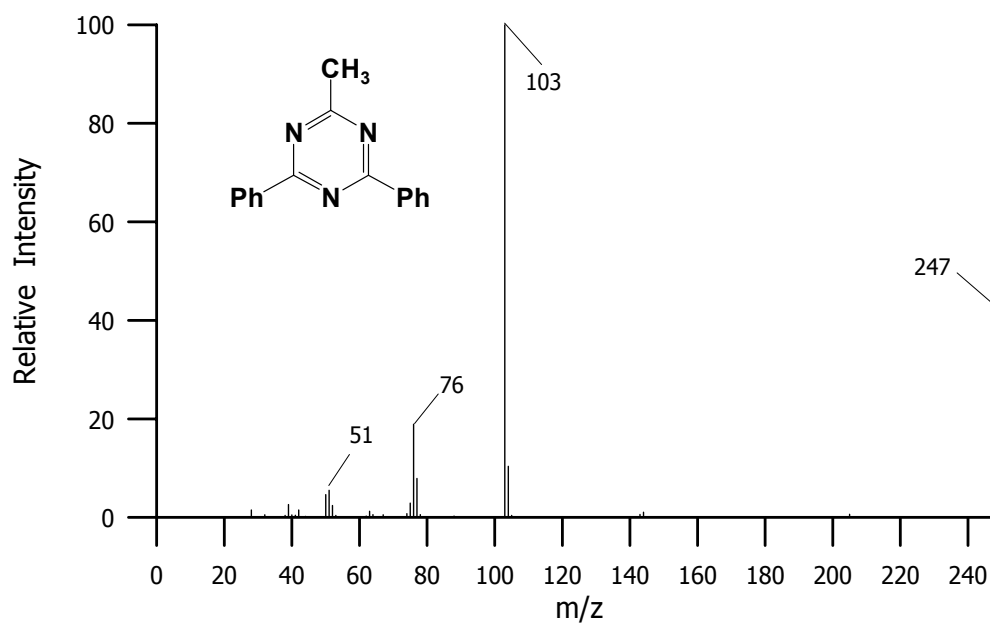
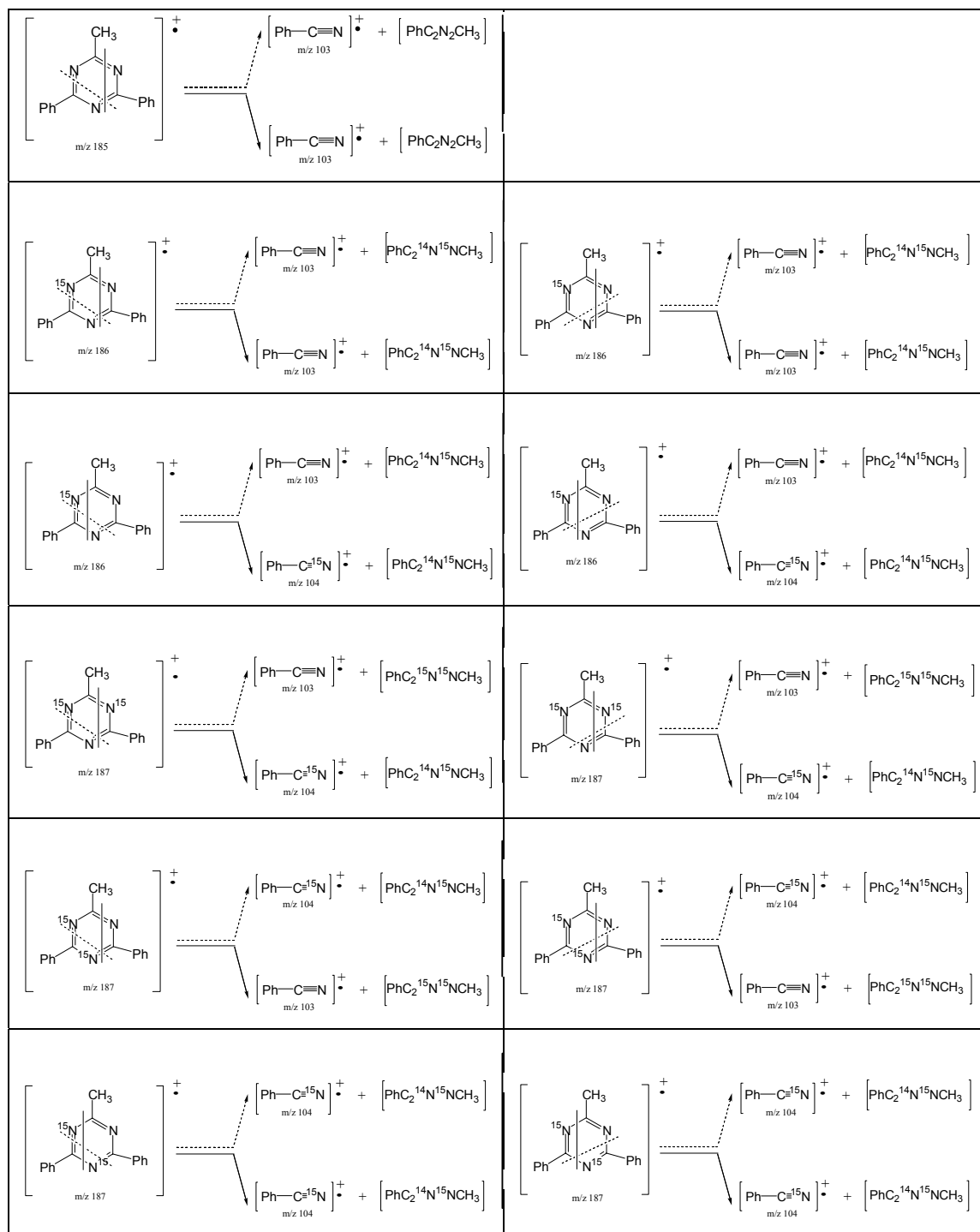


Figure 114: Mass spectrum of 2-methyl-4,6-diphenyl-1,3,5-triazine

The mass spectrum of the un-labelled 2-methyl-4,6-diphenyl-1,3,5-triazine (**66**) (Figure 114) exhibits a base peak at m/z 103 which is due to $[\text{PhCN}]^{+\bullet}$ with the loss of $\text{PhC}_2\text{N}_2\text{H}$ and a very small peak at m/z 104 (2.9% of the base peak after correcting P+1 contribution of the 103 peak). However, the mass spectrum of the triazine containing 1 and 2 ^{15}N atoms (Figure 108f) reveals a peak at m/z 104 as a base peak which is due to $[\text{PhC}^{15}\text{N}]^{+\bullet}$ fragment. The peak at m/z 103 is observed with 91% of the base peak (m/z 104). The observed corrected ratio of 103/104 peaks is 1 : 1.01. Scheme 45 shows the possible fragmentation pathways of this triazine containing one and two ^{15}N atoms. According to Scheme 45, the ratio of 103/104 fragments should be 1 : 1. Interestingly, the observed corrected ratio of 103/104 peaks has a value of 1, which is consistent with the ratio predicted in Scheme 45.

Scheme 45: Possible fragmentation pathways of 2-methyl-4,6-diphenyl-1,3,5-triazine-¹⁵N

2.5.3 Preparative scale photolysis

The preparative photolysis of **54-4**¹⁵N was also studied. A solution of **54-4**¹⁵N in methanol (2.06×10^{-2} M; 25 mL) was irradiated with sixteen > 290 nm lamps for 640 min while the solution was continuously purged with a fine stream of argon. GLC analysis showed that 50% of the reactant had been consumed. The resulting solution turned to a light brown clear solution with a fine solid precipitate. This preparative scale photolysis focused on the isolation of the un-consumed reactant and the phototransposition product. GLC and TLC analyses indicated that 2,4-dimethyl-6-phenyl-1,3,5-triazine (**65**) had chromatographic properties close to that of 3-methyl-5-phenyl-1,2,4-thiadiazole (**54**). Thus, methanol was employed as a solvent for the photoreaction in order to minimize the formation of **65** since previous result showed that the yield of **65** was very low when **54** was irradiated in methanol solvent

The photolyzed solution was filtered, concentrated and subjected to column chromatography [diameter: 1.5cm, silica gel: 8 g, height: 12 cm, hexane:dichloromethane (3:2)]. The column was eluted with hexane–dichloromethane (3:2) (40 mL) and then 10 mL fractions were collected. The polarity of solvent was 10 % increased from hexane:dichloromethane (1:9) → 100 % dichloromethane → dichloromethane : ethyl acetate → 100% ethyl acetate. Finally, 100 % ethanol was applied to the column to elute a yellow band at the base line with the last fraction (40th).

TLC analysis of fractions 16-18 indicated the presence of only one spot with an R_f corresponding to the un-consumed reactant. The ¹H-NMR spectrum of the residue from these combined fractions (Figure 117) exhibits a doublet at δ 2.65 (3H, $J = 2.53$ Hz) and two multiplets at δ 7.43-7.49 (3H) and 7.89-7.92 (2H). The ¹³C-NMR spectrum

(Figure 118a) exhibits major signals at δ 18.0 (d, $J = 8.4$ Hz), 126.3, 128.2, 129.4, 129.5 (d, $J = 6.1$ Hz), 130.8, 173.1 (d, $J = 3.1$ Hz), and 187.0.

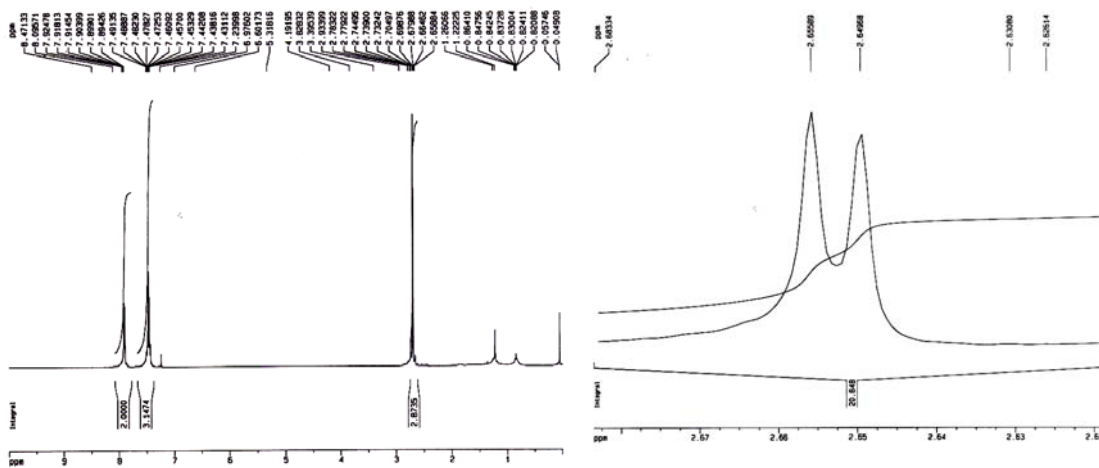


Figure 117: ^1H -spectrum of fractions 16-18 and scale expansion of the doublet at δ 2.65

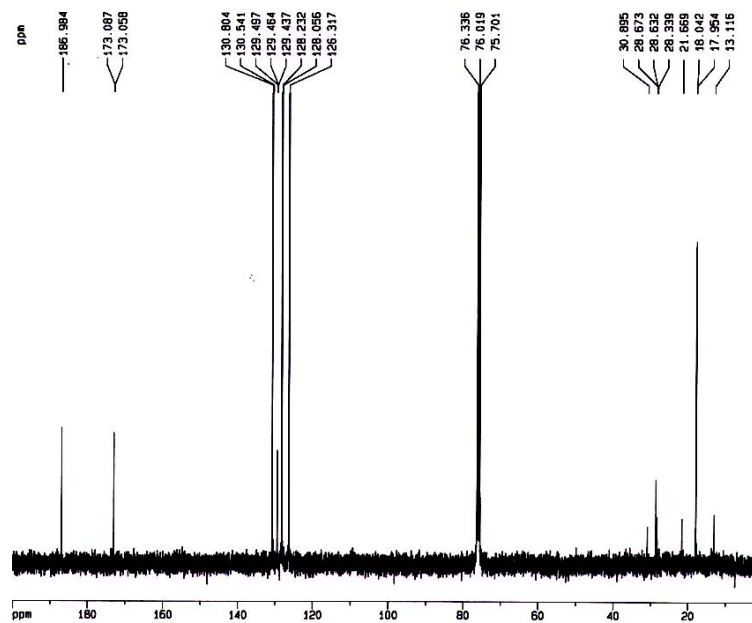


Figure 118a: ^{13}C -spectrum of fractions 16-18

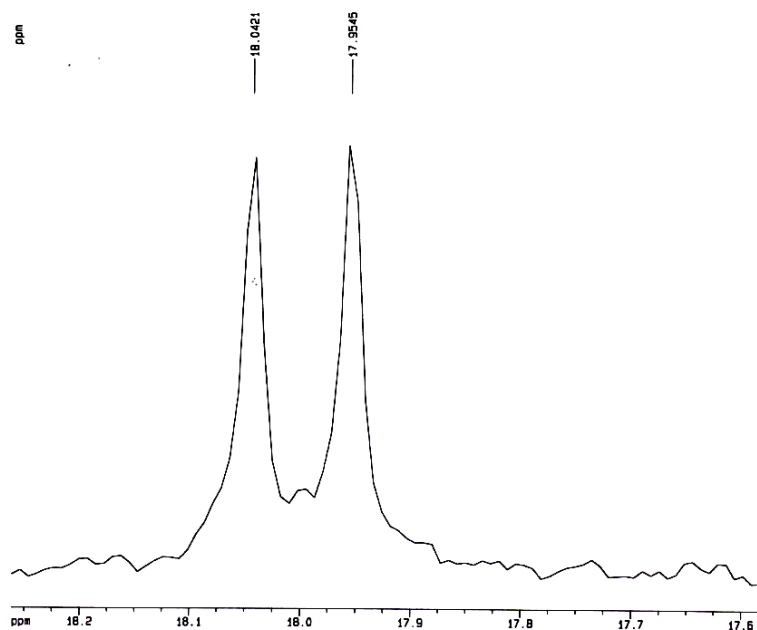


Figure 118b: ^{13}C -scale expansion of a doublet at δ 18.0

A ^{13}C -scale expansion of the doublet at δ 18.0 (figure 118b) reveals a small singlet between the doublet which does not appear in the ^{13}C -spectrum of the reactant before irradiation. Since the previous mass spectral results indicated ^{15}N scrambling in the un-consumed reactant, this small singlet could be due to methyl-carbon of 3-methyl-5-phenyl-1,2,4-thiadiazole-2- ^{15}N (**54-2 ^{15}N**). This methyl-carbon, however, is also expected to appear as a doublet as the methyl-carbon of **54-4 ^{15}N** does. Furthermore, the mass spectrum of this sample (Figure 119a) indicated that **54-4 ^{15}N** underwent 50% photo- ^{15}N -scrambling to **54-2 ^{15}N** . Thus, if this singlet was due to the methyl-carbon of **54-2 ^{15}N** , it should appear as a larger singlet.

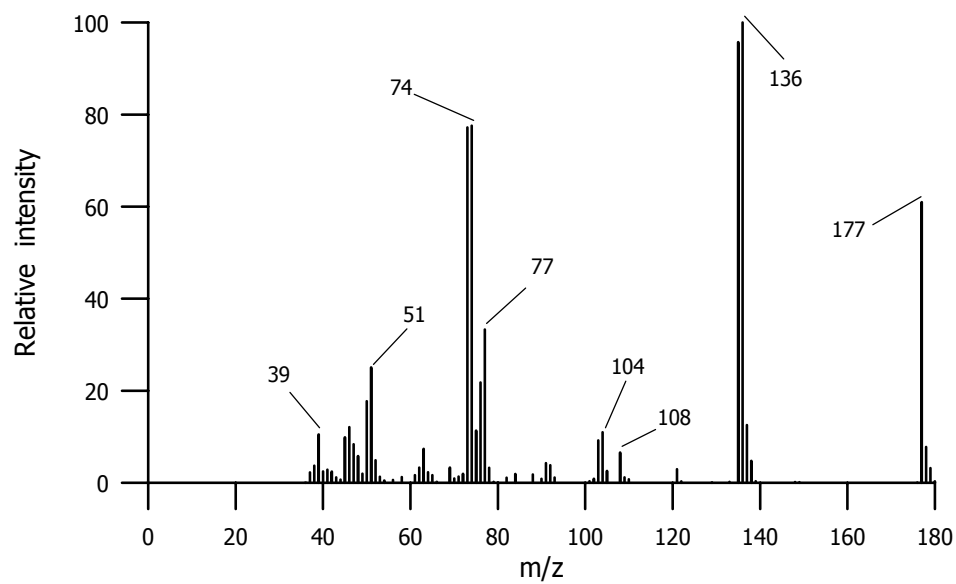


Figure 119: Mass spectrum of the un-consumed reactant at 640 min of irradiation

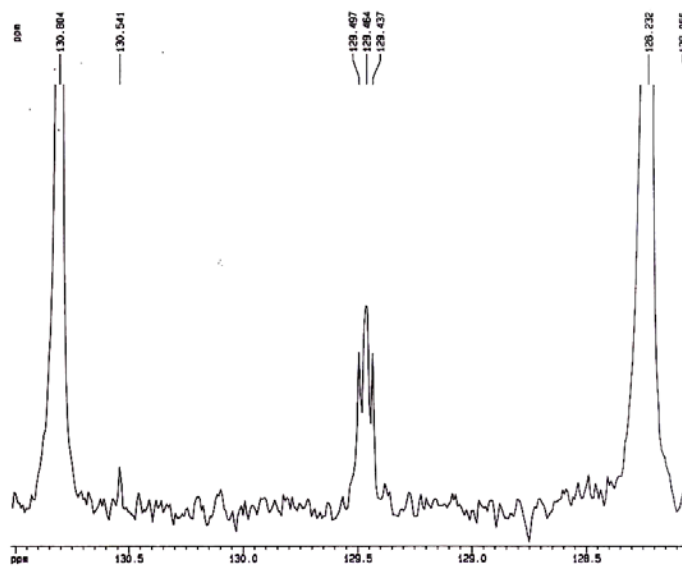


Figure 118c: ^{13}C -scale expansion of a doublet at δ 129.4 and 129.5

The scale expansion of the signals at δ 129.4 and 129.5 (Figure 118c) reveals a singlet at δ 129.4 which is overlapped with a doublet at δ 129.5 (d, $J = 6.1$ Hz). It is interesting to note that this signal, which was assigned to the phenyl-ring carbon at position 1 in the reactant, appeared before irradiation as a clean doublet ($J = 6.1$ Hz) due to long range coupling with the ^{15}N at position 4. The new carbon singlet at δ 129.4 which formed during irradiation is due to the signal of the phenyl-ring carbon at position 1 which is no longer coupled to the ^{15}N atom in 3-methyl-5-phenyl-1,2,4-thiadiazole-2- ^{15}N (**54-2** ^{15}N). The doublet at δ 173.1 (d, $J = 3.1$ Hz) is due to a coupling between the carbon at position 5 of the thiadiazole ring and ^{15}N at position 4 while the signal at δ 187.0 which still appears as a singlet upon an scale expansion is due to the C-3 carbon. The ^{15}N -NMR spectrum of this sample (Figure 120) exhibits a singlet at δ 260.5 and a doublet at δ 301.7 ($J = 2.0$ Hz). This doublet, which was present before irradiation, is assigned to ^{15}N at position 4 of the reactant **54-4** ^{15}N while the new singlet at δ 260.5 is due to ^{15}N at position 2 of **54-2** ^{15}N . This result is consistent with the mass spectral results which indicated ^{15}N -scrambling in the reactant.

TLC analyses and ^1H -NMR analysis of the other fractions did not exhibit any signal which could indicate the presence of 5-methyl-3-phenyl-1,2,4-thiadiazole- ^{15}N . ^{15}N -NMR analysis also did not exhibit any ^{15}N signal which could either indicate that there was no ^{15}N atom present in those fractions or due to the low concentration of ^{15}N atom.

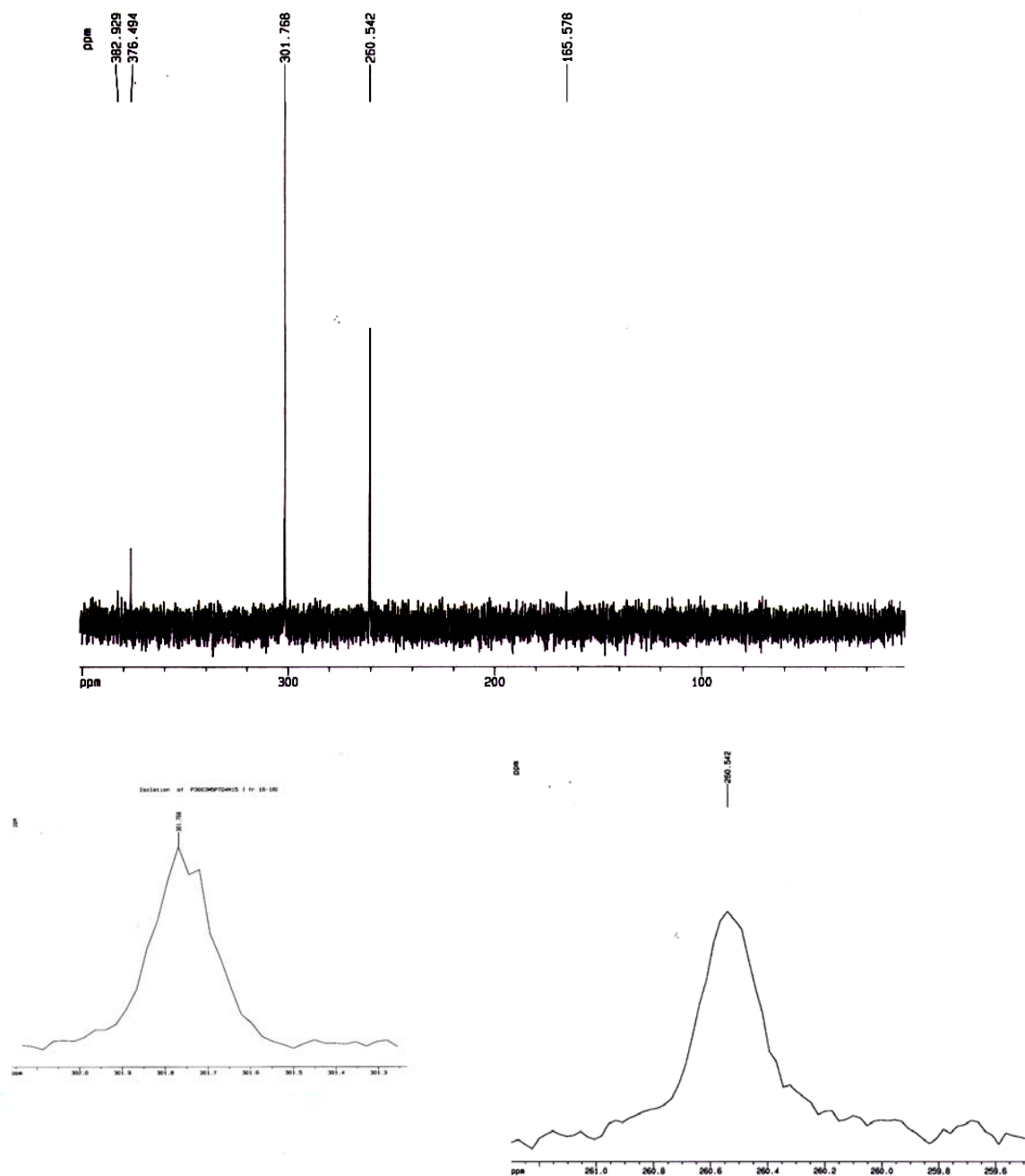
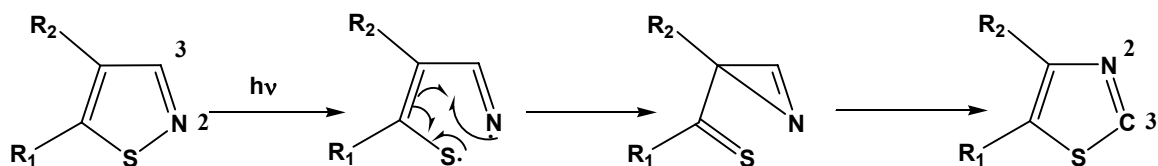


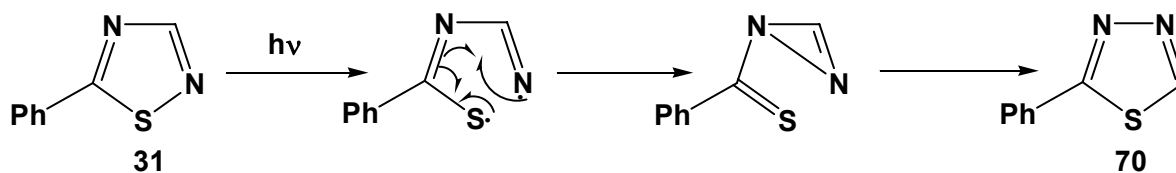
Figure 120: ^{15}N -NMR spectrum of fractions 16-18 and scale expansion of a doublet at δ 301.7 and a singlet at δ 260.5

2.6 Photolysis of 5-phenyl-1,2,4-thiadiazole in the presence of ethyl cyanofornate: attempt to identify the formation of benzonitrile sulfide by 1,3-dipolar cycloaddition reaction

According to the photochemistry of substituted isothiazoles, cleavage of the S—N bond results in the formation of azirine intermediates and eventually to the formation of substituted thiazole products (the N-2 and C-3 interchange product), shown in Scheme 46, has been reported as the major photochemical pathway of 4-substituted isothiazoles⁹. In the case of a 1,2,4-thiadiazole, however, cleavage of the S—N bond and ring contraction would produce a diazirine instead of an azirine (Scheme 47).

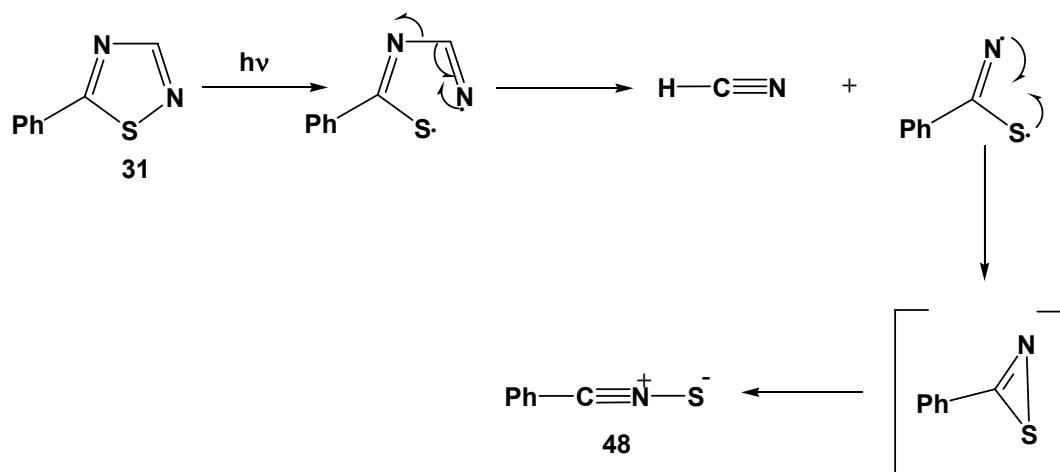


Scheme 46: N-2 and C-3 interchange photochemical pathway of isothiazoles



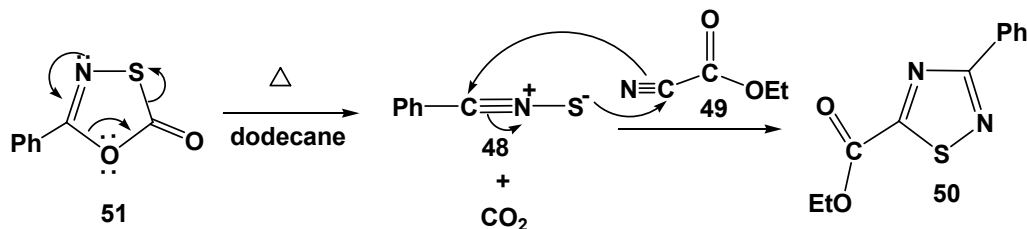
Scheme 47: N-2 and C-3 interchange photochemical pathway of 5-phenyl-1,2,4-thiadiazole

According to the results of the photolysis of 5-phenyl-1,2,4-thiadiazole (**31**), GLC (PE9000) and GC (HP588) analysis of the reaction solution showed no sign corresponding to the formation of 5-phenyl-1,3,4-thiadiazole (**37**), the N-2 and C-3 interchange product. According to Scheme 47, **31** could undergo the photocleavage of the S-N bond leading to the formation of a 1,5-diradical. In the case of phenyl substituted isothiazole, cyclization of the 1,5-diradical (Scheme 46) would lead to the formation of a substituted azirine. In this case of 5-phenyl-1,2,4-thiadiazole (Scheme 47), cyclization of the 1,5-diradical would result not to an azirine but to a diazirine intermediate which would be expected to be an anti-aromatic compound, thus, cyclization of this 1,5-diradical to produce a diazirine would be a high energy pathway. This could preclude the formation of a diazirine. However, this 1,5-diradical could undergo loss of HCN to yield a 1,3-diradical. This diradical could cyclize to the formation of phenyl substituted thiazirine which could eventually rearrange to yield benzonitrile sulfide (**48**), as shown in Scheme 48.



Scheme 48: Possible mechanism for the formation of benzonitrile sulfide

The trapping of thermally generated benzonitrile sulfide (**48**) has been successfully carried out by a 1,3-dipolar cycloaddition reaction using ethyl cyanoformate (**49**) as a dipolarophile to yield ethyl 3-phenyl-1,2,4-thiadiazole-5-carboxylate (**50**),¹² as shown in Scheme 49.



Scheme 49: Trapping of thermally generated **48** by 1,3-dipolar cycloaddition reaction

In order to investigate the possible formation of **48** upon irradiation of **31**, the photolysis of **31** in acetonitrile containing **49** was carried out.

A solution of **31** (2.0×10^{-2} M, 4 mL) and **49** (0.1 mL, 1×10^{-1} M) in acetonitrile was placed in a Pyrex tube and a quartz tube, sealed with rubber septa, purged with argon for 30 min. The solution in the Pyrex tube was irradiated with sixteen > 290 nm lamps and the solution in the quartz tube was irradiated with eight 254 nm lamps. The reactions were monitored by GLC [120°C (5 min), 20°C/min to 160°C (8 min), 20°C/min to 240°C (20 min)] every 30 min of irradiation. Figure 121a exhibits the GC-chromatogram of the reaction solution before irradiation. After 210 min of irradiation, GLC analysis (Figure 121b) reveals the formation of benzonitrile (**43**), 2-phenyl-1,3,5-triazine (**39**), 3-phenyl-1,2,4-thiadiazole (**46**) and 2,4-diphenyl-1,3,5-triazine (**40**), the known photoproducts with retention times of 3, 9, 13 and 23.5 min, respectively. The un-consumed reactant eluted with a retention time of 11 min. The trace also reveals a very small extra peak with a retention time of 19 min, which was not observed upon irradiation of **31** in an absence of **49**.

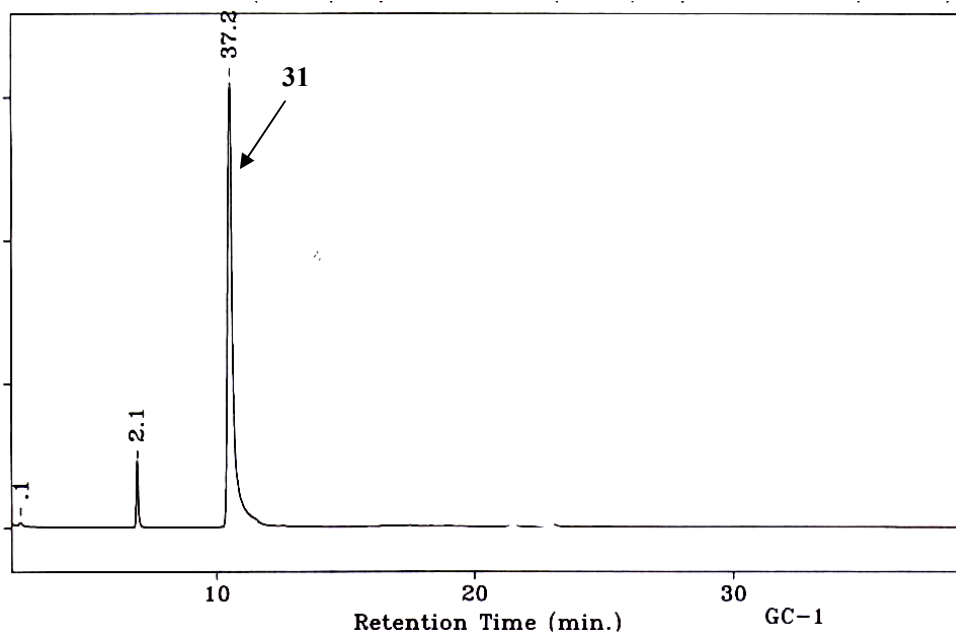


Figure 121a: GLC analysis of solution of **31** containing **49** before irradiation

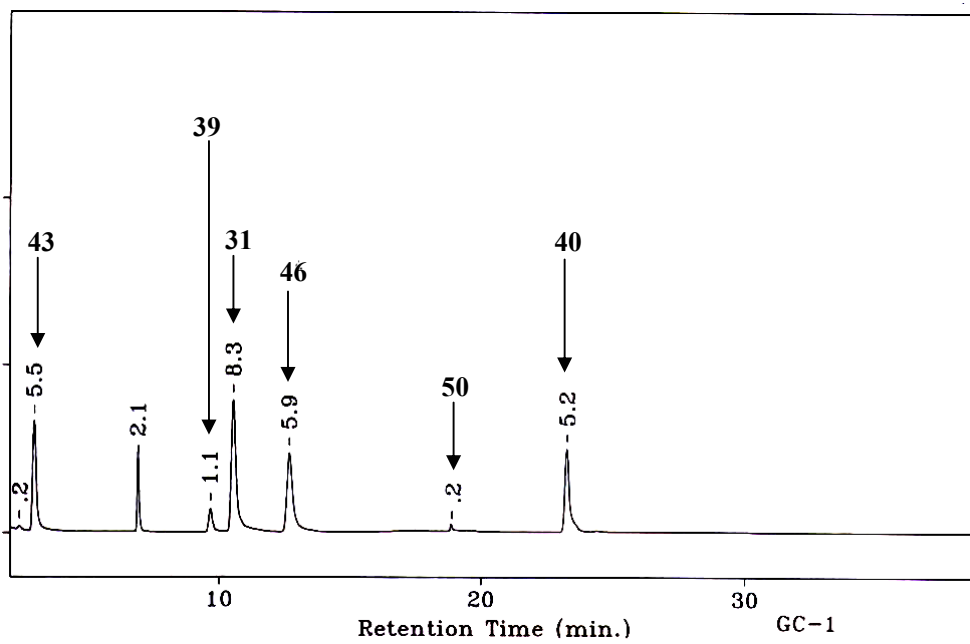


Figure 121b: GLC analysis of solution of **31** containing **49** after irradiation

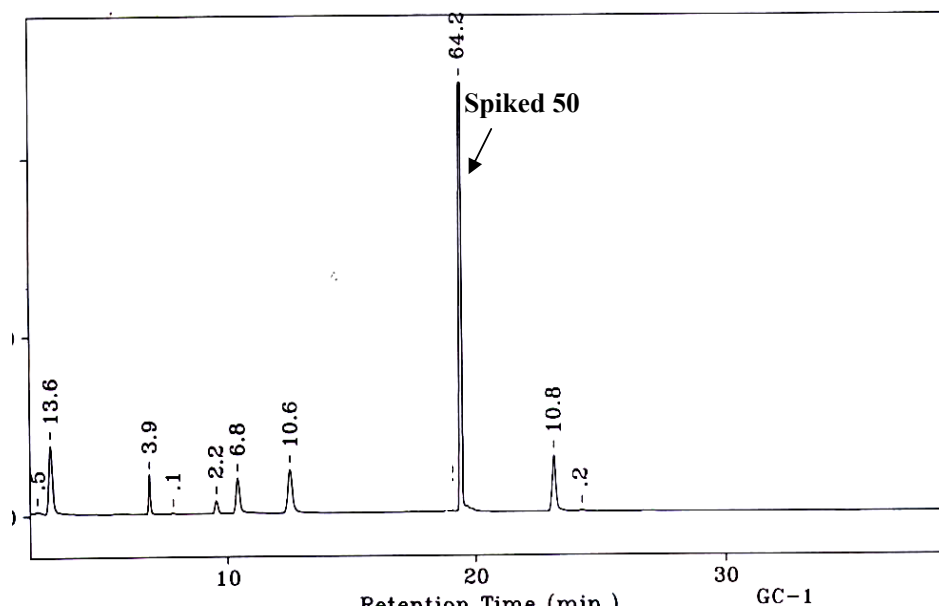


Figure 121c: GLC analysis of the reaction solution spiked with an authentic sample of **50**

A small amount of the reaction solution was removed and spiked with an authentic sample of the expected cycloaddition product, ethyl 3-phenyl-1,2,4-thiadiazole-5-carboxylate (**50**). Figure 121c shows the GLC analysis of the reaction solution spiked with an authentic sample of **50**.

GLC analysis of the spiked solution (Figure 121c) reveals a peak due to **50** with a retention time of 19.5 min which is slightly different from the new photoproduct peak observed at retention time of 19 min in Figure 121b. Thus, photoreaction solution was concentrated and analyzed by the GC (HP588) interfaced with a mass spectrometer. The trace (Figure 122a) [140°C (5 min), 20°C/min to 240°C (20 min)] of the concentrated reaction solution exhibits the formation of the known photoproducts with retention times of 4, 9, 11 and 25 min and the un-consumed reactant with a retention time of 10.5 min. The trace also reveals a very small peak, which eluted with a retention time of 15.4 min. The mass spectrum of this peak (Figure 122b) exhibits a molecular ion at m/z 234, which corresponds to the molecular weight of the expected trapping product, **50** (MW 234).

An authentic sample of **50** also eluted with a retention time of 15.4 min under the same GC (HP588) analytical condition.

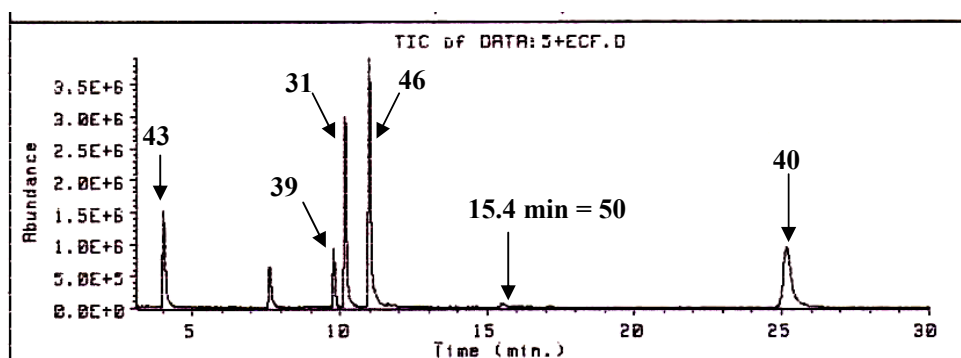


Figure 122a: GC-trace of the concentrated solution after 210 min of irradiation

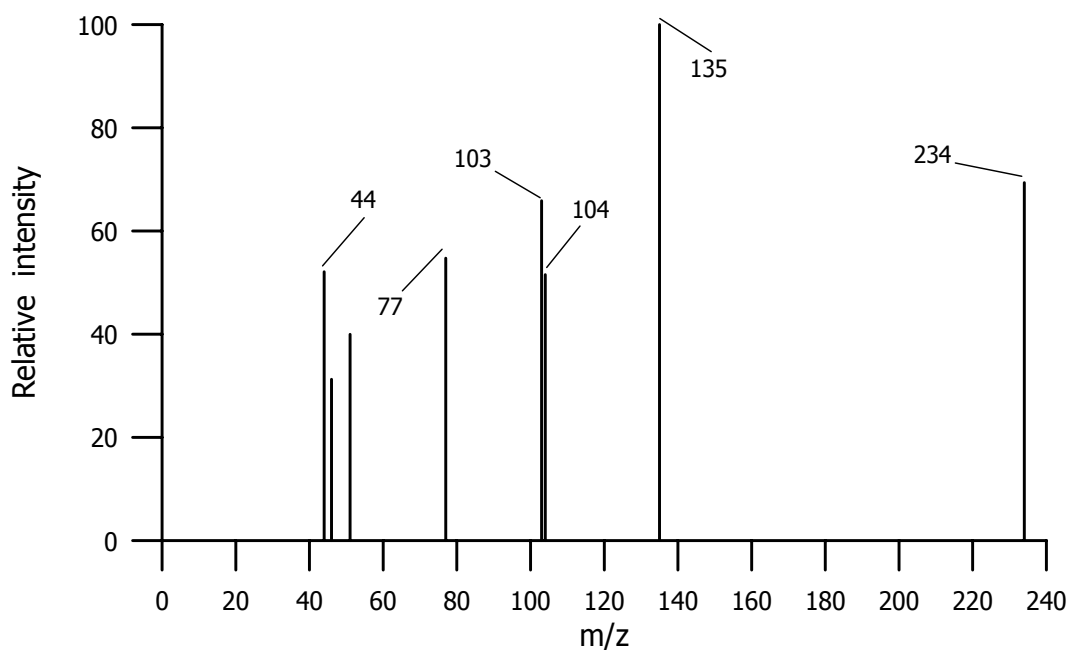


Figure 122b: Mass spectrum of a suspected peak to be **50**

The mass spectrum of the peak which is suspected to be **50** (Figure 122b) exhibits a molecular ion at m/z 234, a base peak at m/z 135 and intense peaks at m/z 104, 103, and 77.

The mass spectrum of an authentic sample of **50** (Figure 123) shows a molecular ion at m/z 234, a base peak at m/z 135 which is due $[C_6H_5CNS]^+$ fragment.

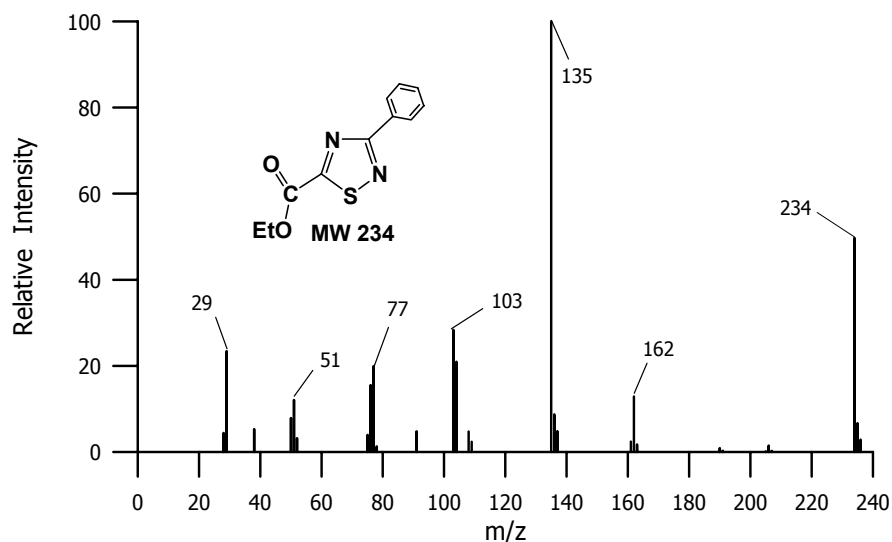


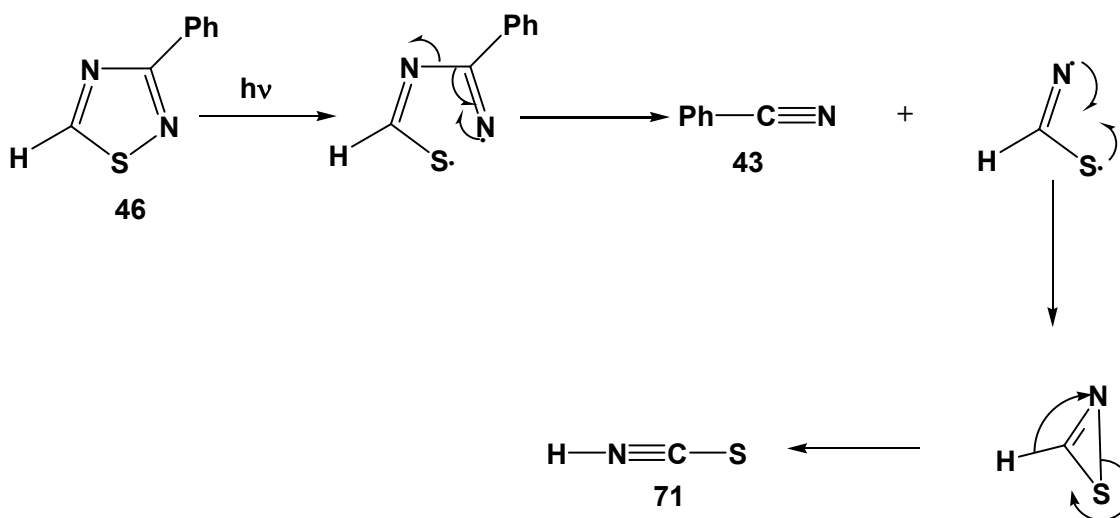
Figure 123: Mass spectrum of an authentic sample of **50**

By comparison of the fragmentation pattern of the mass spectrum of the suspected product with the fragmentation pattern of the mass spectrum of an authentic sample of **50**, it indicates that this suspected product is ethyl 3-phenyl-1,2,4-thiadiazole-5-carboxylate (**50**). However, since the presence of this product in the reaction solution before concentration can be detected by GLC (PE9000) analysis in very trace quantity, this indicates that the formation of benzonitrile sulfide (**48**) can only be a very minor pathway upon photolysis of 5-phenyl-1,2,4-thiadiazole (**31**). This result is consistent with the proposed mechanism for the formation of **48** upon irradiation of **31**, shown in Scheme 48.

This trapping experiment was also irradiated with eight 254 nm lamps. The results also showed trace amount of the formation of the expected cycloaddition product, **50**.

2.7 Photolysis of 3-phenyl-1,2,4-thiadiazole in the presence of ethyl cyanofornate: attempt to identify the formation of benzonitrile sulfide by 1,3-dipolar cycloaddition reaction

In an attempt to trap the expected intermediate, benzonitrile sulfide (**48**), upon irradiation of **31**, the results indicated the formation of very trace amount the expected cycloaddition product. However, in the case of 3-phenyl-1,2,4-thiadiazole (**46**), cleavage of the 1,5-diradical would not finally produce **48**. According to Scheme 50, cleavage of the 1,5-diradical would not finally produce **48**. According to Scheme 50, cleavage of the 1,5-diradical would finally lead to the formation of isothiocyanic acid (**71**), which could be an un-identified photoproduct formed upon irradiation of **46**. Therefore, the formation of **50** could be predicted not to observe upon irradiation of **46** in the presence of **49**.



Scheme 50: The predicted mechanism for the formation of isothiocyanic acid

A solution of **46** (2.0×10^{-2} M, 4 mL) in acetonitrile containing **49** (0.1 mL, 1×10^{-1} M) was placed in a Pyrex tube and a quartz tube, sealed with rubber septa, and purged with argon gas for 15 min. The solution in the Pyrex tube was irradiated with sixteen > 290 nm

lamps and the solution in the quartz tube was irradiated with eight 254 nm lamps. The reactions were monitored by GLC [120°C (5 min), 20°C/min to 240°C (20 min)] every 30 min of irradiation. The solution in the Pyrex tube was photolyzed for 300 min while the solution in the quartz tube was photolyzed for 120 min.

Figure 124a exhibits GLC analysis of the solution before irradiation. After 300 min of irradiation, the trace (Figure 124b) shows the formation of two peaks with retention times of 3 and 12 min and the un-consumed reactant with a retention time of 9 min. The peak which eluted with a retention time of 3 min is benzonitrile (**43**), the known major photoproduct upon irradiation of **46**. The peak which eluted with a retention time of 12 min was not observed upon irradiation of **46** without **49**.

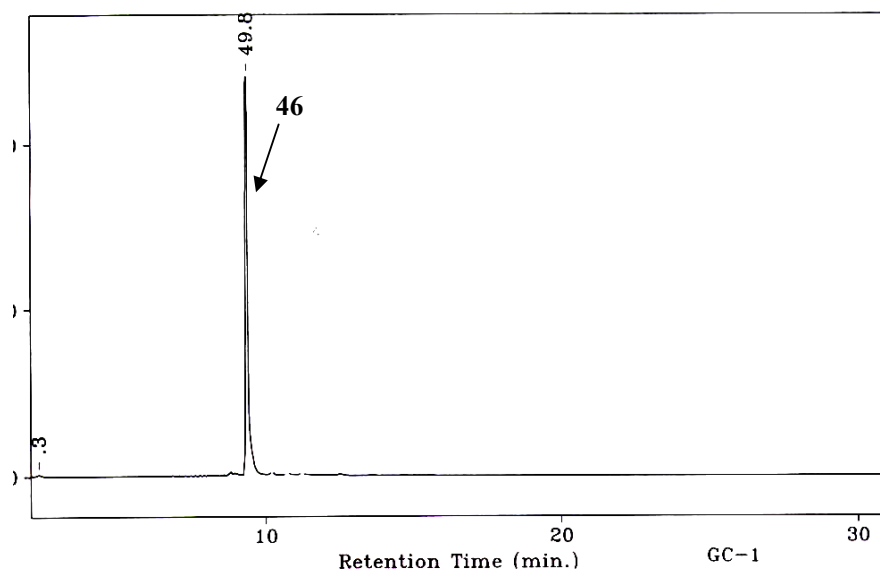


Figure 124a: GLC analysis of the solution before irradiation

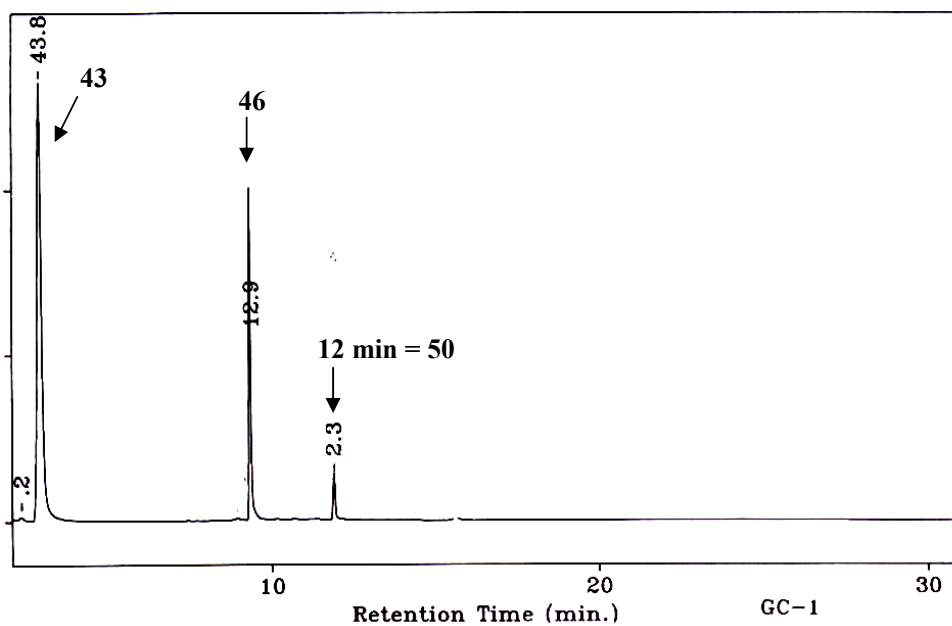


Figure 124b: GLC analysis of the reaction solution after 300 min

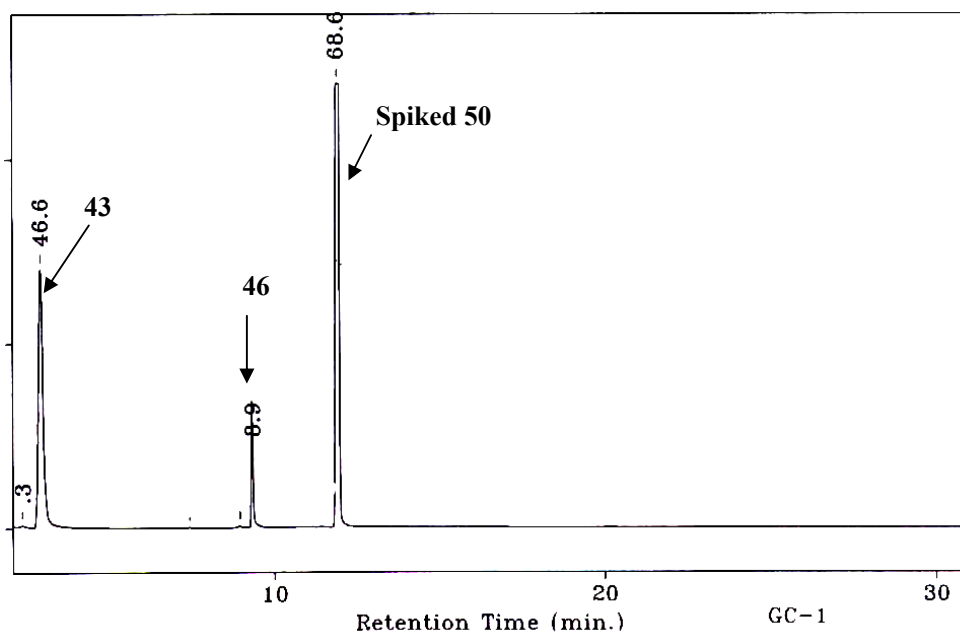


Figure 124c: Co-injection GLC analysis of the reaction solution with an authentic sample of 50

Co-injection GLC analysis of the reaction solution after 300 min with an authentic sample of **50** (Figure 124c) reveals that the peak with a retention time of 12 min has been increased. This would indicate that the new observed product which eluted with a retention time of 12 min upon irradiation of **46** in the presence of **49** is ethyl 3-phenyl-1,2,4-thiadiazole-5-carboxylate (**50**).

The GC (HP588) analysis of the same un-concentrated reaction solution after 300 min of irradiation (Figure 125a) shows three components in this reaction mixture with retention times of 4, 11.5 and 17 min. The mass spectrum of the first eluted component with a retention time of 4 min exhibited a molecular ion at m/z 103 and fragmentation pattern consistent with that of **43**, the known photoproduct. The second eluted component is the un-consumed reactant. The mass spectrum of the third eluted component (Figure 125b), which is strongly suspected to be **50**, exhibits a molecular ion at m/z 234 and a base peak at m/z 135.

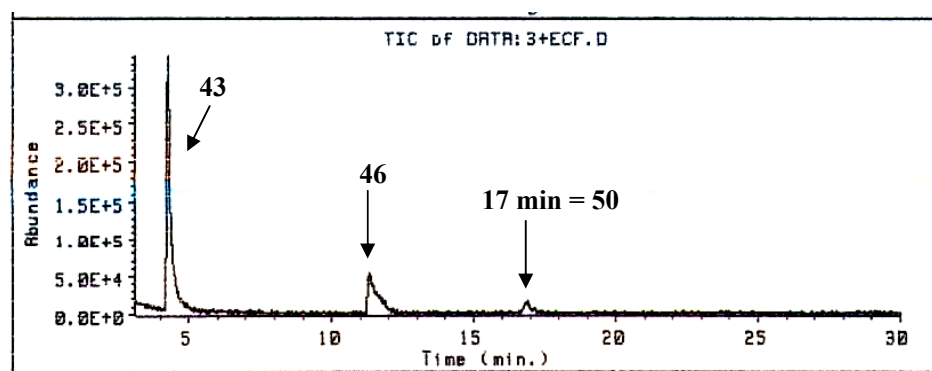


Figure 125a: GC-trace of the un-concentrated reaction solution after 300 min of irradiation

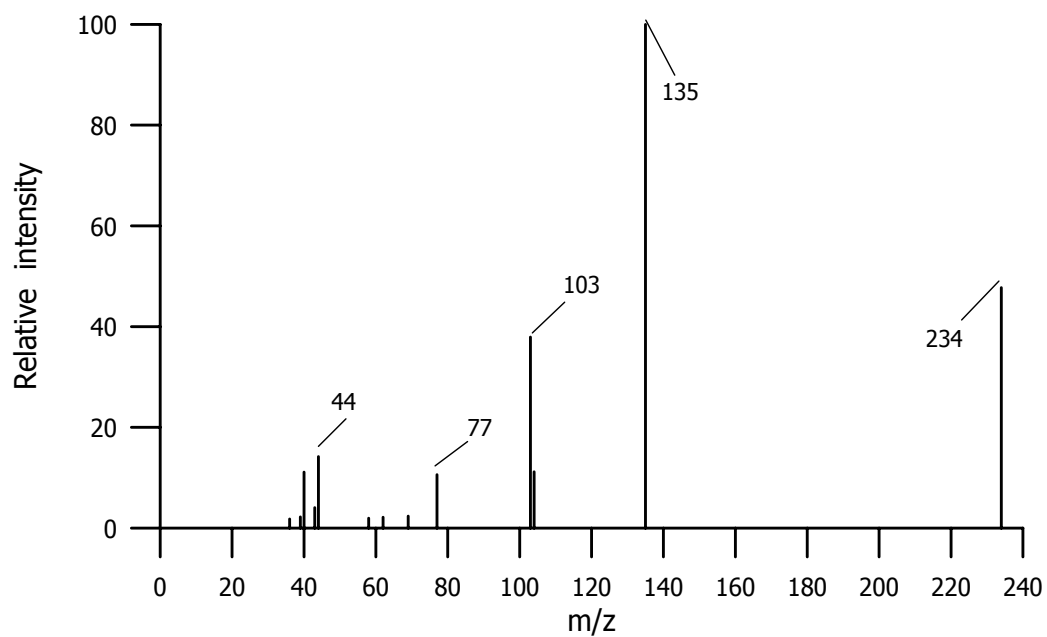


Figure 125b: Mass spectrum of the suspected product at RT 17 min

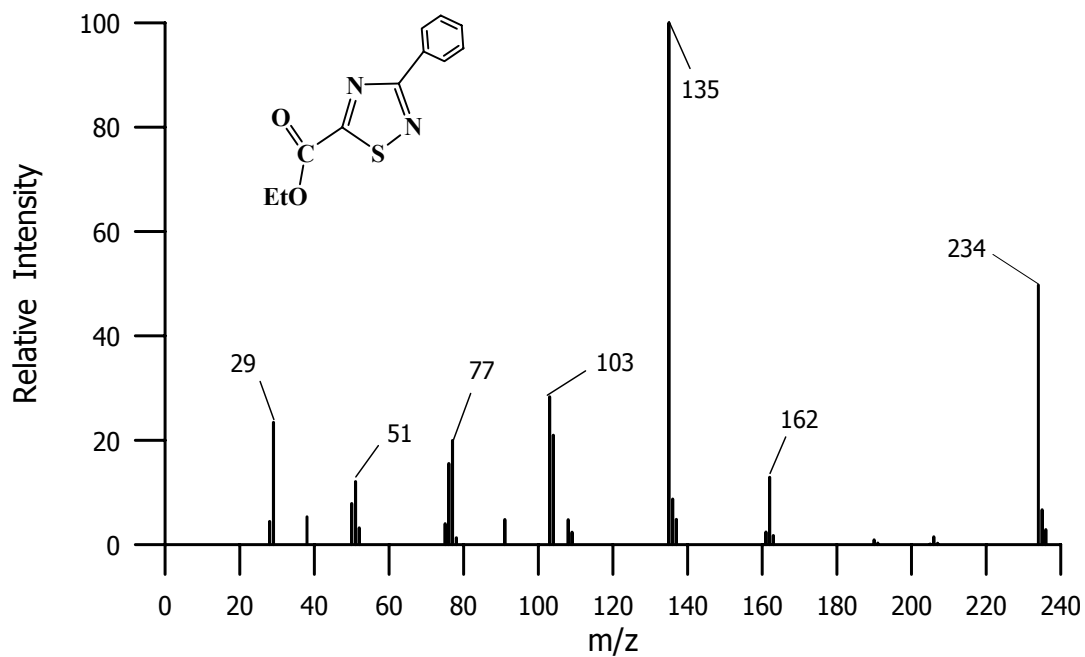
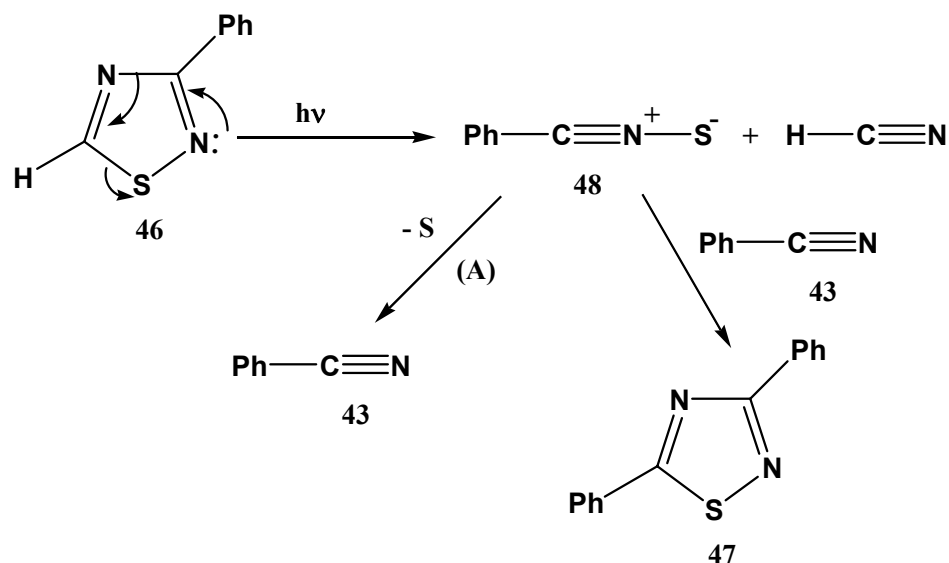


Figure 126: Mass spectrum of an authentic sample of 50

By comparison of the chromatographic and mass spectroscopic properties of the suspected product with the chromatographic and mass spectroscopic properties of an authentic sample of **50**, it can be concluded that the suspected product is ethyl 3-phenyl-1,2,4-thiadiazole-5-carboxylate (**50**). This result indicates the formation of benzonitrile sulfide (**48**). This result also corresponds to the observed formation of diphenyl-1,2,4-thiadiazole (**47**) upon irradiation of **46** which was proposed to arise from a 1,3-dipolar cycloaddition reaction of **48** with benzonitrile (**43**), the observed major product in this photoreaction.

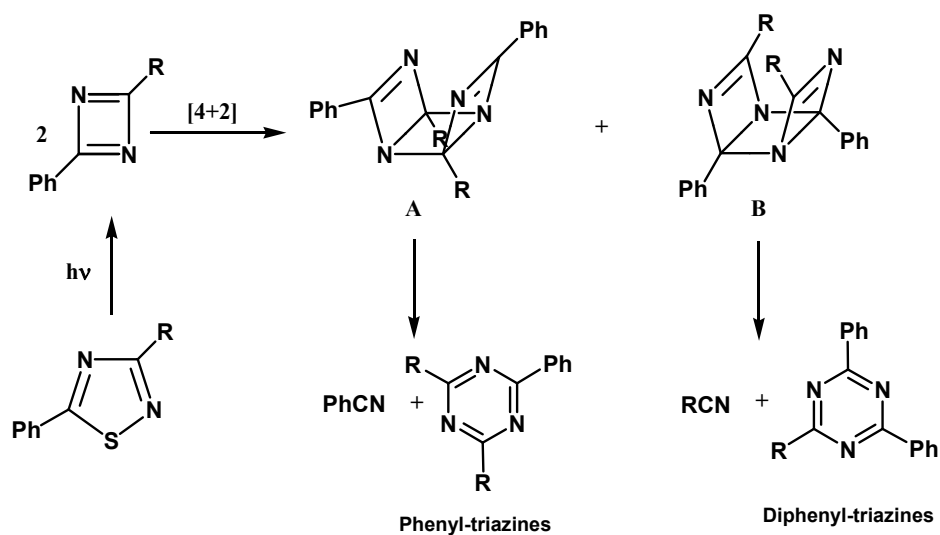
The detection of **48** would suggest direct photocleavage of the thiadiazole ring with the formation of H-CN and **48**. The latter species can undergo cycloaddition with **49** to yield **50**. In the absence of the trapping agent, **48** could split out sulfur resulting in the formation of **43** (A) or could undergo a 1,3-dipolar cycloaddition reaction with **43** to give **47** (B), as shown in Scheme 51.



Scheme 51: The proposed mechanism for the formation of **48** upon irradiation of **46**

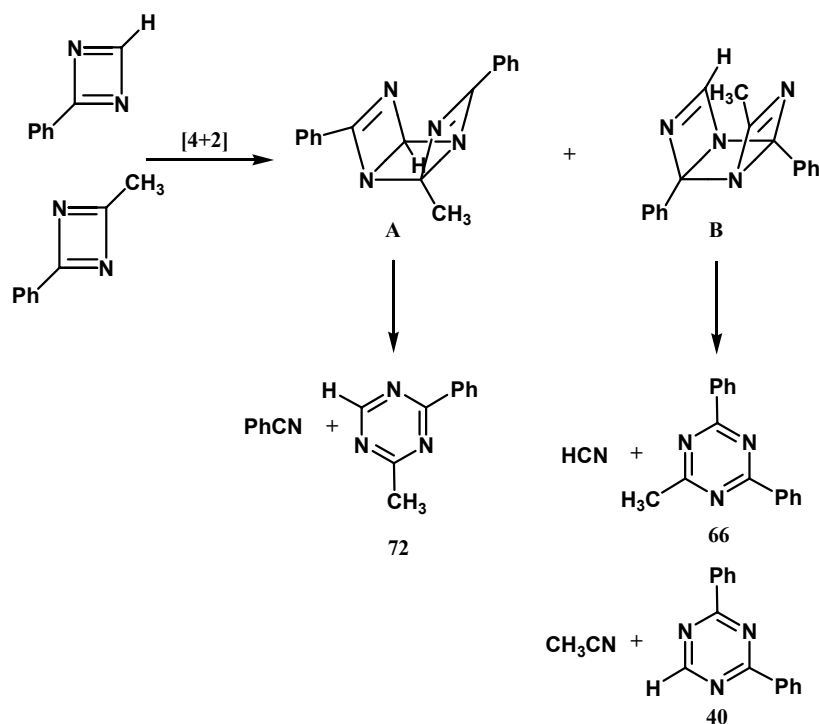
2.8 Photolysis 3-methyl-5-phenyl-1,2,4-thiadiazole and 5-phenyl-1,2,4-thiadiazole mixture in acetonitrile: Identification of phenyltriazines formation via [4+2] cycloaddition reaction of phenyldiazacyclobutadienes by a cross coupling experiment

The formation of triazines was proposed to occur via a [4+2] cycloaddition self-coupling of phenyldiazacyclobutadienes generated upon irradiation of 5-phenyl-1,2,4-thiadiazoles as shown in Scheme 52.



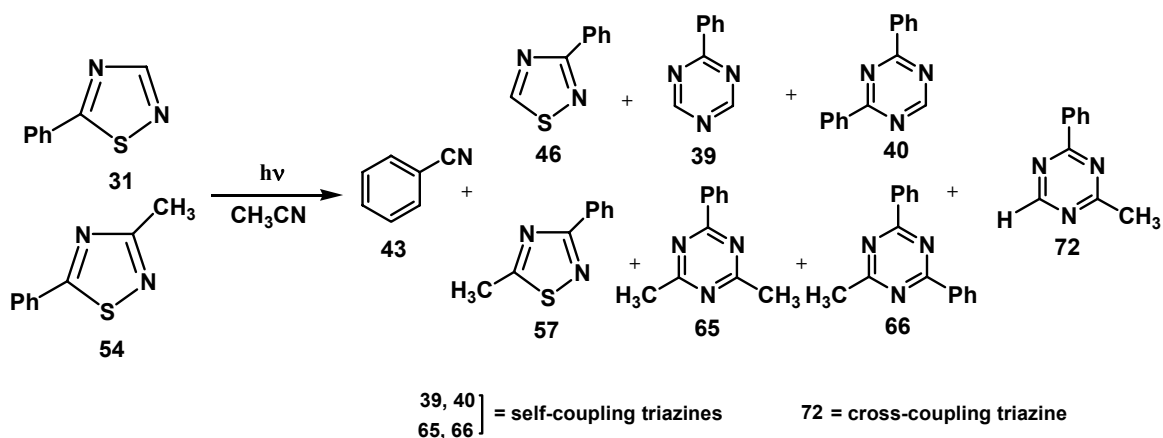
Scheme 52: The proposed mechanism for phenyl-s-triazines formation

In this proposed mechanism, if two different phenyldiazacyclobutadiene intermediates existed in the reaction, the observed triazines formation would not only come from a [4+2] cycloaddition self-coupling leading to the formation of symmetrical triazines but a [4+2] cycloaddition cross-coupling would also be in competition leading to the formation of an unsymmetrical triazine. This can be envisioned as shown in Scheme 53.



Scheme 53: The proposed formation of unsymmetrical phenyltriazine via [4+2] cycloaddition cross-coupling of phenyldiazacyclobutadiene intermediates

Therefore, it was proposed that irradiation of a mixture of 5-phenyl-1,2,4-thiadiazole (**31**) and 3-methyl-5-phenyl-1,2,4-thiadiazole (**54**) in acetonitrile would lead to the formation of 2-methyl-4-phenyl-1,3,5-triazine (**72**), a cross coupling product. Scheme 54 shows possible photoproducts that would be observed upon irradiation of a mixture of **31** and **54** in acetonitrile.

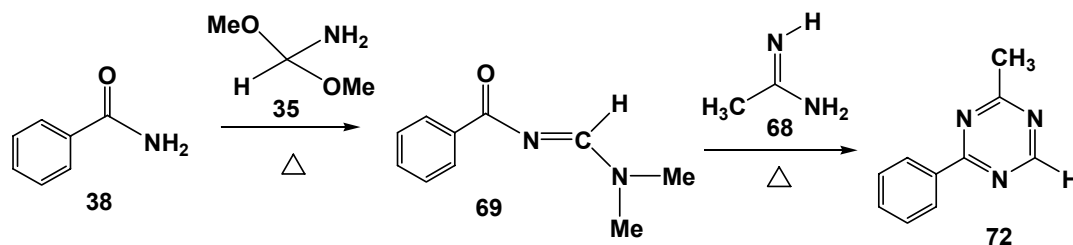


Scheme 54: The possible photoproducts predicted to observe upon irradiation of a mixture of 5-phenyl-1,2,4-thiadiazole and 3-methyl-5-phenyl-1,2,4-thiadiazole

In order to confirm this proposed mechanism, 2-methyl-4-phenyl-1,3,5-triazine (**72**) was synthesized and employed as an authentic sample for photoproduct identification upon irradiation of the thiadiazole mixture.

2.8.1 Synthesis of 2-methyl-4-phenyl-1,3,5-triazine

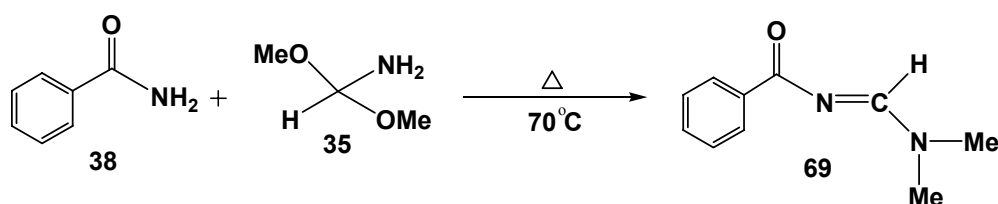
A recent synthesis of un-symmetrically substituted triazines has been reported by Raymond Dengino and colleagues¹³ involving the condensation of N-acylamidines with amidines or guanidines in aprotic solvents. Based on this synthetic method, condensation of N-[(dimethylamino)methylene]benzamide (**69**) with acetamidine (**68**) would yield 2-methyl-4-phenyl-1,3,5-triazine (**72**) as shown in Scheme 55.



Scheme 55: Total synthesis of 2-methyl-4-phenyl-1,3,5-triazine

2.8.1.1 Synthesis of N-[(dimethylamino)methylene]benzamide

In order to synthesize **72** by the synthetic route proposed in Scheme 55, N-[(dimethylamino)methylene]benzamide (**69**) was required as the starting amidine. This amidine **69** was prepared in 50 % yield as colorless crystals by the condensation of benzamide (**38**) with N,N-dimethylformamide dimethylacetal (**35**), as shown in Scheme 56. The colorless crystals were characterized by ^1H -, ^{13}C -NMR and mass spectroscopy.



Scheme 56: Synthesis of N-[(dimethylamino)methylene]benzamide

GC analysis of the colorless crystals (Figure 127a) exhibits only one component that eluted with a retention time of 16 min. The mass spectrum of this component (Figure 127b) shows a molecular ion at m/z 176 which is consistent with a molecular formula of $\text{C}_{10}\text{H}_{12}\text{N}_2\text{O}$ (MW 176). The base peak at m/z 99 is due to cleavage of $[\text{C}_6\text{H}_5]^+$ fragment (m/z 77) from the molecular ion. The peaks at m/z 44 and 105 are consistent with $[\text{C}_2\text{H}_6\text{N}]^+$ and $[\text{C}_7\text{H}_5\text{O}]^+$ fragments, respectively.

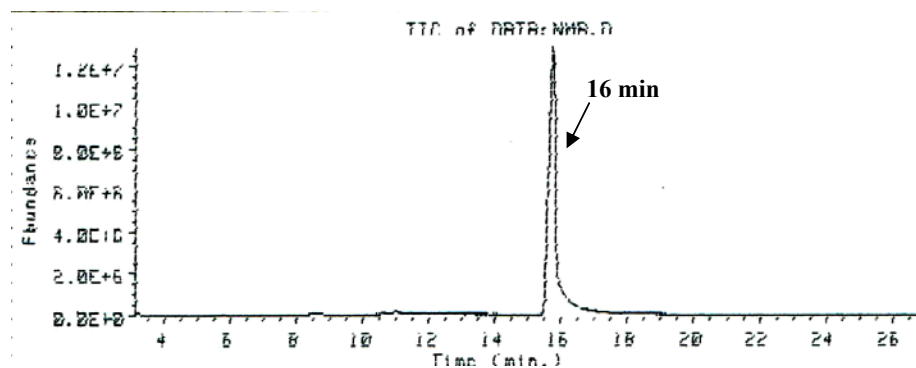


Figure 127a: GC analysis of N-[(dimethylamino)methylene]benzamide

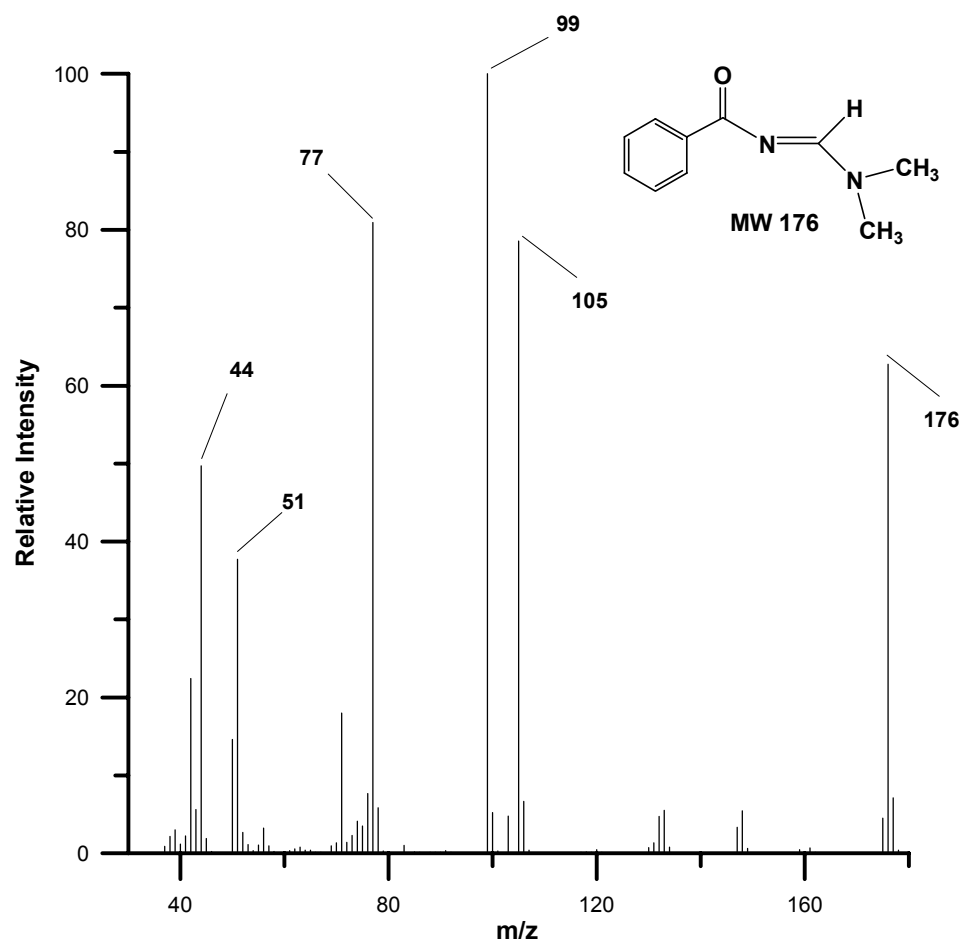


Figure 127b: Mass spectrum of N-[(dimethylamino)methylene]benzamide

Figure 128 shows $^1\text{H-NMR}$ spectrum of the colorless crystals corresponding to the structure of **69**. The spectrum reveals absorptions of the two non-equivalent amino methyl protons as two singlets at δ 3.17 (3H) and 3.21 (3H). The imine proton appears as a singlet (1H) downfield at δ 8.84. The phenyl ring protons are shown as two multiplets at δ 7.38-7.49 (3H) and 8.06-8.25 (2H).

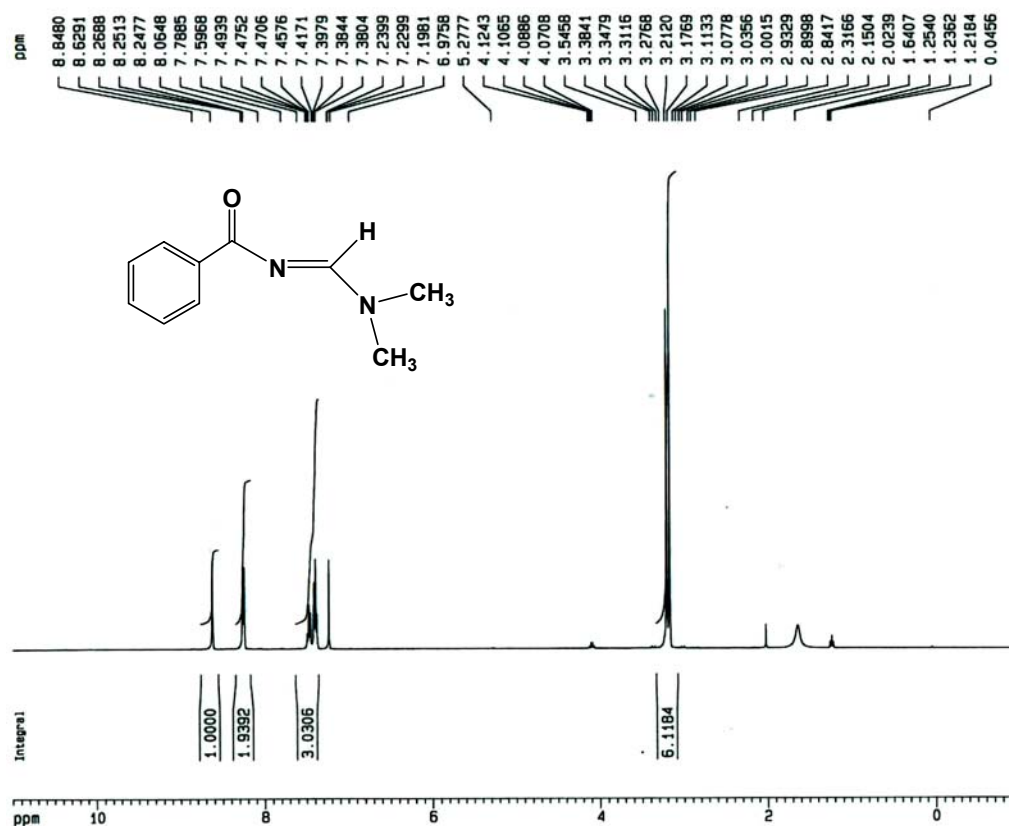


Figure 128: ^1H -NMR spectrum of N-[(dimethylamino)methylene]benzamide

The ^{13}C -NMR spectrum (Figure 129a) is also consistent with the structure of **69**. The carbonyl carbon absorbs downfield at δ 177.6. Based on the previous ^{13}C -NMR spectral assignments of the amidines synthesized in this laboratory, the signal at δ 160.6 can be assigned to the absorption of the imine carbon. The phenyl ring carbons at positions 2,6 and 3,5 appear as two singlets at δ 127.9 and 129.7 while the phenyl ring carbons at positions 1 and 4 absorb at δ 136.3 and 131.9, respectively. The two singlets at δ 35.4 and 41.5 were assigned to the two non-equivalent N-methyl carbons. These assignments are consistent with the ^{13}C -DEPT 135 spectrum (Figure 129b). The two signals at δ 136.3 and 177.6 disappeared in the ^{13}C -DEPT 135 spectrum which are consistent with the assignment of the two signals to the two quaternary carbons of the phenyl ring at position 1 and the carbonyl carbon, respectively. The signals at δ 35.4, 41.5, 127.9, 129.7, 131.9 and 160.6 still appear

in the ^{13}C -DEPT 135 spectrum which are consistent with the assignment to the two non-equivalent amino methyl carbons, phenyl ring carbons positions 2 and 6, 3 and 5, 4 and the imine carbon, respectively.

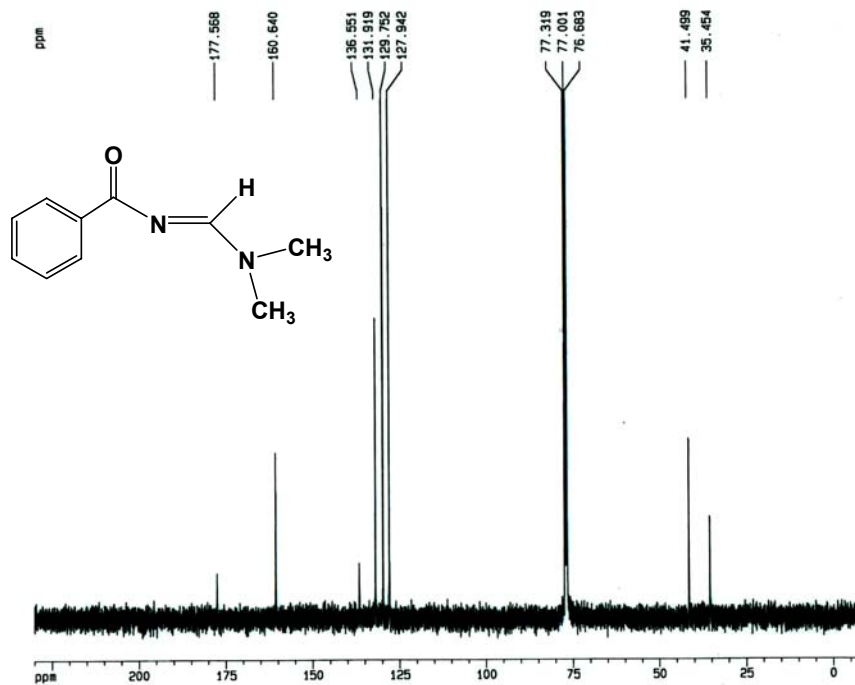


Figure 129a: ^{13}C -NMR spectrum of N-[(dimethylamino)methylene]benzamide

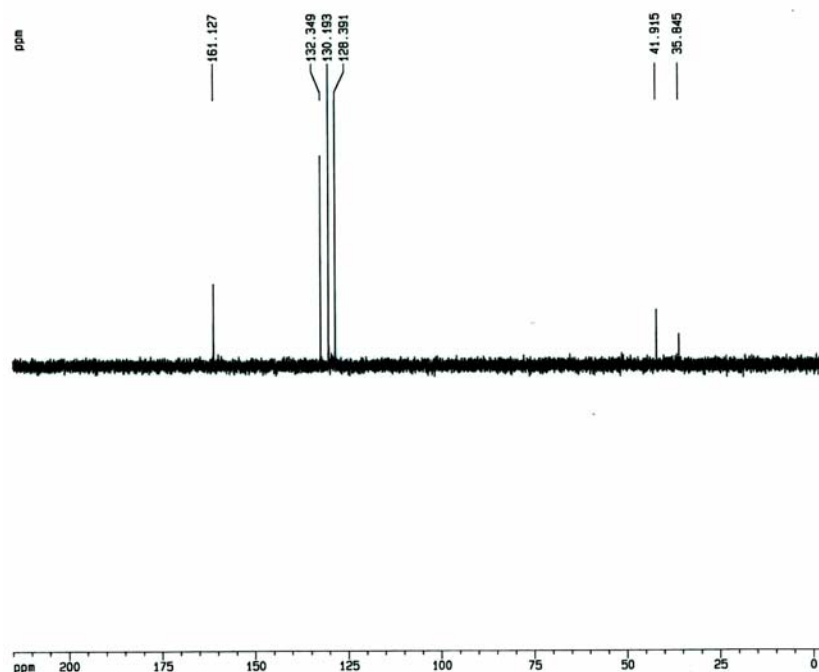
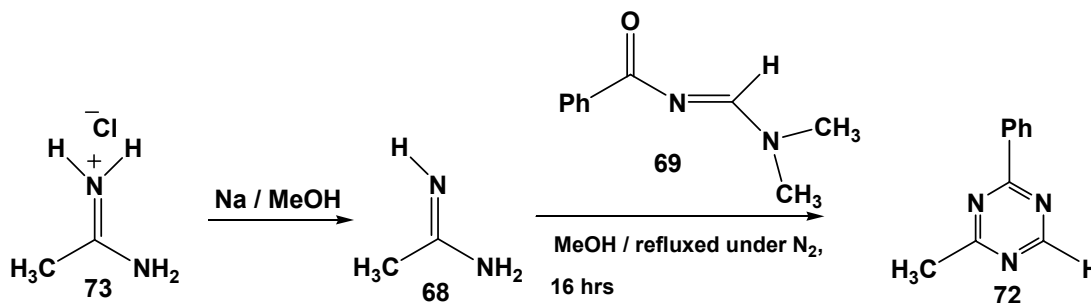


Figure 129b: ^{13}C -DEPT 135 spectrum of N-[(dimethylamino)methylene]benzamide

2.8.1.2 Synthesis of 2-methyl-4-phenyl-1,3,5-triazine

2-Methyl-4-phenyl-1,3,5-triazine (**72**) was synthesized by the method involving a condensation of **68** with amidine **69**. The desired triazine **72** was obtained in 20 % yield as a colorless viscous liquid. The colorless liquid was characterized by ^1H -, ^{13}C -NMR and mass spectroscopy.



Scheme 57: Synthesis of 2-methyl-4-phenyl-1,3,5-triazine

GC analysis of the colorless liquid (Figure 130a) exhibits only one gc-volatile component which was eluted with a retention time of 19 min. The mass spectrum of this component (Figure 130b) shows a molecular ion at m/z 171 corresponding with the molecular weight of 72 (MW 171). The base peak at m/z 103 is due to $[C_7H_5N]^+$ fragment while the moderate intense peak at m/z 104 is due to the m/z 103 fragment with subsequent hydrogen atom abstraction. These fragmentations are characteristic for fragmentation of 2-unsubstituted-4-phenyl-1,3,5-triazines as previously observed in the mass spectra of phenyl- and diphenyl-1,3,5-triazine. The peak at m/z 68 is consistent with elimination of $[C_7H_5N]$ from the molecular ion.

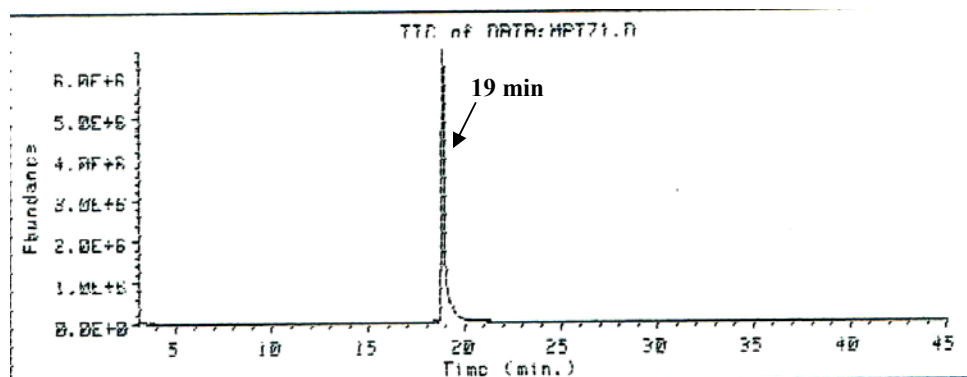


Figure 130a: GC analysis of the colorless liquid; 2-methyl-4-phenyl-1,3,5-triazine

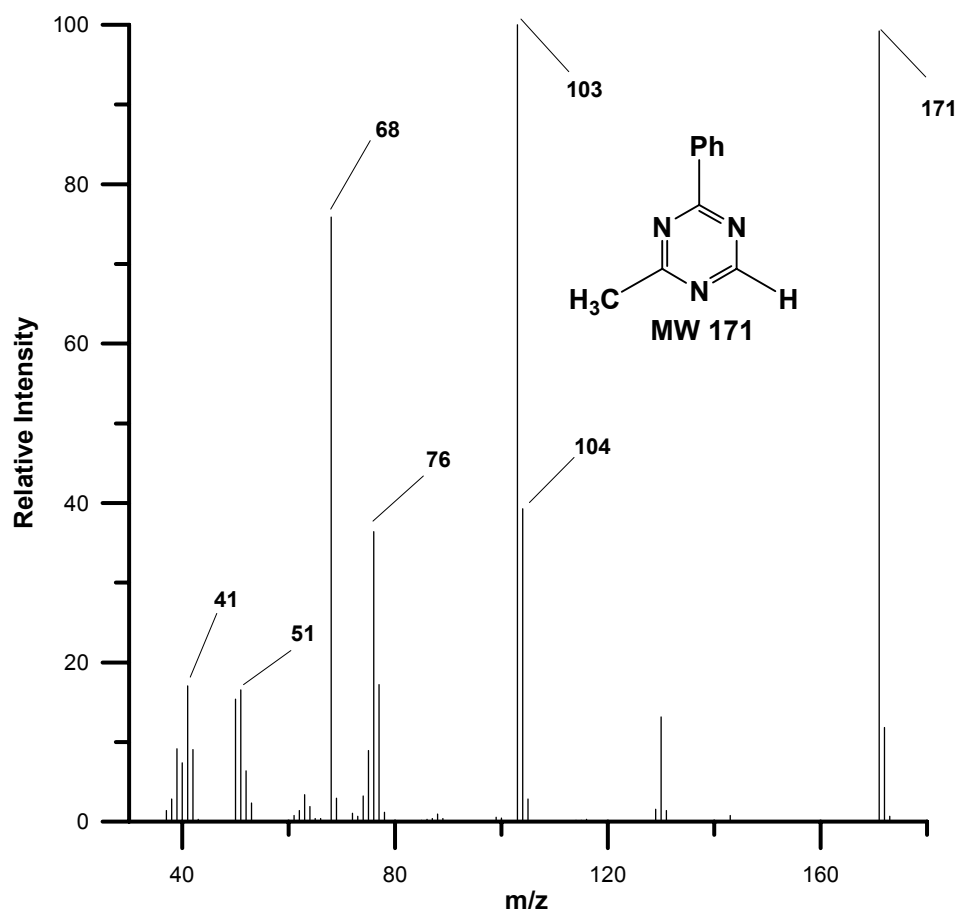


Figure 130b: Mass spectrum of 2-methyl-4-phenyl-1,3,5-triazine

Figure 131 shows the $^1\text{H-NMR}$ spectrum of the colorless liquid product. The spectrum reveals absorption of the proton on the triazine ring at position 6 as a singlet (1H) at δ 9.17. The methyl protons appear as a singlet (3H) at δ 2.71. The phenyl ring protons are shown as two multiplets at δ 7.47-7.57 (3H) and 8.47-8.51 (2H).

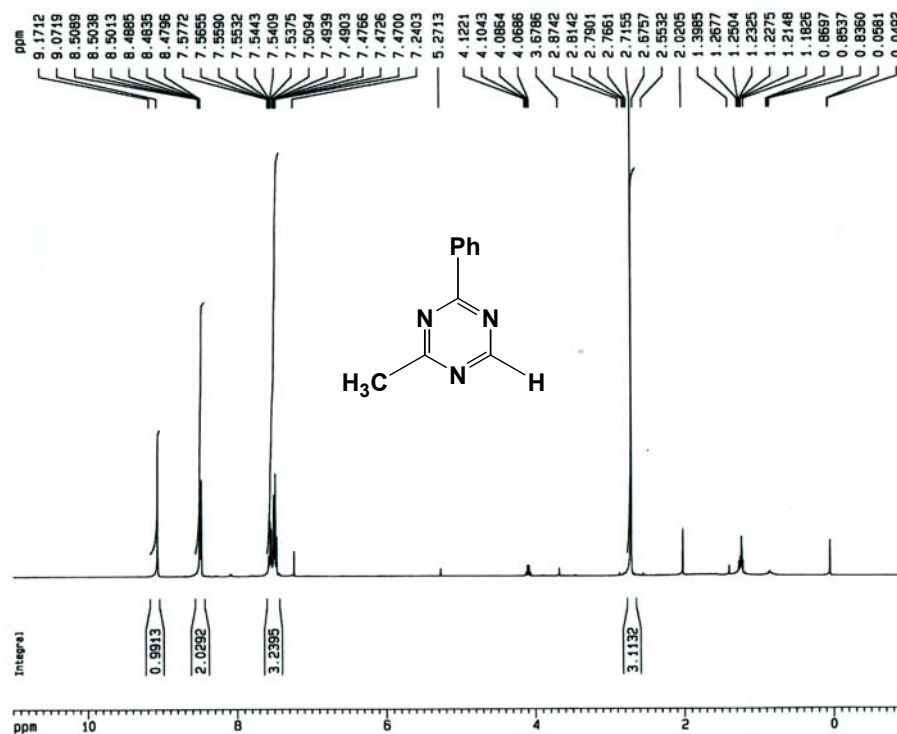


Figure 131: $^1\text{H-NMR}$ spectrum of 2-methyl-4-phenyl-1,3,5-triazine

The $^{13}\text{C-NMR}$ spectrum (Figure 132a) is also consistent with the structure of **72**. The methyl carbon appears at δ 26.3. The phenyl ring carbons at positions 2,6 and 3,5 absorb at δ 129.1 and 129.3 while the phenyl ring carbons at positions 1 and 4 absorb at δ 135.6 and 133.2, respectively. The three singlets at δ 166.5, 171.5 and 177.2 were assigned to the carbons on the triazine ring. These assignments are consistent with the $^{13}\text{C-DEPT}$ 135 spectrum (Figure 132b). The three signals at δ 135.6, 171.5 and 177.2 disappeared in the $^{13}\text{C-DEPT}$ 135 spectrum which is consistent with the assignment of the three signals to the three quaternary carbons of the phenyl ring at position 1 and the two carbons on the triazine ring at position 2 and 4, respectively. The signals at δ 26.3, 129.1, 129.3, 133.2 and 166.5 are still present in the $^{13}\text{C-DEPT}$ 135 spectrum which is consistent with the assignment to the methyl carbon, phenyl ring carbons positions 2 and 6, 3 and 5, 4 and the carbon of the triazine ring at position 6, respectively.

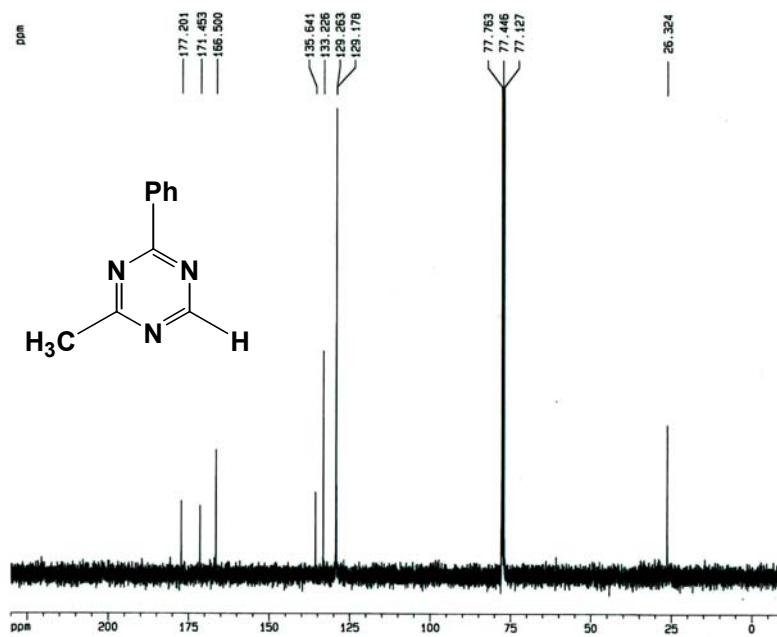


Figure 132a: ^{13}C -NMR spectrum of 2-methyl-4-phenyl-1,3,5-triazine

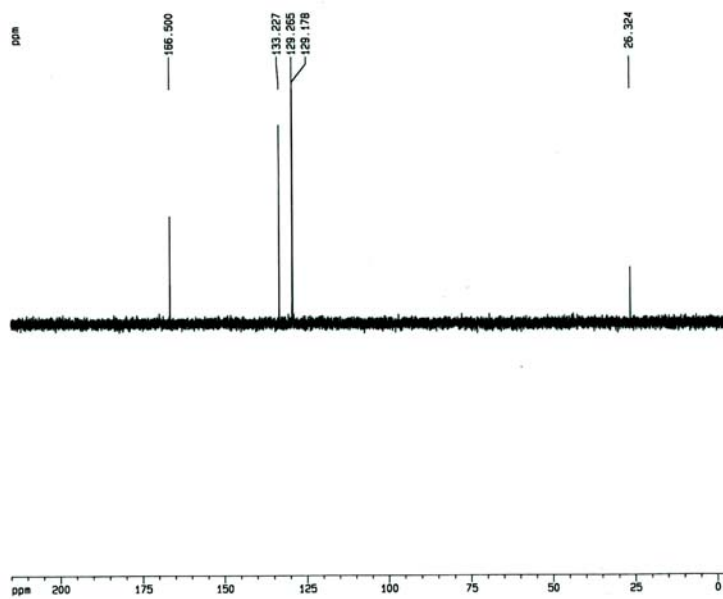


Figure 132b: ^{13}C -DEPT 135 spectrum of 2-methyl-4-phenyl-1,3,5-triazine

2.8.2 Irradiation of 5-phenyl- and 3-methyl-5-phenyl-1,2,4-thiadiazole mixture in acetonitrile

If the formation of triazines occurred via [4+2] cycloaddition self-coupling reaction of phenyldiazocyclobutadiene intermediates, as shown in Scheme 52, irradiation of a mixture of 5-phenyl- and 3-methyl-5-phenyl-1,2,4-thiadiazole (**31**) and (**54**) in acetonitrile should lead to the formation of the unsymmetrical triazine, 2-methyl-4-phenyl-1,3,5-triazine (**72**), arising from a [4+2] cycloaddition cross-coupling reaction of phenyldiazocyclobutadiene intermediates. In order to explore this possibility, irradiation of a mixture of 5-phenyl- (**31**) and 3-methyl-5-phenyl-1,2,4-thiadiazole (**54**) in acetonitrile was carried out. The photoreaction was qualitatively monitored by GLC and GC-MS.

The mixture solution of **31** + **54** (3.5 mL), the solution of **54** (3.5 mL), and the solution of **31** (3.5 mL) in acetonitrile each in sealed Pyrex tubes were purged with argon for 15 min. These solutions were then irradiated simultaneously with fifteen > 290 nm lamps for a total of 650 min. The reactions were monitored by GLC (PE9000) analysis after every 120 min of irradiation. Figure 133 (a-b) and 134 (a-b) show the GC-chromatograms of solutions of **31** and **54** before and after 650 min of irradiation, respectively, revealing the formation of the known photoproducts upon irradiation of these compounds. GC-chromatogram of the mixture before irradiation showed only two components with retention times corresponding to chromatographic properties of each individual thiadiazole **31** and **54**. This confirms that these two thiadiazoles did not undergo any thermal reaction especially leading to the formation of triazines.

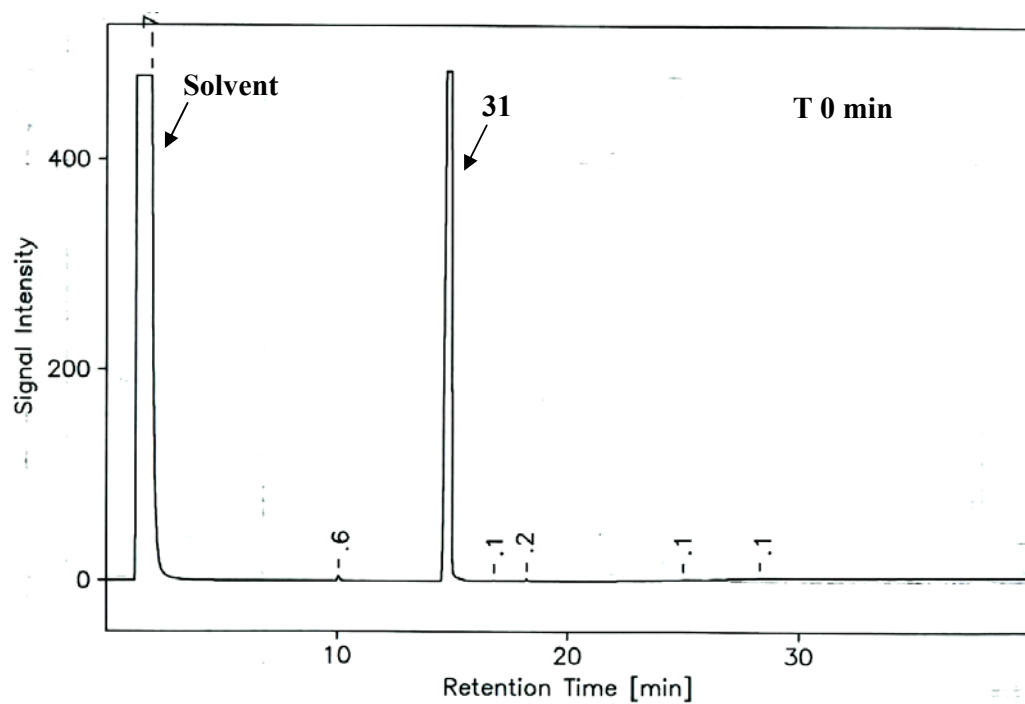


Figure 133a: GLC analysis of **31** in acetonitrile before irradiation

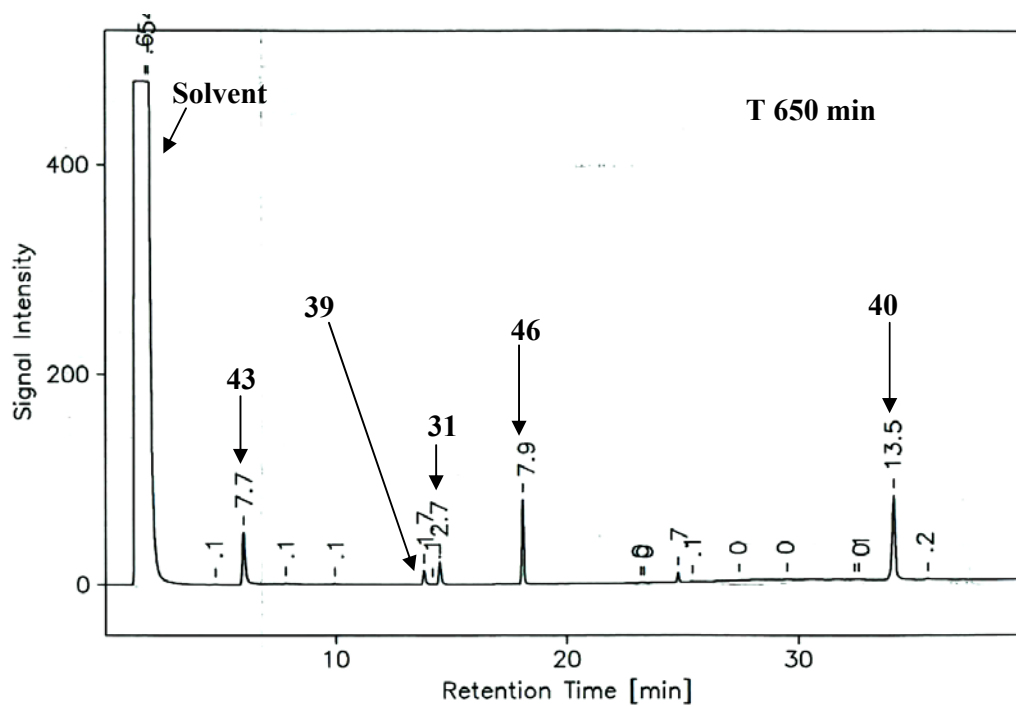


Figure 133b: GLC analysis of **31** in acetonitrile after 650 min of irradiation

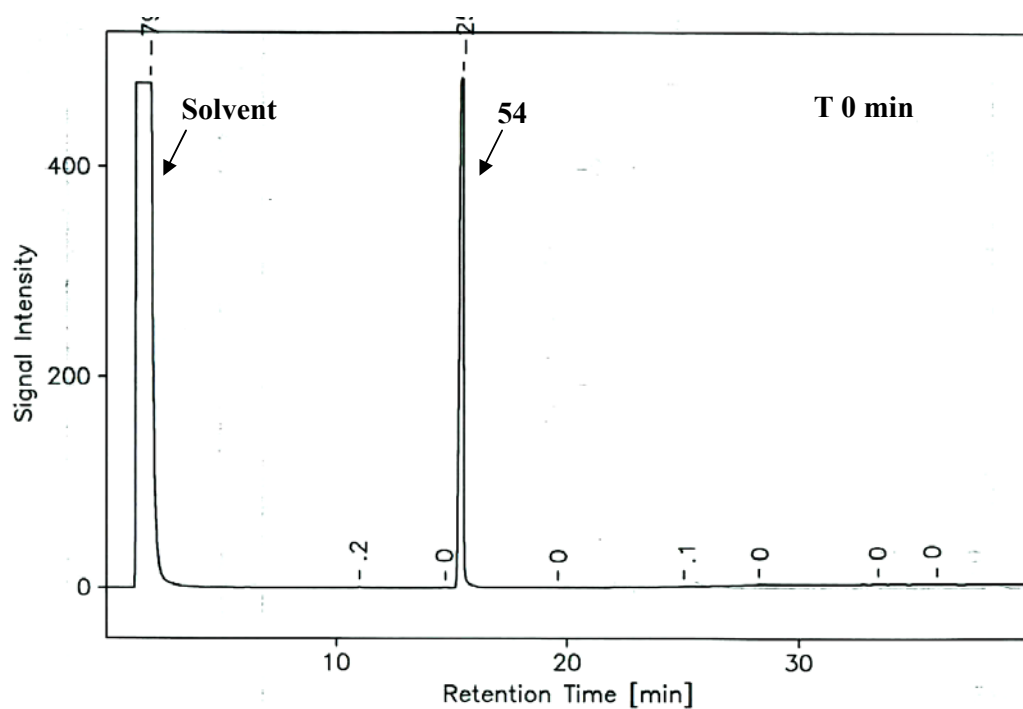


Figure 134a: GLC analysis of 54 in acetonitrile before irradiation

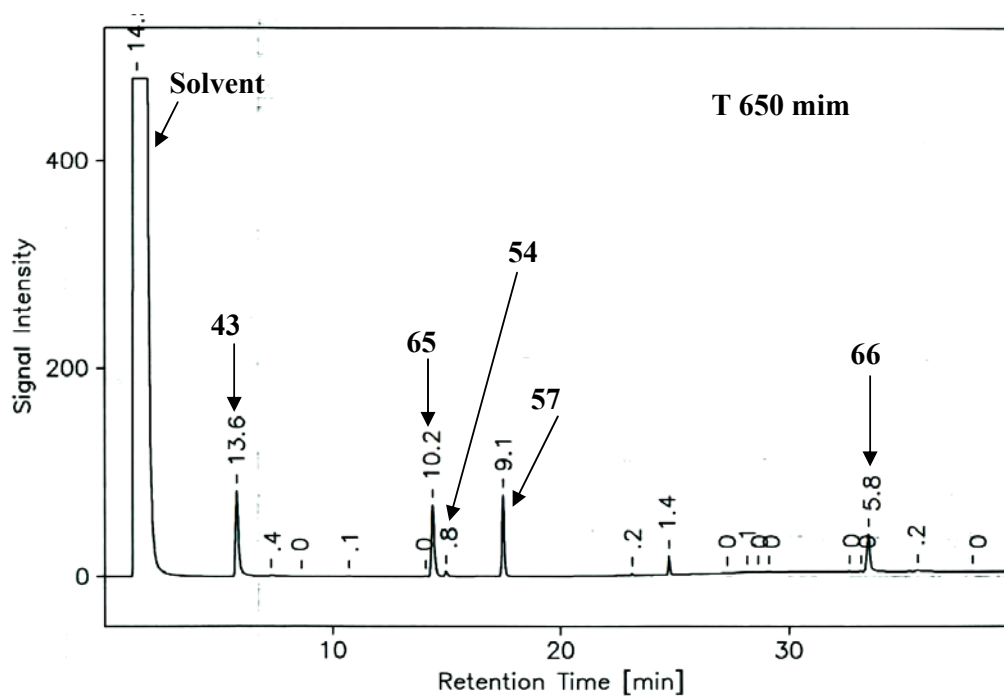


Figure 134b: GLC analysis of 54 in acetonitrile after 650 min of irradiation

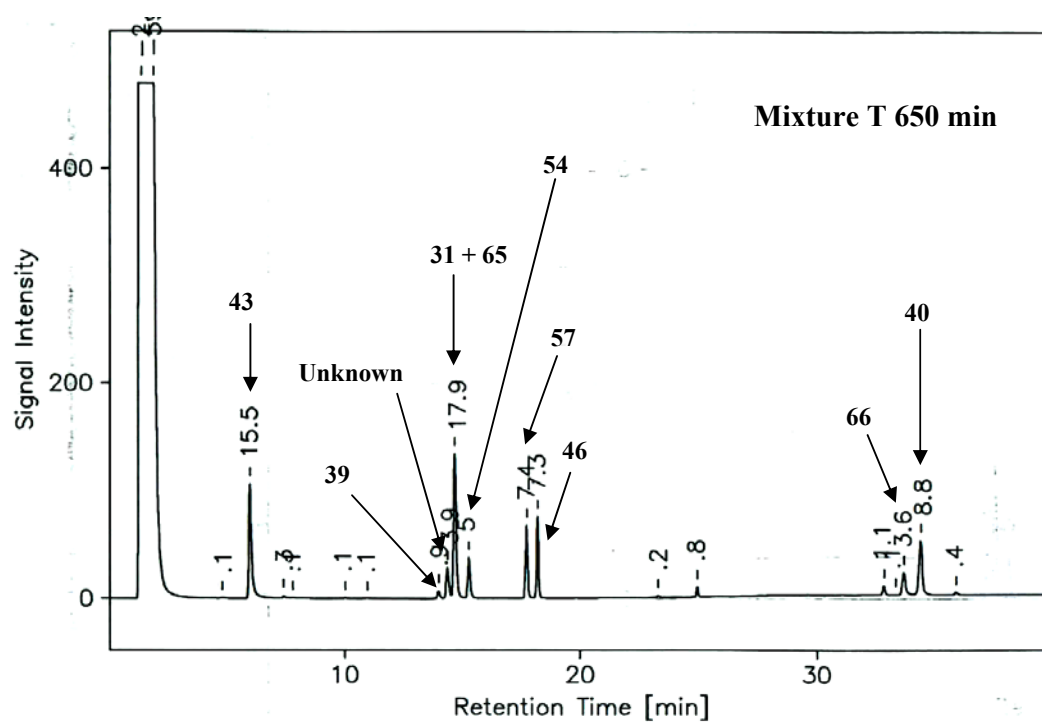


Figure 135: GLC analysis of the thiadiazole mixture solution after 650 min of irradiation

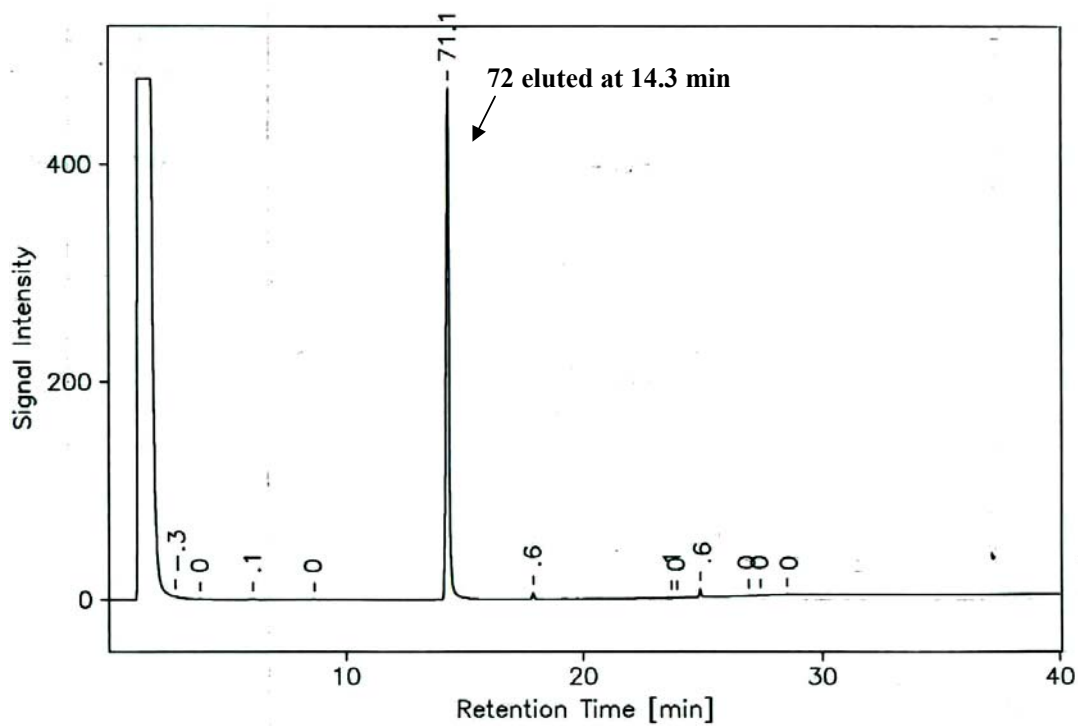


Figure 136: GLC analysis of the authentic sample of 2-methyl-4-phenyl-1,3,5-triazine

Figure 136 shows the GLC analysis of the authentic 2-methyl-4-phenyl-1,3,5-triazine (**72**) under the same analytical condition as employed for the analyses of the photoreactions. The chromatogram reveals the presence of only one gc-volatile component with a retention time of 14.3 min.

After 650 min of irradiation, the solution of **54** and the solution of **31** became yellow brown while the mixture solution appeared as a pale pink-yellow with a colloidal precipitate. Figure 135 shows the GC-chromatogram of the mixture after 650 min of irradiation. The components observed in the mixture reaction after irradiation could be assigned by comparison with the chromatographic properties obtained by GLC analyses of the individual thiadiazole reactions under the same analytical condition (Figure 133b and 134b). Only one component, which eluted with a retention time of 14.3, was not observed in either of the reaction of **54** or **31**.

A small amount of the mixture solution after 650 min of irradiation was removed and spiked with an authentic sample of the expected un-symmetrical triazine, 2-methyl-4-phenyl-1,3,5-triazine (**72**). Figure 137 exhibits the GLC analysis of the irradiated mixture solution spiked with an authentic sample of **72**. The GC-trace reveals an increase of the unidentified peak that eluted with a retention time of 14.3 min. This would indicate that the unknown component, which eluted with a retention time of 14.3 min, is 2-methyl-4-phenyl-1,3,5-triazine (**72**).

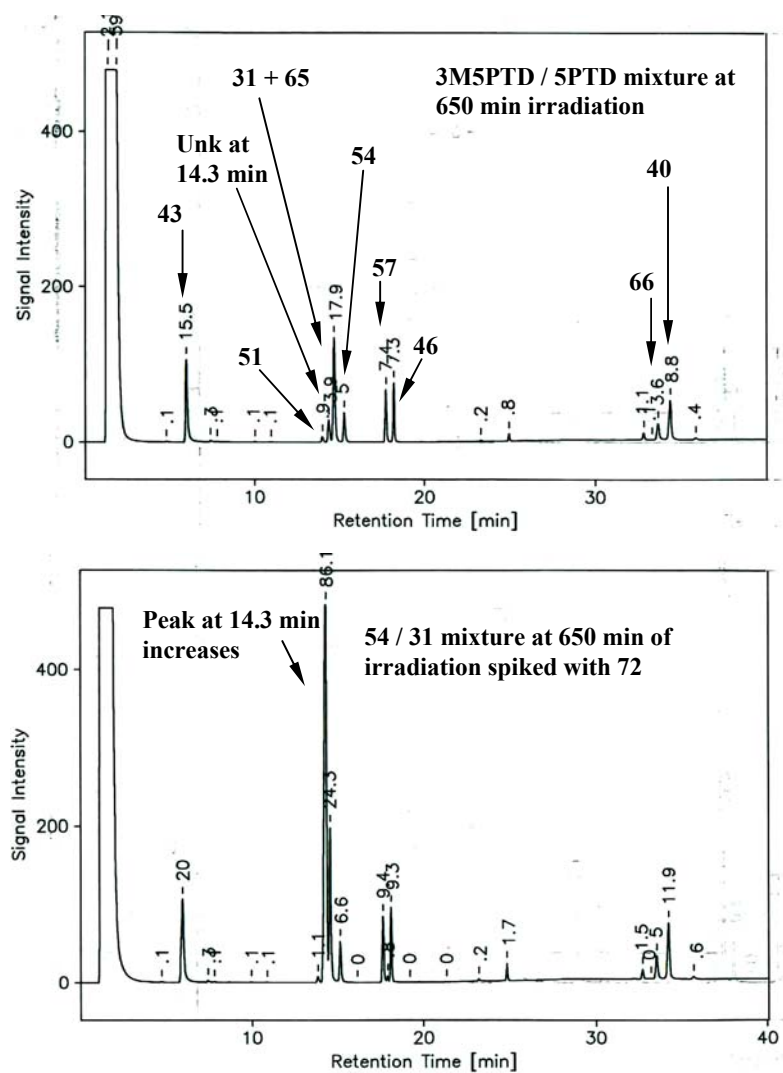


Figure 137: GLC analysis of the irradiated mixture solution spiked with an authentic sample **72**

The mixture solution after 650 min of irradiation was also analyzed by GC-MS. The GC-trace (Figure 138a) exhibits a new unidentified component, which eluted with a retention time of 19.2 min, which was not observed either in the reaction of **31** or **54**. The mass spectrum of this component (Figure 138b) reveals a molecular ion at m/z 171 and its fragmentation pattern corresponding with the molecular ion and fragmentation pattern of an authentic sample of **72**.

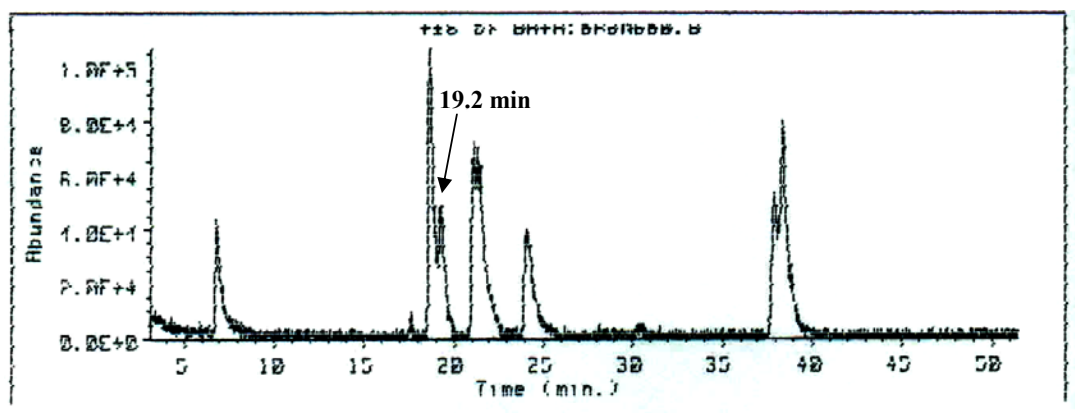


Figure 138a: GC-trace of the mixture solution after 650 min of irradiation

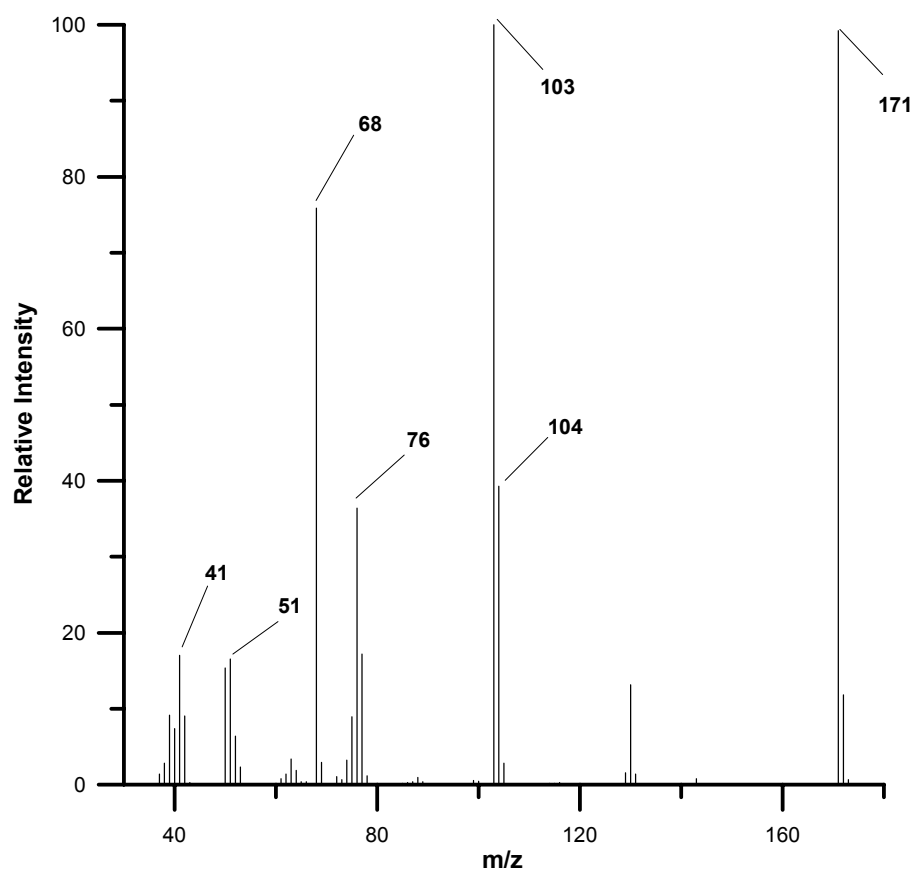


Figure 138b: Mass spectrum of the component eluted with a retention of 19.2 min

The irradiated mixture solution, which was spiked with an authentic sample of **72**, was also analyzed by the GC (HP588) interfaced with a mass spectrometer. The GC-trace (Figure 139a) reveals an increasing of the component that eluted with a retention time of 19.2 min. The mass spectrum of this peak revealed a molecular ion and fragmentation pattern identical to those of an authentic sample of **72**.

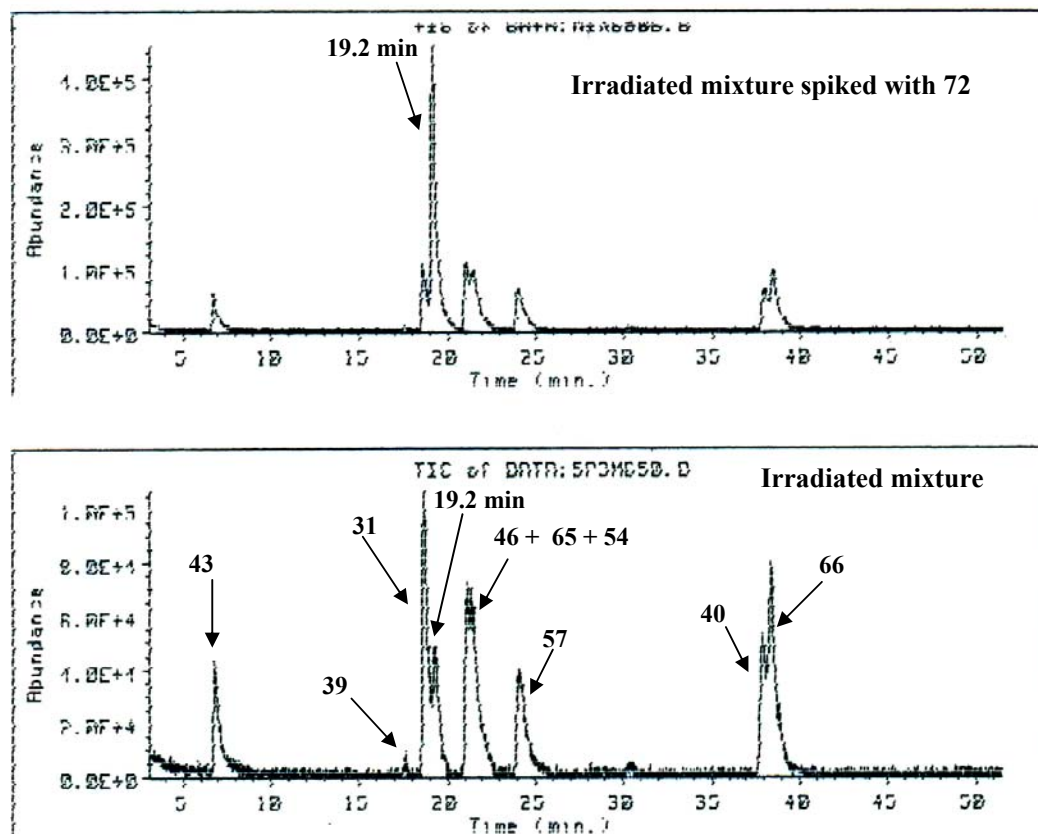


Figure 139: GC-trace (HP588) of the irradiated mixture spiked with an authentic sample of **72**

By comparison of the chromatographic and mass spectroscopic properties of the new photoproduct with the chromatographic and mass spectroscopic properties of an authentic sample of **72**, it can be concluded that this new product is 2-methyl-4-phenyl-1,3,5-triazine (**72**).

This result, therefore, supports the assumption of triazine formation *via* a [4+2] cycloaddition reaction of phenyldiazacyclobutadienes as previously proposed based on the results observed upon irradiation of 5-phenyl-1,2,4-thiadiazole-4-¹⁵N (**31-4¹⁵N**).

It is of interest to note that the analysis with the GC (HP588) interfaced with a mass spectrometer of the concentrated photolysate of **31** (Figure 140a) reveals two unknown peaks that eluted with a retention time of 18.9 min (**Unk1**) and 35 min (**Unk 2**). These peaks were not previously observed in the photolysate of **31**.

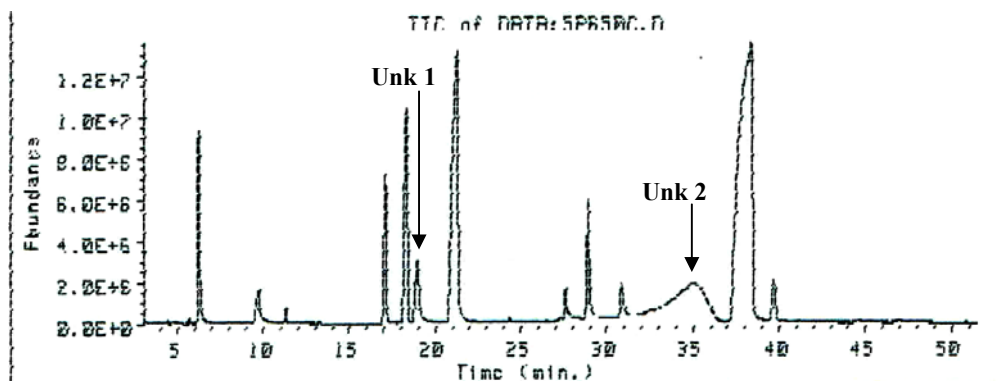


Figure 140a: GC analysis of the concentrated **31** photolysate after 650 min of irradiation

The mass spectrum of the broad peak that eluted with a retention time of 35 min (**Unk2**; Figure 140b) exhibits a molecular ion at m/z 256 which corresponds to a formula of S_8 (FW 256). The fragmentation pattern of this component appears in a P-32 manner which corresponds to loss of sulfur atom in each cleavage. This indicates the presence of elemental sulfur in this photolysate. Since previous photolysis of **31** was carried out for short periods of irradiation, thus, the concentration of elemental sulfur in the mixture was below the detection limit of the GC-MS analytical condition. Thus, no elemental sulfur was previously detected upon irradiation of **31**. This result, therefore, confirms the formation of elemental sulfur upon photolysis of **31** in acetonitrile.

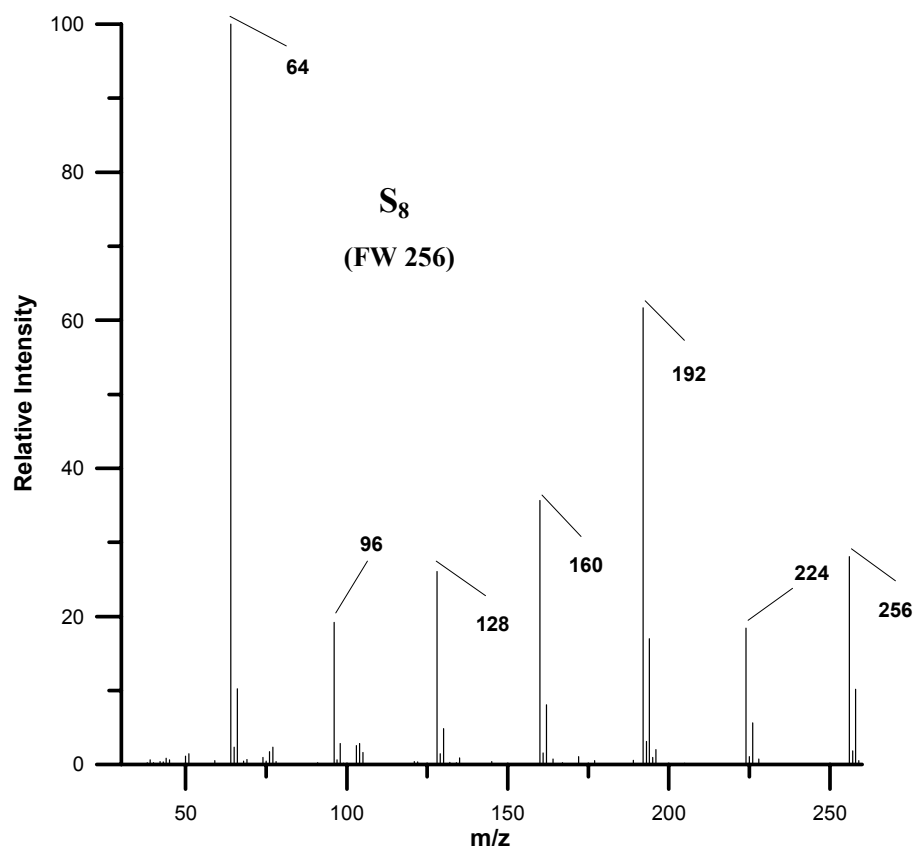


Figure 140b: Mass spectrum of the **Unk2** eluted with a retention time of 35 min

The unknown peak that eluted with a retention time of 18.9 min (**Unk1**) has a molecular ion at m/z 121 (Figure 140c) which corresponds to a molecular formula of C₇H₇NO (MW 121).

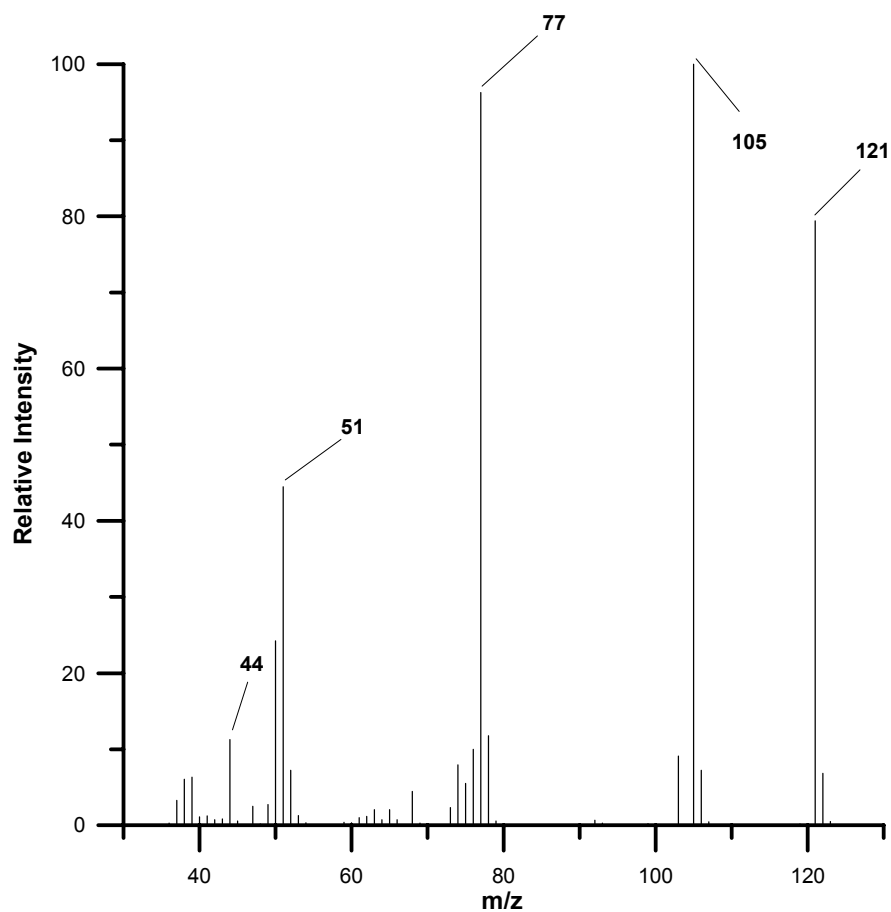


Figure 140c: Mass spectrum of the peak eluted with a retention time of 18 min (**Unk 1**)

Figure 141 show the GC-trace of an authentic sample of benzamide (**38**). This result shows that the **unk 1** in the photolysate of **31** has its chromatographic and mass spectroscopic properties identical to those of an authentic sample of **38**. Thus, it can be concluded that the **unk 1**, which was observed in the photolysis of **31**, is benzamide (**38**).

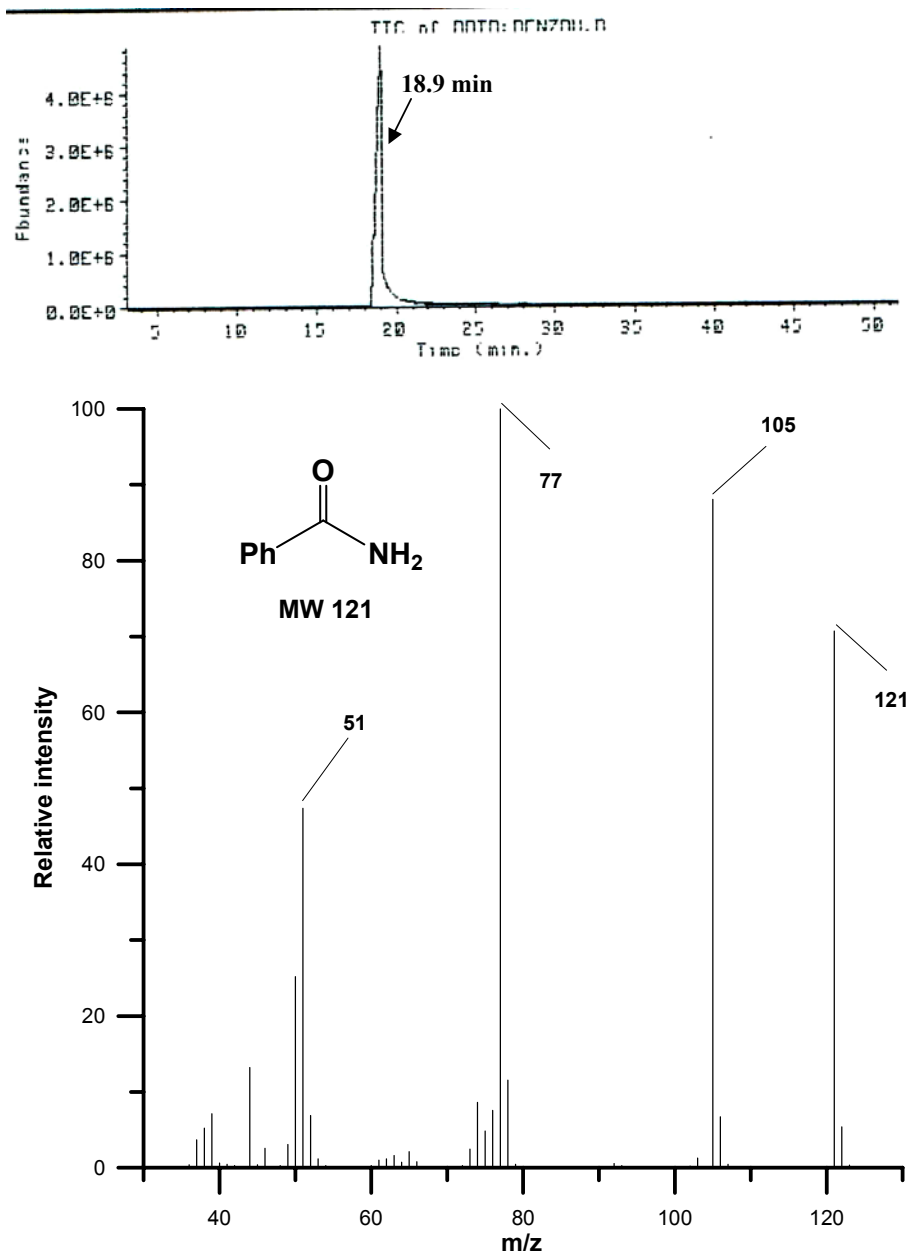
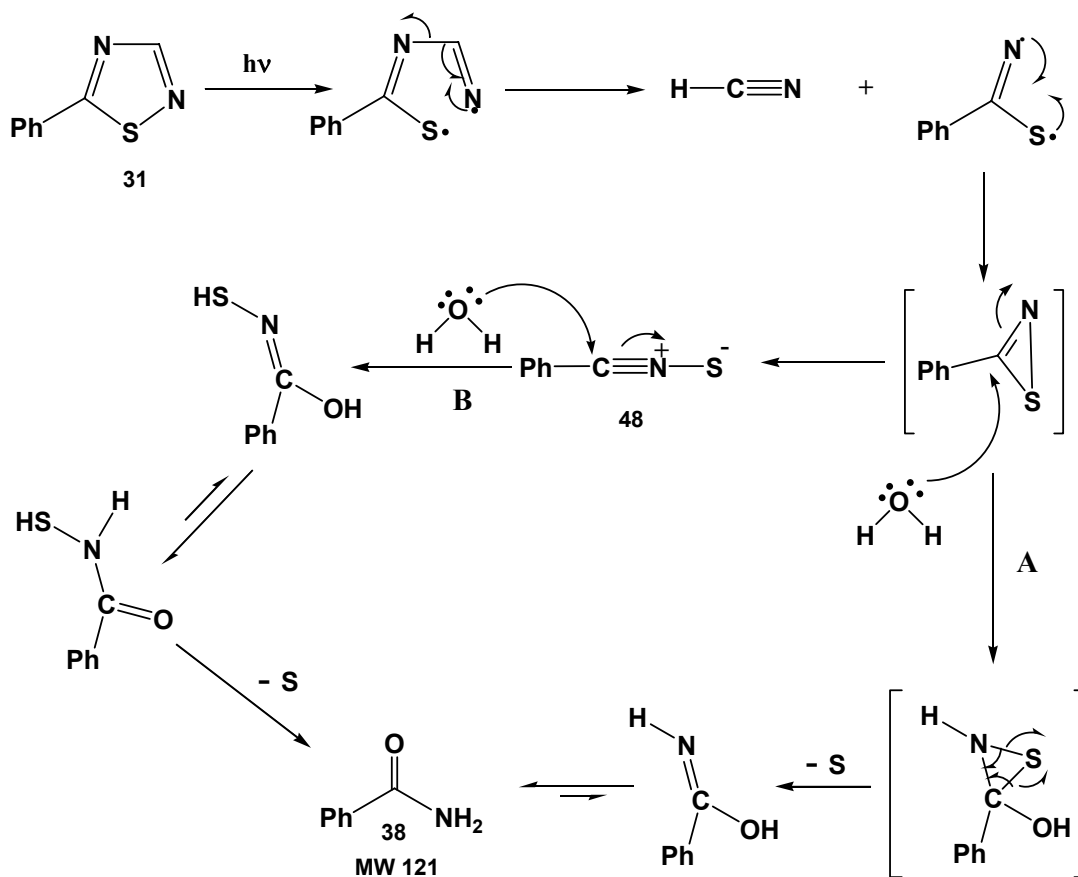


Figure 141: GC (HP588) and mass spectrum of an authentic sample of benzamide

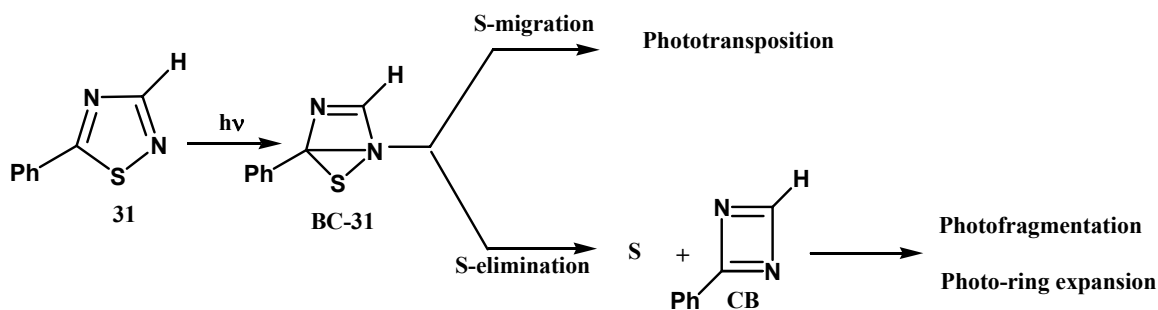
The formation of **38** upon photolysis of **31** was proposed to arise from a nucleophilic ring opening of the phenyl substituted thiazirine due to the presence of water in the reaction media (pathway A) or a hydrolysis of benzonitrile sulfide (**48**) via an unclear mechanism (pathway B) as shown in Scheme 58.



Scheme 58: The proposed formation of benzamide upon irradiation of **31**

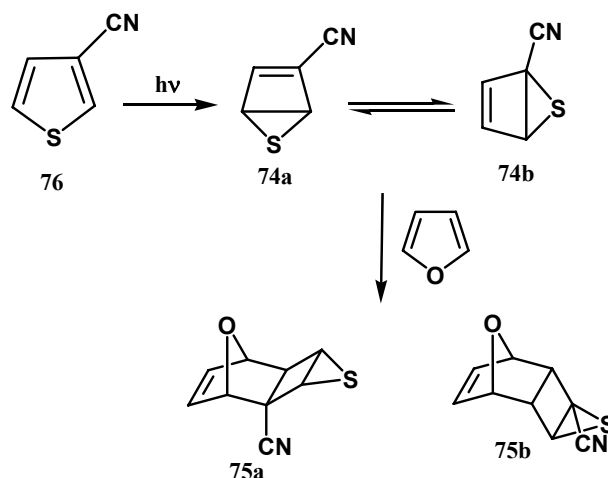
2.9 Photochemistry of phenyl substituted-1,2,4-thiadiazoles in furan solvent: Furan trapping of reactive intermediates

Previous result from the irradiation of 5-phenyl-1,2,4-thiadiazole (**31**) and ^{15}N -labeled 5-phenyl-1,2,4-thiadiazole, have suggested that a photochemically generated 1,3-diaza-5-thiabicyclo[2.1.0]pentene (**BC-31**) is the key intermediate in the photoreaction.¹⁴



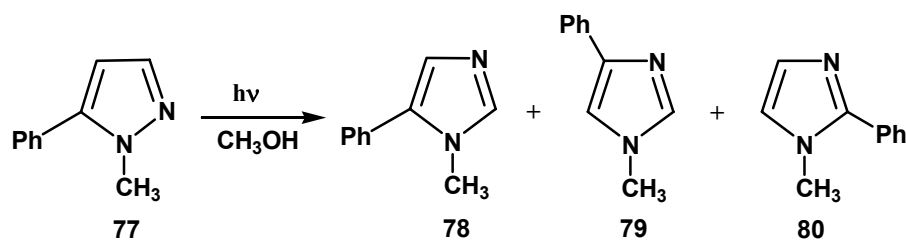
Scheme 59: 1,3-Diaza-5-thiabicyclo[2.1.0]pentene; Key intermediate upon irradiation of 5-phenyl-1,2,4-thiadiazole

There are precedents for trapping such a photochemically generated bicyclic species. Day and Barltrop¹⁵ have suggested that the phototransposition reaction of cyanothiophenes occur via thiabicyclo[2.1.0]pent-2-ene intermediates (**74**). The existence of these intermediates was confirmed by isolation of a 1:1 mixture of furan-thiabicyclo[2.1.0]pent-2-ene adducts (**75a** and **75b**) upon irradiation of 3-cyanothiophene (**76**) in furan solvent as shown in Scheme 60.



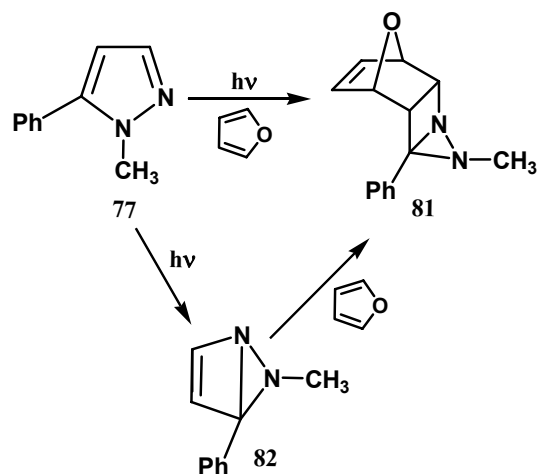
Scheme 60: Photochemistry of 3-cyanothiophene in furan solvent

Work in our laboratory has also shown that 1-methyl-5-phenylpyrazole (**77**) undergoes phototransposition to the three different 1-methylimidazoles (**78-80**) upon irradiation in methanol.¹⁶ These products were not observed, however, if the reaction



Scheme 61: Photochemistry of 1-methyl-5-phenylpyrazole in methanol

was carried out in furan solvent. Instead, irradiation of **77** in furan solvent led to the isolation of the [4+2] adduct (**81**).¹⁶ The formation of the product is consistent with furan trapping of 4-phenyl-5-methyl-1,5-diazabicyclo[2.1.0]pentene (**82**) formed photochemically by electrocyclic ring closure of **77**.



Scheme 62: Irradiation of 1-methyl-5-phenylpyrazole in furan solvent

In an attempt to establish the formation of the bicyclic intermediate upon irradiation of phenyl substituted-1,2,4-thiadiazoles, irradiation of phenyl substituted-1,2,4-thiadiazoles in the presence of furan solvent were carried out in an attempt to trap the bicyclic species as a Diels-Alder adduct.

2.9.1 Photochemistry of 5-phenyl-1,2,4-thiadiazoles in furan solvent

2.9.1.1 Irradiation of 5-phenyl-1,2,4-thiadiazole in furan solvent

Solutions of 5-phenyl-1,2,4-thiadiazole (**31**) in furan (2.4×10^{-2} M; 3.5 mL) and **31** in acetonitrile (1.72×10^{-2} M; 3.5 mL) in sealed Pyrex tubes were purged with argon gas for 20 min. These solutions were simultaneously irradiated with sixteen > 290 nm lamps in a Rayonet reactor for a total of 120 min. Figure 20a and 21a show the GLC analyses of **31+Furan** and **31+AcCN** solutions before irradiation, respectively. Furan is eluted with a retention time within the solvent delay (2 min) and, thus, will not be observed in this GLC analysis. Figure 142a reveals that no ground state reaction between **31** and furan has occurred.

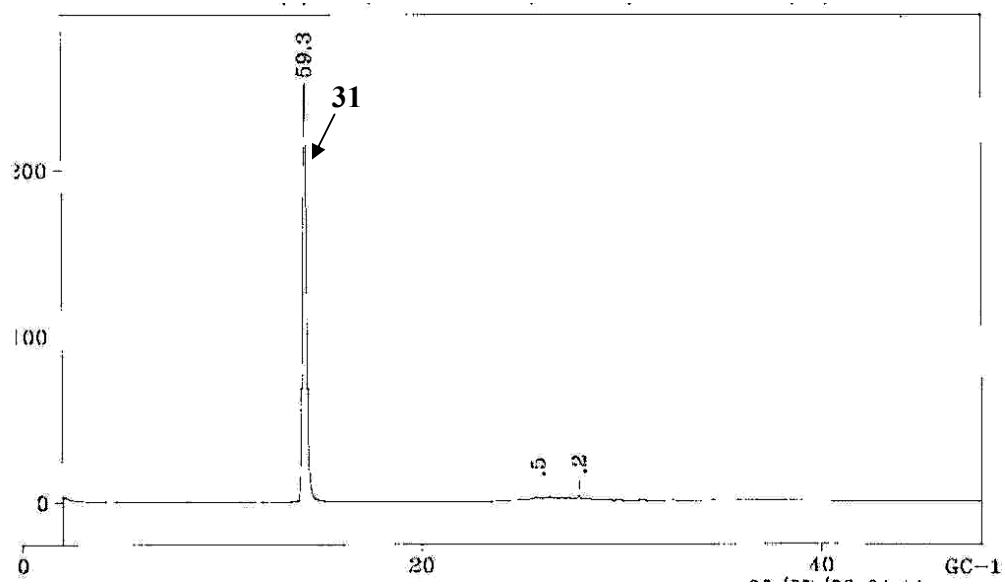


Figure 142a: GC-trace of 31+Furan before irradiation

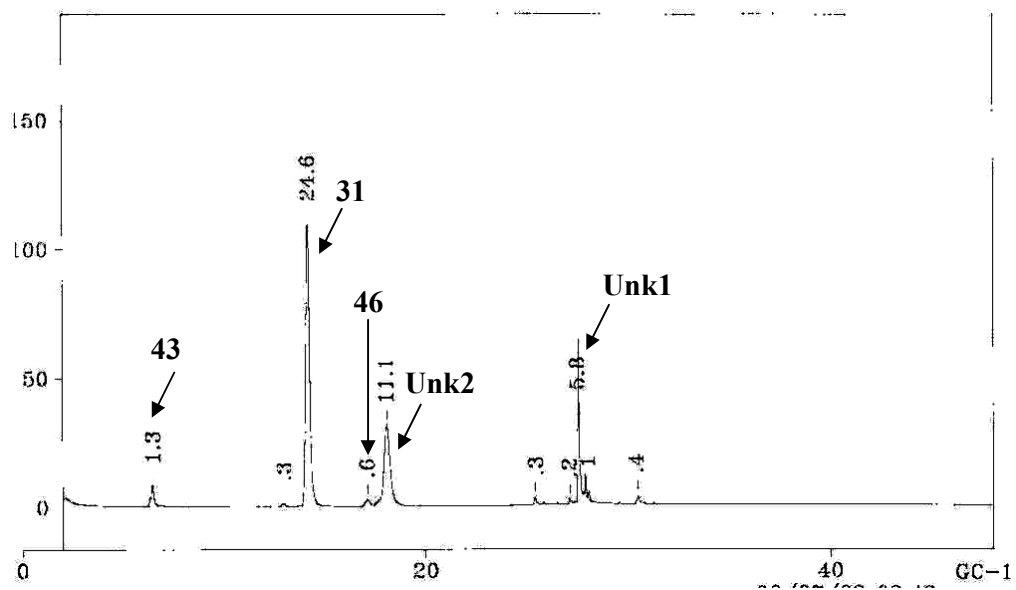


Figure 142b: GC-trace of 31+Furan after 120 min of irradiation

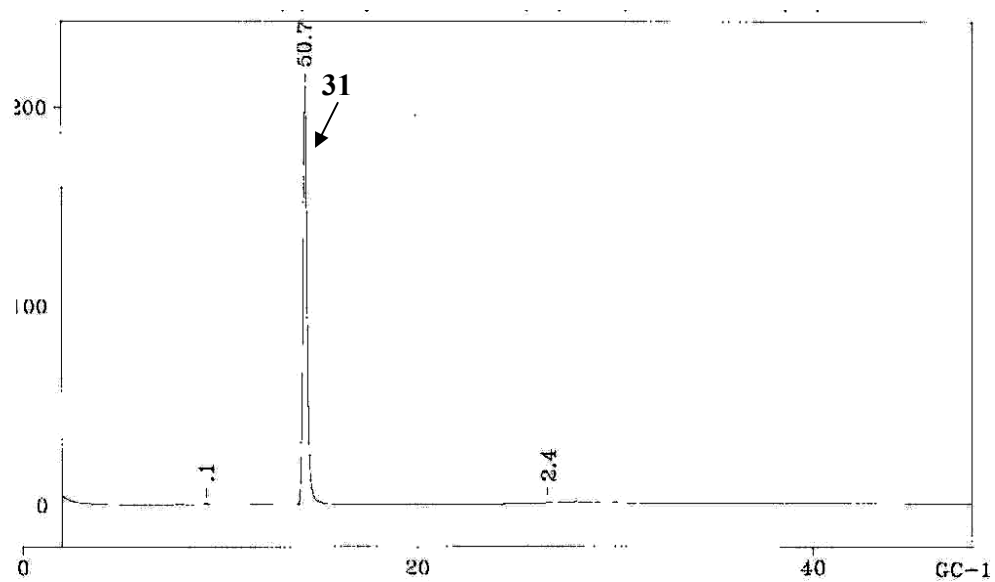


Figure 143a: GC-trace of **31** in AcCN before irradiation

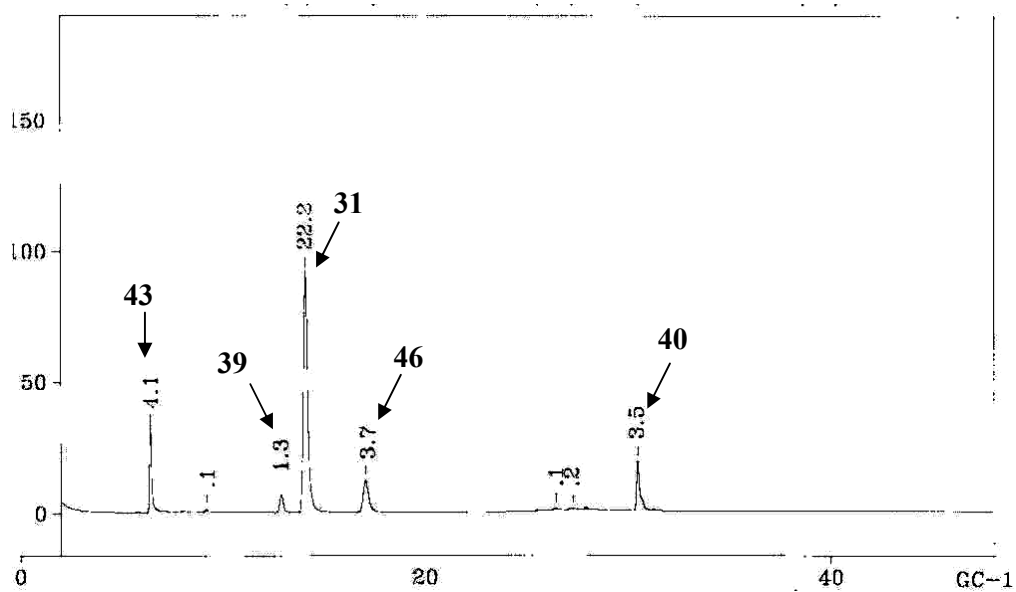


Figure 143b: GC-trace of **31** in AcCN after 120 min of irradiation

Figure 142b shows the GC trace of the **31+Furan** solution after 120 min of irradiation. For comparison, Figure 143b shows the GC trace of the **31+AcCN** solution after 120 min of simultaneous irradiation on the merry-go-round apparatus. This trace shows that the expected products, benzonitrile (**43**), 2-phenyl-1,3,5-triazine (**39**), 3-phenyl-1,2,4-thiadiazole (**46**), and 2,4-diphenyl-1,3,5-triazine (**40**) have been formed. Figure 142b reveals, however, that the peaks due **43** and **40** are substantially smaller than the peaks observed in Figure 143b in the absence of furan while the peaks due to the two triazines (**39** and **40**) are not observed at all in Figure 142b. Thus, Figure 142b shows that during irradiation of **31** in furan, the formation of **43**, **46**, **39**, and **40** have been quenched. In addition to these changes, the GC-trace shows the formation of two new peaks eluting at retention times of 17.9 (**Unk2**) and 28.8 min (**Unk1**) that were not observed when the irradiation was carried out in acetonitrile.

The irradiated **31+Furan** solution was also analyzed using the gas chromatograph (HP588) interfaced to the mass spectrometer detector. As shown in Figure 144a, this GC trace shows the peaks due to **43**, **31** and **46** and two new products eluting at retention times of 24.7 (**Unk1**) and 26.2 min (**Unk2**).

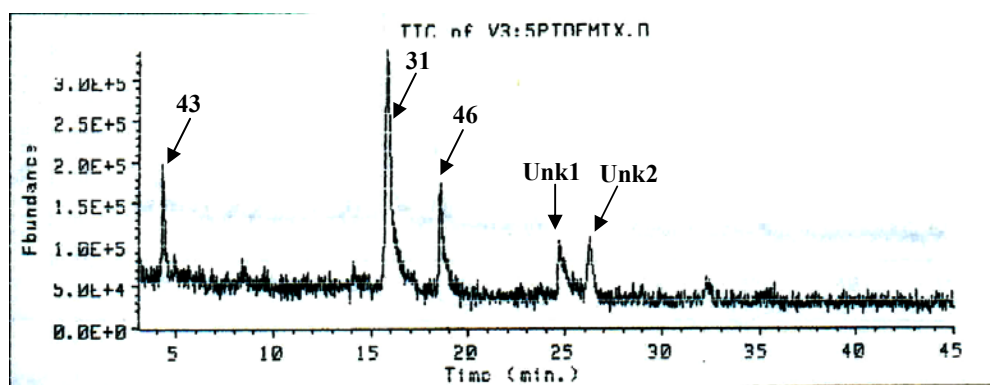


Figure 144a: GC-trace of **31+Furan** solution after 120 min of irradiation

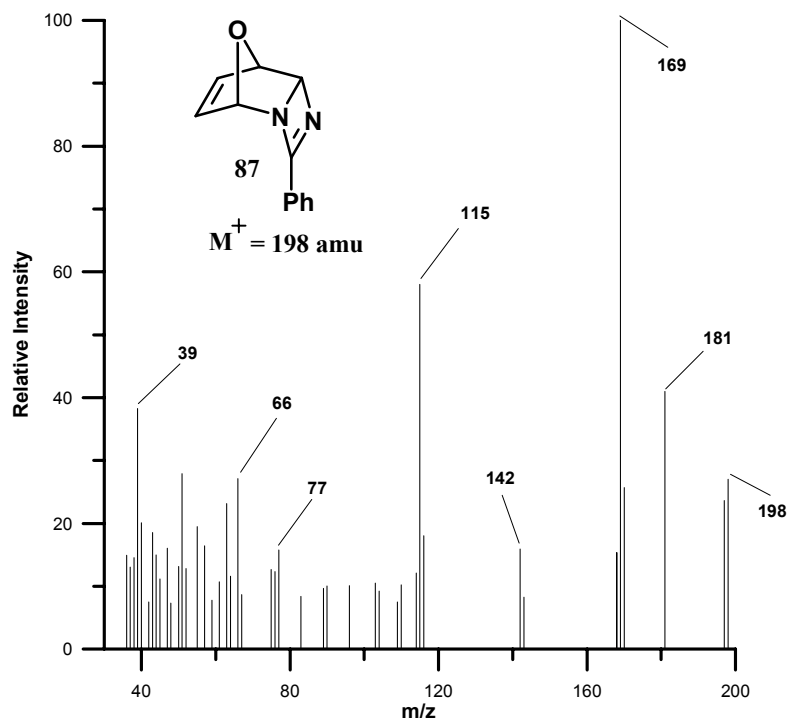


Figure 144b: Mass spectrum of Unk1 (24.7 min)

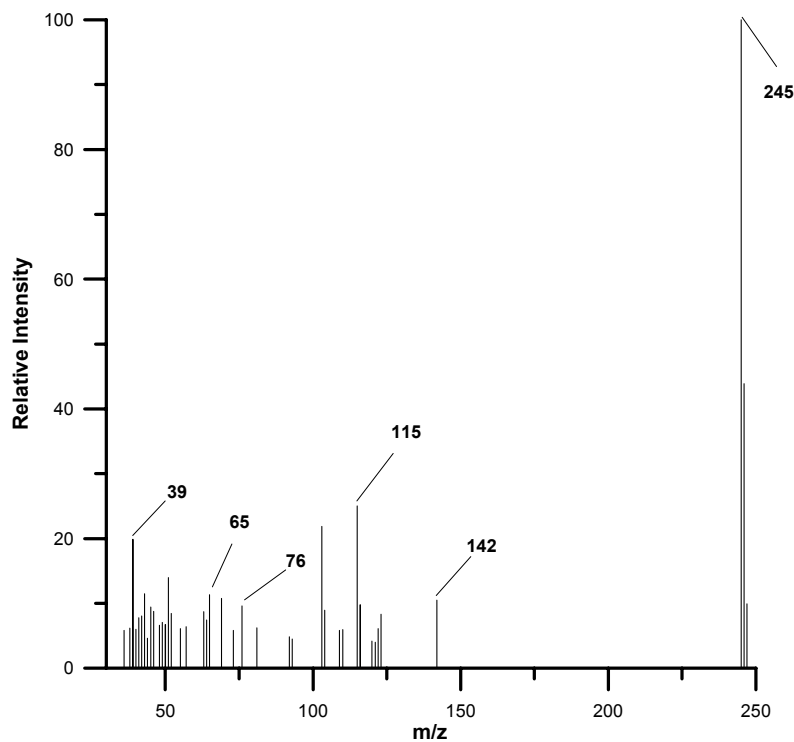
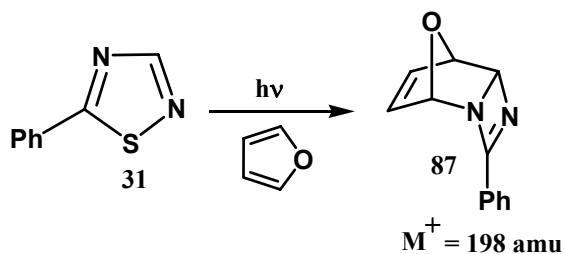


Figure 144c: Mass spectrum of Unk2 (26.2 min)

The mass spectra of these new products are shown in Figure 144b (**Unk1**) and 144c (**Unk2**) and reveal molecular ions at m/z 198 and 245, respectively. Although the latter mass is larger than the mass of a 1:1 5-phenyl-1,2,4-thiadiazole-furan adduct, a mass of 198 would be consistent with a 1:1 adduct minus sulfur (**87**) as shown in Scheme 63.



Scheme 63: Formation of furan-phenyldiazacyclobutadiene adduct upon irradiation of **31+Furan**

The irradiated **31+Furan** solution was also concentrated in a warm water bath (60-70 °C) under vacuum to give a dark brownish viscous liquid and analyzed by GC-MS. No additional product was observed.

2.9.1.2 Irradiation of 3-methyl-5-phenyl- and diphenyl-1,2,4-thiadiazoles in furan solvent

Irradiations of 3-methyl-5-phenyl-1,2,4-thiadiazole (**54**) (7.1×10^{-2} M, 3.5 mL) in neat furan was carried out with sixteen > 290 nm lamps.

Figure 145a shows GC analysis of the photoreaction of **54** in neat furan after 210 min of irradiation. The trace shows a peak at 18 min due to an unresolved mixture of the reactant (**54**) and one of the expected photoproducts, 2,4-dimethyl-6-phenyl-1,3,5-triazine (**65**), very small peaks due to benzonitrile (**43**) and 5-methyl-3-phenyl-1,2,3-thiadiazole (**57**), the expected photocleavage and phototransposition products, respectively, and two new peaks due to **unknowns 3** and **4**, products not observed in the absence of furan. Figure 145b-c show the mass spectra of these unknown products revealing molecular ions at m/z 188 (Figure 145b; **Unk3**) and m/z 212 (Figure 145c; **Unk4**).

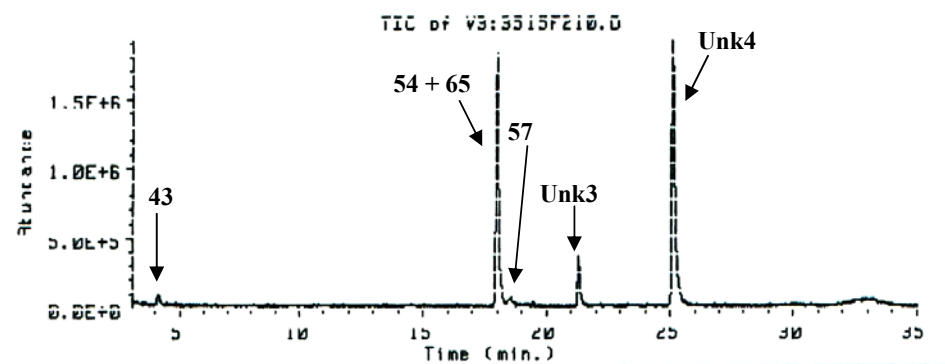


Figure 145a: GC trace of photoreaction of **54** in furan after 210 min of irradiation

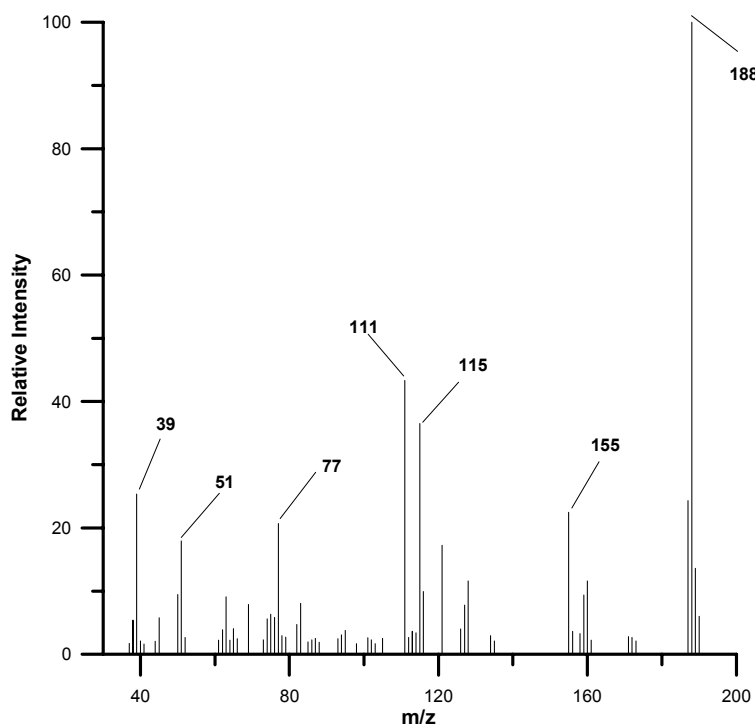


Figure 145b: Mass spectrum of Unk3; 54+Furan reaction

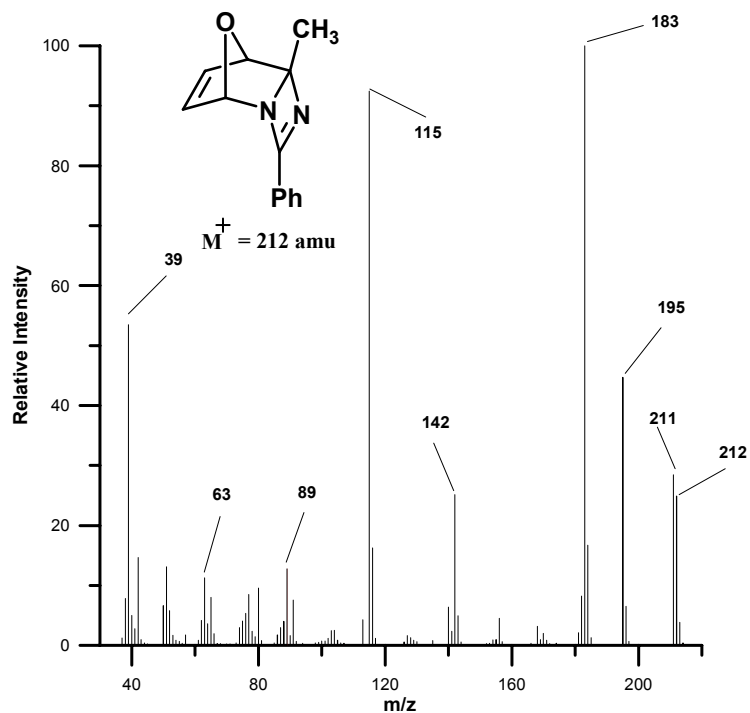
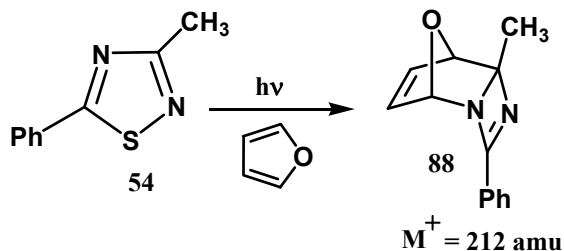


Figure 145c: Mass spectrum of Unk4; 54+Furan reaction

This shows that the major new photoproduct with a retention time of 25.5 min has a mass consistent with a 1:1 adduct of 3-methyl-5-phenyl-1,2,4-thiadiazole (**54**) and furan minus sulfur (**88**) as shown in Scheme 64.



Scheme 64: Formation of furan-phenyldiazacyclobutadiene adduct upon irradiation of **54**+Furan

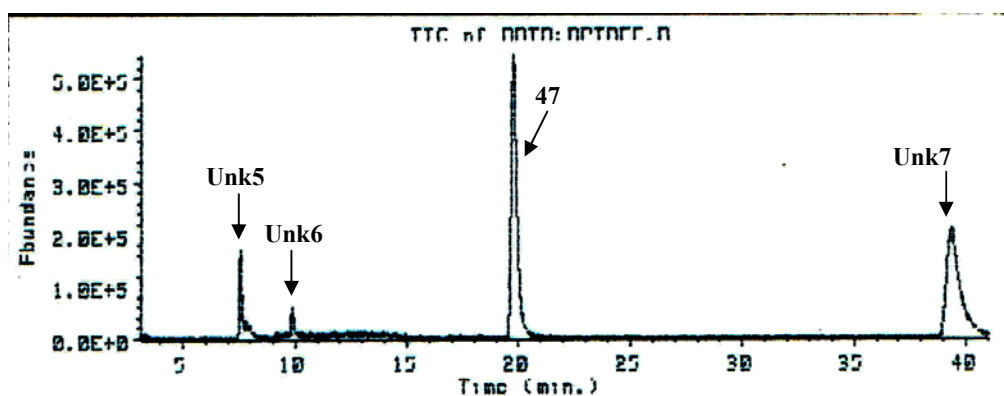


Figure 146a: GC-trace of photoreaction of **47** in furan after 210 min of irradiation

Solution of diphenyl-1,2,4-thiadiazole (**47**) (3.2×10^{-2} M, 3.5 mL) in neat furan was also irradiated with sixteen > 290 nm lamps. Figure 25a shows the GC-analysis of the irradiated **47**+furan solution after 210 min of irradiation. In addition to the unconsumed **47**, the trace reveals the formation of three new photoproducts labeled **Unk5**, **Unk6** and **Unk7** which were not observed in the absence of furan. This GC trace also reveals that **43** and 2,4,6-triphenyl-1,3,5-triazine (**86**), the photoproducts formed in acetonitrile, were not formed when irradiation was carried out in furan.

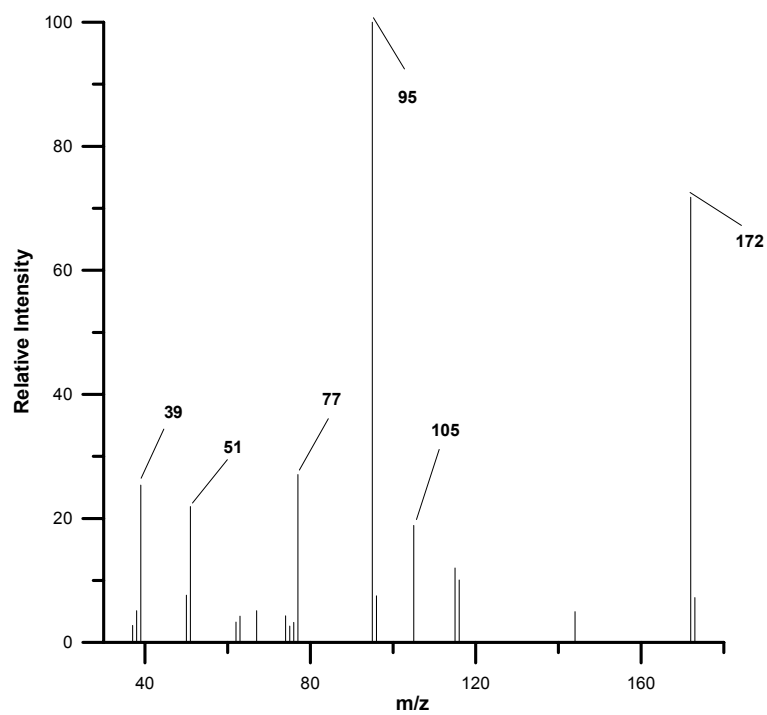


Figure 146b: Mass spectrum of Unk5; 47+Furan reaction

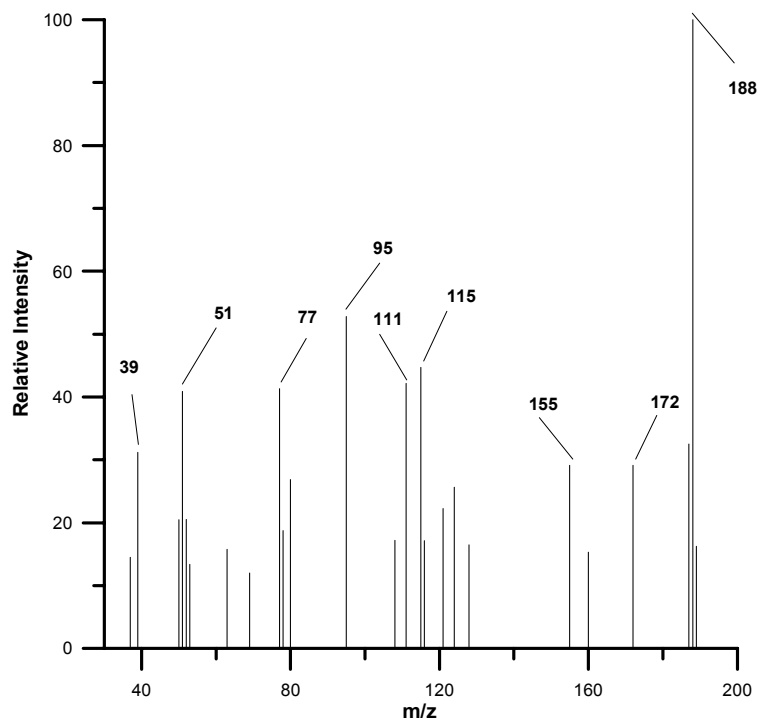


Figure 146c: Mass spectrum of Unk6; 47+Furan reaction

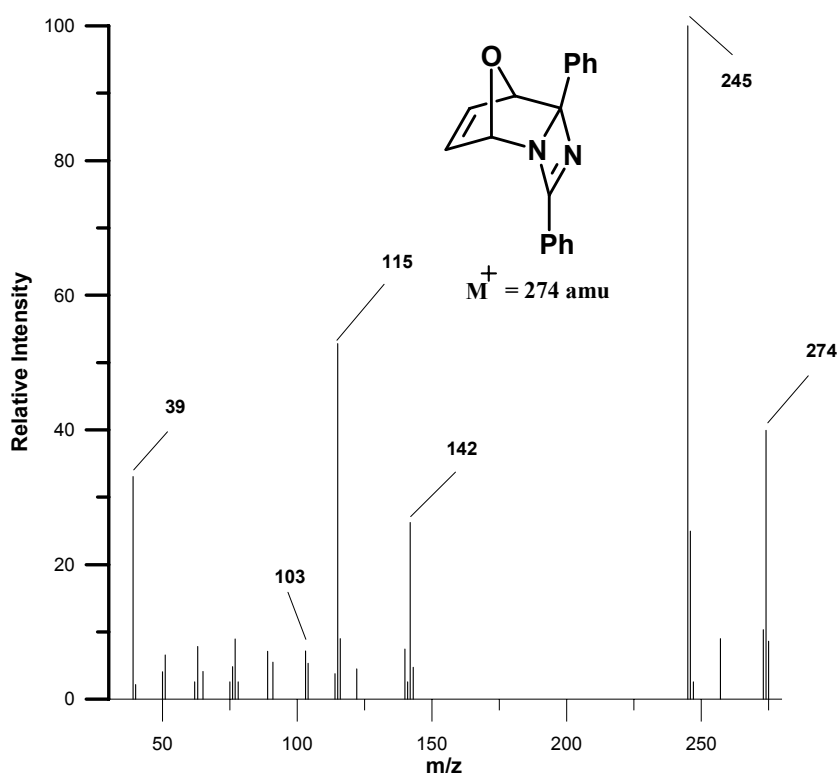
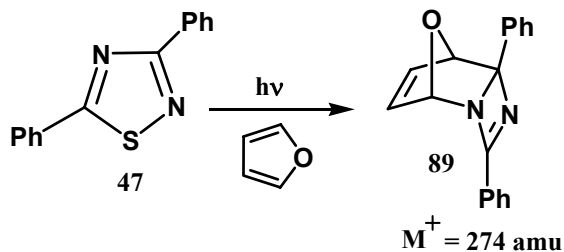


Figure 146d: Mass spectrum of Unk7; 47+Furan reaction

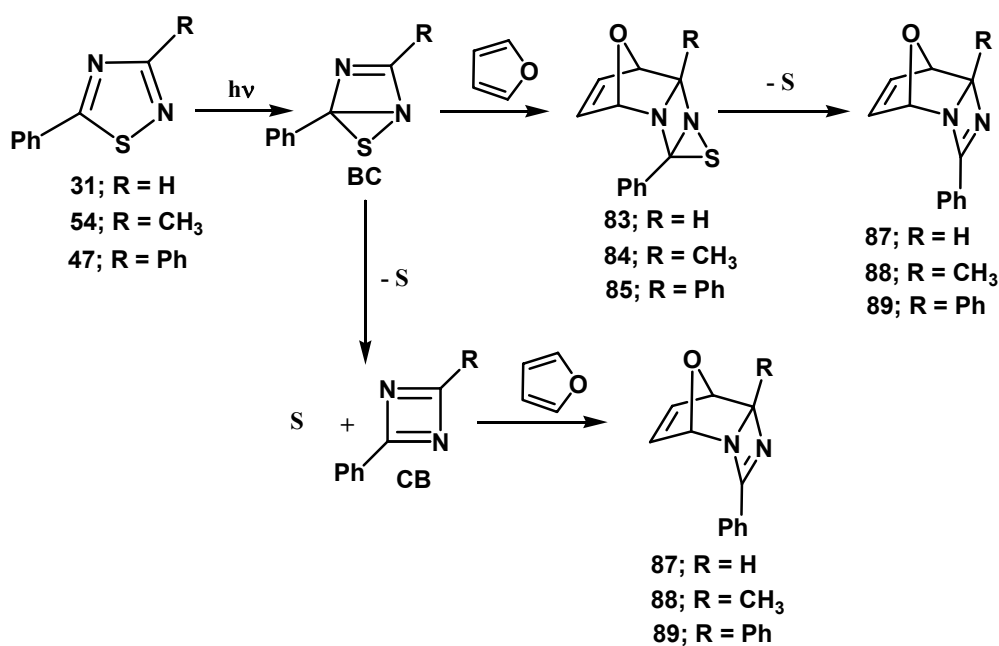
The mass spectra of **unknowns 5, 6, and 7** are shown in Figure 146b, 146c and 146d, respectively. These new products have molecular ions of m/z 172, 188 and 274, respectively. Of these three products, the major new product (**Unk7**) has a molecular ion at m/z 274 consistent with the formation of a 1:1 adduct of diphenyl-1,2,4-thiadiazole (**47**) and furan minus the sulfur atom (**89**) as shown in Scheme 65.



Scheme 65: Formation of furan-phenyldiazacyclobutadiene adduct upon irradiation of 47+Furan

These results show that irradiation of 5-phenyl-1,2,4-thiadiazole (**31**), 3-methyl-5-phenyl-1,2,4-thiadiazole (**54**) or diphenyl-1,2,4-thiadiazole (**47**) in furan solvent results in quenching of the formation of the products observed in the absence of furan and in the formation of new products which their molecular weights are consistent with the formation of 1:1 adducts of the thiadiazole and furan with loss of sulfur.

Such adducts could be formed by furan trapping of the initially formed diazathiabicyclo[2.1.0]pentene (**BC**) to form a sulfur-containing adduct (**87-89**) which eliminates sulfur, possibly under the condition of our GC-MS analysis, or by furan trapping of the phenyldiazacyclobutadiene (**CB**) after the initial adduct eliminates sulfur as shown in Scheme 66.



Scheme 66: Possible formation of the observed adducts

Trapping of the initially formed bicyclic intermediate (**BC**) would be accompanied by quenching the formation of the phototransposition, photofragmentation and photo-ring expansion products since these products all arise from this intermediate. Alternatively, trapping of only the phenyldiazacyclobutadiene species (**CB**) would be accompanied by quenching of the photofragmentation and ring-expansion products which are both derived from this species but would not quench the formation of the phototransposition product since that product is derived only from the initially generated bicyclic species.

It should, however, be noted that all previous GC analyses revealed that the formation of the known photoproducts upon irradiation of 5-phenyl-1,2,4-thiadiazoles have been quenched. In order to determine the effect of added furan on the yields of the photoproducts, the irradiation of **31** in acetonitrile containing various concentrations of furan was carried out.

Solutions of **31** (1.7×10^{-2} M; 5 mL) in acetonitrile with the presence of furan from 0-90% were sealed in Pyrex tubes, purged with a fine stream argon gas for 15 min and simultaneously irradiated with sixteen > 290 nm lamps in a Rayonet reactor. The photoreactions were monitored by GLC at 60 min intervals.

Figure 147a-d show plots that reveal the effect of increasing the furan concentration on the yield of the product in the absence of furan divided by the yield of the product observed at the various furan concentrations. In these plots, a positive slope indicates that the yield of the product decreases with an increase in the furan concentration.

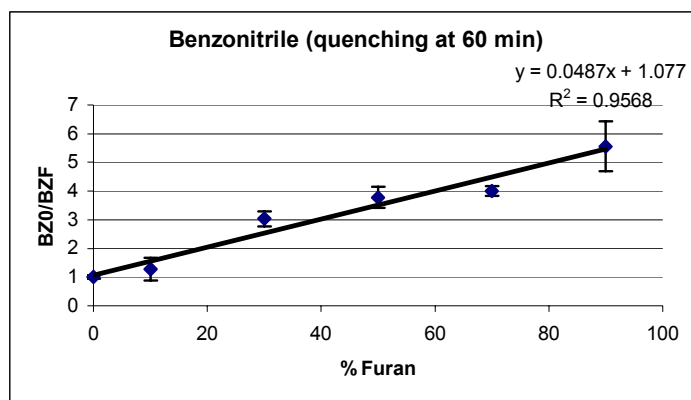


Figure 147a: Furan quenching of the formation of **50** in the photoreaction of **1**

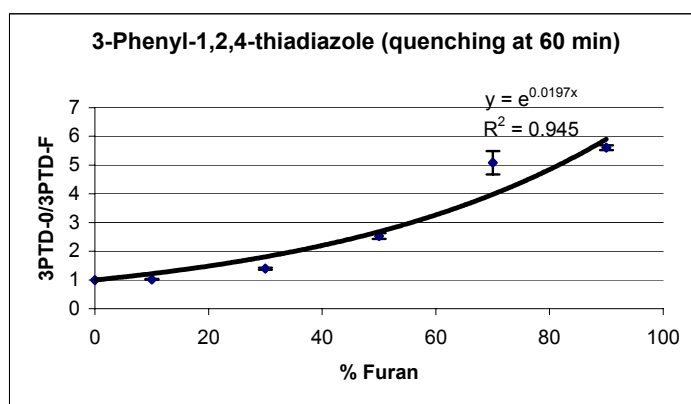


Figure 147b: Furan quenching of the formation of **4** in the photoreaction of **1**

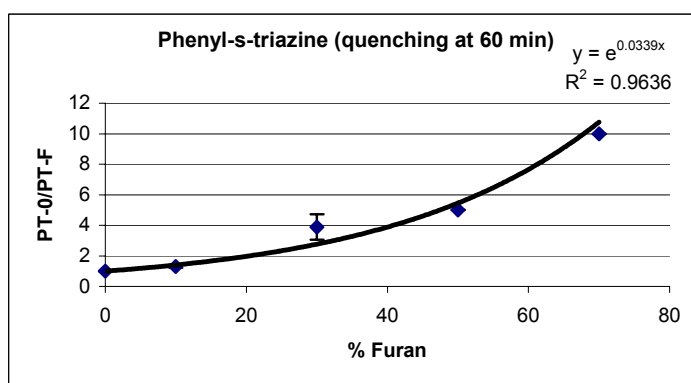


Figure 147c: Furan quenching of the formation of **51** in the photoreaction of **1**

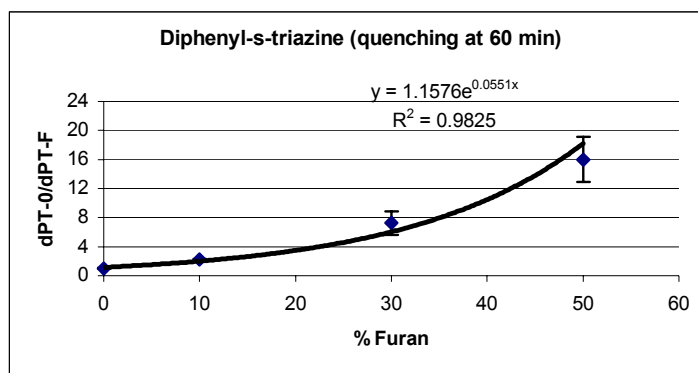


Figure 147d: Furan quenching of the formation of **52** in the photoreaction of **1**

Figure 147a shows a linear decrease in the yield of benzonitrile (**43**) with increasing furan concentrations until at 90% furan concentration, the yield of **43** is 80% quenched. The next three plots (Figure 147b-d) show that the yields of 3-phenyl-1,2,4-thiadiazole (**46**), the phototransposition product, and the yields of phenyl- and diphenyl-1,3,5-triazines (**39**) and (**40**) are also substantially quenched by added furan. In these cases, they appear to be a parabolic relationship between product quenching and furan concentration.

Since furan quenches the formation of all products, the quencher must be reacting with a species which is a precursor of all four products, namely the 4-phenyl-1,3-diaza-5-thiabicyclo[2.1.0]pentene (**BC-31**) as shown in Scheme 59. These results, however, do not rule out the possibility that furan is also reacting with the phenyldiazacyclobutadiene species (**CB**).

2.9.1.3 Preparative scale photolysis of diphenyl-1,2,4-thiadiazole in furan solvent

In attempts to isolate the furan-trapping adducts, preparative scale photolysis of diphenyl-1,2,4-thiadiazole (**47**) in neat furan was carried out.

Solution of diphenyl-1,2,4-thiadiazole (**47**) in neat furan (2×10^{-2} M; 25 mL) in a sealed Pyrex tube was irradiated with sixteen > 290 nm lamps for a total of 360 min resulting in 94% consumption of the starting material. The reaction solution was concentrated by rotary evaporation to give a dark brownish residue. The brown residue (120 mg) was subjected to a column chromatography (column; 0.5×30 cm, silica gel 12 g). The column was eluted with ethyl acetate-hexane 3:7. GC (HP588) analysis of each fraction showed that fractions 1-2, 3-5, 7 and 9-10 contained major components with molecular ions at m/z 309, 238, 274 and 172, respectively. Mass spectra analysis indicated that the components in fractions 1-2 and 3-5 were consistent with 2,4,6-triphenyl-1,3,5-triazine (**86**), the known product in this photoreaction, and the starting thiadiazole, **12**, respectively. The molecular ion at m/z 274 corresponds to the molecular ion of the 1:1 adduct of diphenyl-1,2,4-thiadiazole (**47**) and furan minus the sulfur atom. Thus, fraction 7 was concentrated to give a yellow viscous liquid (**F7**). This sample was dissolved in CDCl_3 and analyzed by ^1H -, ^{13}C -NMR, and the GC interfaced with a mass spectrometer.

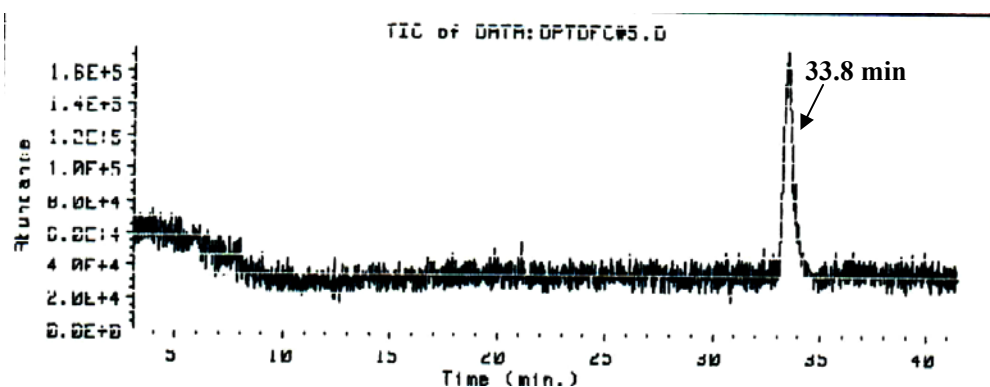


Figure 148a: GC-trace of the concentrated fraction 7

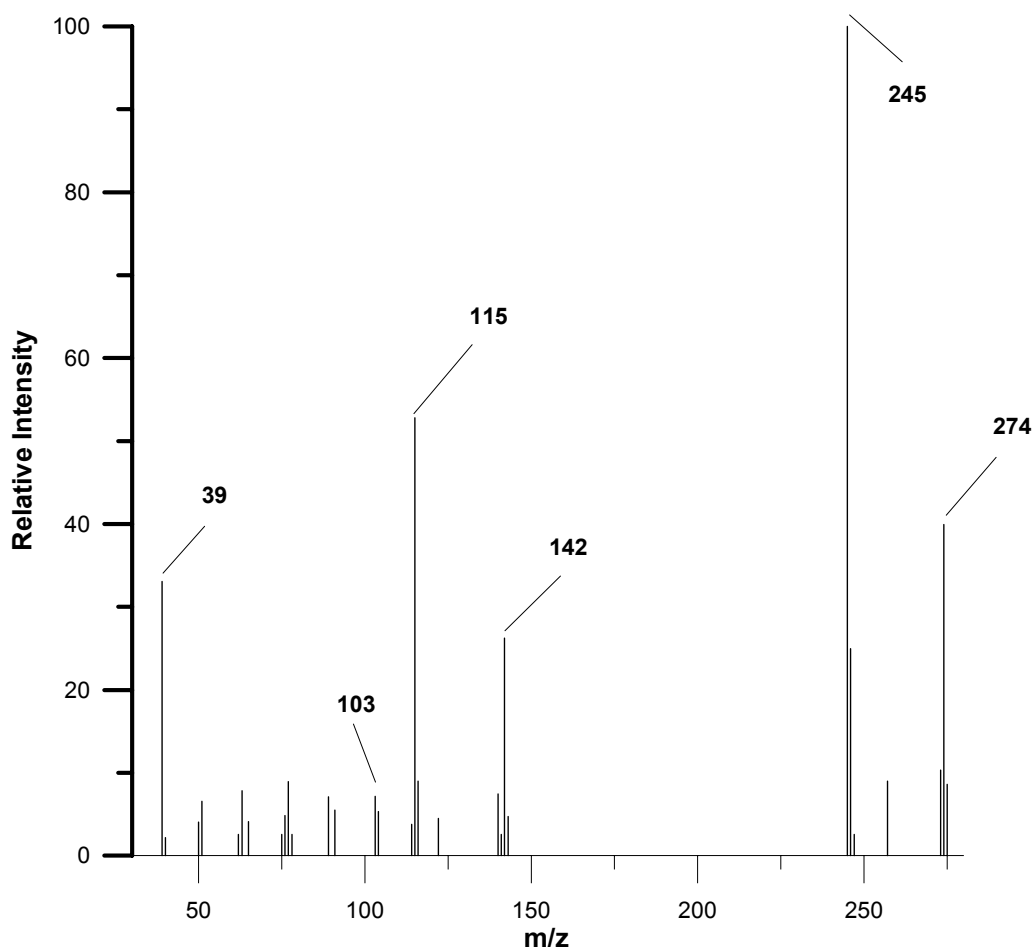


Figure 148b: Mass spectrum of the concentrated fraction 7

Figure 148a shows GC trace of the yellow liquid sample **F7**, in CDCl_3 . The trace reveals a major component eluted with a retention time of 33.8 min. Figure 148b shows the mass spectrum of this component revealing a molecular ion at m/z 274 and a base peak at m/z 245. The molecular weight of this sample (**F7**) is consistent with the molecular weight of the 1:1 adduct of diphenyl-1,2,4-thiadiazole (**12**) and furan minus the sulfur atom (**72**; MW 274). For a molecule containing sulfur atoms, its mass spectrum should exhibit a $M^+ + 2$ peak due to a natural abundance of ^{34}S atom. Since the natural abundance of ^{34}S

atom is approximately 4.42 %, thus, the number of sulfur atom in the molecule can also be determined from the ratio of $[M^+ + 2]/[M^+]$ as shown below:

$$[(M+2)^+]/[M^+] = n (0.042)/(0.9503) = n \times 0.0442$$

$$n = \text{number of } ^{34}\text{S}$$

In Figure 148b, however, no $M^+ + 2$ peak is observed. This confirms that this molecule does not contain a sulfur atom.

Figure 149a-b shows the $^1\text{H-NMR}$ spectrum and the scale expansion spectrum of the sample **F7** in CDCl_3 . The $^1\text{H-NMR}$ spectra of these adducts usually exhibit complicated splitting due to homonuclear long range couplings. Figure 149a shows that the isolated **F7** is not in a highly pure state and is, therefore, very complicated. In contrast, the ^{13}C -spectra, with complete decoupled, is more simple and characteristic of these adducts. Table 3 shows the ^{13}C -chemical shifts of 7-oxabicyclo[2.2.1]hept-2-ene and some derivatives.

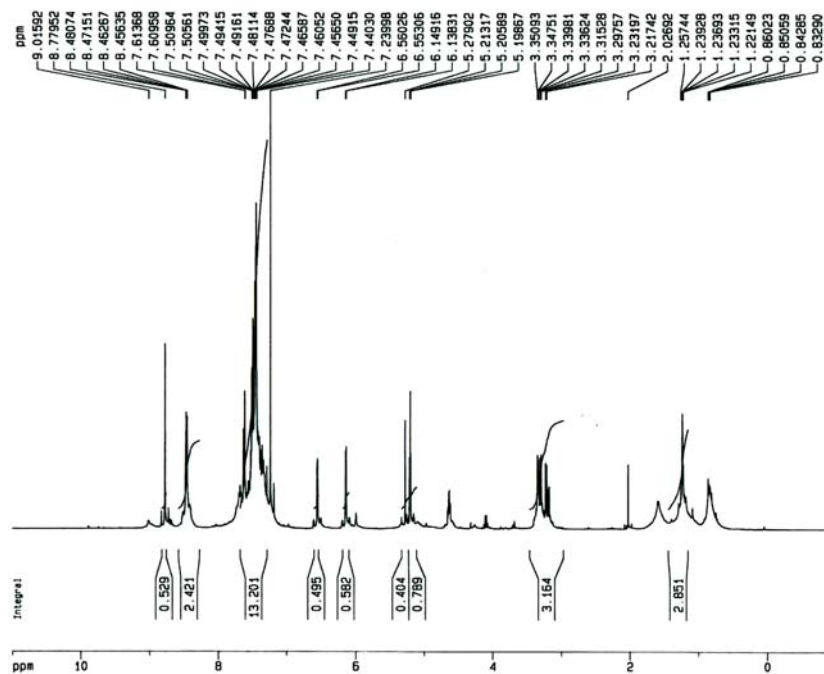


Figure 149a: $^1\text{H-NMR}$ spectrum of the unknown sample F7; the expected adduct

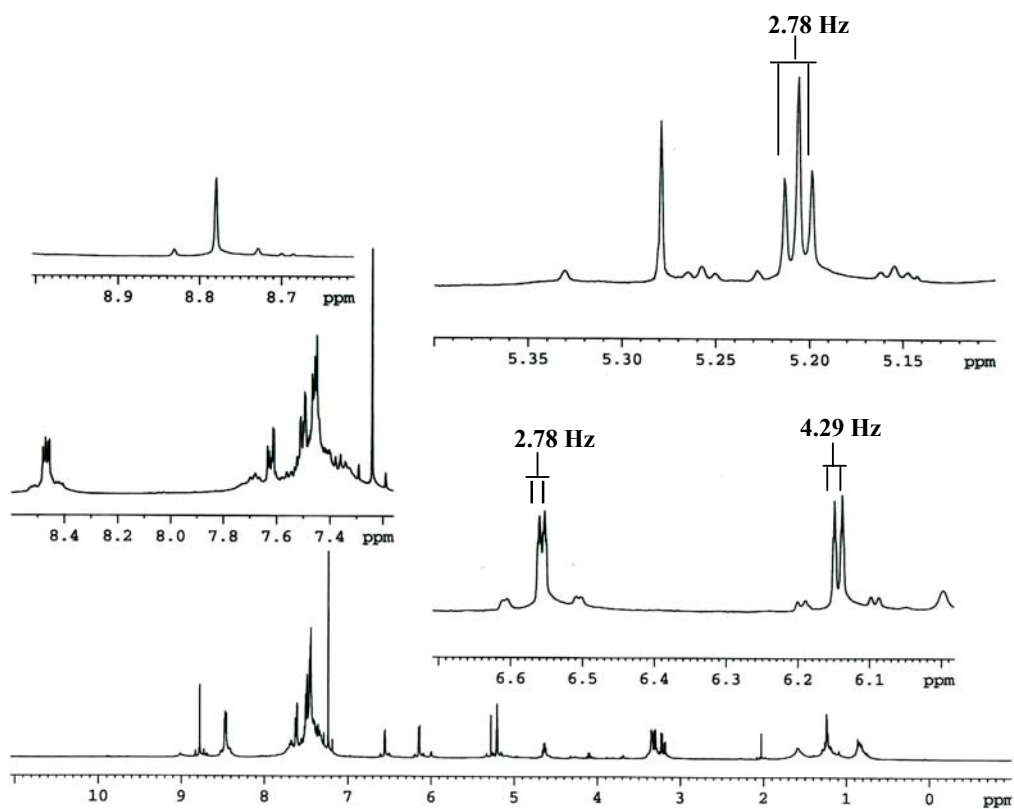
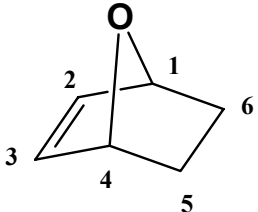
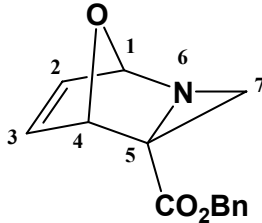
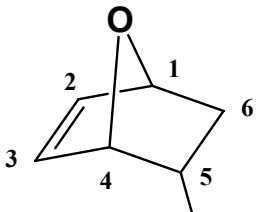
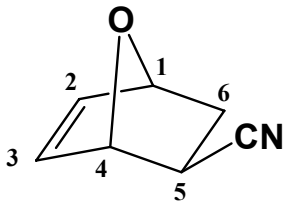
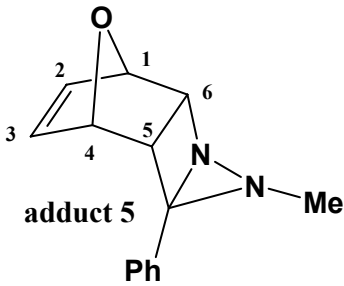
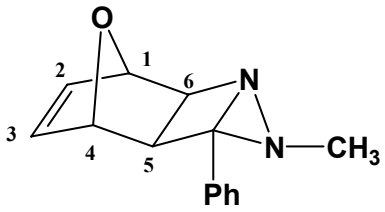


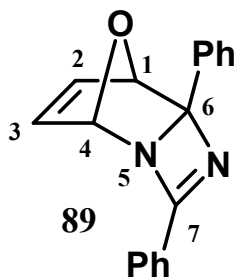
Figure 149b: $^1\text{H-NMR}$ scale expansion of spectrum of the unknown sample F7

Table 1: ^{13}C -chemical shifts of 7-oxabicyclo[2.2.1]hept-2-ene and some derivatives

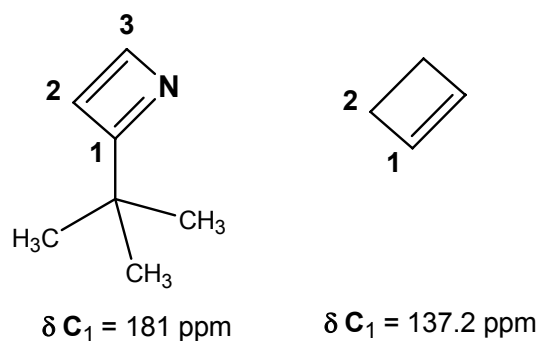
Compound	Assignments (δ in ppm)	Compound	Assignments (δ in ppm)
Ref. 17  adduct 1	C1 = 77.7 C2 = 134.6 C3 = 134.6 C4 = 77.7 C5 = 23.4 C6 = 23.4	Ref. 18  adduct 2	C1 = 93.2 C2 = 138.9 C3 = 128.5 C4 = 76.1 C5 = 48.3 C7 = 41.9
Ref. 19  adduct 3 CN	C1 = 78.9 C2 = 137.9 C3 = 133.1 C4 = 78.9 C5 = 26.2 C6 = 31.6 CN = 120.8	Ref. 19  adduct 4	C1 = 78.0 C2 = 137.4 C3 = 133.9 C4 = 81.4 C5 = 27.6 C6 = 31.6 CN = 122.8
Ref. 16  adduct 5	C1 = 80.0 C2 = 137.4 C3 = 147.4 C4 = 103.5 C5 = 56.5 C6 = 62.1	Ref. 16  adduct 6	C1 = 79.3 C2 = 135.7 C3 = 149.6 C4 = 102.3 C5 = 55.3 C6 = 63.0

7-Oxabicyclo[2.2.1]hept-2-ene (**adduct 1**) would be considered as basic structure of the adducts shown in Table 1. Table 1 shows the ^{13}C -chemical shifts of this compound (**adduct 1**) revealing the absorption of the two equivalent bridge head carbons at δ 77.7. The carbons at positions 6 and 5 are shown at δ 23.4. The two equivalent methylene carbons appear at δ 134.6. Table 1 shows that when the C6 is replaced with a nitrogen atom, the C1 of the **adduct 2** appears downfield of 15.5 ppm, relative to the shift of C1 observed in the **adduct 1**. This also leads to 4.3 ppm deshielded of the C2 in the **adduct 2**. In the **adduct 5**, the C4 is 25.8 ppm deshielded relative to the C4 in the **adduct 1**. This would be due to a secondary magnetic field from the phenyl ring. The C3s in the **adduct 3** and **4** absorb at δ 133.1 and 133.9, respectively, while the C3s in the **adduct 5** and **6** are approximately 10 ppm downfield from the C3s in the **adduct 3** and **4**. This additional deshield effect of C3s in **adduct 5** and **6** would also be expected due to a secondary magnetic field from the phenyl ring. In **adduct 5** and **6**, the C5s and C6s are shown approximately two-fold further downfield from the observed shift in C5 and C6 in the **adduct 1**. The deshielding in these cases would be due to the electronegative nitrogen atom and the phenyl ring in the **adduct 5** and **6**.

The mass spectrum of the isolated **F7** sample (Figure 148b) showed a molecular ion at m/z 274 corresponding with a 1:1 adduct of diphenyl-1,2,4-thiadiazole (**47**) and furan minus the sulfur atom (**89**) which the structure of this adduct would be expected as shown below:



Although, the ^1H -NMR spectrum of this sample, shown in Figure 149a-b, is quite complicated, the ^{13}C -spectra (Figure 150a-b) show a clearer spectrum. The ^{13}C -NMR signals of this new product, **F7**, could be assigned based on the ^{13}C -chemical shifts analysis of 7-oxabicyclo[2.2.1]hept-2-ene and some derivatives as shown in Table 3. Since the C1 in the **adduct 2**, which is adjacent to a nitrogen atom, appears downfield at δ 93.2 while the C4 in the **adduct 5** is deshielded, due to an effect from the phenyl ring, to δ 103.5. Therefore, the singlet at δ 107.4 would be expected due to the absorption of the C4 in **89** while the C1 would be expected to absorb upfield at δ 90.4 due to shielding effect of the phenyl ring attached to the C6 as observed in the **adduct 5** and **6**. Since the C6 in **adduct 5** appears at δ 62.1, the C6 in **89**, that is adjacent to two nitrogen atoms and attached to a phenyl ring, would be expected to absorb downfield at δ 103.8. The sp^2 carbons at C2 and C3 of **89** would correspond to the two singlets at δ 148.5 and 159.0, respectively. The C3 of **89** was expected to appear more downfield than the C3s of adducts shown in Table 3 since nitrogen atom at position 5 and the phenyl ring attached to the C7 would contribute deshielding effect to the C3 more than to the C2 of **89**. Although, the cyano carbon of the **adduct 3** and **4** are shown at δ 120.8 and 122.8, respectively.



The carbon chemical shift of cyclobutene at position 1 (as shown above) has been reported at 137.2 ppm.²¹ When the carbon at position 1 is attached with a nitrogen atom as in the azete, shown above, the shift of the carbon at position 1 has been reported at 181 ppm.²⁰ Although this azete has one additional double bond in the ring when compared with cyclobutene, the downfield approximately 50 ppm of the carbon at position 1 in the azete relative to cyclobutene would likely be due to a deshield effect of the electronegative nitrogen atom. Based on this information, the signal at δ 192.0, in Figure 150a, would correspond to the carbon at position 7 of **89** since it attaches to two nitrogen atoms and a phenyl ring. These assignments corresponded to the ¹³C-DEPT 135 spectrum revealing the signals at δ 90.4, 107.4, 148.5 and 159.0 in positive direction indicating the absorptions of tertiary carbons. The signals at δ 103.8 and 192.0 appeared in the ¹³C-CPD spectrum as the least relative intensity signals and disappeared in the ¹³C-DEPT 135 spectrum corresponding to the assignments to the quaternary carbons at C6 and C7, respectively. The signals in the region of δ 127.0-131.0 would be due to absorption of the phenyl ring carbons.

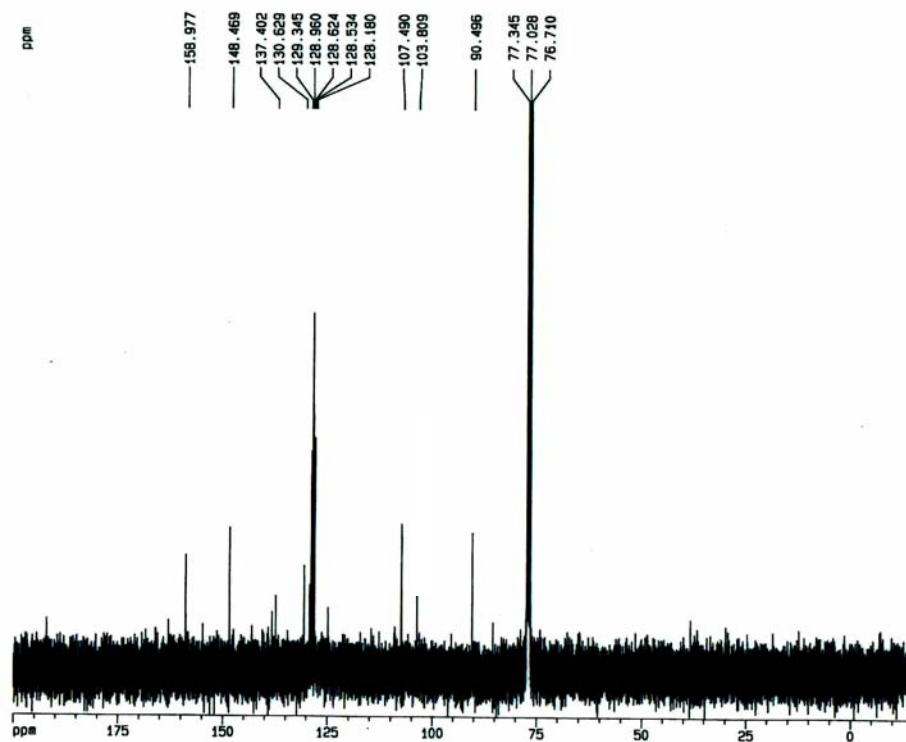


Figure 150a: ^{13}C -NMR spectrum of the unknown sample F7; the expected adduct

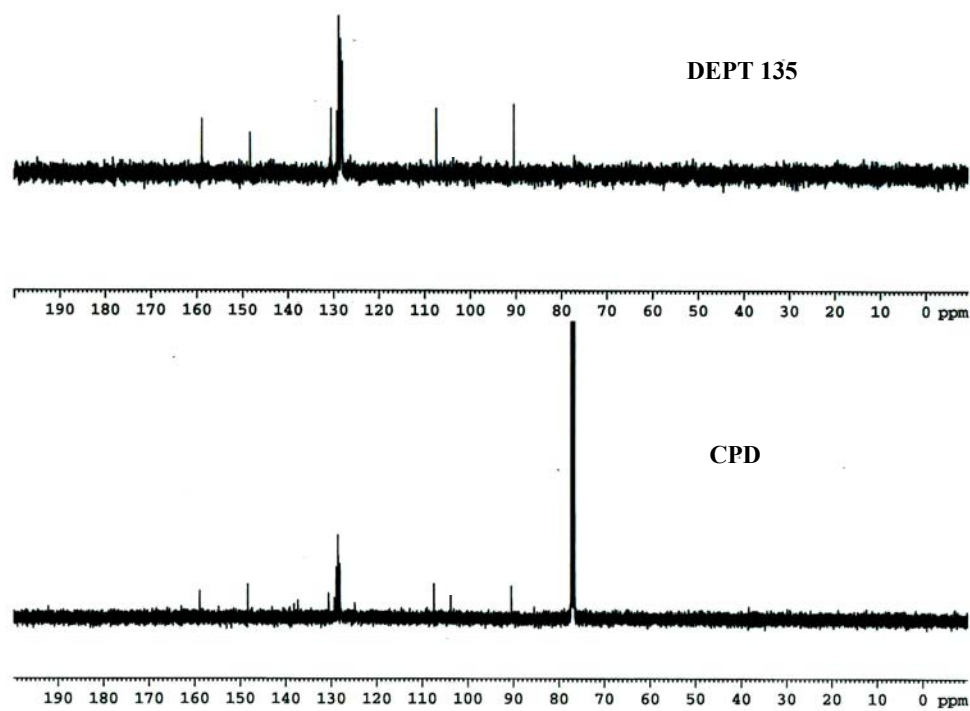
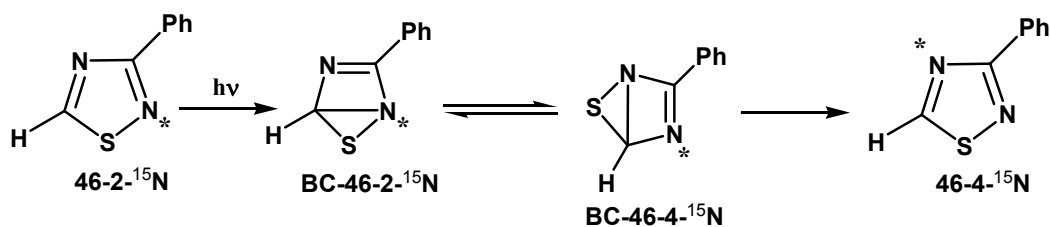


Figure 150b: ^{13}C -DEPT 135 spectrum of the unknown sample F7; the expected adduct

The mass spectral results observed in the photolysis of 5-phenyl-1,2,4-thiadiazole (**31**), 3-methyl-5-phenyl-1,2,4-thiadiazole (**54**) or diphenyl-1,2,4-thiadiazole (**47**) in furan solvent and the ^{13}C -NMR spectral analysis of the product isolated from the photoreaction of **47** in furan solvent, are strongly evidence for the formation 1:1 adducts of the thiadiazole and furan with loss of sulfur. These adducts could result from trapping of the photochemically generated 1,3-diaza-5-thiabicyclo[2.1.0]pentenes (**BC**) with furan and subsequent elimination of elemental sulfur or from trapping of phenyl-1,3-diazacyclobutadienes (**CB**) with furan.

2.9.2 Irradiation of 3-phenyl-1,2,4-thiadiazole in furan solvent

Previous work in this laboratory has shown that irradiation of 3-phenyl-1,2,4-thiadiazole-2- ^{15}N (**46-2- ^{15}N**) does not lead to ^{15}N -scrambling in the 3-phenyl-1,2,4-thiadiazole ring.¹⁴ Irradiation of this compound leads only to the formation of benzonitrile- ^{15}N (**43- ^{15}N**), the photofragmentation product. This indicates that **46-2- ^{15}N** does not undergo electrocyclic ring closure. If it did, the initially formed bicyclic species, **BC-46-2- ^{15}N** , would be expected to be in equilibrium with the isoenergetic species **BC-46-4- ^{15}N** . Rearomatization of the latter species would give 3-phenyl-1,2,4-thiadiazole-4- ^{15}N (**46-4- ^{15}N**). This was not experimentally observed. In view of these results, it was of interest to see if the photochemistry of **46** would be affected by the presence of furan.



Scheme 67: The expected ^{15}N -scrambling in 3-phenyl-1,2,4-thiadiazole-2- ^{15}N

Solutions of 3-phenyl-1,2,4-thiadiazole (**46**) in furan (1.1×10^{-2} M; 4 mL) and **46** in acetonitrile (1.1×10^{-2} M; 4 mL) in sealed Pyrex tubes were purged with argon gas for 15 min. These solutions were simultaneously irradiated with sixteen > 290 nm lamps in a Rayonet reactor for a total of 120 min. Figure 151 shows the GC trace of the **46**+Furan solution before irradiation revealing that no ground state reaction between **46** and furan was observed. Furan is eluted with a retention time within the solvent delay (2 min) and, thus, was not observed in this GLC analysis.

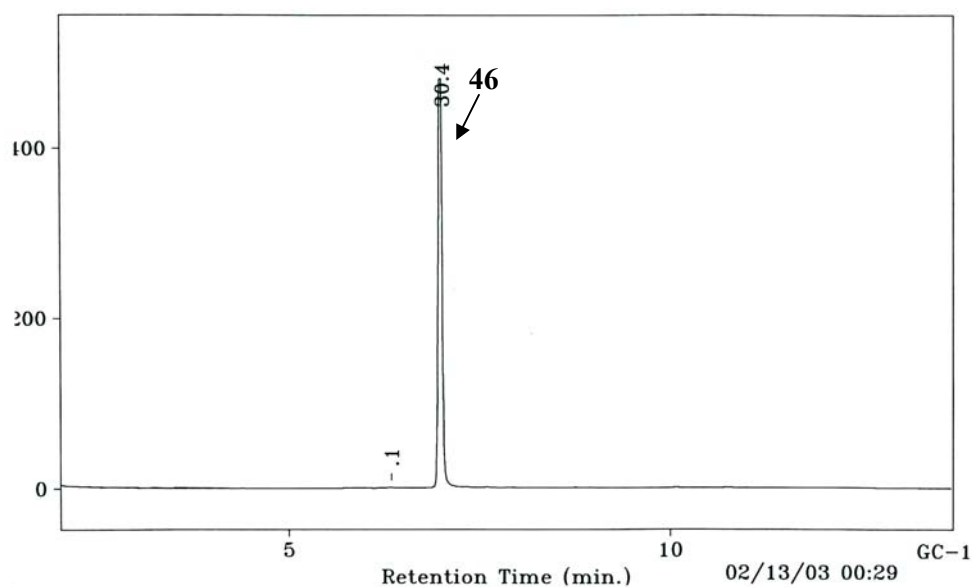


Figure 151: GLC analysis of **46**+Furan solution before irradiation

After 120 min of irradiation, the **46**+Furan solution was analyzed by the GC interfaced with a mass spectrometer. The trace reveals (Figure 152) the presence of only two major components which eluted with retention times of 4.3 and 18.5 min. Mass spectra analyses of these components were consistent with the structures of benzonitrile (**43**), the known photofragmentation product observed upon irradiation of **46** in an absence of furan, and the starting thiadiazole **46**, respectively. Even after concentration, the GC-trace did not show the formation of any new GC-volatile components in this concentrated photolysate.

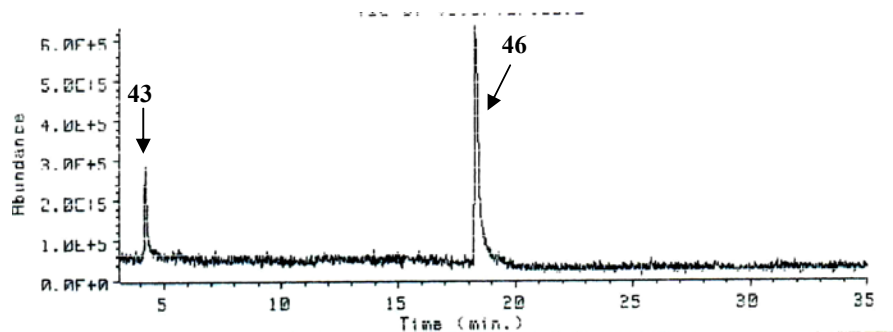


Figure 152: GC-trace of **46**+Furan solution after 120 min of irradiation

These results show that irradiation of 3-phenyl-1,2,4-thiadiazole (**46**) in neat furan leads only to the formation of benzonitrile (**43**). No furan-phenyldiazacyclobutadiene could be detected in this case. These results show that when electrocyclic ring closure does not occur, no reaction occurs with furan. This is further evidence that in the case of 5-phenyl-1,2,4-thiadiazoles **31**, **54**, and **47**, furan reacts with the photochemically generated 1,3-diaza-5-thiabicyclo[2.1.0]pentenes (**BC**) and possibly also with the diazacyclobutadienes (**CB**) derived from the bicyclic species.

These results are thus consistent with the conclusion reached from ^{15}N -labeling experiments. These results did show, however, that the yield of benzonitrile (**43**) formation is decreased upon changing solvent from acetonitrile to neat furan. In order to gain more quantitative information, irradiations of **46** with various furan concentrations were carried out.

Solutions of **46** in acetonitrile (1.1×10^{-2} M; 4 mL) with the presence of furan from 0%-90% were placed in Pyrex tubes, sealed with rubber septa and purged with argon gas for 15 min. The solutions were simultaneously irradiated by sixteen > 290 nm lamps in a Rayonet reactor. The photoreactions were monitored by GLC at 30 min of intervals.

Figure 153 shows a plot of the furan concentrations V_s the yield of **43** in the absence of furan divided by the yield of **43** observed at the various furan concentrations after 60 min of irradiation. This plot reveals that, increasing the concentration of furan is initially accompanied by a decrease in the yield of **43** until the furan concentration reaches approximately 60% which led to 40% quenching of the yield of **43**. After that point continued increasing the furan concentration has no additional effect on the yield of **43**. In classical Stern-Volmer kinetics, such a quenching curve is generally taken to mean that a long-lived species is initially being quenched and is totally quenched by 60% quencher. Beyond that concentration, benzonitrile (**43**) is being formed only from a very short-lived species which cannot be quenched.

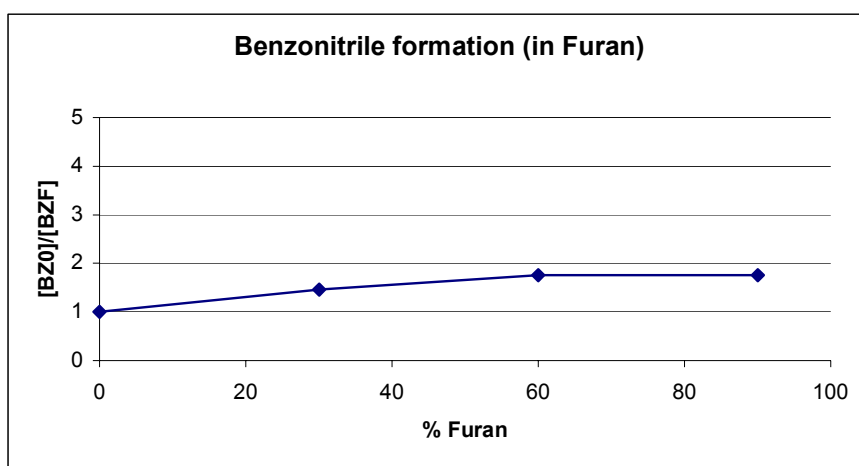


Figure 153: Plot of the furan concentrations V_s the yield of **43** in the absence of furan divided by the yield of **43** observed at the various furan concentrations

Figure 154 and 155 show plots between irradiation time *Vs* consumption of **46** upon irradiation in acetonitrile and furan solvents. These plots clearly indicate that after 60 min of irradiation the consumption of **46** in furan solvent is less than the consumption of **46** in acetonitrile solvent. This change of reactivity could be due to a change in solvent polarity upon changing from acetonitrile to furan or to a direct quenching interaction between **46** and furan.

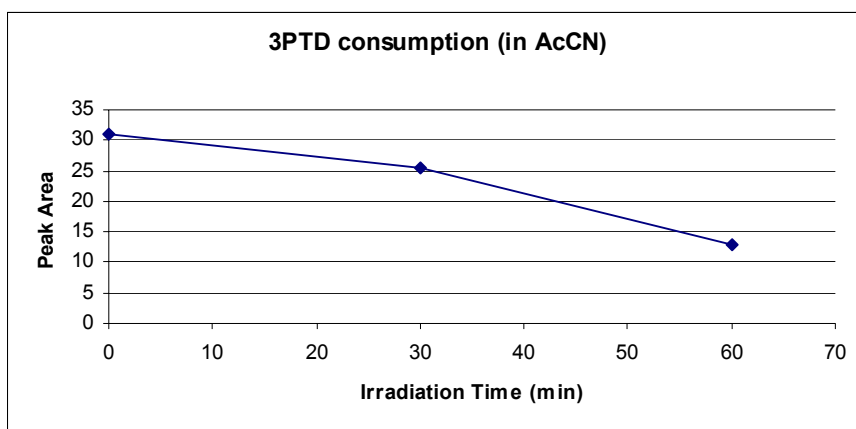


Figure 154: Plot between irradiation time *Vs* consumption of **46** in acetonitrile solvent

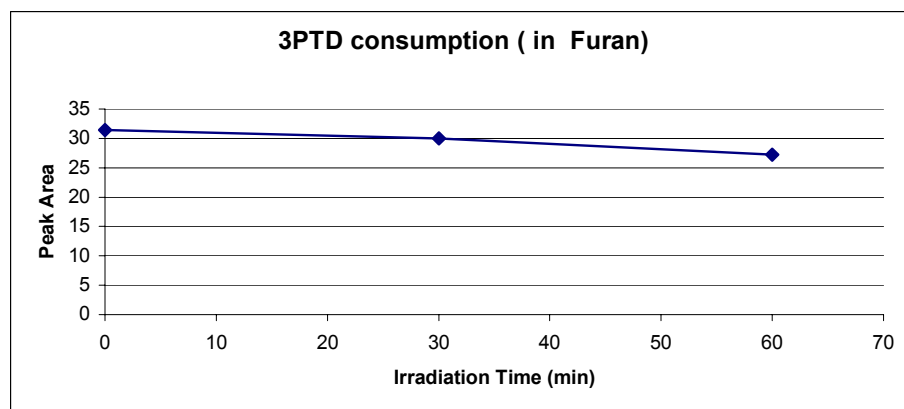


Figure 155: Plot between irradiation time *Vs* consumption **46** in furan solvent

In order to clarify this assumption, irradiation of **46** in tetrahydrofuran solvent was carried out. Tetrahydrofuran is expected to have similar polarity to furan but no interaction between the solvent and either the ground state or excite state of **46** is expected to occur.

2.9.3 Irradiation of 3-phenyl-1,2,4-thiadiazole in tetrahydrofuran solvent

Solutions of 3-phenyl-1,2,4-thiadiazole (**46**) in tetrahydrofuran (1×10^{-2} M; 3.5 mL) and **46** in acetonitrile (1×10^{-2} M; 3.5 mL) in sealed Pyrex tubes were purged with argon gas for 20 min. These solutions were simultaneously irradiated with sixteen > 290 nm lamps in a Rayonet reactor for a total of 90 min. Figure 156a shows the GLC analysis of **46**+THF solution before irradiation revealing that no ground state reaction between **46** with THF was observed.

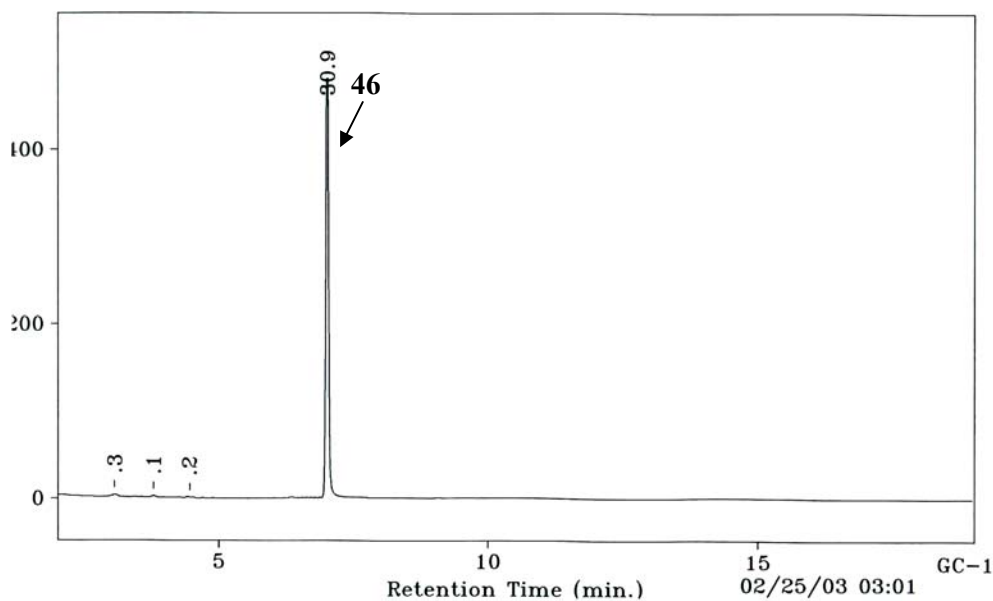


Figure 156a: GC-trace of **46**+THF solution before irradiation

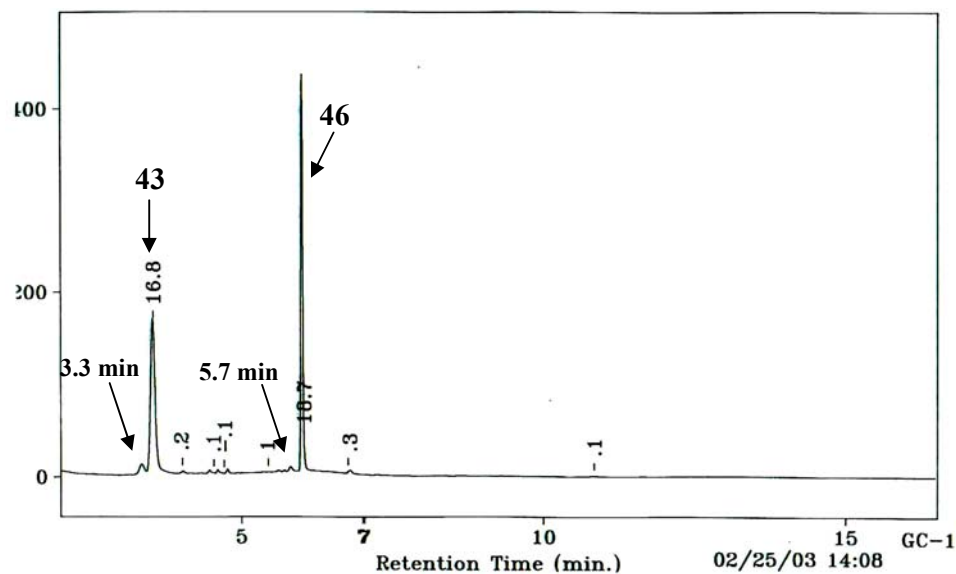


Figure 156b: GC-trace of **46+THF** solution after 90 min of irradiation

The GC-trace of the **46+THF** solution after 90 min of irradiation (Figure 156b) reveals the formation of **43** eluting at retention time of 3.5 min and the two minor products eluting at retention time of 3.3 and 5.7 min. After concentration, the concentrated photolysate was analyzed by the GC interfaced with a mass spectrometer. Figure 157a exhibits a GC-trace of the concentrated **46+THF** photolysate revealing the presence of two major components, which eluted with retention times of 7.5 and 17.7 min, and three minor components which eluted with retention times of 7, 17 and 34.5 min. Figure 157b-d show mass spectra of the three minor components. Mass spectra analysis of the two major components at 7 and 17 min was consistent with benzonitrile (**43**) and the starting thiadiazole (**46**), respectively. Mass spectra analysis of the three minor products indicates that the components eluting with retention times of 17 and 34.5 min, which have molecular ions at m/z 121 and 238, respectively, are consistent with the structures of benzamide (**38**) and diphenyl-1,2,4-thiadiazole (**47**). The component which eluted with a retention time of 7 min, that has a molecular ion at m/z 86, has not been un-identified.

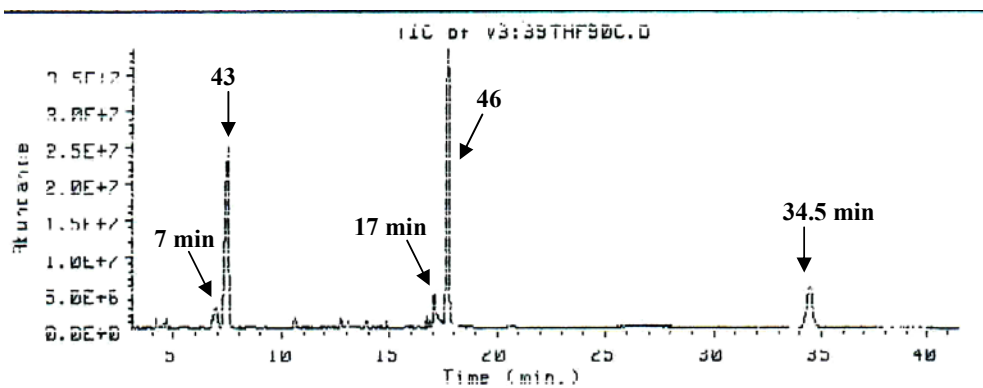


Figure 157a: GC trace of the concentrated **46+THF** photolysate

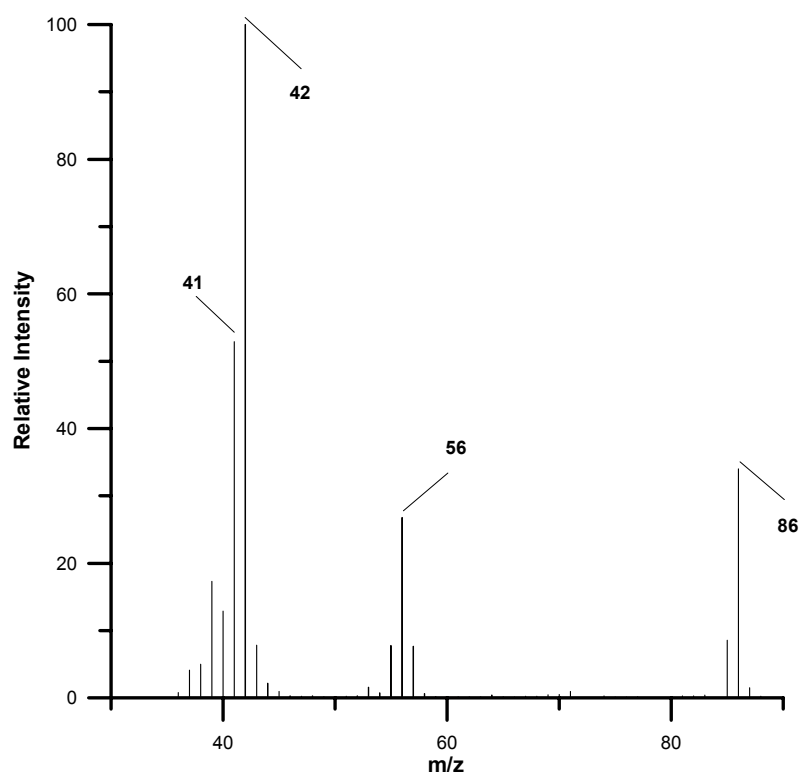


Figure 157b: Mass spectrum of the component at retention time of 7 min

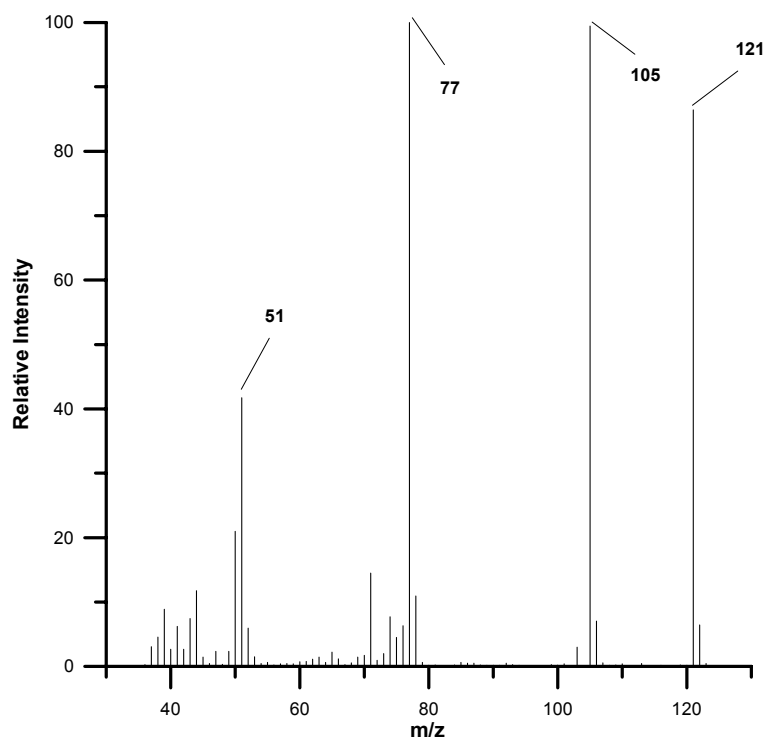


Figure 157c: Mass spectrum of the component at retention time of 17 min

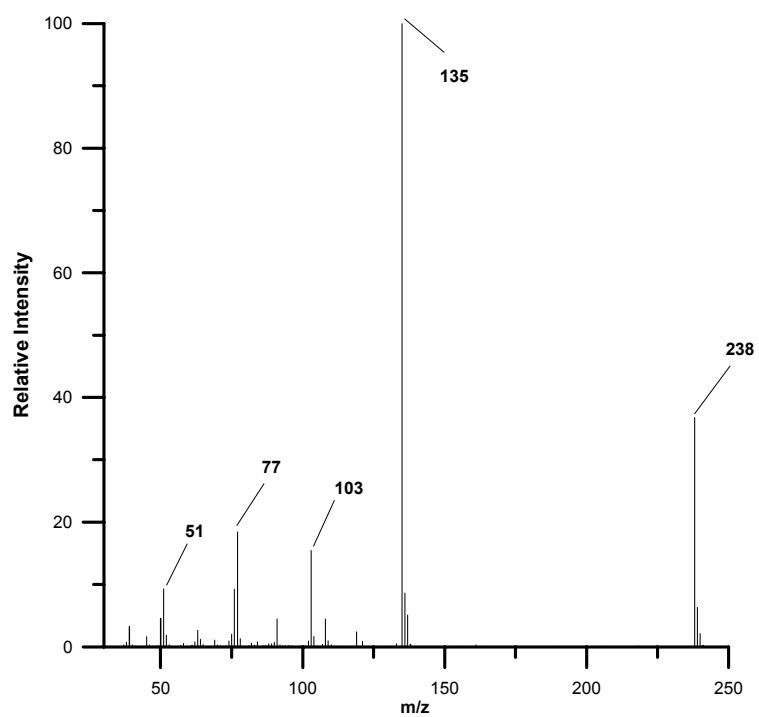
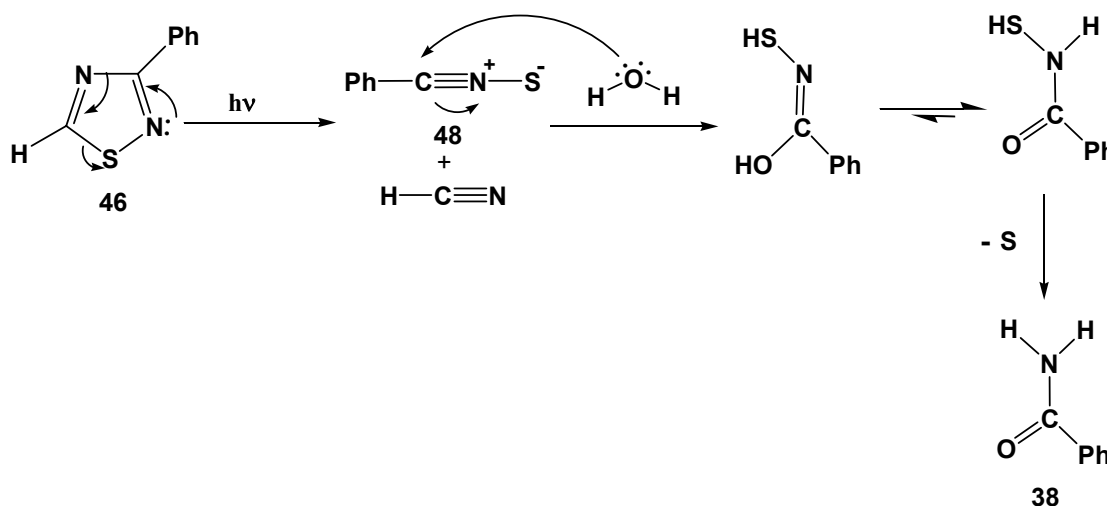


Figure 157d: Mass spectrum of the component at retention time of 34.5 min

Benzamide (**38**) was also observed as a minor product formed from the photoreaction of 5-phenyl-1,2,4-thiadiazole (**31**) in acetonitrile solvent. In that case, the formation of **38** was suggested to occur by reaction of either a thiazirine or nitrile sulfide intermediates with water present in the solution. Since 3-phenyl-1,2,4-thiadiazole (**46**) is not expected to isomerize *via* a thiazirine intermediate, benzamide (**38**) would have to result from reaction of benzonitrile sulfide with water in the solution as shown in Scheme 68.



Scheme 68: Possible formation of benzamide upon irradiation of **46**

Irradiation of **46** in acetonitrile with tetrahydrofuran at various concentrations was also carried out. Solutions of **46** in acetonitrile (1.1×10^{-2} M; 4 mL) containing tetrahydrofuran from 0%-90% were placed in Pyrex tubes, sealed with rubber septa and purged with argon gas for 15 min. The solutions were simultaneously irradiated by sixteen > 290 nm lamps in a Rayonet reactor equipped with a merry-go-round apparatus. The photoreactions were monitored by GLC at 30 min of intervals.

Figure 158 shows a plot between tetrahydrofuran concentrations *Vs* the yield of benzonitrile (**43**) in an absence of THF divided by the yield of **43** observed at various tetrahydrofuran concentrations after 30 min of irradiation. This plot reveals that tetrahydrofuran has no significant effect on the formation of **43** relative to the formation of **43** observed in the reaction in the absence of tetrahydrofuran.

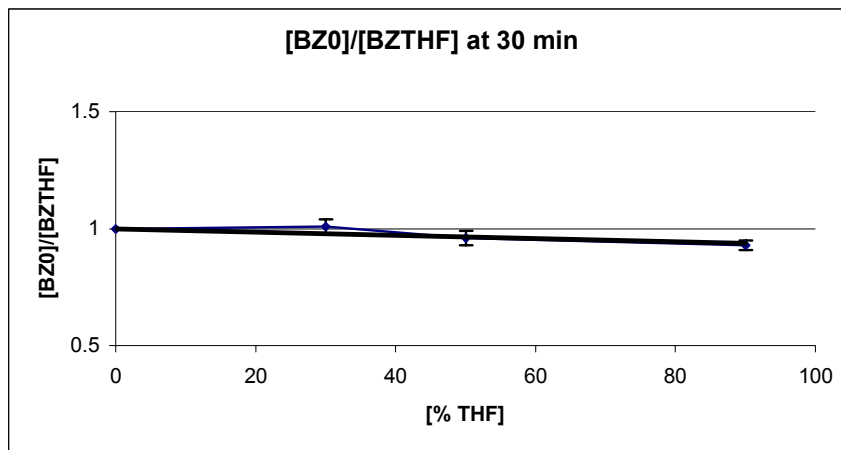


Figure 158: Plot of THF concentrations *Vs* the yield of **43** in the absence of THF divided by the yield of **43** observed at the various THF concentrations

Figure 159 shows a plot between the tetrahydrofuran concentrations *Vs* the consumption of **46** in the absence of tetrahydrofuran divided by the consumption of **46** observed at various tetrahydrofuran concentrations after 30 min of irradiation. This plot clearly reveals that tetrahydrofuran also has no effect on the consumption of **46** relative to the consumption of **46** in the photoreaction in the absence of tetrahydrofuran.

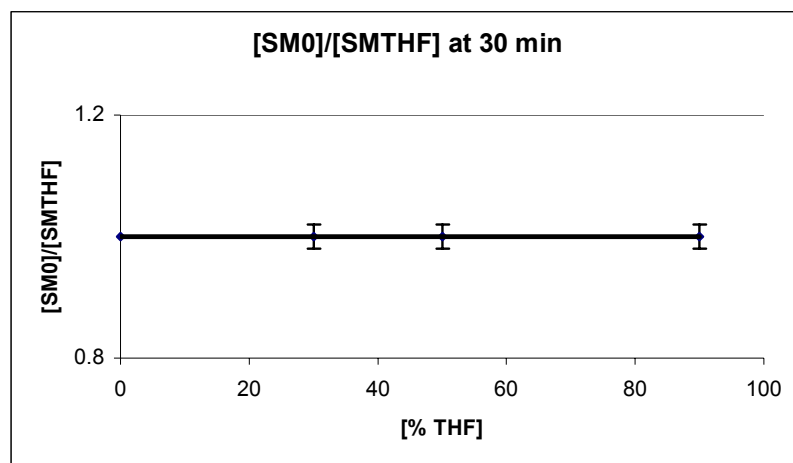


Figure 159: Plot of THF concentrations *Vs* the consumption of **46** in the absence of THF divided by the consumption of **46** observed at the various THF concentrations

Since tetrahydrofuran and furan are similar in the polarity, if the photoreactivity change of 3-phenyl-1,2,4-thiadiazole (**46**) upon changing from acetonitrile to furan was due to an effect of solvent polarity, irradiation of **46** in acetonitrile containing tetrahydrofuran at various concentrations should also reveal a similar decrease in the photoreactivity of **46**. The result upon irradiation of **46** in acetonitrile with various tetrahydrofuran concentrations, however, indicated that tetrahydrofuran had no effect either on the consumption of **46** or the formation of benzonitrile (**43**). This indicates that solvent polarity of furan has no effect on the reactivity of **46**. Thus, the observed decrease in the photoreactivity of **46** in the presence of furan would be due to a direct quenching interaction between **46** and furan via an unclear mechanism. The S_1 and T_1 state energies of furan have been reported at 129 and 74 kcal/mol, respectively.²² With the observed S_1 and T_1 state energies of 3-phenyl-1,2,4-thiadiazole (**46**) at 97 and 68 kcal/mol, respectively, and under the irradiation condition at > 290 nm, the possibility that furan may act as a singlet or triplet quencher can be ruled out since these processes are energetically unfavorable.